5TH INTERNATIONAL CONFERENCE ON

Timber Bridges

EFFECTIVE • EFFICIENT • RESILIENT

Rotorua, New Zealand • 29 June – 2 July 2025

PLATINUM SPONSOR

IBUILT PNGFP ENGINEERED WOOD PRODUCTS

HOSTS

NZTDS NEW ZEALAND TIMBER DESIGN SOCIETY

NZ TRANSPORT AGENCY WAKA KOTAHI

5th International Conference on Timber Bridges

Conference Programme

29 JUNE – 2 JULY 2025

ROTORUA, NEW ZEALAND

5TH INTERNATIONAL CONFERENCE ON
Timber Bridges
EFFECTIVE • EFFICIENT • RESILIENT

Rotorua, New Zealand · 29 June – 2 July 2025

Conference Programme - Sunday 29 June 2025

13.30	**Bus tickets must be pre-booked** Bus Departs Auckland CBD	**Auckland**
14.30	Bus Departs Auckland International Airport	
PM	Own time to explore local activities	**Rotorua**
15.00 – 19.00	Registration Open	**Sir Howard Morrison Centre**
17.30 – 19.00	**Mihi Whakatau - Welcome Reception**	**Sir Howard Morrison Centre**

Monday 30 June 2025

08.00 – 18.30	Registration Open	**Sir Howard Morrison Centre**
08.30	**Conference Opening** **Welcome from Conference MC**, Andrew Hewitt, Vice-President, New Zealand Timber Design Society **Welcome from Rotorua Mayor**, Tania Tapsell **Welcome from Conference Organising Committee** Sulo Shanmuganathan Daniel Moroder Andy Buchanan **Welcome from Platinum Sponsor**	**Haumoko Theatre**
09.00	**Keynote 1** Daniel Moroder **Chair:** Moustafa Al-Ani *Timber Bridges in Aotearoa New Zealand – Honouring the Past, Shaping the Future*	**Haumoko Theatre**
09.30	**Keynote 2** Steffen Franke *Long-Span Timber Highway Bridges as a Contribution to Global Decarbonization*	**Haumoko Theatre**
10.00 – 10.30	**Coffee Break & Exhibition**	**Te Whakaruruhau Banquet Room**
10.30 – 12.00	**Technical Session 1** **Chair:** Thomas Lim **Room:** Haumoko Theatre	**Theme**
10.30	*Durability of Wooden Bridges: Insights from Historical Service Test Data in New Zealand* **Tripti Singh**	**Durability**
10.52	*Extended Design Rules to Improve the Durability of Timber Structures* | **Roland Maderebner**	**Durability**
11.15	*Monitoring Technologies for the Long-Term Evaluation of Timber Bridges* | **Andreas Rödel**	**Monitoring**
11.37	*131 M Span Timber Cycle-Pedestrian Bridge: Structural Design and Calculation, Wind Tunnel Testing and Implementation of Vibration Control System* | **Mario Suárez Álvarez**	**Dynamics**
12.00 - 13.00	**Lunch & Exhibition**	**Te Whakaruruhau Banquet Room**
13.00	**Keynote 3** David Moses **Chair:** Bettina Franke *Breathing New Life into Timber Bridge Engineering in Canada*	**Haumoko Theatre**
13.30 – 15.00	**Technical Session 2** **Chair:** Andy Buchanan Room: Haumoko Theatre	**Theme**
13.30	*Design of Timber Bridges in Europe* | **Steffen Franke**	**Bridge Design**
13.52	*Design of Timber Bridges in France - New Technical Guide from the French Association of Civil Engineering* | **Valentina Bruno Hure**	**Bridge Design**
14.15	*Analysis of the Collapse of the Timber Bridge over the Duratón River, in Peñafiel (Spain)* **Alfonso Lozano**	**Bridge Design**
14.37	*Kakanui Replacement Bridge – Design of a New 162m Long Timber Road Bridge in New Zealand* **Anton Kivell**	**Bridge Design**
15.00	**Coffee Break & Exhibition**	**Te Whakaruruhau Banquet Room**

5TH INTERNATIONAL CONFERENCE ON
Timber Bridges
EFFECTIVE • EFFICIENT • RESILIENT

Rotorua, New Zealand · 29 June – 2 July 2025

Monday 30 June 2025

15.30 – 17.00	**Technical Session 3** **Chair:** Andy Van Houtte **Room: Haumoko Theatre**	**Theme**	**Technical Session 4** **Chair:** Jeremiah Shaw **Room: Matatea**	**Theme**
15.30	*Ageing Resistance of Bonded Joints in Externally Exposed Glued Laminated Timber Elements* **Gary Raftery**	Durability	*Smooth-Shank Nail Withdrawal Capacity: Effects of Wood Relaxation and Moisture Content* **Yuhao Zhang**	Connections
15.48	*Investigation of Cross-Laminated (CLT) Decks for Bridge Applications in the USA* **Justin Dahlberg**	Decks	*Dowel-Type Connection Behaviour of High-Density Naturally Durable Hardwood* **Milad Lezgi**	Connections
16.06	*Investigations on ATCC Components Using Fiber-Optical Sensors for Structural Analyses* **Andreas Kirchner**	Decks	*Austenitic Stainless-Steel Self-Tapping Screws in Timber Bridge Design: A Preliminary Performance Analysis* **Rodrigo Mendes & Ömer Şişman**	Connections
16.24	*Analysis of the Timber Moisture Content of ATCC-Road Bridge Superstructure Segment* **Johannes Koch**	Decks	*Modular Timber Arch Bridge for New Zealand* **Oliver De Lautour & Moustafa Al-Ani**	Structural Design
16.42	*Stauffacher Bridge, Timber-UHPC Composite Structure* **Edgar Kälin**	Decks	*A Restraint System for Vertically Laminated Glulam Bridge Girders – A Design Engineer's Perspective* | **Michael Campbell**	Structural Design
17.00 – 18.30	**Technical Session 5** **Chair:** Gang Yu **Room: Haumoko Theatre**	**Theme**	**Technical Session 6** **Chair:** Oliver De Latour **Room: Matatea**	**Theme**
17.00	*Development for the Composite Hybrid Bridge – A Novel Solution for a Low Carbon Future* **Royce Liu**	Sustainability	*CLT Timber Bridges: Experimental and Numerical Study* **Reza Masoudnia**	Construction
17.18	*Adding Broader Value to Aotearoa New Zealand – How Timber Bridges can Create Regional Economic Growth while Reducing Carbon Emissions* **Liz Root**	Sustainability	*SH 26 Onetai Stream Bridge - New Zealand's First Modern Timber State Highway Bridge in Decades* **Cameron Douglas**	Construction
17.36	*Methods of Life Cycle Assessment of Bridge Constructions and Exemplary Investigation of Different Bridge Constructions of Pedestrian and Cycle Bridges* **Sven Steinbach & Christoph Kunde**	Sustainability	*The Rakaia Gorge Bridge Deck Replacement and Seismic Strengthening* **Andrew Bradfield**	Construction
17.54	*Longevity and Service Life Considerations for Vehicle Timber Bridges in New Zealand* **Hanshen Wang**	Durability	*Tharwa Bridge Restoration and Maintenance* **Marcia Prelog**	Construction
18.12	*Effects of Brown-Rot Decay and Corrosion on Polymer Composition on Radiata Pine Connectors* **Camilo Montoya**	Durability	*Emerging Technology in Timber Bridge Deck Replacement: Recent Use of Engineered Plywood Panels in New Zealand* **Jeremiah Shaw & John van Rij**	Construction
18.30	**Own Time** Recommended meeting point for evening socialising: Tutanekai Street - Also known as 'Eat Street'			

5TH INTERNATIONAL CONFERENCE ON
Timber Bridges
EFFECTIVE • EFFICIENT • RESILIENT

Rotorua, New Zealand · 29 June – 2 July 2025

Tuesday 1 July 2025

08.00 – 18.00	**Registration Open**	
08.30 – 10.00	**Technical Session 7** **Chair:** Henri Baillères **Room: Haumoko Theatre**	**Theme**
08.30	*GLVL Panels for a New Timber Footbridge over the Brussels Ring* | **Benoît Hargot**	Pedestrian Bridges
08.52	*Sustainable Spans - Timber's Role in New European Pedestrian and Cycling Networks* **Frank Miebach & Lukas Osterloff**	Pedestrian Bridges
09.15	*Bridges in Switzerland - Experience of Bridges for Pedestrians, Traffic and Wildlife Overpass* **Stefan Zöllig**	Pedestrian Bridges
09.37	*SH1 Papakura to Drury Shared Use Path Timber Bridge* | **Tony Pham**	Pedestrian Bridges
10.00	**Coffee Break & Exhibition**	**Te Whakaruruhau Banquet Room**
10.30	**Keynote 4** Ralph Belperio **Chair:** Hugh Morris *Past, Present And Future Of Timber Bridges In Australia*	**Haumoko Theatre**
11.00 – 12.30	**Technical Session 8** **Chair:** Anton Kivell **Room: Haumoko Theatre**	**Theme**
11.00	*Best Practices in Timber Railway Overbridge Asset Management: Queensland Case Studies* **Dan Schneider & Daniel Anstice**	Rail Bridges
11.22	*Test-Based Asset Life Management of Timber Railway Bridge Members* | **Evie Anderson**	Rail Bridges
11.45	*Emergency Repair of Timber Howe Truss Bridge After Vehicle Strike* | **Murray Johnson**	Repairs
12.07	*The Rehabilitation Design of the West Montrose Covered Bridge* | **Andrew Lehan**	Repairs
12.30 – 13.30	**Lunch And Exhibition**	**Te Whakaruruhau Banquet Room**
13.30 – 15.00	**Technical Session 9** **Chair:** Gary Raftery **Room: Haumoko Theatre**	**Theme**
13.30	*Timber Circularity: Sustainable Wood Resource Management in Australia* | **Tripti Singh**	Sustainability
13.48	*Timber Bridge Asset Management* | **Gang Yu**	Asset Management
14.06	*Analysis of a Mechanically Connected Timber Arch Section and Steel Hinge Connection for an Arch Bridge* | **Jens Bergenudd**	Structural
14.24	*Pre-Fabricated Stress Laminated Timber Bridges in New Zealand* | **Edwin Douglass**	Pre-Stressed Bridges
14.42	*Prestressing Losses in a Stress Laminated Timber (SLT) Logging Bridge* | **Andy Buchanan**	Pre-Stressed Bridges
15.00 – 15.30	**Coffee Break & Exhibition**	**Te Whakaruruhau Banquet Room**
15.30	**Panel:** *What is the Future of Effective, Efficient,and Resilient Timber Bridge Design?* **Chair:** Moustafa Al-Ani **Panellists: Andrew Lehan, Tripti Singh, Anton Kivell, Stefan Zöllig and Borjen Yeh**	**Haumoko Theatre**
17.00	**Conference Closing** **Chair:** Hugh Morris **Expression of Interest for 6th ICTB in 2029:** Bettina Franke **Conference Close:** Sulo Shanmuganathan	**Haumoko Theatre**
17.30	**Bridge Testing Competition** **Chair:** Thomas Lim	**Entrance Foyer**
19.00 – Late	**Conference Dinner** **Sponsored By Rothoblaas NZ** rothoblaas Solutions for Building Technology	**Te Whakaruruhau Banquet Room**

5TH INTERNATIONAL CONFERENCE ON
Timber Bridges
EFFECTIVE • EFFICIENT • RESILIENT

Rotorua, New Zealand · 29 June – 2 July 2025

Wednesday 2 July 2025

08.45	Bus Departs from outside Sir Howard Morrison Centre	
09.00 – 10.30	**Red Stag TimberLab CLT Factory Site Visit**	**Scion - Te Whare Nui o Tuteata Site Visit**
10.45	Bus Departs from outside Sir Howard Morrison Centre	
11.00 – 12.30	**Red Stag TimberLab CLT Factory Site Visit** Bus will return to Sir Howard Morrison Centre after site visit including a drop at Scion as per below.	**Scion - Te Whare Nui o Tuteata Site Visit** Bus will return to Sir Howard Morrison Centre after site visit including a drop at Scion as per below.
12.30 **13.30**	**Optional** **Lunch in Scion Café (at own cost)** **Redwoods Treewalk $5 discount promocode: 2025TWTIMBER** **Redwoods Altitude Treewalk $10 discount promocode: 2025ALTTIMBER** Bus departs to Sir Howard Morrison Centre	
14.00 **16.00** **18.00** **19.00**	**Auckland bus tickets must be pre-booked** Bus Departs from outside Sir Howard Morrison Centre including stops: » **Onetai Timber Bridge (weather dependent)** » **Auckland Airport** » **Auckland CBD**	

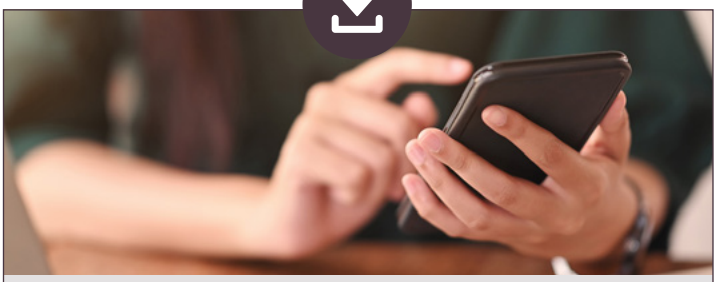

ICTB 2025 APP

Have you downloaded the conference mobile event app? If not, come and see us at the registration desk and we'll get you set up.

- Submit questions to the presenters for Keynote and Panel Sessions
- View the full conference programme
- Read speaker biographies and presentation abstracts
- Receive notifications for important notices straight to your device during the conference
- Scan the QR code on delegate nametags to share contact details.

Conference Organising Committee

- **Sulo Shanmuganathan**, Chief Engineer, New Zealand Transport Agency (Convenor)
- **Andy Buchanan**, Principal, PTL Structural & Fire (Chair, Scientific Committee)
- **Daniel Moroder**, Technical Director, PTL Structural & Fire, Past President, NZ Timber Design Society (Co-Convenor)
- **Bettina Franke**, Head of Research and Marketting, Timbagroup Holding AG, Switzerland (Chair, 4th ICTB)
- **Moustafa Al-Ani**, Lead Advisor Structures, New Zealand Transport Agency
- **Hyungsuk Thomas Lim**, WIDE Trust Senior Lecturer, University of Canterbury
- **Hugh Morris**, Technical Manager, Timber Unlimited
- **Gary Raftery**, Senior Lecturer and Co-Director of CIRCUIT Research Centre, University of Auckland
- **Tripti Singh**, Senior Scientist, Scion, Rotorua and Director, National Centre for Timber Durability & Design Life, Australia

Special Dietary Requirements

If you indicated your dietary requirement during the online registration, this has been forwarded to the caterers. Depending on your requirement, the main food may be suitable for you, or a separate table will have your food. Please make yourself known to the catering staff who will assist or please see the Registration Desk for assistance.

5TH INTERNATIONAL CONFERENCE ON
Timber Bridges
EFFECTIVE • EFFICIENT • RESILIENT

Rotorua, New Zealand · 29 June – 2 July 2025

Scientific Committee

Chair of Scientific Committee : Andy Buchanan, PTL Structural & Fire, New Zealand

International Committee	National Committee
» Ralph Belperio, Australia	» Henri Bailleres, Scion
» Valentina Bruno-Hure, France	» Ben Browne, Novare Design
» Keith Crews, Australia	» Kwan Chin, WSP
» Per Anders Fjellstron, Sweden	» Liam Coleman, KiwiRail
» Steffen Franke, Switzerland	» Paul Corbett, Jacobs
» Caroline Frenette, Canada	» Oliver De Lautour, Aurecon
» Liu Jie, China	» Matt Ireland, Holmes NZ
» Benjamin Kromoser, Austria	» Anton Kivell, Hoffcon
» Andrew Lehan, Canada	» Sam Leslie, Redstag
» Thomas Lim, New Zealand	» Lisa Oliver, Holmes NZ
» Kjell Arne Malo, Norway	» Ranjit Rajasingh, AECOM
» David Moses, Canada	» John Roebuck, Holmes Solutions
» Hideyuki Nasu, Japan	» Jeremiah Shaw, Beca
» Gary Raftery, New Zealand	» Charlotte Toma, University of Auckland
» Antje Simon, Germany	» Andy Van Houtte, Potius
» Tripti Singh, Australia and New Zealand	» Mike Wall, Fletcher Projects
» Julio Vivas, Spain	» Gang Yu, Auckland Transport
» James Wacker, USA	

Notes

5TH INTERNATIONAL CONFERENCE ON

Timber Bridges

EFFECTIVE • EFFICIENT • RESILIENT

Rotorua, New Zealand · 29 June – 2 July 2025

The conference organising committee gratefully acknowledges the conference sponsors for their generous support:

Platinum Sponsor

IBUILT™ / PNGFP

ENGINEERED WOOD PRODUCTS

Gold Sponsors

RED STAG TIMBERLAB®

Eurotec® | Marshall INNOVATIONS CONSTRUCTION SOLUTIONS

Silver Sponsors

NZ TRANSPORT AGENCY WAKA KOTAHI

aurecon

Bringing ideas to life

Te Uru Rākau New Zealand Forest Service

Bronze Sponsors

BIG RIVER

WIDE WOOD INDUSTRY DEVELOPMENT AND EDUCATION TRUST

Conference Dinner Sponsor

rothoblaas

Solutions for Building Technology

Coffee Cart Sponsor

BG&E

Lunch & Refreshment Break Sponsor

Responsible Wood

PEFC

PEFC/21-1-1

International Media Partner

Bridge

DESIGN & ENGINEERING

ICTB 2025. 5th International Conference Timber Bridges
Rotorua, New Zealand, 29 June to 2 July 2025.

TEST-BASED ASSET LIFE MANAGEMENT OF TIMBER RAILWAY BRIDGE MEMBERS

Evie Anderson[1], Liam Coleman[2]

ABSTRACT

KiwiRail maintains an extensive railway network in New Zealand, where hundreds of in-service bridges have spans and piers that are comprised of Australian Hardwood with an average age greater than 100 years. This far exceeds international best practice recommendations for operational life of this type of timber. The replacement cost for these bridges is significantly higher than funding KiwiRail receives. Consequently, remedial solutions have been employed to extend the life of these bridges. Previous strategies have included visual assessment, invasive investigation via core drilling of timber members, and field engineering-type remedial solutions.

To mitigate risk, understand the reliability of aged timber with different types of defects, and quantify the effectiveness of remedial solutions, KiwiRail engaged Holmes Solutions LP to undertake testing on beams, pile caps, and piles removed from service.

Based on the testing to date, we learned:

- Beam clamp remedial solutions did not materially increase the capacity of a member, as they were intended.
- Strength loss in piles resulting from weathering and defects was not inherently as significant as expected.
- Split cylinder pile repairs are an effective means of remediating damaged piles and increasing their capacity.

The outcome of testing provided more confidence in the methods currently used to establish condition scores for members, validated the assessment methodology currently employed, which considers an age factor and condition factor, and provided quantitative data to inform KiwiRail about the effectiveness of remedial solutions.

1 KIWIRAIL'S STORY

The first commercial steam railway in New Zealand was from Christchurch to Lyttleton, which opened in 1863. The network continued to grow to its peak in 1953 with a length of 5656 km. Today, the network is circa 4000 km and has over 1300 active bridges, which equates to over 52 km of bridge length. When the network opened in 1863, timber was the most assessable material and Australian Hardwood was the species of choice. As a result, a large portion of the rail bridges in New Zealand were constructed from Australian Hardwood timber. Today approximately 15% of piers and 8% of spans on the active network are timber with an average age greater than 100 years. International best practice guides suggest the operational life of hardwood timbers in service should be 60 years, which KiwiRail have exceeded. The timber bridges that remain in the KiwiRail network have a replacement cost of $2 billion NZD, and KiwiRail currently get funding of $50-80 million per annum. Consequently, KiwiRail are not in a position to replace all their life-expired timber bridges in a suitable timeframe. For this reason, KiwiRail seek to better understand their timber bridges to establish if the timber is life-expired, and if not, how they can extend the life of the timber to increase the reliability of its performance and maintain their currently levels of service and safety requirements.

[1] Structural Engineer, Holmes Solutions LP, Christchurch, New Zealand
e-mail: evie.anderson@holmessolutions.com,
[2] Professional Head (Structures) - Infrastructure, KiwiRail

Degradation of timber members manifests itself in many ways. Examples of defects observed in the field are illustrated in Figure 1.

Figure 1: Examples of defects observed in the field in timber pile and beam elements.

1.1 Standard Timber Remediation Strategies

Over the years, KiwiRail developed remedial strategies based on qualitative methods to attempt to extend the life of timber assets. Through testing, KiwiRail and Holmes Solutions aimed to increase understanding of these remedial solutions and what capacity they would generate for repaired members. Some solutions KiwiRail developed include:

- Placing steel clamps on beams and pile caps (refer to Figure 5).
- Removing a section of a timber pile and reinstating with a new section (stump repair). This approach has evolved from solutions such as the examples in Figure 2 where the new and old sections were spliced together using steel members and bolts, to the current approach shown in Figure 3. The current approach introduces a compression force into the new and old sections using a simple bolted jack. The stump jack is then wrapped with a steel jacket (sleeve or split cylinder) and filled with concrete or high strength grout as shown in Figure 3 and Figure 9.
- In addition to its application in stump repairs, the split cylinder method can also be applied to an in-situ single timber section with defects.

Figure 2: [Left] Historic stump repair on a pile segment removed from service. [Right] Stump repair in service.

Figure 3: Current process for installing a stump repair.

2 PRELIMINARY TESTING

From visual assessment and implicit consideration, it is understood that the strength and performance of timber degrades over time, particularly when exposed to adverse environmental factors. However, the extent and consequences of this have not been previously investigated sufficiently to inform assessment procedures with a reasonable degree of certainty. To begin removing uncertainty, beams, pile caps, and piles were removed from service and supplied to Holmes Solutions for initial testing. Testing included:

- STAGE 1 – Initial investigation into the effectiveness of beam clamp remedial solutions.
- STAGE 2 – Evaluation of beam and pile cap capacity versus Condition Score.
- STAGE 3 – Evaluation of pile capacity, considering various ages, defects, and Condition Scores, and the performance of remedial solutions.

As part of KiwiRail's inspection standards, their beams, pile caps, and piles had been assigned condition scores categorising them as containing a certain level of defects as defined in Figure 4. The KiwiRail assessment guide[1] provides examples of what type of defects may place the element into a particular category. For example, a Condition Score 3 member may contain checks up to 1500 mm long and/or present fungal decay (e.g. white rot). Per KiwiRail's assessment procedure, this Condition Score is used to obtain a strength reduction factor applied to the capacity that is determined as a function of timber age.

Code	Description
1	As new condition or defect has no significant effect on the component (visually or functionally).
2	Early signs of deterioration, minor defect / damage, no reduction in functionality of component.
3	Moderate defect / damage, some loss of functionality could be expected.
4	Severe defect / damage, significant loss of functionality and / or component is close to failure / collapse.
5	The component is non-functional / failed.
NR	Not Reported component has not been inspected.

Figure 4: Excerpt from the KiwiRail condition assessment guide[1] defining Condition Scores.

Piles were supplied with various defects documented. Inspections via drilling small diameter core holes had been undertaken by KiwiRail historically and immediately prior to testing. Core samples only provide information about a local section of timber; consequently, defects may go undetected. Testing provided an opportunity to evaluate the limits of this inspection method by showing to what extent significant defects go undetected.

2.1 Beam Testing

The average age of timber components on KiwiRail's network is over 100 years, and the material properties are not fully known. Through testing, KiwiRail wanted to better understand the capacity of this timber to help inform their standards and validate their assessment methodology. In the past, KiwiRail have clamped decayed timber with the hope of increasing its capacity; however, they did not know to what extent this solution was effective. To understand the merit of this theory, three beams were subjected to 3-point bend tests. One beam had no clamps, one had clamps providing horizontal restraint (refer to Figure 5), and the third had clamps providing vertical restraint. Beams were tested to failure and deflection was recorded at the point of load application.

Figure 5: A beam specimen with horizontal restraint clamps.

Results indicated the clamps did not increase the capacity of the members and were ineffective for that remedial intent (refer to Figure 6).

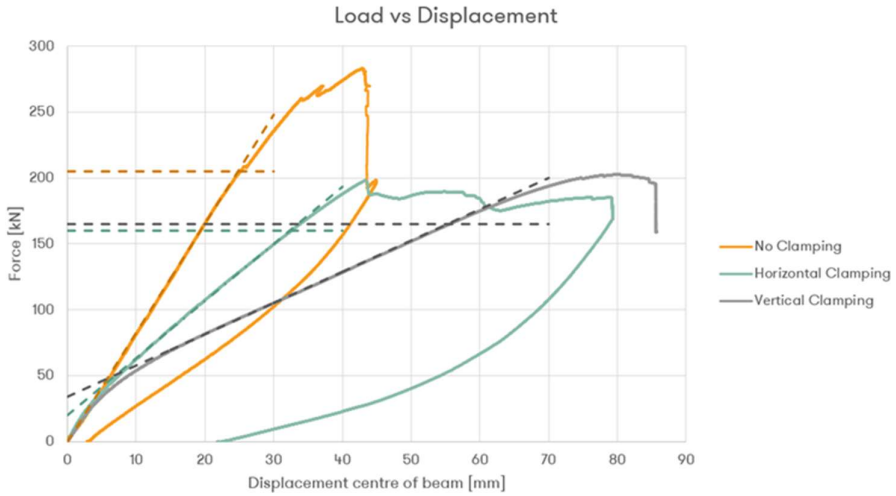

Figure 6: Results from the initial investigation of the beam clamp remedial solution.

Subsequently, an additional 14 beams and pile caps were subjected to 3-point bend testing to evaluate the capacity of members with different Condition Scores (refer to Figure 7 for an example test specimen).

Figure 7: Test setup configuration for initial pile cap testing.

Specimens ranged from Condition Score 1 to 4 and were installed between 1904 and 2011. Load and deflection results obtained from the testing (refer to Table 1) were used to determine Young's Modulus of Elasticity for comparison to the grades defined in NZS AS 1720.1:2022[2] Table H2.1. Stress grade, based on Young's Modulus, had previously been selected by KiwiRail as a means of categorising timber and providing probable capacity values for use in assessments. For beams, new Ironbark hardwood is considered to have a stress grade of F27. This round of testing provided KiwiRail with insight into the reduction in stress grade with Condition Score for comparison to the results they obtain for their current assessment approach.

Table 1: Summary of Beam and Pile Caps Tested in the Preliminary Round of Testing

ID	Condition Score	Year Installed	Max. Force [kN]	E [GPa]	Grade [1]
Pier 3	1	2011	458	11.4	F11
Pier 9	1	2000	649	12.6	F14
Pier 10	1	1986	440	14.4	F17
Span X	2	2011	543	15.8	F17
Span 12	2	2011	408	9.8	F8
Pier 1	3	1904	276	12.9	F14
Pier 5	3	1904	186	10.2	F8
Pier 8	3	1904	328	13.5	F14
Pier 11	3	1904	282	9.8	F8
Pier 12	3	1973	254	9.0	F7
Pier 13	3	1904	301	10.8	F11
Span 1	3	1904	320	12.1	F14
Pier 2	4	1904	309	10.7	F11
Pier 4	4	1904	249	6.6	F4
Pier 6	4	1904	233	13.9	F14

Notes:

[1] Grade is defined in accordance with NZS AS 1720.1:2022[2] Table H2.1 and based on the calculated Young's Modulus of Elasticity value from the testing results, per the assessment approach employed by KiwiRail.

2.2 Pile Testing

Segments of timber piles removed from service were subjected to compression testing to establish the capacity and performance of defects observed in the field. Additionally, testing provided the opportunity to evaluate the effectiveness of repair strategies, consider whether improvements can be made to the existing methodologies, and how failure mechanisms may change once remediation has occurred. The age of several piles was known, and Condition Scores had been assigned; thus, the test failure load could be compared to the capacity that the assessment method would have produced for these piles.

The types of defects observed on tested piles included:

- Section loss from rot and/or erosion, including asymmetrical section loss.
- Rot of the core of the pile.
- Significant splits and checks.
- Historic bolt holes.
- Significant weathering.

Remediation methods evaluated during this round of testing included stump repairs and split cylinders. One pile was supplied with a stump repair. Split cylinders were added to a pile after it was initially tested (refer to Figure 9) and another pile with significant section loss prior to testing.

Failure mechanisms observed included:

- "Mushrooming" near an end,
- Buckling, particularly at defects or locations with asymmetric cross-sections, and
- Crushing.

The "mushroom" failure mechanism appeared to be most common in piles that were relatively large diameter and exhibited longitudinal weathering and splits. Pile 12, which was one of the piles that failed in this manner (see Figure 8), was the pile repaired with a split cylinder and subjected to repeat testing.

Figure 8: Compression of Pile 12 resulted in radial buckling, "mushroom", along splits.

In its original condition, Pile 12 reached a maximum axial load of 1510 kN. The pile displayed signs of significant internal rot in the failed region when inspected after testing. KiwiRail applied their standard split cylinder repair over the zone of failure. The high strength grout was cured for just over two days, and the pile was retested. The repaired pile reached an axial load of 2926 kN.

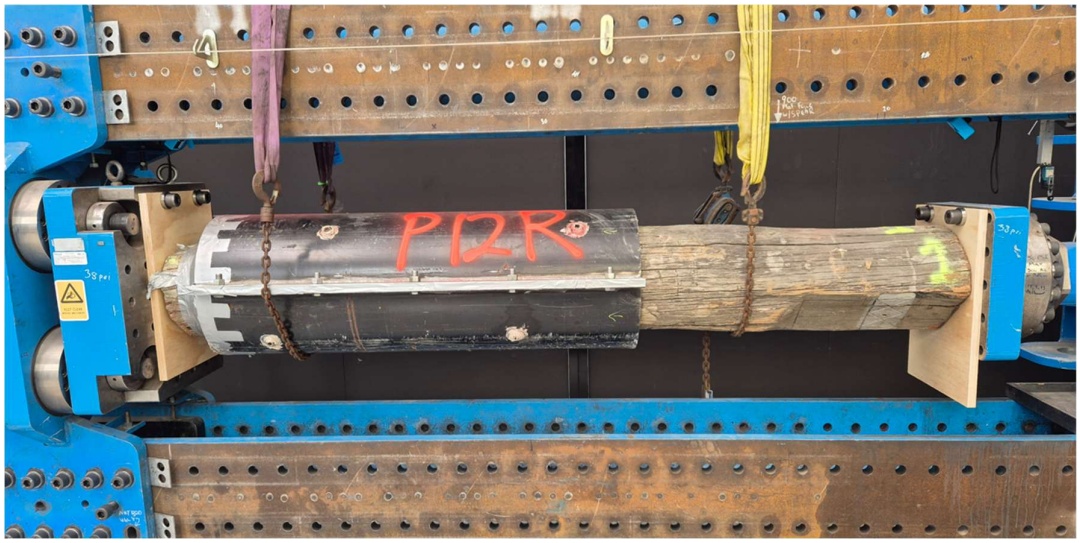

Figure 9: Pile 12 repair test setup with split cylinder and high strength grout.

Considering the results from the other pile tested with a split cylinder repair and the ability to directly compare the results from a pile tested with and without the repair provided valuable insight. Learnings included:

- Understanding the impact of the repair methodology on different types of defects.
- Factors in the split cylinder design that impact its effectiveness.
- Preliminary information about the grout curing time versus quantifiable benefit of the repair. Awareness of the impact of grout curing time on the performance of the repair allows KiwiRail to understand when it is safe for trains to pass over the repaired bridge.

Some factors that appeared to impact the performance of the split cylinder included:

- The capacity of the bolts clamping the steel flanges.
- Grout thickness, strength, and integration with the pile (i.e. filling large voids).

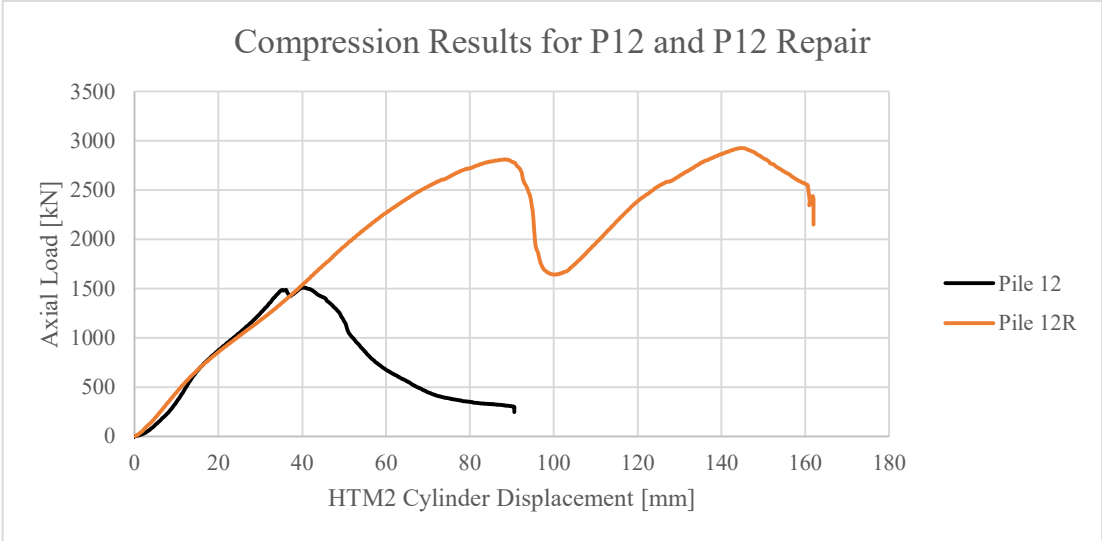

Figure 10: Comparison of pile performance before and after implementation of a split cylinder repair.

Despite different pile lengths, diameters, and original defects, the two piles repaired with the split cylinder reached similar compression stress capacities upon failure. In both cases, the repair was effective at significantly increasing the capacity of the pile compared to its original condition and assessed capacity.

New Ironbark hardwood piles are considered to have a stress grade of F34. In KiwiRail's assessment approach, this grade is reduced as a function of age and another reduction factor is applied to account for

the visually assigned Condition Score. Of the piles that were tested, ones that exhibited a mushroom failure mechanism reached the most consistent compression stress capacities regardless of Condition Score. Piles with a crushing failure mechanism appeared to be the most linked to Condition Score. Piles with a buckling failure mechanism presented a large standard deviation relative to Condition Score, and appeared to be the most influenced by defects, especially asymmetrical section loss and degradation (see Figure 11).

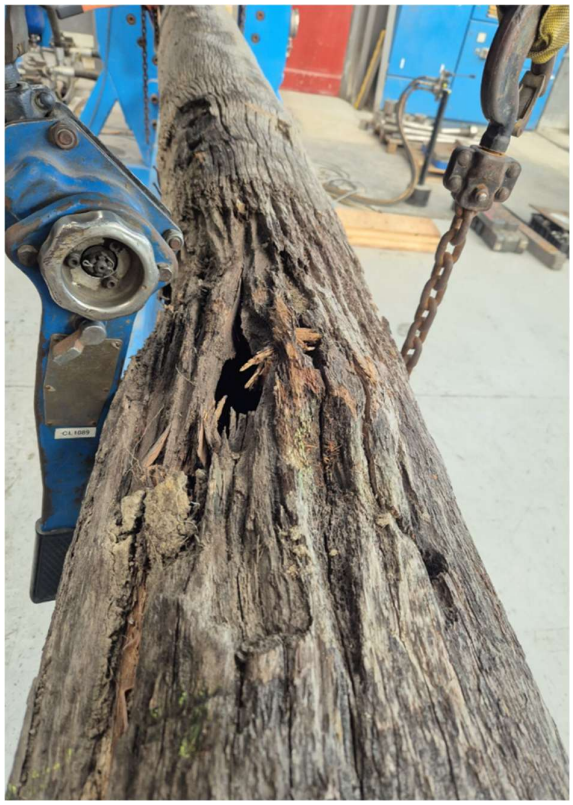

Figure 11: Pile 10 contained a void and significant degradation on the left side of the pile and buckled at the worst location, which was near the gravity support.

3 FUTURE TESTING AND USE OF RESULTS

KiwiRail started testing timber components with Holmes Solution over two years ago. The initial testing helped inform the current KiwiRail assessment standards. As testing has progressed with large suites of specimens, the standards have been refined, and initial conservatism has been removed. Additionally, a better understanding of KiwiRail's aging timber helps ensures timber is not removed before it has reached the end of its useful life.

The latest round of pile testing has informed KiwiRail on methods for strengthening, such as "entombing" timber in steel and concrete jackets (e.g. the split cylinder method), which has proven through testing that significant additional capacity is possible when adopted. These test results will be reviewed with a plan to develop internal task instructions so this standardised strengthening technique can be rolled out across the engineering team. Using the split cylinder repair has the potential to be a quarter of the costs of a typically pier replacement, which is a significant saving for KiwiRail.

Over the next 12-24 months KiwiRail intend to trial other low-tech repair solutions to add to the growing suite of strengthening techniques developed, which are extending the life of timber on their network.

4 CONCLUSIONS

The testing of Australian Hardwood railway bridge components removed from service by KiwiRail and Holmes Solutions has yielded several valuable insights for asset management. Beam clamp remedial solutions were found to be ineffective at increasing member capacity. Timber pile testing provided useful

data points regarding qualitative defects and performance, including the opportunity to correlate failure mechanisms to condition types and some physical features. Mushroom failure mechanisms were associated with the most consistent compressive stress results regardless of condition score, crushing failures resulted in the closest link between condition score and compressive stress capacity, and piles that experience buckling failures were most influenced by asymmetrical degradation. The split cylinder repair methodology proved highly effective, nearly doubling the capacity of a damaged pile repaired after initial testing, and it offers the opportunity for significant cost savings compared to a full pier replacement. The quantitative data obtained from testing allows KiwiRail to refine their assessment standards, remove unnecessary conservatism, extend the service life of timber components beyond the typical 60-year recommendation, and develop standardised strengthening techniques for their timber bridge network.

REFERENCES

1. KiwiRail, 2024. Structures Standard: Rail Bridge Assessment. Document No. B-ST-AS-3121. This document is available upon request from KiwiRail.
2. Standards New Zealand and Standards Australia. NZS AS 1720.1:2022. Timber Structures Part 1: Design Methods. 155pp.
3. Holmes Solutions LP test reports delivered to KiwiRail are confidential and therefore not referenced.

ICTB 2025. 5th International Conference Timber Bridges
Rotorua, New Zealand, 29 June to 2 July 2025.

ANALYSIS OF A MECHANICALLY CONNECTED TIMBER ARCH SECTION AND STEEL HINGE CONNECTION FOR AN ARCH BRIDGE

Jens Bergenudd[1], Jean-Marc Battini[2], Roberto Crocetti[3], Georgi Nedev[4]

ABSTRACT

This article investigates the dynamic and static behaviour of a novel steel hinge connection for the arch of a recently built pedestrian timber bridge. A full-scale model of an arch section was built in laboratory and experimentally tested at four different stages of construction to properly evaluate the material properties, degree of composite action between the timber members and the stiffness of the connection. The results showed that the composite action was partial with an approximately 70 % reduction of the second moment of area and torsional constant when comparing the numerical and experimental results. The dynamic rotational stiffness of the connection was around 0.9-3.4 MNm/rad (out-of plane bending) and 10.0-27.0 MNm/rad (in-plane bending). The static results indicated that the rotational stiffness was around 2.5-7.5 MNm/rad (out-of plane) and 1.9-9.1 MNm/rad (in-plane). The compressive stiffness could potentially be around 2-8 times larger (4 times on average) than the tensile stiffness of the steel hinge connection.

1 INTRODUCTION

Timber bridges typically include several joints which, due to their load-slip behaviour, can significantly reduce the stiffness of the structure. This phenomenon needs to be properly addressed, especially regarding the dynamic assessment of timber bridges. The stiffness in timber structures due to the presence of joints has been studied in previous research. Rönnquist et al. [1] investigated the dynamic response of a pedestrian timber bridge and found that a reduction of the stiffness of a specific connection was required to calibrate the numerical model. Similar results were found by Hawryszków & Biliszczuk [2] on a pedestrian timber cable-stayed bridge.

Malo et al. [3] and Sandhaas [4] perfomed tensile static tests on glulam specimens with connections made from slotted-in steel plates and steel dowels. Comparisons with the expression for the slip modulus (K_{ser}) in Eurocode 5 were performed and some discrepancies between the experiments and K_{ser} could be found. Solarino et al. [5] evaluated the rotational stiffness of a similar type of joint and found deviations compared with K_{ser}. Jockwer et al. [6] also mentions deviations of the slip modulus, e.g. depending on the diameter of the dowel. Landel et al. [7] studied the joints of a truss structure from dynamic experiments by applying detailed models and comparing them with simplified models applying springs with K_{ser} for dowels. The spring model showed promising results for modes of vibration in 2D, i.e. the in-plane modes of the truss. Studies of the axial withdrawal strength ($K_{ser,ax}$) of self-tapping screws was performed by Blaß et al. [8] where expressions based on the density of the timber member as well as length and diameter of the screw was determined. Similar expressions can be found in research [9] and several design guides discussed by [10]. A new expression for $K_{ser,ax}$ is evaluated for the new Eurocode 5 [11].

This article investigates a novel steel-hinge connection for an arch bridge in Sweden. A full-scale arch section was constructed in laboratory and tested both statically and dynamically. The arch section was tested at different stages to determine the material parameters, partial composite action and finally the bending stiffness of the connection.

[1] PhD student, KTH Royal Institute of Technology, Sweden,
e-mail: jbergenu@kth.se,
[2] Professor, KTH Royal Institute of Technology
[3] Professor, KTH Royal Institute of Technology. Structural engineer, Timber Bridge Specialists.
[4] Structural engineer, Timber Bridge Specialists.

2 UDDEBO BRIDGE

Uddebo bridge is a newly built pedestrian hybrid bowstring arch bridge with a modular design [12] and span of 39.8 m located in Uddebo, Sweden, see Figure 1. The modularity is achieved by applying standardised timber beams, i.e. without the need for prefabricated elements. The timber structure consists of an arch, vertical columns as well as upper and lower crossbeams. The arch is mainly loaded in compression whereas a bottom steel member carries the tension forces and bending moments. Cross-bracing is achieved with steel rods between the vertical columns as well as between the upper crossbeams.

Figure 1. Uddebo bridge.

2.1 Arch section

Each of the two arches consists of 10 arch sections which are made from four straight glulam beams (90x405 mm) with a length of 3.95 m. The four beams are divided into two pairs, where the ends are connected with steel joints, see Figure 2. The four beams are mechanically connected with steel rods at four positions along the section. Timber spacers (45x200x190 mm) and sharp metal plates (Rothoblaas SHARP501200) are placed in between with a characteristic value on the slip modulus of 3.0 N/mm^3.

2.2 Steel hinge connection

The arch sections are connected with a novel joint, see Figure 2. The joint consists of two "door hinge-type" connections applied at the top and bottom of each end of the straight elements of the arch section. Due to its configuration, with two separate hinges placed at a distance to one another, the joint can transfer bending moment from one arch element to the next. Steel fittings are fastened with screws (Rothoblaas VGS EVO 9x280 mm) at the ends with a 45º angle. The steel fittings are then connected with dowels (d = 30 mm), creating a moment stiff connection.

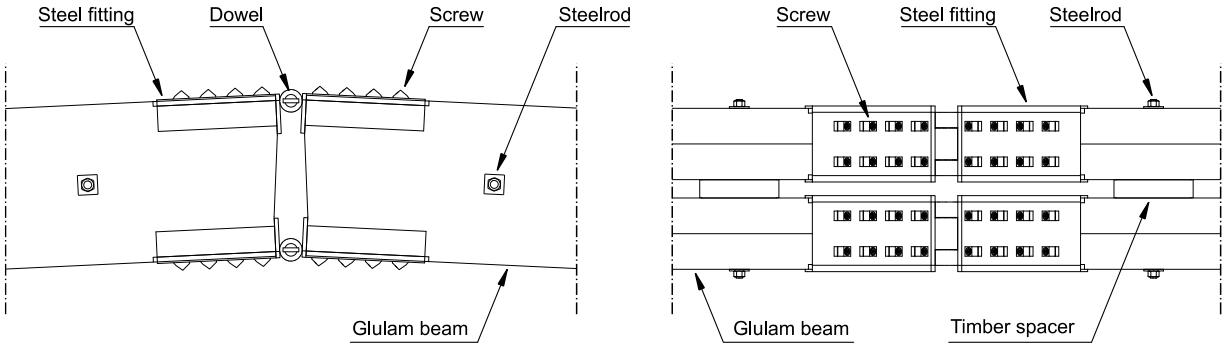

Figure 2. Steel hinge connection.

3 EXPERIMENTAL TESTING

3.1 Static and dynamic tests

The dynamic and static testing were performed on a full-scale piece of the bridge arch that included the novel joint, see Figure 3. The dynamic tests consisted of impulse excitation and recording of the subsequent accelerations. The structure was suspended by straps during the dynamic tests to achieve free-free boundary conditions. Static tests were carried out in accordance with EN-408 four-point loading [13].

Figure 3. Left) Static four-point loading. Right) Dynamic testing with free-free boundary conditions.

3.2 Stages of testing

Dynamic and static tests were performed at four stages, see Table 1 and Figure 4. Testing with and without a compression force was also performed at stage 4 to simulate the conditions of the arch section on the bridge, since the arch is mainly in compression. Two steel hollow box beams were placed at each end with a tensioned steel wire between them providing an axial compressive force.

Table 1. Stages of the experimental testing.

Stage	Description	Investigation
Stage 1	**Individual timber elements**	Dynamic elastic moduli (E, G)
Stage 2	**Mechanically connected member type 1 (MC1)** *Two glulam elements connected with steel rods and end joints.*	Composite action
Stage 3	**Mechanically connected member type 2 (MC2)** *Two MC1s connected with steel rods, timber spacers and sharp metal plates.*	Composite action
Stage 4	**Mechanically connected member type 3 (MC3)** *The MC2s are cut in half and connected with dowels at the end joints.* *Tested both with/without axial compression force.*	Bending stiffness of the joint

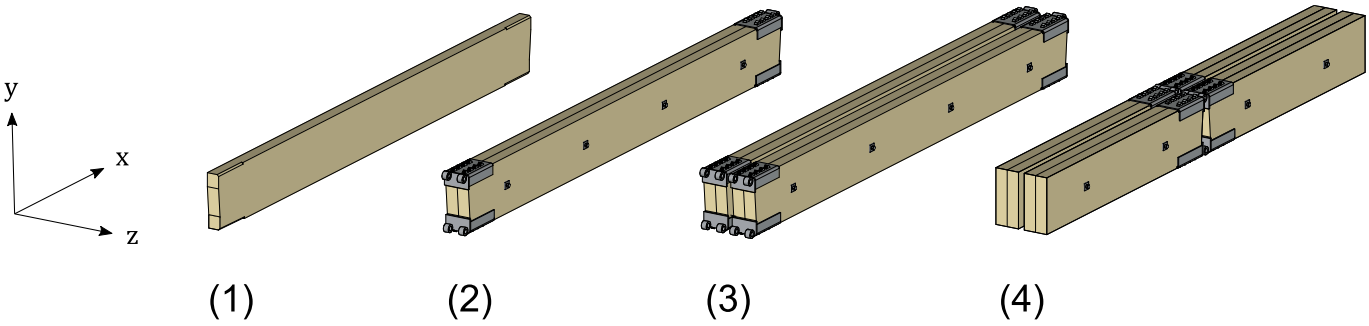

Figure 4. Stages of the experimental testing.

4 STIFFNESS OF THE CONNECTION

4.1 Theoretical stiffness

The theoretical stiffness of the steel hinge connection can be evaluated based on expressions of the slip modulus for the shear plane ($K_{ser,sh}$) and axial withdrawal ($K_{ser,ax}$) stiffness of the screws. The slip modulus for shear stiffness of steel-to-timber connections ($K_{ser} = 2\rho^{1.5}d/23$) according to Eurocode 5 is applied [14]. Several expressions for $K_{ser,ax}$ are evaluated, see Table 2. The combined stiffness of the fasteners including the number of screws per steel fitting ($n_{sc} = 8$ screws) can be expressed according to Equation (1). Note that the stiffness equals the perpendicular (shear) stiffness $K_{\perp}$ at $\alpha = 0°$ and the parallel (axial) stiffness at $\alpha = 90°$. The rotational stiffness ($k_{\theta,s}$) for one MC1 end connection (see Figure 4) can be expressed based on the cross-sectional height (ℓ) and an equivalent stiffness ($K_{s,eq}$) if the stiffness differs in compression ($K_{s,c}$) and tension ($K_{s,t}$), see Equation (2) and Figure 5. The total stiffness of the connection can then be determined based on two springs in series ($k_{\theta,i,ss}$), see Equation (2). The stiffness of the steel

dowel is assumed to be very stiff and much larger than the stiffness of the embedded screws and compression of the timber. The compression of the steel fitting on the timber member cannot easily be evaluated and is therefore disregarded for the values in Table 2, i.e. $K_{s,c} = K_{s,t} = K_s$.

$$K_s = n_{sc}\left(K_{ser,sh}\cos^2\alpha + K_{ser,ax}\sin^2\alpha\right) = n_{sc}\left(K_\perp\cos^2\alpha + K_\parallel\sin^2\alpha\right) \tag{1}$$

$$k_{\theta,s} = \frac{K_{s,c}K_{s,t}}{K_{s,c}+K_{s,t}}\ell^2 = K_{s,eq}\ell^2 \quad \Rightarrow \quad \begin{cases} k_{\theta,y} = K_{s,eq}\ell_z^2 \\ k_{\theta,z} = K_{s,eq}\ell_y^2 \end{cases} \quad \Rightarrow \quad k_{\theta,i,ss} = \frac{1}{\frac{1}{2k_{\theta,i}} + \frac{1}{2k_{\theta,i}}} \tag{2}$$

Table 2. Evaluation of the rotational stiffness of the steel hinge connection ($\ell_y = 380$ mm, $\ell_z = 225$ mm) for different expressions of $K_{ser,ax}$ based on timber density ($\rho = 480$ kg/m^3), embedded length (ℓ_s) and diameter of the screws (d_s).

	Blaß et al. (2006)	ETA11/0190	Stamatopoulos et al. (2020)	Hegeir et al. (2023)	Average
Reference	[8]	[15]	[9]	[11]	
$K_{ser,ax}$ [N/mm]	$234(\rho d_s)^{0.2}\ell_s^{0.4}$	$25 d_s \ell_s$	$\frac{50000\left(\frac{d_s}{20}\right)^2\left(\frac{\rho}{470}\right)^2 k_{l,K}}{0.4\cos^{2.3}\alpha + \sin^{2.3}\alpha}$	$160\left(\frac{\rho}{420}\right)^{0.85} d_s^{0.9}\ell_s^{0.6}$	
K_s [MN/m]	80.5	284.9	96.5	185.2	161.8
$k_{\theta,y,ss}$ [MNm/rad]	2.0	7.2	2.4	4.7	4.1
$k_{\theta,z,ss}$ [MNm/rad]	5.8	20.6	7.0	13.4	11.7

4.2 Experimental stiffness

The horizontal displacements (u) were measured with LVDTs at the top and bottom of the joint to determine the rotation (θ) of the steel hinge connection during the static testing at stage 4, see Figure 5. An expression of the rotational stiffness can then be expressed based on the assumption of equilateral triangles, see Equations (3) and (4). The moment (M) is determined based on the force applied to the specimen.

$$\theta_1 = \theta_2 \Rightarrow \frac{u_1}{\ell_1} = \frac{u_2}{\ell_2} \Rightarrow \begin{cases} \ell_1 = \frac{u_1}{u_1+u_2}\ell \\ \ell_2 = \frac{u_2}{u_1+u_2}\ell \end{cases} \tag{3}$$

$$k_\theta = \frac{M}{\frac{1}{2}(\theta_1+\theta_2)} = \frac{M\ell}{u_1+u_2} \tag{4}$$

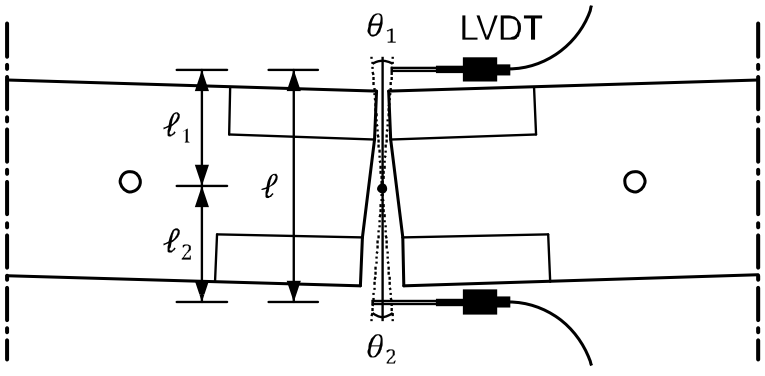

Figure 5. Experimental setup and measurement of the rotations at stage 4.

5 MECHANICALLY CONNECTED MEMBERS (γ-METHOD)

The γ-method is a simplified approach to estimate the reduced bending stiffness $(EI)_{ef}$ for mechanically connected beams [16] with a maximum of three connected members, see Equation (5). The bending stiffness is calculated by applying γ_i $(0 \leq \gamma_i \leq 1)$ to the Steiner part $(\gamma_i A_i a_i^2)$ for the second moment of area where a_i is the distance from the member to the neutral axis of the composite cross-section. γ_i is based on the area (A_i), distance between the connections (s_i), slip modulus for the fasteners (K_i) and length of the beam (L). In this article, the γ-method is applied at stage 3, see Figure 4. The MC1s are assumed to have a massive cross-section, the distance between steel rods is $s_i = 3000/(n_{sr} - 1)$ mm and the shear stiffness of the timber spacers and slip modulus of the sharp metal plates is determined as $K_i = 81.6$ MN/m.

$$(EI)_{ef} = \sum_{i=1}^{3} (E_i I_i + \gamma_i E_i A_i a_i^2) \quad \text{where} \quad \gamma_i = \frac{1}{1 + \frac{\pi^2 E_i A_i s_i}{K_i L^2}} \tag{5}$$

6 FINITE ELEMENT MODELS

Two finite element (FE) models were implemented with python scripting in the commercial software Abaqus. The orthotropic material modelling described in [17] was applied for the timber beams. Timoshenko shear flexible beam elements (B32) were applied for the mesh. The mass properties of the steel fittings were added as point-masses along the ends and rotary inertia around the beam centre of gravity. The four steel rod connections along the section were added as point-masses. The slenderness ratio of the beam regarding bending is $L/h \approx 10$ which is above the general criteria for applying beam theory. The material parameters in the FE models were set according to the average experimental results at stage 1, see Section 7.1.

6.1 Simplified beam model (SBM)

The arch segment is modelled with one beam using the generalised beam section in Abaqus. The partial composite action is implemented by reducing the second moment of area around the y-axis (I_y) and the torsional constant (K_v) with a reduction factor. Rotational springs $(k_{\theta,y}, k_{\theta,z})$ were applied at the steel hinge connection at stage 4, see Figure 6. The purpose of the simplified beam model was to determine the reduction factors for I_y and K_v and to calibrate the dynamic rotational stiffness of the connection. This simplified model is then used for the analysis of the bridge.

Figure 6. Simplified FE model at stage 4.

6.2 Detailed beam model (DBM)

The arch segment is modelled using four beams with rectangular cross-sections, see Figure 7. The two timber beams for the MC1s were tied together at the locations of the steel rods and along the steel hinge connection ($L = 300$ mm), see Figure 4. The shear stiffness of the timber spacers and slip modulus of the sharp metal plates were added as translational springs (k_x, k_y) at stages 3-4. Rotational springs $(k_{\theta,z})$ and longitudinal springs (k_x) were applied at the steel hinge connection at stage 4. $k_{\theta,z}$ had half the magnitude compared to the simplified beam model. The magnitude of the longitudinal springs (k_x) were derived from $k_{\theta,y}$ for the simplified beam model, see Equation (2). The main purpose of the detailed models is to be able to predict the partial composite action.

Figure 7. Detailed FE model at stage 4.

7 RESULTS

7.1 Material parameters

The elastic and shear moduli were estimated from the resonance frequencies at stage 1, see Figure 8. The first axial ($f_{n,ax}$), bending around the y-axis ($f_{n,b}$) and torsional ($f_{n,t}$) resonance frequencies were determined for the individual beams. The bending around the y-axis (weak axis) could be analysed without Timoshenko shear effects. The elastic and shear moduli were then derived from the equations in Table 3. The material properties in the FE models were based on the values in Table 3 and were set to: $E_0 = 13$ GPa, $G_0 = 750$ MPa and $\rho = 480$ kg/m^3.

Table 3. Material parameters for the timber beams of strength GL 30c with standard deviation in parenthesis. The analytical natural frequencies are formulated as: $f_{n,ax} = \frac{n}{2L}\sqrt{\frac{E}{\rho}}$, $f_{n,b} = \frac{c_n}{2\pi L^2}\sqrt{\frac{EI}{\rho A}}$ and $f_{n,t} = \frac{n}{2L}\sqrt{\frac{GK_v}{\rho I_p}}$.

Beam	ρ [kg/m3]	$E_{0,b,dyn}$ [MPa]	$E_{0,ax,dyn}$ [MPa]	$G_{0,dyn}$ [MPa]
1	475	12797	13127	761
2	469	12699	13140	731
3	479	13140	13618	741
4	500	13085	13664	764
Average	480.8 (11.7)	12930.3 (252.7)	13411.6 (301.2)	749.3 (32.9)

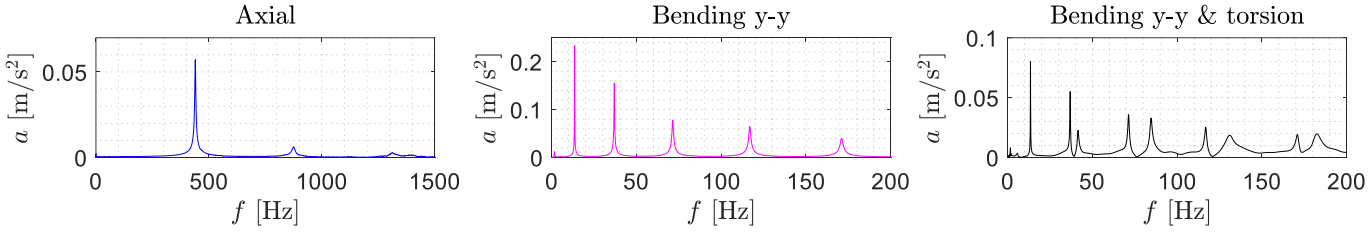

Figure 8. FFTs at stage 1 showing the resonance frequencies for free-free boundary conditions.

7.2 Modes of vibration

The analysed modes of vibration are the first bending modes around the y- and z-axis (B1y and B1z) and the first torsional mode (T1). The experimental mode shapes have a similar appearance at stages 1-4 and only the experimental mode shapes for the finished arch section at stage 4 are presented, see Figure 9.

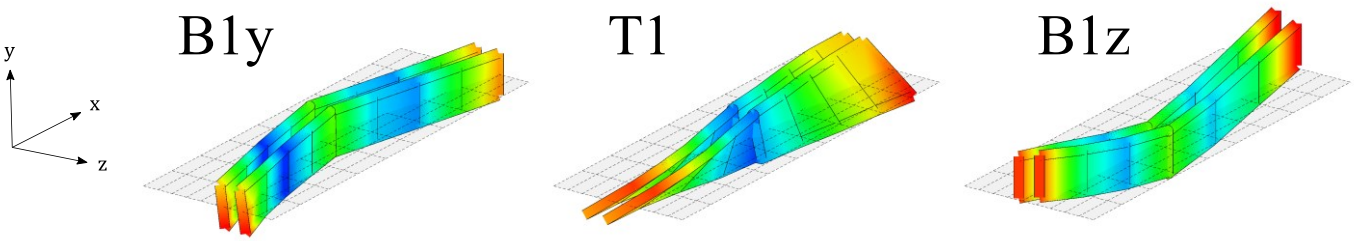

Figure 9. Experimental mode shapes for the finished arch section at stage 4 (MC3). The horizontal grid is in the xz-plane.

7.3 Partial composite action

The natural frequencies at stages 2-3 for the simplified and detailed beam models described in Section 6 are presented in Table 4. A reduction factor was applied to I_y to calibrate B1y for the simplified beam model. T1 could thereafter be calibrated by reducing K_v since it also depends on the polar moment of inertia ($I_p = I_y + I_z$). A significant reduction was necessary for B1y and T1 showing that the composite action is partial and reduced with around 70 % dynamically. The experimental and numerical results are the same for B1z at stage 3, i.e. no reduction of I_z was necessary at stages 2-3. The slip modulus of the sharp metal plates for the detailed beam model had to be calibrated to 9.5 N/mm^3 at stage 3 to match B1y. However,

the original value of 3.0 N/mm^3 provided reasonable results as well, but underestimated B1y with around 10 %. The experimental and numerical frequency response functions (FRFs) are presented in Figure 10.

Table 4. Experimental resonance frequencies and numerical natural frequencies for the FE models at stages 2-3. SBM: Simplified beam model. DBM: Detailed beam model.

Stage	Model	Reduction factor [−]			Natural frequencies [Hz]		
		I_y	I_z	K_v	B1y	B1z	T1
Stage 2 – MC1	**Exp.**				**44.5**	**-**	**50.2**
	SBM	0.87	1.00	0.43	44.5	99.2	49.8
	DBM	-	-	-	44.7	99.2	50.8
Stage 3 – MC2	**Exp.**				**58.2**	**100.1**	**41.5**
	SBM	0.27	1.00	0.32	58.3	99.2	41.9
	DBM	-	-	-	58.2	99.1	40.9

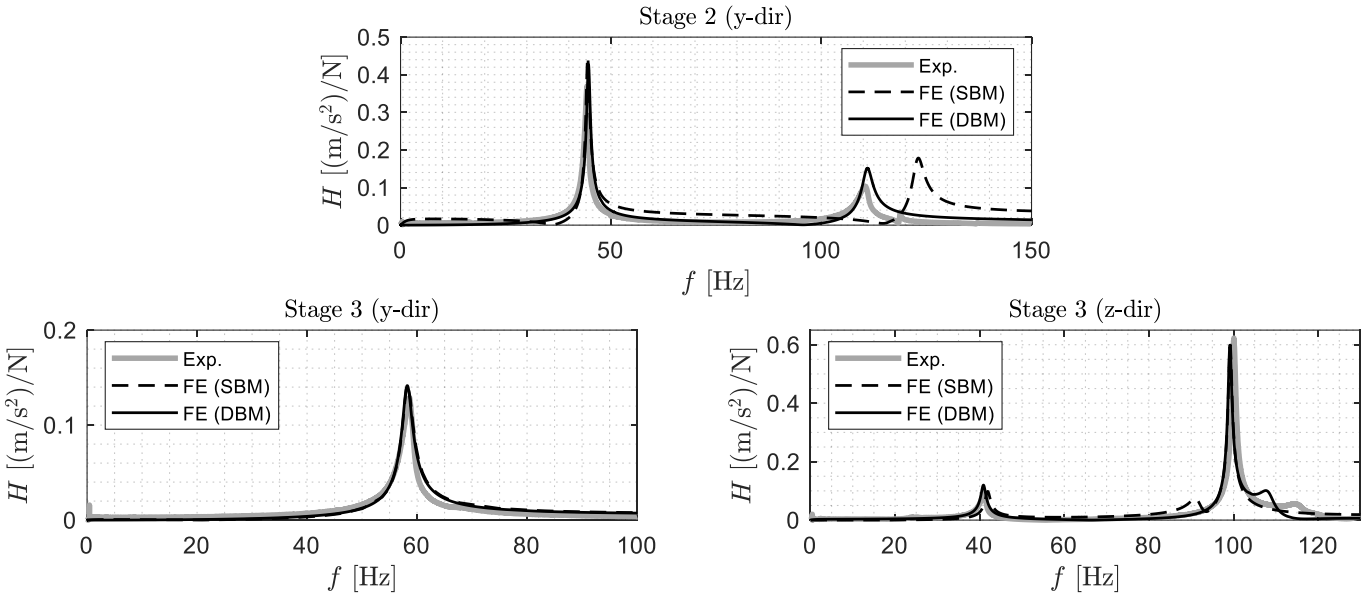

Figure 10. FRFs at stages 2-3 from hammer excitation and acceleration in the y- and z-direction.

7.4 Reduction factor

Natural frequencies for the first bending mode (B1y) with the detailed beam model based on different number of steel rod connections (n_{sr}) were determined at stage 3. The simplified beam model was then adjusted to exactly match B1y for the detailed model by reducing I_y with a reduction factor. Results by applying the γ-method from Section 5 were then compared with the numerical results, see Figure 11. The results are shown to be very similar, i.e. an estimation of the reduction factor can be obtained in the design phase using Equation (5). Increasing the number of steel rods is a simple way of increasing the buckling capacity of the arch. E.g. applying $n_{sr} = 8$ increases the bending stiffness with 50 % compared to $n_{sr} = 4$.

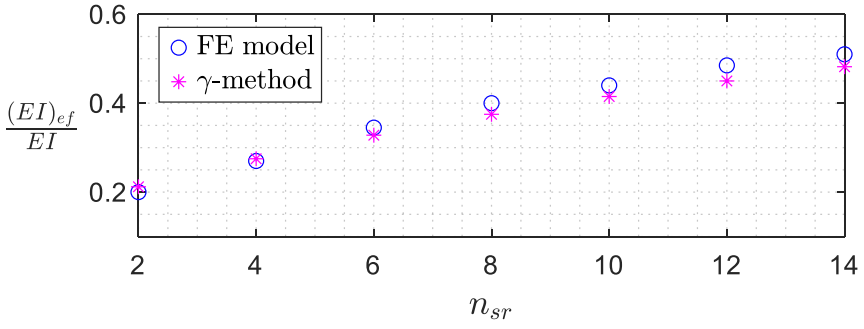

Figure 11. Reduction factor $\frac{(EI)_{ef}}{EI}$ based on number of steel rod connections (n_{sr}) along the MC2.

7.5 Dynamic rotational stiffness of the connection

The experimental resonance frequencies and numerical natural frequencies at stage 4 are presented in Table 5. The reduction factors from stage 3 in Section 7.3 were kept the same at stage 4 for the simplified beam model. The stiffnesses in the simplified and detailed beam models were then calibrated to match the experimental resonance frequencies. The simplified and detailed beam models provided the same results with the same stiffness ($k_{\theta,y}$), indicating that the reduction factors did not change. The dynamic rotational stiffness of the joint ($k_{\theta,y}$, $k_{\theta,z}$) had to be increased for the calibration of the tests with axial compression. Deriving the axial stiffness for one steel fitting (K_s) from the experimental values gives an average value of $\bar{K}_s \approx 87.0\ \mathrm{MN/m}$ (without compression) and $\bar{K}_s \approx 254.1\ \mathrm{MN/m}$ (with compression), c.f. with the values in Table 2. The experimental and numerical FRFs are presented in Figure 12. The detailed and simplified beam model gives reasonable responses compared to the experimental vibrational modes.

Table 5. Experimental resonance frequencies and numerical natural frequencies for the FE models at stage 4. SBM: Simplified beam model. DBM: Detailed beam model.

Stage	Model	Rotational stiffness [MNm/rad]		Natural frequencies [Hz]		
		$k_{\theta,y}$	$k_{\theta,z}$	B1y	B1z	T1
Stage 4 – MC3 (without axial compression)	**Exp.**			**23.5**	**66.8**	**57.9**
	SBM	0.9	10.0	23.9	67.2	58.6
	DBM			23.3	67.2	56.0
Stage 4 – MC3s (with axial compression)	**Exp.**			**36.3**	**76.9**	**53.3**
	SBM	3.4	27.0	36.5	76.8	51.9
	DBM			36.4	76.9	53.3

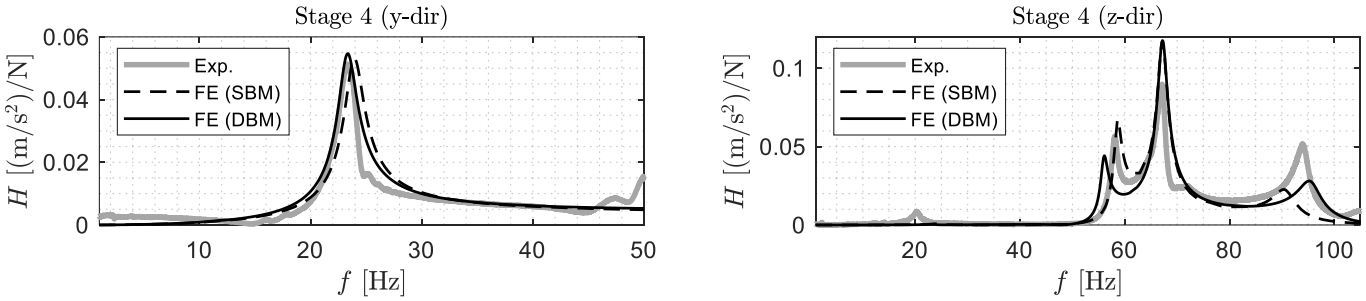

Figure 12. FRFs at stage 4 from hammer excitation and acceleration in the y- and z-direction.

7.6 Static rotational stiffness of the connection

The experimental horizontal displacements at stage 4 were not exactly equal at the top and bottom of the connection, see the top graphs in Figure 13. This indicates that the stiffness in tension and compression are not exactly equal. This is most likely due to the contact pressure of the steel fitting on the timber beam. The stiffness in compression is therefore around four times larger on average (or 2-8 times based on max/min values) than the stiffness in tension, i.e. $K_{s,c} = \ell_2/\ell_1 \cdot K_{s,t} \approx 4K_{s,t}$ see Equation (3). The rotational stiffness appears to be larger at small rotations, whereas a softening occurs after some time which cannot be fully explained, see the bottom graphs in Figure 13. The magnitude of the rotational stiffness is in a similar range compared to the theoretical values. Deriving the stiffness for one steel fitting (K_s) in Equation (2) from the experimental values gives an average value of $\bar{K}_s \approx 136.9\ \mathrm{MN/m}$, c.f. with the theoretical values in Table 2.

8 CONCLUSIONS

This article evaluates the dynamic and static behaviour of an arch section with a novel steel hinge connection for an arch bridge. A full-scale model was constructed in laboratory and tested at four stages of

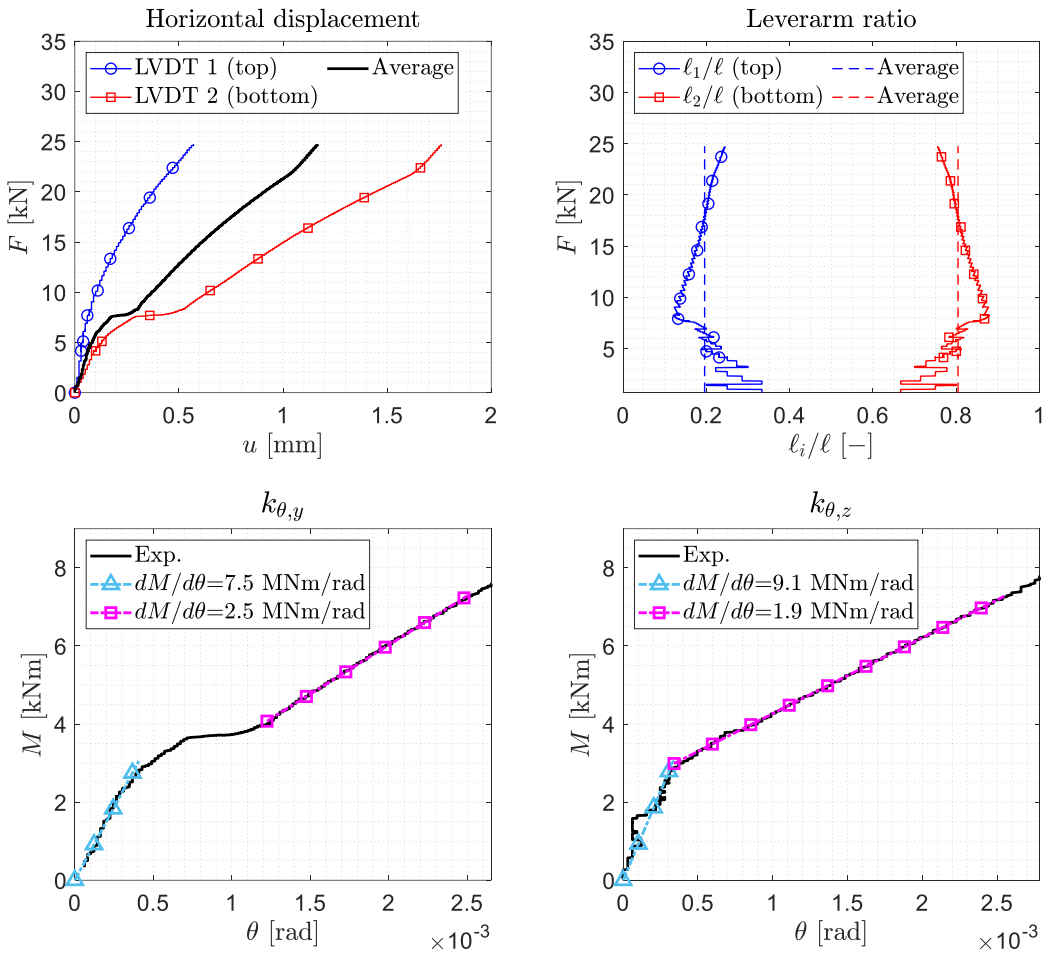

Figure 13. Top left) Horizontal displacements during the static tests of the finished arch section (see Figure 5) for bending around the y-axis. Top right) Leverarm ratios a_1 (compression) and a_2 (tension) for the upper and lower forces. Bottom left) Rotational stiffness around the y-axis, $k_{\theta,y}$. Bottom right) Rotational stiffness around the z-axis, $k_{\theta,z}$.

construction: 1) individual timber beams, 2) 2 beams mechanically connected, 3) 4 beams mechanically connected and 4) 2 sets of 4 beams mechanically connected with a steel hinge connection in-between. The main purpose of the study was to evaluate the partial composite action for the arch section and the bending stiffness of the connection. The main conclusions from the experimental testing and numerical models are:

- The second moment of area around the y-axis (I_y) and the torsional constant (K_v) had to be reduced in the numerical models to simulate the partial composite action of the mechanically connected beams. Reduction factors were applied to these constants indicating that I_y and K_v required a reduction of around 70 % respectively to agree with the dynamic experiments. The results were compared with the γ-method for composite beams which showed similar results.
- The horizontal displacements for the LVDTs at the upper and lower edges of the beams to evaluate the rotations during the static tests showed an asymmetry, indicating that the stiffness of the steel connection could potentially be 2-8 times larger (4 times on average) in compression than in tension.
- The static rotational stiffness of the steel hinge connection was around 2.5-7.5 MNm/rad ($k_{\theta,y}$) and 1.9-9.1 MNm/rad ($k_{\theta,z}$) with a derived average value of the steel fitting stiffness in the x-direction ($\bar{K}_s$) of 136.9 MN/m.
- The dynamic rotational stiffness of the steel hinge connection was around 0.9-3.4 MNm/rad ($k_{\theta,y}$) and 10.0-27.0 MNm/rad ($k_{\theta,z}$) without and with axial compression respectively. This indicated an average stiffness of the steel fitting in the x-direction ($\bar{K}_s$) of 87.0-254.1 MN/m.

9 ACKNOWLEDGEMENTS

This project is a cooperation between KTH Royal Institute of Technology and the company Timber Bridge Specialists (TBS). The authors would like to thank the Swedish Transport Administration and J. Gustaf Richert foundation for the financial contribution.

REFERENCES

1. A. Rönnquist, E. Strømmen, and L. Wollebæk, 2008, "Dynamic properties from full scale recordings and FE-modelling of a slender footbridge with flexible connections," *Struct. Eng. Int. J. Int. Assoc. Bridg. Struct. Eng.*, vol. 18, no. 4, pp. 421–426, doi: 10.2749/101686608786455162.
2. P. Hawryszków and J. Biliszczuk, 2022, "Vibration Serviceability of Footbridges Made of the Sustainable and Eco Structural Material: Glued-Laminated Wood," *Materials (Basel).*, vol. 15, no. 4, doi: 10.3390/ma15041529.
3. K. A. Malo, R. B. Abrahamsen, and M. A. Bjertnæs, 2016, "Some structural design issues of the 14-storey timber framed building 'Treet' in Norway," *Eur. J. Wood Wood Prod.*, vol. 74, no. 3, pp. 407–424, doi: 10.1007/s00107-016-1022-5.
4. C. Sandhaas, "Mechanical Behaviour of Timber Joints With Slotted-in Steel Plates," Delft University of Technology, 2012.
5. F. Solarino, L. Giresini, W. S. Chang, and H. Huang, 2017, "Experimental tests on a dowel-type timber connection and validation of numerical models," *Buildings*, vol. 7, no. 4, pp. 1–14, doi: 10.3390/buildings7040116.
6. R. Jockwer, D. Caprio, and A. Jorissen, 2022, "Evaluation of parameters influencing the load-deformation behaviour of connections with laterally loaded dowel-type fasteners," *Wood Mater. Sci. Eng.*, vol. 17, no. 1, pp. 6–19, doi: 10.1080/17480272.2021.1955297.
7. P. Landel and A. Linderholt, 2022, "Reduced and test-data correlated FE-models of a large timber truss with dowel-type connections aimed for dynamic analyses at serviceability level," *Eng. Struct.*, vol. 260, no. February, p. 114208, doi: 10.1016/j.engstruct.2022.114208.
8. H. J. Blaß, I. Bejtka, and T. Uibel, *Tragfähigkeit von Verbindungen mit selbstbohrenden Holzschrauben mit Vollgewinde*, vol. 4. 2006.
9. H. Stamatopoulos and K. A. Malo, 2020, "On strength and stiffness of screwed-in threaded rods embedded in softwood," *Constr. Build. Mater.*, vol. 261, p. 119999, doi: 10.1016/j.conbuildmat.2020.119999.
10. H. Stamatopoulos, *Withdrawal Properties of Threaded Rods Embedded in Glued-Laminated Timber Elements Withdrawal Properties of Threaded Rods Embedded in Glued-Laminated Timber Elements Thesis for the Degree of Philosophiae Doctor*, vol. 3. 2016.
11. O. A. Hegeir and H. Stamatopoulos, 2023, "Experimental investigation on axially-loaded threaded rods inserted perpendicular to grain into cross laminated timber," *Constr. Build. Mater.*, vol. 408, no. October, p. 133740, doi: 10.1016/j.conbuildmat.2023.133740.
12. Timber Bridge Specialists, "Referensprojekt Uddebo." Accessed: May 27, 2024. [Online]. Available: https://timberbridgespecialists.se/uddebo-lattvikt-gc-bro/
13. European Committee for Standardization (CEN), 2012, "SS-EN 408. Timber structures – Structural timber and glued laminated timber – Determination of some physical and mechanical properties".
14. European Committee for Standardization (CEN), "Eurocode 5: Design of timber structures – Part 1-1: General – Common rules and rules for buildings," 2009.
15. Deutsches Institut für Bautechnik, "European Technical Assessment ETA-11/0190," Berlin, 2018.
16. H. J. Blaß and C. Sandhaas, "Timber Engnering Principles for Design," *Scientific Publishing*. Karlsruher Institut für Technologie (KIT), Karlsruhe, p. 644, 2017.
17. J. Bergenudd, J. M. Battini, and R. Crocetti, 2024, "Dynamic analysis of a pedestrian timber truss bridge at three construction stages," *Structures*, vol. 59, no. December 2023, p. 105763, doi: 10.1016/j.istruc.2023.105763.

ICTB 2025. 5th International Conference Timber Bridges
Rotorua, New Zealand, 29 June to 2 July 2025.

THE RAKAIA GORGE BRIDGE DECK REPLACEMENT AND SEISMIC STRENGTHENING

Bradfield, Andrew[1], Routledge, Peter[2]

ABSTRACT

The Rakaia Gorge No. 1 Bridge on SH77 is a 55m span wrought iron truss constructed circa 1882. The bridge is a Category 1 Historic Place on the NZ Heritage List/Rārangi Kōrero [1], and the structural form is internationally unique.

To ensure that this important structure continued to provide a safe and resilient transport route, the deteriorating historic timber deck required replacement. Numerous complexities needed to be considered in the design including limited load capacity, heritage effects, operational safety, seismic resilience, constructability and traffic management. Several innovative solutions were developed to address these issues.

The project sensitively balanced the conflicting objectives of state highway operations and heritage preservation – replacing the deck with a modern timber system, refurbishing timber handrails and providing seismic resilience to this strategically important structure, whilst respecting the heritage significance and successfully preserving the exceptional landmark appearance of the bridge.

1 INTRODUCTION

The Rakaia Gorge No. 1 Bridge is a State Highway bridge and a Category 1 Historic Place [1]. This paper discusses some of the interesting challenges encountered when the deteriorating timber deck required replacement. It also describes how these were overcome through innovative solutions developed for this project using modern engineered timber.

2 DESCRIPTION OF THE ORIGINAL STRUCTURE

The Rakaia Gorge No.1 Bridge is a 55-metre span wrought iron truss bridge which carries State Highway 77 across the Rakaia Gorge. The bridge was constructed by the Public Works Department circa 1882 and is one of the oldest wrought iron bridges in New Zealand.

The focus of this paper is on the modifications to the timber deck and balustrades. However, this section also describes the underlying steel truss to provide context to the site, structure and complexities associated with the timber deck and balustrade works.

The wrought iron superstructure is unusual. The structural form has many similarities to both Bollman and Fink Trusses, in that it comprises a girder supported at mid-span and quarter-span points by vertical posts which in turn are supported by a series of diagonal tie plates (Figure 1). There are very few surviving Bollman or Fink trusses in the world. In Bollman and Fink trusses, the diagonal ties would be anchored to the ends of the girders which would act as the compression chord formed by truss action. Rakaia Gorge Bridge differs in that the diagonal ties are anchored at each end within concrete-filled sockets tunnelled into the rock outcrops on which the abutments are founded.

[1] Senior Bridge & Civil Structures Engineer | Team Leader, WSP NZ Ltd, e-mail: andrew.bradfield@wsp.com
[2] Technical Principal – Bridge Design, WSP NZ Ltd

The girders are supported completely independently on cast iron pedestals and do not act as a compression chord; hence the bridge is not strictly a truss. Consequently, Engineering New Zealand (EngNZ, formerly IPENZ) have identified the bridge to be unique in the world [2].

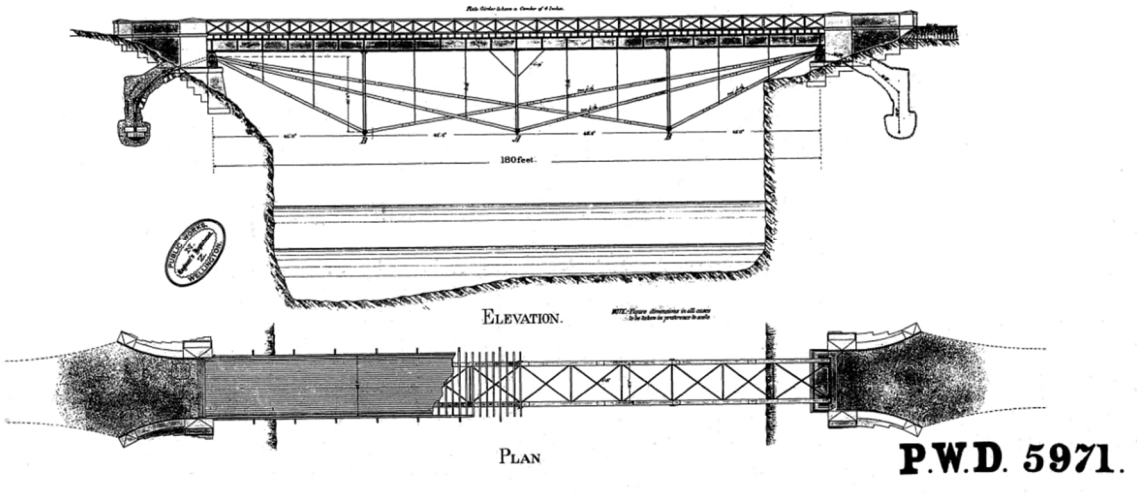

Figure 1. Extract from Historic Drawings – Plan and Elevation.

The main girders are of traditional riveted wrought iron plate girder construction using flange angles, web angles, and splice plates. Whilst the bridge 'truss' is a single span, the main girders behave as four-span continuous beams supported on vertically stiff abutments with sprung intermediate supports at the vertical post locations (Figure 2).

The main girders are braced together with cross bracing in the plane of both the top and the bottom flanges and there is also vertical cross bracing at each plan bracing node.

The bridge deck is chip sealed and carries a single bi-directional traffic lane. The deck was of timber construction comprising 75 mm thick diagonal softwood running planks, overlaying 80 mm thick longitudinal hardwood deck planks. The deck planks spanned 610 mm between hardwood transoms which in turn spanned 3650 mm between the two main girders.

Figure 2. Elevation of Bridge.

3 FACTORS INFLUENCING DESIGN

3.1 Poor condition of the original timber deck

The condition and extent of decay to the original timber deck had been monitored for many years by WSP through their role as Structures Management Consultant (SMC) for Canterbury.

During that time, several timber transoms had been augmented with steel flitch beams where decay was considered severe. The deck planks were also deteriorating with increasing maintenance (Figure 3). Through timber-drilling investigation, the extent of decay was found to have increased such that continuing to augment selected transoms was no longer considered practical or sufficient to remediate the decay without compromising on the live load capacity. Consequently, it was concluded that the timber deck had reached the end of its useful life and required replacement.

Figure 3. Poor deck condition (prior to replacement) and kerb delineation.

3.2 Significant heritage importance of the structure

The Rakaia Gorge Bridge is a Category 1 Historic Place. A Heritage Effects Assessment indicated that the following elements have exceptional heritage value:

- Wrought iron trusses including girders and original bracing elements
- Concrete abutments and parapet walls
- Timber transoms and decking
- Timber balustrades

The heritage importance was a significant factor which influenced many of the decisions on the project.

3.3 Limited vehicle live load capacity

The capacity of the structure to carry live load is limited (suitable for 50MAX vehicles[3]). The current live load capacity was justified by restricting the carriageway width to 3.5 m using timber kerbs and flexible delineation devices (Figure 3). This was to prevent traffic from driving eccentrically on the relatively wide 5 m deck, which would cause uneven loading of the two trusses. Therefore, the weight of the replacement deck was a critical constraint to ensure that the level of service would not be reduced.

3.4 Difficult access conditions

The bridge deck is 16 m above the water and the obstruction presented by the diagonal ties makes access for inspection and maintenance difficult.

This restricted the ability to undertake survey and confirm existing details during the design. The difficult access constraint also needed to be considered from a Safety in Design perspective regarding constructability and future maintenance.

[3] 50MAX is a permitted vehicle that can have a total weight of up to 50 tonnes. They have an additional (9^{th}) axle when compared to a legal vehicle and legal axle mass limits still apply.

3.5 Seismic vulnerability

A seismic screening undertaken by New Zealand Transport Agency Waka Kotahi (NZTA) in 2000 had identified a number of seismic vulnerabilities with this structure. Whilst some issues were addressed, the structure did not satisfy the funding requirements for a Detailed Seismic Assessment (DSA) at that time. However, this deck replacement project provided an opportunity to undertake other strengthening works whilst good access to the underside of the bridge was temporarily available. Consequently, NZTA commissioned WSP to undertake a DSA as part of this project to determine the strengthening requirements.

3.6 Significant traffic route importance

As the bridge is a single lane structure, it needed to be completely closed to traffic to enable deck replacement. A closure of the bridge requires a 95km detour via SH1 at Rakaia River Bridge. Any closure of the bridge would be highly disruptive to users of SH77 and so only night closures were permitted. Therefore, the bridge deck needed to be replaced in stages during a series of 7-hour night closures, with the bridge reopened to traffic by 5:00am each morning.

A further complication is that the bridge is the only viable diversion route available if SH1 (a Primary Lifeline Route) needs to be closed due to an emergency. The closure of SH1 and emergency diversion via SH77 has occurred several times in recent years typically due to a vehicle accident on the SH1 Rakaia River Bridge.

A contingency plan needed to be in place during the night closures to enable the Rakaia Gorge No.1 Bridge to be reopened within about 30 minutes, prior to the arrival of diverted traffic following a closure of the SH1 Rakaia River Bridge.

3.7 Existing structure details

The design and detailing of the new deck system and strengthening needed to accommodate existing bridge features in order to avoid clashes. This was further complicated by the difficult access available to measure-up and confirm existing details prior to construction. Elements of the existing structure which required particular consideration in the design included (Figure 4):

- Wind bracing and associated gusset plates and rivets
- Girder splice plates and associated varying girder flange level and rivets
- Rivets for the web-flange angles
- Rivets for the web-stiffeners

Figure 4. Original timber transoms notched to accommodate girder features.

4 SOLUTIONS AND INNOVATIONS

4.1 Engineered laminated timber deck panels and steel transoms

The obvious deck replacement solution was a like-for-like replacement using new hardwood transoms and decking planks. However, there was opportunity for several improvements by using modern engineered timber in the solution.

WSP identified an alternative deck system using an engineered laminated timber product called NiuDeck (Figure 5). This product has been used on deck replacements throughout Australia but had never been used on a State Highway Structure in New Zealand at the time.

The system is a laminated timber product, essentially a thick plywood, specifically engineered for use as a bridge decking material. It is available in standard thicknesses from 27 mm to 198 mm and supplied in standard widths of 1200 mm and lengths up to 14 m [3].

The replacement deck consisted of new steel transoms, which would span transversely between the two existing wrought iron girders, with the NiuDeck panels spanning longitudinally between the transoms. This proposal offered several advantages over a like-for-like replacement, including:

- The NiuDeck panels are lighter than hardwood.
- The NiuDeck panels and steel transoms are stronger than the original planks and transoms (at the same total depth) which allowed the transom spacing to be doubled.
- The weight savings due to increased transom spacing and lighter deck panels led to increased capacity for vehicle loading.
- The NiuDeck panels could be detailed to contribute to improved seismic resilience.
- Orienting the full width NiuDeck panels transversely provided significant flexibility to the Contractor in terms of the extent of deck to be replaced in each night closure.
- The use of NiuDeck panels and steel transoms allowed preassembly of a number of transoms and deck panels into units enabling rapid installation during the night closures (Figure 6).

Figure 5. NiuDeck panels ready for installation.

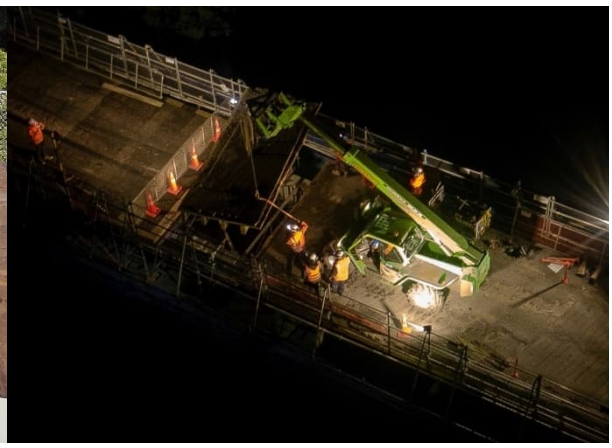

Figure 6. Installation of prefabricated deck sections during night closures.

4.2 Removal of timber transoms

As described in Section 3.1, the extent of decay in the original hardwood transoms was such that these elements could not be saved without compromising on the live load capacity of the structure. Options to replace the transoms like for like with hardwood were considered, however, sourcing suitable material would be problematic. It would also preclude re-use of original heritage fabric in the design and would not provide the additional benefits (listed in Section 4.1 above) associated with the modern engineered timber deck option.

This led to the proposal to replace the deck with steel transoms and a modern plywood deck. This would change the appearance of the bridge, and this was considered detrimental to the heritage values of the structure. The original hardwood transoms were a highly visual element of the bridge when viewed from the riverbank below and from the approaches either side. The transoms typically end flush with the timber balustrade bottom rail and so the ends of all the transoms are clearly visible. Additionally, every sixth original transom extends out as a cantilever beyond the balustrade to accommodate a diagonal out-rigger which provides support to the timber balustrade posts (refer Figure 7).

The solution was to design the steel transoms to have spliced timber ends (Figure 8). Furthermore, the timbers would be the actual heritage fabric salvaged from the original transoms. The steel transoms would extend almost to the deck edge with the bottom flange removed to accommodate the hardwood end piece. The longer cantilever transoms would similarly be spliced to support the balustrade out-riggers – the salvaged hardwood was relied upon structurally to provide this function. False ends were placed between new transoms to match the original transom spacing.

Timber that was considered unsuitable for re-use with a structural purpose was able to be donated to neighbouring landowners for use in information boards (Figure 9), bollards and benches (Figure 10) on their Taniwha walking track at the western end of the bridge.

Figure 7. Longer transoms (every sixth) supporting balustrade outriggers.

Figure 8. Spliced hardwood end piece (from original timber transom).

Figure 9. This walking track sign on the Taniwha Track uses original hardwood transoms from the Rakaia Gorge Bridge No. 1.

Figure 10. Hardwood benches made from the original transoms and deck planks, gifted back to the community.

4.3 Deck drainage

The original deck was horizontal with no notable cross-fall, and water would tend to drain through the gaps between planks. The NiuDeck panels are much larger units than the deck planks and the joints between units are sealed. This has the benefit of eliminating or significantly reducing the amount of water draining through the deck onto the wrought iron

structure below. However, it also introduces a drainage issue with increased potential for water ponding on the new deck, presenting a hazard to the road user in wet weather and in icy conditions.

To address this risk, a cross fall was introduced into the new deck system. Rather than create the cross fall with variable thickness surfacing, which would have increased the weight of the deck, the transoms were installed with a cross fall.

4.4 Deck panel hold-downs

The Safety in Design process identified that difficult access to the underside of the deck would make maintenance of the deck panel hold-down bolts difficult if conventional nuts were used on the underside of the transoms. Although it is expected that the need for maintenance of the hold-down bolts should be significantly less frequent than the original deck fastenings, a blind fastening detail was desirable which could be installed and tightened from the deck surface, and which would not vibrate loose under traffic loading.

The solution was to weld a nut cradle to transom flange cleats, allowing the bolt to be wound in from the deck surface and preventing the nut vibrating loose. The cradle restrained the nut on three faces, allowing the nut to be temporarily removed to enable site drilling of the NiuDeck panels to suit the predrilled holes in the transom cleats (Figure 11).

To prevent the bolt vibrating loose, a locking plate with a hex-shaped hole cut to match the bolt head, was screwed down into the NiuDeck panel over the installed bolt head (Figure 12).

Figure 11. Transom and deck panel connections.

Figure 12. (Inset) Innovative locking plate (Main) Locking plate installed and screwed down with central strip of BRP Road Patch partially pre-applied.

4.5 Deck surfacing

The deck panels were installed in a series of night closures with the bridge reopened to traffic each morning. Conventional chip sealing methods would have needed to wait until all the deck panels had been installed prior to sealing. This would have led to direct trafficking of the deck panels leading to ‘smoothing’ of the deck surface which can adversely affect the chip seal bond. The solution for this project was to use BRP road patch – a proprietary bituminous paper with pre-coated aggregates. The road patch was pre-applied to the central portion of the deck panels and a further strip was placed over the panel joints in situ (Figure 12).

This reduced the time of closures, avoided premature trafficking and enabled the works, including the surfacing, to continue through the winter months (which would not have been feasible using conventional chip seal).

4.6 Detailed seismic assessment of truss structure

The unusual bridge superstructure presented a challenge for seismic analysis and assessment. A three-dimensional analysis model was developed in Microstran to idealise the entire superstructure (Figure 13).

The seismic assessment highlighted the importance of bracing elements (particularly plan bracing to the main girders) in the structure's response to seismic loading. Since the bracing comprises a series of cross-braced frames, any tendency of the compression members to buckle would redistribute load to the tension members without damage to the compression members Various modelling methods were used to account for this, identifying areas where compressive buckling was critical and also significantly reducing the number of members requiring strengthening where redistribution to tension members was appropriate.

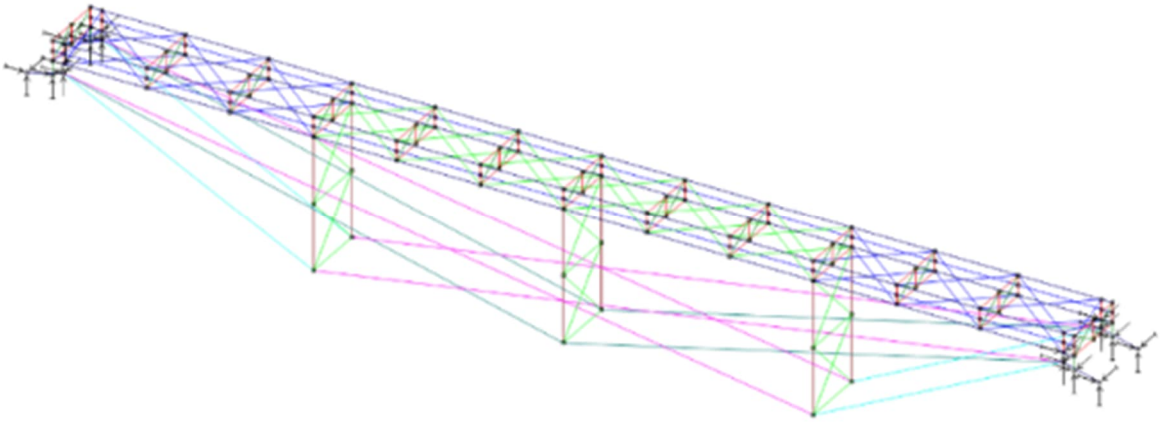

Figure 13. Seismic analysis model.

4.7 Robustness for maximum considered earthquake and important role of timber in strengthening

The seismic assessment identified that seismic response was uncertain if one of the bracing connections exceeded its capacity. Failure of the connection would be brittle and would lead to a significant reduction in lateral stiffness and possible progressive failure of adjacent bracing bays. Therefore, designing for Damage Control Limit State (DCLS) in this case would not demonstrate reliable capacity to withstand without collapse a major earthquake exceeding the DCLS capacity. One way to ensure collapse avoidance would be to design the bracing members to withstand the Maximum Considered Earthquake (MCE) but this would require considerable strengthening to the bracing and their connections.

It was recognised that a further advantage in using the NiuDeck timber deck system is that it has the potential to act as a diaphragm in the plane of the top flange of the main girders. The contribution provided by the diaphragm was dependent upon the stiffness of the fixings between the deck and the transoms and also between the transoms and the main girder. This was not relied upon for DCLS design but provided a reliable secondary load path to avoid collapse in a major earthquake.

The connection stiffness was governed by potential movement of bolts within their holes. To minimise the slippage in connections, all deck to transom and transom to girder connections were specified with close-tolerance holes (1 mm rather than the standard hole size of 2 mm). This used-up construction tolerance and so match-drilling on site was specified to achieve the close-tolerance holes. To minimise the quantity of site drilling, holes in the transom bottom flange and the deck panel hold-down cleats were drilled during shop fabrication. When the transoms had been set down in position on the bridge, match drilling through the top flange of the existing girders was required to achieve the close-tolerance holes. Similarly, match-drilling through the deck panels was done during pre-assembly of transom and deck sections, prior to closures. The remainder of hold-down bolt holes were match-drilled after setting down a section of deck in position (Figure 14).

Figure 14. Deck partially removed and replaced.

4.8 Timber balustrade refurbishment

Replacing the deck necessitated removal of the balustrades, one of the most important visual elements of the bridge (other than the wrought iron truss itself). This required significant liaison with Heritage New Zealand Pouhere Taonga given risk assessment considerations for road user safety.

The existing timber balustrades were replaced like-for-like re-using as much of the original components as their condition permitted and supplementing with new hardwood (Purpleheart) material (Figure 16). Minor safety improvements were also made to the signage and line markings on the approaches to the bridge to improve hazard warning and encourage reduced speeds.

The balustrades were deconstructed (Figure 15) and reconstructed in accordance with heritage conservation best practice and matching original joinery details. Each member of the balustrade was individually numbered, its condition assessed, and the extent of heritage fabric suitable for reuse was defined on this basis. The original iron straps were cleaned, repainted and reinstated, and new fixings selected to be in keeping with the originals.

Figure 15. Numbering and deconstruction of balustrades.

Figure 16. Reconstruction of balustrades (combination of refurbished original and new hardwood).

5 CONCLUSION

The Rakaia Gorge No.1 bridge is a Category 1 Historic Place and is a unique example of Kiwi ingenuity by the early settlers [4]. The heritage significance of the structure created some interesting complex constraints in addition to what would have already been a relatively complex bridge deck replacement project.

Innovative solutions were adopted to resolve these constraints. For example, re-using the existing timber transoms on the ends of the new steel transoms enabled deck replacement with a modern lighter-weight timber product whilst maintaining the spectacular historic appearance.

Through use of modern engineered timber, this project has ensured that the bridge will remain a viable asset for continued public use on the State Highway with increased live load capacity and seismic resilience. This was achieved whilst preserving the heritage values and fabric. Moreover, this was achieved without changing the exceptional appearance of the bridge which has been preserved to be admired for generations to come (compare Figure 17 and 18).

Figure 17. View along bridge **before** refurbishment.

Figure 18. View along bridge **after** refurbishment.

REFERENCES

1. Heritage New Zealand Pouhere Taonga. New Zealand Heritage List/Rārangi Kōrero. Entry no. 272 – Old Rakaia Gorge Bridge. Available at: https://www.heritage.org.nz/places
2. Astwood K, 2013. IPENZ Engineering Heritage Register Report. Rakaia Gorge Bridge.
3. PNGFP, 2023. NiuBridge & NiuDeck Construction Manual. Available at: Technical Downloads - NiuBridge / NiuDeck
4. WSP Opus, 2017. Rakaia Gorge No.1 Bridge Conservation Management Plan.

ICTB 2025. 5th International Conference Timber Bridges
Rotorua, New Zealand, 29 June to 2 July 2025.

DESIGN OF TIMBER BRIDGES IN FRANCE - NEW TECHNICAL GUIDE FROM THE FRENCH ASSOCIATION OF CIVIL ENGINEERING

Jean-Baptiste Simon[1], Valentina Bruno-Huré[2], Robert Leroy[3]

ABSTRACT

In 2013, the French Association of Civil Engineering (AFGC), a prominent hub in France for experts in the field of civil engineering, published a technical guide on the design of timber bridges. This guide was the result of three years' work by a small group of French specialists gathered to bring to the table of AFGC the topics specific to timber structures.

At that time, this publication was one the first guides in France aiming to provide an overview of the key aspects to be addressed for the design of durable timber bridges.

In 2023, a new working group was created within AFGC to update the existing guide and to bring fresh momentum to timber structures in civil engineering. As such, the new publication contains updates on topics discussed in the previous guide as well as new chapters on eco-design, on wooden-specific features and on monitoring/maintenance of timber bridges.

The aim on the authors is to provide a practical guide to complement Eurocode 5 (the European Design Code on timber structures) and help democratizing the use of timber as a bridge material. This means raising awareness among French civil engineers – more prone to steel and concrete structures – to timber alternatives and showcasing the dependability of well-designed timber bridges to potential clients and infrastructure owners.

A first version of the new guide will be published at the end of 2025.

1 INTRODUCTION

The French Association of Civil Engineering (AFGC, *Association Française de Génie Civil*) serves as a prominent hub for meetings and experience-sharing between its members (engineers or technicians, architects, professors, or students). This association has existed since 1934 and has some 1400 members.

Its main purposes are to help strengthen the links between research, design, construction, and maintenance and to enhance the interest of students in civil engineering.

At the beginning of 2010, a small group of 3 experts (Robert Le Roy, Jean-Marc Tanis et Nicolas Didier) gathered to bring to the table of AFGC the topics specific to timber structures. In 2013, their works resulted in the publication of a technical guide on the design of timber bridges [1] (see Figure 1).

At that time, France had only two methodological guides on the durability [2] and maintenance and inspection [3] of timber bridges. The AFGC publication was then the first guide in our country, aiming to provide an overview of the key aspects to be addressed for the design of durable timber bridges.

[1] Structural engineer, Bouygues Travaux Publics Régions France,
e-mail: jb.simon@bouygues-construction.com,
[2] Structural engineer, setec tpi
[3] Professor, Ecole Nationale d'Architecture Paris Malaquais

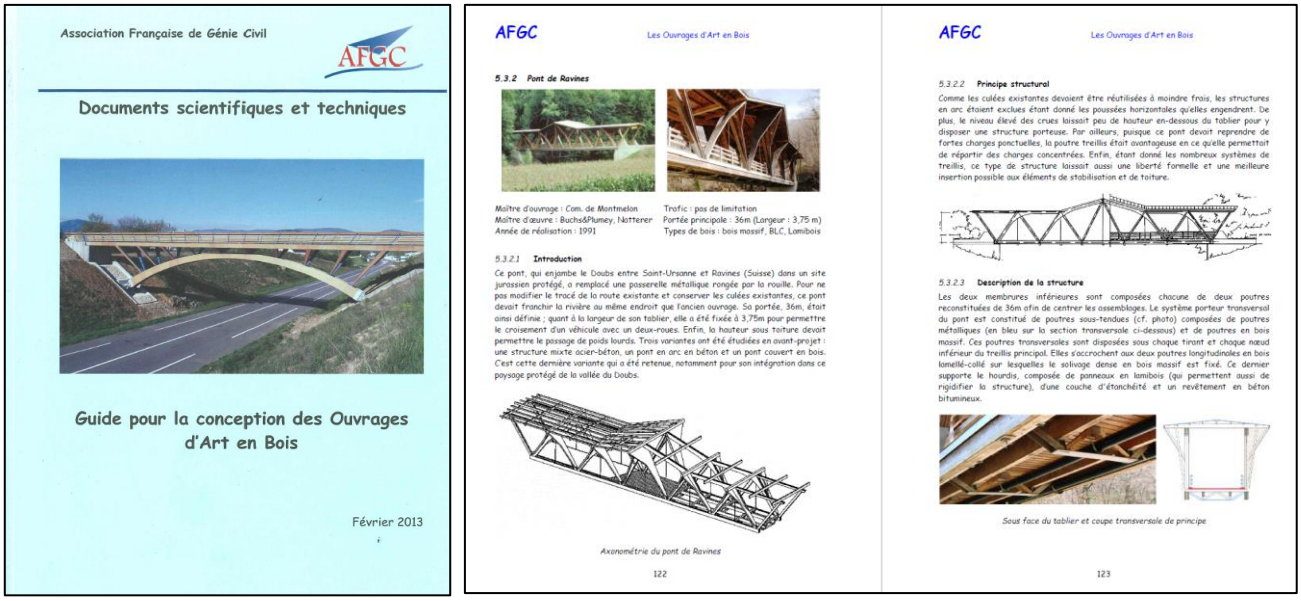

Figure 1. Cover and extracts of the AFGC design guide of 2013 [1]

In 2022, the AFGC decided to revive the topic of timber as a bridge material, and a new working group was formed at the beginning of 2023 with the aim of updating the guide published in 2013. This group is composed of about twenty members from various organizations (project management, engineering firms, universities, companies, project owners, etc.). The goal is to publish this new version by the end of 2025.

2 CHANGES IN THE CONTENT OF THE GUIDE

The table of contents of the 2013 guide [1] was designed to provide an educational review of timber and civil engineering structures built with this material (mainly bridges). Table 1 below presents the table of contents of this first version and that of the upcoming update. The chapters added as part of the update are highlighted in bold.

Table 1. Comparison of the tables of contents between the 2013 and 2025 versions

First version of the guide (2013)		Updated version of the guide (2025)	
Chapter number	Chapter title	Chapter number	Chapter title
1	Introduction	1	Introduction
2	Wood material	2	Wood material
3	Calculations of timber elements	**3**	**Features specific to timber structures**
4	Assemblies	4	Calculations of timber elements
5	Structural typologies	5	Assemblies
6	Durability	6	Structural typologies
7	Research and developments	**7**	**Eco-design of timber structures**
8	Monography	8	Durability
		9	**Monitoring and maintenance of timber structures**
		10	Innovations*
		11	Monograph

* The "Research and Developments" chapter changes its name into "Innovations"; its purpose remains the same.

3 DETAILED REVIEW OF THE MAIN EVOLUTIONS OF THE GUIDE

3.1 Resource challenges

In the introductory chapter, the guide presents the evolution of European and French forests, particularly from the perspectives of stock and annual flux. As Europe strives to meet its decarbonization commitments by 2050, the development of large-scale timber structures in the construction sector is often seen as a panacea, given that long-life timber structures serve as effective carbon sinks. Consequently, increased pressure on forest exploitation can be anticipated.

This chapter aims to provide engineers with the most accurate information possible on the use of forest resources, enabling them to make informed decisions regarding the choice of wood species and dimensions, thereby balancing resource utilization with sustainability.

Regarding the French forest - the fourth largest in Western Europe by surface area - data from the period 2013–2021 indicate that the net annual timber production (75 million cubic meters) has exceeded the annual harvesting rate (52 million cubic meters). However, this trend masks a progressive decline in resource availability due to disease and the effects of global warming [4].

French forest is closely monitored by national institutions such as the French Geographic Institute (IGN, *Institut National de l'information Géographique et forestière)* and the National Forest Office (ONF, *Office National des Forêts*), which conduct research programs to track timber use with greater precision, species by species, from harvesting to final application.

A distinctive feature of French forests is their composition: two-thirds hardwood and one-third softwood. This imbalance presents a challenge, as structural timber demand remains predominantly focused on softwood. To address this, researchers are exploring ways to shift demand towards the more abundant hardwood resources. Achieving this goal requires reintroducing engineers to a deeper understanding of forest resources and developing technical solutions for utilizing so-called "non-noble" species in construction.

3.2 Features specific to timber structures

New Chapter 3 dedicates to timber-specific features and properties. It is aimed at an audience that is not specialized in this material and offers an in-depth analysis of several fundamental aspects to consider when designing a timber structure. Some of the topics presented below were already addressed in the 2013 version of the guide [1], but not in a targeted and detailed manner. The objective here is to provide the reader with a focus on the challenges of the material.

The first aspect addressed concerns the shrinkage and swelling of wood depending on its moisture content. This rheological characteristic, unique to this material and absent in other common construction materials, significantly influences the sizing of structures.

The behavior of wood in fire situations is also discussed. While wood has a combustible mass that can be perceived as a constraint, it nevertheless retains its mechanical properties even under the effect of fire, which is an asset in terms of structural stability.

Furthermore, under the effect of accidental actions such as earthquakes, wood exhibits specific behavior, particularly at the level of its joints. Depending on their design, these joints can allow significant energy dissipation, thus influencing the dynamic response of timber structures.

Another point of interest is the resistance of wood to aggressive environments, particularly to chlorides, which are frequently present in certain types of structures. This resistance gives advantages to wood-based materials in contexts where other materials might degrade more quickly.

Regarding manufacturing, timber structures are generally prefabricated in factories, sometimes located far from the construction site. Consequently, issues related to transportation and lifting become predominant and present specific challenges compared to other construction materials.

Finally, the chapter addresses measures for protecting timber during the construction phase. It is indeed essential to limit excessive moisture exposure during this period, which may require the implementation of specific provisions to preserve the integrity of the material and ensure the longevity of the structure.

3.3 Verification of members and assemblies

Chapters 3 (Calculations of timber elements) and 4 (Assemblies) of 2013 guide [1] were heavily focused on calculation sections, featuring a significant number of formulas and calculation procedures, most of which were derived from Eurocode 5 [5].

For the update of the guide, the working group decided to present the design principles specific to timber structures according to the philosophy of Eurocode 5, but to limit the calculation formulas to aspects specific to bridges. This decision was taken for two reasons mainly:

- The new guide is not intended to replace publications that specifically describe the calculation methods for elements and assemblies, as many guides already exist on this topic (see for example [6] [7]);
- The update of Eurocode 5, scheduled to be effective in 2027, may render some of the formulas and calculation methods obsolete. In this context, warnings are added to the main text to inform the reader of the expected changes between the current and future versions of Eurocode 5.

The new chapter on assemblies has also been reorganized with an introductory section on the general design of timber joints, a brief section on carpentry joints (rarely used in recent timber bridges), and a more substantial section on joints with metal fasteners (predominantly used in timber bridges). Connections using bonded-in-rods have also been included, as they are increasingly used by timber constructors.

3.4 Structural typologies and Monograph

Chapter 5 of the 2013 guide [1] detailed different structural typologies recurrent in timber structures:

- Simple beam bridges.
- Truss beam bridges.
- Under-tensioned beam bridges.
- Frame and bowstring bridges.
- Cantilever bridges.
- Arch bridges.
- Cable-stayed and suspension bridges.

Each typology was illustrated by the presentation of 2 existing references, a road bridge and a footbridge. The bridges presented were, with few exceptions, located in France.

For the update of the guide, the working group decided to keep the same classification by structural typology, as it is still relevant today. However, the new chapter is enriched with around ten new references, including number of international structures. These include, for example:

- Engelskirchen footbridge (Engelskirchen, Germany), new reference of a suspension footbridge.

Figure 2. Photos of the intrados of the deck (left) and metallic connecting parts with the stay cables (right) [8]

- Steien bridge (Alvdal, Norway), new reference of bow-string road bridge.

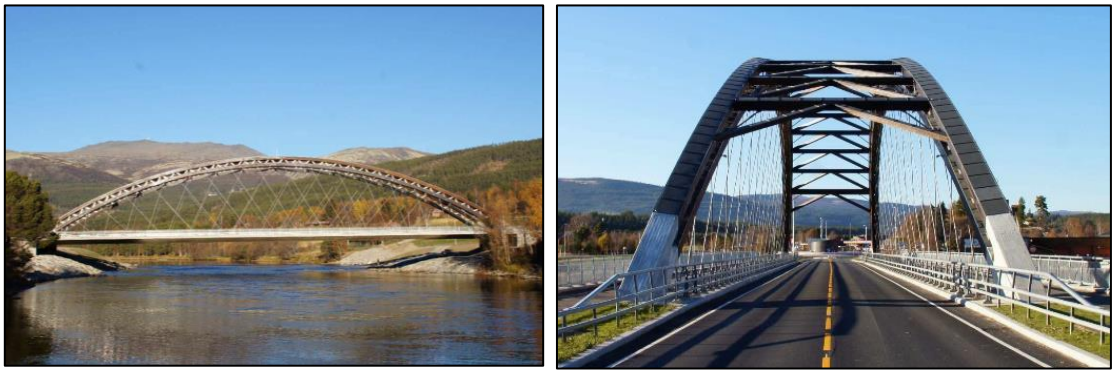

Figure 3. Photo of the structural principle of the bridge (bridge) and out-of-plane stabilization (right) [9]

- Footbridge over the Renaison (Roanne, France), new reference of truss footbridge.

Figure 4. Photo of the structure being assembled (left) and during crane lifting (right) [10]

Information, photos and data new references have been collected by some members of the working group directly contacting the stakeholders involved in the projects (wood industry professionals, architects, project managers, designers, etc.).

Following this illustrated presentation of the main structural typologies, the different types of deck are described: timber decks, composite timber-steel or timber-concrete decks, etc.
It is worth noticing, in the 2013 version of the guide [1], composite timber-concrete decks were not explicitly detailed; they were shortly addressed in the chapter dealing with innovations as this technique was still in its early days in France.
Since then, composite timber-concrete decks have been used for several structures (particularly road bridges), largely thanks to the work of Cerema (see 3.6) who published two guides on the design, calculation

and construction of beam bridges with composite timber-concrete decks ([11] and [12]). For this reason, this technique is now presented and discussed more comprehensively based on existing bridges.

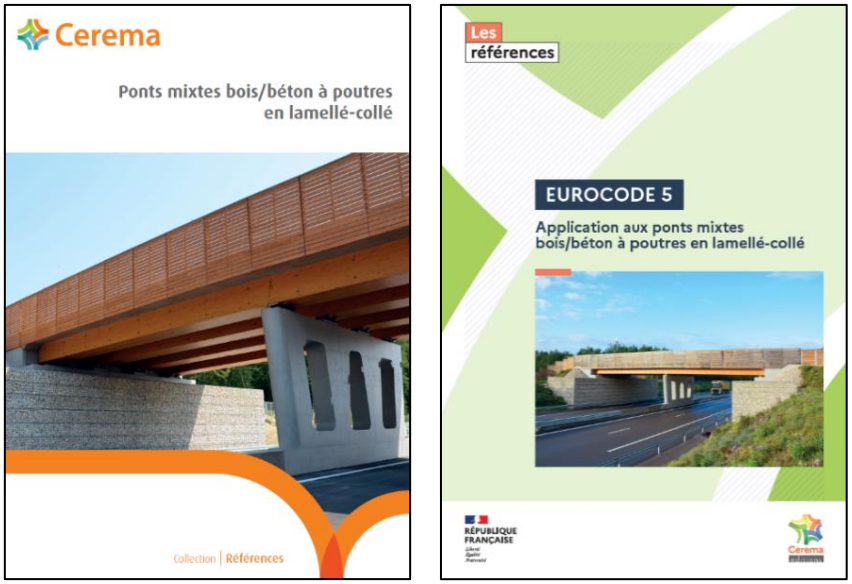

Figure 5. Covers of design guide [11] (left) and calculation guide [12] (right) on timber-concrete decks from Cerema

Finally, it is planned to enrich the brief monograph present at the end of the guide with works from the Oceania region, particularly those constructed in Australia and New Zealand. In the 2013 version [1], this concluding chapter categorizes timber bridges references based on geographical zones (North America, Asia, and Europe).

In parallel with these searches for new references, a collaborative map (see figure 6) has been created and populated by the group members to inventory French timber bridges.
Currently, there are about ten timber road bridges in France, mostly located in the South-East quarter of the country. While the list of road bridges and wildlife crossings appears to be nearly exhaustive, it is not the case for pedestrian footbridges, due to their significant number. It is therefore challenging to have a precise overview of these types of structures.

Figure 6. Collaborative map for inventorying timber bridges

3.5 Eco-design of civil engineering timber structures

In 2022, a working group focused on the eco-design of civil engineering structures was established within the AFGC [13]. The objective was to provide understanding and tools to help civil engineering stakeholders (project owners, project managers, companies, etc.) integrate the eco-design approach into their fields of action. The work led to the development of four main principles of eco-design and ten associated concrete criteria (biodiversity, decarbonization, resource preservation, etc.). This working group then divided into several sub-groups addressing more specific topics, such as concrete and steel or structure maintenance.
To support this dynamic, Chapter 7 is added as part of the guide's update specifically to address eco-design of timber structures. It is organized as follows:

- A comparative review of greenhouse gas emissions from the three major construction materials (concrete, steel, and timber). The aim is to demonstrate the benefits of wood-based products and provide estimates of emission reductions using timber as a bridge material.
- A discussion on the use of adhesives and preservative treatments, which are heavily criticized by a significant part of the civil engineering community. It is noted here that, though these products can indeed have high toxicity, they constitute a very small proportion compared to the mass of wood used.
- A summary of a 2024 study by the Swiss Federal Roads Office (OFROU, *Office Fédéral des ROUtes*) [14], presenting a comparative analysis of the environmental impacts of various bridge designs (concrete, steel-concrete composite, timber-concrete composite). This provides a more comprehensive view of the impacts through practical examples of design approaches and across the entire lifecycle of the infrastructures.
- A non-exhaustive list of "best practices" for eco-design, such as the use of naturally durable species, the choice of lower-carbon transport modes, maximized prefabrication in workshops, and the use of mixed materials (especially timber-concrete composite decks). The goal is to broaden the eco-design reflection beyond the CO2 emissions from the manufacturing of elements.

The chapter closes with a presentation of the state of the art on the end-of-life for timber structures in France. It is specifically explained that the direct reuse of structural elements remains marginal at present (2.5%), and that wood waste is primarily directed towards waste disposal (7.5%) energy recovery (42%) and material recycling (48%). These data are derived from a study by the French wood organization (FCBA, *Forêt Construction Bois Ameublement*) [15].

To change this paradigm, it is proposed, beyond sustainable design aspects, to initiate a reflection on the dismantlability of structures from the design phase and to enhance the transmission of information throughout the life of the project (drawings, types of materials, design assumptions, construction data, maintenance operations, etc.).

3.6 Durability, Maintenance and Monitoring of timber bridges

The current version of Eurocode 5 – the set of calculation codes on timber structures in Europe – does not provide requirements specific to timber bridges in terms of design service life. This choice is in most cases up to the client or to the future infrastructure owner. However, the 2nd generation of Eurocode 5 (due to come into force in 2027) sets the “standard” design service life of timber bridges equal to that of concrete or steel bridges, i.e. 100 years. This requirement for long-lasting timber bridges, together with considerations related to the costs of maintenance and repair operations, make durability one of the main issues when designing such structures.
Durability can be achieved by appropriate constructive measures, protections, preservative treatments or the use of a wood species with high natural durability, but also by a mix of the above. To be effective, these design choices must be followed by monitoring and inspection campaigns throughout the lifetime of the structure.

For this reason, the chapter on durability (already present in the previous version of the guide) has been split into two sections and expanded.
The first section focuses on different types of pathologies for timber structures and on the ways to prevent them. Firstly, biological degradation of timber due to fungi and/or insects depending on timber moisture content is described. Mechanical and aesthetic pathologies are discussed as well. Then, different methods to prevent those disorders are covered, form the choice of the wood species, to constructive measures (such as protection claddings or planks), to chemical treatments.
The second section describes the operations of inspections and maintenance specific to timber bridges and the more common techniques for moisture and temperature monitoring. For each part of the bridge (deck, expansion joints, cladding, abutments and bearings, etc…) the chapter provides and overview on how to inspect it effectively and presents the possible corrective measures to be taken in case of identified failure, up to heavy structural rehabilitation.

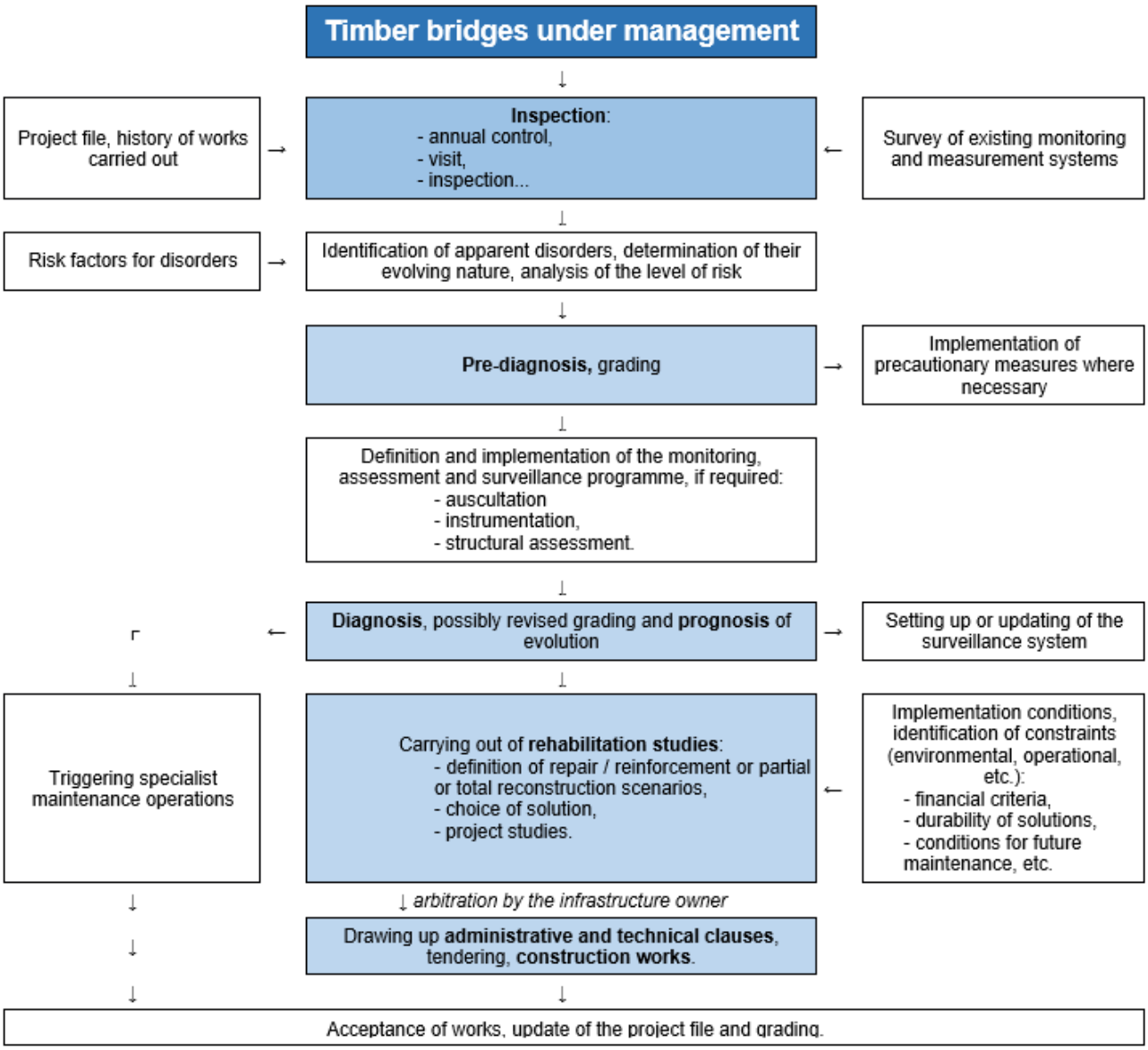

Figure 7. Inspection and maintenance approach

The text update has been carried out by two experts of the Cerema, a public institution under the supervision of the French Ministry for Ecological Transition and Regional Cohesion. Its technical department is a

benchmark on road infrastructure, and it has been at the origin of the design and construction of several timber and timber-concrete bridges in France ([11] and [12]). Its technicians are also among the most experienced in bridge monitoring, which makes these two chapters are a wealth of valuable information for designers as well as for the infrastructure owners.

3.7 Innovations

One of the new chapters of the guide focuses on recent technical innovations, particularly those expected to emerge in the future based on the insights of the members of the working group. As it would be impossible to provide an exhaustive overview, the objective is rather to highlight the potential of timber and to spark deeper curiosity among designers. Innovations at multiple scales is explored, from the material level to structural applications, including assembly techniques.

From a material perspective, the chapter reviews transformation processes aimed at enhancing the physical and mechanical properties of timber. Regarding assemblies, new gluing applications are discussed, such as edge gluing for CLT. Additionally, a state-of-the-art review on the composite action of timber and ultra-high-performance concrete decks is presented.

Finally, the chapter focuses on the "non-standard" use of solid timber (see Figure 11), whether in small or large cross-sections – solutions that are often overlooked by designers despite their significant potential for long-span structures.

A final section is dedicated to the reconstruction of Notre-Dame de Paris, discussing the use of green oak and the scientific and technical challenges that this has brough to engineers, which should be of particular interest to readers.

Figure 8. Covering of a highway with a whole log timber crossing structure(left) and Prof of concept of the crossing structure made of a composite concrete-log timber structure (right). (STENT project: https://www.archipente.com/stent-bois/)

4 CONCLUSION

The guide update aims to democratize the use of timber as a structural material for bridges in France, especially for “standard” ones. The wish of the authors is in fact to help provide the same momentum to timber construction for bridges as it is the case today for buildings.

Achieving this goal involves two key actions: first, raising awareness among French civil engineers – who traditionally favour steel and reinforced/prestressed concrete structures – to timber alternatives; second, showcasing the dependability of well-designed timber bridges to potential clients and infrastructure owners.

Timber bridges completed in recent years or currently in the design phase in France are proof that the move towards more eco-friendly and sustainable infrastructures is well underway in our country. Against this backdrop, the updated guide aims at becoming a practical and comprehensive handbook for the construction industry to support this trend by highlighting national expertise and drawing on examples from around the world.

The publishing of the updated guide is planned for the end of 2025.

REFERENCES

[1] AFGC, 2013. Guide pour la conception des Ouvrages d'Art en Bois. Paris, France, in French.

[2] Sétra, 2006. Les ponts en bois, Comment assurer leur durabilité. Bagneux, France, in French.

[3] Laboratoire Central des Ponts et Chaussées, 2008. Recommandations pour l'inspection détaillée des ouvrages en bois. Marne-La-Vallée, France, in French.

[4] IGN, 2023. Memento, IGN website. https://www.ign.fr/files/default/2023-10/memento_oct_2023.pdf, in French

[5] NF EN 1995-1-1 - Design of timber structures, Part 1-1 General- common rules and rules for buildings, ISSN 0335-3931.

[6] Y. Benoit, B. Legrand and V. Tastet, 2019. Calcul des structures en bois - Guide d'application des Eurocodes 5 (structures en bois) et 8 (séismes) - 4e édition revue et mise à jour. Eyrolles, Paris, France. In French.

[7] Y. Benoit, 2014. Construction bois : l'Eurocode 5 par l'exemple. Eyrolles, Paris, France. In French.

[8] F. Miebach, 2021. Zeitgemäße Rad- und Fußwegbrücke in Engelskirchen in nachhaltiger Holzbauweise - Schrägseilbrücke mit baulich geschütztem Brettschichtholz-Blockträger, Holzbau.

[9] J. Veie, R. B. Abrahmsen, 2013. Steien Network Arch Bridge, 2nd International Conference on Timber Bridges – ICTB. Las Vegas, USA.

[10] Loïc Couton, 2024. Apaisement de l'équilibre, Séquence bois numéro 141. Paris, France. In French.

[11] Cerema, 2019. Guide Ponts mixtes bois/béton à poutres en lamellé-collé. Sourdun, France.

[12] Cerema, 2023. Guide méthodologique Eurocode 5. Application aux ponts mixtes bois/béton à poutres en lamellé-collé. Sourdun, France, in French.

[13] AFGC, 2023. Kit Ecoconception des ouvrages de Génie Civil, AFGC website. https://www.afgc.asso.fr/ressources/kit-ecoconception-des-ouvrages-de-genie-civil/

[14] Z. Mukhamadiyeva and R. Hischier, 2024. Potentiel de réduction des émissions de CO2 dans le domaine des ouvrages d'art. Office Fédéral des Routes. St. Gallen, Switzertland. In French.

[15] FCBA, 2022. Gestion des déchets bois du bâtiment – GDBAT, Phase 1 : Gisement et devenir des déchets bois issus de la construction neuve, de la démolition et de la rénovation du bâtiment. Bordeaux, France. In French.

ICTB 2025. 5th International Conference Timber Bridges
Rotorua, New Zealand, 29 June to 2 July 2025.

PRESTRESSING LOSSES IN A STRESS-LAMINATED TIMBER (SLT) LOGGING BRIDGE

Andy Buchanan[1], Cameron Douglas[1], Daniel Moroder[1]

1 INTRODUCTION

A post-tensioned timber box-girder logging bridge was designed and built in 2010, with a span of 6.0m and a width of 4.0m. This paper describes construction of the bridge, stressing of the transverse post-tensioning tendons, and measurement of post-tensioning losses over 15 years of use (PTL, 2012). The bridge is on private land so it did not need to comply with the NZ Bridge Manual, except for the vehicle loading and required load combinations.

As far as we know, this is the first transversely post-tensioned timber bridge to be built in New Zealand. Earlier stress-laminated timber highway bridges were constructed in Canada and Australia, following research and development, especially that by Crews (2001, 2002). Stress-laminated timber bridge decks have become very popular in Scandinavian countries, often used on structural systems of timber arches or timber trusses.

An earlier bridge in the North Island of New Zealand had a longitudinally post-tensioned timber deck supported on steel beams, as shown in Figure 1, but no records are available to the authors. No other bridges of this type are known of. Longitudinal post-tensioning in timber bridge decks creates difficulty in maintaining stress levels over time, as anchorage points are often inaccessible and creep perpendicular to the grain leads to a reduction in the length of the bridge.

More recent post-tensioned timber bridges in New Zealand are described by Douglass et al. (2024, 2025).

Figure 1(a). Longitudinally post-tensioned timber deck supported on steel beams.

Figure 1(b). Post-tensioning in progress.

[1] Structural Engineer, PTL | Structural & Fire, e-mail: a.buchanan@ptlnz.com

2 STRUCTURAL FORM

The timber box-girder bridge is 6.0m long, 4.2m wide and 600mm deep, supported on reinforced concrete abutments. Each of the 10 LVL webs is a 36mm cross-banded LVL plank, 600mm wide and 6.0m long, from Nelson Pine Industries. The top and bottom flanges are made from 80 rough sawn timber boards, nominally 150mm by 50mm. All webs and boards were cut to size and pre-drilled before preservative treatment and delivery to site. The boards were not dried after treatment. The timber bridge was attached to the concrete abutments by screwed-in brackets, designed for earthquake and flood loads, with slotted holes to allow for movement from post-tensioning distortion.

Figure 2 shows the bridge being constructed board by board, threading boards over the white plastic water pipes, used to protect the tendons from the Copper-Chrome-Arsenic (CCA) treated timber. The sawn timber members were pre-treated to Hazard Class H5 in accordance with NZS 3602 (SNZ, 2003). The LVL webs were autoclave treated with the same process used to achieve H5, but due to the presence of glue lines the interior layers may not all have achieved the level of retention required in the standard.

The bridge is unsealed but has running boards to limit wear and deterioration of the structural timber in the top of the box girders. Figure 3 shows the bridge after it was built in one day, before tensioning.

Figure 2. Boards being threaded one-by-one, over white plastic water pipes to locate and protect the tendons.

Figure 3. The timber bridge after construction in one day, before tensioning.

3 STRUCTURAL DESIGN

The timber structure was designed to accommodate full highway loads (HN loading) in accordance with the NZTA Bridge Manual (NZTA, 2005).

4 DESIGN OF STRESSING SYSTEM

The post-tensioning provides the clamping force and hence friction necessary to hold all the boards and webs together for full composite action, with no need for any other fasteners such as nails, screws or adhesives. Seven top and bottom post-tensioning tendons (evenly-spaced at 860mm) provide the friction between boards.

The post-tensioning was designed to give a compressive pressure between timber boards of 1.0 MPa at transfer and a minimum long-term pressure of 0.5 MPa, in accordance with the Australian recommendations at the time (NSW, 1995). For tendon spacing of 860mm and a deck thickness of 150mm, these stresses give stressing forces of 129kN and 65kN respectively. In the Australian Standard for Timber Bridge Design AS

5100.9 (AS, 2017), the minimum in-service pressure due to prestress for softwood decks has increased to 0.55 MPa. This would mean that the minimum post-tensioning force for this bridge should be increased to 71kN.

Eurocode 5 Part 2 (EC5, 2005) requires that "the long-term prestressing force shall be such that no inter-laminar slip occurs". It also gives design rules based on coefficients of friction, and states that the long-term residual prestressing pressure "may normally be assumed to be greater than 0.35 N/mm^2 (0.35 MPa), provided that the initial prestress is at least 1.0 N/mm^2 and the moisture content at the time of prestressing is not more than 16%." For sawn timber decks, the new draft of Eurocode 5 Part 2 (EC5, 2023) requires that to compensate for long-term stressing losses, the initial prestressing force should be 2.0 times the value of $F_{p,min}$, the minimum long-term residual compressive force calculated to ensure sufficient friction. It also requires that in areas subjected to concentrated loads, the minimum long-term residual compressive force between boards, $F_{p,min}$, should be greater than 80 kN/m (69 kN per tendon in this bridge).

5 MAINTENANCE

There is no guidance in AS 5100.9 regarding maintenance or relaxation of the prestressing strand due to creep in the timber. An Australian guide (NSW, 1995) required that the drawings shall indicate maintenance procedures for the stress-laminated bridge deck including "maintain adequate prestress, monitoring and restressing when required". It also refers to a forthcoming procedural guide for maintenance which has not been found at the time of writing.

The draft of Eurocode 5 Part 2 (EC5, 2023) requires "a maintenance program for the prestress system to monitor long term losses, including regular inspections and re-stressing of the prestress system a number of times during its design service life".

6 OPTIONS FOR STRESSING SYSTEMS

The tendons in this bridge are commercially supplied 7-wire BBR strands, as typically used for post-tensioned concrete structures. The tendons were purchased from Contech in Christchurch. The tendons were nominal 0.5-inch diameter with a cross-section area of $100mm^2$ and an ultimate tensile stress of 1860 MPa (ultimate resistance of 186 kN). The BBR post-tensioning design data gives the minimum proof load as 158.1 kN, and the modulus of elasticity as 185 to 205 GPa. Each single tendon was supplied in a pre-greased PVC conduit. Figure 4 shows the tendons being post-tensioned, and Figure 5 shows a fully-loaded logging truck crossing the finished bridge.

Two other stressing options considered were Macalloy and Reidbar. The Macalloy 1030 system has bars from 20mm to 75mm diameter with a nominal ultimate tensile strength of 1030 MPa and a nominal 0.1% proof stress of 835 MPa, and modulus of elasticity of 170 to 205 GPa. The Reidbar design data shows bar diameters of 12mm to 32mm, with minimum yield stress of 500 MPa, and modulus of elasticity as 200 GPa. The 7-wire strands were selected because the higher yield strength would result in lower losses from creep or shrinkage, and for easier supply than Macalloy bars.

Australian Standard AS 5100.9Clause 5.8.1 (SA, 2017) states that the minimum prestressing element size shall be selected to maximize the elongation of the element, supporting the use of high tensile steel of minimum diameter.

Figure 4. Post-tensioning in progress.

Figure 5. Fully-loaded logging truck on bridge.

7 STRESSING OPERATION

A full-length steel channel was provided to distribute the point forces at the anchorage points into a uniform stress in the timber. An alternative to the steel channel would have been localized steel plates with closely spaced screws in the timber laminates at the anchorage point, as proposed by Crocetti and Kliger (2010). The galvanised steel channels were chosen as a conservative, but more expensive option.

The 14 stressing tendons were purchased from Contech in greased plastic sleeves, with two different custom anchorages for the fixed end and the stressing end. The tendons were inserted into the plastic water pipes, and end washers were placed before stressing each tendon from the north end using a hand-operated hydraulic jack. This jack is specially designed for stressing 7-wire strands in post-tensioned concrete structures.

Re-stressing was carried out seven times in the first year between 2010 and 2011, during the logging activities. There was then a delay of almost ten years before re-stressing in 2020, and another 5 years to 2025. Measurement of the existing stressing force is approximate, because it requires visual recording of the hydraulic jack pressure associated with a sudden clicking sound when the wedges release during the re-stressing operation. More accurate readings could be obtained by the use of load cells, but this is not considered necessary, for practical reasons.

8 MOISTURE CONTENT

Despite specifying dried timber. the bridge was constructed with wet timber because none of the boards had been dried after treatment. The moisture content was well over the fibre saturation point of 30%, maybe even double that value. In the 15 years since construction, the timber has been able to air dry in-situ, but the moisture content has remained very high. The boards in the bottom flange appear to have reached equilibrium at about 22% moisture content. The bottom surface of the bridge is in a damp location two metres above a flowing stream. The boards in the top flange have much more variable moisture content, measured at about 14% close to the exposed surface, but over 30% when measured by 30mm long probes. The measurements were carried out only in the sawn timber members, and correction factors due to the presence of copper based preservatives were applied.

On the basis of these measurements of moisture content, shrinkage from drying of the timber will not have significantly affected the loss of prestressing forces. However, it is almost certain that unknown changes in moisture content have contributed to mechano-sorptive creep.

9 CREEP

A summary of creep in timber structures is given by Granello and Palermo (2019). They quote figures showing that the creep in timber loaded perpendicular to the grain can be eight times more than when loaded parallel to the grain. Also, that the process of mechano-sorptive creep depends on the accumulation of moisture cycles within the element that increases the rate of creep.

Mechanical response of wood perpendicular to grain subjected to changes of humidity is described by Svensson and Toratti (2002). They point out that deformation of wood perpendicular to the grain is the summation of free shrinkage, thermal expansion/contraction, elastic strain, mechano-sorptive strain and visco-elastic strain. The observed creep deformations in our bridge are likely to be from mechano-sorptive strain. Svensson and Toratti measured mechano-sorptive strain that was 10 times the initial elastic strain. They show that it is possible to predict the stress distribution in timber if the climate history and moisture gradients are known, but this is only of limited use for this bridge, because of the inability to track small changes in the moisture content, which remains very high.

10 STRESSING LOSSES

Figure 6 shows the loss of post-tensioning force with time over 15 years. This is the average force in all 14 tendons. At the 2025 stressing, the average force in the top 7 tendons was 96% of the average force in the bottom 7 tendons, so this difference is not significant. In Figure 6 the top horizontal line (134 kN) is the design stress of 1.0 MPa and the lower dotted line (62 kN) is the minimum long-term stress of 0.5 MPa.

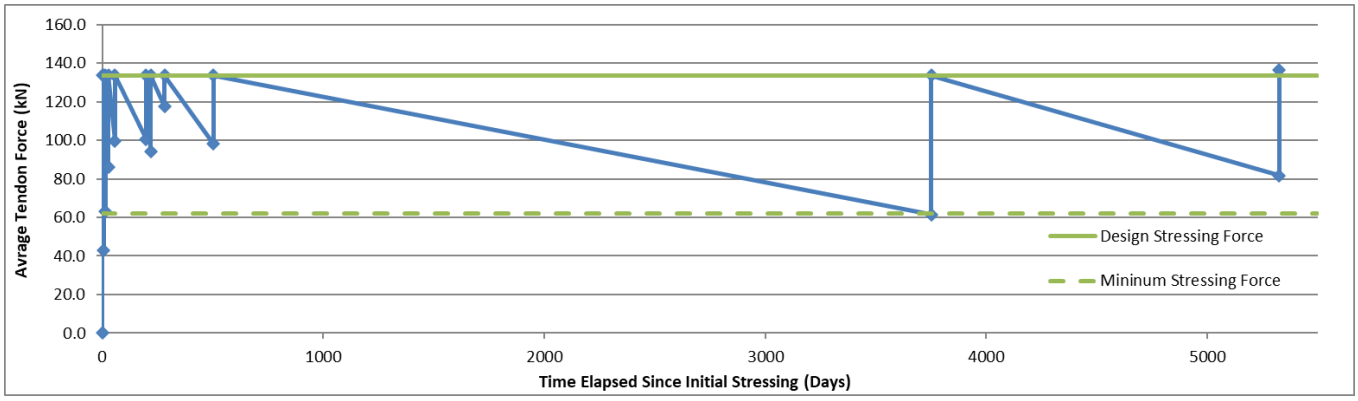

Figure 6. Loss of post-tensioning force with time over 15 years.

Figure 7 shows the compressive distortion of the bottom chord compared with the predicted values, showing that the width of the underside of the bridge has reduced by almost 100mm (2.5%) over 15 years. Distortion of the top flange was too difficult to measure. There is nothing in Eurocode 5 or AS 5100.9 about predicted narrowing of the bridge deck. Figure 8 shows the same data as in Figure 7, plotted to show compressive distortion of the bottom chord over 15 years. The black line is a creep curve fitted to the data points using a logarithmic approximation. Figure 9 is the same as Figure 8, with an extended axis to show the extrapolated compressive distortion of the bottom chord over 50 years, being approximately 110mm.

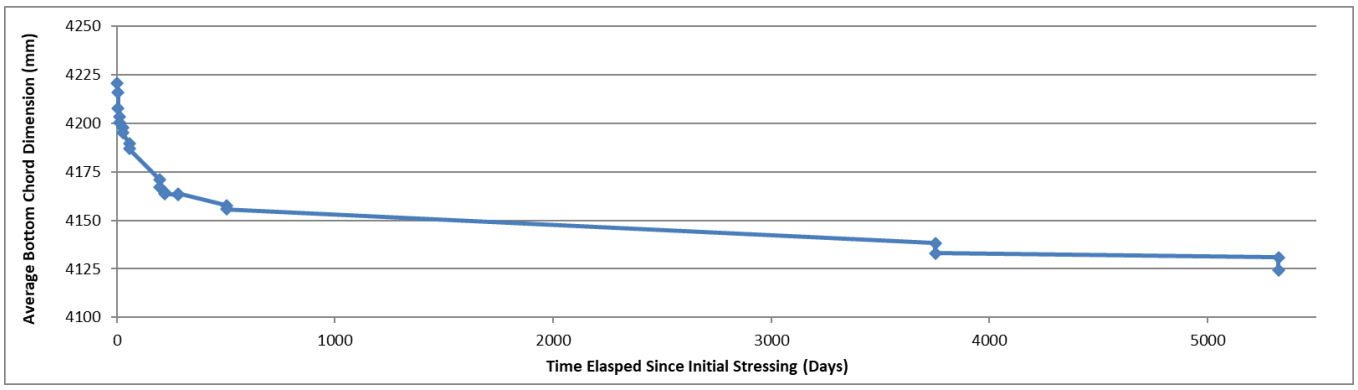

Figure 7. Narrowing of bottom chord of the bridge deck over 15 years.

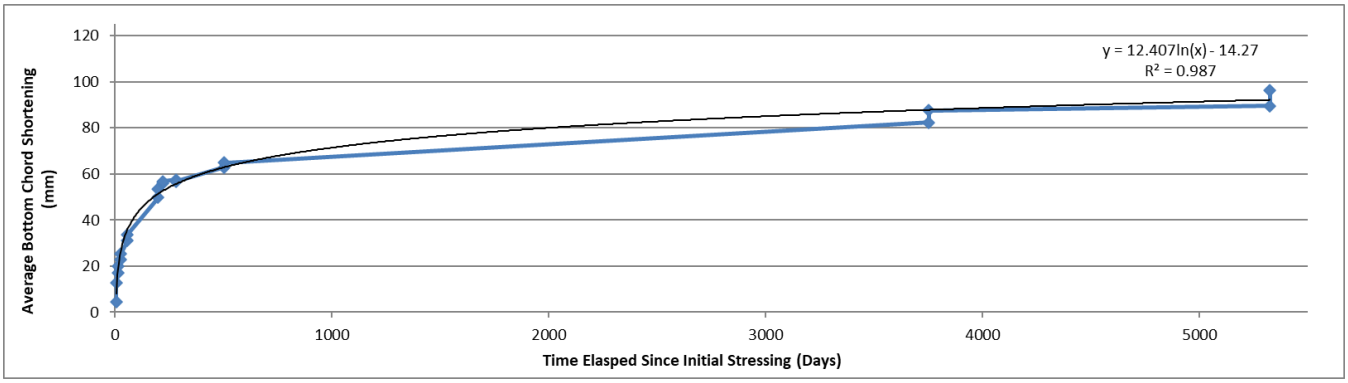

Figure 8. Compressive distortion of the bottom chord over 15 years, with creep curve.

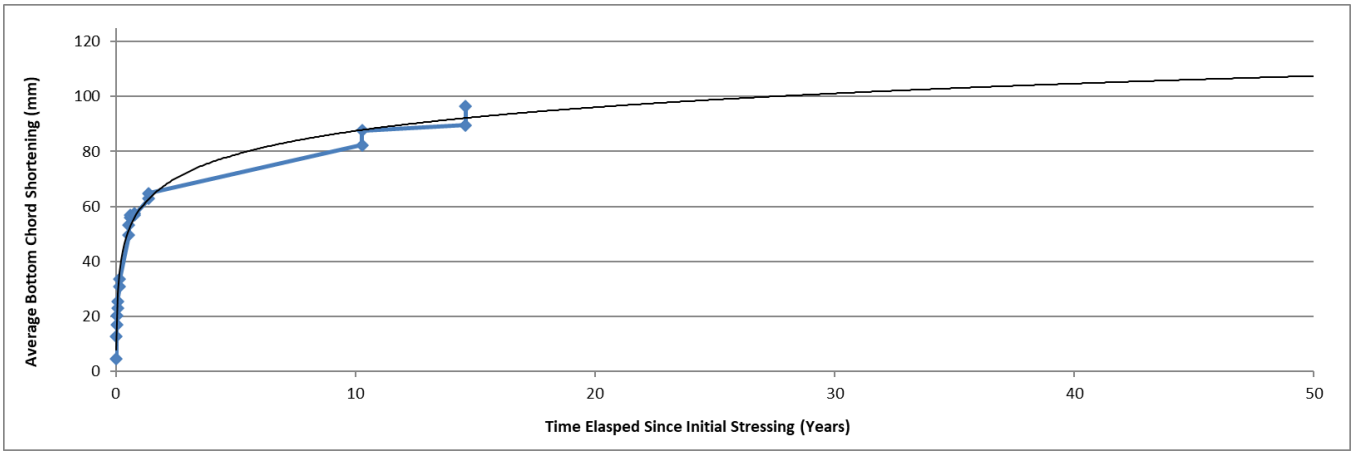

Figure 9. Predicted compressive distortion of the bottom chord over 50 years.

In summary, the performance of the bridge over 15 years shows that routine maintenance must include regular re-stressing, recommended to be at weekly then monthly intervals immediately after construction, yearly for the first 10 years, and no greater than five yearly intervals over the life of the bridge, especially if high levels of loading are expected.

11 DURABILITY

Preservative treatment of the wood has been described above. The 14 stressing tendons were purchased from BBR Contech in greased plastic sleeves. These protected tendons were inserted into the white plastic water pipes which had been used to align all the boards. This provided three layers of protection between the CCA treated timber and the tendons, being two layers of plastic pipe and one layer of grease. At the stressing end of the tendons, they pass through a short length of steel pipe containing a grease nipple. Grease has been pumped in on a regular basis to maintain the grease protection at the stressed end of the tendon.

The anchorages at the non-stressing end of the tendons were wrapped with Densotape. The anchorages at the stressing end must remain available for routine stressing, so they are exposed to the weather. A surface coating of grease has been hand-applied to these anchorages and projecting tendons from time to time.

After 16 years in service, no noticeable rust or other deterioration of the steel channel or tendons has been noted. The timber box girders also performed well, with no noticeable deterioration. The running boards, which are not structural, were not regularly cleared of organic matter and show some signs of deterioration, hence might require replacement in the future, depending on the level of traffic.

There is no reason why the bridge should not have a 100 year design life, provided that regular inspections and maintenance are carried out.

12 CONCLUSIONS

The performance of the bridge over 15 years shows that regular maintenance must include monitoring and re-stressing the transverse post-tensioning in the bridge. Initial stressing should be at short intervals after construction, and long-term routine maintenance should include regular re-stressing, at no greater than five yearly intervals over the full life of the bridge.

ACKNOWLEDGEMENTS

Many thanks to all those who assisted with construction of the bridge in 2010, and re-stressing the bridge since then. Thanks also to the engineering staff at PTL Structural & Fire for their assistance on this and other timber bridges. Edwin Douglass is thanked for his support for the commercialisation of pre-stressed timber bridges in New Zealand. Special thanks to University of Canterbury technicians Russell McConchie and John Maley for assistance with stressing on many occasions.

REFERENCES

Crews, K. (2001). An Overview of the Development of Stress Laminated Cellular Timber Bridge Decks for Short to Medium Span Applications in Australia. International Conference on High Performance Materials in Bridges, Hawaii, 2001.

Crews, K. (2002). Behaviour and Critical Limit States of Transversely Laminated Timber Cellular Bridge Decks. PhD thesis, University of Technology, Sydney, Australia.

Crocetti, R. and Kliger, R. (2010). Anchorage systems to reduce the loss of pre-stress in stress-laminated timber bridges. International Conference on Timber Bridges, ICTB 2010.

Douglass, E., Moroder, D., Buchanan, A. (2024). Case Study: Pre-fabricated Stress Laminated Timber Bridge. Glen Alton Forest, Clarence River Valley. NZ Timber Design Journal, 2024.

Douglass, E., Moroder, D., Buchanan, A. (2025). Pre-fabricated Stress Laminated Timber Bridges in New Zealand. International Conference on Timber Bridges, Rotorua, June 2025.

EC5 (2005). EN 1995-2:2005. Eurocode 5: Design of timber structures - Part 2: Bridges, European Committee for Standardization, Brussels.

EC5 (2023). FprEN 1995-2:2025-02-03 Eurocode 5: Design of timber structures - Part 2: Bridges, European Committee for Standardization, Brussels.

Granello, G., Palermo, A. (2019). Creep in timber: research overview and comparison between code provisions. New Zealand Timber Design Journal, Vol 27, Issue 1.

NSW (2012). Guide for the design of stress laminated timber bridge decks, Part 1 – Design Procedures, Part 2 – Commentary, Version 2.2, NSW Transport, Roads and Maritime Services, March 2012.

NZS (2003). NZS 3602:2003 Timber and wood-based products for use in building, Standards New Zealand, 2003.

NZTA (2005). Bridge manual - 2nd edition, NZ Transport Agency Waka Kotahi.

PTL (2012). NZ Timber Design Awards 2012. PTL Structures & Fire, Christchurch. https://ptlnz.com/projects/other/stress-laminated-timber-bridges/

SA (2017). AS 5100.9:2017. Bridge Design, Part 9 Timber. Standards Australia, 2017.

Svensson, S, & Toratti, T. (2002). Mechanical response of wood perpendicular to grain when subjected to changes of humidity. Wood Science and Technology 36 (2002) 145-156.

ICTB 2025. 5th International Conference Timber Bridges
Rotorua, New Zealand, 29 June to 2 July 2025.

A RESTRAINT SYSTEM FOR VERTICALLY LAMINATED GLULAM BRIDGE GIRDERS – A DESIGN ENGINEERS PERSPECTIVE

Michael Campbell[1], Cameron MacPherson[2]

ABSTRACT

A 30m span glulam girder pedestrian bridge has been designed in the Ōtākaro Avon River Corridor, an area of Christchurch severely affected by soil liquefaction and lateral spreading during the 2010-11 Canterbury Earthquakes. Due to fabrication limitations and cost efficiency, each girder comprises of two mechanically laminated vertical billets. Global restraint for the bridge consists of cross bracing below the deck structure and moment resisting restraint frames at each end. To determine the global girder buckling capacity, both the composite out-of-plane and torsional stiffness of the laminated girders, and the restraint system effects on flexural lateral torsional buckling were assessed. For the composite stiffness of the laminated girders, methods within recent research papers were used to determine an effective composite design width two-thirds the gross width. Current analytical methods for flexural lateral torsional buckling were limited and assume uniform rigid restraints. To verify global restraint system effects, geometric non-linear static FEA was used to determine critical buckling moments 8% lower than those found by analytical methods. Recommendations were made for the consideration of system effects of tension flange restraint systems in design, design methods for vertical lamination, and future research to inform design standards.

1 INTRODUCTION

The project involves construction of a new 30m span pedestrian bridge over the Ōtākaro Avon River in Christchurch's residential red zone, an area severely impacted from soil liquefaction and deemed infeasible to rebuild on. Running from the City Centre to the eastern seaside suburbs, the bridge is part of a new City to Sea Pathway and is part of the overall regeneration of the red zone. This is the fourth bridge for Christchurch City Council (CCC) on the pathway, with previous bridges using traditional steel and concrete.

In conjunction with architects Isthmus, the concept design was developed in conjunction with University of Canterbury. For cultural, environmental, engineering and architectural reasons, a glulam timber bridge concept was selected. The concept was developed through to detailed design by Isthmus, structural engineers Ruamoko Solutions, engineering peer reviewers PTL and geotechnical engineers, Tonkin & Taylor. The bridge has been designed, consented, and construction is due to be completed in mid-2025.

This paper briefly describes the bridge structure, design loadings, compliance pathway, design challenges, the design process used for the mechanical lamination of the glulam girder billets, and methods for determining the global girder capacities when considering the restraint system effects.

[1] Structural Engineer, Ruamoko Solutions, BE.Hons(Civil), MEngNZ
e-mail: michaelc@ruamoko.co.nz,
[2] Director, Ruamoko Solutions, ME (Dist), BE.Hons(Civil), CMEngNZ, CPEng, IntPE

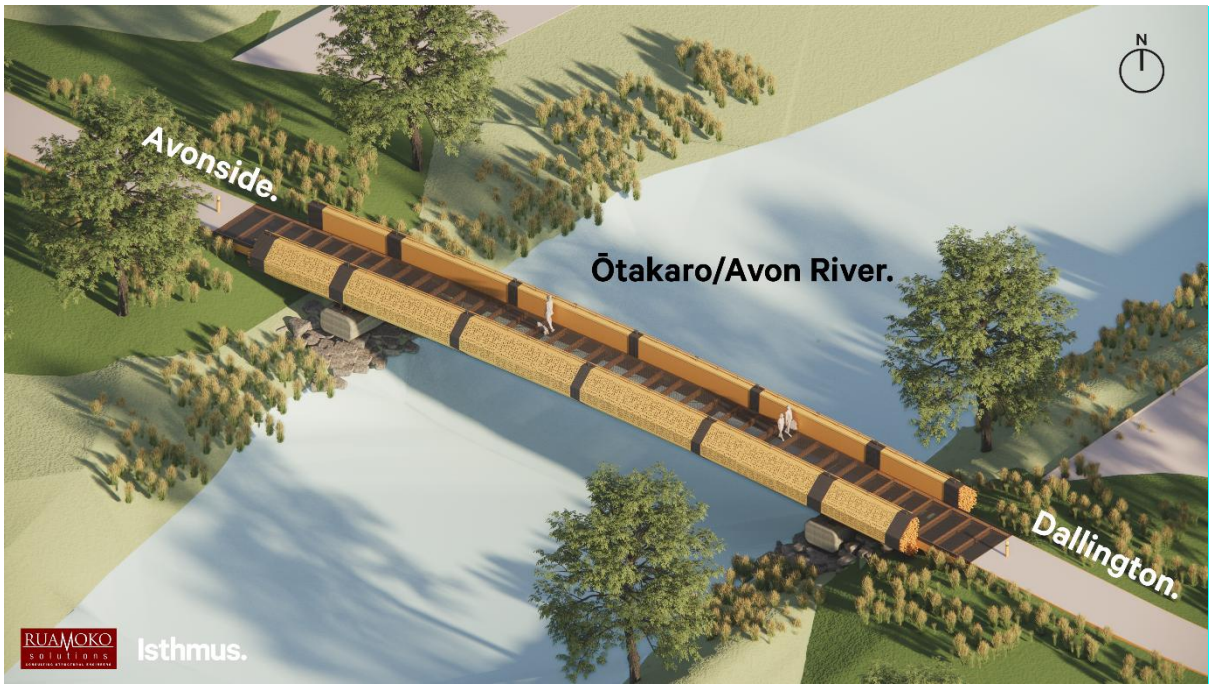

Figure 1. Architectural render of the proposed bridge (image courtesy of Isthmus)

2 DESIGN OVERVIEW

2.1 General Description

The main bridge span is 30m, the deck width 3.65m, with additional 9.5m long suspended timber approach structures. The primary structure features glulam girders, glulam deck beams, permeable FRP decking and a structural steel restraint structure. The foundations comprise of precast concrete pile caps and one 30m deep 1.2m diameter bored concrete pile each end. An architectural render of the proposed bridge is illustrated in Figure 1.

The vertical load resisting structure for the bridge superstructure consists of two primary 2m deep by 0.45m wide overall glulam girders spanning to a single pile cap each end on bored in-situ piles. The deck structure consists of 50mm deep Mini Mesh FRP panels spanning between glulam secondary beams at 1.2m spacings. Secondary cladding structure consists of timber trusses at 1.25m spacings cantilevering off the primary glulam girders.

The lateral load resisting structure for the bridge superstructure in the transverse direction is provided by a tension only steel rod cross bracing system extending between glulam restraint struts at 3.6m spacings below the deck, supported via a custom fabricated steel moment resisting ‘H’ restraint frame each end with a shear key to the pile cap and piles. Longitudinal bracing is provided by a pile cap catch frame designed to prop the primary glulam girders through a shear key to the pile cap and piles. Figure 2 illustrates the general bridge structure, including the restraint frames and connection to the pile caps.

2.2 Design Compliance

The bridge was designed in accordance with the joint Australian and New Zealand loadings standard, AS/NZS 1170, and the NZTA Bridge Manual. The structure has been classified as Importance Level 2 (Normal) and has a design life of 50 years. In addition to B1/VM1 compliance documents for steel and concrete, the new Timber Structures standard NZS-AS 1720.1:2022 [1] was used as an Alternative Solution to achieve compliance with the New Zealand Building Code. The design was independently peer reviewed by PTL Limited and granted building consent by Christchurch City Council.

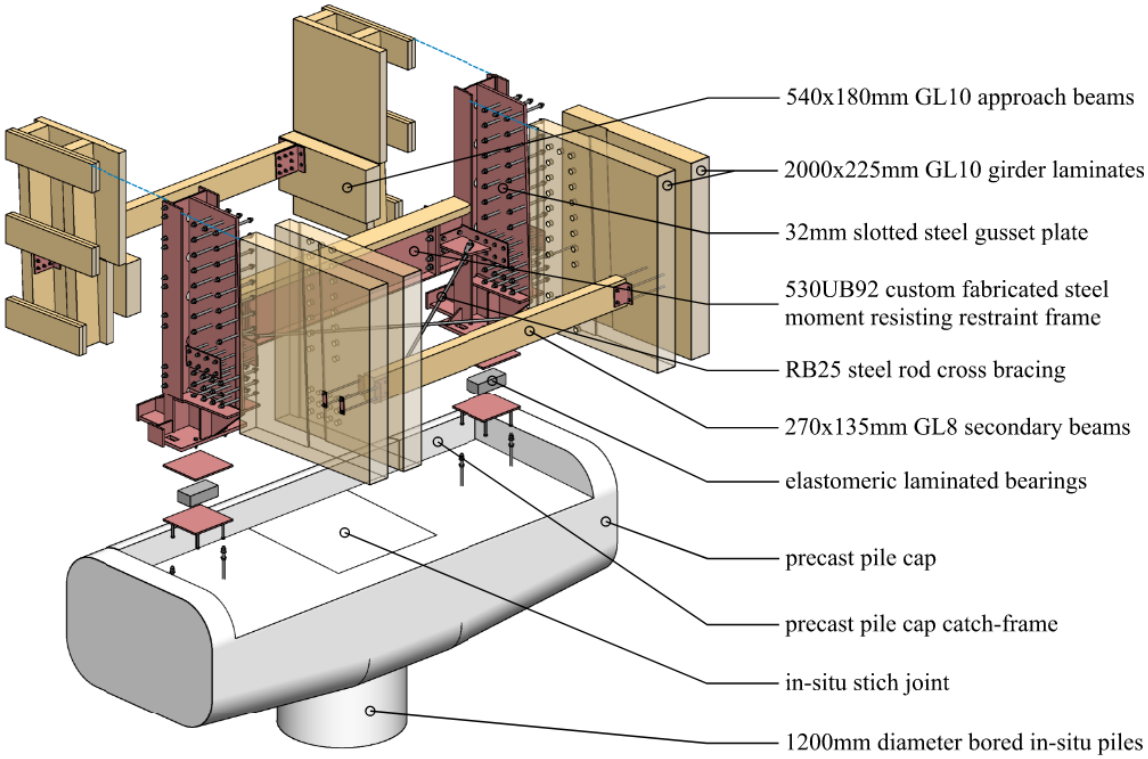

Figure 2. Exploded 3D model image of the superstructure at the end of the bridge main span

2.3 Design Actions

The earthquake design considered four limit states; Serviceability Limit State (SLS) with an 1/25 annual probability of exceedance, Ultimate Limit State (ULS) and Damage Control Limit State (DCLS) with an 1/500 annual probability of exceedance, and Collapse Avoidance Limit State (CALS) with 1.5 × DCLS intensity, ensuring no collapse despite extensive damage, applying to both the superstructure and foundations.

The bridge was designed for 5kPa live loading suitable for a dedicated footbridge, with bollard protection specified to ensure no accidental vehicle loading was possible. Wind and snow loads, temperature effects, construction and maintenance, and barrier loads were also allowed for. The bridge height and camber was based on ensuring ample freeboard above flood levels, to allow for boat passage, as well as sea level rise during the bridge's design life.

2.4 Key Design Considerations

Following the initial design concept phase where multiple structural options were considered, the use of glulam girders was chosen as the primary structural form. Preliminary design for the glulam girders also addressed tension flange restraint of the deep girder members through positioning and layout of the deck structure, and the axial loading from earthquake induced lateral spreading and pile displacements.

Once the overall girder section was designed, the practicalities of fabrication, transportation, construction and cost was considered with feedback from New Zealand's leading mass timber suppliers and fabricators. These fabrication limitations and cost efficiency led to each girder comprising of two mechanically laminated vertical billets, with the difficulty of block gluing large members, lifting weights during workshop fabrication and transportation to site, and the simplified construction methodology for the end restraint and slotted connections key factors.

Further challenges included design of the restraint frame to pile cap connection to allow for translational and rotational movement as well as transferring the large axial loads from lateral spreading and pile displacements.

3 MECHANICAL LAMINATION

3.1 Theory

Design provisions within international design standards for the composite strength and stiffness of mechanically laminated timber members is limited. Known provisions such as the *'Gamma Method'* within EN 1995-1-1: Eurocode 5 [2] provides design methods to compute the effective bending stiffness and fastener demands of mechanically jointed beam sections but does not address the composite member effects for flexural lateral torsional (FLT) buckling. Due to this, alternative research-based analytical methods were reviewed to consider the effects of mechanical lamination on FLT buckling for the design of the bridge girders.

The first paper referred to was Engineering Structures "*Lateral-Torsional Buckling of Vertically Layered Composite Beams with Interlayer Slip Under Uniform Moment*" [3], which presented an analytical model to compute the critical buckling moment of a vertically layered composite section under pure bending, un-restrained between two pin supports with torsional restraints, taking into consideration fixing pattern and stiffness through refined kinematics. Figure 3 shows the refined kinematic model under lateral-torsional deformation at the onset of buckling.

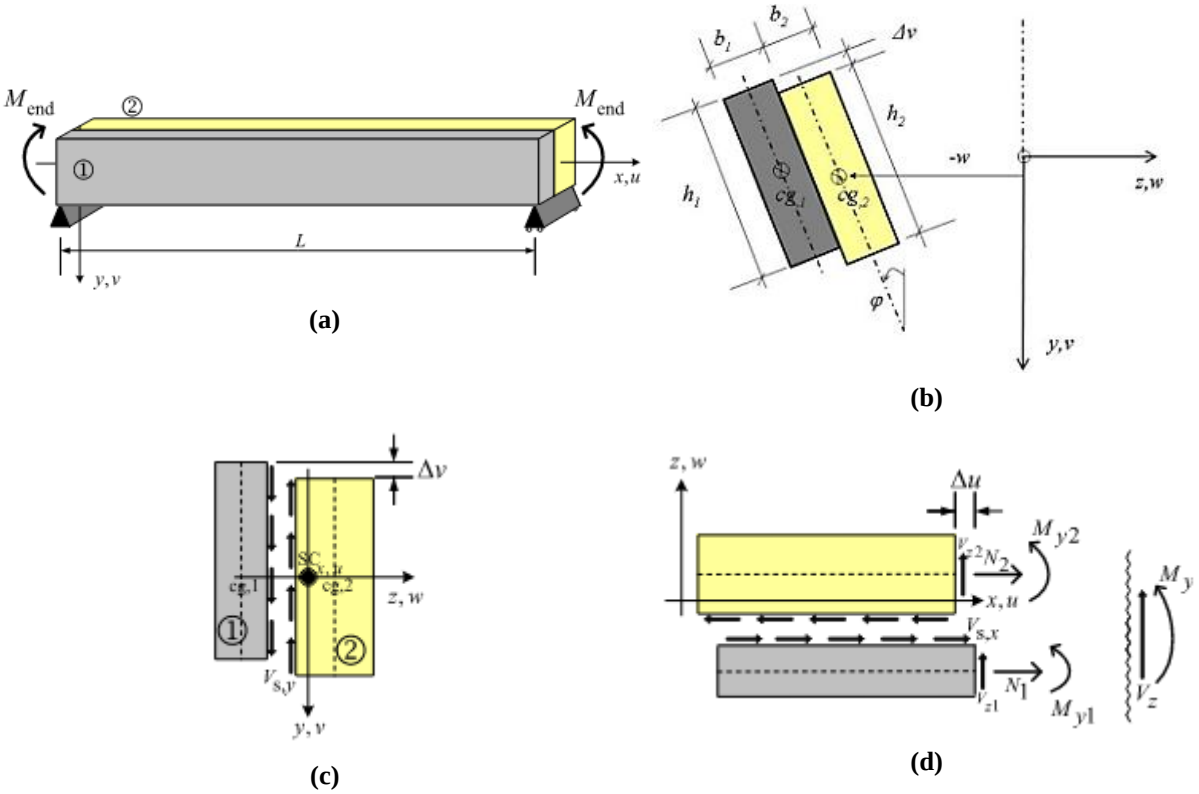

Figure 3. (a) Beam member boundary conditions for analytical model. **(b)** Simplified kinematics of a partially vertically layered composite section. **(c)** Cross section view of beam with slip forces in the cross-longitudinal or vertical direction. **(d)** Vertical view of beam element with transverse forces and moments defined positive as shown, including slip forces in the longitudinal or horizontal direction [3]

Through the refined kinematic model, an analytical solution was derived as shown in Equation (1) which accounts for fastener stiffness and joint slip in the longitudinal and transverse direction due to lateral and torsional displacements.

$$\bar{M}_{end}{}^2 = \left[E_1 I_{z1} E_2 I_{z2} \left(\frac{n\pi}{L}\right)^4 + K_{across} E I_{z0}\right]\left[E_1 A_1 E_2 A_2 \left(\frac{n\pi}{L}\right)^2 + K_{along} E A_0\right] = \left(\frac{n\pi}{L}\right)^2 \left\{GJ_0 E_1 I_{z1} E_2 I_{z2} \left(\frac{n\pi}{L}\right)^4 + K_{across}\left[GJ_o E I_{z0} + b_o{}^2 \left(\frac{n\pi}{L}\right)^2 E_1 I_{z1} E_2 I_{z2}\right]\right\} \cdot \left[E I_{y0} E_1 A_1 E_2 A_2 \left(\frac{n\pi}{L}\right)^2 + K_{along}\left(E I_{y0} E A_0 + b_0{}^2 E_1 A_1 E_2 A_2\right)\right] \quad (1)$$

Where:
- $\bar{M}_{end}$ - critical buckling end moment
- Subscripts *'1' & '2'* – each vertical laminate
- Subscript *'0'* – summation of the two laminates
- b_0 - half the gross width
- E – parallel-to-grain modulus of elasticity
- G – shear modulus
- A – cross section area
- I – moment of inertia
- J – polar moment of inertia
- L – member span between support restraints
- n – buckling mode 1 for the first mode shape
- K_{across} - transverse fastener stiffness
- K_{along} - longitudinal fastener stiffness

The second paper referred to was University of Ottawa's, Robabeh Robatmili's thesis paper on "*Lateral Torsional Buckling of Timber Built-up Beams"* [4], which tested the analytical model presented in [3] through Finite Element Analysis (FEA). The paper concluded that the analytical model provided conservative results when compared to the numerical model, and considering the composite action of two-ply vertically laminated members under pure bending resulted in critical buckling moments 40% that of the gross solid section.

3.2 Adopted Design Approach

The analytical model within [3] was adopted to compute the un-restrained critical buckling moment of the girders. Due to the boundary conditions of the actual bridge structure differing to the assumed boundary conditions for the analytical model, where the bridge structure has continuous tension flange restraint, an effective composite FLT buckling width *'b_{eff}'* was calculated for an equivalent solid section. This was calculated by equating the critical buckling moment from the analytical model with the critical buckling moment from the design provision within Appendix E6.3 *'Beams with No Intermediate Buckling Restraints but with Torsional Restraints at the Ends'* [1], and solving for an effective width as shown in Equations (2) to (4). This effective width then allowed for the use of other design provisions that better represented the actual boundary conditions of the bridge girders as discussed further in Sections 4 and 5.

$$M_{cr} = \frac{h_2}{L_{ay}}[(EI)_y (GJ)]^{1/2}\left\{1 - h_3 \frac{y_h}{L_{ay}}\left[\frac{(EI)_y}{(GJ)}\right]^{\frac{1}{2}}\right\} = \bar{M}_{end}\ (eqn.1) \quad (2)$$

$$I = \frac{b_{eff} d^3}{12} \quad (3)$$

$$J = \frac{d b_{eff}{}^3}{3}\left(1 - 0.63\frac{b_{eff}}{d}\right) \quad (4)$$

To match the boundary conditions of the analytical model for beams loaded only by end moments, the height above the centroid of the point of load application *'y_h'* was taken as 0, moment factor *'h_2'* was taken as 3.1, and moment factor *'h_3'* was taken as 0, as per the design provisions within [1].

3.3 Fastener Stiffness

The fastener stiffness plays a critical role to the amount of partial composite action contributing to FLT buckling. Design provisions within Section ZZ4A.8 *'Deformation'* [1] were used to compute the fastener stiffness 'K_{ser}' for coach screws through Equations (5) to (7).

$$k_{ser,0} = (0.0075\rho' - 0.29) k_{sp} k_{15} \quad (5)$$

$$k_{ser,90} = (0.0075\rho' - 0.29) k_{90} k_{15} \quad (6)$$

$$k_{90} = 2.12 D^{-0.45} \quad (7)$$

The characteristic density *'ρ'* was assumed to be 415kg/m^3 for New Zealand-verified seasoned SG10 timber, the steel side plate factor *'k_{sp}'* was assumed to be 1.0, the fastener moisture content factor *'k_{15}'* assumed to be 0.7 for coach screws, and the fastener deformation factor *'k_{37}'* taken as 1.5 for the ULS load case 1.35DL + 1.5FP (loading 5 minutes to 2 weeks).

3.4 Comparison of Gross and Composite Section Properties

Using the adopted design approach, the developed design solution comprised of stainless steel G316 M12 x 400mm coach screw fasteners at 500mm centres perpendicular to the grain and 1200mm centres parallel to the grain as shown in Figure 4 below.

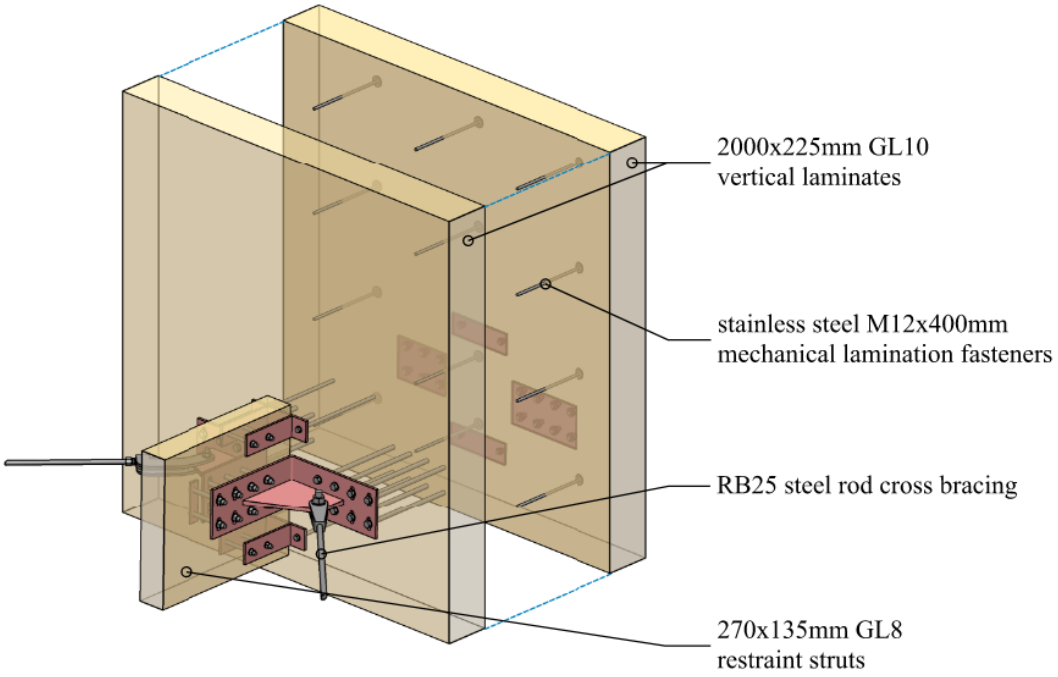

Figure 4. Exploded 3D model image of the mechanical lamination fixings

With the design fixing pattern, the effective composite width for FLT buckling was found to be 305mm considering the un-restrained critical buckling moment. This was approximately two-thirds of the total gross width of 450mm. Table 1 shows the un-restrained critical buckling moments for the gross and effective width, along with a sensitivity check on the effective width by doubling and halving the parallel to grain fixing spacing. The combined individual laminates was also provided as a point of reference. The effect of mechanical lamination was found to have a 67% reduction in critical buckling moment from the gross width, and about a 22% increase in critical buckling moment when compared to the combined individual laminates.

Table 1. Gross vs effective width critical buckling moments

	Width(mm)	Critical Buckling Moment (kNm)	Percentage of Gross Width (%)	Percentage Gross Critical Buckling Moment (%)
Gross Width	450	5269	100	100
Individual Laminate Width (combined)	2-225	1370	50	26
Effective Design Width	305	1677	67	32
50% of Design Fasteners	297	1562	66	29
150% of Design Fasteners	315	1850	70	35

4 RESTRAINT SYSTEM EFFECTS

4.1 Known Analytical Methods

Design provisions within international design standards generally capture most types of restraint systems, however, there appears to be limitations to these methods. Initially, Section 3 *'Design Capacity of Basic Structural Members'* [1] was considered for restraint system effects on member design, which considers a slenderness factor *'S_1'*, and stability factor *'k_{12}'* to reduce the member design bending capacity. Although these design provisions have methods for both discrete and continuous restraint to both the compression and tension flange, there appeared to be no consideration to the position of the restraint across the member depth and the restraint system stiffness.

To consider the above, Appendix E6 *'Slenderness Coefficients for Beams'* [1] was reviewed to provide more detailed design provisions. Appendix E6.4 *'Continuously Restrained Beams'* [1] presented design provisions which gave the closest approximation of the actual restraint conditions of the bridge girders by calculating critical buckling moments and slenderness factors for tension flange restraint at some point below the neutral axis. Although this appeared suitable, the method has an underlying assumption that the member is effectively continuously restrained against lateral displacement but does not define or provide means for checking this assumption. This raised the question of whether a slender long span steel rod cross bracing system sufficiently fulfils this assumption.

4.2 End Restraints

An important underlying assumption for any of the design provisions is the end restraint. In all design provisions, it is assumed that the ends of the member at its supports are effectively restrained against twisting. To achieve this in practice, the design provisions within Appendix E6.2 *'End-supported Beams'* [1] were used, where the steel restraint frames at each end of the girders were designed to provide a torsional rigidity exceeding that determined by Equation (8), where '*G'* is the shear modulus, *'J'* is the polar moment of inertia of the girder, and *'L'* is its span between end restraints, which governed the design of these frames.

$$k > \frac{20(GJ)}{L} \tag{8}$$

4.3 Restraint System Stiffness and Force Demands

Appendix E7 *'Buckling Restraints'* [1] was reviewed for design provisions for the restraint system stiffness. The design provision states *"for most design situations, the effectiveness of buckling restraints need not be checked. Where a check is needed, it is appropriate to assess the capacity of the restraint system using the following equations"* and notes Equations (9) and (10) below, which only appear to be the basic relationship of force, displacement and stiffness.

$$N^*_R > K_A \Delta_A \tag{9}$$

$$T^*_R > K_B \theta_B \tag{10}$$

Again, this design provision doesn't define or provide the means for checking the required restraint stiffness *'K'* or limiting displacement *'Δ'*, and only provides further design provisions for forces on lateral restraints in Appendix E7.4.2 *'Force on Lateral Restraints'* [1]. Although these equations are useful to check the additional forces in the restraint system for strength, verification of the restraint system stiffness was still deemed necessary, which led to the use of FEA modelling and is discussed in the following section.

5 GLOBAL FLEXURAL LATERAL TORSIONAL BUCKLING

5.1 Finite Element Analysis Model

To verify the restraint system assumptions made using the analytical design provisions, and to capture the global restraint system effects on FLT buckling, a 3D FEA ETABS model was developed to perform a non-linear static buckling analysis. To determine the critical buckling moment, the model included an initial geometric non-linearity of out-of-straightness to the girders and was analysed with large P-Delta effects. For stability analysis within [2] a maximum initial out-of-straightness of L/500 is assumed for glulam members, which was adopted for the FEA modelling.

Three models were developed as shown in Figure 5. The purpose of the single girder model was to verify the results of the first two cases against known analytical solutions, providing a point of reference for comparison of the full bridge model.

(a) single girder with torsional restraints at ends (Appendix E6.3 [1])

(b) single girder with torsional restraints at ends, and continuous lateral restraint to the tension flange (Appendix E6.4 [1])

(c) full bridge model including end restraint frames, tension flange cross brace and strut restraint system, and both girders

Figure 5. Visual representation of 3D ETABS models developed to verify analytical solutions

5.2 Modelling Parameters

The bridge girders were modelled as shell elements with the effective width of 305mm assumed from the adopted design approach for mechanical lamination. ETABS modification factors were then used to modify the section properties to account for the actual gross section stress areas, the orthotropic properties of timber parallel and perpendicular to the grain, and the reduced out-of-plane and weak axis moment of inertias calculated in accordance with the *'Gamma Method'* [2] for jointed beam sections. These modification factors are shown in Table 2, with further notes on how they were derived.

Table 2. ETABS modification factors for mechanical lamination

Modification Factor		Calculation	Factor	Notes
membrane stress	f11 & f12	450mm/305mm	1.475	scaling up to actual gross area
membrane stress	f22	$\frac{450mm}{305mm}.\frac{280MPa}{7000MPa}$	0.06	scaling up to actual gross area, then scaling down to perp-to-grain modulus of elasticity
bending	m11	$\frac{(450mm)^3}{(305mm)^3}.0.25$	0.8	scaling up to actual para-to-grain gross bending stiffness, then scaling down for effective mechanical lamination stiffness based on Gamma Method para-to-grain

bending	m22	$\frac{(450mm)^3}{(305mm)^3}.0.01$	0.032	scaling up to actual perp-to-grain gross bending stiffness, then scaling down for effective mechanical lamination stiffness based on Gamma Method perp-to-grain
torsion	m12	-	1.0	effective width for FLT buckling modelled
shear	v13 & v23	450mm/305mm	1.475	scaling up to actual gross area

5.3 Critical Buckling Moment

A displacement-controlled non-linear static analysis was run to determine the critical buckling moments for the three cases. Table 3 summarises the analytical and numerical critical buckling moments. The analytical solution was found to be non-conservative when compared with the numerical solution, with critical buckling moments varying by 2-10%. The full bridge model indicated a critical buckling moment that was significantly greater than a girder with no lateral restraints, but notably 6-8% less than the girder with continuous lateral restraint along the tension edge when compared with both the analytical and numerical solutions.

Table 3: Primary Glulam Girder Critical Buckling Moment Comparison

Boundary Conditions	Design Method	Analytical Critical Buckling Moment (kNm)	Numerical Critical Buckling Moment (kNm)
Torsional restraints at ends only	Appendix E6.3 [1]	1765	1600
Torsional restraints at ends and lateral restraint to the tension edge	Appendix E6.4 [1]	5820	5750
Full bridge model	FEA	-	5416

5.4 Design outcomes

Due to the full FEA bridge model indicating that global restraint system stiffness does influence the critical buckling moments when compared to analytical solutions, the critical buckling moments from the FEA model were adopted for design and used to calculate slenderness factor *'S_1'* in accordance with Appendix E6 [1] and *'k_{12}'* in accordance with Section 3 [1]. For additional robustness and to account for discrepancies between the analytical and numerical solutions, the fastener spacing parallel-to-grain was halved, with the number of fixings doubled, making the effective design width 315mm for the detailed design solution.

6 OTHER CONSIDERATIONS

An important design consideration to note is how moisture content effects the member capacity. The girders were designed as GL10 Seasoned (manufactured with a moisture content percentage MC% of 10-15%), with the in-service ULS MC% assumed to be 25%. The factor *'k_4'* (moisture condition factor) was applied to the characteristic stresses in accordance with Section 2 of [1]. Although the use of *'k_4'* for the modulus of elasticity and rigidity is not explicitly intended for this application within [1], it is known that these moduli decrease with increasing moisture content, which is an important consideration when calculating critical buckling moments from first principles as it effects both lateral and torsional rigidity, which has a direct impact on the critical buckling moment.

7 CONCLUSIONS

A 30m span glulam girder pedestrian bridge was designed in Christchurch, New Zealand. Each girder consisted of two mechanically laminated vertical billets for cost efficiency and fabrication feasibility. Fundamental design considerations included evaluating the composite lateral and torsional stiffness of the laminated girders and the restraint system's effect on flexural lateral torsional buckling.

Design methods for the mechanical lamination of vertically laminated timber members are limited. From the design review of research papers, mechanical lamination significantly effects the member critical buckling moments. With the adopted design approach, an effective composite design width two-thirds that of the gross width was calculated, resulting in critical buckling moments 68% less than the gross solid section. We therefore recommend:

- Further research and experimental testing are undertaken to further validate the findings and inform future design provisions.
- Introducing a guidance document with provisional reduction factors for designers, and ultimately design provisions within standards such as NZS-AS 1720.1 for the reduction in member capacity of mechanically laminated timber beams.

Furthermore, geometric non-linear static FEA analysis revealed critical buckling moments approximately 8% lower than those predicted by analytical methods, indicating that restraint system stiffness does influence the member capacity. We therefore recommend:

- Further research and testing into the sensitivity and effect of restraint system stiffness on flexural lateral torsional buckling of timber members.
- Introducing design provisions within standards such as NZS-AS 1720.1 for the required restraint system stiffness to justify the use of analytical design provisions, similar to standards such as NZS 3404 [5] for steel structures.

ACKNOWLEDGEMENTS

The authors would like to acknowledge the contributions of all involved with the project, and in particular: David Little and Samantha Morris (Christchurch City Council) for their leadership and vision, Adjunct Professor Alessandro Palermo (University of Canterbury) for his early enthusiasm and drive for a timber bridge concept, Nik Kneale, Scott McKerrow and Joshua Joe (Isthmus) for their creativity and craft leading the design process, Daniel Moroder (PTL) for his expertise and support as engineering peer reviewer, Scott Forster (Tonkin & Taylor) for his critical role in the foundation design, and both Techlam and Red Stag Timberlab for their early contractor involvement, providing valuable input into material selection and constructability considerations.

REFERENCES

1. Standards NZ, 2019. *"NZS-AS 1720.1: Timber Structures. Part 1: Design Methods".* Wellington, New Zealand
2. European Committee for Standardization, 2004. *"Eurocode 5: Design of timber structures - Part 1-1: General rules and rules for buildings"* (EN 1995-1-1). Brussels, Belgium: European Committee for Standardization.
3. Noel Challamel, Ulf Arne Girhammar, 2012 *"Lateral-torsional Buckling of Vertically Layered Composite Beams with Interlayer Slip under Uniform Moment".* Engineering Structures, Volume 34, 2012.
4. Robabeh Robatmili, 2022, *"Lateral Torsional Buckling of Timber Built-up Beams"*. University of Ottawa
5. Standards NZ, 1997. *"NZS 3404:Part 1:1997 Steel Structures Standard"* Wellington, New Zealand

ICTB 2025. 5th International Conference Timber Bridges
Rotorua, New Zealand, 29 June to 2 July 2025.

INVESTIGATION OF CROSS-LAMINATED (CLT) DECKS FOR BRIDGE APPLICATIONS IN THE USA

Justin M. Dahlberg[1], Zhengyu Liu[2], James P. Wacker [3], Douglas R. Rammer[4]

ABSTRACT

Cross-Laminated Timber (CLT) panels have been primarily developed for the building industry. But there have been few instances where CLT panels have been used for bridge deck applications in North America. CLT is prefabricated, lightweight, dimensionally stable, and environmentally sustainable. The use of CLT in bridge structures has been limited and the adoption of CLT into governing bridge design codes has been slow-going in North America. The objective of this project was to investigate the feasibility of CLT as a primary structural material for highway bridge deck applications. To achieve the objective, two CLT interconnected deck panel configurations were investigated in the laboratory for their structural performance characteristics under simulated wheel loads. Configurations consisted of longitudinal deck panels that span the abutments and transverse deck panels supported by simply-supported longitudinal girders.

1 INTRODUCTION

Cross-laminated timber (CLT) has gained significant popularity over the past decade, driven by advances in research and construction projects, particularly in Europe. It has been widely adopted in vertical construction, where some of its key features—prefabrication, lightweight properties, dimensional stability, and environmental sustainability—make it a viable alternative to traditional materials like concrete and steel. Despite these successes, CLT's application in bridge structures remains limited, with few notable examples in North America, such as the Mistissini Bridge (2014) and Maicasagi Bridge (2011) in Quebec. Furthermore, its integration into governing bridge design codes has been entirely absent, limiting its widespread adoption.

In the United States, CLT is not yet recognized in the AASHTO *LRFD Bridge Design Specifications* (2020), hindering its broader implementation in bridge projects. By contrast, glue-laminated timber has been accepted for decades. While CLT shares many similarities with glulam, it has benefits of two way action and dimensional stability and additional research or proof-of-concept projects are needed to establish CLT's viability for bridge applications.

This paper summarizes the efforts to characterize the structural performance of CLT bridge decks under typical traffic loads. The material shows promise as a complementary or alternative construction material for bridge decks, offering benefits such as dimensional stability and the potential to incorporate underutilized timber species. With continued research and data supporting its durability and performance, CLT could become a viable option for inclusion in AASHTO bridge design codes, paving the way for its use in modern infrastructure.

To complete the study, a comprehensive literature review and manufacturer inquiries were conducted to evaluate current practices and manufacturing capabilities related to CLT in bridge construction. Laboratory tests assessed the strength and serviceability of CLT panels under typical highway loads in two

[1] Justin M. Dahlberg, Director, Bridge Engineering Center, Iowa State University, Co-Director, National Center for Wood Transportation Structures, Ames, USA, dahlberg@iastate.edu
[2] Zhengyu Liu, Adjunct Assistant Professor, Civil, Construction, and Environmental Engineering, Iowa State University, Ames, USA, zhengyu@iastate.edu
[3] James P.Wacker Research Engineer, USDA Forest Products Laboratory, Co-Director, National Center for Wood Transportation Structures, Madison, USA, james.p.wacker@usda.gov
[4] Douglas R. Rammer, Research Engineer, USDA Forest Products Laboratory, Madison, WI USA, douglas.r.rammer@usda.gov

configurations: spanning longitudinally as a complete superstructure and spanning transversely across longitudinal girders, functioning as the deck.

2 BACKGROUND

2.1 CLT Construction and Materials

CLT panels are composed of adjacent lumber boards in a flatwise orientation. Each layer is arranged crosswise, typically at 90-degree angles, and bonded together on their wide faces, with occasional bonding on the narrow faces. Modern CLT originated from industry-academia collaborations in Austria during the mid-1990s. Its use expanded significantly in Europe in the early 2000s, driven by the green building movement, improved efficiencies, product approvals, and enhanced marketing and distribution channels.

While CLT is well established in Europe but not yet fully adopted by the Eurocode, its implementation in the United States and Canada began more recently, in the 2010s. The U.S. edition of the *CLT Handbook* (2013) was published to support the U.S. design and construction industry, covering only glued CLT products and systems, and CLT was recognized in the NDS (2015) in 2015.

A typical CLT panel consists of at least three glued layers of boards placed flatwise and oriented orthogonally. Lumber thickness ranges from 16 mm to 51 mm, and widths range from 60 mm to 240 mm. Individual boards are finger-jointed with structural adhesives and kiln-dried. Panel sizes vary by manufacturer, with typical widths of 0.6 m, 1.2 m, 2.4 m, and 3.0 m, lengths up to 18 m, and thicknesses up to 500 mm.

CLT offers high in-plane and out-of-plane strength and stiffness, providing two-way action similar to the behavior of reinforced concrete slabs, except that flexural continuity across panel joints is difficult to establish. The cross-lamination increases splitting resistance in connection systems. For floor and roof systems, outer layers align parallel to the main span direction to optimize load capacity.

In North America, CLT design values adhere to the ANSI/APA PRG 320 standard (2018) and are certified through rigorous testing. While Annex A of PRG-320 outlines representative layups for validation, manufacturers can develop and certify custom configurations. For this project, the selected layup was not among those specified in PRG-320 and required independent certification to ensure it met the strength and stiffness requirements for bridge live-load conditions.

2.2 CLT Panel-to-Panel Connection Designs

Panel-to-panel connection designs for CLT have been successfully implemented in vertical construction, with potential adaptability for bridge applications. Common connection types, as outlined in the *CLT Handbook* (Gagnon, 2013), include:

1. **Single/Double Wooden Splines:** Internal splines joined with self-tapping screws and structural adhesive. Double splines provide greater resistance to out-of-plane loads but require precise profiling.
2. **Single/Double Surface Splines:** External splines attached with screws and optional adhesive, offering easier assembly but lower performance compared to internal splines.
3. **Half-Lapped Joint:** Overlapping panels secured with long screws. Quick to assemble and capable of handling normal and transverse loads but prone to splitting under uneven loading.
4. **Tube Connection:** Steel tubes with glued-in or screwed rods connect panels. This system requires minimal edge profiling and relies on pullout resistance for strength.

Panel-to-girder connections for bridge decks are less documented. Adaptable options include self-tapping screws and metal brackets. Screw connections are cost-effective but weaker when installed in the narrow side or end grain of panels. Angled installation improves strength. Metal brackets, such as “L” or “T” shapes, provide strong, efficient connections with simplified construction access.

A couple of case studies highlight the potential of CLT’s for bridge decks with different connection details. The Hundorp Bridge in Norway used timber screws, steel brackets, and lag bolts for adjacent panel and girder connections, ensuring simplicity and reliability (Abrahamsen and Nylokken, 2017). Similarly, the

Mistissini Bridge in Quebec featured a CLT walkway with integrated guardrail connections (Lefebvre and Richard, 2014).

2.3 Research on Adhesives and Treatments

Recent studies have focused on improving CLT performance for exterior applications. For example, Han et al. (2017) demonstrated that treating CLT panels with superheated steam reduced delamination failures by 50%. Tripathi and Lim (2018) and Lim et al. (2020) evaluated adhesive systems for treated CLT, finding that polyurethane adhesives performed better than others like melamine and resorcinol formaldehyde for bonding treated Southern Yellow Pine. Such findings highlight the need for appropriate pairing of lumber pre-treatment with adhesive selection to improve durability in wet environments.

2.4 Standards and Challenges for Exterior Use

CLT standards like PRG 320 primarily address indoor applications, limiting exterior use due to moisture and durability concerns. Adhesives used in CLT panels must meet standards such as ASTM D2559 for exterior exposure. While some adhesives already meet these criteria, further development of testing methods is needed to address the unique grain orientation in CLT and ensure durability under outdoor conditions.

2.5 Innovations in Lamination Type and Orientation

Adjusting lamination orientation has been shown to enhance performance. Buck et al. (2016) found that orienting transverse layers at 45° instead of 90° increased bending strength by 35% and reduced mid-span deflection, while Masoudnia et al. (2016) observed similar improvements in structural reinforcement. Composite laminated panels (CLP), using structural composite lumber for transverse layers, have also shown increased shear strength and stiffness compared to traditional CLT (Zhou et al., 2018).

2.6 Size Limits of CLT Panels in the United States

The project team surveyed CLT manufacturers and pressure treatment facilities across North America to determine the size limitations of CLT panels suitable for pressure treatment.

The ability to pressure-treat full panels after fabrication is constrained by current manufacturing capabilities. Feedback from several CLT manufacturers indicated that typical pressure treatment chambers in the United States limit panel widths to approximately 2.1 meters. This makes the process less economical than treating wider panels, such as those up to 3 meters. Protecting CLT panels for exterior use is critical to ensuring long-term structural integrity as with other timber bridge types.

Pressure-treating individual timber members before assembling them into CLT panels is cost-prohibitive. Treating before bonding requires plant quality control testing to ensure glue bonds meet quality standards, as the bonding process becomes more complex with treated boards. Typically, the lumber must be re-dried after treatment to achieve the necessary adhesive performance, further adding to the costs and complexity of the process.

2.7 Challenges and Future Research

CLT's adoption in bridge construction faces several challenges, such as moisture resistance, adhesive testing, seismic resistance, and standardization. Effective pressure treatments and waterproof adhesives are critical for durability and affect timber's mechanical properties. New methods are required to evaluate adhesive performance in alternating grain orientations under exterior conditions. Enhancing CLT panel connections and diaphragm performance is vital for seismically active regions. Expanding standards like PRG 320 to include exterior durability tests is necessary for broader acceptance in bridge applications.

3 LABORATORY INVESTIGATIONS

At the Iowa State University Structures Laboratory, the project team conducted load tests on CLT panels in two configurations – spanning longitudinally (left photo) and transversely (right photo), in Figure 1.

The longitudinal deck panel system consisted of two single-span panels with a 9-lam layup measuring 314 mm deep × 2.48 m wide (see Figure 2). These panels spanned 7.62 m longitudinally between two concrete blocks serving as abutments.

The transverse deck panel system consisted of three panels with a 5-lam layup measuring 175 mm deep × 2.48 m wide (see Figure 2). These panels spanned transversely across longitudinal, simply-supported W-shape steel girders at two interval spacings.

All layers of the panels were constructed from visually-graded, untreated Douglas fir (Pseudotsuga menziesii) lumber. Select-structural grade lumber was used in the primary span direction, while #2 grade lumber was used for the transverse layers. Notably, the select-structural grade lumber in layers oriented with the primary span direction exceeds the typical quality of basic CLT grades. This addresses the higher structural demands imposed by highway service loads compared to those on standard panels of similar thickness.

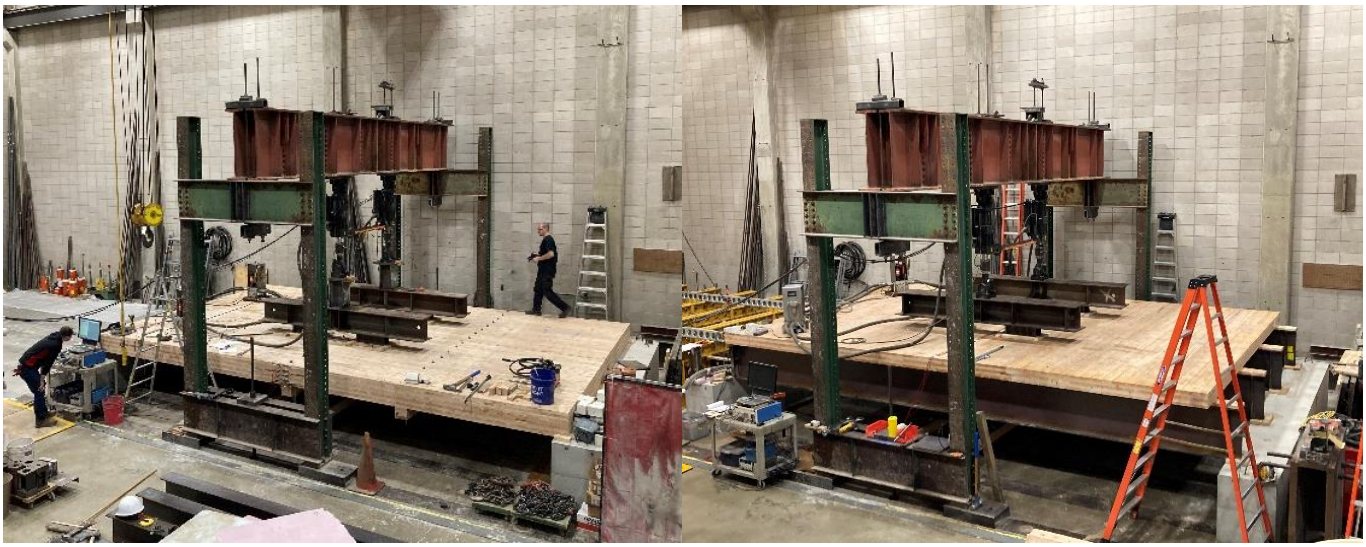

Figure 1. Load Tests of Longitudinal (left photo) and Transverse CLT Panels (right photo)

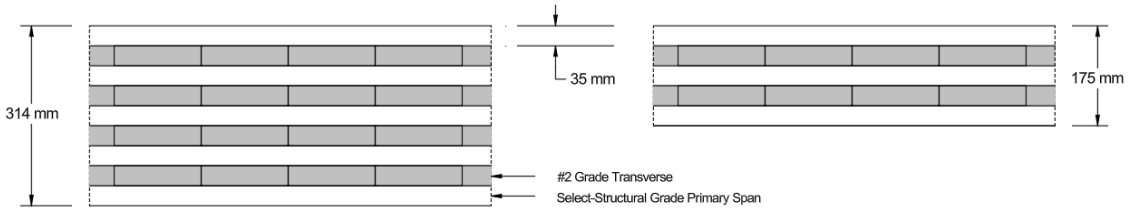

Figure 2. Layup of Longitudinal (left) and Transverse CLT Panels (right)

3.1 Laboratory Testing of Longitudinal Deck Panel System

The laboratory test setup featured two equal-width CLT panels placed side-by-side and spanning longitudinally, as illustrated in Figure 3 (left). The total deck width was 4.88 meters, constituting about half the width of an in-service bridge. To simulate bridge conditions, three built-up spreader beams (each made of four boards measuring 38 mm × 191 mm and connected with screws for a total cross-section of 152 mm × 191 mm) were attached to the underside of the deck. These beams were secured using 19 mm diameter threaded thru-rods spaced at 305 mm, consistent with AASHTO specifications.

These longitudinal panels were joined along their edges using a half-lap joint, a common connection detail employed with CLT in vertical construction panels and nail-laminated timber bridge deck panels. The overlap width was 76 mm, with screws securing the joint using an inclined configuration designed for higher stiffness and load capacity. Vertical screws (8 mm diameter × 302 mm length) and inclined screws (9.5 mm diameter × 400 mm length) were used to enhance joint performance.

Tests included both static and cyclic loading to simulate highway service loads. For the static tests, four load cases were applied to simulate the rear tandem axle of a dump truck, with loads positioned to maximize shear and bending reactions (see Figure 3). The cyclic tests were performed for only Load Case 2, applying a tandem axle load of 111.2 kN (55.6 kN per tire), consistent with HL-93 AASHTO design truck loading.

Instrumentation included strain and deflection gauges to monitor structural behavior. Vertical deflection gauges were placed transversely at the midspan and along the longitudinal joint to measure deflection and joint movement. Horizontal gauges along the joint captured relative motion or gapping. ST350 strain gauges (Bridge Diagnostics, Inc.) were installed at the top and bottom edges of the panels and at approximately 1.52 meters from the edges. Additional strain gauges were placed on individual laminations at one panel edge to assess the strain profile under loading. A horizontal displacement gauge was added to the lowest transverse lamination to monitor any gapping between members.

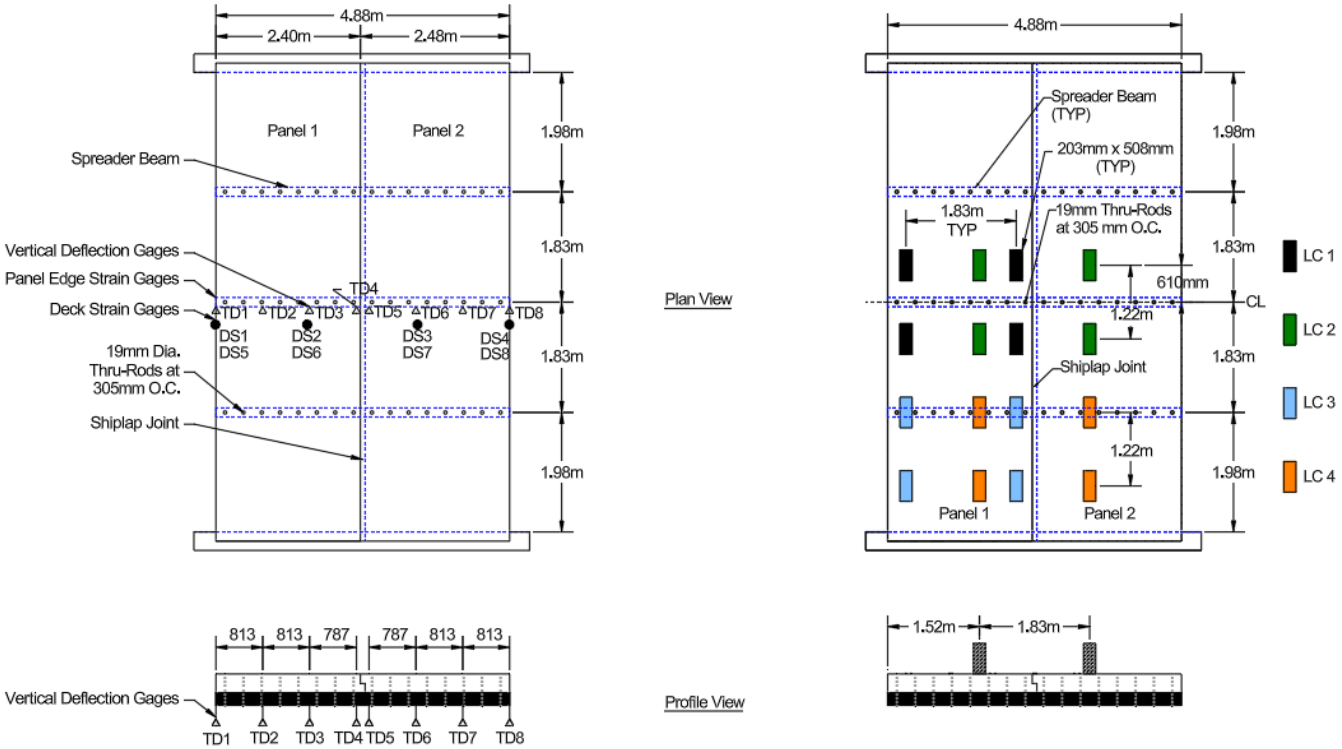

Figure 3. Longitudinal Panel Configuration, Instrumentation, and Load Case Position

3.2 Equivalent Strip Width

3.2.1 Equivalent Strip Width (ESW) Calculation for CLT Bridge Decks

The AASHTO LRFD Bridge Design Specifications (2020) prescribe an equivalent strip width (ESW) for longitudinal bridge deck strips to estimate the portion of the slab engaged in resisting live loads from vehicles. This method is commonly used for cast-in-place concrete slabs, stress-laminated wood decks, and glued/spiked wood panels with a spreader beam. While the AASHTO equations tend to be conservative, the actual ESW can be determined using strain and deflection measurements.

ESW is typically calculated by integrating the area under the moment distribution curve and dividing it by the maximum moment**.** Assuming uniform stiffness, deflection data can also be used for ESW determination (Equation 1):

$$ESW = \frac{\sum_{i=1}^{n}(deflection_i \times d_i)}{deflection_{max}} \qquad (1)$$

where, n is the total number of deflection sensors, $deflection_i$ is the deflection reading of the *i*-th sensor, $deflection_{max}$ is the maximum deflection measured by the sensors, and d_i is the spacing of adjacent deflection gauges. Using this approach, ESW values were calculated for longitudinal CLT deck panels under various load cases.

When the load was applied across both panels (Load Cases 2 & 4)**,** the ESW increased by approximately 70% compared to when the load was applied to a single panel (Load Cases 1 & 3)**.** This indicates greater engagement of the bridge width in load resistance. However, transverse load distribution was significantly reduced when the load was isolated to one panel. While the spreader beam rigidity (62 kN-m^2) was greater

than the rigidity required by AASHTO design specifications (23 kN-m^2), a stiffer spreader beam could potentially improve load-sharing behavior.

3.3 Laboratory Testing of Transverse Deck Panel System

A full-scale bridge section using steel girders and transverse CLT panels was constructed and load-tested The test setup included two girder configurations to assess the performance of the same CLT deck under different girder spacings – a four girder (see Figure 4) and three girder (see Figure 5) configuration. The clear span of the girders was 7.62 m, and the bridge deck width was 4.88 m, equivalent to half of a full bridge width. Girder spacings ranged from 1.40 m to 2.10 m. Design calculations using glulam girders spaced at 2.10 m were completed and resulted in using a 24F-V3, 838 mm deep x 172 mm wide Spruce Pine glulam girders with a rigidity of 10,442 kN-m^2. Steel girders with near-equivalent rigidity were used in lieu of glulam girders due to lead time and availability. The W610x82 steel girders had a rigidity (E_{stl} x I_{xx}) of 11,235 kN-m^2, about 7.5% greater than the glulam.

The setup included three equal-width panels with the major strength direction in the transverse direction were connected to the top flange of the girders with flatwise 38 mm × 191 mm boards secured by 13 mm dome-head thru-bolts spaced 305 mm apart. The panels were joined using half-lap joints, a common technique in vertical construction. The joints featured a 76 mm overlap, secured with ASSY VG CYL 8 mm × 159 mm vertical screws and ASSY VG CSK 9.5 mm × 219 mm inclined screws. Inclined screws were chosen to provide higher stiffness and load capacity at inter-panel connections.

Two static test series were conducted. The first used the four-girder configuration with 1.40 m spacing, and the second used the three-girder configuration with 2.10 m spacing. Each test involved four load cases simulating the rear tandem axle of a dump truck, with a maximum load of 111.2 kN per axle (55.6 kN per tire), consistent with the AASHTO HL-93 design tandem loading (see Figure 4 and Figure 5).

The three-girder configuration was subjected to 500,000 cycles at the same load level and position as Load Case 2 to simulate several years of truck traffic. A static test followed to compare pre-and post-cyclic performance.

Strain and deflection gauges were used to monitor performance. Instrumentation included deflection gauges installed beneath each girder at midspan to measure vertical deflection and on the bottom side of the CLT panels at panel joints to monitor spacing changes. Strain gauges were placed at the bottom flange of the steel girders at midspan and on the top and bottom of the CLT panels in the strong direction, evenly spaced between girders.

The load cases were designed to maximize shear and bending reactions within the panels and to analyze force distribution across the bridge deck. Load Case 2 was specifically selected for cyclic testing due to its potential to stress the longitudinal joints and influence lateral load distribution. The 0 m transverse position in the results figures corresponds to the deck edge nearest Load Cases 1 and 3.

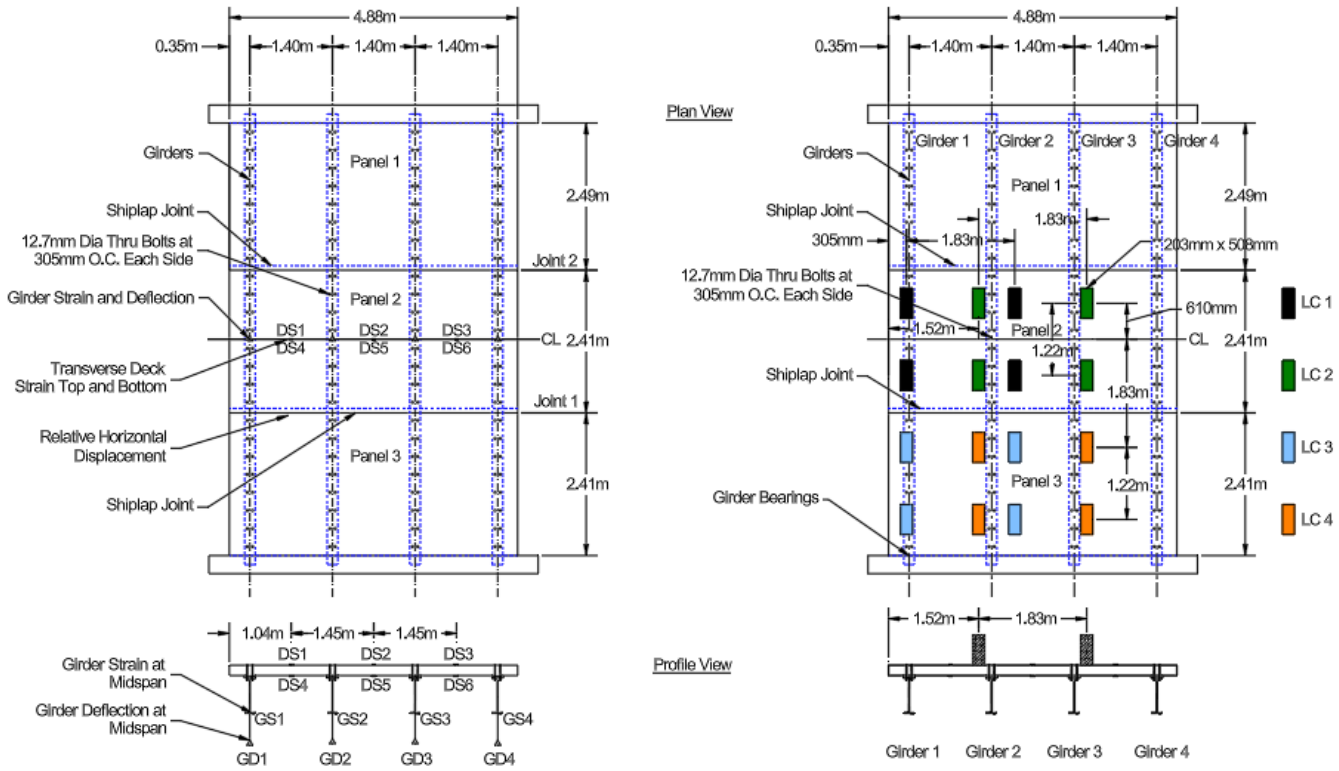

Figure 4. Four Girder Transverse Panel Configuration, Instrumentation, and Load Case Position

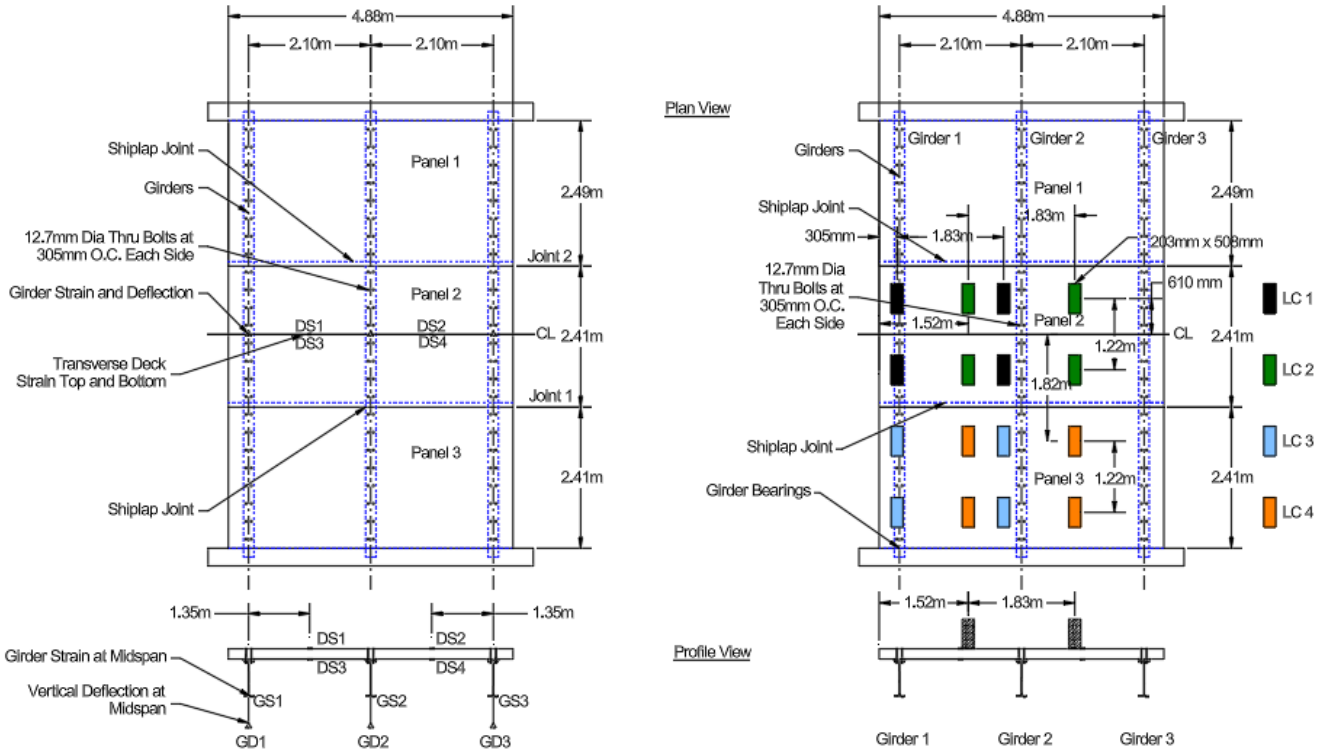

Figure 5. Three Girder Transverse Panel Configuration, Instrumentation, and Load Case Position

4 TEST RESULTS

For brevity, only the static and cyclic load test results for Load Case 2 of the longitudinal and transverse panel tests will be discussed in this paper.

4.1 Longitudinal Panel Deck System Test Results

The static load test results for Load Case 2 are summarized below. Load Case 2 was conducted twice – once before and after the cyclic loading test – to assess any changes in structural performance after 500,000 load cycles.

The midspan strain (DS1 – DS8) and deflection plots (TS1 – TS8) at maximum load are provided in Figure 6 (left) For Load Case 2, the load was symmetrically applied to both panels—the maximum deflection was 21.6 mm at the longitudinal joint, corresponding to an L/D of 351. Deflection decreased uniformly from the joint to the panel edges, with minor reductions overall.

Strain values were relatively symmetric, ranging from 279 microstrain (compression) to 260 microstrain (tension) at the panel edge. The strain profile was linear through the panel depth, with a peak strain of 401 microstrain in compression at the top of the first interior position. Using a modulus of elasticity of 11,700 MPa for select structural Douglas Fir, the corresponding maximum stress was 4.8 MPa. Similar to the deflection behavior, strain values decreased slightly at the panel edges.

Figure 6 (right) also compares the static test results from before and after the completion of the cyclic loading. The comparison of strain and deflection values indicates that there is no appreciable change in the structure behavior as a result of the cyclic testing.

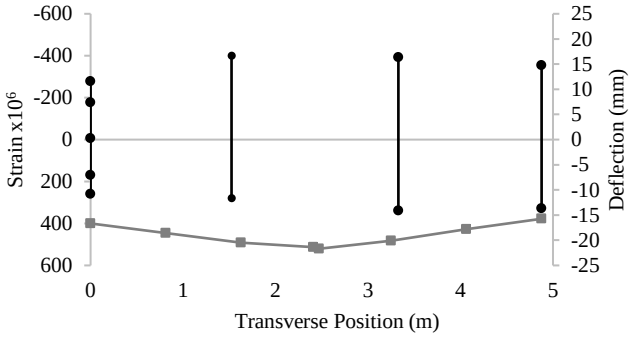

DS1-DS4 (Top, L-R) Compression, DS5-DS8 (Bottom, L-R) Tension

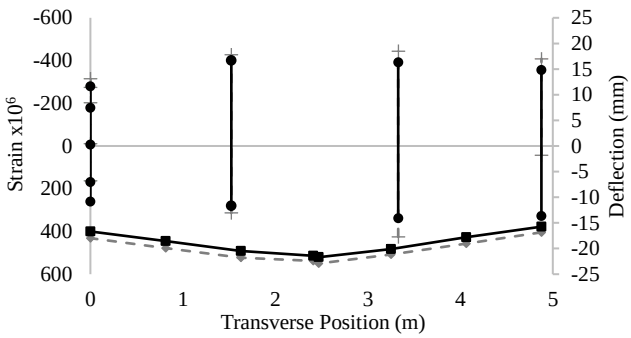

Pre-Cyclic = Black, Post-Cyclic = Grey

Figure 6. Load Case 2 Static Load Test Results Pre- (left) and Post-Cyclic Testing (right) for Longitudinal Panel Deck System

4.2 Transverse Panel Deck System Test Results – Four Girder Assembly

For Load Case 2, the midspan girder strain and deflection values at maximum load are shown in Figure 7. The highest deflection (5.3 mm) and bottom-flange tensile strain (265 microstrain) occurred near the transverse load location. These values correspond to a span-to-deflection ratio (L/D) of 1,371 and a live-load steel stress of 55.2 MPa, both within acceptable limits based on service deflection criteria and steel yield strength. CLT strain measurements (see Figure 7) across three transverse locations showed peak tensile and compression strains of 165 and 134 microstrain, respectively. Using a modulus of elasticity of 11,700 MPa for select structural Douglas Fir, these correspond to maximum stresses of 1.93 MPa (tension) and 1.59 MPa (compression).

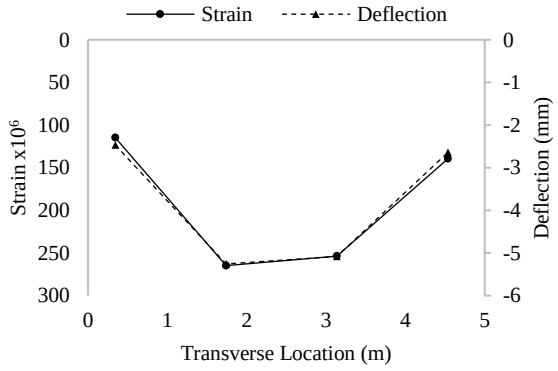

GS1-GS4 (L-R), GD1-GD4 (L-R)

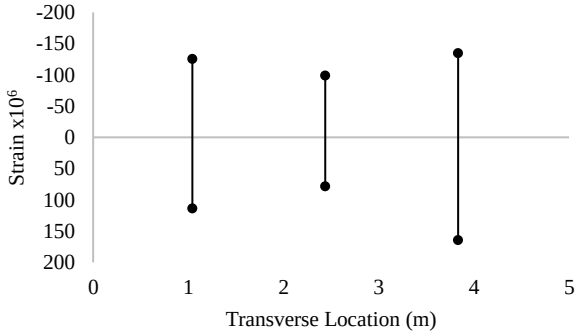

DS1-DS3 (Top, L-R) Compression, DS4-DS6 (Bottom, L-R) Tension

Figure 7. Girder Strain and Deflection (left) and Transverse CLT Panel Strain (right) - Four Girder Assembly

4.3 Transverse Panel Deck System Test Results – Three Girder Assembly

For Load Case 2**,** the midspan girder strain, deflection, and CLT strain values at maximum load are shown in Figure 8. The highest deflection (7.6 mm) and bottom-flange tensile strain (197 microstrain) occurred near the transverse load location. These values correspond to a span-to-deflection ratio (L/D) of 960 and a live-load steel stress of 41.4 MPa, both within acceptable service deflection limits and steel yield strength. Strain measurements across two transverse locations showed peak tensile and compression strains of 443 and 301 microstrain, respectively. Using a modulus of elasticity of 11,700 MPa for select structural Douglas Fir, the corresponding maximum stresses were 5.17 MPa (tension) and 3.52 MPa (compression).

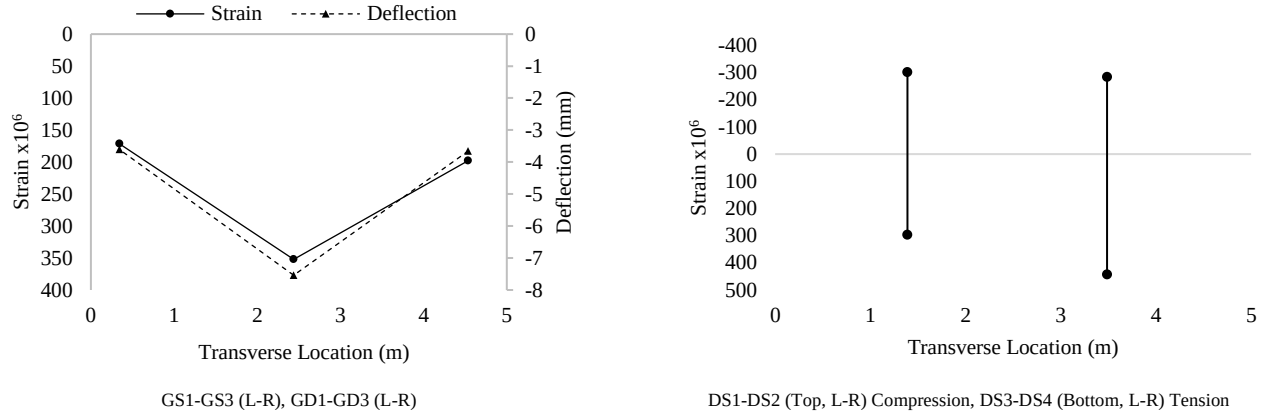

Figure 8. Girder Strain and Deflection and Transverse CLT Panel Strain – Three Girder Assembly

After the cyclic test, an additional static test was conducted for Load Case 2 to assess any structural changes due to repeated loading. A comparison of midspan strain and deflection values before and after 500,000 load cycles is provided in Figure 9. The results show that post-cyclic structural performance remained nearly identical to pre-cyclic values. No significant changes in strain or deflection were observed. This indicates that cyclic loading had no appreciable effect on the CLT panels' strength or stiffness, confirming their durability and stability under prolonged load conditions.

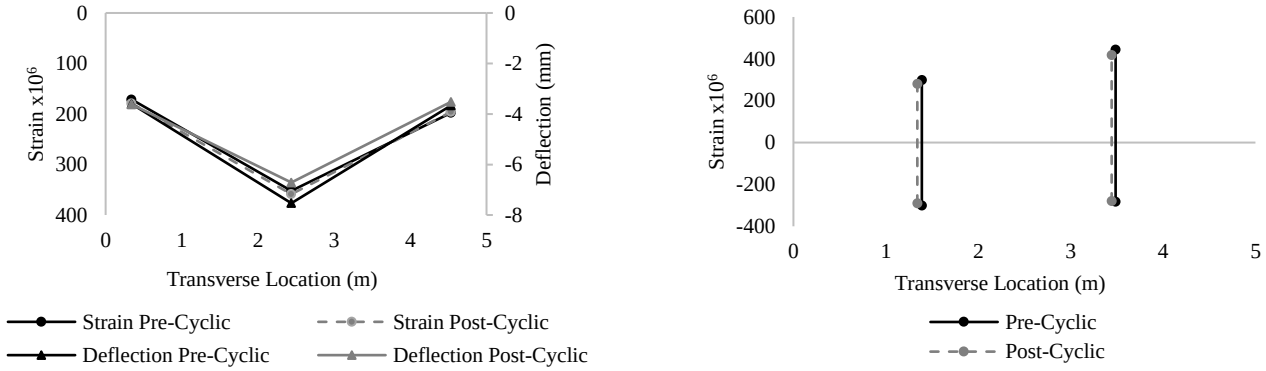

Figure 9. Load Case II Comparison of the Girder Strain, Deflection, and Transverse CLT Panel Results – Pre- and Post-Cyclic

5 CONCLUSIONS

CLT panels have been widely used in vertical construction but remain largely unexplored for bridge decks in North America. Challenges include limited pressure treatment capabilities and high costs associated with treating individual components before assembly. Further research is needed to develop cost-effective protection against environmental exposure.

CLT is prefabricated, lightweight, dimensionally stable, and environmentally sustainable. However, existing North American standards (PRG 320, CLT Handbook, NDS) currently restrict its use primarily to indoor applications. This study examined two CLT configurations under highway loads: longitudinal panels spanning between abutments and transverse panels supported by girders**.**

For longitudinal panels, static tests assessed equivalent strip width (ESW) and load distribution. When a single panel was loaded, ESW decreased by 40% compared to when both panels were loaded. Load distribution results aligned with previous slab-type timber bridge tests. Identifying methods to improve the transverse load distribution in CLT bridge decks would benefit future designs and ratings of these bridges. The panels performed consistently, though AASHTO LRFD guidelines for deflection limits (L/425) were exceeded in some cases. Increasing panel depth, improving transverse load distribution, or reducing span lengths could mitigate these serviceability concerns.

For transverse CLT decks, static and cyclic tests evaluated deflection, strain, and joint behavior across four-girder and three-girder configurations. The panels performed consistently within AASHTO LRFD deflection guidelines.

Cyclic tests subjected CLT panels to 500,000 load cycles simulating years of traffic. Post-cyclic static tests showed no significant change in strength or stiffness, confirming durability under sustained loads.

Code adoption challenges remain for bridge structures in North America. CLT lacks standardized exterior durability testing, and PRG 320 does not permit wet-use adhesives. Research on waterproof adhesives, pressure treatment, and performance under moisture exposure is essential for regulatory acceptance which will lead to broader CLT bridge construction in the future.

REFERENCES

The references should be in a numbered list in the order the references first appear in the paper. Reference numbers in the paper should be in square brackets, e.g. [1].

1. AASHTO 2020. AASHTO Load and Resistance Factor Design (LRFD) Bridge Design Specifications. Ninth Edition, LRFD BDS-9 American Association of State Highway and Transportation Officials, Washington, DC.
2. Abrahamsen, Rune B., and Nylokken, Trond E., (2017), the deck rehabilitation using cross-laminated timber on Hundorp bridge. Downloaded at https://docplayer.net/22615250-Hundorp-bridge-bridge-deck-rehabilitation-using-cross-laminated-timber-authors-structural-engineers-rune-b-abrahamsen-and-trond-e-nylokken.html (2022)
3. APA - The Engineered Wood Association. Standard for Performance-Rated Cross-Laminated Timber, ANSI/APA PRG 320. Tacoma, Washington, U.S.A. 2018.
4. Buck, D., Wang, X. A., Hagman, O., & Gustafsson, A. (2016). Bending properties of cross laminated timber (CLT) with a 45 alternating layer configuration. BioResources, 11(2), 4633-4644.
5. Gagnon, Sylvain, et al. "CLT Introduction to cross-laminated timber." In: CLT handbook: cross-laminated timber/edited by Erol Karacabeyli, Brad Douglas. U.S. ed. 2013; pp. 1-45. (2013): 1-57.
6. Han, Y., Park, Y., Chang, Y. S., Chung, H., Eom, C. D., & Yeo, H. (2017). Improvement of shear strength, wood failure percentage and wet delamination of cross-laminated timber (CLT) panels made with superheated steam treated (SHST) layers of larch wood. Holzforschung, 71(11), 873-879.
7. Lefebvre, D., & Richard, G. (2014, December). Design and construction of a 160-metre-long wood bridge in Mistissini, Quebec. In Proceeding of Internationales Holzbau-Forum (pp. 3-5).
8. Lim, H., Tripathi, S., and Tang, J., (2020). Bonding performance of adhesive systems for cross-laminated timber treated with micronized copper azole type C (MCA-C). Construction and Building Materials 232 (2020)
9. Masoudnia, Reza; Pouyan Zarnani, Ashkan Hashemi, Pierre Queneville (2016) Introducing New Board Lamination to Cross Laminated Timber, The University of Auckland.
10. Tripathi, Sachin and Hyungsu Lim (2018, August). Evaluation of Adhesive Systems for Treated Cross-Laminated Timber (CLT). In Proceedings of the 15th World Conference on Timber Engineering.
11. Zhou, J., Niederwestberg, J., Chui, Y. H., & Gong, M. (2018, August). Bending properties of innovative multi-layer composite laminated panels. In Proceedings of the 15th World Conference on Timber Engineering (pp. 20-23).

ICTB 2025. 5th International Conference Timber Bridges
Rotorua, New Zealand, 29 June to 2 July 2025.

MODULAR TIMBER ARCH BRIDGE FOR NEW ZEALAND

Oliver de Lautour[1], Moustafa Al-Ani[2]

ABSTRACT

A concept design for a modular tied timber arch bridge to cross typical State Highway expressways in New Zealand has been developed. The use of timber allows alternative building materials, a reduced carbon footprint and new structural forms for bridge construction.

The modular concept has been developed on a typical span requirement of 35m. This allows sufficient width for a typical expressway cross section and allows direct comparison with other typical bridging solutions. This paper outlines key structural considerations for the arch design and compares the embodied carbon of the design with a conforming precast concrete design.

1 INTRODUCTION

Modern timber bridges are rarely constructed in New Zealand (NZ), however, timber bridge construction offers opportunities as a renewable resource, potential boarder economic benefits in growing a high-value timber products, reduced carbon footprint and urban design outcomes. This paper develops a concept for a modular tied timber arch bridge spanning 35m that is suitable for typical local road crossing on major State Highway expressway projects. Modular construction offers advantages in quality, cost and construction programme. The tied timber arch span provides a module for use with other standard components, e.g. abutments, wingwalls etc to provide a modular design solution.

This paper represents the concept design development for the timber arch, outlines key structural considerations and includes a comparative carbon assessment.

2 DESIGN CRITERIA

2.1 Design standards

The NZ Transport Agency Bridge Manual, Edition 3 Amendment 4 (Bridge Manual) [1] has limited technical guidance of the design of modern glue laminated bridges. Interim advice issued by the NZ Transport Agency in TAN #22-02 stated the use of NZ, Australian or European standards dependent on the complexity of the design. Given the complexity and structural elements involved this concept design adopting the following material design standards in order of preceedance;

- General elements and arch – Eurocode 5, including parts BS EN 1995-1-1, BS EN 1995-1-2 and BS EN 1995-2 for design.
- Stress laminated timber deck – AS5100.9
- General elements – NZS AS 1720.1

[1] Title, Aurecon NZ,
e-mail: oliver.delautour@aurecongroup.com,
[2] Title, New Zealand Transport Agency
e-mail: moustafa.al-ani@nzta.govt.nz

2.2 Design life

NZ standards do not currently provide a technical pathway to demonstrate a 100-year design life for timber bridges. Studies of existing timber bridges in NZ indicate that with the correct materials, detailing and maintenance a 100-year life is viable.

2.3 Design loading

Design loading for the bridge adopts the HN-HO-72 traffic model within the Bridge Manual.

The requirements for hanger replacement and loss as outlined in Clause 4.9 of the Bridge Manual for network and tied arch bridges where not considered in the concept as discussed below.

3 CONCEPT DEVELOPMENT

The proposed concept arrangement consists of a glue laminated timber tied arch module supported by pad foundations on a Mechanically Stabilised Earth (MSE) abutment wall, refer Figure 1. The concept adopts a local road overpass arrangement as this typically provides the optimal design solution with minimum bridge deck area. An arch span of 35.0m has been selected for the concept as this provides sufficient length for a dual lane expressway, horizontal clearance to the MSE wall and remaining width for a Shared Use Path (SUP) and/or drainage, refer Figure 1. The bridge cross section provides a typical local road cross section with two 3.5m traffic lanes, two 1.0m shoulders and a single 3.0m SUP, refer Figure 2.

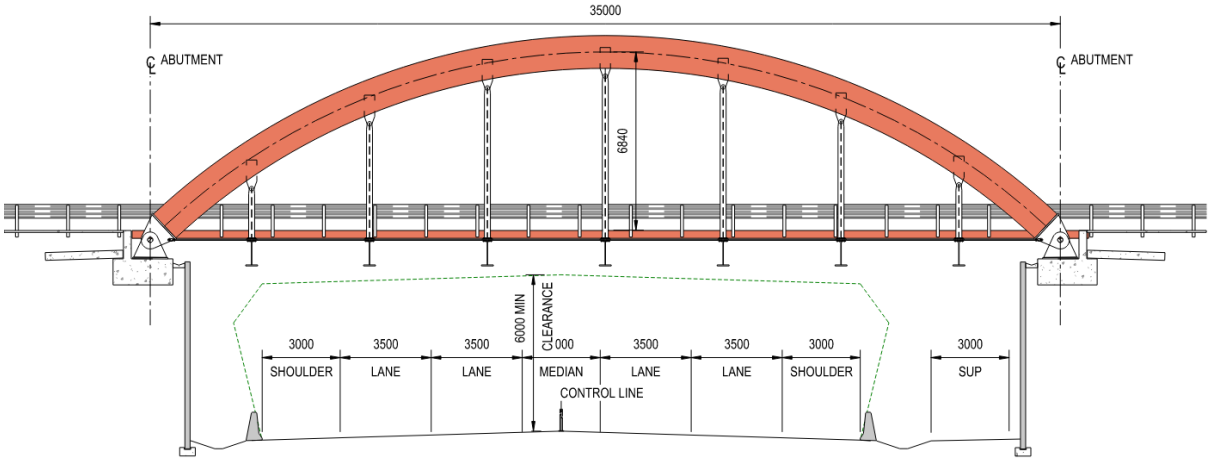

Figure 1 Concept general arrangement long section.

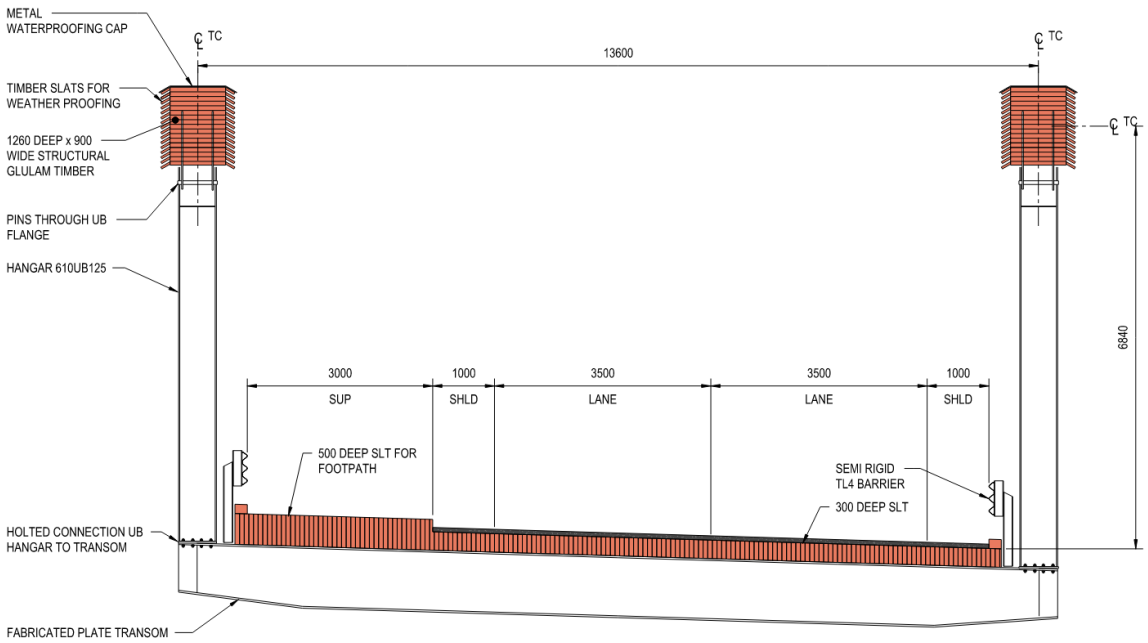

Figure 2 Concept general arrangement cross section.

The arch is proposed to be un-braced to permit a 6.0m vertical clearance envelope with a span to rise ratio of approximately 6. To provide stability to the arch, frame action is provided transversely by the hangers and transoms. The six hangers are spaced at approximately 5.0m centres. For constructability, a three pinned arch is used to permit fabrication and transportation. The tied arch form is used to avoid thrust forces acting on the foundations and permit the use of the pad foundation and MSE wall, proving a robust and economical sub-structure. The tied arch solution has been used internationally previously and could be removed should site ground conditions permit a traditional arch. The deck is a Stress Laminated Timber (SLT) deck that spans longitudinally between the hanger/transoms. Edge protection on timber is proposed to be a propriety TL-4 thrie beam section.

3.1 Timber arch

The arch was sized to be 1260mm deep by 900mm wide using commonly available Grade GL10 timber. The arch was unbraced and buckling analysis obtained an out-of-plane buckling mode factor of approximately 7. **Error! Reference source not found.**Figure 3 shows the first mode buckled shape. This provided compression capacity in the arch of approximately 8.9MN compared to a demand of 4.0MN.

Arch bending capacity was found to be governed by tension perpendicular to grain due to the curve profile. The arch has a low curvature ratio of 0.04. Eurocode provides values for curvatures for values d/R below 0.1 unlikely NZS AS 1720.1. A flexural capacity of approximately 1.7MNm was obtained compared to a demand of 1.4MNm.

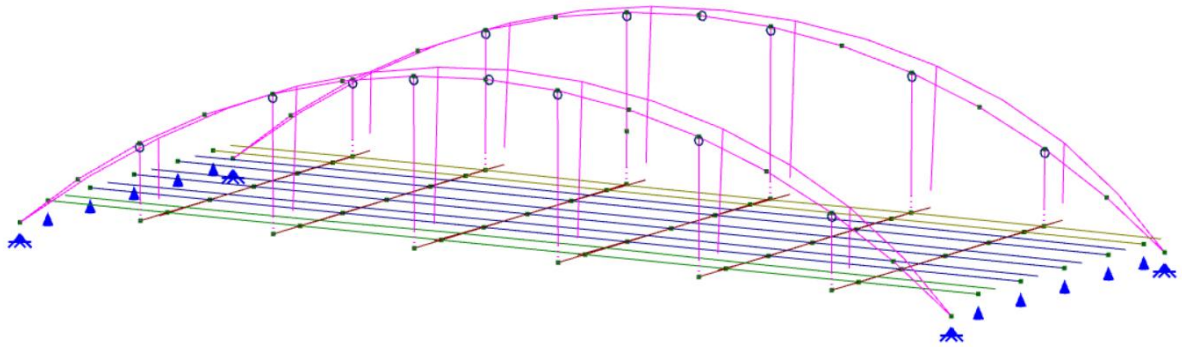

Figure 3 Arch buckling shape.

Perfect hinges in the arch ware provided using stainless steel pins connected via steel plates embedded into the timber arch.

3.2 Hangers and transoms

The arch supports six rigid U-frame hangers. The hangers where sized to be 610UB125 sections to provide sufficient stiffness to restrain the arch and provide a degree of resistance to impact loading. The hangers are pinned longitudinally to the arch and bolted to the transoms with a moment connection.

As noted above, arch hanger loss and replacement cases as outlined in the Bridge Manual have not been applied to the concept design as these are not considered appropriate for the proposed structural arrangement. The concept uses rigid hangers that do not require replacement within the design life of the bridge and are more robust to impact loading and damage than high tensile elements. Relaxing of the hanger loss and replacement cases is further justified with the typically lower volume and speed environment of a local road.

For concept development, the hangers where design for TL-4 collision loading from Table B3 of the Bridge Manual acting on a single hanger. The hangers are also protected with a semi-rigid TL-4 thrie beam as discussed below.

3.3 Stress laminated deck

The SLT deck spans longitudinally approximately 5.0m between the transoms. The deck was sized to be 300mm deep and constructed from commonly available sawn timber grade SG8. Transverse stressing was sized to be 26mm diameter stress bar at 1.2m centres with an initial jacking force of approximately 400kN. The anchorage detail as proposed in AS5100.9 Figure 5.3.1.

3.4 Traffic barrier

Timber decks have limited ability to resist the high torsional forces generated by traffic barrier loading. Typical, rigid TL-5 concrete road barriers are not practical for timber decks. Internationally, various semi-rigid post and rail systems constructed from timber and/or steel have been developed via testing. For this concept, a TL-4 thrie beam system developed in the United States has been adopted, refer Figure 4. The detail uses a tie to distribute tension loading into the deck. The barrier section would require modification to include a top rail to achieve a total 1100mm height and mesh in-fill to meet NZ building code for pedestrian safety.

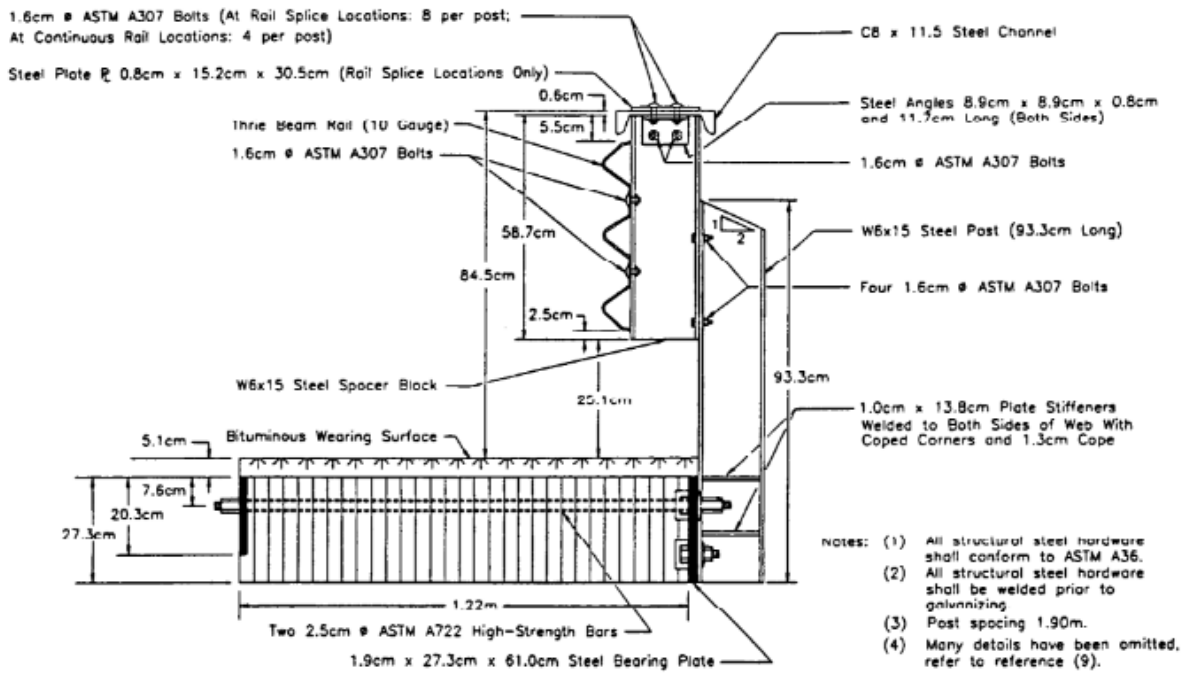

Figure 4 Example Tl-4 barrier detail reproduced from Transport Research board [2]

3.5 Durability

As outlined above, a 100-year design life is proposed for the concept design. NZ building code does not provide a technical pathway to demonstrate a 100-year design life. Older glulam bridges constructed in NZ circa 60 years old have been assessed to be performing well with limited deterioration. Internationally, there are many examples of timber bridges exceeding 100 years old.

It is proposed to achieve a 100-year design life in NZ conditions using a combination of H5 timber treatment and structural protection using either cladding and/or a weather resistance layer will be required for unsheltered elements. This is similar to international examples e.g. Nordic bridges.

Timber connections need to match the design life of the bridge as these are difficult to replace. Material selection for connection plates is an important durability concern. Typical connection feature “cast-in” plates and dowelled connections where the embedded surfaces cannot be inspected or maintained. This concept assumes that stainless steel plates would be used to guarantee the 100 year design life, however, this introduces costs. An alternative would be to use epoxy coated galvanised steel plates with increased maintenance requirements for the external surfaces. Internal surfaces would rely on the steelwork coating and structural protection / weather resistance provided to the timber arch to ensure durability.

4 FABRICATION

There are several fabricators in NZ that have sufficient expertise and capability to manufacture large glulam elements required for timber bridge construction

To control fabrication costs associated with multiple glulam pressings to build large arch elements there is opportunity to consider the use of several narrower width arch sections to form a built-up section or sections. These individual sections could be spaced transversely and structurally connected to achieve a similar level of out-of-plane stiffness to a complete unit.

5 CARBON ASSESSMENT

A high-level embodied carbon assessment between the concept and a typical conforming precast concrete beam design was undertaken. The precast concrete solution adopted 1525mm super-tee girders to provide a 35.0m span solution.

The timber arch super-structure was estimated to have an embodied carbon expressed as equivalent tonnes of CO_2 of 0.51 tCO2e / m^2 compared to 0.89 tCO2e / m^2 in the baseline Super-tee design. The timber design presents a reduction of approximately 40%. Including the concrete sub-structure in the comparison, assumed to be equivalent in both options this saving reduces to 30%. The largest contribution to the timber value was the steelwork required for the transoms, hangers and connections. Using recycled steel would further improve the footprint of the timber solution.

6 CONCLUSIONS

Timber offers new opportunities for construction of road bridges in the NZ market. Timber arches are suitable for single span crossings of expressways with a span of approximately 35m. The arch arrangement is suitable to be incorporated into a modular design approach. Concept sizing of the arch indicates significant reduction in carbon footprint can be achieved with timber construction.

To progress into detailed design and construction, further effort is required to develop design criteria, durability and edge protection requirements for timber bridges.

REFERENCES

1. NZTA, 2022. Bridge Manual SP/M/022 Edition 3, Amendment 4. NZTA, New Zealand.
2. Rosson, B.T., Faller, R.K., Ritter, M.A., 1995, Performance Level 2 and Test Level 4 Bridge Railings for Timber Decks, Transportation Research Record, USA.

ICTB 2025. 5th International Conference Timber Bridges
Rotorua, New Zealand, 29 June to 2 July 2025.

SH 26 ONETAI STREAM BRIDGE - NEW ZEALAND'S FIRST MODERN TIMBER STATE HIGHWAY BRIDGE IN DECADES

Cameron Douglas[1], Daniel Moroder[2], Liam Edwards[3], Andy Buchanan[4]

ABSTRACT

The Onetai Stream Bridge is a State Highway (SH) bridge located on SH 26, north of Paeroa in New Zealand's North Island. The original bridge was built in 1976, the 9-meter bridge carried two lanes of traffic and consisted of steel girders supporting a 150mm-thick nail-laminated timber deck. The deck was in poor condition, and long-term maintenance was deemed not cost-effective, necessitating its replacement. The replacement bridge served as a modern timber prototype under the New Zealand Transport Agency (NZTA) Waka Kotahi Engineered Timber Bridge Initiative, aimed at reducing carbon emissions. This paper examines lessons from notable timber bridge examples, the structural design of the Onetai bridge, including key considerations for specifying and designing timber, including detailing, durability, and construction. As a pilot project, the Onetai Stream Bridge aims to demonstrate timber as a viable alternative to conventional steel and concrete structures.

1 INTRODUCTION

The original Onetai stream bridge on SH 26, North of Paeroa (see Figure 1) was constructed in 1976. It spanned 9 metres and was 7.2 metres wide and consisted of steel girders supporting a 150mm thick Nail-Laminated Timber deck. A routine inspection, as part of the 2014/2015 Life Cycle Management Plan, identified the need for intervention within four to six years. Due to the high cost of long-term maintenance, replacing the bridge was deemed the most viable option.

Over the last decades, Engineered Wood Products (EWP) have gained increasing popularity in the vertical building industry due to their fast installation, strong strength-to-weight ratio, carbon sequestration capabilities, and aesthetic appeal. As a result, there is now also growing national interest in adopting EWPs for more sustainable roading infrastructure. The replacement bridge was hence selected to become New Zealand's prototype as part of NZTA's Engineered Timber Bridge Initiative [9]. PTL | Structural & Fire designed the timber superstructure, while Beca was responsible for the bridge substructure, foundations, and civil works as well as project and contract management.

This paper describes a pilot timber highway bridge project in New Zealand, with the goal of achieving a 100-year design life. The project explores appropriate design philosophies for NZ and identifies gaps in the design processes. It also served as the foundation for the NZ Timber Bridges Design Guide, a summary of which will be presented at the ICTB [6].

Figure 1. Bridge location (left) [17] and previous SH26 Onetai stream bridge (right) [3].

[1] Structural Engineer, PTL | Structural & Fire, e-mail: c.douglas@ptlnz.com,
[2] Technical Director, PTL | Structural & Fire,
[3] Technical Director - Bridges and Civil Structures, Beca,
[4] Principal, PTL | Structural & Fire.

2 BACKGROUND

2.1 Engineered Wood Products (EWP)

Sawn timber has been a common construction material for thousands of years. However, its quality and hence material properties can be inconsistent, depending on factors such as knots, splits, grain direction, and warping. Sawn timber members are limited in size, limiting its use for larger structural members. It has traditionally been used for truss bridges and as bridge decking, often mechanically fastened, and more recently stress-laminated (SLT), to form a monolithic element.

Over the past 30 years, advancements in Engineered Wood Products (EWP) have led to the development of stronger and stiffer timber materials, with much larger dimensions. Most notably, glued laminated (glulam) timber, formed by gluing sawn timber in a parallel arrangement, is frequently used for bridge girders and arch members due to its reduced defects and customisable sizing. Plywood, made from thin veneers bonded under heat and pressure with plies oriented in orthogonal directions, creates a stiff plate element commonly used for bridge decking. Refer to Figure 2 for cross-section illustrations of these two timber elements.

Other common EWPs, such as Cross Laminated Timber (CLT) and Laminated Veneer Lumber (LVL), are also widely used for buildings, though they are not currently suitable for exterior applications in New Zealand due to current treatment-related issues and unknown long-term performance.

Figure 2. Common timber bridge construction materials: sawn timber (left), glulam (middle), and plywood (right).

2.2 Existing Timber Bridges in New Zealand

According to NZTA Waka Kotahi, there are approximately 4,200 highway bridges in New Zealand, of which only 14 are constructed from timber, representing just 0.3% of the total stock [16]. A study of these existing timber bridges was conducted by Scion Research and found that Copper Chrome Arsenate (CCA) treated New Zealand glulam beams in service for up to 60 years had experienced very few durability issues [19]. Typically, deterioration occurred due to mechanical decay [7, 23].

2.3 Notable Timber Bridges

Timber bridges remain an important aspect to the transport infrastructure both nationally and internationally. Notable examples are outlined below with key findings integrated into the Onetai Bridge project where possible.

- The Tretten Bridge, located in Øyer Norway, was constructed in 2012. Consisting of a glulam truss girder supporting a SLT deck via steel decking beams, spanning 148 metres over three spans [12]. Inspections prior to its failure indicated some moisture damage at the connections, but the bridge was generally considered to be in good conditions. However, in August 2022, the bridge collapsed catastrophically due to a likely brittle block shear failure at a connection, where one of the timber diagonals was loaded in tension (see Figure 3). This sudden failure triggered an ‘unzipping’ effect, as the load could not be effectively redistributed. Investigations revealed that the designers had not adequately accounted for brittle failure modes in the connections, which was a provision in Eurocode 5 but were not explicitly covered by the Norwegian standard at that stage [13]. Brittle failure modes in timber connections must be explicitly checked in design to prevent catastrophic collapse.
- Another Norwegian bridge is the Skogsrud Bridge, located in Tangen, which is a four-lane structure with a total span of 49 metres [5] (see Figure 3). It features two three-pin glulam arches and a SLT deck supported by steel beams. To enhance durability of the timber, sacrificial louvres were installed

on the face of the glulam arches, providing protection while allowing airflow to prevent water from being trapped.

- A logging bridge in Okuti Valley, New Zealand, utilises SLT technology, incorporating LVL webs and sawn timber boards in a cellular arrangement. Steel tendons stress the structure, clamping the boards to enable monolithic behaviour. However, over time, creep leads to tensioning losses, necessitating regular maintenance [2]. This approach was considered for the Onetai Bridge, but NZTA opted against it due to the preference for low-maintenance solutions.

These examples underscore the importance of structural robustness in the design of public transportation networks, particularly when using timber. These learnings (i.e. avoidance of brittle failure modes, and enhanced durability by appropriate detailing and protection) have been incorporated into the design of the Onetai Stream bridge where possible.

Figure 3. Tretten Bridge following the failure of a connection [1] (left) and Skogsrud Bridge with sacrificial fascia (right).

2.4 Engineered Timber Bridge Initiative

In 2021, the NZTA Waka Kotahi launched an initiative to transform the construction approach for state highway bridges in New Zealand in a safe manner [9].

As part of this initiative, the SH26 Onetai Stream Bridge was identified as a suitable candidate for a pilot project for an engineered timber bridge. Its design and construction are documented in the next sections.

3 KEY DESIGN CONSIDERATIONS

3.1 Importance Level & Design Life

The bridge was considered as an Importance Level 3 (IL3) structure. As a highway bridge, it was designed with the goal of achieving a 100-year design life to comply with the NZTA Bridge Manual [15] and AS 5100.9 [25]. NZTA released a memo on guidance for durability related design techniques [8] with reference to a SCION durability report [19]. A Technical Advice Note (TAN) for timber bridges is currently being prepared to complement the bridge manual.

3.2 Environmental Factors

The bridge is located downstream of the Onetai Stream, which historically, floods regularly with the potential to fully submerge the deck. See Section 5.2 for the designed flood levels.

The bridge is located near Thames with an earthquake hazard factor of 0.16, which is relatively low risk. This is approximately half of the design load compared with Christchurch for seismic loading.

3.3 Daily Traffic

The bridge has been estimated to have an average annual daily traffic (AADT) of 3,462 vehicles, with 11.4% classified as heavy vehicles. Traffic volumes are projected to grow at an average rate of ~3% per year [18], meaning that the AADT is expected to exceed 4,000 vehicles within the next five years.

3.4 Differential Temperature & Moisture Effects

The coefficient of thermal expansion for timber is relatively small and not typically problematic especially for short spans.

However, differential moisture effects cause shrinking and swelling of timber members. Moisture changes perpendicular to the grain cause the greatest dimensional changes and were accounted for in the design.

3.5 Barrier

Based on the AADT and the presence of heavy commercial vehicles, a TL-4 barrier is the minimum required for the new structure. See Section 4.7 for further information on the barrier system.

3.6 Construction

The bridge was designed using a modular prefabrication approach, with girder segments manufactured off-site and lifted and installed on-site in a short amount of time. Deck panels were fastened in situ. The road closure duration, including foundation and roading work, was three weeks, aimed to minimise infrastructure disruption.

3.7 Performance Monitoring

As part of the prototype pilot project, several design assumptions were required to be monitored to support the confident construction of future engineered timber bridges. This involved installing accelerometers to monitor dynamic movements and moisture meters to capture the change of moisture content of the girders during the seasons and after larger rainfall events.

4 STRUCTURAL FORM & ELEMENTS

4.1 General Arrangement

The new carriageway has a width of 9.4 metres between the barrier faces, consisting of two 3.5-metre-wide lanes and 1.2-metre-wide shoulders. Additionally, a 0.9-metre allowance was included from the barrier to the outer edge of the kerb. The total bridge width is 11.2 metres. The bridge spans 9.0 metres from each abutment, refer to Figure 4 below.

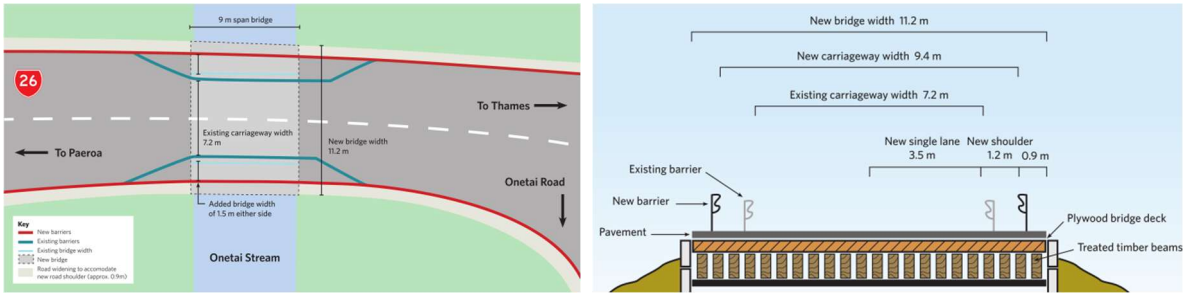

Figure 4. Plan view of the proposed bridge (left) and the proposed bridge cross-section (right) [17].

4.2 Superstructure

The structural form of the replacement bridge consists of 100 mm thick F14 structural plywood decking panels of Hoop Pine (Araucaria Cunninghamii), supported by twenty-two 675 mm deep by 225 mm wide GL10 glued laminated (glulam) timber girders (Pinus Radiata), spaced at 500 mm across the deck width. The girders are simply supported between abutments. Seven rows of blocking members (vertical diaphragms) connect the glulam girders to provide stability and also provide additional support for the longitudinal edges of plywood decking to minimise any vertical differential movement.

The plywood deck panels are fastened to the glulam girders and blockings using stainless-steel engineered wood screws along all edges and intermediate supports, forming a horizontal diaphragm capable of transferring lateral loads, such as flood and log impact forces, to the concrete abutments. A 4mm nominal gap was detailed between panels to allow for moisture-related movement. The plywood panels allow for load sharing between adjacent glulam girders.

4.3 Substructure

The abutments consist of a precast reinforced concrete abutment beam with wingwalls, and precast settlement slabs designed to minimise on-site construction time and mitigate any soil settlement.

The bridge abutments are supported on a Mechanically Stabilized Earth (MSE) retaining wall utilising proprietary Stone Strong facing blocks to provide long-term scour protection [30]. The abutment beam and MSE wall are founded on the existing low strength soils, with weak materials being undercut and replaced. The lightweight timber superstructure aided in enabling a shallow footing to be selected for the project site.

4.4 Surfacing

The pavement system was proposed by NZTA subject matter experts in a specific memo [10]. The plywood was first covered with an epoxy emulsion and chipseal. To accommodate any vertical or horizontal movement of the decking panels, an attenuation layer made of a tapered medium traffic surfacing layer was applied, incorporating a central crown with a 2% crossfall. The nominal gap between the plywood panels,

to accommodate shrinkage and swelling, was filled with construction sealant and taped off with a self-adhesive membrane.

4.5 Abutment Connection

Vehicle braking and seismic actions are transferred to the concrete foundation by bespoke stainless-steel brackets. The brackets are designed to resist braking loads in the bridge's longitudinal direction. They also resist DCLS (Damage Control Limit State) seismic loads from the bridge superstructure, as well as the soil pressures when abutments tend to move towards each other due to earthquake-induced soil movements. Under a CALS (Collapse Avoidance Limit State) seismic event, the bolts connecting the brackets are likely to fail, allowing the abutments to move further until the gap between the girder ends and the abutments has completely closed. In the event of severe flooding, the brackets can resist horizontal loads perpendicular to the bridge span.

Any horizontal loads are resisted by friction of the shallow foundations and settlement slab on the supporting soil.

Hold-down anchors in combination with a steel PFC beam bearing against the upper edge of the glulam girders are used to tie the bridge to the concrete abutments to prevent floatation in severe flooding events.

4.6 Expansion Joint

An asphaltic plug joint system that can meet the displacement requirements of the design has been proposed to minimise surfacing maintenance. Due to the short span of the bridge and negligible thermal movement of the timber structure, the predicted differential movement between the superstructure and abutments is minor and less than 5mm.

4.7 Barrier System

The bridge is 11.2m wide including the barrier system. The TL-4 proprietary barrier system, CrocGuard, free spans the length of the bridge with no barrier fixings to the deck. By avoiding intermediate barrier posts, the timber bridge superstructure did not require any specific detailing to resist the overstrength demand from the barrier system during impact loading.

5 STRUCTURAL ANALYSIS & DESIGN

The proposed timber structure was designed according to the NZTA Bridge Manual [15] and the Technical Advice Note #22-02 [14].

5.1 Modelling of the Timber Superstructure

The demands on the structural elements were determined assuming a first-order linear analysis due to the simple geometry allowing for internal forces to be computed based on the conditions of geometry. This analysis does not consider any forces due to deformations that may occur with compression members, where a second-order analysis may be more appropriate.

The Finite Element Modelling (FEM) software, Dlubal RFEM, was used. Refer to Figure 5 below for an illustration of the 3D model. The plywood decking was analysed as an orthotropic plate element to account for its varying structural properties based on span orientation. This approach was used to assess the plywood's two-way spanning and load-sharing capability with the supporting girders. The material properties were taken as for F14 plywood [24] with layer geometry of 3/34-31-11 ply as per manufacturer's specifications. The girders themselves are modelled as beam elements with isotropic material properties for GL 10 [29]. The design did not consider T-beam composite action.

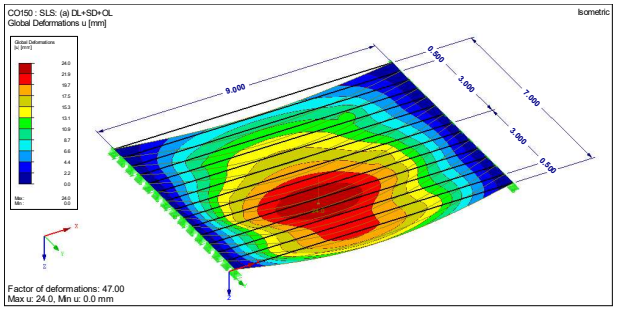

Figure 5. Dlubal RFEM for Onetai Stream Bridge showing calculated deflection under HN loading.

5.2 Design loads

Superimposed (SDL) and HN/HO traffic loadings were applied to the structure in accordance with the NZTA Bridge Manual. Dead loads of the timber had been computed using NZS AS 1720.1:2022 [29]. The bridge was designed to accommodate a 70 mm nominal thickness of asphaltic surfacing, tapering transversely to form a central crown, incorporating a 2% crossfall.

Additionally, the bridge was designed to withstand 2-year, 100-year, and 1000-year flood events, which may partially or fully submerge the bridge deck. Seismic demands for the superstructure were determined using the equivalent static method for a 1000-year event, ensuring the structure remains elastic during DCLS and CALS seismic loading.

The bridge was not specifically designed to accommodate significant pedestrian or cycle traffic. As a result, the vibration criteria outlined in the Bridge Manual were not considered applicable.

5.3 Member Design

The girders and plywood decking elements were assessed to meet AS 5100.9:2017 [25] in combination with AS 1720.1:2010 [24] and NZS AS 1720.1:2022 [29]. Noting that NZS AS 1720.1 takes priority for design equations and capacity factors (strength reduction factors). Some notable assumptions for member design are shown below:

- k_4: Seasoned timber was assumed that is subjected to conditions in which the average moisture content for a 12-month period is expected to be 20%.
- k_9: Load sharing attributes are not allowed for glulam members (only for sawn timber). So, k_9 was set to 1.0.
- k_{24}: Size factor was conservatively taken as 1.0, from NZS 3603 [27].

5.4 Connection Design

The design of connections was conducted using NZS AS 1720.1:2022, which allows for the determination of the failure load (embedment of timber or yielding of the metal fasteners) and has provisions for checking brittle failure modes in connections.

The bespoke bracket at the abutment was designed so that during a DCLS event, the bolts will yield before any brittle failure occurs, with group tear-out being the likely brittle mode of failure.

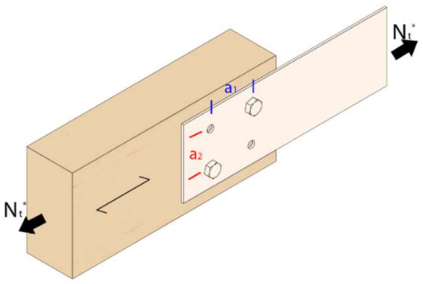

Figure 6. Connection schematic of steel plate-to-timber.

6 DURABILITY & DETAILING

Demonstrating the durability requirement for a 100-year design life as per the NZTA Bridge Manual [15] is a key challenge for timber bridges in New Zealand due to there being no clear compliance pathway within the New Zealand Building Code framework for timber products [11], or the NZTA Bridge Manual. Research from current practice within NZ and internationally, including a study conducted by Page et. al [19] led to a series of key details and material choices for the project with the aim of achieving a 100-year design life. The design ultimately followed the provisions outlined in a NZTA durability memo [8], which represents the only pathway to fulfil the durability requirement until further criteria and guidance are introduced by either the Bridge Manual or any design or material standards. The following key considerations have been followed to achieve the 100-year design life.

- Detailing to Prevent Entrapment of Water – All holes from fixing through the plywood decking are plugged with an epoxy emulsion. Where possible, drainage and ventilation spaces are provided so that any water can drain out.

- End & Side Grain Protection – Bitumen emulsion was applied to the end grain, top, and upper side surfaces of the glulam girders. The top surface of the plywood was sealed with epoxy emulsion, which is also part of the pavement system.
- Rain & UV Protection – Sacrificial weatherboard cladding with a ventilated cavity was provided on the vertical faces of the outer girders. Protection of the timber kerb member and plywood panel edges utilised stainless steel flashing with a ventilation cavity.
- Steel Components – All connections and brackets are fabricated with grade 316 stainless steel. This is especially important, as any mild steel in contact with CCA treated timber will have a much higher corrosion rate.
- Timber Adhesives & Treatment – All glulam girders were made of laminations which were individually treated to Hazard Class H5 with Copper Crome Arsenic (CCA) treatment before being laminated, in accordance with NZS 3640 [28]. All laminations are glued with resorcinol-formaldehyde adhesive as recommended by the SCION report [23]. The plywood panels were veneer-treated to Hazard Class H5 with Alkaline Copper Quaternary ACQ to AS/NZS 1604.1 before being laminated [26]. These specified treatment requirements, which are unique to Australia and New Zealand, ensure that the same level of treatment can be achieved throughout the girders and the decking.

7 INSTRUMENTATION

The in-service moisture content of timber bridges within NZ has little historical data. The target upper limit to avoid decay is a moisture content of 20% [8]. The moisture content of structural timber members will be regularly monitored, with measurements taken at both the surface and core of the girders. The non-structural (sacrificial) glulam blockings have been designed for removal and testing to evaluate the long-term performance of the timber from time-to-time in the future.

8 SUSTAINABILITY

Timber was chosen as a construction material for its carbon sequestration properties compared to steel and concrete. Additional benefits include reduced volume of the concrete foundation due to the light-weight superstructure, using locally sourced materials, and reduced wastage due to pre-fabrication.

A carbon calculation assessed emissions associate with bridge deck across its the product stage (A1-A3) and end-of-life (C4 and D). The calculation used specific Environmental Product Declarations (EPDs) and assumed a 100-year design life. During its lifetime, the bridge deck stores an estimated 26.2 tonnes CO_2 equivalent of sequestered carbon and emits 37.4 less tonnes CO_2 equivalent than an alternative concrete deck design.

To put the carbon figures into perspective, the net carbon sequestered offsets the emissions of a single passenger taking five round-trip flights between Auckland and London. This calculation assumes an emission rate of 148 g CO_2 equivalent per km for a long-haul flight [22].

9 MANUFACTURING & CONSTRUCTION

The glulam beams were manufactured at the Red Stag TimberLab (RSTL) factory [21], Auckland, where they were coated with bitumen emulsion, and the abutment brackets were fastened, as shown in Figure 7. The plywood panels (NiuDeck [4]) were manufactured in Papa New Guinea by PNGFP [4, 20]. As required by NZTA, all materials were thoroughly inspected and tested in accordance with the structural drawings, specifications and manufacturing standards. Only materials strictly conforming with the outlined requirements were accepted on site.

The construction of the bridge and civil works was conducted by HEB Construction NZ. During construction, a real time camera was positioned to allow for remote monitoring of the bridge. In progress construction snapshots are shown in Figure 8 below, where the installation of the girders and plywood deck took approximately 4 days to complete.

Figure 7. Timber girder modules (left), abutment bracket (middle), and bracket notch (right) at RSTL Factory, Auckland.

Day 0

Day 10

Day 16

Day 19

Day 23

Day 45 (completion)

Figure 8. In progress construction photos.

10 LESSONS LEARNED

Upon completion of the bridge, there were several lessons learned and are noted below for future reference.

- Tolerances – Timber is a variable material prone to dimensional changes with changes in moisture content. While the girder modules and panels were manufactured to the specified tolerances, they were not stored flat on site, leading to some distortion. This was allowed for by aligning abutment bracket anchors with Drossbach ducts and site-cutting infill glulam blocking.
- Timber expertise on site – bridge contractors have limited experience with engineered wood products. This resulted in minor issues in terms of storage (plywood panels had slightly warped as they were stored on an uneven site), handling (some timber members got damaged during installation), and remediations on site (site cutting, remediation of damage due to impact, etc). Contractors will gain this experience over time or could opt to engage or subcontract specialist timber contractors or carpenters.
- Bitumen/Epoxy Emulsion – The timber absorbed bitumen emulsion coatings more than expected. For future projects, applying minimum x3 layers of coating are advised to achieve better protection.
- Pavement Crown – During design, a crossfall was considered for the plinth to maintain a consistent pavement thickness. However, this approach would introduce a longitudinal deck joint, creating an additional interface for possible water infiltration. To mitigate this, the crossfall was instead implemented through the pavement, requiring milling and additional work. For future projects, alternative solutions in coordination with pavement engineers could be explored.
- Availability of Stainless-Steel Screws – Although NZTA require the use of stainless steel 316 fasteners, the required partially threaded engineered wood screws were only available as grade 304. Instead, fully threaded screws were used, which made it challenging to provide adequate clamping between the plywood decking and the girders.

11 RESEARCH NEEDS

Several items require further research to streamline and enhance the design of timber bridges.

- Pavement compatibility – The adhesion interface between road surfacing and timber is not yet fully understood, but research is currently underway to gain a better understanding. Most pavement solutions are very sensitive to differential movement, which is likely to be encountered at decking panel splices (both in terms of in-plane and out of plane movements).
- Plug joints – There is little information regarding the plug joint performance for timber.
- Moisture content – Data will be regularly monitored for the Onetai Bridge for further analysis.
- Interpretation of Manufacturing Standards – Some interpretation is required for manufacturing standards, e.g. rules for delamination and finger joint testing.

12 CONCLUSION

The SH 26 Onetai Stream Bridge replacement is a modern timber prototype as part of the NZTA Waka Kotahi Timber Bridge Initiative. The design and construction of this bridge aimed to demonstrate the design of timber bridges as a viable substitute for traditional steel and concrete bridges. The learnings of the Onetai stream bridge project have been incorporated in the New Zealand design guide for timber [6]. Additionally, several lessons learned from the bridge's construction can inform future timber highway bridge projects.

13 ACKNOWLEDGEMENTS

The authors would like to acknowledge staff at NZTA Waka Kotahi, and all material suppliers, for their support given during the design and construction of the bridge.

REFERENCES

1. Associated Press. *Norway bridge collapses, drivers of 2 vehicles rescued*. 2022; Available from: https://nypost.com/2022/08/15/norway-bridge-collapses-drivers-of-2-vehicles-rescued/.
2. Buchanan, A., C. Douglas, and D. Moroder, *Prestressing Losses in a Post-Tensioned Timber Logging Bridge.* ICTB 2025 Conference Proceedings, 2025.
3. Edwards, L., D. Moroder, and C. Douglas, *SH26 Onetai Stream Bridge Replacement - Structures Design Statement: Detailed Design*. November 2022.
4. IBuilt. *NiuDeck - Plywood Decking*. 2025; Available from: https://nzwoodproducts.co.nz/products/details/plywood-bridge-decking/38/.
5. Legg, C. and D. Tingley, *Viability of Modern Timber Highway Bridges*. 2019, Wood Research & Development.
6. Moroder, D., et al., *New Zealand Timber Bridges Design Guide. NZ Transport Agency Waka Kotahi Draft.* 2025.
7. Morris, P., *Durability of Wood Bridges*. 2018, Wood Protection Group, FPInnovations.
8. Netley, J., *Design life and durability for Onetai Stream Bridge Replacement (Memo).* NZTA Waka Kotahi, 2023.
9. Netley, J., *Engineered Timber Bridges for Highways in New Zealand.* Austroads Bridge Conference 2022, 2022.
10. Netley, J., *Surfacings for SH26 Onetai Bridge replacement (Memo).* NZTA Waka Kotahi, 2022.
11. New Zealand Building Code (NZBC). *Building Regulatory Framework*. 2021; Available from: https://www.building.govt.nz/building-code-compliance/how-the-building-code-works#jumpto-building-regulatory-framework.
12. Norwegian Safety Investigation Authority, *Sub-report 1 on the bridge collapse at Tretten on 15 August 2022*, in *Road traffic report 2023/03*. 2023.
13. Norwegian Safety Investigation Authority, *Sub-report 2 on the collapse of Tretten bridge on 15 August 2022*, in *Road traffic report 2024/03*. 2024.
14. NZ Transport Agency Waka Kotahi. *#22-02 Interim technical standards for the design of timber bridges*. 2022; Available from: https://www.nzta.govt.nz/resources/22-02-interim-technical-standards-for-the-design-of-timber-bridges/?back=10211.
15. NZ Transport Agency Waka Kotahi, *Bridge Manual SP/M/022 (Third Edition)*, ed. N.Z. Government. 2022.
16. NZ Transport Agency Waka Kotahi. *Bridges and structures*. 2024; Available from: https://www.nzta.govt.nz/roads-and-rail/bridges-and-structures/#:~:text=There%20are%20still%20185%20single,timber%20bridges%20on%20state%20highways.
17. NZ Transport Agency Waka Kotahi. *New Zealand Transport Agency (NZTA) Waka Kotahi - SH26 Onetai Bridge Replacement*. 2024; Available from: https://www.nzta.govt.nz/projects/sh26-onetai-bridge-replacement/.
18. NZ Transport Agency Waka Kotahi. *State highway traffic volumes 1975-2020*. 2020; Available from: https://www.nzta.govt.nz/resources/state-highway-traffic-volumes/.
19. Page, D. and T. Singh, *The durability of preservative-treated Glulam in New Zealand*. 2022, SCION Research: Rotorua.
20. Papua New Guinea Forest Products (PNGFP). *Homepage*. 2025; Available from: https://pngfp.com/.
21. Red Stag TimberLab. *Homepage*. 2025; Available from: https://redstagtimberlab.co.nz/.
22. Ritchie, H. *Which form of transport has the smallest carbon footprint?* Our World in Data 2023 [cited 2025; Available from: https://ourworldindata.org/travel-carbon-footprint.
23. Singh, T. and D. Page, *Case studies on the history and use of timber bridges in New Zealand.* Wood Material Science & Engineering, 2018.
24. Standards Australia, *AS 1720.1:2010 - Timber structures Part 1: Design methods*. 2010.
25. Standards Australia, *AS 5100.9:2017 - Bridge Design Part 9: Timber*. 2017.
26. Standards Australia/Standards New Zealand, *AS/NZS 1604.1:2021 - Preservative-treated wood-based products - Part 1: Verification requirements*. 2021.
27. Standards New Zealand, *NZS 3603:1993 - Timber structures standard.* 1993.
28. Standards New Zealand, *NZS 3640:2003 - Chemical Preservation of Round and Sawn Timber*. 1992.
29. Standards New Zealand, *NZS AS 1720.1:2022 - Timber structures Part 1: Design methods*. 2022.
30. Stone Strong. *Homepage*. 2025; Available from: https://stonestrong.co.nz/blocks/.

ICTB 2025. 5th International Conference Timber Bridges
Rotorua, New Zealand, 29 June to 2 July 2025.

Pre-fabricated Stress Laminated Timber Bridges in New Zealand.

Edwin Douglass[1] , Daniel Moroder[2] , Andy Buchanan[3]

ABSTRACT

This paper describes new developments in the design of pre-fabricated Stress Laminated Timber (SLT) bridges in New Zealand. The example "TrailGate" bridge has two six-metre spans. It is designed for "lightly trafficked rural" applications such as farm road infrastructure and secondary public road bridges. The design choices are aimed at preserving the simplicity of assembly and use of standard farm machinery (farm tractor, fence post driver and digger) in the construction and assembly phase. Individual components of the bridge are sized so that they can easily be handled by two persons.

The design choices allow the bridge to be manufactured using trade skills and commercially available components, with no specialised equipment for the manufacture of individual component parts. Design choices are guided by simplicity and oriented towards "low tech" solutions making the bridge design and construction accessible to small and medium size contractors with construction capabilities and skills available throughout New Zealand.

Photo 1. Completed TrailGate bridge in service use.

[1] *Edwin Douglass (BE, MBA), Kiwood Ltd. Email:* E_douglass@bluewin.ch, www.kiwood.co.nz
[2] *Daniel Moroder (dott. ing., PhD), PTL Structural & Fire*
[3] *Andy Buchanan (BE, MS, PhD), PTL Structural & Fire*

1. PROJECT OVERVIEW

1.1 Description

The TrailGate bridge is located on private land at Glen Alton Forest, Clarence river valley, near Kaikoura. It is 12m long consisting of 2 x 6m spans of pre-fabricated Stress Laminated Timber (SLT) beams supported on a timber substructure. The bridge was designed by Kiwood Ltd and is targeted towards "lightly trafficked rural" applications [3] such as farm road infrastructure and secondary public road bridges.

1.2 TrailGate bridge project purpose

Aside from its functional use, the TrailGate bridge is built to demonstrate the viability of using structural timber, construction simplicity, and to further promote the use of structural grade Radiata pine rough sawn timber for road bridge infrastructure in New Zealand.

2 DESIGN METHODOLOGY

2.1 Stress Laminated Timber bridges

SLT bridges were originally conceived as a method for rehabilitating deteriorated nail laminated timber bridge decks in Canada in the 1980s. They have since been widely used in North America and Australia [1]. The primary concept of stress laminated timber bridges is the use of transverse post-tensioning forces to provide friction between the timber elements in lieu of glue, screws or nails. The first stress laminated timber box-girder bridge in New Zealand was a 6.0m single span logging bridge designed and built near Christchurch in 2010 [2].

2.2 Design for Vehicle Loading

Vertical loading is dominated by 0.85 x HN truck loading as defined in the NZTA Bridge manual [3]. The bridge deck is designed as a stress laminated plate structure [4, 5].

2.3 Design for Earthquake Loading

The bridge is designed as an elastically responding structure for a design acceleration of 1.0g. A combination of the effects of orthogonal seismic actions are applied to the structural elements to account for the simultaneous occurrence of earthquake shaking in two perpendicular horizontal directions. However, the bridge responds as a locked-in structure in the longitudinal direction (direction of traffic flow) as it is effectively wedged between the two abutment timber retaining walls and hence the transverse direction (orthogonal axis to the direction of traffic) is the critical axis for consideration of lateral earthquake forces.

The equivalent static force method of analysis is used as the basis of seismic analysis and design.

Each span of the Stressed Laminated Timber deck acts as a rigid single plate element supported by the abutment and central mid span support structure. The stress lamination of the prefabricated box girders ensures the bridge deck acts as a single plate structure. The abutment and mid-span support structure is designed as a rigid frame to the bridge deck and the driven timber piles are assumed to be pinned at the base.

2.4 Design codes and conflict resolution

The primary structural design methods and codes are taken from relevant Australian and New Zealand design standards [6 – 13]. As can be witnessed by the relatively long list of reference standards, care is needed to resolve eventual code conflicts between standards, especially relating to the characteristic stresses of radiata pine or other softwoods when comparing New Zealand and Australian codes. The Code compliance path is summarized as follows; (i) Loads to NZTA Bridge Manual, (ii) Design principles for timber bridge design to AS 5100.9 with reference to AS 1720.1, (iii) material strength

factors and design properties of NZ graded timber to NZS 3603 (at the time of the design of the bridge, as NZS AS 1720.1 was not yet published).

3 STRUCTURAL SYSTEMS

3.1 Bridge deck: Prefabricated timber box girder modules

The prefabricated timber bridge box girder modules were assembled with 25mm full-length cross-banded LVL web panels and top and bottom flanges formed from 150 x 50 rough sawn timber, all with holes drilled at 600mm centres for the transverse stressing bars. The individual 150 x 50 sawn timber sections of the top and bottom flange and the LVL web elements were nail laminated together for construction assembly and transport of the completed box girder modules. Timber blocking was added to each end of the box girder and the whole modular assembly was preservative treated via envelope penetration to H4 as a pre-fabricated unit. Whilst a good level of carpentry skills are required, the whole box girder assembly was fabricated with readily available carpentry tools and does not require specialized manufacturing technology or equipment.

Photo 2: Pre-fabricated timber box girder module.

Photo 3. Assembly of the bridge deck/superstructure.

3.2 Bridge deck/Superstructure stress laminated system

Following the placement of the pre-fabricated box girders on the bridge support structure, the bridge deck/superstructure was stress laminated. The deck structure was stress laminated to service design compression levels by tightening the 32mm diameter Reidbar^{TM} threaded stressing bars to 6 tonnes (60kN) tension by applying a design torque of 1000Nm. The Reidbar^{TM} nuts were tightened using a spanner and impact drill with socket that delivered the desired torque/tension relationship [14] hence tensioning the stressing bars. The correct torque application was further calibrated by using a custom-made stressing bridge arrangement in combination with a hydraulic jack as shown in Photo 4. Calibration of the pre-stressed rods, on a sample of the stressing bars, was achieved by using the hydraulic jack to tension the stressing bar to the design tension, at which time the anchorage nut becomes loose if the pre-tensioned bar is correctly tensioned using the torque method. Results from the calibration exercise demonstrated that the torque method reliably delivered the design tension force in the stressing bar.

Photo 4: Hydraulic jack and stressing bridge used to calibrate the design tension in the pre-stressing bars stressed by applying torque.

Photo 5: Stress laminated bridge deck.

The design choice of tightening a nut on a threaded rod to apply tension was made to simplify the stress laminating process and periodic maintenance of the compression stress level in the laminated deck structure. As a subsequent step, the stressing nuts and bearing plates were removed one at a time then reassembled and tightened after 4x SPAX stainless steel fully threaded screws were added behind each of the stressing bearing plates to reduce the local loss of pre-stress [15]. The stress laminating of the bridge deck was carried out prior to attachment of the bridge deck to its support brackets. This sequence was to avoid impeding the clamping action of the stressing bars.

A major advantage of Reidbar^{TM} threaded stressing bars is the ease of construction and maintenance. Some other SLT bridges have used 7-wire prestressing strands from the concrete industry. These have the disadvantage of requiring specialised stressing equipment, but they have an advantage of less reduction in pre-stressing force for given levels of timber shrinkage, because of the higher yield strength steel.

Photo 6: Stress laminated bridge deck stressing bar and bearing plate assembly.

Photo 7: Fully threaded screws added behind the bearing plate to reduce pre-stressing losses.

3.3 Abutment and mid span support structure

The bridge deck foundation structure was formed with driven 300mm SED timber piles and two levels of 290 x 90mm transverse timber beams on either side of the piles. The bridge support beams were diagonally braced between levels forming a braced frame support structure under the bridge deck. The seven timber piles at each end of the bridge deck spans were spaced so as to be directly under each web section of the box girder modules. Vertical forces are directly transmitted to the foundation piles via shear in the webs of the box girder modules and direct bearing on the timber pile support structure. The braced frame pile support structure is designed to resist laterally induced earthquake forces.

The bridge abutment retaining walls were formed with driven timber plies and 200 x 50 timber sections placed laterally behind the timber piles. The bridge deck structure left a 100mm space at each end of the deck spans and at mid-span for construction tolerance purposes. With the use of galvanized steel retention brackets, timber packing was placed to fill the tolerance void, effectively wedging the bridge deck superstructure against the abutment retaining walls and at the bridge mid-section. Since timber has a negligible coefficient of thermal expansion, no expansion joint was required.

Photo 8: Abutment and mid-span support structure.

Photo 9: Bridge deck to abutment retaining wall detail, showing timber packing retention brackets.

3.4 Abutment retaining wall and support structure

The foundation structure was formed using driven timber piles. Whilst each bridge site foundation design requires specific geotechnical and hydraulic investigation and engineering design, the use of driven timber piles can offer a viable solution for commonly encountered situations.

Photo 10: Abutment retaining wall driven timber piles.

Photo 11: Tractor-mounted post driver used to drive timber piles for the support structure and the abutment retaining wall.

3.5 Bridge barrier

The bridge barrier has 150 x 150mm timber posts spaced at 1200mm centres, each formed from three 150 x 50mm timber sections nail laminated together. Lateral and vertical load resistance is provided at the post base by galvanised coach screws into the top and bottom flanges of the outer box girders. The timber barriers were designed based on loadings for pedestrian, cyclist and equestrian barriers, however, these would require a departure from the roading authority for full compliance with the NZTA Bridge manual.

Photo 12: Bridge barrier posts.

Photo 13: Timber lattice mat wearing course under construction.

3.6 Timber lattice and gravel wearing course

The bridge wearing course consists of a sacrificial timber mat lattice and fine river gravel surface. The timber mat lattice was built from continuous 100 x 50mm treated H4 timber and interspaced with 400 x 100 x 50mm timber blocking at 800mm centres. The timber lattice was nail laminated together to form 1200 wide x 3000 long x 100mm deep timber mats. The lattice mats were subsequently filled and covered by a 50mm layer of fine river gravel after placing a fine waterproof and tear-resistant geo-textile layer on the bridge deck, to prevent incursion of the fine river gravels into the bridge superstructure. The timber lattice mats and river gravel finish is contained on each side by the bottom rail of the bridge barrier.

Photo 14: Nail lamination of timber lattice mat.

Photo 15: Timber lattice wearing course after application of the gravel surface.

4 DURABILITY AND MAINTENANCE

4.1 Durability considerations

The TrailGate bridge is designed for a 50 year design life.

The authors note that the 100 year design life specified in the NZTA Bridge manual currently introduces an unresolved dilemma for the use of structural timber for bridge infrastructure projects in New Zealand. The current treatment regime for timber has largely been driven by the use of treated timber in buildings with a code requirement of 50 years durability. The authors suggest that there is an industry need for systematic monitoring of the durability aspects of in-service timber infrastructure projects, including the moisture content of the wood, in order to resolve and better understand the long-term durability aspects for use of preservative-treated structural timber in bridge infrastructure projects.

For the TrailGate bridge all timber above ground was CCA treated to H4 and the timber piles to H5. In order to mitigate concerns around the penetration of the CCA treatment through the glue lines of LVL the completed bridge modules were treated after assembly without any modification, exposing all critical surfaces such as holes to direct exposure to the CCA treatment.

The galvanized steel elements (anchorage system bearing plate, nuts and washers, tensioning bars, retention brackets and bolts) are designed to be accessible and removable for eventual replacement

in case of need. The bridge maintenance regime includes a periodic (every 10 years) sample inspection of galvanized steel elements and replacement if required.

Although the structural timber is designed assuming a wet (moisture content ≥25%) in-service condition, careful detailing of the bridge superstructure has been undertaken to avoid ponding and prolonged period of exposure to moisture; (i) The bridge deck is sloped at 2 percent in its longitudinal direction to ensure rain runoff, (ii) a waterproof and tear-resistant membrane layer is included between the timber box girders and the timber lattice and gravel wearing course and (iii) the flashing detail at the bridge deck edge protects the end grain of the outer LVL box girder web section and forces any water dripping to occur outside the vertical plane of the outer box girder's exposed face. All exposed timber surfaces are additionally painted with CD50 timber preservative treatment.

4.2 Maintenance

The maintenance schedule to ensure the ongoing performance of the TrailGate bridge is as follows:

Annually, for the first three years and every five years thereafter; (i) visual inspection and resolution of any obvious deficiencies, (ii) checking and restressing of the stressing bars, (iii) removal of vegetation restricting the airflow around the bridge deck to retaining wall space and (iv) every ten years sample removal of galvanized steel elements and inspection for corrosion and eventual replacement if required.

During the third annual maintenance of the TrailGate bridge the moisture content of the exposed box girder sections on the underside of the bridge deck was measured at the surface of 12 locations on the underside of bridge and directly above the stream water flow with an average moisture content measured of 13.8% ± 2% accuracy with maximum and minimum values of 19.6% and 10.3% respectively. The maintenance intervention was taken on 24th March 2025 (late summer in New Zealand) and one week after a significant rain event at the bridge location. Recalibration of a sample (4x) stressing bars revealed compression of the box girder module laminates was being maintained above the minimum service level compression stress requirements.

5 BROADER APPLICATIONS

5.1 Stress laminated timber bridge 12m and 25m clear span designs

Kiwood has developed designs for 12m (shown in Figure 1) and 25m clear span versions of the TrailGate stress laminated box girder bridge described earlier. These designs allow for both "lightly trafficked Rural" and full HN/HO truck loadings.

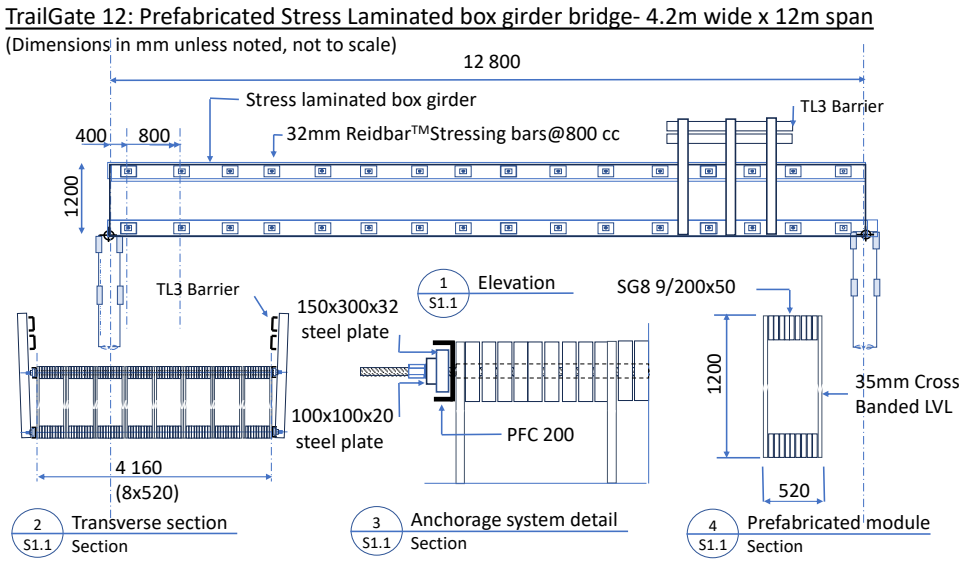

Figure 1: Concept design sketch of TrailGate 12: Stress laminated box girder bridge (12m span)

Practical constraints were encountered around the requirement that the Cross Banded LVL web section of the box girders are continuous over the span. The inherent stiffness of box girder and cell structure, once stress laminated, means this type of road bridge is well suited to STL timber construction and scales to full HN/HO loadings and longer spans.

Further Kiwood designs include Stress Laminated Suspended Arch Timber bridges named the "FarmGate" (12m span) and the "HighGate" (25m span and shown in Figure 2.) bridge respectively designed for HN/HO and "Lightly Trafficked Rural " loadings. In these designs, there is a single layer stress laminated timber deck spanning onto transverse steel beams suspended from the timber arch on each side of the bridge. Vertical tension members consisting of 2 – RM32 rods at each end of the deck support beams carry vertical loads to timber arch top chord connection. Each diagonal arch member takes compression loads directly from top chord points to a reinforced concrete pile cap which effectively shares the vertical abutment load between adjacent timber piles.

The top chord of the timber arch is stabilised by a horizontal truss and braced laterally at each end of the bridge at two chord points with RB32 Galv. bracing rods from the timber arch top chord to the extended pile cap.

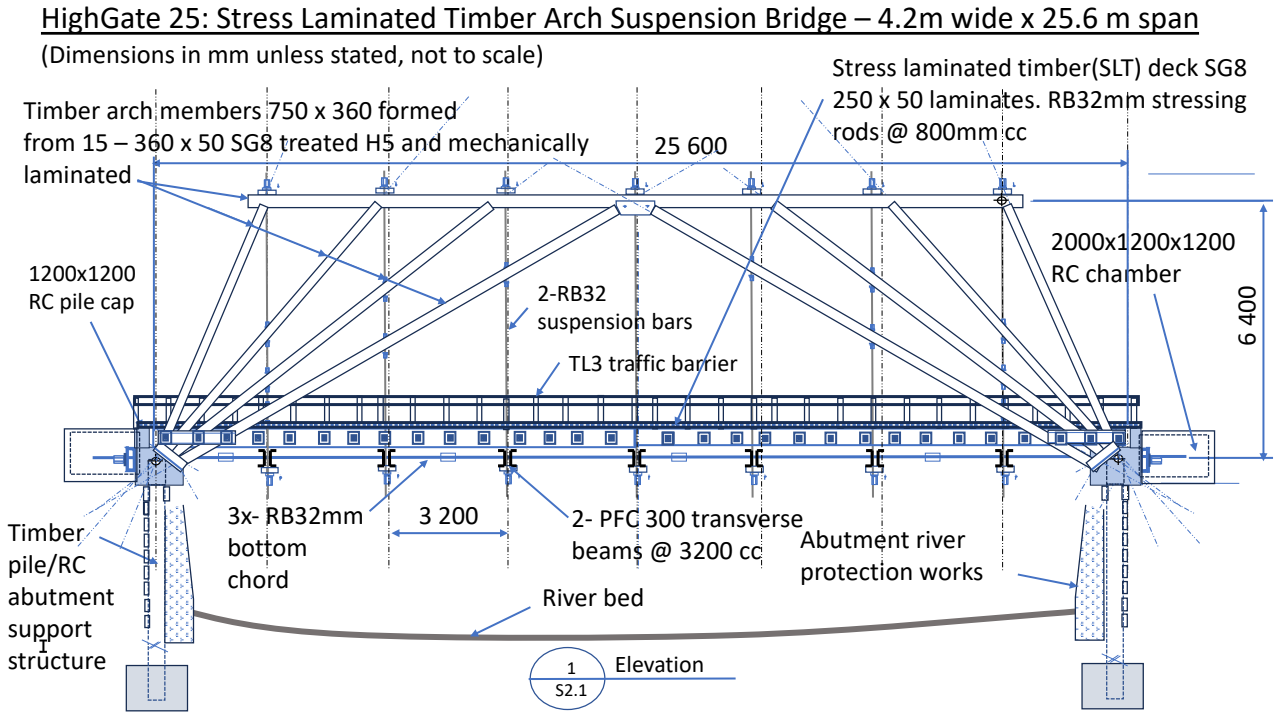

Figure 2: Concept design sketch of HighGate 25: Stress Laminated Timber Arch Suspension Bridge (25m span)

Stress laminated timber bridges have a high potential for use in broader applications for road transport infrastructure.

6 CONCLUSIONS

The realization of the TrailGate Stress laminated timber bridge further demonstrates that the use of structural grade rough sawn timber, LVL webs, and timber piles provides a viable option for the construction of road bridges with the potential for much broader applications and longer clear spans.

The regulatory framework and relevant engineering design codes currently in use in New Zealand and Australia provide a framework for the design and construction of timber road bridges. However, further elaboration and simplification of design codes and practitioner guides specifically focussed

on the use of New Zealand timber in bridges would further promote and assist in the adoption and acceptance of structural timber use for infrastructure projects.

Design choices orientated towards simplicity of construction and low-tech solutions could render the design and construction of timber bridge infrastructure accessible to a wider range of construction practitioners and skilled tradespeople available throughout New Zealand.

There is a case for further documentation and monitoring of the durability aspects of in service timber infrastructure projects in order to overcome current limitations and better understand the long term durability aspects for use of structural timber in bridges.

7 REFERENCES

[1] Keith Crews. An Overview of the Development of Stress Laminated Cellular Timber Bridge Decks for Short to Medium Span Applications in Australia. International Conference on High Performance Materials in Bridges, Kona, Hawaii, 2001. https://opus.lib.uts.edu.au › bitstream › 10453 › 2010 › 1 › 2003001332.pdf (Ref., 6.12)

[2] NZ Timber Design Awards 2012. PTL Structures & Fire, Christchurch. https://ptlnz.com/projects/other/stress-laminated-timber-bridges/

[3] NZTA Bridge Manual SP/M/022, Third edition, Amendment 3, October 2018.

[4] NSW (AU) Transport, Roads and Maritime Services, Guide for the design of stress laminated timber bridge decks, Part 1 – Design Procedures, Version 2.2, March 2012.

[5] NSW (AU) Transport, Roads and Maritime Services, Guide for the design of stress laminated timber bridge decks, Part 2 Commentary, Version 2.2, March 2012.

[6] AS 5100.9. Bridge design. Part 9 Timber. Standards Australia, 2017.

[7] NZS 3603, including amendments 1,2 and 4. Timber Structures Standard. Standards New Zealand, 1993.

[8] AS/NZS 1170.0. Structural Design Actions. Standards Australia, 2002

[9] NZS 1170.5. Structural Design Actions, Earthquake Actions – New Zealand. Standards New Zealand, 2004.

[10] NZS 3602. Timber and Wood Based Products for Use in Buildings. Standards New Zealand, 2003.

[11] NZS 3404. Part 1, Steel Structures Standard. Standards New Zealand, 1997.

[12] NZS 3101. Concrete Structure Standard, Standards New Zealand, 2006.

[13] AS 1720.1. Timber structures. Part 1 Design methods. Standards Australia, 2010.

[14] Reidbar™ Reinforcing solutions design guide, NZ edition. Reid Construction Systems, Auckland.

[15] Roberto Crocetti and Robert Kliger. Anchorage systems to reduce the loss of pre-stress in stress-laminated timber bridges. Paper presented at the International Conference on Timber Bridges, ITCB 2010.

ICTB 2025. 5th International Conference Timber Bridges
Rotorua, New Zealand, 29 June to 2 July 2025.

DESIGN OF TIMBER BRIDGES IN EUROPE

Matthias Gerold [1], Steffen Franke[2]

ABSTRACT

Design rules of Timber Bridges are published as EN 1995-2:2010-12 [1]. The second generation implements new knowledge gained the last 20 years. The aim especially was to improve the structure and clarity of the code family. Consolidation on European design practice has been a great part of the work. Although the calculation of timber bridges has become a common practice, the protection of timber is as much a tradition as it is an architectural taste. A timber bridge according to the Eurocode is expected to resist for its design service life independent on being located far south or far north in Europe, in the Alpes at high altitude as well as on a windy coast. The term protected timber bridge is introduced, where weathering is not expected to govern the design service life. All parts of EN 1995-2 [1] have been examined and updated if needed, as presented here.

Keywords: Timber Bridges, Design rules, Eurocode

1 INTRODUCTION

In 2004, the EU (including GB) and several EFTA states introduced uniform design codes, the so-called EUROCODEs (ECs). The goal of the European Committee for Standardization (CEN) was to replace the member states differing or even missing design guidelines by a common set of technical rules that provide the same level of safety and thereby to further minimise barriers within Europe. In 2012, the European Commission issued a mandate for the development of a 2 generation of the ECs to ensure their long-term applicability and reflect the constant technical developments and knowledge gains, see Figure 1.

In the work of 2nd generation ECs, updates in EC 0 and 1 forced updates for the other EC's. For the series of standards "EN 1995 – Design of timber structures" (EC 5) experts regularly prepared drafts for specific topics in timber construction (see [2]). After extensive revision of the entire EC 5 series, new versions were available for all members states for Formal Vote (FV), which ends 2025-04 and publication around 2027 [3], [4].

The meaning of the used verb forms are as follows (in all EC's):

shall **requirement;** strictly to be followed ➔ former ()P principle
should **recommendation** (highly); alternative approach where technically justified
may **permission** within the limits of Eurocodes
can **possibility** and capability ➔ only in NOTEs

Figure 1. European design codes – Eurocodes (Source: European Commission, 2021)

[1] Matthias Gerold, Harrer Ingenieure Gesellschaft Beratender Ingenieure VBI mbH, Germany, m.gerold@harrer-ing.net
[2] Dr. Steffen Franke, ETH Zürich, steffen.franke@ibk.baug.ethz.ch

2 SUSTAINABLE TIMBER BRIDGE CONSTRUCTION

One of the main topics of editing EN 1995-2 [1] was the implementation of the specifications of EN 1990 [5] and EN 1991-2 [6], in particular requirements for reaching a design service life of 100 years. Since construction professionals speak the language of implementation planning, a new Annex D is suggested with simplified figures exemplifies how timber bridges can be protected given proper service. Service is topic in another new suggested Annex E covering inspection and maintenance of timber bridges. Both annexes are informative and may be subject to changes nationally.

Like the building construction code, the code for timber bridges was extended to include requirements and regulations for the durability of structures, taking into account the issues of corrosion protection, and special structures like transvers post-tensioned timber decks or timber-concrete composites. The creep factors for concrete in timber-concrete composite bridges are different from those in building constructions, as the cross-sections are significantly larger. Accordingly, a new normative Annex A of FprEN 1995-2 [7] provides relevant conditional equations. Most regulations on timber decks (deck plates) were now added to the normative Annex C of FprEN 1995-1-1 [8].

Eurocode 8, Part 2 ("Design of structures for earthquake resistance"), takes in 2nd generation also timber bridges into account. In an Informative Annex C of FprEN 1995-2 [7], additional hints for the design of bearings are given. It is also relevant to point to the Informative Annex B, which contains suggestions to be considered in view of deformations and dimensional changes of timber constructions under changing environmental conditions such as temperature or timber moisture, and notes on transversely prestressed timber deck plates (among other things for the "cupping" of the deck sides) [2]. It was also decided to move fatigue requirements into the general part 1-1 as these may be necessary also for buildings with cyclic loads such as industrial buildings, crane structures, highway traffic sign posts, wind turbine tower, or bell towers.

With the technical work being done, the document is being translated into German and French. The remaining steps of the standardisation process are shown in [3] and [4].

3 DURABILITY

3.1 Durability of wooden members

General requirements regarding expected service life, i.e. design service life T_{lf}, that form the basis for all bridge design in Eurocodes are given in EN 1990, A.2 [5]. Together with recommendations on Quality Management the requirements on Durability as well as on Inspection and Maintenance form the basis of a bridge building. These are defined as:

Definition **Maintenance:** Set of activities performed during the service life of the structure so that it fulfils the requirements for reliability.

Chapter 6 **Durability:** All structural parts that rely on a design to satisfy their durability requirements over the design service life **shall** be designed to permit inspection and maintenance. Matters of durability, moisture and moisture content **shall** be given particular attention in the design, see 4.1.2 and 6. Bridges shall be designed to avoid damages from excessive deformation during the intended design service life.

Subclause **Quality Management:** Appropriate quality-management measures **should** be implemented to provide a structure corresponds to the design requirements and assumptions. The following quality-management measures **should** be implemented:

- organizational procedures in design, execution, use and maintenance
- controls at the stages of design, detailing, execution, use and maintenance.

Based on this, different categories are defined for design service life. For bridges, 100 years is the basic option or choice - independent of material types. Lower service life may be relevant for simple bridges used for instance in recreational purposes where consequence of failure is very little, but still 50 years are expected. Further, lower service life is given for replaceable structures (25 years) and temporary or unprotected structures (10 years).

For the design of durable timber bridges the term **Protected and Unprotected Member** are included. The definitions are:

Protected Member

Structural member not exposed to direct weathering such as rain, snow, or other sources of moisture ingress.

Examples of protected timber bridges are given e.g. in Figure 2.

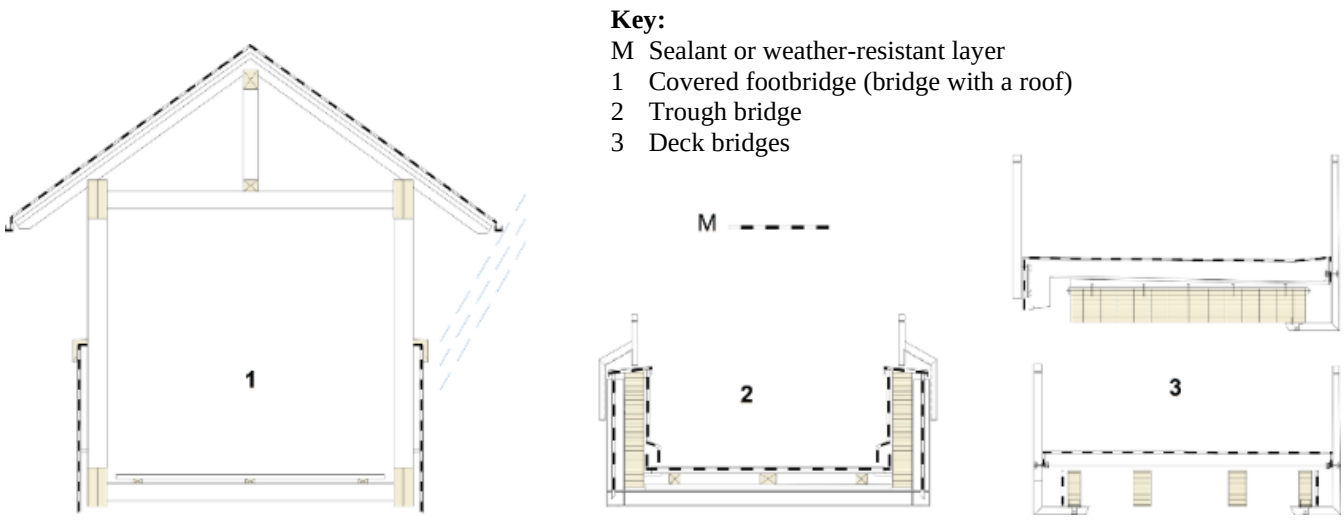

Figure 2. Examples of protected bridges (Source: FprEN 1995-2, Figure 3.2 [7])

Unprotected Member

Structural member that is not protected or partially unprotected from weathering but is within the limits of Service Class (SC) 3.

The methodology is that a protected timber bridge is expected to last for 100 years. When parts of a structures are not within the definition of a protected member these must either be easily replaceable or the expected service life will be less than 100 years. Durability and thus sustainability ensure the economic viability of timber structures. Therefore, the following so-called “magic triangle” must be observed, Figure 3:

Requirements on basic structural protection are given in FprEN 1995-1-1 [8] and EN 1995-2 [1], in some countries with additional nation requirements. This leads to a higher robustness of the expected service life, expecting to lower maintenance costs.

2nd generation of EN 1995-2 includes detailing by figures in Annex D how timber bridges can generally be protected. Five possibilities for basic structural timber protections are given (see Figure 4), together with more detailed examples on expansion joints between superstructure and road (three possible solutions) and bridge caps (2 examples). Furthermore, a suggested monitoring scheme is included as monitoring timber bridges may be a useful addition to inspection, in some European countries mandatory. Currently an arch bridge is taken as example showing which part of the bridge is expected to be critical and thus wise instrumenting, also with regard to the Use Class (UC) according to EN 335 [9].

Because of translation of European standards all figures are language neutral, creating rather lengthy keys to each figure, e.g. in Figure D.4 FprEN 1995-2 [7], see Figure 4.

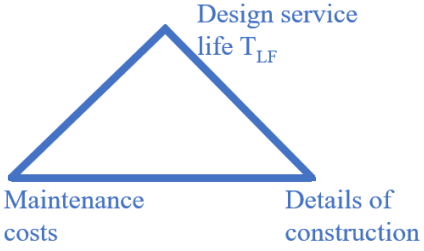

Figure 3. Magic Triangle (Source: Matthias Gerold)

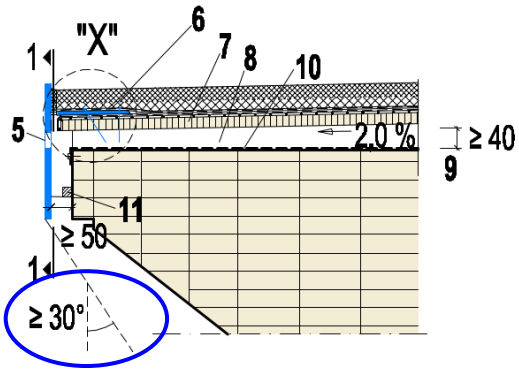

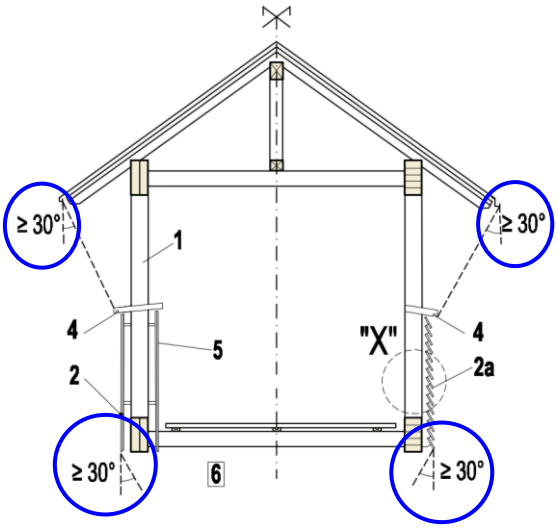

The angle of at least 30o to the vertical at which windblown rain is assumed to fall is shown in blue

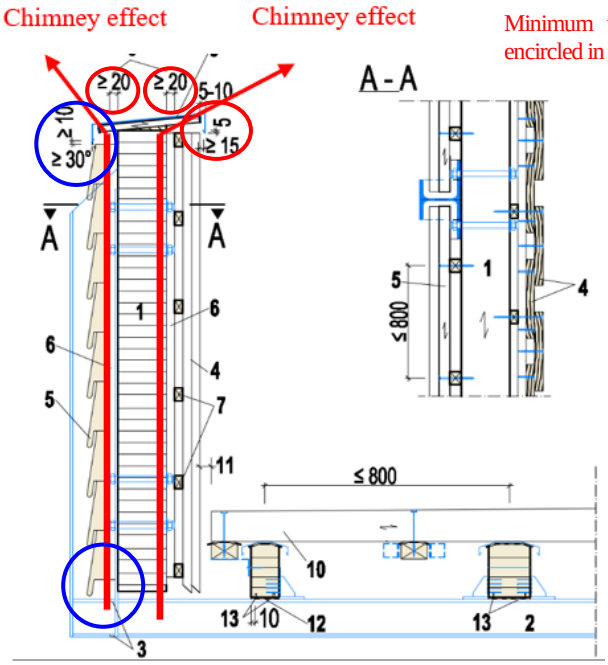

Minimum ventilation openings for the chimney effect encircled in red

Key

M Sealant or weather-resistant layer
A-ASection A-A
1 main girder
2 steel frame
3 borehole in top and bottom flange
*4 cladding (generally outside) *)*
*5 vertical weather boarding (outside) *)*
6 vertical battens
7 horizontal battens
8 ventilation openings, horizontal ≤ 100 cm³/m, vertical ≤ 50 cm²/m
9 aluminium plate or equivalent
10 insect mesh
11 grooved deck planks
**) Shuttering elements partially easy to dismantle for inspection.*

Figure 4. Constructional wood protection - possibilities:
top: Asphalt surface (Source: FprEN 1995-2, Figure D.5 [7])
middle: Roof and claddings (Source: FprEN 1995-2, Figure D.3 [7])
bottom: Sheating of through bridge (Source: FprEN 1995-2, Figure D.4 [7])

3.2 Durability of steel members

For steel members the updated standard gives requirements of protection of steel members in wooden structures by declaring a timber exposure category T_E. Different protection levels depending on an atmospheric exposure category C_E, the service class SC and the design service life of 100 years [in brackets 50 years] results in different recommendations of minimum protection either by steel grade or zinc coverage (see Table 1). Requirements of protection of steel in general is covered by Eurocode 3.

Informative typical atmospheric exposures are given in FprEN 1995-2 [7], Table 6.2; e.g. in case of TE3/TE4 and CE2: L_{sea} > 10 km and L_{street} > 100 m and/or low polluted area (< 5 µg/m³ of SO_2).

Table 1. Timber exposure T_E-categories and atmospheric exposure C_E-categories with examples of minimum requirement for thicknesses for pure zinc coating, hot-dipped galvanized coating, and types of stainless steels for timber bridges (outdoor) with a design service life of 100 years [50 years] (Excerpt from source: FprEN 1995-2, Table 6.2 [7])

Situation	***Timber exposure category T_E***	***Atmospheric exposure category C_E***	***Examples of minimum***	
			zinc thickness	***stainless steel grade (type)***
Protected outdoor with access of pollution (SC2 and SC3)	*T_E3/T_E4*	*C_E2*	*T_R3: 40 µm (n/a if T_E4)* *[20 µm (55 µm if T_E4)]*	*CRC II (e.g. 1.4301)*
	T_E3/T_E4	*C_E3*	*C_R3: 110 µm* *[80 µm]*	*CRC III (e.g. 1.4401)*
	T_E3/T_E4	*C_E4*	*C_R4: n/a* *[110 µm]*[j]	*CRC III (e.g. 1.4401)*
	T_E3/T_E4	*C_E5*	*C_R5: n/a*[j]	*CRC III (e.g. 1.4529)*
Permanent in contact with ground- or fresh-water (SC4)	*T_E5*	*n/a*[g]	*C_R5: n/a*	*CRC III to CRC V*

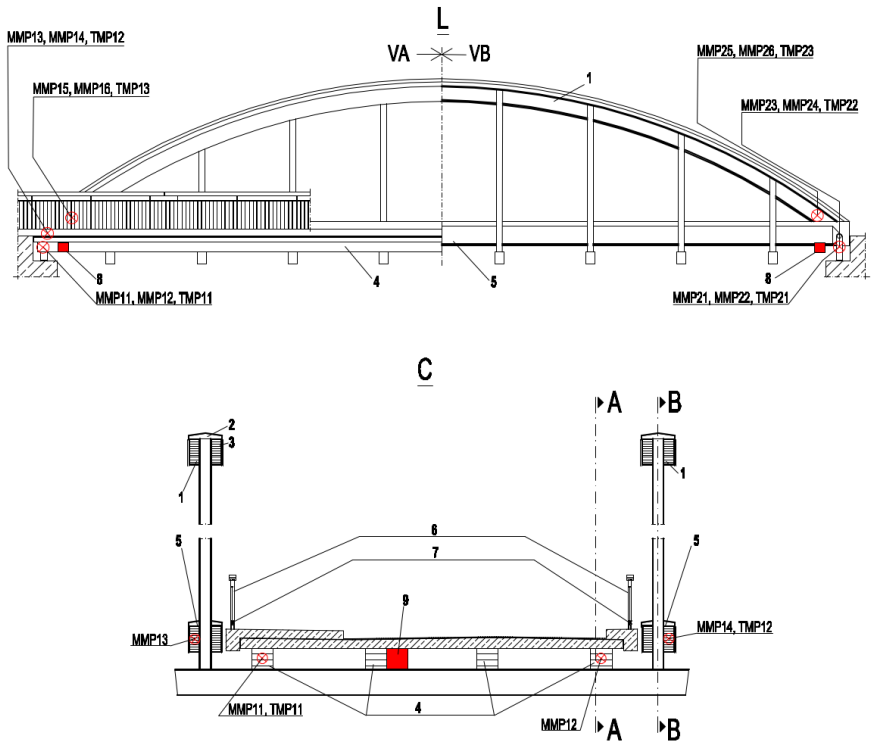

Key

1 arch truss UC 2
2 roof board
3 lead sheet
4 longitudinal beam UC 2
5 pliers beam UC 2
6 railing vertical components UC 3.1
7 railing horizontal component UC 3.2
8 instrument box 1 (or 2)

MMP Moisture measurement point
TMP Temperature measurement point

Figure 5. Moisture monitoring – example arch truss (Source: FprEN 1995-2, Figure D.13 [7])

4 INSPECTION AND MAINTENANCE

See introduction clause 2 and subclause 2.1 (→ Annex B)

Regarding sealant systems see [12].

As already mentioned, a monitoring of timber bridges may be a useful in addition to inspection. Currently an arch bridge is taken as example (see Figure 5) showing which part of the bridge is expected to be critical and thus wise instrumenting, also with regard to the Use Class (UC) according to EN 335 [9] (Table 2).

5 OTHER MEMBERS

5.1 Timber-Concrete Composites (TCC) and Integral abutments

TCC decks are included in the updated bridge standard, giving requirements on design and recommendations on durability and design. In the Technical Specification CEN TS 19103 the load-bearing capacity and deformation behaviour of a notched connection in a girder as a shear connection is regulated. Looking on the uplift forces of the notch the loading for the waver-head screw (see Figure 6) are given.

Table 2. Components of an arch road bridge (example), Source: FprEN 1995-2 [7], Table D.1

Component	***Use class (UC)*** ***[Service class SC]*** ***EN 350 [10]*** ***[FprEN 1995-1-1]***	***Protective measure*** ***FprEN 1995-2 Sample drawings***	***Wood type*** ***EN 13556*** ***[11]***	***Durability Class (DC)*** ***EN 350 [10],*** ***Table B.1***
Longitudinal beam	*2 [4]*	*Weather protection through roadway slab and deck planks and transition, protection of the edges (grain-cut timber), protection against insect attack through technical drying, visibility and control of insect infestation*	*Larch or Pine or Douglas fir as glulam*	*4*
Arch truss / pliers beam	*2 [4]*	*Weather protection by cladding and shuttering, protection against insects by technical drying and insect protection grid, visual inspection every 6 years by removal of claddings*	*Larch or Pine or Douglas fir as glulam*	*4*
Railing	*Vertical: 3.1 [2]* *Horizontal: 3.2 [2]*	*None, maintenance component*	*European larch*	*3*

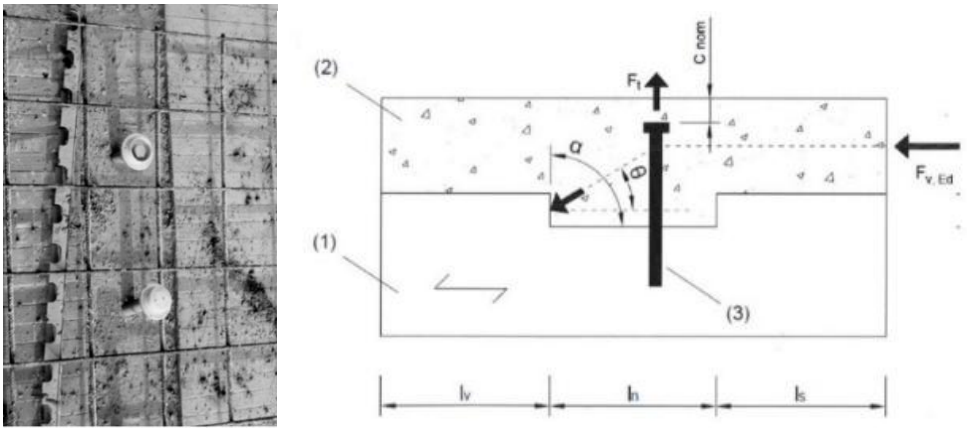

Figure 6. Weaver head screws and notched connection, Source: Mattias Gerold, CEN/TS 19103

Based on the research mainly made at the University of Stuttgart the rheological material behaviour (shrinkage and swelling) is temporary conversely. Therefor the period from 3 to 7 years has to be taken into account.

Creep must be evaluated carefully and as such this is also topic in the updated draft. Basically, all connectors regulated by a national technical approval or European Technical Assessment (ETA) may be used.

Integral timber bridges, bridges with a flexural connection to a concrete abutment (see Figure 6 and Figure 7 showing the Rokoko- and the Bahnhofsbrücke in Schwäbisch Gmünd, Germany) have gained some experience and are also included in the timber bridge code.

Figure 7. Examples of integral timber bridge designs, Source: Matthias Gerold

5.2 Timber Deck Plates

Timber deck plates comprise decks made of solid-wood beams arranged side by side in the direction of span, clamped together (see Figure 8). As a result, the (punctual) wheel loads can be distributed over several beams. Nowadays, these deck plates (timber decks) are largely used in Scandinavian and Baltic states often using glued laminated timber (GL) as beams and stressed together with steel rods. Requirements regarding these structures have been updated representing state of the art including newer research on the topics.

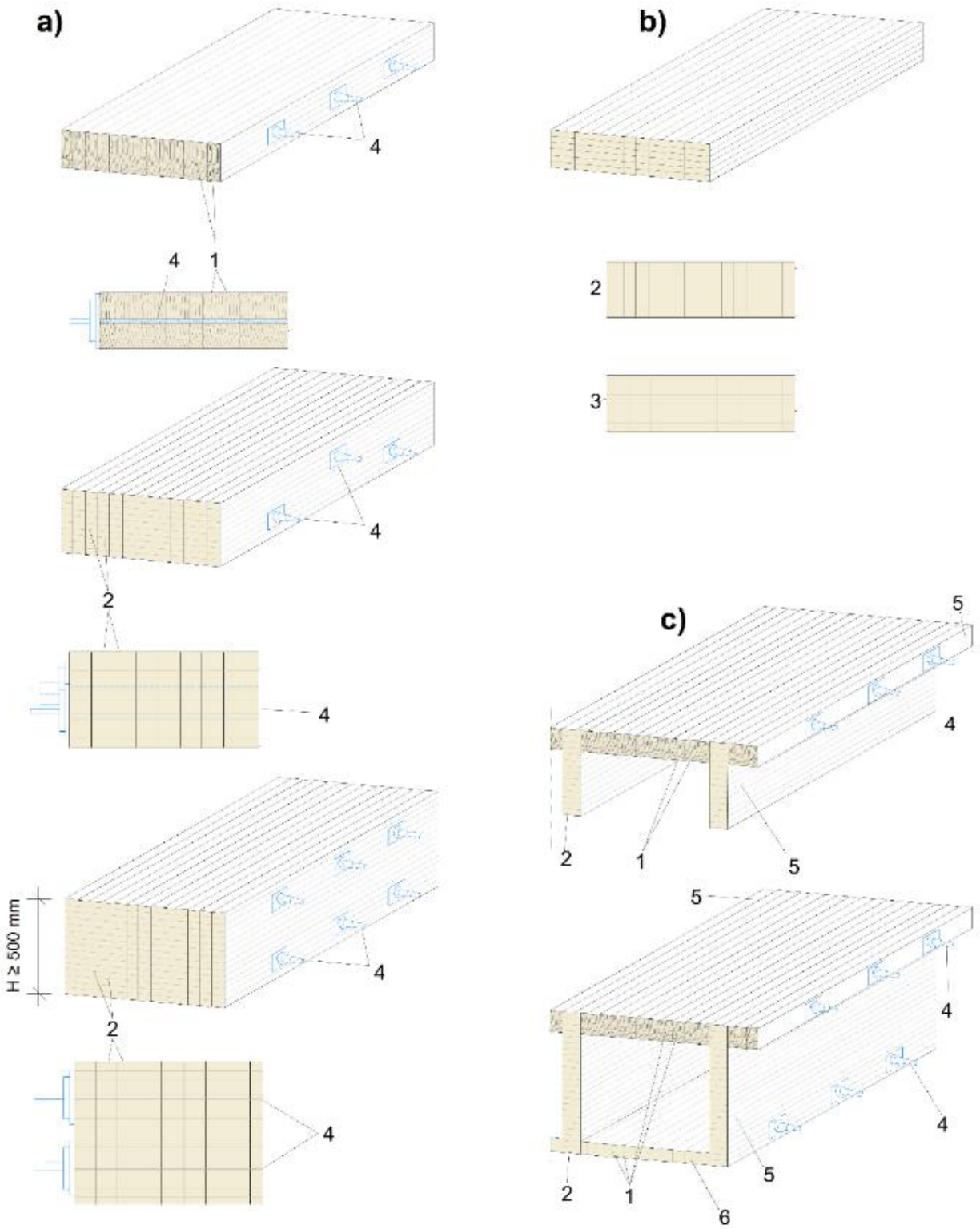

Key

a) Stress-laminated decks, b) Solid timber or glulam beams, c) Stress-laminated T-beams and box girders

1	solid timber beam	4	prestressing bar or tendon
2	glulam beam	5	glulam / GLVL beams as web
3	block glued glulam beam		

Figure 8. Examples of transvers post-timber decks for bridges made of lamellas, Source: FprEN 1995-2, Figure 8.1 [7]

6 SERVICE LIMIT STATE

6.1 Deflections and deformations

Requirements on deflections due to traffic-load and wind-force have been updated (see Table 3) due to the requirements in EC 0 [5]. These actions should be verified and limited in order to prevent unwanted dynamic impact due to traffic, infringe of required clearances and cracking of surfacing layer, ensuring also sufficient run-off from standing water.

Table 3. Limiting values for deflections of timber beams, plates and trusses (NDP)

Action (Frequent load value)	**Range of limiting values**	
	vertical	**horizontal**
Traffic loads on road bridges	L/500 to L/650	-
Low traffic loads on footways, cycle tracks and pedestrian bridges	L/500 to L/900	-
Wind forces	-	L/600 to L/1500

6.2 Vibrations/Oscillations and damping

A rather large update has been conducted on the subjects vibrations and damping. Simplification regarding requirements given in other parts of Eurocodes are introduced in the timber bridge part, Annex F. An example is shown in Figure 9, where different requirements are gathered in one requirement, see black line in Figure 9.

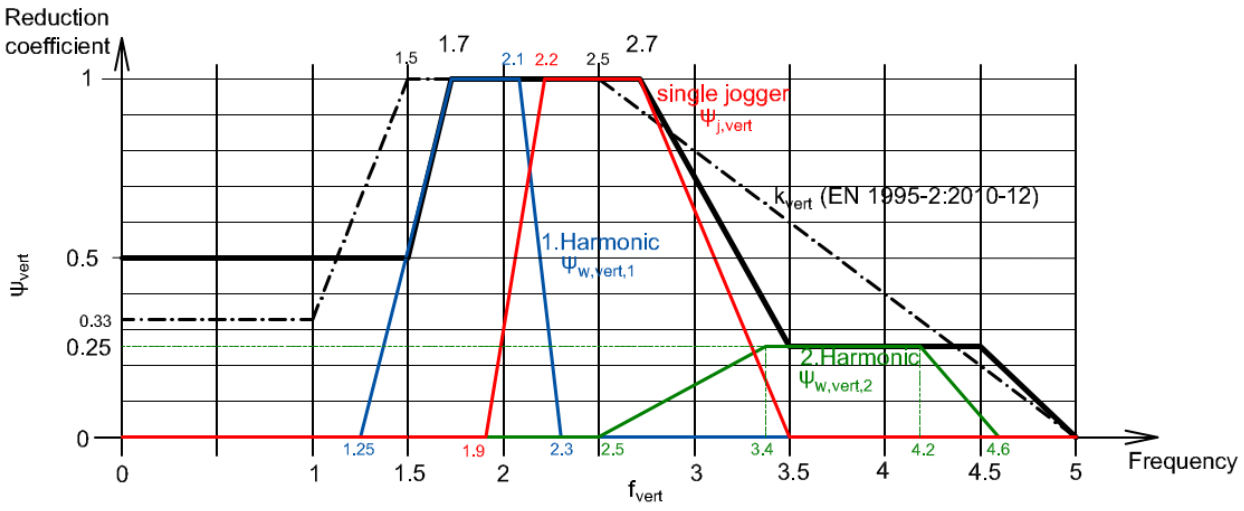

Figure 9. Relationship between the vertical eigenfrequency f_{vert} and the coefficient ψ_{vert} (Source: Matthias Gerold, Patricia Hamm)

7 FATIGUE

As already mentioned it was decided to move fatigue requirements into the general part FprEN 1995-1-1 [8]. This means that in FprEN 1995-2 [7], only those parts were kept that are relevant for timber bridges.

Basis in fatigue verification is the stress ratio R_T as the arithmetical minimum stress to the maximum stress of a particular stress cycle in timber design. Since the factor representing the reduction of fatigue strength with number of load cycles k_{fat} values depend on R_T, a simplification is given in the background document (BGD) to offer a real advantage over the 'full' k_{fat} verification. Therefore, it is proposed to consider only whether the fatigue loading is alternating or not and to use the k_{fat} values for $R_T = 0$ or $R_T = -1$, respectively.

The k_{fat} values were evaluated for two lanes and 2 x 106 cycles (trucks), giving anticipated 100 years design service life using an ß-factor equal to 3 (substantial consequences). This yields a design load cycle number of 1.2 x 109.

8 CONCLUSIONS

The completion of the work on the European timber construction standards is scheduled for 2026/2027. Current status for the timber bridge code is that the comments given in the public Enquiry 2023 (together with all other parts on timber structures; i.e. part 1-1 General rules and rules for buildings, part 1-2 Fire design and part -3 Execution) were answered. After FV, no new technical content will be added; only changes to what is suggested will be made, thus most of the essential changes are already known.

The scope of the standard will inevitably grow, as new timber construction products need to be considered and known design approaches need to be extended and optimised. The update is guided by the central interest of increasing the user-friendliness – not only by profiting from digital availability and efficient search options but also by restructuring, homogenising, and simplifying the regulations.

Nevertheless, as with the adjustment of the first generation of EC 5, an additional process of learning, training, and education will be necessary, with this process starting already prior to the final publication. In conclusion, it may be stated: the second generation of EC 5 is not a revolution but an evolution that consistently builds on the experiences and principles of the previous version.

Common practice design examples of a variety of bridge structures are presented e.g. in [13].

REFERENCES

1. EN 1995-2:2010-12 Eurocode 5: Design of timber structures - Part 2: Bridges, European Committee for Standardization, Brussels
2. Simon, A.; Gerold, M.; Burkart, H.; Müller, A. 2025 The 2nd generation of the Eurocode on Timber Bridges. In.: World Conference on Timber Engineering 2025 (WTCE), Brisbane (Australia)
3. Schenk, M.; Werther, W.; Gerold, M. 2022 The Next Generation – Die Weiterentwicklung der Holzbaubemessung nach Eurocode 5. In: Quadriga, H. 6, p. 16–19
4. Gerold, M. 2022 The further Development of the Design of Timber Structures according to Eurocode 5 – Part 2: Timber Bridges. Overview EN 1995-2 and Annex D Examples for Detailing. In.: 4th International Conference on Timber Bridges ICTB2021PLUS, Switzerland
5. EN 1990:2023 Eurocode - Basis of structural and geotechnical design. European Committee for Standardization, Brussels
6. EN 1991-2:2023 Eurocode 1: Actions on structures - Part 2: Traffic loads on bridges and other civil engineering works. European Committee for Standardization, Brussels
7. FprEN 1995-2:2025-02-03 Eurocode 5: Design of timber structures - Part 2: Bridges, European Committee for Standardization, Brussels
8. FprEN 1995-1-1:2023 Eurocode 5 - Design of timber structures — Part 1: General rules and rules for buildings, European Committee for Standardization, Brussels
9. EN 335:2013 Durability of wood and wood-based products – Use classes: definitions, application to solid word and wood-based products, European Committee for Standardization, Brussels
10. EN 350:2016 Durability of wood and wood-based products - Testing and classification of the durability to biological agents of wood and wood-based materials, European Committee for Standardization, Brussels
11. EN 13556:2003 Round and sawn timber - Nomenclature of timbers used in Europe, European Committee for Standardization, Brussels
12. Müller, A.; Schiere, M.; et al. 2022 Details for timber bridges with asphalt wearing surfaces. Creating a connection between asphalt surface and timber deck bridges. In.: 4th International Conference on Timber Bridges ICTB2021PLUS, Biel (Switzerland)
13. Zöllig S., Franke B., Rüegsegger L., Burgherr A. (2025) Bridges in Switzerland - Experience of bridges for pedestrians, traffic and wildlife overpass, In.: 5th International Conference on Timber Bridges ICTB2025, New Zealand

ICTB 2025. 5th International Conference Timber Bridges
Rotorua, New Zealand, 29 June to 2 July 2025.

GLVL PANELS FOR A NEW TIMBER FOOTBRIDGE OVER THE BRUSSELS RING

Laurane Néron[1], Thijs Van Roosbroeck[2], Benoît Hargot[3], Samuel Blumer[4]

ABSTRACT

As part of the R0 East ring optimization in Brussels, a 67.5-meter span timber footbridge is being constructed over the Vier Armen intersection to provide a direct connection for cyclists and pedestrians. The footbridge features Glued-Laminated Veneer Lumber (GLVL) panels as the main structural material, showcasing a novel approach to the construction of covered timber bridges.

1 INTRODUCTION

The Flemish Government is seeking to reconnect the areas inside and outside the Ring of Brussels, through the project "*Werken aan de Ring*" led by *De Werkvennootschap.* The new bicycle and pedestrian bridge over the busy Vier Armen intersection will be an important link on the yet-to-be-built F29 cycle highway connecting Brussels, Tervuren and Leuven. *Ney and Partners* has been selected as the architectural and structural design office for these projects. In collaboration with *WOW Engineering*, the Vier Armen footbridge was an ideal opportunity to explore innovative ways to construct bridges with timber.

2 BRIDGE DESIGN

2.1 Integration in the surroundings

The bridge is situated in the eastern part of Brussels at the intersection of Tervuren Avenue and the ring road. This intersection is characterized by its high traffic volume, with vehicles, bicycles, and trams all traversing at ground level. This configuration poses significant safety concerns for all road users. Consequently, the client sought to redesign the intersection to enhance safety and improve the experience for all users.

The bridge creates a bicycle and pedestrian connection between two green areas from the Sonian forest separated by the R0 ring road. The bicycle bridge is designed as an integrated element within the forest areas rather than an additional infrastructure element on top of the existing roads. The design emphasizes safety, comfort, and integration into the environment, with as little interaction as possible with the underlying busy intersection and tunnel of the ring road.

The bridge was constructed from a single 67.5m span to minimize interaction with the infrastructure. The choice of timber in the bridge design is obvious in this forested environment. However, timber was not only used for cladding and finishes, but also for the load-bearing structure. The single span requires a structural height that is provided above the bridge deck in order to keep the bridge deck as low as possible, minimizing the height to be climbed by cyclists and increasing cycling comfort. A timber box structure made of GLVL panels gives the bridge its required structural height. Cyclists ride through the structure and are shielded from the busy road below at the *Vier Armen* junction. The landings are made of reinforced earth with green slopes that also blend into the green environment.

[1] Laurane Néron, Structural engineer, WOW Engineering, Belgium, lane@wow-engineering.com
[2] Thijs Van Roosbroeck, Partner, Ney and Partners, Belgium, tvr@ney.partners
[3] Benoît Hargot, Managing director & co-founder, WOW Engineering, Belgium, bha@wow-engineering.com
[4] Samuel Blumer, Consulting engineer, sblumer, Austria, samuel.blumer@sblumer.com

Figure 1. Views of the footbridge crossing the Vier Armen junction ©Corentin Haubruge – Ney and Partners

2.2 Construction system

The concept draws inspiration from the historical tradition of covered timber bridges, which have long demonstrated the durability and structural efficiency of timber in bridge construction. One of the oldest existing examples is the Kapellbrücke in Lucerne, Switzerland, dating back to 1333.

The structural system of those old timber bridges combines two classic principles: that of a truss and an arch. This hybrid behaviour ensures efficient load transfer along the span, while the two main load-bearing axes, running longitudinally on either side of the deck, also serve as guardrails for user safety. The construction involved the use of small pieces of lumber, which were connected to achieve a longer span. The roof plays a key role in stabilizing the structure horizontally and protecting the timber elements from rain and UV exposure, significantly improving the long-term durability of the structures.

Figure 2. Historic pictures of covered timber bridges

2.3 GLVL as building material

The bridge is entirely constructed using Kerto Q panels, which are supplied by MetsaWood. The standard panels are glued together to form a robust and substantial cross-section, up to 216 mm in thickness, for the bridge's walls. The selection of Kerto Q was influenced by its strength in two directions and its dimensional stability. The cross layer functions as a locking layer, thereby restraining the swelling or shrinkage of the wood. This is particularly crucial for a structure of such magnitude, where it is imperative to mitigate the expansion of the wood.

The timber box girder is comprised of a bottom flange, side plates, and a top flange, each of which is made of Kerto® GLVL-Q panels and serves a primary function in the main load-bearing structure of the bridge. The design is an integrated solution, with each component fulfilling multiple functions. The bottom flange serves as the bridge deck. The lateral panels serve to protect the users from vehicular traffic and also function as parapets. The top flange serves as a protective roof, shielding users and the underlying timber structure from rain.

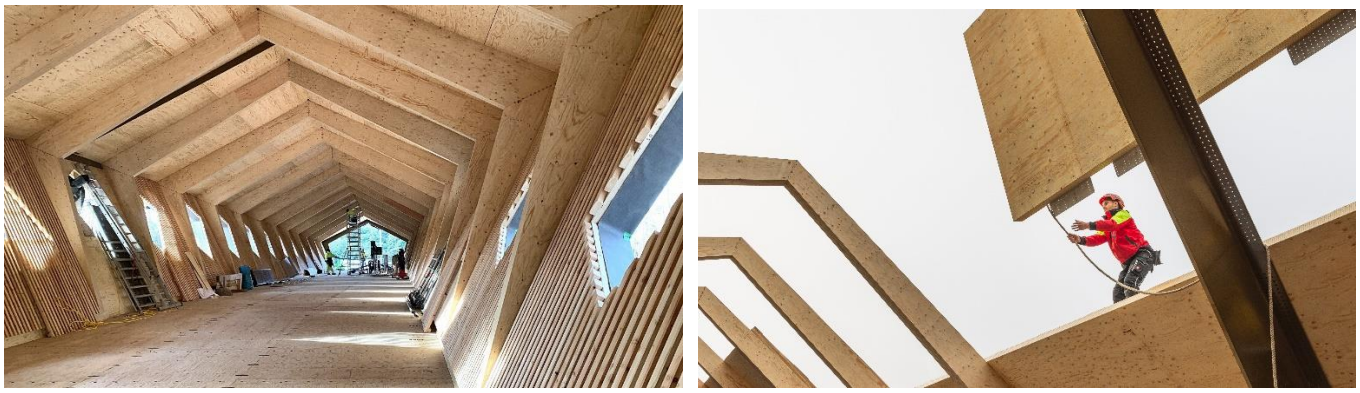

Figure 3. GLVL panel installation

3 DURABILITY AND RISK MANAGEMENT

In the field of timber construction, effective water management is crucial for ensuring the durability and longevity of the structures. This was a fundamental consideration in the design of this bridge, and several measures were implemented to achieve a robust solution that would protect the structural elements from humidity.

3.1 Geometry

The roof's geometry is specifically designed to prevent driving rain from coming into contact with the structure. In both transverse and longitudinal sections, the roof extends far enough to shield the structure from rain at an angle of 45°. The bridge deck incorporates a 2% longitudinal slope, allowing any water that reaches the deck to drain towards the abutments.

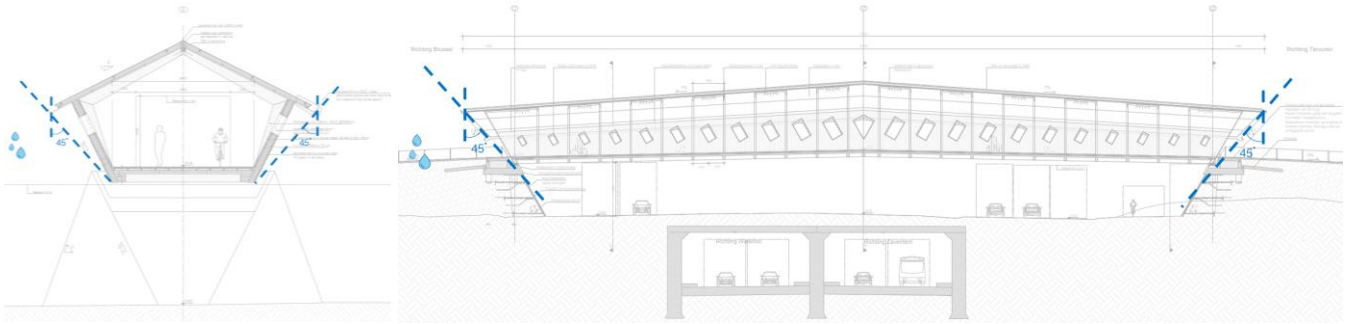

Figure 4. Geometric rules to protect timber from rain

3.2 Monitoring

Furthermore, a series of sensors has been installed with the objective of monitoring the timber elements over time and detecting the presence of moisture. Three distinct types of sensors are employed:

- Moisture content sensors: Pins connected by electrical wires are embedded in the GLVL panels at critical joints of the deck, façade, and roof to measure moisture content.
- Leakage detection system: A membrane (smartex® by Progeo) covers the entire deck area, complemented by detection stripes along the perimeter of the roof to identify potential leaks.
- Inclinometers are also place near the support to measure the deformation of the bridge

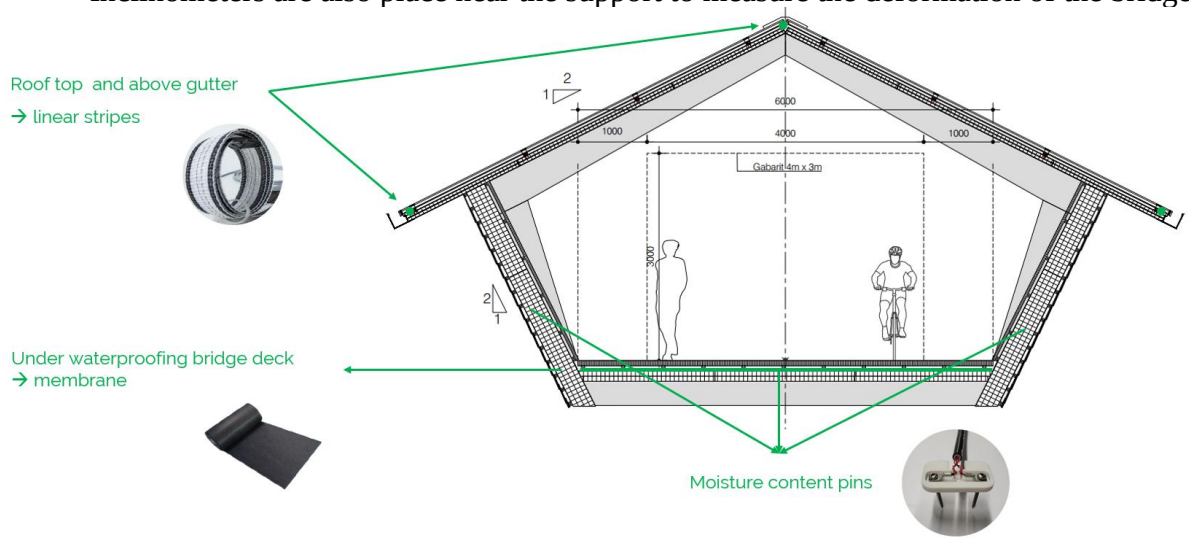

Figure 5. Implementation of monitoring system

All data is collected by the client, and alerts are triggered if threshold values are exceeded. This monitoring system, combined with regular visual inspections, enables early detection of any anomalies, allowing for timely interventions to prevent damage from escalating. This thoughtful approach to water control not only improves the durability of the timber structure but also demonstrates timber's viability as a resilient material in modern, weather-resistant construction.

3.3 Finishes

The bridge incorporates a range of high-quality finishes to ensure durability, functionality, and aesthetic appeal:

- The roof is clad with aluminium panels, providing robust protection against the elements.
- With a usable width of 6 meters, the walking surface on the bridge deck is con-structed from wooden larch planks with anti-slip grooves to enhance safety.
- The inner surfaces are lined with a secondary structure of larch slats. This secondary layer, commonly used in wooden bridges, protects the main structure and can be replaced if necessary. In addition, the non-planar surface design helps to deter graffiti, as the irregular texture makes it difficult to apply and maintain graffiti.
- The facades are covered with Western Red Cedar shingles. This traditional wood tile technique provides effective protection for the GLVL panels while maintaining the natural, warm appearance of timber.

Figure 3: Finishes of deck, façade and roof

4 STRUCTURAL FEATURES

4.1 Timber box girder

The structural bearing system of the bridge is ensured by a timber box girder made of GLVL panels acting as flanges and webs, and combined with transversal frames of the same material. The roof operates primarily in compression, the deck in tension, and the facades channel shear forces toward the supports.

A distinctive feature of the construction is that the four LVL layers that comprise the walls have been angled prior to the application of adhesive. At mid-span, all the layers were oriented longitudinally in order to primarily transfer tension and compression forces. However, as the distance from the supports is reduced, the external layers rotate towards 90°. This rotation of the cross layers has been shown to enhance the structure's vertical stiffness. This approach enabled the transfer of a greater proportion of the compression forces from the roof to the abutments. This results in the formation of an arch effect, which in turn serves to reduce shear forces within the panels and optimise their dimensions.

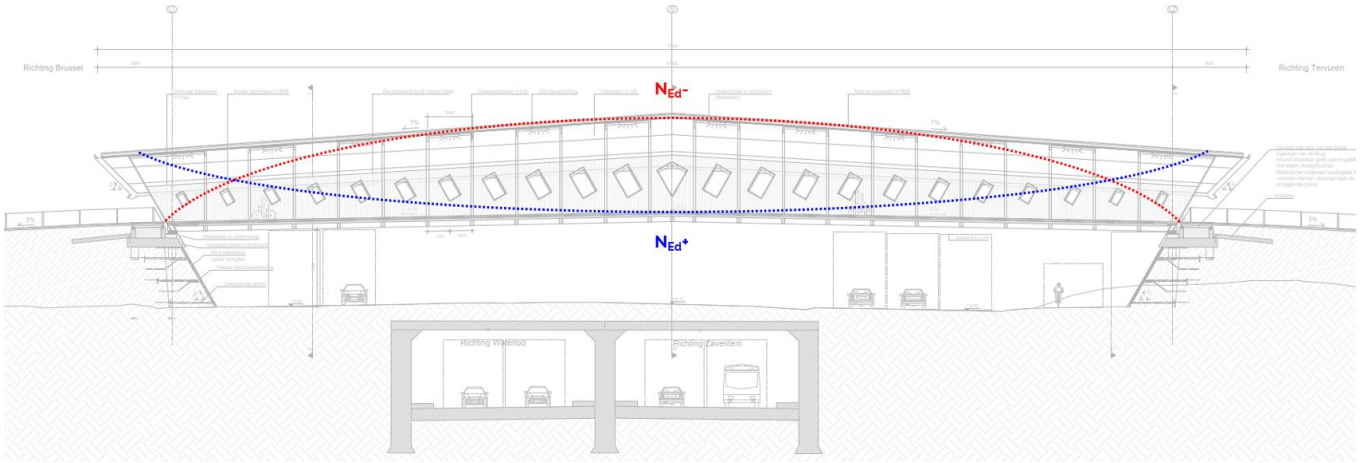

Figure 6. Flow of forces in the timber box girder

The structural height of the timber box increases toward the mid-span, where a higher sense of space is achieved, enhancing the user experience. This geometric configuration also aligns with the structural demands, as additional inertia is required at the centre of the span, where the bending moment is highest. Consequently, the structural height above the bridge deck ranges from 5.6 to nearly 7 meters.

To increase the incidence of natural light and provide cyclists with a view of the exterior, openings are cut in the side plates at a fixed rhythm of 3 metres. The openings become smaller towards the support points,

where more structural material is required, and increase in size at mid-span, where the structure allows material to be removed from the side plates. The shape of the openings is based on structural logic on the one hand and is determined by the regulations for parapets on the other. The bottom of the openings is sufficiently high above the tread so that no additional features are required as parapets.

Achieving the final structural geometry required an iterative design process, refining the dimensions, joints, and façade openings to meet both engineering and architectural specifications. This process accounted for numerous construction parameters, including standard LVL plate sizes, press dimensions for gluing, transportation constraints, and assembly techniques. Integrating these considerations allowed the design team to arrive at an optimized and functional geometry that aligns with architectural and structural requirements.

4.2 Structural modelling and verification

The construction was optimized through a collaboration between the timber construction contractor Holzbau Amann and the structural engineering firm sblumer, which specializes in timber construction and modeling.

4.2.1 Experimental tests

The deck, wall, and roof elements consist of up to four different LVL panels bonded into a single hybrid section with a thickness of up to 216 mm. The layers were symmetrically and orthogonally, or parallel as appropriate, glued together. Various bending tests have been conducted to determine the mechanical properties of the base material. Tension tests were carried out to evaluate the resistance and spring stiffness of the connections. The tests have been executed at the Material Testing Center in Stuttgart.

Figure 7: Three point bending tests for determination of the mechanical parameters (Left: plate, right: slab)

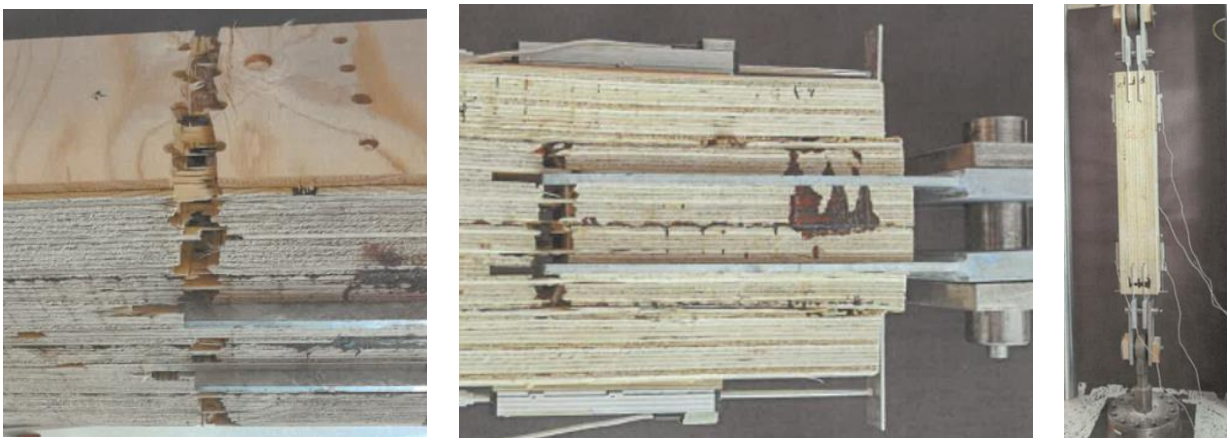

Figure 8: Tensile tests: left failure in the net section. Right failure: bloc-shear.

4.2.2 Optimizing of the structure

In the execution, the tender proposal has been optimized for a more resource-efficient solution. This was achieved through more detailed modeling, smaller dowel diameters for better ductility, fewer dowels in a row, and optimizing the structural system by removing a wall opening in the support region. The main connection details have been designed with three or, at most, four dowels in a row. The reason for this simplification was the limitation of cutting depth and ductility. Additionally, tension tests were adapted to all possible connection configurations of the project. Even though the modifications were made, the sophisticated initial architectural and structural design was preserved.

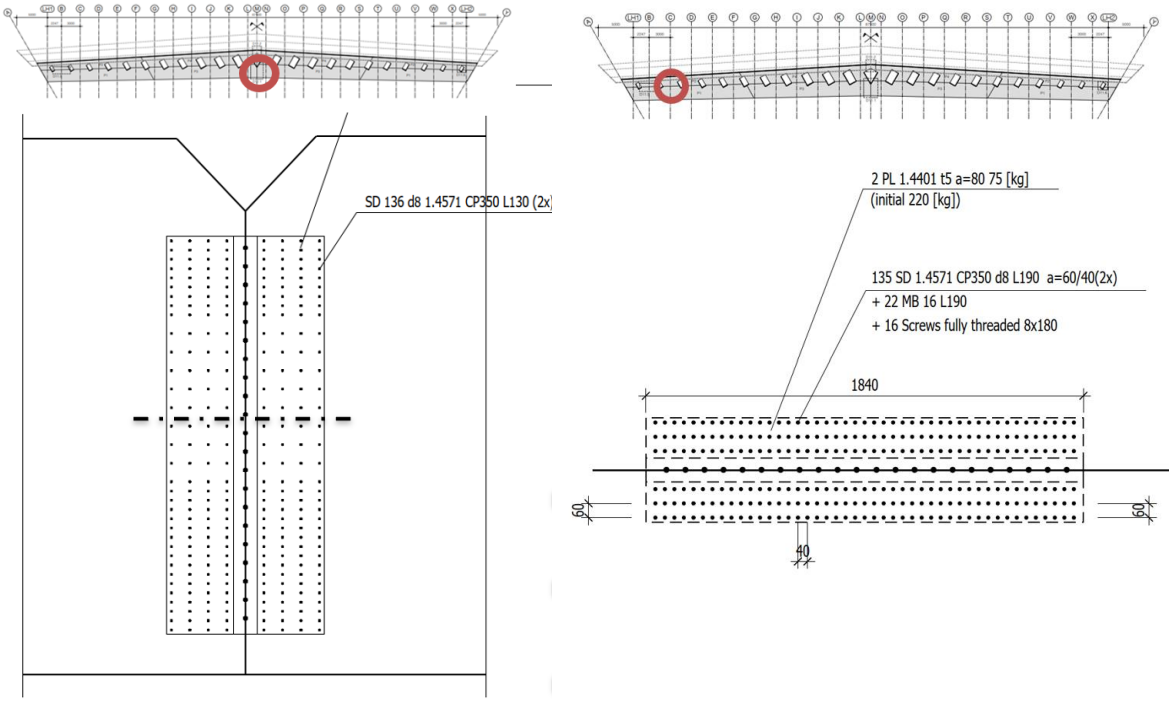

Figure 9. Connection: Left main joint in the middle of the bridge, right: Shear joint of the wall. ©sblumer

4.2.3 From FE modeling to detailing and production

The stiffnesses and material properties determined from the tests were implemented into the FE model. Since the spring stiffnesses of dowel connections differ between various standards (e.g., Eurocode and SIA), a limit analysis for the stiffnesses was carried out. To reduce sources of error, a consistent numbering of the elements and connections was developed. The following illustration shows the closed loop between modeling and detailing.

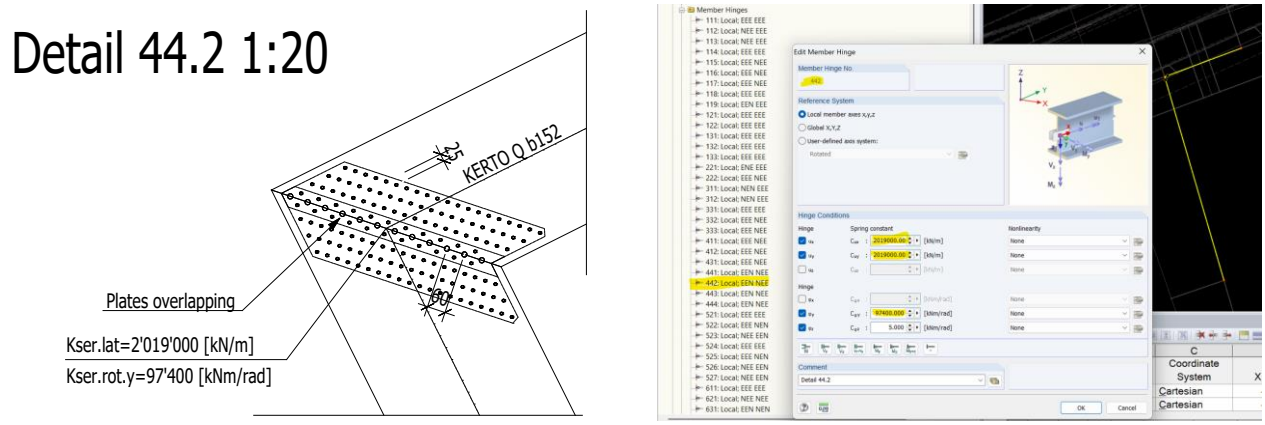

Figure 10. Consistent modelling: Detail Nr. 44.2 correpsond hinge 442. ©sblumer

For verification of the modular connection (ductile dowel connection with max. 4 dowels in a row and the properties of material different test series have been performed. The test results of the three point bending tests and tension test delivered the material properties of the four layered panels consisting of KERTO Q - GLVL.

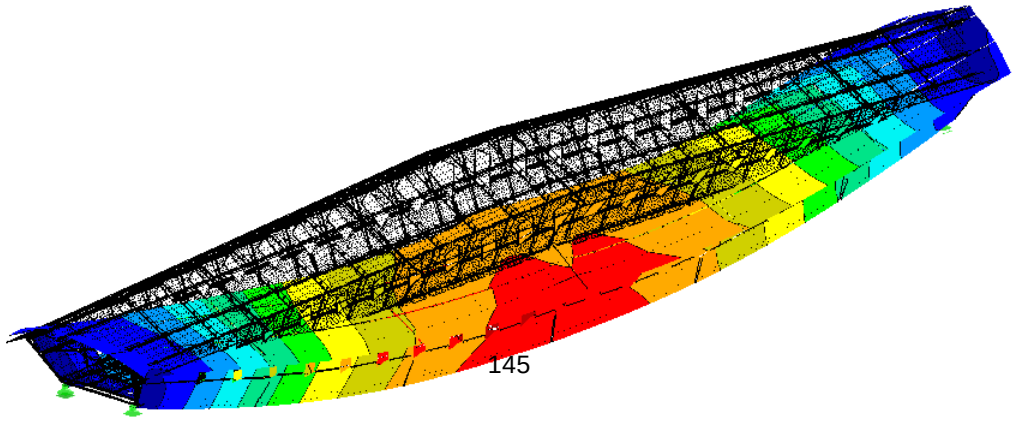

Figure 11. Vertical deformation of the bridge under self-weight (less than 5% variation to measurement) ©sblumer

4.3 Connections of GLVL panels

Three main types of connections were used to assemble the bridge:

- Continuity joints: Steel plates and dowels embedded within the structure were employed to transfer tension and compression forces between segments, maintaining longitudinal continuity.
- Diaphragm Joints: For large planar surfaces, shear connections were managed through steel plates and nails in the roof, while aluminium blocks inserted into grooves facilitated the deck's shear resistance.
- T-sections: To connect the deck, façade, and roof, inclined fully-threaded screws were used, providing a secure and cohesive assembly.

For both aesthetic and durability purposes, the design emphasizes invisible connections, which not only maintain the visual integrity of the timber structure but also shield the steel components from environmental exposure, enhancing long-term resilience.

Figure 12. Assembly of GLVL panels on the prefabrication area ©Ney & Partners

5 FABRICATION AND MOUNTING

Given the bridge's significant span, it was divided into six segments, each no longer than 12 meters, to meet standard transportation limits. The segments were prefabricated in Holzbau Amann's workshops in Germany and then assembled on-site near Tervuren Avenue, approximately 800 meters from the final

installation site. This approach minimized on-site construction, facilitating a rapid assembly process that was completed within four weeks.

To ensure protection during assembly, the division into six segments allowed each GLVL panel section to be quickly covered. After each segment was installed, it was immediately protected with its roof and a waterproofing membrane before the next segment assembly began. This method prevented water accumulation and safeguarded the timber structure.

On October 21, 2024, the bridge, weighing 290 tonnes, was transported from the prefabrication site to its final position. Mounted on Self-Propelled Modular Transporters (SPMT) by Sarens, it was driven to the Vier Armen junction. The final placement on its supports occurred during the night, drawing a crowd of spectators to witness this precise operation.

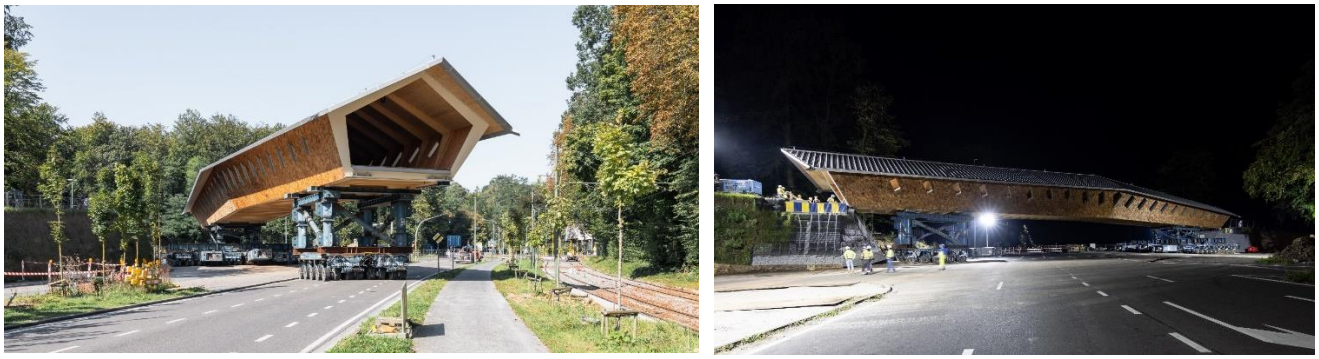

Figure 13. Transportation of the footbridge on SPMT from the prefabrication site to its final location ©Corentin Haubruge

6 ENVIRONMENTAL IMPACT

In an era where reducing carbon emissions is essential to combat climate change, timber bridges offer a promising approach to minimizing environmental impact. By quantifying all emissions associated with a project in terms of CO_2 equivalents, the Global Warming Potential (GWP) serves as a comprehensive metric for evaluating and comparing the environmental impact of different materials and construction techniques.

As shown in the GWP comparison chart of Ney & Partners' bridge projects (Figure 8), the Tervuren timber footbridge achieves a notably low GWP compared to other bridges constructed from conventional materials. The inclusion of timber's biogenic carbon storage further reduces its overall GWP with 280 $kgCO^2eq/m^2$, placing the Tervuren footbridge as one of the most environmentally favourable options.

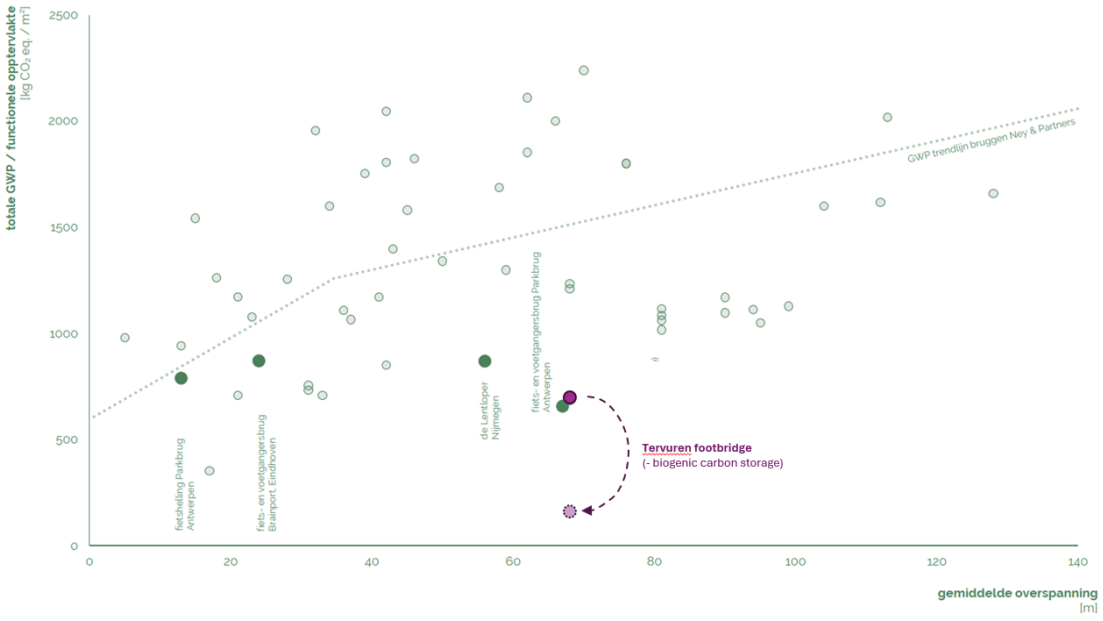

Figure 14. GWP comparison of Ney & Partners bridge projects

7 CONCLUSIONS

The 67.5-meter span timber footbridge, constructed using glued GLVL panels as the primary structural material, represents an innovative and sustainable approach to covered timber bridge design. This project demonstrates the feasibility of achieving long spans without intermediate supports, underscoring the potential of timber in applications traditionally dominated by concrete and steel. By incorporating a bio-sourced material, the bridge not only reduces embodied carbon but also aligns with modern environmental goals for minimizing the ecological footprint of infrastructure.

8 ACKNOWLEDGEMENT

The following participants, among others, were involved in the project:

Projectteam:	Fietsbrug over Vierarmenkruispunkt
Client:	De Werkvennotschap BE-1210 Brussel
Architect, structural design:	Ney & Partners WOW Engineering BE-1170 Brussel
General contractor:	Viabuild! BE-2870 Puurs-Sint-Amands
Timber construction:	Holzbau Amann GmbH DE-79809 Weilheim-Bannholz
Executive timber engineering:	sblumer ZT A-8042 Graz
Tests GLVL and joints:	FMPA Stuttgart DE-70569 Stuttgart

REFERENCES

1. “Fietssnelweg F29”, Werken aan de ring, August 2022, https://www.werkenaandering.be/nl/werken-aan/fietsinfrastructuur/fietssnelweg-f29 (accessed on 26.06.2024).

ICTB 2025. 5th International Conference Timber Bridges
Rotorua, New Zealand, 29 June to 2 July 2025.

EMERGENCY REPAIR OF TIMBER HOWE TRUSS BRIDGE AFTER VEHICLE STRIKE

Johnson, Murray[1]

ABSTRACT

During the early to mid part of the 20th century, the expansion of the road network in the rugged province of British Columbia, Canada into more remote portions of the province depended heavily upon water crossings built of timber Howe truss spans. Hundreds of these bridges were built, taking advantage of plentiful Douglas Fir timber and requiring minimal amounts of iron or steel materials. Today just 20 of these bridges remain, with a total of 25 Howe truss spans, but many of these are on roads that serve as the only link into remote or small communities. One such bridge is the Kispiox River Bridge, with two 130 ft (40m) timber Howe through truss spans completed in 1955. This bridge provides the only access into an area that includes the Gitxsan First Nation village of Kispiox, with over 600 inhabitants. In the winter of 2021, the bridge was struck by a snowplough truck passing over it, heavily damaging multiple members along one of the trusses and requiring an immediate closure of the bridge. This had an enormous impact upon the lives and well-being of the people dependent upon the bridge and an emergency repair to re-open the bridge was called for to be completed as soon as possible. The paper describes the damage, assessment, initial re-opening, and repairs, including a discussion about the nature of timber Howe trusses, which while having a lack of redundancy, are also receptive to the replacement of individual truss members with relatively simple methods.

1 INTRODUCTION

The Province of British Columbia (BC) in Canada is a largely mountainous region with extensive forests and innumerable river and stream crossings. When construction of roads began in the mid-1800's, the bridges needed were built mostly from the most plentiful material available, timber. The construction of timber bridges of many types continued through the 20th century, and timber bridges actually dominated the Province's road bridge inventory until about 1980. The most popular timber bridge type for longer spans was the Howe truss. Invented in 1840 by William Howe of Massachusetts, the Howe truss, with timber chords and diagonal members and iron (later steel) vertical rods and connection blocks, was the most popular bridge design in the United States during the last half of the 19th century, and is the structure within many of the covered bridges remaining within the USA today. In BC, the timber readily available near most bridge sites, and the small amount of steel required to build a Howe truss bridge, made the Howe truss a very practical choice for clear spans of up to 55m. Many Howe truss bridges, some nearly a century old, still carry traffic in BC today [1].

Today, the BC Ministry of Transportation and Transit (BCMoTT) maintains a total of 20 water crossings that include timber Howe truss spans. Within these bridges there are a total of 25 truss spans, with 4 deck trusses and 21 through trusses. Few of the timber Howe truss bridges remain on numbered highways in BC, most are on secondary roads serving smaller communities with primarily local traffic, relatively low traffic volumes, and often with available alternate routes for heavy or oversize vehicles.

One of these crossings is the Kispiox River Bridge, in a fairly remote area of Northern BC, built with two 130 ft (40m) timber Howe through truss spans and two short sawn timber approach spans (See Fig 1). Completed in 1955, this bridge provides the only access into an area that includes the Gitxsan First Nation

[1] Senior Bridge Engineer, Elevation Technical Services.
e-mail: Murray@elevationtech.ca

village of Kispiox, with over 600 inhabitants, along with an extensive valley beyond it with about 200 inhabitants along the Kispiox River.

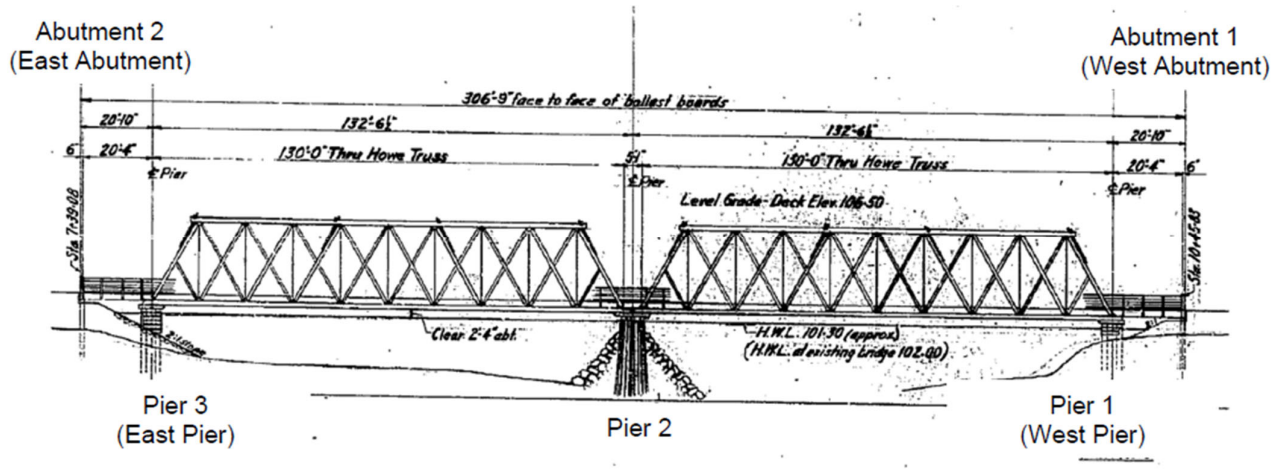

Figure 1. Original Elevation Drawing of Kispiox River Bridge

The Kispiox River Bridge has a 5.5m wide roadway, which by modern standards is a wide single lane, although it's possible for two light vehicles to pass on the bridge. Like most of the Howe trusses in BC, it was constructed of creosote-treated Douglas Fir sawn timber, steel tension and bracing rods, and cast-iron angle blocks. The top (compression) chords are built up from five vertically-oriented plies of 305mm deep timbers with a total width of 635mm while the bottom (tension) chords are built up of six plies of vertically-oriented timbers 356mm deep with a total width of 635mm. Chord plies are bolted together. Main (compression) diagonals are pairs of sawn timbers ranging in size from 203mm x 254mm up to 279mm x 305mm. Counter diagonals are single members of 152mm x 203mm or 203mm x 203mm. Tension rods are provided in groups of three at each panel point, with diameters ranging from 29mm to 44 mm. The floor system on the bridge includes sawn timber floorbeams resting on the truss bottom chords and longitudinal deck planks. Timber curbs and railings on both sides of the bridge form the traffic barriers. (See figs 2 and 3 for views of the bridge).

As previously mentioned, the bridge is the only river crossing for the road network it serves. There is no detour route, and it does not have a load posting (it carries full legal truck loads)

Figure 2. Kispiox River Bridge

Figure 3. End View of Kispiox River Bridge

2 BRIDGE DAMAGE INCIDENT

On February 04, 2021, at about 8:00 a.m., in the middle of the cold Northern BC winter, the bridge was extensively damaged when a snowplough blade projecting from a truck crossing the bridge accidentally struck most of the timber diagonals on the inner side of one of the spans along with several diagonals on the second span. The impact dislodged the first member it hit, a main diagonal at the end of the bridge (end post), moving it laterally off its support by half its width. The interior diagonals struck sustained damage varying from complete fracture to a lesser degree of section loss (see Figs 4, 5, and 6). Several tension rods were also hit, but did not appear to sustain significant damage.

Figure 4. Dislodged End Diagonal (End Post)

Figure 5. Badly Damaged Inner Diagonals

Figure 6. Inner Diagonal With Lesser Damage

With the bridge badly damaged, but still standing, action was taken to immediately close the road to all traffic, vehicular and pedestrian. This effectively cut the community off from the rest BC and from many of their services, including groceries, fuel, schools, medical and emergency services. The emergency response to address the problem is described later in this paper, however to help understand the response, some background information on timber Howe trusses is provided first.

3 HOWE TRUSSES: LACKING REDUNDANCY

Bridge historian Eric DeLony wrote, "The Howe truss may be the closest that wooden-bridge design ever came to perfection. For simplicity of construction, rapidity of erection, and ease of replacing parts, it stands without rival." [2].

The truss design developed by William Howe featured heavy timber diagonal members in compression and lighter, vertical iron (later steel) members in tension, with parallel timber chords. The arrangement of members and connections ensured that compression members could only act in tension, and tension members could only act in tension. Howe's design catered to the limited methods of analysis available at the time: the completely statically-determinate form meant that real forces and stresses could be accurately computed and efficiency achieved while creating a safe structure. The form of a Howe truss is shown in

Fig. 7. The bold lines represent members in compression, the top chord and the main diagonals. Lighter lines indicate members in tension, the bottom chord and the vertical tension rods. The dashed lines are counter-diagonals, which help control the geometry of the bridge but also, in the more central region, counter shear reversal due to the passage of live loads.

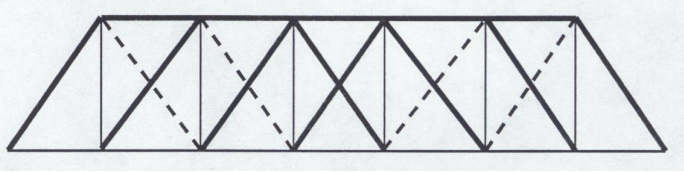

Figure 7. The General Form of a Howe Truss

This is a very efficient design, using the properties of the two materials, timber and iron/steel, to best effect. The ease and accuracy of analysis also allowed for selection of member sizes closely matched to the force effects, hence we see for example, the tension rods and diagonal members varying by quite small increments from panel to panel. The features of the design that made the truss easy to accurately analyse and allowed for such efficiency in materials, however, also make it vulnerable to collapse. With respect to entire truss members, there are no redundancies in the design; with only a single load path throughout, damage that removes or excessively weakens a single member will result in collapse of the entire system. In BC, a number of Howe though-truss bridges have collapsed after being struck by a vehicle or the load on a vehicle, often after one vulnerable member, such as the end diagonal (see Fig. 8). Note while the design lacks redundancy for complete members, there is some redundancy of individual elements of a web member, as the main diagonals are paired timbers, and there are two or three tension rods at each panel point. This feature became extremely important in the case of the Kispiox River Bridge

Figure 8. Willow Bridge Collapse After Vehicle Strike

4 HOWE TRUSSES: SIMPLICITY IN REPAIR

The use of threaded, adjustable iron tension members, secured by nuts, was the feature that made Howe the first bridge designer to devise a method of adjusting a timber truss to keep joints tight. Other versions of timber trusses, which included vertical tension members of wood, were difficult to detail in an efficient manner that would keep joints tight, and Howe's simple, elegant solution of replacing these timber verticals with iron rods resulted in a truss that was not only easy to erect but could be adjusted and have parts replaced while remaining in service [3].

The connections at the truss panel points are at the heart of the success of the Howe truss design. The detail at both the top and bottom chords employs a cast iron "angle block" which is made with bearing surfaces at the correct angle to allow diagonal members with a square-cut end to simply bear against it, with no other connection. (see Fig. 9). In a truss with two vertical tension rods (as in Fig 9), the angle block has two holes through it to allow the rods to pass,

Figure 9. Typical Howe Truss Connection

while in a truss with three vertical rods, the angle block has a single hole for the middle rod, and the two outer rods pass outside the block and the chord. Tension rods are anchored against the bottom chord, and the top of the top chord, by nuts bearing on a steel "gib plate" which bears against the timber. There is no connection between the timber diagonals and the angle block, other than a very small centring pin to locate the timber while the truss is being constructed; in service, this whole joint assembly is kept tight together by the dead load of the bridge itself and the pre-loading of the counter-diagonals resulting from tightening the tension rods.

All of the Howe trusses remaining in BC are similarly constructed. The top and bottom chords are assembled from multiple plies of timber that is creosote pressure-treated prior to assembly with bolts. This creates a robust member that is very resistant to decay, the most common enemy of timber bridges. The chords, being continuous members vital to the functioning of the truss, are difficult to repair, but they are seldom subject to damage from other sources. The timber diagonal members comprise a pair of matching sawn timbers, usually also pressure-treated, but more vulnerable to decay due to the single layer of protection and breaching of the protection due to weathering, checking, or other defects. In the case of through-trusses (most of the inventory), they are also much more vulnerable to damage from vehicles, as in the case of Kispiox River Bridge. The vertical steel tension rods are essentially unprotected, are subject to deterioration from corrosion where they pass through the connection blocks and timber at the bottom chords, and are also somewhat vulnerable to vehicular impact damage.

Howe's design, however, greatly facilitates the feasibility and ease of replacing these more vulnerable members, diagonals and tension rods, in maintaining and prolonging the life of these bridges. This is a significant factor in the fact that many of the surviving bridges are approaching 100 years in age; many of them have had multiple web members replaced over the years. Because the diagonals are paired timbers, and the tension rods comprise a group of two or three, the removal and replacement of a single member is readily achieved without compromising the integrity of the bridge. Loosening of a tension rod aligning with the top of a compression diagonal member will loosen the diagonal and allow for its replacement. Because the diagonal has no connections to the chords, it simply bears on the angle blocks, once it is unloaded it can simply be slid out and a new one cut to the same length inserted. Similarly, removing the top nut of a tension rod allows the rod to be dropped all the way down through the chords and a new threaded rod inserted in reverse.

Typically, the dead load component of force in the truss members is on the order of half of the total design force, so in theory one could remove one of two timbers or tension rods without temporary support. In practice, however, due to potential or known deterioration in the remaining member, and the need for some live load capacity during replacement, it is common to provide some temporary support while replacing the member. In the case of diagonal replacement, this will consist of a jacking strut alongside a diagonal member, loaded by hydraulic jack or a wedge arrangement, while for tension rods a simple clamp between chords with additional threaded rods can be used.

5 KISPIOX RIVER BRIDGE: ASSESSMENT AND INITIAL RE-OPENING

When the Kispiox River Bridge was badly damaged, it was immediately closed to all traffic, including pedestrians. With the loss of their only road connection to the rest of BC, the local community was understandably highly concerned and desiring of the soonest possible restoration of service to the bridge.

The bridge owner, MoTT, assigned an engineering consultant, Stantec (this author's employer at the time) to provide emergency engineering response under an existing service contract. The road maintenance contractor, Dawson Road Maintenance, was already on site and provided initial assessment and road closure measures. The MoTT engaged a bridge contractor from the region, Formula Contractors, who were familiar with work on the bridge type, to immediately deploy to site to help with initial stabilization and ultimate repairs. Multiple stakeholders affected by the closure of the bridge were involved in helping determine immediate needs and ongoing priorities.

With the consulting engineer more than 1000 km and a full day's travel away from the bridge site, the initial engineering assessment, on the day of the damage, relied on descriptions and photographs from those on

site. Concurrently, record drawings for the bridge were obtained from the MoTT's system and an analysis of the bridge begun, with an initial focus on dead loads effects. The immediate concern was the dislodged end diagonal (Fig. 4). The displacement of this critical member off its support, amounting to 50% of its width, reduced the nominal capacity of the member to less than the calculated dead load effect, meaning the bridge appeared to be in danger of imminent collapse, so the initial response was to keep even pedestrians off the span. A more informed assessment of the capacity of the individual timbers within a diagonal was then undertaken based on extensive experience analysing these bridges. This assessment used the actual length of timbers in a diagonal as the buckling length, given the comparative rigidity of the end details, which was about 93% of the workpoint-to-workpoint length generally assumed. In addition, it used a slenderness factor of 0.85 instead of the 1.0 usually assumed, based on the end restraint afforded to the relatively stocky timber members. Based on the results of this analysis, the bridge was deemed to be safe to support its own weight plus the very small live load resulting from pedestrian traffic. This allowed foot traffic to use the bridge with residents parking cars on both sides of the bridge, alleviating some of the isolation from losing the bridge, on the same day the accident occurred. A pedestrian lane was demarcated along the side of the bridge opposite the damaged truss.

Site review indicated that it would be possible to shore up the damaged truss at the first panel point in from the dislodged end post, with cribbing supported off the ground at the edge of the riverbank (see Fig 10). This would remove the load from the dislodged end post and reduce the load on other damaged diagonals. Analysis of the truss with this new end support, along with the member capacity analysis described above, then showed that the bridge could safely support a live load of 8000 kg in a single lane against the undamaged truss, with traffic control and slow speeds. Work was undertaken to install this shoring (see Fig. 11) and a specified load was jacked into the support point to ensure that the reaction was transferred at this location.

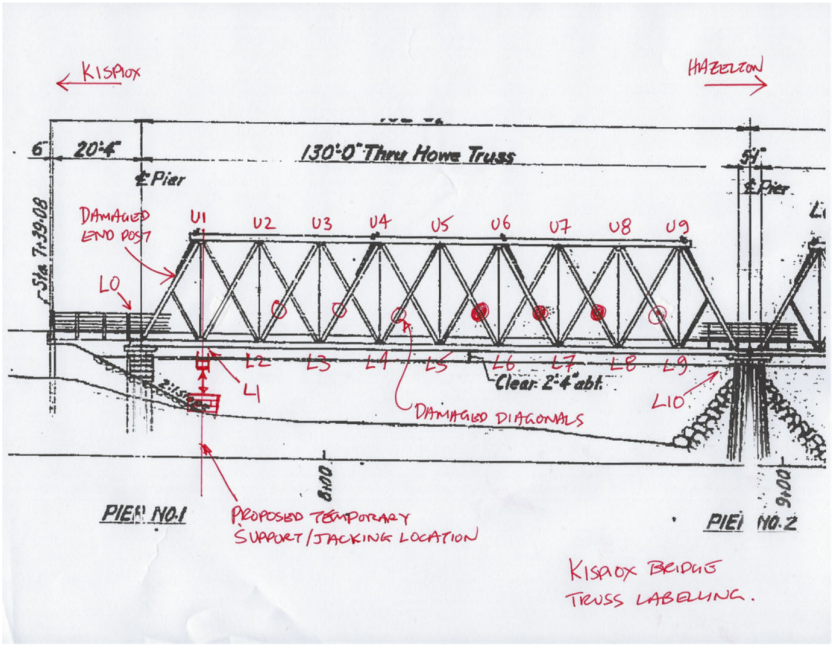

Figure 10. Sketch Showing Damaged Diagonals and Temporary Shoring Point

Figure 11. Temporary Shoring Installed Under Panel Point

On Saturday evening, February 06, the bridge was reopened to light traffic, allowing passenger vehicles, pickup trucks, and light delivery vehicles to cross. This significant milestone was achieved just two days after the extensive damaged was incurred, and was a great relief to those isolated by the incident after initial reports indicated that it might take weeks to reopen. While design and preparations were underway for permanent repairs, the engineering team undertook some evaluations to allow for special loadings requested by the community, including a school bus and a small propane delivery truck.

6 REPAIRS: DESIGN AND EXECUTION

With the initial stabilization of the bridge complete and the reopening to light traffic accomplished, attention turned to permanent repairs and restoration of full traffic loading on the bridge. By this time the engineering consultant had an engineer on site, and a more detailed assessment of damage was conducted. This indicated that to restore the bridge to its previous condition, replacement of the following members would be required (Span 3 was the first span struck, Span 2 was the second):

- All ten inner main diagonal members in Span 3
- Three counter-diagonal members in Span 3
- One portal brace member in Span 3
- One sway brace member in Span 3
- Two inner main diagonal members in Span 2

Consistent with the original construction, the replacement members would be Douglas Fir #1 Grade. With the diagonals 7520mm long, stock material of the size needed in this grade and length were not available, and the timbers would be custom-sawn. This meant that it was not feasible to use pressure-treated material and have the bridge restored quickly; the time needed to season, pressure-treat and dry the timbers would have been on the order of months. In consultation with the MoTT, the decision was made to proceed with untreated material for the repairs. In the colder, dryer northern climate, experience from some other Howe trusses where some untreated timbers have been used is that they will not deteriorate significantly for 10 or 20 years. It was felt that within this time frame, the Kispiox River Bridge may be replaced with a more robust, modern structure; if not, any deteriorated members could again be replaced.

Replacement of counter-diagonals and braces would be straightforward, they could be removed and replaced quickly at a time with no live load or wind load in the members. Replacement of main diagonals under load would be more complex, involving a jacking strut to unload the affected diagonal and carry load while the new one was installed. Two of the diagonals in Span 3 were fractured so extensively during the incident that they were already removed, but the jacking strut would still be used for these to take construction loading and allow for insertion of a new diagonal member at the correct length, so that it would accept its share of the load.

An existing jacking strut was considered and found not suitable for the Kispiox geometry, and so a custom jacking strut was designed and fabricated while timbers were being sawn and other preparations for repairs completed. The strut comprised steel HSS members with an integral hydraulic jack and end details to fit around the truss angle blocks (See Fig 12).

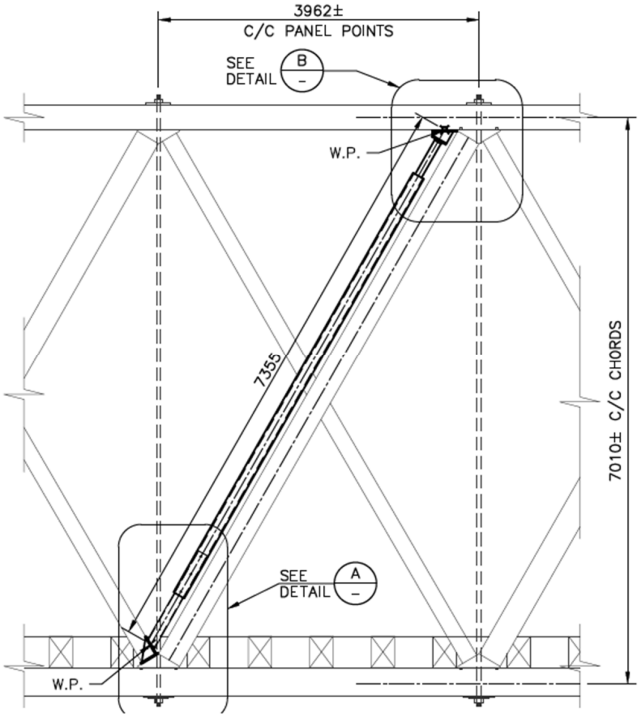

Figure 12. General View of Deployed Jacking Strut

The basic procedure using the jacking strut was to install the strut in place above the diagonal member to be replaced, set bottom restraints, ease off the tension rod nut at the top of the diagonal, jack until the member was just unloaded, remove the damaged member, cut the new member to matching unstressed length, insert the new member, release the jack to load the new member, and tighten the tension rod nut. Expected jacking loads for each member, including the effects of nearby equipment in addition to dead loads, were calculated and provided to the contractor, along with upper-bound restrictions.

The engineering team worked closely with the contractor throughout the repairs, designing the jacket strut and procedures to suit the contractor's methods. This collaboration including determining how construction live loads could be applied, including a telehandler and a boom lift. To allow for these loads and to provide working room for the contractor, once repairs commenced public traffic was held at the bridge and released once an hour for twenty minutes. This provided the contractor with forty minute periods when he owned the bridge and could use the full bridge width for the work.

The relatively small size of the individual truss members facilitated handling manually, using such equipment as chain hoists and cable pullers, in addition to the worker access provided by the boom lift.

Priorities were assigned to each member to be replaced, beginning with the damaged end post (see Fig 13), then to two main diagonals that had been completely removed, then to the next few most damaged diagonals. Once these higher priority members were replaced, the temporary load limit for the bridge was increased from 8000 kg to 30,000 kg, allowing for some commercial traffic. This was accomplished on Feb 19, two weeks after the damage incident.

Following completion of the remaining replacements, members that had lesser damage, counter-diagonals, and braces, the bridge was reopened to unrestricted traffic (63,700 kg maximum legal weight), on Tuesday February 23, nineteen days after the damage incident.

Figure 13 Replacement of Damaged End Post in Span 3

Figure 14 Re-tightening Tension Rod

Figure 15 Ongoing Diagonal Replacement Work

Figure 16 Completed Repairs

7 CONCLUSIONS

The timber Howe truss design was “the bridge that built BC”, and hundreds of them were constructed, largely from local materials, as the Province expanded its road network in the first half of the 20th century. Today, only 20 of these bridges remain, but some are on vital routes serving small communities. While these bridges were a very efficient design and easily built, they lack redundancy in many respects and through-trusses especially are vulnerable to damage from vehicle impact. The Kispiox River Bridge was in danger of collapse when it was struck by a snowplough which damaged many timber diagonals, resulting in closure of the bridge, but the ease of analysis and simple nature of construction of the bridge enabled a staged reopening of the bridge; to pedestrians almost immediately, to light traffic in two days, to medium traffic in two weeks, and to full traffic in nineteen days. This was achieved by a collaborative effort between the bridge owner, engineering consultant, general contractor, road maintenance contractor, and multiple area stakeholders.

REFERENCES

1. Johnson, Murray and Farnden, Gary. *Historic Howe Truss Bridges of British Columbia*, International Conference on Timber Bridges, Sweden 2017.
2. DeLony, Eric. "*The Golden Age of the Iron Bridge*." I&T: Invention and Technology, 1994.
3. Parsons Brinkerhoff & Engineering and Industrial Heritage, *A Context for Common Historic Bridge Types*, NCHRP Project 25-25, Task 15, 2005.

ICTB 2025. 5th International Conference Timber Bridges
Rotorua, New Zealand, 29 June to 2 July 2025.

STAUFFACHER BRIDGE, TIMBER-UHPFRC COMPOSITE STRUCTURE

Edgar Kälin[1], Peter Rogenmoser[2], Leonardo Dominguez[3]

1 INTRODUCTION

The municipality of Steinen in Switzerland sought a solution for a new crossing over the Steineraa River to establish a connection between the village's historic centre and a recently developed residential area.

The decision was made to utilise timber construction in combination with Ultra-High-Performance Fibre-Reinforced Composite (UHPFRC), a cement-bonded fibre construction material. This construction could be produced almost entirely with local materials and by local companies.

The bridge has been designed as a trough bridge, incorporating two glulam beams and a slender UHPFRC bridge deck. The integration of timber and UHPFRC has resulted in a ductile overall system, with the two materials ideally complementing each other. The resultant structure is both slender and rigid.

Figure 1: Northern view of the bridge

Figure 2: Southern view of the bridge

Figure 3: View of the walkway

Figure 4: Aerial view

[1] Edgar Kälin, dipl. Ing. ETH/SIA, Ingenieurbüro Edgar Kälin AG, Switzerland, e.kaelin@ingenieurkaelin.ch
[2] Peter Rogenmoser, Holzbauingenieur, neue Holzbau AG, Switzerland, peter.rogenmoser@neueholzbau.ch
[3] Leonardo Dominguez, Architect ETSAC und CAS Holztragwerke BFH, HTB-Ingenieure AG, Switzerland, l.dominguez@htb-ag.ch

2 UHPFRC

This unassuming bridge's key feature is the innovative use of UHPFRC (Cement Bonded Ultra-High-Performance Fibre-Reinforced Composite). Another abbreviation used is UHPC (Ultra-High-Performance Composite). Building with UHPFRC, a material that is neither steel nor concrete but a new type of building material with an independent mode of action, is regulated in Switzerland in the 2052 standard of the SIA (Swiss Society of Engineers and Architects).

UHPFRC has been used on bridges in Switzerland for over 20 years, and its durability has been proven. The Stauffacher Bridge is expected to have significantly lower maintenance costs than conventional concrete or timber-concrete constructions.

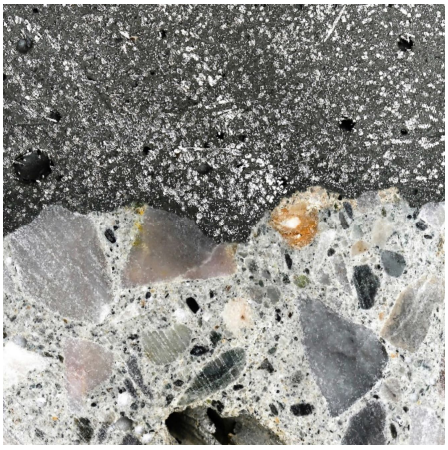

Figure 5: Comparison of UHPFRC and concrete [1]

Figure 6: UHPFRC on a roughened concrete surface

Figures 5 and 6 show the apparent pictorial difference between the two building materials. UHPFRC consists of cement, other fines and hard particles (quartz) with a maximum size of 1 mm. The packing density of these particles is optimised so that the resulting building material no longer has any voids (pores). This cement-bound building material is reinforced by slender, short fibres in high dosage. These fibres are made of steel, 15 mm long and 0.2 mm thick. They make up at least 3% of the building material volume. The amount of water needed to set the cement (binder) is so small that during the hardening process of UHPFRC, the added water is completely consumed for the cement setting. Since there is no more free water, no drying process can occur, as is usual with mortar and concrete, leading to the formation of capillary pores. The capillary pores common in conventional concrete are interconnected and thus allow water to enter the concrete from the outside. Water is the necessary precondition for corrosion of the steel reinforcing bars or chemical reactions in the concrete (alkali-aggregate reaction), the two most common damage mechanisms of reinforced concrete. In contrast, UHPFRC - as previously explained - has no capillary pores, which means that no water ingress can occur, and thus, no damage to the building material can occur. The building material UHPFRC is waterproof. This watertightness has been proven by many tests. In addition, tests have shown that UHPFRC is waterproof even under tensile stress. These properties guarantee that the building material UHPFRC is highly durable against climatic influences with water and de-icing salts.

Due to the UHPFRC’s impermeability and the very high abrasion resistance, the sealing and waterproofing work required for a concrete or timber bridge can be omitted, and no wear layer is necessary for the roadway.

UHPFRC has a characteristic compressive strength of 120 to 150 MPa and a characteristic plastic tensile strength of 7.7 to 12.0 MPa, which can be used for structural safety verifications. UHPFRC shrinks similarly to concrete; its creep is slightly lower, and its temperature expansion is identical to concrete's. At >= 45 MPa, the modulus of elasticity is higher than that of concrete.

Typically, UHPFRC structures are lightly reinforced, but unlike in concrete, no shrinkage reinforcement is required to minimise cracks – UHPFRC is crack-free in service condition! The high strength,

impermeability, and needed reinforcement cover of only 15 mm allow the construction of very slender structures.

The cost of UHPFRC m^3 is approximately 20 times higher than that of concrete. However, due to its unique and diverse properties, more favourable solutions can often be found than with conventional constructions.

UHPFRC is not only used in bridge construction. The range of applications includes repairs, sealing and strengthening. In addition, UHPFRC constructions are suitable for use in architecture as slim, eye-catching features. The following pictures show typical applications of UHPFRC.

Figure 7: 4.5 m long and 6 cm thin UHPFRC bridge, Einsiedeln, Switzerland

Figure 8: Repair of a historic bridge using UHPFRC, Lauperswil, Switzerland

Figure 9: Strengthening of a ceiling using UHPFRC, Reichenburg, Switzerland

Figure 10: Slender UHPFRC staircase, Einsiedeln Switzerland

3 DESIGN OF THE STAUFFACHER BRIDGE

The municipality of Steinen already had a project proposal for a timber bridge, but it was inadequate regarding moisture protection. So, they contacted us, and we convinced them with our project.

The bridge is designed as a trough bridge made of glulam beams with a UHPFRC bridge deck. Except for the inner cladding and the beam cover board, it was prefabricated entirely in the factory.

The two longitudinal beams were placed on a formwork to which the tension and shear connections for the bridge slab had previously been glued. The UHPFRC bridge deck, which has a thickness of only 60 mm, is reinforced to 97 mm under the longitudinal beams and has transverse reinforcements at 2 m intervals with a total thickness of 100 mm. To minimise the consumption of UHPFRC, 40 mm thick 3-layer timber panels were inserted into the slab. We use UHPFRC only where it is really necessary.

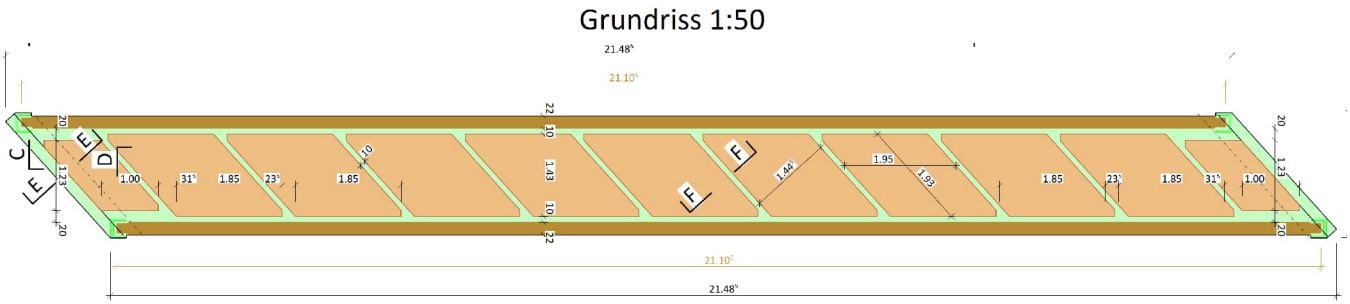

Figure 11: Layout of the bridge slab with the 3-layer timber panels

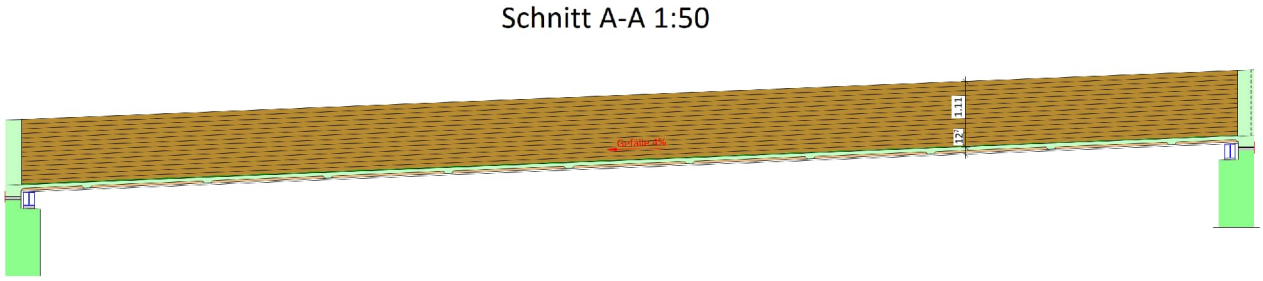

Figure 12: Longitudinal section

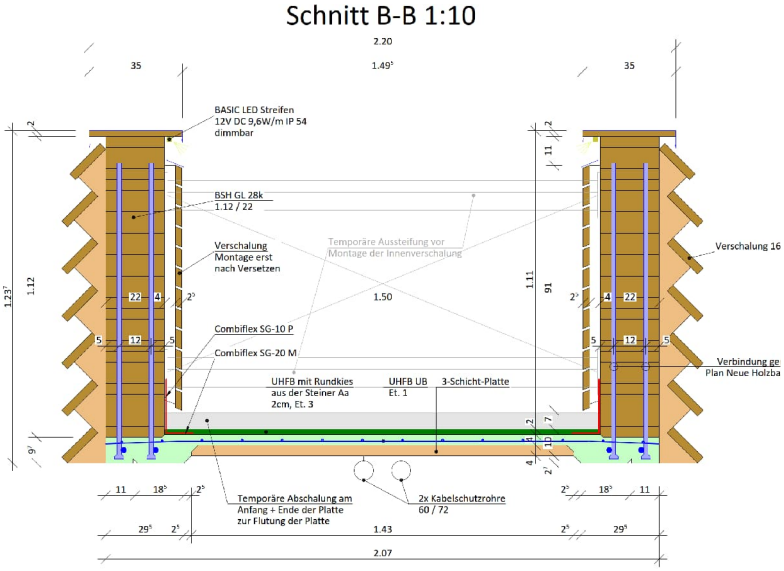

Figure 13: Cross section

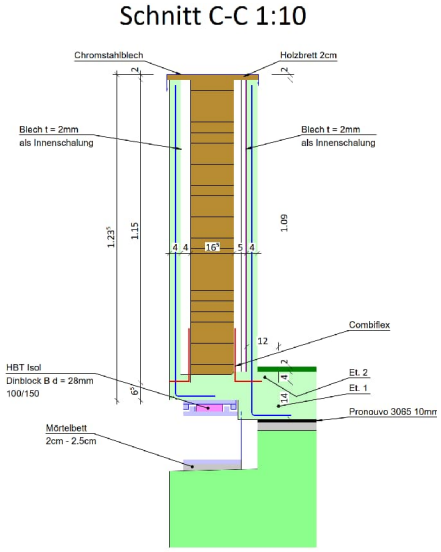

Figure 14: Abutment detail

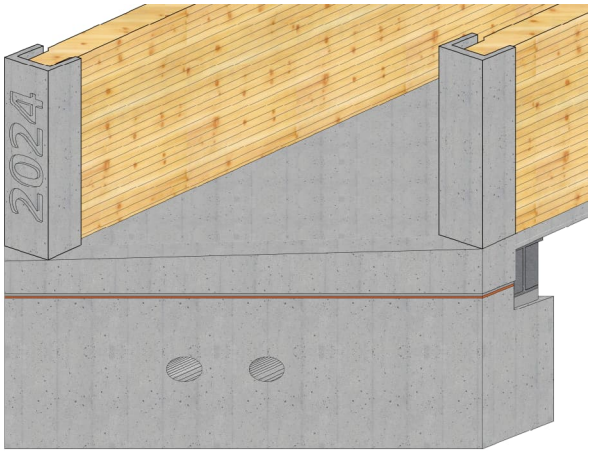

Figure 15: Isometric view of the tilt protection

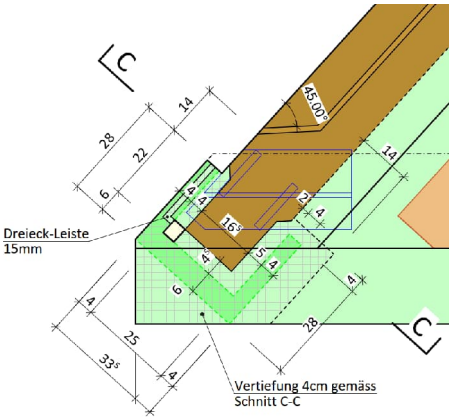

Figure 16: Detail of the tilt protection

The longitudinal beams are secured against tilting with vertical UHPFRC beams at the abutments. These beams, which have wall thicknesses of 40 mm and 60 mm, respectively, are fixed in the edge-reinforced plate.

The bridge slab is a two-layer UHPFRC construction. The first layer consists of a conventional UHPFRC with steel fibres. The second layer is a UHPFRC-gravel matrix without fibres with a thickness of 20 mm. The gravel required was taken directly from the Steineraa River. The Steineraa River is a mountain stream once crossed by a ford at this location. The stream has gravel that is ideally suited as an admixture to the gravel matrix UHPFRC of the bridge slab. For this purpose, the children from the village of Steinen contributed by sifting out the correct grain fraction of the gravel in a gravel works. Instead of crossing the stream through the ford as they did a long time ago, the people of Steinen now walk over the new bridge - on the gravel from the Steineraa River that their children sifted out. This ensures a strong emotional bond with the bridge.

Figure 17: The gravel of the Steineraa River

Figure 18: Sifting the gravel

Figure 19: The proud children of Steinen, after filling a big bag with its own gravel

Figure 20: The finished walkway surface

The stresses resulting from shrinkage remain lower than the tensile strength of the UHPFRC. In addition, because the modulus of elasticity of the timber is about five times lower, the stresses in the UHPFRC are reduced to about half. In the ultimate limit state, stresses in the composite system due to impeded deformation at an early age, particularly stresses due to impeded shrinkage in the UHPFRC, may be neglected, according to SIA 2052.

Unlike conventional TCC bridges, the UHPFRC layer is below the timber beams. Therefore, the shrinkage's positive (upward) effects impact the bridge deflections.

4 CONSTRUCTION OF THE STAUFFACHER BRIDGE

The construction of the Stauffacher Bridge was straightforward because the entire structure, including the UHPFRC components, had been prefabricated in a factory less than 1 km from the construction site.

UHPFRC rapidly attains substantial strengths. Typically, the compressive strength exceeds 100 MPa within a week. Consequently, the bridge could be transported to the construction site within a short time following the casting of the bridge slab.

Figure 21: The timber beams on the formwork

Figure 22: Detail of the pull- and shear connection

Figure 23: The reinforcement for the tilt protection

Figure 24: Mixing the UHPFRC on site

Figure 25: Casting of UHPFRC

Figure 26: Smoothing the surface of the 1st layer

Figure 27: Detail of the tilt protection

Figure 28: Lifting the bridge from the formwork

Figure 29: Detail of the fixed support and service lines

Figure 30: Transport of the bridge through Steinen

Figure 31: Moving the bridge with a mobile crane

Figure 32: The bridge resting on the abutments; the temporary stabilisation of the timber beams is visible

5 COMPOSITE OF TIMBER AND UHPFRC

Due to the high material properties, the UHPFRC slab should not only form the flooring but also fulfil a load-bearing function. This made it possible to dispense a U-shaped steel construction required in timber construction to stabilise the bridge beams, resulting in a simple and economical bridge cross-section. The consequence of this approach was to combine the beam and bridge deck into a hybrid overall structure. The connection had to be designed for the following tasks:

- bring in vertical dead and live loads of the bridge deck into the beams
- shear connection for the vertical bending

- beams tilt bracket
- stabilisation for horizontal wind loads and horizontal loads in case of human crowding

GSA technology could solve this multifaced task. GSA is a high-performance and ductile Timber connection system that includes the GSA-HBV (TCC) solution, which is ideal for connecting the high-strength UHPFRC with timber. The GSA technology is based on threaded rods glued into timber or, in the case of the TCC system, on glued-in reinforcing steel. The system is designed so that the reinforcing rods fail ductility in the fracture state, excluding the brittle failure modes of the timber or the adhesive.

The bridge deck is suspended in the beams by GSA 16.8 @400mm. An additional reinforcement perpendicular to the grain is not necessary. This connection also generates longitudinal shear forces in the connectors on account of the bending load. This combined load must be analysed and should not be ignored. The vertical GSA alone cannot absorb the shear forces near support. Therefore, GSA-HBV connectors were placed in this area. These are considerably stiffer and can absorb the forces and relieve the vertical GSA. The lateral offset of the vertical GSA creates a resistance to bending in cross direction to transfer the horizontal loads into the bridge deck.

GSA technology creates a rigid U-shaped bridge cross-section, resulting in a uniform hybrid overall system. The connection technology contributes significantly to the bridge's overall stability and stiffness.

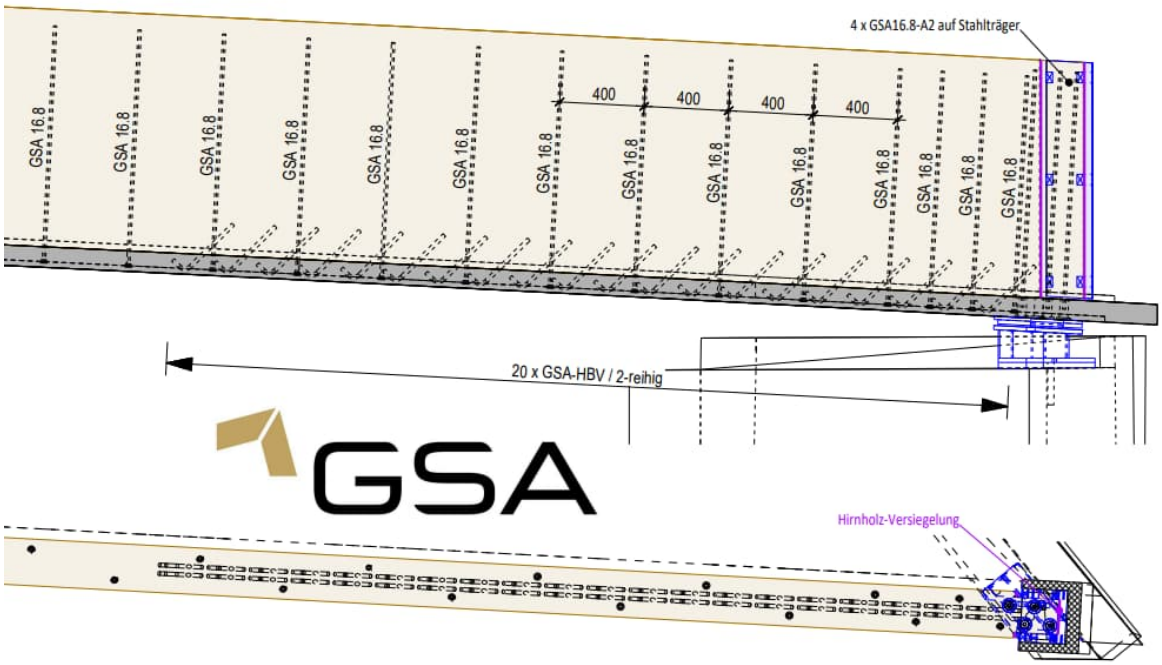

Figure 33: Arrangement of GSA connectors near the support

6 MOISTURE PROTECTION

Various protective measures have been implemented to ensure the longevity of the bridge. The ends of the beams have been sealed to prevent moisture from penetrating. The bridge is fitted with ventilated timber cladding inside and outside, ensuring proper ventilation and preventing moisture accumulation.

Another key element is the sealing in the inner corner where the bridge deck transitions to the timber beams. Since standing water from the roadway can accumulate in this area, special attention has been given to this section. A high-quality dynamic waterproofing membrane (Sikadur-Combiflex) has been bonded to the first UHPFRC layer and the beams. The second UHPFRC layer was then poured over it. This waterproofing ensures that no water can penetrate the timber beams from the roadway. Additionally, a weather groove has been installed on the underside of the bridge deck to direct flowing water away from the cladding panels. Finally, a cover board with a metal sheet is mounted on top of the beams to protect them from direct exposure to the weather.

7 DYNAMIC ANALYSIS

7.1 Assumptions and calculations

A 3D structural model has been used to calculate the bridge's mode shapes and natural frequencies. The model considers all relevant mass and stiffness of the bridge.

Vibrations of the pedestrian walkway due to the live loads on the deck were investigated and assessed to evaluate the pedestrians' comfort. To ensure adequate comfort, the natural frequencies should be $f > 4.5$ Hz or $f < 1.6$ Hz for vertical vibrations in accordance with SIA 260. The calculations showed a minimum vertical natural frequency of $f = 4.58$ Hz. Therefore, a detailed dynamic analysis is necessary to verify this issue. The horizontal vibrations were also examined. However, the calculations showed that they are in an uncritical range.

The design was completed in accordance with the "Hivoss project—Guidelines and background documentation for the design for human-induced vibrations on pedestrian bridges" [2], considered the most up-to-date publication on theoretical design and practical examples of existing footbridges.

According to the calculations, the horizontal vibrations were in an uncritical range and were not analysed further.

The literature does not indicate what damping can be assumed for a timber-UHPFRC composite structure. Since the main beams are timber, a damping of $\xi = 1.5\%$ has been considered.

7.2 Results

The Hivoss publication defines comfort classes according to the acceleration obtained. Maximum comfort is assumed for a vertical acceleration of < 0.5 m/s^2. Average comfort is given at an acceleration between 0.5 m/s^2 and 1.0 m/s^2. Unacceptable comfort corresponds to an acceleration > 2.5 m/s^2. For the Stauffacher Bridge, the aim was to achieve a medium level of comfort.

The calculations showed that with the selected assumptions, a vertical acceleration of 0.55 m/s^2 occurs at a density of 1.0 persons/m^2, i.e. a medium level of comfort is guaranteed. With less than 0.5 persons/m^2, the vertical acceleration is 0.27 m/s^2, corresponding to maximum comfort.

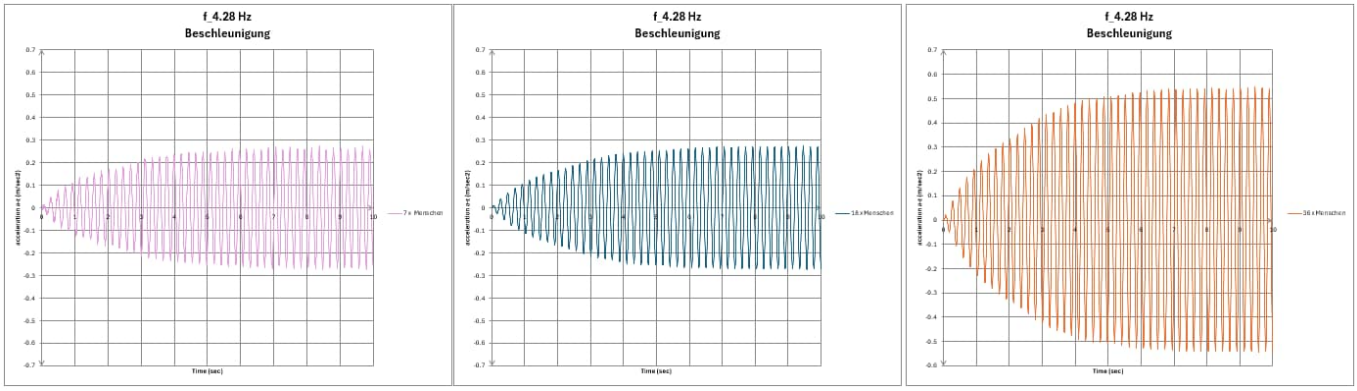

Figure 34: Vertical accelerations at some specific Vertical accelerations at a particular point on the footbridge for 7, 18 and 36 persons (0.2 – 1.0 persons/m^2)

No unpleasant vibrations have occurred during use so far. However, measurements were not taken when writing this text. Measurements will be carried out in spring 2025.

8 SUSTAINABILITY

Timber bridges have significant advantages over conventional concrete or steel constructions in terms of global warming potential and resource consumption. The same applies to timber-UHPFRC composite constructions.

In the 'Assessment of the Environmental Impacts of Bridge Designs Involving UHPFRC' [3], various bridge constructions (concrete, timber-UHPCFRC composite, UHPFRC) were compared in terms of sustainability using the specific example of the Fruttli Bridge [4], a timber-UHPFRC-composite road bridge. Due to the low material consumption rate and high durability rating, the resulting UHPFRC constructions can be rated as very sustainable. This is despite the composition of the UHPFRC, which has a high cement and steel content.

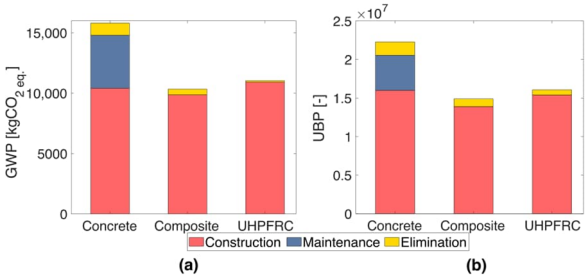

Figure 35: Environmental impacts of bridge designs: (**a**) Global warming potential; (**b**) Ecological scarcity (UBP points)

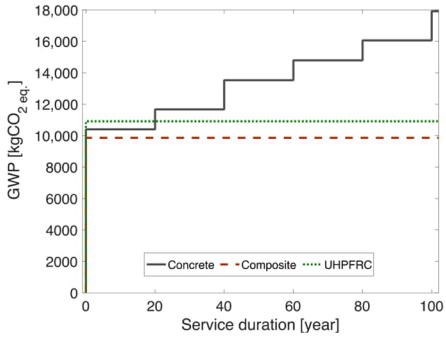

Figure 36: Influence of the service duration on the environmental impacts of bridge designs

9 CONCLUSIONS

UHPFRC is a highly versatile and proven building material. Combined with timber, it allows the construction of highly sustainable and durable bridges, making it a suitable option for pedestrian and heavy-duty bridges.

High-performance connections are required to create efficient structures with high-performance materials. The GSA technology fulfils these requirements.

Due to the low component thicknesses, timber-UHPFRC constructions remain lightweight, unlike TCC constructions, and are very stiff.

The absence of a seal or covering allows for accelerated construction, minimised sources of error and reduced costs.

REFERENCES

1. Brühwiler, E. (2018). Structural UHPFRC to Enhance Bridges. Proceedings of the 2nd International Conference on UHPC Materials and Structures UHPC 2018 - China 129, Fuzhou, China, November 7–10, 2018, p140.
2. Feldmann, M., Heinemeyer, C. and Lukić, M., Directorate-General for Research and Innovation, *Human-induced vibration of steel structures (Hivoss)*, Publications Office, 2010, https://data.europa.eu/doi/10.2777/79056
3. Bertola, N., Küpfer, C., Kälin, E., Brühwiler, E., "Assessment of the Environmental Impacts of Bridge Designs Involving UHPFRC", Sustainability, vol. 13, no. 22, 2021, p. 12399, https://doi.org/10.3390/su132212399
4. Kälin, E., Rogenmoser, P., Fruttli-and Rigiaa-Bridge, Timber-UHPC composite structure, Proceedings of the 4th ICTB Conference (2022) – Switzerland, Biel, May 9 – 12, 2022, p41, https://www.bfh.ch/dam/jcr:8373b846-9eb8-4549-ac9a-9fbab55feb3c/ictb-2021-conference-proceedings-bfh.pdf

ICTB 2025. 5th International Conference Timber Bridges
Rotorua, New Zealand, 29 June to 2 July 2025.

INVESTIGATIONS ON ATCC COMPONENTS USING FIBER-OPTICAL SENSORS FOR STRUCTURAL ANALYSES

Martin Ganß[1], Andreas Kirchner[1,2], Henri Paetow[2], Martin Kästner[2], Johannes Koch[3], Antje Simon[3], Matthias Kraus[2]

ABSTRACT

Timber-concrete composite (TCC) road bridges offer promising ecological and economic advantages, particularly for short to medium spans ranging from 10 to 30 meters. While the construction of TCC bridges typically relies on discontinuous, semi-rigid joining techniques, adhesive bonding enables a continuous, rigid connection between timber and concrete, optimizing stress transfer and enhancing load resistance. Additional benefits of adhesive bonding include efficient prefabrication and improved sealing properties. However, the long-term performance of adhesively bonded TCC (ATCC) bridges largely depends on the durability of the adhesive joint. Therefore, it is essential to investigate both the production technology and the composite properties of the ATCC, as well as to develop structural health monitoring (SHM) concepts. In this context, this study explores the structural behaviour of large-scale ATCC components i.e. ATCC-beams and a superstructure segment using integrated fibre-optic sensors. Furthermore, the potential of fibre-optic sensors and measurement techniques for a detailed analysis of the adhesive layer will be presented.

1 INTRODUCTION

1.1 Adhesively bonded timber-concrete composite (ATCC)

The timber-concrete composite (TCC) construction method using adhesive bonding technology has been the subject of research since the 1960s. This includes methods such as ‘wet-on-wet’ joining (bonding timber to fresh concrete) and dry bonding (bonding a prefabricated concrete component). In [1] an overview is given about TCCs. Mineral-filled, epoxy resin-based adhesives (also known as polymer mortar) have proven to be suitable for joining prefabricated concrete and timber components, as well as for compensating manufacturing tolerances between these components. This has also been demonstrated in own studies on the short-term load-bearing behaviour of ATCC components at Bauhaus-University Weimar [1]. Since bridge construction aims for a service life of 100 years, the long-term load-bearing behaviour and durability of the bonded joint are of great importance. In this context, Eisenhut [2] conducted long-term hygro-thermal tests on ATCC components. However, no studies have yet been established on the long-term behaviour of bridge components under environmental conditions. Due to the different thermal expansion coefficients of concrete and timber, significant constraining stresses can develop. A major challenge in structural design is therefore to accurately determine the thermal reactions within the hybrid structure. Current design standards, such as EN 1991-1-5, only provide temperature profiles for superstructures made of steel and concrete.

Consequently, a segment of the superstructure of an ATCC road bridge has been manufactured in the collaborative research project “Hybrid timber bridges with adhesive bond - quality assurance and structural health monitoring using integrated sensors (HBVSens)” to analyse hygro-thermal effects, temperatures and the structural response under real environmental conditions. The ATCC superstructure segment was equipped with various moisture, temperature, and strain sensors for a detailed analysis. In particular, it is important to integrate sensors during production to detect changes in the adhesive joint. Here, the sensors should not influence the structural behaviour. Very thin fibre-optic sensors could be suitable in this context, as they allow a large number of measurement points on a single sensor without affecting the structure itself. The following section briefly presents selected semi-distributed and distributed fibre-optic sensors and measurement methods.

---

[1] Materials Research and Testing Institute Weimar; Germany, e-mail: andreas.kirchner@mfpa.de; martin.ganss@mfpa.de

[2] Bauhaus-University Weimar, Germany; e-mail: martin.kaestner@uni-weimar.de; henri.paetow@uni-weimar.de; matthias.kraus@uni-weimar.de

[3] University of Applied Sciences Erfurt, Germany; e-mail: johannes.koch@fh-erfurt.de; antje.simon@fh-erfurt.de

1.2 Semi-distributed and distributed fibre-optical sensors and measuring techniques

Fibre-optical measuring technologies offer a powerful tool for the analysis and monitoring of structures, components, and buildings by measuring strain and temperature in real time using thin optical fibres and/or fibre-based cables. With appropriate measurement technologies, sensor data can be collected along a fibre sensor at different positions in and on a structure. Distributed fibre-optic sensors can be categorized in semi-distributed and distributed sensor systems.

Fibre Bragg Grating (FBG)-sensors are an established technology for strain measurement and damage detection in civil engineering structures [3, 4] and composite materials [5]. They enable real-time monitoring of temperatures, mechanical strains and structural changes at defined points on the fibre-optical sensor. FBG-sensors are light guiding optical fibres with zones where the refractive index in the fibre core is periodically modulated. The zones with modified optical properties are called Bragg gratings [6]. When broadband light is passed through the FBG, a wavelength-selective reflection of the light occurs. The light is reflected at the Bragg wavelength λ_B [6]. If temperature or mechanical strain is applied to the FBG along the fibre axis, the Bragg wavelength increases or decreases depending on the situation. The Bragg wavelength correlates to the applied strain or temperature and thus the strain and temperature can be calculated by accounting the temperature and strain sensitivity. For strain measurements at constant temperature, the peak shift of the Bragg wavelength is typically converted into a measurement of strain along the axis of the optical fibre. If the temperature is not constant, temperature effects must be separated from mechanical strain effects using temperature compensation techniques.

For strain measurements, the FBG-sensors are normally attached to the surfaces of the structure of interest using structural adhesives or by using other joining techniques. It has been shown that FBG-sensors can also be used as embedded sensors in laminated composite structures [7] as well as in adhesive layers of structural joints [8, 9, 10]. FBG-sensors offer the possibility to analyse strain and temperature at many predefined points (semi-distributed) with high resolution and long-term stability.

In recent years, distributed fibre-optical sensors (DFOS) and measuring systems are strongly in the focus of research and on the way to practical application. These measurement techniques use the light scattered back from ‘defects’ and ‘inhomogeneities’ in the optical glass fibre itself. The optical fibres contain a characteristic reflection signal whose defined changes under the influence of temperature and mechanical strain are analysed to determine temperature and strain. Special interferometer measurement techniques and defined tuneable laser light sources are used to evaluate the light scattered back into the fibre. Optical frequency domain reflectometry (OFDR) uses frequency analysis to evaluate the Rayleigh components in the backscattered light. The measurement systems consist of a tuneable narrow-band laser and a Mach-Zehnder interferometer with one arm used as a sensor and the other as a reference [11]. By using special analysis techniques and algorithms, strains and/or temperatures can thus be continuously recorded over the entire optical fibre (over a length of up to 100 m) with high spatial resolution in the lower millimetre range. Usual optical fibres and optical fibre cables can be used for this measurement technique. With other measurement techniques, the Raman and Brillouin components in the backscattered light are analysed. These techniques can measure over distances of tens of kilometres, but their spatial resolution is limited [11].

2 EXPERIMENTAL STUDIES ON ATCC COMPONENTS

2.1 Bending tests on ATCC beams – design, preparation and testing

For both ATCC components, discussed in the manuscript, the adhesive joint between concrete and timber was realized by using a highly mineral-filled, epoxy resin-based adhesive (i.e. polymer mortar). The highly rigid joint assures the connection between concrete and timber as well as tolerance compensation and sealing functions. In the past, different systems of two-component epoxy adhesive with high mineral filler content have been investigated [12, 13]. A research project [14] carried out at the Bauhaus-University Weimar included four-point bending tests on ATCC beams. The aim of the investigations was to determine the maximum load-bearing capacity of the ATCC beams and the detection of local damage by means of sensors. Therefore, fibre-optic sensors were used for a detailed analysis of the adhesive joint of two test specimens (beam HBV-11 and HBV-12) [15]. The ATCC beams had a T-shaped cross-section, consisting

of a reinforced concrete slab arranged in the compression zone and a block glued glulam beam underneath. General information on the test specimens and boundary conditions are given in Figure 1.

For beam HBV-11 the concrete slab was bonded to the glulam beams using the polymer mortar system ‘COMPONO 100 S’ (Bennert GmbH, Germany) [16]. For HBV-12, an alternative but comparable polymer mortar system was considered. The polymer mortar was applied on the entire timber surface. The average thickness of the adhesive joint measured approximately 13 ± 3 mm. To prevent sudden failure of the wood, the block glued glulam beams were reinforced with both tensile and shear reinforcements [1, 13]. An image of the deformed ATCC beam HBV-12 at the end of the bending test is shown in Figure 3.

Prior joining, a fibre-optical sensor (FOS) was applied over the entire length on the timber surface (see FOS in Figure 1). The used sensor was made of a single-mode optical glass fibre with polyimide coating having an overall diameter of 150 µm. To produce a sensor from the optical fibre, a 1.5 m long pigtails were spliced to the glass-fibre using a Fusion Splicer (Fujikura 70S, Japan). The fibre end was prepared so that no light could be backscattered from the fractured surface of the fibre end.

The load was applied displacement controlled in four consecutive load cycles until failure at the end of the fourth cycle (see Figure 4). Using inductive displacement transducers at different points of the composite beam, the global and local deformations were measured according to DIN EN 408 as well as the relative displacement between timber and concrete components. In addition, local measurements of longitudinal strains were realized using electrical strain gauges (SG) in different areas of the composite beam (SG: see Figure1). The measured strains of SG10, SG11 and SG12, applied on the upper surface of the block glued glulam beam, were used for comparison with the fibre-optical sensor data. The fibre-optic measurements were performed with a single channel coherent frequency domain reflectometer type ODiSI-B of Luna Innovations Incorporated (USA). The system allows measuring temperature and strain over few meters of an optical fibre with a spatial resolution of 0.65 mm.

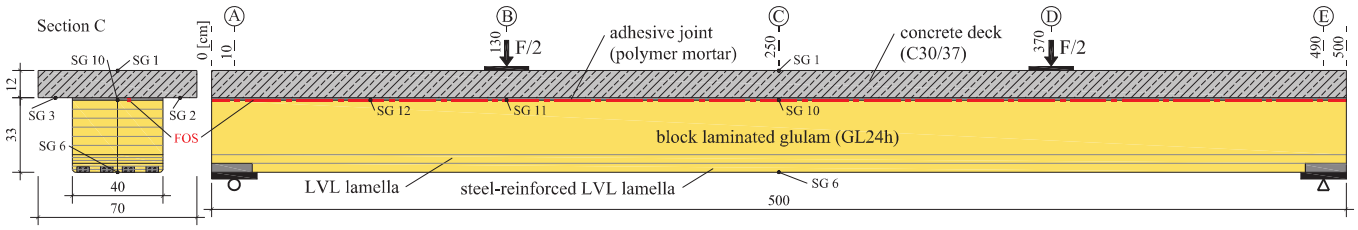

Figure 1: Specimen dimensions of the ATCC beams HBV-11 and HBV-12 used for the four-point bending tests with fibre-optical strain measurement along the adhesive joint

2.2 ATCC superstructure segment – design, preparation and testing

The ATCC superstructure segment was designed based on a parameter study for TCC bridges [17]. The cross-section (Figure 2) represents half of a double-girdered T-beam cross-section required for a single-lane road bridge with a span of 10 meters. The segment mainly consists of a block-glued glulam beam (b × h = 100 cm× 60 cm, GL24h) and a prefabricated reinforced concrete slab element (b × h = 200 cm× 22 cm, C40/50). The cement in the bonding zone of the concrete slab was washed out using a surface deactivator to create a rough contact surface. Since the thermal conductivity in the wood fibre direction is about twice as high as in the transverse direction, the segment length of the superstructure was set to 2.5 meters. This represents 2.5 times the width of the glulam beam. The chosen dimensions should ensure that the central section of the component remains unaffected at a length of 50 cm by heat and moisture transport along the segment.

The block glued glulam beam with the concrete slab was joined using the polymer mortar ‘COMPONO 100 S’ (Bennert GmbH, Germany) [16]. The polymer mortar was applied on the timber surface in five stripes using framework, each with a height of 18 mm. During the positioning of the concrete slab on the timber, the polymer mortar was allowed to spread with the aim of achieving a nearly full-surface bonding. The final height of the adhesive joint was approximately 10 mm.

For monitoring and detailed analysis, different temperature sensors, wood moisture sensors, and fibre-optical sensors, such as FBG-sensors and DFOS, were integrated into the structure. This contribution

focuses in particular on the fibre-optic sensors. Based on the geometry of the ATCC superstructure, the FBG-sensors were designed with respect to the FBG length, sensor positions, Bragg wavelength, and coating. The positioning of the Bragg gratings on the fibre was chosen such that changes close to the end grain area of the structure are recorded with higher spatial resolution. Details on the FBG-sensors and DFOS can be found in Figure 2. The FBG-sensors were produced by the FBGS Technologies GmbH (Germany) by inscribing the Bragg grating using a femtosecond laser process in 150 µm thick, bend-insensitive optical glass fibres. The Bragg grating length measures 4 mm. For temperature measurements, FBG- sensors with OrmocerT coating were integrated into a thin metallic capillary (outer diameter 1 mm) to avoid mechanical strain on the sensor. For strain measurements, FBG-sensors with polyimide (PI) coating were directly applied on the timber surface or in a timber groove. FBGS Technologies GmbH provided the sensor coefficients. The Bragg wavelength at a temperature of 22.0 ± 0.5 °C was estimated in a thermally insulated tube in an air-conditioned laboratory at the MFPA.

For distributed fibre-optical sensors, single-mode optical fibres with a PI coating and an overall diameter of 150 µm were used. The sensor coefficient for strain measurement is known from the literature. Two DFOS measuring paths are implemented in both the longitudinal and transverse directions of the ATCC. On the bottom of the timber, one DFOS measuring path is provided. Prior to joining the parts, the sensor fibres were applied to the surface and protected by a thin layer of a modified polymer mortar formulation with reduced grain size. Furthermore, optical glass fibres were integrated into the timber part before block gluing of the glulam components at the timber factory (STRAB Ingenieurholzbau Hermsdorf GmbH, Germany). In this respect, one thin PI-coated fibre and one “thicker” single-mode glass fibre (diameter: 900 µm; soft coating) were applied in a flat, sawn groove using a two-component epoxy resin adhesive (EasyMix S50, Weicon GmbH, Germany). Subsequently, the individual timber components were glued together to the glulam component and transported to final fabrication in Weimar. The locations of the fibre-optical sensors are marked with red outlines in the schematic illustration of the ATCC superstructure (Figure 2).

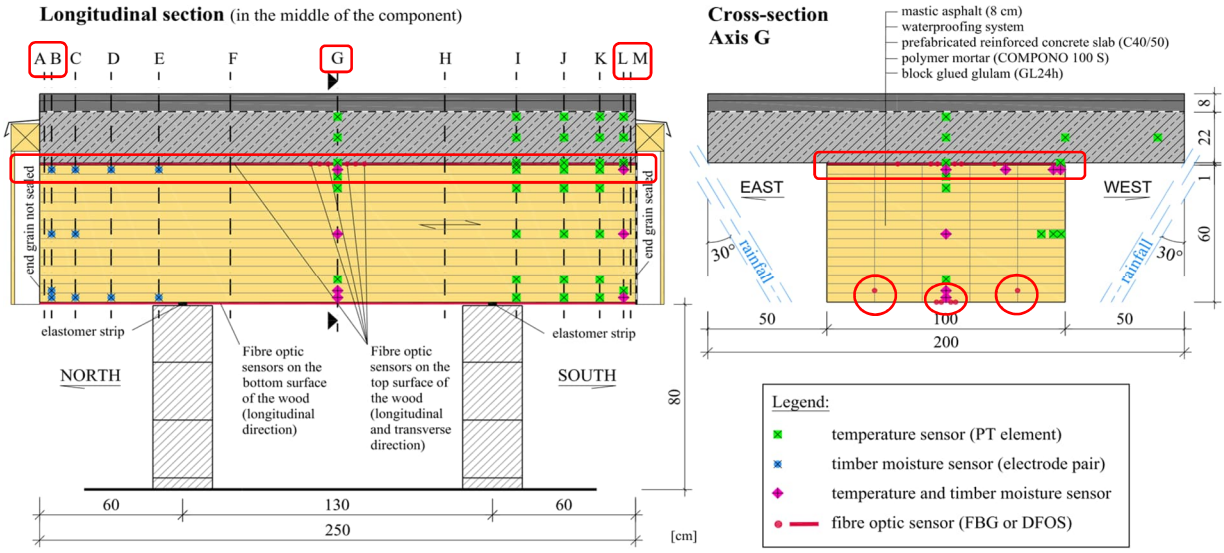

Figure 2: Superstructure segment the sensor positions (A to M). (The positions of the fibre-optical sensors are marked in red.)

Further details regarding the fabrication of the ATCC superstructure segment, sensor application, and analysis of temperature and timber moisture content can be found in [18, 19]. After fabrication and hardening of the polymer mortar, the ATCC superstructure was transported to an external location in Weimar and placed on foundations. Subsequently, a bituminous sealant and a mastic asphalt layer were applied to the concrete surface corresponding to the specification in Germany. Due to the selected setup, the effect of the top layer on the temperature distribution can be determined in accordance with the standards. Adequate weather protection for the timber is provided by the overhang of the concrete slab and by cladding at both end grain zones. The south-facing end grain was vapour-tight sealed.

The monitoring of the FBG-sensors was done using an 8-channel FBG interrogator system from Advanced Optics Solutions GmbH, Germany. The sensors are connected to the monitoring system via fibre-optical field cables. The connectors are protected from dust and weather by moisture-proof junction boxes. The FBG-sensors are continuously read every 5 minutes. A weather station of the company Ahlborn Mess- und Regelungstechnik GmbH (Germany) was placed nearby the superstructure and collects local climate information. Parallel to the condition monitoring with the FBG-sensors, measurement campaigns on DFOS are being realized using a four-channel coherent optical frequency domain reflectometry system ODiSi-6 of Luna Innovations Incorporated (USA). Measurement campaigns are preferably conducted over several days during the Christmas time and summer holidays.

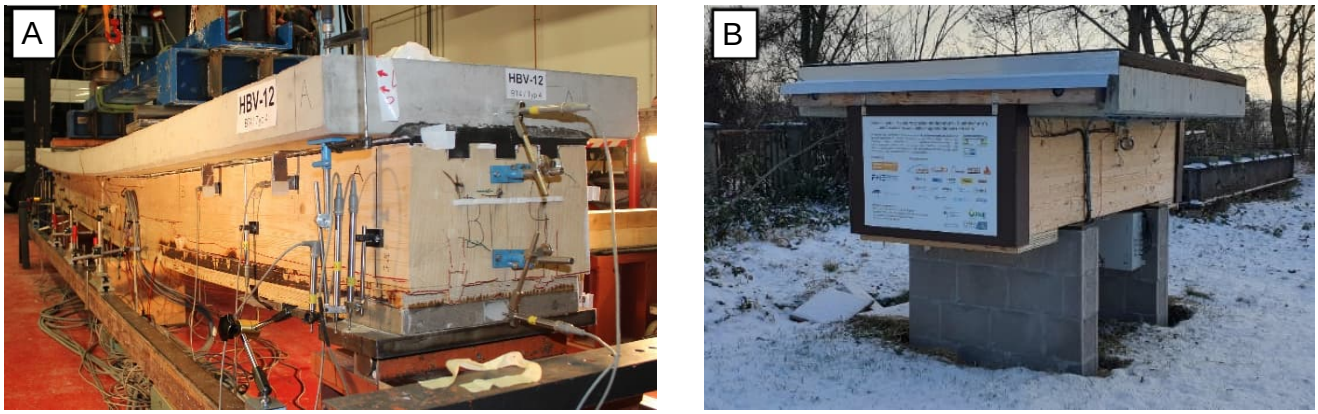

Figure 3: A) ATCC beam HBV-12 under bending load and B) ATCC-superstructure segment in outdoor climate in Weimar, Germany (January 2024)

3 RESULTS AND DISCUSSION OF POSSIBILITIES USING FIBER-OPTICAL SENSORS FOR MONITORING OF ATCC

3.1 Strain evaluation during mechanical loading of an ATCC-beam

As mentioned in section 2.2 for HBV-11 and HBV-12, the DFOS were integrated in the adhesive layer near the timber surface during the fabrication of the beam. It was therefore possible to measure strain changes in the adhesive layer already during the application of the polymer mortar, joining of the timber with the concrete slab and hardening of the polymer mortar. During the fabrication of the ATCC-beam (HBV-11), strain changes in the range of -200 to 200 µm/m were recorded over the entire fibre length. Events such as loading due to the application of the concrete slab and strain reduction due to the curing of the adhesive could be identified. However, the observed strain changes due to reaction- and temperature-induced adhesive shrinkage were relatively small.

The fibre-optic sensors were integrated primarily to analyse the strain behaviour and local damage at an early stage in the adhesive joint of the ATCC. Strain measurements using the OFDR were started concurrently with the loading of the ATCC beam in the four-point bending tests. The beam HBV-12 was subjected to four consecutive load cycles, which is shown in the force-time curves in Figure 4B. An overview of the temporal and local strain development measured with DFOS in combination with OFDR during the complete four-point bending test is shown in Figure 4A. The plot in Figure 4A (bottom-left) represents the change in the time–position history of the strains measured during the test. The x-axis represents the coordinates along the fibre-sensor in meters (longitudinal direction of the beam), while the y-axis represents the testing time in seconds. The strain values are shown in colour (see the legend on the right of Figure 4A). Figure 4A (top) highlights the strain distribution as a function of the sensor position by presentation of selected strain curves at specific time intervals. The times correspond to defined loads, which are marked on the load-time curve in Figure 4B. The strain curves illustrate that DFOS can be used to analyse strain events with high spatial resolution. In the strain data, the load application points (axis B and D) are particularly evident due to significant strain peaks at sensor positions of approximately 3.97 m and 6.41 m. At these positions, the local tensile strains increase with higher external load and reach a maximum of 600 µm/m. In the middle area of the beam, negative strains of up to approx. -370 µm/m occur between the load application points. The negative strains increase as the force increases until a testing time

of approx. 2000 s. The fibre sensor is largely located within the bending compression area due to the geometry and the stiffness of the rigid-bonded ATCC beam. Slight variations in the strain data can be attributed to inhomogeneities in the polymer mortar or timber structure. Münzer and Dill-Langer [20] already showed for DFOS-measurements on a glued-laminated timber beam that strain profiles give deeper insight into the very uneven strain distributions of common quality timber with growth defects such as knots and inclined wood fibres.

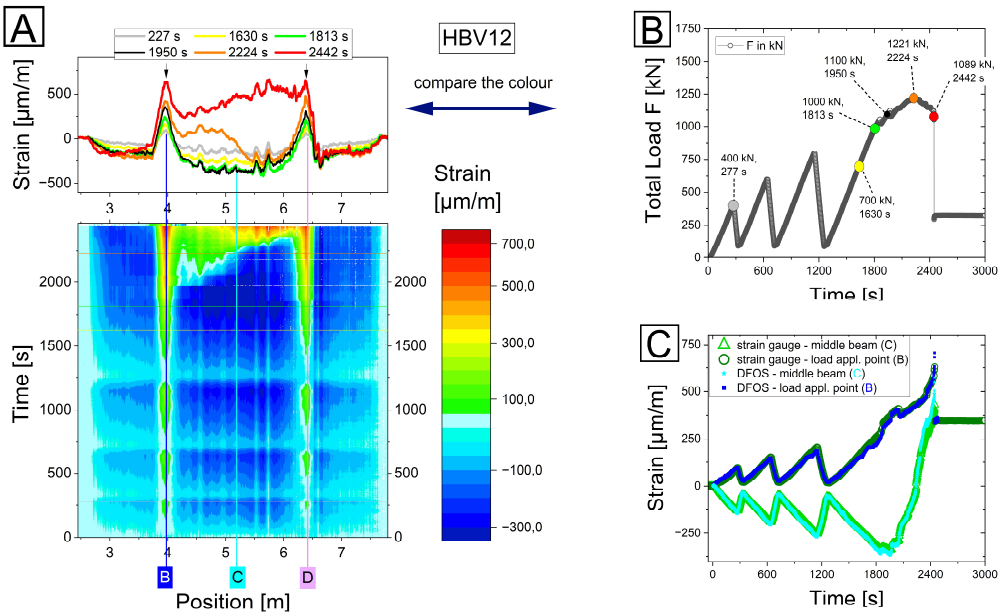

Figure 4: Fibre-optical strain data of the ATCC beam HBV-12 estimated during testing: A) Overview-plot with strain data as function of time and position; B) Load versus time plot with marked load levels for correlation to A; C) Strain-time-curves for electrical strain gauges and DFOS for load application point (axis *B*) and in the middle of the beam (axis *C*, see Figure 1)

In general, the negative strain values in the middle section become magnifying as the load on the ATCC beam increases until a time of approx. 1950 s is reached, which corresponds to an overall load of 1100 kN (see Figure 4B). Beyond 1813 s and 1950 s, a small drop in load indicates a non-linear deformation behaviour and possibly localized damage. Although the strain data from electrical strain gauges indicate a change in deformation behaviour (see Figure 4C, above 1800 s). In principle, the results of the strain measurements obtained using strain gauges and the fibre-optic measurement method reveal a high level of correlation. This is illustrated in Figure 4C, where the DFOS strain is compared to the strain measured by electrical strain gauges at similar positions in the structure (i.e., in the middle of the beam and at load application point in axis B). At a testing time above 2000 s, a significant strain redistribution is observed in the DFOS strain data in the middle of the beam (see coloured strain plot in Figure 4A). Exemplary, an asymmetric strain profile at 2224 s with an overall load of 1221 kN is shown in the strain vs. position graph (Figure 4A, top). The asymmetric strain distribution indicates an initial damage of the structure. Shortly afterwards, the global failure of the structure occurs at a time of 2442 s (load: 1089 kN). Here, the strain data in the middle of the beam shifts strongly to positive strains (see Figure 4A, top: red curve). Thus, it could be shown that DFOS can be used to analyse strain distributions with high local resolution in the joint. Therefore, it is possible to detect changes in strain due to damage.

In another subsequent beam test (HBV-11), even shrinkage cracks in the concrete slab could be observed using distributed fibre-optical sensors. The beam was loaded as shown in the load-time history of Figure 5A. No failure occurred up to loads of 1000 kN. A significant drop in the maximum load at 1100 kN indicates a “global” failure of the beam. The strain profiles along the length of the sensor fibre showed significant strain peaks even at low load levels. The strain peaks can be correlated with the locations of the shrinkage cracks in the concrete slab. In Figure 5C, this is illustrated for two overall load levels (120 kN and 971 kN). The positions of the cracks are indicated with red lines and match very well with the local strain peaks of the DFOS measurements. Initially, as the loading started, the cracks in the concrete were

compressed. Following the initial compression of the shrinkage cracks, the strain peaks remained almost constant with further load increase.

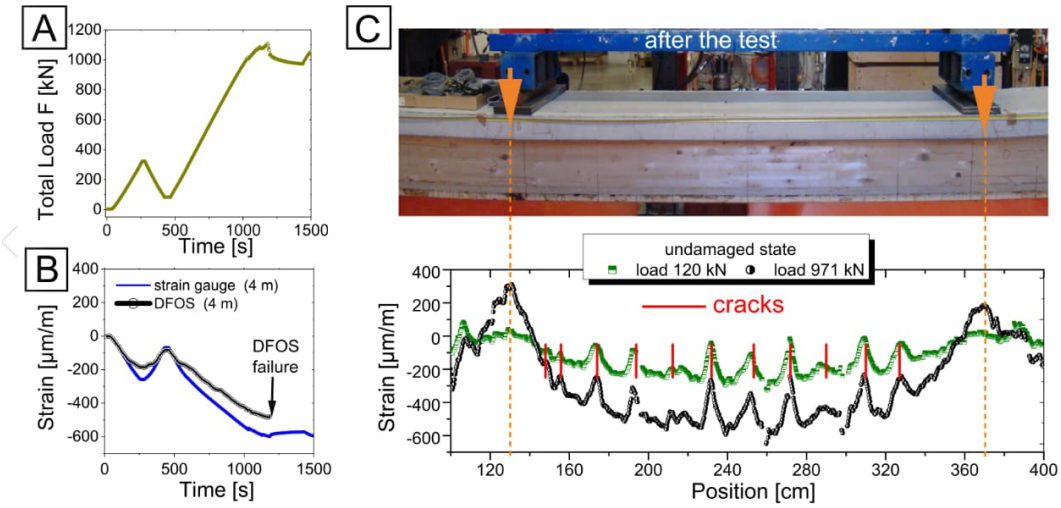

Figure 5: Load and strain data from four-point bending test of ATCC beam HBV-11; A) Load-time curve B) Strain vs. time from electrical strain gauges and DFOS in the middle of the beam (axis C) and C) Strain vs. position for loads of 120 kN and 971 kN and identified cracks (red lines) in the concrete slab

3.2 Monitoring of an ATCC superstructure segment in outdoor climate

For redundancy reasons, significantly more fibre-optic sensors were installed in the ATCC superstructure segment than can ultimately be measured by the available equipment. This applies particularly to the DFOS. Notably, with the exception of one sensor, all installed sensors remained intact throughout production, transportation, and outdoor storage on-site. The monitoring of the ATCC superstructure segment started in June 2023. For the discussion of the potentials of FBG-sensors and DFOS, results from selected time periods or measurement campaigns are presented here.

Contrary to investigations under constant temperatures (see 3.1), it is particularly important to separate mechanical from temperature effects for strain monitoring under environmental conditions. This was achieved by simultaneously measuring temperature and strain at comparable sensor positions within the ATCC structure. Each strain value is compensated with the corresponding temperature from the FBG-sensor. The temperature-curves from April 10, 2024 to May 5, 2024 measured by the fibre-optic temperature sensors, shade air temperature (weather station), and a conventional thermocouple from inside the structure (electrical sensor “UPM_G” – located axis G on the top surface of the block glued beam) are presented in Figure 6A. The measured temperatures of the FBG-sensors in the middle (green: axis G) and close to the end grain (black: axis B/north, blue: axis L/south; see Figure 2) of the ATCC superstructure segment follow the daily temperature variation. The temperatures from FBG-sensors agree well with temperature data from the electrical temperature sensor in the ATCC (compare TFOS_K4_G (green line) with UPM-G (orange line)). Minimal deviations in the range of 2-3 K may result from slight differences in sensor positioning as well as sensor-specific properties. For instance, using a ceramic capillary for encapsulation would be optimal for fibre-optic sensors, as it reduces the capillary's thermal conductivity. Similarly, the supply cables of electrical sensors can be affected by heating due to solar radiation, leading to slight changes in temperature. Both effects can contribute to deviations from the actual temperatures. Over the considered time-period, the temperatures measured by the integrated sensors always lag behind the shade air temperature. This can be explained by the good heat storage capacity of wood and concrete. Furthermore, the maximum and minimum temperatures measured inside the ATCC superstructure segment at the adhesive joint are slightly higher than the corresponding maximum and minimum daily shade air temperatures recorded by the nearby weather station. The higher temperatures inside the adhesive layer can be due to the intense heating of the dark mastic asphalt layer as a result of direct solar radiation. For more detailed analyses of the temperature distributions measured in the superstructure segment see [18]. The direct embedding of the FBG-sensors enables the measuring of mechanical strains and temperature-induced

strains (thermal expansions or thereof resulting strains). The measured values also contain a temperature influence, which is corrected by temperature compensation using the FBG-sensors temperature measurements. Due to the storage conditions of the ATCC with small support distances and the absence of mechanical load on the structure, the proportion of mechanical strain is negligible. Thus, mainly temperature-induced strains and perhaps moisture-induced strains of the structure are recorded. It should be noted, that the strain behaviour of the ATCC superstructure segment after installation at the outdoor location with a temperature of 20 °C (temperature in the structure) was set as the reference state (zero state). All strains should be expressed as changes in strain relative to the selected reference state. This is necessary because strains (residual strain/stress) have already been induced into the structure during fabrication caused by load application of the concrete slab, shrinkage of the polymer mortar during hardening and visco-elastic effects.

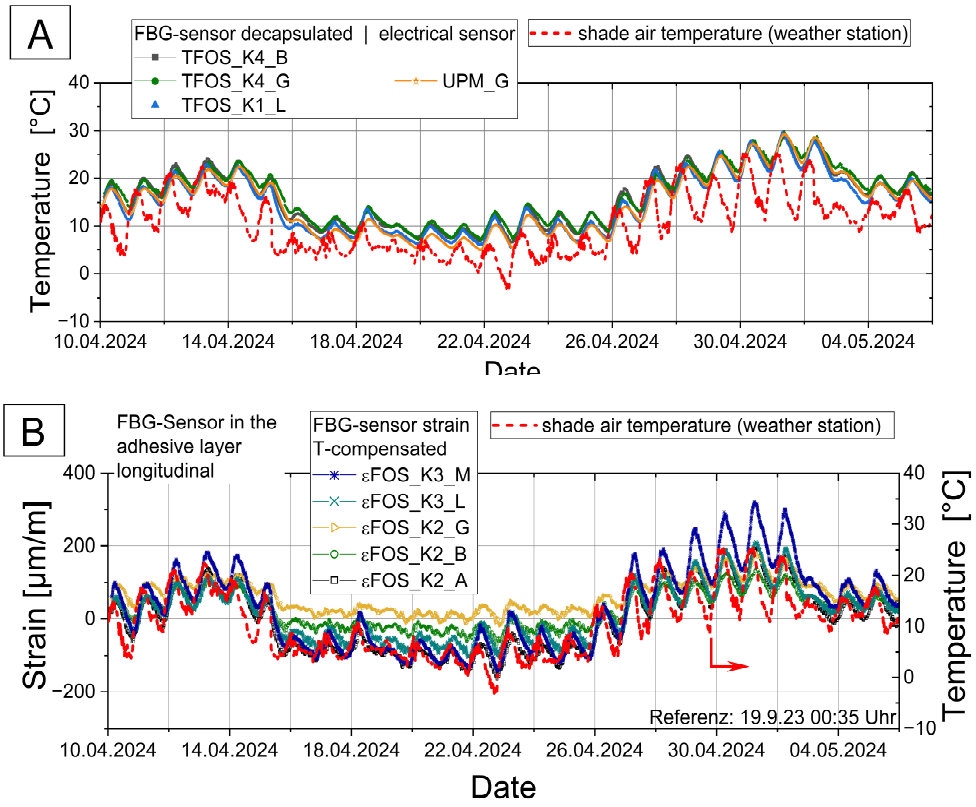

Figure 6: FBG-sensor data from the ATCC superstructure segment for approx. one month in outdoor climate Weimar, Germany: A) Temperature; B) Strain data compared with shade air temperature from weather station

The temperature-compensated strain changes are shown in Figure 6B for FBG-sensors in the longitudinal direction (axis A, B, G, L, M, refer to Figure 2). The daily strain minima and maxima are in particular comparable to the temperature data; however, they occur with a time delay in relation to the external temperatures. Bragg gratings close to the end grain of the structure (axis A: black, axis M: blue) react much stronger to the external environmental conditions compared to Bragg gratings in the middle of the structure (axis G: yellow), where the daily minima and maxima are less pronounced. In particular the FBG-sensor in southern orientation (axis M: blue) shows the highest strain values. In principle, it is therefore possible to describe temperatures and the local strain changes in the adhesive of the ATCC superstructure segment with FBG-sensors.

A major advantage of distributed strain measurements is the high spatial resolution and thus the gain in additional local information. Figure 7 shows the strain changes from DFOS measurements as function of the position in the adhesive layer in longitudinal direction of the ATCC superstructure segment. There various times at different temperatures in the structure ranging from -4.9 °C to 30.3 °C are presented. The temperature value refers to a sensor in the middle of the structure in axis G. In addition to the temperatures inside the ATCC structure, the shade air temperatures are also indicated in the graph (Figure 7, right). The

influence of the inner temperature on the course of the strain can be seen in Figure 7 by shifts of the strain profiles. At high temperatures, the strain profile is shifted to positive strain with a slight increase in strain close to the end grain of the structure (see green curves at temperature of ca. 30 °C). At low temperatures, i.e. -4.9 °C (purple curve) the strain profile is shifted to negative strains with higher negative strains at the edge of the structure (see position 0.05 m and 2.45 m) compared to the middle part at sensor position of approx. 0.75-1.75 m. Furthermore, local strain peaks occur in the profiles. The strain peaks are more pronounced the higher the strains are and the further the distance to the reference temperature of the sensor (here 20 °C) is. The strain peaks are most probably produced by inhomogeneities. This concerns not only knots, growth defects, or inclined wood fibres on the timber surface (already discussed in [20]), but can also result from inhomogeneities in the adhesive layer and geometry irregularities. Last concerns strain peaks in the centre area of the structure. In this area, grooves were made in the timber surface into which fibre sensors were inserted to measure strains in the transverse direction. The spatially resolved strain measurement can detect faults in the structure near the sensor.

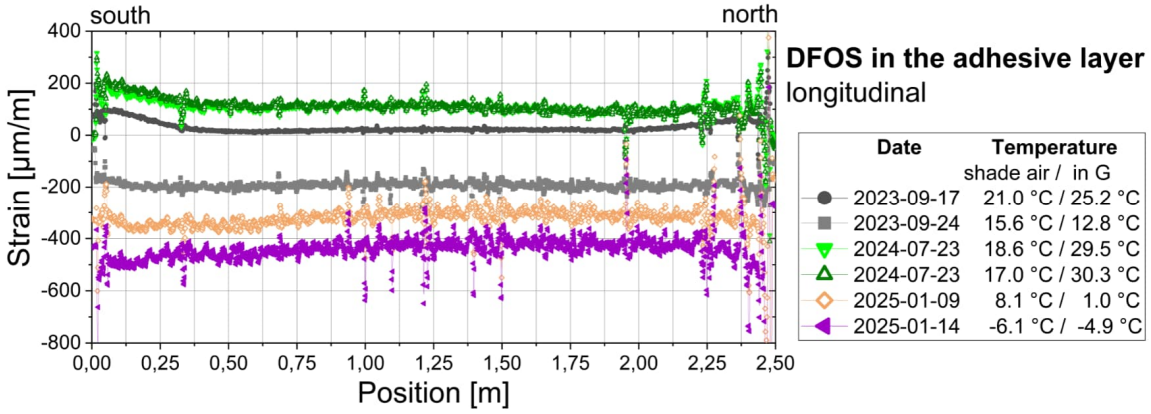

Figure 7: DFOS-data with spatial resolution of 1.3 mm from measuring campaigns of the ATCC superstructure segment in outdoor climate Weimar, Germany

4 CONCLUSIONS AND OUTLOOK

The results of the study demonstrate the potential of using thin fibre-optic sensors to measure strain and temperature values in the adhesive joints of ATCC along their entire length with high spatial resolution. The sensor data can be used to gain insights into local strain conditions and to detect localized damage in the component. Investigations on an ATCC superstructure segment show that fibre-optic sensors can be integrated into the adhesive layer. With appropriate protective measures, the sensors can withstand the fabrication process and transportation. Semi-distributed and distributed fibre-optic sensors enabled the monitoring of temperatures and strains of the ATCC superstructure segment, which is stored in outdoor climate. This allows to obtain detailed information of corresponding values at various positions of the superstructure segment. Thus, the sensor data may offer valuable information for the development and implementation of new construction methods, such as adhesively bonded timber-concrete. FBG-sensors can therefore be highly effective for structural health monitoring. The use of DFOS enables detailed analysis with high spatial resolution.

ACKNOWLEDGEMENT

Many thanks go to the Fachagentur Nachwachsende Rohstoffe e.V. (FNR) and to the Federal Ministry of Food and Agriculture (BMEL) of Germany for funding the ongoing research project ‘HBVSens’ (FNR-project no.: 2221HV097). Special thanks go to partners from industry Bennert GmbH, STRAB Ingenieurholzbau Hermsdorf GmbH, Beton Fertigteilbau Erfurt GmbH, HEBAU GmbH, STRABAG AG and Sika Deutschland GmbH, FBGS GmbH, AOS GmbH and Polytec GmbH for strong support and fruitful discussion during the project. Thanks also go to the staff of the testing facility “Versuchstechnische Einrichtung” at the Bauhaus-University Weimar and the MFPA colleagues for their support in the fabrication of the ATCC and for preparation and help during testing.

REFERENCES

1. Kästner, M.: Zum Tragverhalten von Polymermörtel-Klebverbindungen für die Anwendung bei Straßenbrücken in Holz-Beton-Verbundbauweise. Dissertation, Bauhaus-Universität Weimar, 2019.
2. Eisenhut, L.: Geklebter Verbund aus Holz und hochfestem Beton – Untersuchungen zum Langzeitverhalten. Dissertation, Universität Kassel, 2015.
3. Yassin, M.H.; Farhat, M.H.; Soleimanpour, R. et al.: Fiber Bragg grating (FBG)-based sensors: a review of technology and recent applications in structural health monitoring (SHM) of civil engineering structures. Discov Civ Eng 1, 151 (2024). https://doi.org/10.1007/s44290-024-00141-4.
4. Zhou Z.; Graver, T. W.; Hsu L.; Ou J. P.: Techniques of advanced FBG sensors: Fabrication, demodulation, encapsulation and their application in the structural health monitoring of bridges. in: Pacific Science Review 5(1): pp. 116–121, 2003.
5. Schroeder, K.; Ecke, W.; Apitz, J.; Lembke, E.; Lenschow, G.: Fibre Bragg Grating Sensor System Monitors Operational Load in a Wind Turbine Rotor Blade. in: Measurement Science and Technology 17 (5), pp. 1167-1172, 2006.
6. Peters, K.: Fibre Bragg Gratings Sensors, Chapter 61, p. 1103: in Boller, C.; Chang, F.-K.; Fujino, Y.: Encyclopedia of Structural Health Monitoring, Vol. 2, Wiley & Sons, 2009.
7. Kuang, K.S.C.; Kenny, R.; Whelan, M.P.; Cantwell, W.J.; Chalker, P.R.: Embedded fibre Bragg grating sensors in advanced composite materials, Composites Science and Technology 61, 1379–1387, 2001.
8. Ganß, M.; Daum, M.; Breidenbach, M.L.; Beinersdorf, H.; Kuhne, M.; Hildebrand, J.: Untersuchungen an thermo-mechanisch beanspruchten Glasklebverbindungen mit integrierten faseroptischen Sensoren, in Glasbau 2015, S.361, 2015, Ernst&Sohn, ISBN:978343303101-8.
9. Ganß, M.; Barnickel, J.; Kuhne, M.; Beinersdorf, H.; Hildebrand, J.; Bergmann, J. P.; Könke, C.: Zustandserfassung von strukturellen Klebverbindungen mittels faseroptischen Sensoren: Untersuchungen an geklebten Stahl-CFK-Verbindungen, in Smarte Strukturen und Systeme, p. 51, Tagungsband des 4Smarts-Symposium, ISBN: 978-3-8440-5083-7, 2017.
10. Wachter, N.; Ganß, M.;. Baudone, T.; Baitinger, M.; Teich, M.; Thiel, T.: Zustandsmonitoring von strukturellen Silikonklebverbindungen mit faseroptischen Sensoren – Möglichkeiten und Herausforderungen in B. Weller; F. Nicklisch; S. Tasche (Hrsg.): Klebtechnik im Glasbau. Berlin: Ernst & Sohn, 2022, ISBN: 978-3-433-03391-3.
11. Samiec, D.: Verteilte faseroptische Temperatur- und Dehnungsmessung mit sehr hoher Ortsauflösung. in: Photonik (6), pp. 34-37, 2011.
12. Kästner, M.; Jahreis, M.; Hädicke, W.; Rautenstrauch, K.: Development of continuous composite joints on the basis of polymer mortal with matched properties. in: Proceedings of the World Conference on Timber Engineering (WCTE 2014), Quebec City, Canada, 2014.
13. Kästner, M.; Rautenstrauch, K.: Polymermörtel-Klebverbindungen für Holz-Beton-Verbundbrücken Teil 1+2. in: Bautechnik 98, SH Holzbau, Ausgabe 1, pp. 23–39, 2021.
14. Kästner, M.; Rautenstrauch, K.: Entwicklung einer ökologischen Straßenbrückenbauweise aus Holz und Beton mit kontinuierlichem Klebeverbund auf Basis (bio-)polymerer Reaktionsharzsysteme – Ein Beitrag zum Einsatz nachwachsender Rohstoffe für Verkehrsbauten. Final report of the FNR Project 22000612, Bauhaus-Universität Weimar, 2017.
15. Ganß, M.; Hildebrand, J.; Beinersdorf, H.; Kuhne, M.; Könke, C.: Monitoring von Klebverbindungen mittels faseroptischem Messsystem – MOFAS. Final report of the IGF project 17777 BR, Bauhaus-Universität Weimar, 2015.
16. Allgemeine bauaufsichtliche Zulassung Nr. Z-10.7-282: Polymerverguss zur Verstärkung von Holzbauteilen. Bennert GmbH Klettbach, Deutsches Institut für Bautechnik, 2021.
17. Simon, A.: Analyse zum Trag- und Verformungsverhalten von Straßenbrücken in Holz-Beton-Verbund-bauweise. Dissertation, Bauhaus-Universität Weimar, 2008.
18. Kästner, M.; Ganß, M.; Kirchner, A.; Paetow, H.; Koch, J.; Simon, A.; Kraus, M.: Adhesively bonded timber-concrete composite bridges – analysis of thermal actions on the superstructure. in: Proceedings of the World Conference on Timber Engineering (WCTE 2025), Brisbane, Australia, 2025.
19. Koch, J.; Simon, A.; Kästner, M.; Ganß, M.: Analysis of the timber moisture content of an ATCC-road bridge superstructure segment. in: Proceedings of the 5th International Conference on Timber Bridges (ICTB 2025). Rotorua, New-Zealand, 2025.
20. Münzer, A.; Dill-Langer. G.: Monitoring of Timber Structures by Fiber-optic Sensors: Concept and First Results, Otto Graf Journal Vol. 22, 2023.

ICTB 2025. 5th International Conference Timber Bridges
Rotorua, New Zealand, 29 June to 2 July 2025.

KAKANUI REPLACEMENT BRIDGE – DESIGN OF A NEW 162M LONG TIMBER ROAD BRIDGE IN NEW ZEALAND

Anton Kivell[1], Andy Van Houtte[2], Mike Harrison[3], Tom Armstrong[4]

ABSTRACT

After serving the people of Kakanui, New Zealand, for 124 years, the Waitaki District Council have decided in 2023 that the existing timber bridge across the Kakanui River is to be replaced with a single lane, 11 span, 162m long, modern, durable engineered timber bridge. The inspiration behind considering the timber option was the fact the existing bridge is 124 old and still operational, therefore clearly a suitable material for this intent and environment. This paper discusses the project background, selection process for the timber option, and technical challenges with the adoption of this new bridge form for New Zealand conditions. Some of these technical challenges differ to those encountered in other parts of the world. It also discusses the cost competitiveness of timber bridges when compared against traditional precast concrete girders and what the future looks like for timber bridges in New Zealand.

1 INTRODUCTION

The bridge is located in Kakanui, 100km north of Dunedin in the South Island of New Zealand, and crosses the Kakanui River. The new bridge replaces an existing timber bridge which was constructed in 1900 and is still operating, though at a reduced capacity.

Figure 1: Existing Kakanui Bridge

The Waitaki District Council sought a cost effective, resilient new bridge that was able to replicate the functionality of the existing bridge. Hoff Consultants Limited (Hoffcon) were engaged to develop the design of the bridge from the initial concepts through to detailed design. Timber was always considered an option, but the Council's primary driver was cost. A series of concept designs were developed that considered timber, prestressed concrete and steel for

[1] Head Bridge Engineer, Hoff Consultants Limited
e-mail: anton.kivell@hoffcon.pro
[2] Director, Potius Building Systems Limited
[3] Project Manager – Major Transport Projects, Waitaki District Council
[4] Associate Structural Engineer, Hoff Consultants Limited

the replacement Bridge's superstructure. Through development of the design options, and subsequent pricing, the timber option was selected to be progressed through to detailed design.

2 BRIDGE DESCRIPTION

The proposed Kakanui Replacement bridge is 162m in length, consisting of nine 15.6m internal spans and two 10.7m long end spans. It caters for one lane of full HN-HO-72 (Waka Kotahi NZ Transport Agency, 2022) traffic along with a 1.5m wide footpath. At the bridge location, the Kakanui river opens out into an estuary, and is approximately 750m from the ocean.

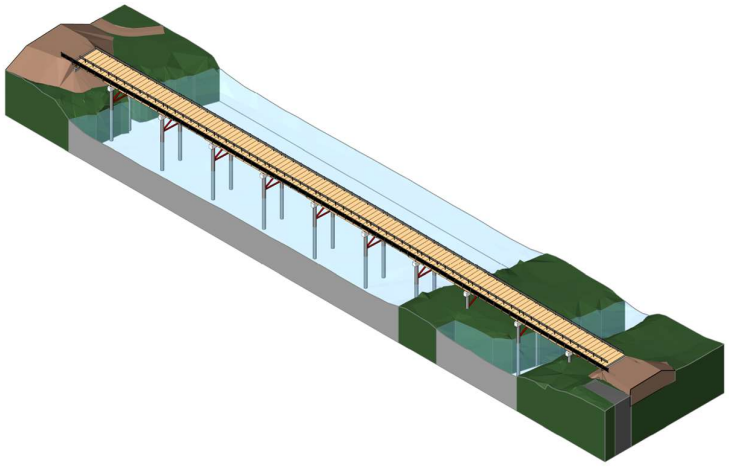

Figure 2: Isometric image of the model of the Kakanui Replacement Bridge

The bridge utilises a traditional concrete and steel substructure with an engineered timber superstructure made up of glulam girders supporting a plywood deck as is shown in Figure 3. The timber girders lap over the piers and inter-lock to provide moment continuity. Glulam blocking is also provided to assist with load distribution, stability of the beam sofit under debris impact and in construction. The bridge also supports a series of water, sewer, and telecommunications utilities.

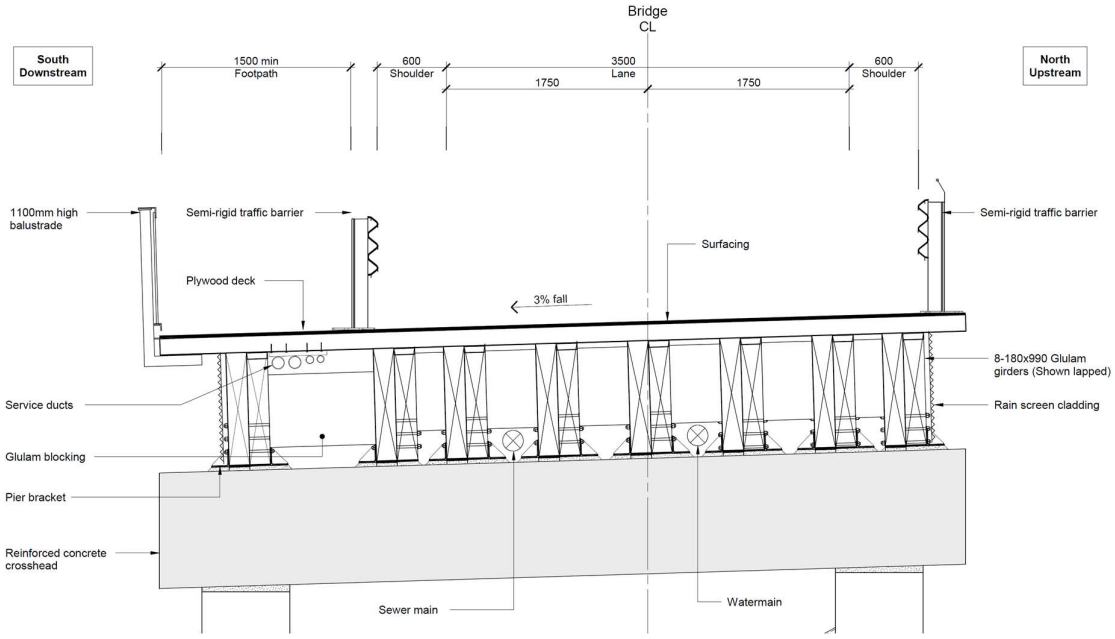

Figure 3: Typical bridge cross section at piers.

3 DESIGN PHILOSOPHY

3.1 General

The design philosophy for the bridge was to produce a structural form that could be constructed by local contractors, largely manufactured off site, be able to be assembled on site rapidly with minimal craneage, and that was relatively simple in its form and detailing. Control of cost was a key consideration for WDC, and having a bridge which fulfilled these criteria was seen as being critical to achieving value for money.

3.2 Articulation

The main girders of the bridge were made continuous over the piers to reduce structural depth requirements to control strength requirements and vibration concerns. The shorter end spans were simply supported at the abutments and provided with a single seal expansion joint to allow for movement of the 162m long superstructure.

The piers consisted of two 760mm diameter reinforced concrete cast in place piles which extended to a precast concrete crosshead. These cantilevered in the longitudinal direction of the bridge which provided adequate flexibility to accommodate movements of the superstructure. The superstructure was supported on elastomeric strip bearings at the piers, with lateral restraint provided by galvanised steel bracket. Seismic and breaking loads were able to be resisted by the piers and abutments without the need for ductility, largely due to the light weight of the superstructure.

The dominant loading on the bridge piers comes from debris under flooding which is applied primarily in the transverse direction with a magnitude approximately three times the seismic loads. The high flood levels and velocities, combined with significant level of scour necessitated the inclusion of a triangulated brace between the piles above ground.

3.3 Durability

The bridge is located approximately 750m from the ocean. This places considerable level of chlorides in the air which was a consideration for concrete and steel elements.

The Waka Kotahi NZ Transport Agency (Waka Kotahi) requires that bridges be designed for a 100 year design life. There is no pathway for demonstrating this for timber through the acceptable solutions within the NZ Building Code (Ministry of Business, Innovation & Employment, 2023). However, Waka Kotahi have been, and are still at the time of writing, developing guidance on the steps that are required to demonstrate acceptable durability performance (Waka Kotahi NZ Transport Agency, 2022). These guidance documents focus on the treatment and detailing of timber elements to control moisture ingress and promote ventilation to allow moisture to escape if ingress does occur.

3.3.1 Treatment

Unlike much of the world, New Zealand's primary source of timber is Pinus Radiata, which grows in abundance in plantation forests in NZ. While the mechanical properties of radiata are unexceptional, its ability to be pressure treated to achieve full penetration of modest sized (<50-100mm thick) sections means that concerns around hidden degradation are greatly reduced. Treatment to H5 (Standards New Zealand, 2003) using CCA is easily achieved and commonplace. This treatment is considered suitable for achieving a design life of 50 years for timber elements in contact with the ground. For bridge superstructure, when this is combined with well-considered detailing to reduce the potential for moisture build up in timber elements, it is considered suitable for achieving a 100-year design life.

The design utilises 140mm thick plywood deck panels. Unfortunately, these are not currently produced in New Zealand, requiring them to be imported from either Australia or Papua New Guinea. These utilise a veneer treatment process that allows for full penetration of the section

to H5 using ACQ and are generally screw laminated. The screw lamination is only utilised to provide temporary clamping in manufacture but creates the undesirable long term potential for the screw to corrode and leave cavities within the plywood for moisture to become entrapped. The screw lamination allows for the section to be fully treated to H5, whereas other systems which do not utilise screws in manufacture are only envelope treated after the full plywood section is built up. Ideally, stainless steel screws would be used for the re-laminating of the plywood decks, however these carry with them a significant price premium, and are unproven in being able to develop the temporary clamping that is required. With both approaches presenting some deficiencies, bond performance was prioritised over the potential moisture pathways presented by zinc plated screws and conventional screwing was accepted provided the upper face of the deck was not penetrated by the temporary screws.

3.3.2 Fixings

Use of copper rich treatments in the timber elements necessitated the use of 316 stainless steel fixings throughout the structure. The large engineered wood screws required for the bridge connection have limited availability in 316 stainless steel in New Zealand, requiring a 3+ month lead time in the quantities required.

3.3.3 Detailing

Detailing for durability focused on the principles outlined in *AS5100.9:2017 Bridge design Timber* (Standards Australia, 2017). The primary defence against water ingress was the two coats of chip seal applied to the top of the plywood deck panels after they were installed. This, combined with the 3% crossfall of the bridge provides a robust mechanism for surface water to sheet off the deck and away from the timber elements below. This was supplemented by an edge flashing at the down-slope side of the deck to further protect the end-grain of the plywood in addition to the paint/bitumen applied to it.

Cavity fixed roofing iron was provided to the exterior faces of the outermost girders as a screen to minimise the potential for rain and sunlight exposure, and associated checking and degradation.

3.4 Movements

Like other materials, timber is subject to changes in dimension under fluctuations of moisture and temperature levels. There was limited information around for the application to bridges constructed from Pinus Radiata. These movements influence the design of expansion joints on the bridge, amongst other elements.

3.4.1 Thermal

AS 5100.9 (Standards Australia, 2017) Cl6.2.3.1 states that the coefficient for thermal expansion of timber shall be taken as zero. Hence, no thermal effects are required to be considered in the design of the timber elements. However, for a bridge of the length being considered, and the superstructure continuity provided, some allowance was made for thermal effects in the design and strip seal joints were provided at abutments.

The co-efficient for thermal expansion was assumed to be $1.2 \times 10^{-5}/^{o}C$. For the 162m long bridge, with an average temperature of 15°C and a service temperature range of +/-20°C, the anticipated movement range at each abutment was expected to be in the order of +/-20mm. This is considered in the design of the abutment bearings and expansion joints.

3.4.2 Moisture effects

The moisture content considered in AS5100.9 (Standards Australia, 2017) is the Equilibrium Moisture Content (EMC). Variation in EMC is likely to occur on a seasonal basis, rather than being influenced by daily cycles. Data for Oamaru Airport from (Macara, 2015), which shows that there is an annual variation in the monthly average of up to 77.5%RH in May, down to 68.5%RH in September. (Herritsch, 2007) was used to determine an EMC for a range of RH = 68.5% to RH = 77.5% of EMC = 12.5% to 18.7%.

(Chiniforush, 2019) included testing of GL13 Radiata Pine (RP) sourced from New Zealand. Their findings were that the RP samples at 15^{o}C presented average sorption and desorption longitudinal strain co-efficient of 0.081×10^{-3} mm/mm/%MC.

From this it was determined that the total length from the bridge may increase by 78mm from install (at 12%MC) to its maximum expect moisture content in service (18.7%), with a seasonal variation of ~30mm.

For strength checks to AS/NZS 1720 a 20%EMC was used.

4 DESIGN DETAILS

There are no standardised timber road bridge designs available in New Zealand to provide an initial reference, so the entire design was clean sheet. This presented a large degree of freedom but also meant that careful consideration needed to be made around all details. It was appreciated that road bridges are subject to significant, repeated, dynamic loading, and that robust detailing would be required. Generally design was undertaken to AS/NZS1720 (Standards New Zealand, 2022) though this was supplemented with Eurocode 5 part 1 (European Standard, 2004) and part 2 (European Standard, 2008). This section discusses some of the details that were adopted for the design.

4.1 Lapped Girders

The lapped girder arrangement at the piers is a critical detail to create an efficient, easy to construct design. The detail creates moment continuity over the piers, while also increasing the flexural capacity of the glulam girders over the piers where moment demands are the largest. To achieve this, triangular continuity corbels are provided on the side face of the girders which engage with the cut-down end of the opposing girder as shown in Figure 4. The corbels are simply cut from the initially rectangular girders. This couple acts to lock the adjacent spans together through the transfer of vertical shear and prying between the corbels.

4.1.1 Installation

The design intention is to allow cassettes to be assembled offsite or on the riverbank, before being lifted into place. Figure 4 outlines the intended construction sequence. Cassettes consisting of 3 girders weigh in at 8-9t, where as a single prestressed concrete hollowcore for the same span would typically be ~20t. The expectation is that the cassette system will allow for rapid installation of girder spans, with minimal cranage.

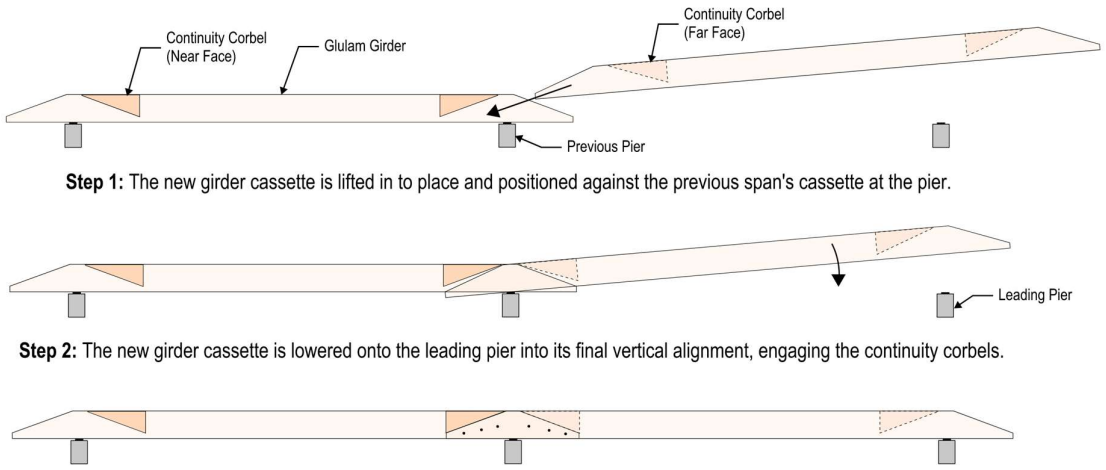

Figure 4: Intended construction sequence for girder installation.

4.1.2 Corbel Detail

The continuity corbels were designed so that they could be fabricated from the cut-out corner of a typical rectangular glulam beam. Their set-out needed to account for the precamber and vertical curvature of the girders to provide confidence that they would engage suitably. The corbels are attached to the girder side using inclined and perpendicular screws which supplemented a glued interface.

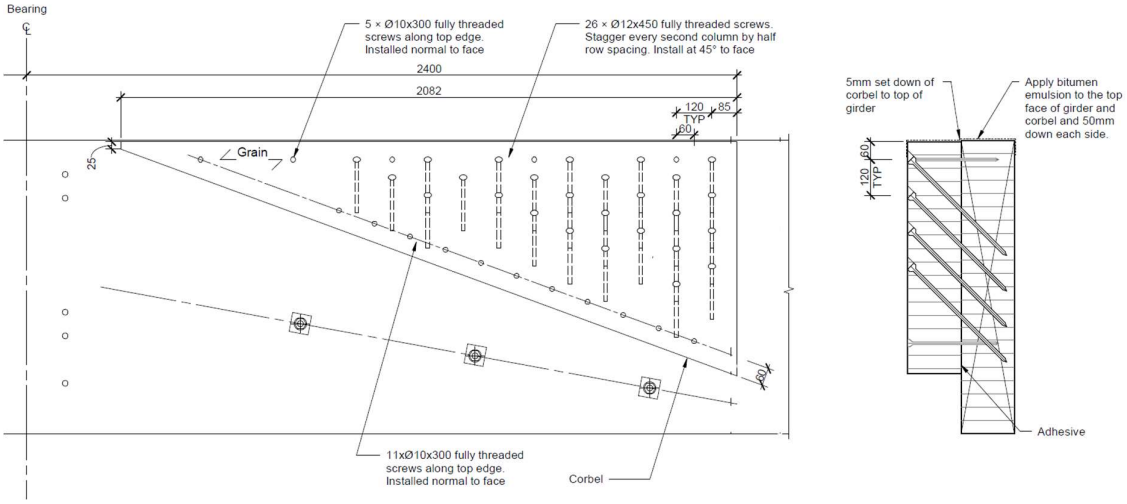

Figure 5: Continuity corbel details

A similar effect could also be achieved without the corbel detail through the use of traditional fixings at these locations. However, the practicalities of installing such a large number of fixings in a confined space on site, particularly when allowing for tolerance/site drilling was seen as too labour and time intensive, as well as potentially unsafe.

Some bolts were ultimately included in the design to allow for more reliable transfer of longitudinal loads, and to avoid any potential unseating from lateral movement of the corbel/girder under flood/debris loading.

4.2 Deck-girder Connection

The connection between the deck panels and girders below needed to be able to transfer vehicle breaking loads, as well as allowing for vertical and horizontal load distribution. Ideally the top surface of the deck would not be penetrated by fixings. However, this makes installation of the plywood deck panels impractical and structurally inefficient. To create a robust connection, inclined screws were utilised as shown in Figure 6. The heads of these screws were recessed into the plywood deck panels that were plugged with bitumen. These screws were fully threaded, raising the possibility that the interface between the plywood and girder may open slightly and the screw is wound in. This could expose the screws to repeated loading from vehicle axles passing above, potentially resulting in fatigue. To give greater confidence that the vertical loads would be transferred directly through the timber rather than the screws, additional partially threaded screws were provided to clamp the panels down prior to the fully threaded screws being installed.

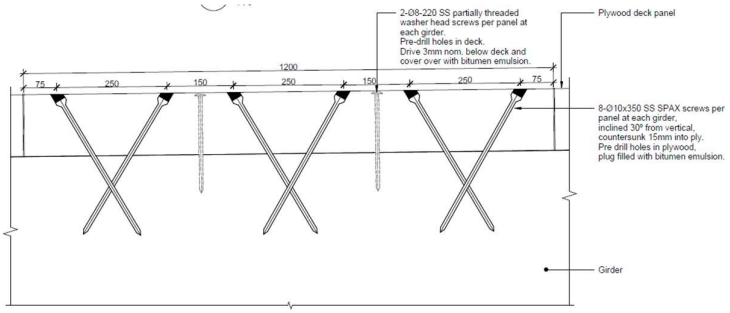

Figure 6: Plywood deck panel to girder connection detail

4.3 Blocking Detail

The role of transverse superstructure elements in bridges is typically to assist with stability of the primary elements as well as assisting in distribution of concentrated loads. The initial design of the blocking attempted to achieve moment and shear fixity. The detail required to develop this fixity proved to be costly and difficult to construct.

Considering this, the design philosophy around blocking was revised so that they primarily would provide stability in construction, along with assisting to transfer any flood debris loading which may be applied to the girder soffit.

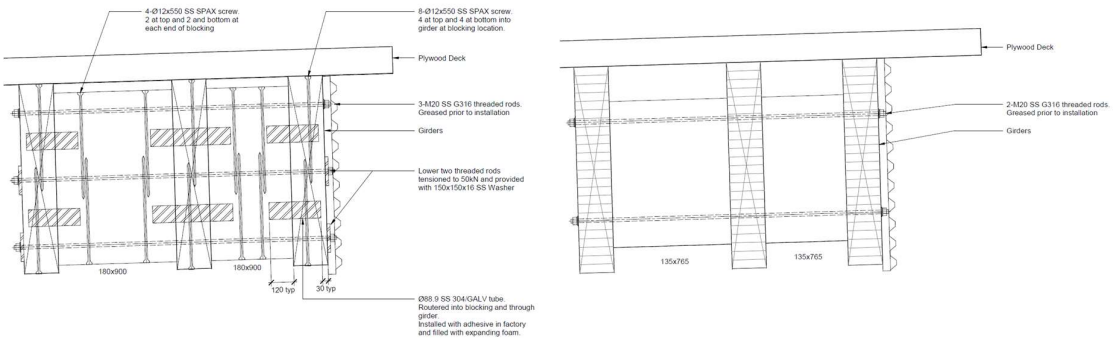

(a) (b)

Figure 7: (a) Initial 'rigid' blocking detail, (b) Revised 'pinned' blocking detail.

4.3.1 Implications on girder size

While the revised approach to the blocking design simplified the blocking detail significantly, it did come at the cost of reduced load distribution between girders. This resulted in the need to increase the more heavily loaded upstream outer three girder sections from 180x990 to 180x1080 at the mid-spans. The girder depth was locally increased over the middle 10.8m of the girder, with the ends were kept consistent with the typical girders.

4.4 Expansion Joint Detail

Expansion joints are one of the most susceptible elements of a bridge to damage and degradation due to their direct exposure to repeated intensive wheel loading. The most common and NZTA preferred form of expansion joint is a single seal joint. These are typically housed in reinforced concrete elements and suppliers are reluctant to deviate from their standard design arrangements without costly testing. With this in mind, it was decided to introduce a reinforced concrete end beam to the bridge deck to house the expansion joint. This was connected into the surrounding timber structure with starter screws.

5 COST COMPARISON

A cost comparison was undertaken at the concept stage of the bridge. This indicated that the engineered timber design offered a modest cost benefit over a traditional prestressed concrete hollowcore superstructure design.

The Waitaki District Council chose to procure the construction of the bridge based on the lowest price of conforming tender, while also making the tender open to alternative designs. The selection of Lowest Price Conforming was not made easily. The Councils fiscal limitation required an analysis of what benefit could come with a quality premium. Hoffcon provided a fully detailed set of construction drawings and specifications. The engagement during the scoping and design phases provided a robust a deliverable specification with drawings. Innovation comes from experience and cutting-edge projects carry an amount of assumed risks.

Five tenders were received, with an alternative design also being submitted that utilised a hollowcore superstructure. Three tenders were within the client's allocated budged, with the hollowcore alternative being the one with the lowest price and being awarded the construction contract.

A comparison of costs for the timber options compared against the concrete alternative is presented in Table 5-1. Also included is the difference when considering a 'pseudo' submission made up of the lowest cost elements across all timber tenders.

Table 5-1: Cost comparison of timber option against the concrete alternative (Bridge only, excluding roading works etc.)

Cost Element	Lowest Tenderer - Timber	Pseudo Timber Tenderer
Temporary Works (inc. P&G)	-20%	-20%
Substructure	-33%	-34%
Superstructure	+99%	+72%
Total:	**+14%**	**+5%**

It is worth noting that the lowest conforming (Timber) price included cost elements for traffic management, project P&G, dayworks, and supply of glulam which, which when compared to

the prices submitted by other tenderers for these elements increased their project tender price by 13%. Had a conforming tenderer (timber) been able to achieve the lowest price from across all the cost elements, then the costs would have been equal to the concrete alternative.

6 OUTCOMES AND DISCUSSION

The final outcome for the Kakanui Replacement Bridge is that it will be constructed from concrete. Construction is scheduled to commence in March 2025. However, there are some positive aspects that demonstrate that timber bridges of this type can be competitive in the New Zealand bridging market. Some of these are discussed below.

6.1 Why did concrete win?

- **Industry maturity:** New Zealand has not built a significant timber road bridge in the last 50 years. It is a fledgling part of the industry where designs, details, manufacturing processes, and construction methods and systems are still being developed. Timber is competing against the well-established precast concrete industry which is set up with standardised bridge beam designs, details, and moulds. The successful contractor has their own precast plant and are self-performing beam manufacture.
- **Risk:** We are unable to determine the mark-up and risk allowance that was made by tenderers to account of the novel aspects of the timber design and its construction, but it is likely to be significant. As the industry becomes more familiar with the risks and opportunities associated with timber bridges, it would be hoped that these allowances can be reduced. Conversely, the successful contractor builds several hollowcore bridges yearly, so is well aware of the risks and carries an added level of confidence and experience that they can be managed effectively.
- **Distance from manufacturers:** The largest glulam suppliers in NZ are located in the central and bottom of the North Island, and at the top of the South Island. Kakanui is located near the bottom of the South Island, a 675km drive to the nearest supplier and a ferry crossing + 800 to 1200km drive to the others. While the design was intended to allow for flat packing for transport, it is difficult to compete with the 240km drive the successful Contractor's precast yard for the delivery of beams. The 140mm thick plywood was also sourced from either Australia or Papua New Guinea, introducing a significant transport component to the price.
- **Variability in prices:** The range of prices received for the supply and installation of glulam elements and their fixings varied significantly (35%). This was similar to the plywood supply and install (40%).
- **Flood load/seismic:** As was observed in this design, the light weight of the timber superstructures allows for significant savings in the foundations and substructure. The high seismicity in many parts of New Zealand means that having a superstructure that has a structural weight of ~2.5kPa compared to that for hollowcores (~15kPa) is a significant benefit to the design. However, flood levels and flood loading on the Kakanui Bridge are very large, dominating the substructure design and not allowing for the benefits of the significantly lighter superstructure to be fully realised.

6.2 Is there a place for timber road bridges in New Zealand?

While the authors of this paper are supremely disappointed that the timber design was not progressed for the Kakanui bridge, this project has demonstrated that timber bridges are a viable roading solution in New Zealand and could be cost competitive. The compounding factors listed in Section 6.1 led to a specialist concrete bridge builder, that has a finely tuned delivery model for hollowcore bridges, being able to propose an alternative design for 15%

less than a traditional contractor building a timber bridge for the first time. This difference seems far from insurmountable. As designers and the industry matures, and when bridges are located closer to manufacturers or in regions of higher seismicity, it seems apparent to the authors that there is indeed a bright future for timber road bridges in New Zealand. This is just the first step.

7 ACKNOWLEDGEMENTS

The development of timber bridges in New Zealand owes a lot to the belief of Sulo Shanmuganathan (Chief Engineer at Waka Kotahi NZ Transport Agency) who grasped the potential that they offered when presented with the concept three years ago. This has been a journey for all involved and there are many others who have provided support in the development of this concept and this project. In particular; Daniel Moroder and Andy Buchannan (PTL), Sam Leslie (Reg Stag), Brett and Roy Hamilton (Techlam), John Woodman (Prolam), Bill Blackmore (ibuilt) and Peter Robinson (PNGFP).

Special acknowledgement needs to go to Andy Van Houtte of Potius building systems who completed the peer review of the timber design, contributing ideas and experience to improve the design and develop pragmatic solutions.

It is also important to acknowledge the team at Hoffcon (Tom, Kaitlin, Hawaiki, Josh, Dean, Dave, and Tessa) for the effort that has gone into the development of this project and enduring belief in one another that we can change the way construction done in Aotearoa.

8 REFERENCES

Chiniforush, A. (2019). Moisture and temperature induced swelling/shrinkage of softwood and hardwood Glulam and LVL: An experimental study. *Construction and Building Materials*, 207:70-83.

European Standard. (2004). Eurocode 5: Design of timber structures - Part 2: Bridges . *EN 1995-2*.

European Standard. (2008). Eurocode 5: Design of timber structures - Part 1-1: General Common rules and rules for buildings . *EN 1995-1-1 :2004+A 1*.

Herritsch, A. (2007). Investigation on Wood Stability and Related Properties of Radiata Pine. *Thesis*.

Macara, G. (2015). The Climate and Weather of Otago. *NIWA Science and Technology Series*.

Ministry of Business, Innovation & Employment. (2023). Acceptable Solutions and Verification Methods Prepared by the Ministry of Business, Innovation and Employment For New Zealand Building Code Clause B1 Structure. ISBN: 987-1-99-100871-8.

Standards Australia. (2017). Bridge Design - Timber. *AS 5100.9*.

Standards New Zealand. (2003). Chemical preservation of round and sawn timber. *NZS 3640*.

Standards New Zealand. (2022). Timber Structures. *NZS AS 1720.1*.

Waka Kotahi NZ Transport Agency. (2022). #22-02 Interim technical standards for the design of timber bridges. *Technical Advice Notice*.

Waka Kotahi NZ Transport Agency. (2022). The Waka Kotahi NZ Transport Agency Bridge manual SP/M/022.

ICTB 2025. 5th International Conference Timber Bridges
Rotorua, New Zealand, 29 June to 2 July 2025.

ANALYSIS OF THE TIMBER MOISTURE CONTENT OF AN ATCC-ROAD BRIDGE SUPERSTRUCTURE SEGMENT

Johannes Koch[1], Antje Simon[2], Martin Kästner[3], Martin Ganß[4]

ABSTRACT

The collaborative research project "HBVSens" aims to develop a high-performance superstructure for road bridges by creating a rigid bond between main timber girders and prefabricated concrete deck elements using a highly filled adhesive system (polymer mortar). The project focuses on a robust manufacturing technology, a reliable quality assurance concept and structural health monitoring. To analyse the effects of outdoor conditions on moisture, temperature and strain distributions in adhesively bonded timber-concrete composite bridges, a superstructure segment was constructed and equipped with a large number of sensors. The following paper describes the design, fabrication and setup of the adhesively bonded timber-concrete composite superstructure segment. Additionally, the monitoring concept and sensor integration are explained with a particular focus on timber moisture content. Finally, initial results of the moisture measurements are presented.

1 INTRODUCTION

To date, only discontinuous semi-rigid joining techniques have been used to construct timber-concrete-composite (TCC) road bridges. The collaborative research project "Hybrid timber bridges with adhesive bond - quality assurance and structural health monitoring using integrated sensors (HBVSens)" aims to create a high-performance superstructure for road bridges with a rigid bond between main timber girders and prefabricated concrete deck elements. The technology of adhesively bonded timber-concrete composites (ATCC) is a promising approach to design ecological and economical road bridges with spans up to 30 m. The Bauhaus-University Weimar (BUW), the Materials Research and Testing Institute at the Bauhaus-University Weimar (MFPA) and the University of Applied Sciences Erfurt (FHE) are collaborating on the project to provide a practical manufacturing technology, a proper concept for quality assurance and a concept for Structural Health Monitoring (SHM) for the ATCC construction method.

Figure 1. left: ATCC superstructure segment in outdoor climate conditions; right: Polymer mortar in strip-shape applied on the timber girder just before the concrete slab is applied from above

[1] Johannes Koch, University of Applied Sciences Erfurt, Germany,
e-mail: johannes.koch@fh-erfurt.de
[2] Antje Simon, University of Applied Sciences Erfurt, Germany
[3] Martin Kästner, Bauhaus-University Weimar, Germany
[4] Martin Ganß, Materials Research and Testing Institute at the Bauhaus-University Weimar, Germany

The ATCC construction method needs to be analysed in detail in outdoor climate conditions because the varying temperature and air humidity result in high internal strains within the structure. Therefore, an ATCC superstructure segment, as displayed in Figure 1, was set up to analyse the moisture and temperature distribution as well as the internal strains within the components and the adhesive joint in outdoor conditions. The superstructure segment was designed as a part of a bridge in practical dimensions and equipped with a substantial number of humidity, temperature and strain sensors.

2 DESIGN AND FABRICATION OF THE SUPERSTRUCTURE SEGMENT

2.1 Conceptual design

The design of the superstructure segment is based on a parameter study of TCC bridges [1]. The segment represents the half cross-section of a single lane bridge with a span of 10 m. The original bridge consists of two block glued glulam beams connected to the concrete deck slab with stud connectors.

In the case of the superstructure segment, one wooden girder has been glued to a concrete deck slab. The length of the superstructure segment was set at 2.5 m. This length was chosen to guarantee that a section in the middle of the segment was not affected by the more rapid heat and moisture transport in the longitudinal direction from the end grain. Furthermore, one of the end grain zones was sealed vapour tight to disable moisture diffusion between the ambient air and end grain of the girder. Claddings were applied on both end grains to prevent the wood from precipitation as recommended for durable wooden structures in outdoor conditions.

The superstructure segment was erected in outdoor conditions at a test site of the MFPA in Weimar. It was placed approximately 0.8 m above the ground to reduce the impact of the ground's temperature and moisture on the distribution of temperature and moisture of the superstructure segment. On the upper side of the concrete deck slab, a standardised system with a sealing, a protective and a wearing surface layer was applied in order to achieve a realistic behaviour, for example, in terms of sun-induced heating on the upper side.

2.2 Materials and fabrication

The wooden girder for the superstructure segment was fabricated using five glulam beams (GL24h), each measuring 0.2 m in width and 0.6 m in height. The spruce lamellas (Picea abies) for the glulam were conditioned to approximately 15 % moisture content, aiming to match the expected moisture level in outdoor environments. These beams were block glued together to achieve a final size of 1.0 m in width and 0.6 m in height. The surface to be bonded was planed at the production site.

The prefabricated concrete deck slab (C40/50) measured 2.0 m in width and 0.22 m in height. To create the best bond connection, the underside of the element, which was to be glued, had an exposed aggregate surface as shown in Kästner [2] developed this surface preparation for adhesive connections between wood and concrete elements. Pull-off bond strength tests [3] and delamination tests [4] also confirmed the suitability of this surface modification. To create the exposed aggregate surface, a deactivator (“Reactive CSE® Concrete Surface Deactivator version pro type 70” produced by HEBAU GmbH) was applied to the formwork before the concrete was poured. The targeted exposure depth of the aggregate was approximately 3 mm. After the formwork was removed, the surface was pressure washed to reveal the aggregate.

Both, the wooden girder but also the concrete slab has been transported to the technical centre of the BUW. After sanding the wooden surface to be bonded, most of the sensors were integrated as described in chapter 2.3. However, sanding or planing the surface again within the 24 hours before bonding, as it is typically done, could not be undertaken due to the sensors that had already been installed. The surface was cleaned with Acetone before joining.

The adhesive joint was produced with the highly filled polymer mortar “COMPONO 100 S” which is a composition of a cold curing epoxy system and a quartzitic aggregate mixture with a maximum grain size of 3 mm. “COMPONO 100 S” was originally developed as a reinforcing system for the pressure zone of timber beams in timber ceilings. However, this has also been investigated in other applications before [2][5][6]. The original mixture “COMPONO 100 S” of the Bennert GmbH, Germany covered by a national technical approval [7] was used for the superstructure segment.

Figure 2. Fabrication of the superstructure segment; from the left to the right: Exposed aggregate surface; polymer mortar stripes; PMMA primer; pouring mastic asphalt; sealed end grain zone

The thickness of the polymer mortar should allow for compensation the manufacturing tolerances of the timber and concrete components. The polymer mortar was applied in 18 mm thick stripes (see Figure 1 and Figure 2) on the wooden surface, while the concrete surface was primed with the reaction resin mixture COMPONO without aggregate to improve adhesion. The concrete slab was applied on the polymer mortar stripes from above (see Figure 1). Its dead weight was used to expand the stripes in width by compression to a final thickness of 10 mm. This ensured the filling of the exposed aggregate surface and an almost full-surface adhesive bond without air pockets.

Before the superstructure segment was transported to the test site, one of the end grains was sealed with the end grain sealing paste “ferax®-Hirnholzversiegelung” and also with a self-adhesive vapour barrier “VSK DS 1500 SYN” by Riwega GmbH as shown in Figure 2.

The upside of the concrete slab was sealed at the production site as standardised for bridge decks in Germany [8]. The surface was grinded, primed with the PMMA resin “Sika® Ergodur Pronto Pro” (see Figure 2) and sealed with the polymer-modified bitumen membrane “SikaShield® Ergobit Pro”, both by Sika AG. At the test site, the mastic asphalt layer with a thickness of 80 mm has been applied as displayed in Figure 2.

2.3 Sensor integration and measurement methods

To measure the distribution of temperature and moisture, as well as strains in the joint and the joining components, a total of 72 PT 100 elements, 32 pairs of electrodes, 54 Fibre Bragg Gratings (FBG), and additional optical glass fibres were integrated. To organise them, the superstructure segment was divided into 13 measurement planes in the cross-sectional direction, labelled as axis A to M in Figure 3. With respect to the more rapid heat and moisture transport in the longitudinal direction, the measurement planes near to the end grain zones were positioned closer together than in the middle of the superstructure segment. The moisture measuring points are labelled as follows: Three characters-one consecutive number. The first character is “F”, which means it is a moisture measuring point. The second character stands for the location of the measuring point and represents the measurement plane in axis A to M. The third character is “H”, which means that the measuring point is located in the timber girder. The consecutive number starts at one in each measurement plane. For example: FBH-2 is the second moisture measuring point in the timber girder in axis B.

PT elements are used for the temperature measurement working according to the electrical resistance method. They are concentrated on the south-facing half of the component in axes G, I, J, K, and L, while the moisture measuring electrodes are mostly concentrated on the north-facing half of the component to minimise collisions of the cables. The PT elements are placed at varying heights and distances within the component's cross-section in both wood and concrete, fixed in pre-drilled holes, which are filled with thermal conductive paste respectively attached to the concrete reinforcement before pouring. Results of the temperature measurements are given in [9].

Two types of fibre optic sensors (FOS) were used for temperature and strain measurement: FBG sensors and distributed fibre optic sensors (DFOS). Depending on their function, they are installed in stainless-steel capillaries to prevent mechanical strains, or they are rigidly mounted with epoxy. The FBG sensors provide high-resolution and stable measurement at specific points, while the DFOS offer continuous strain or temperature monitoring along their length with spatial resolution in millimetre range. The high potential of FOS in Structural Health Monitoring (SMH) is described more in detail in [10].

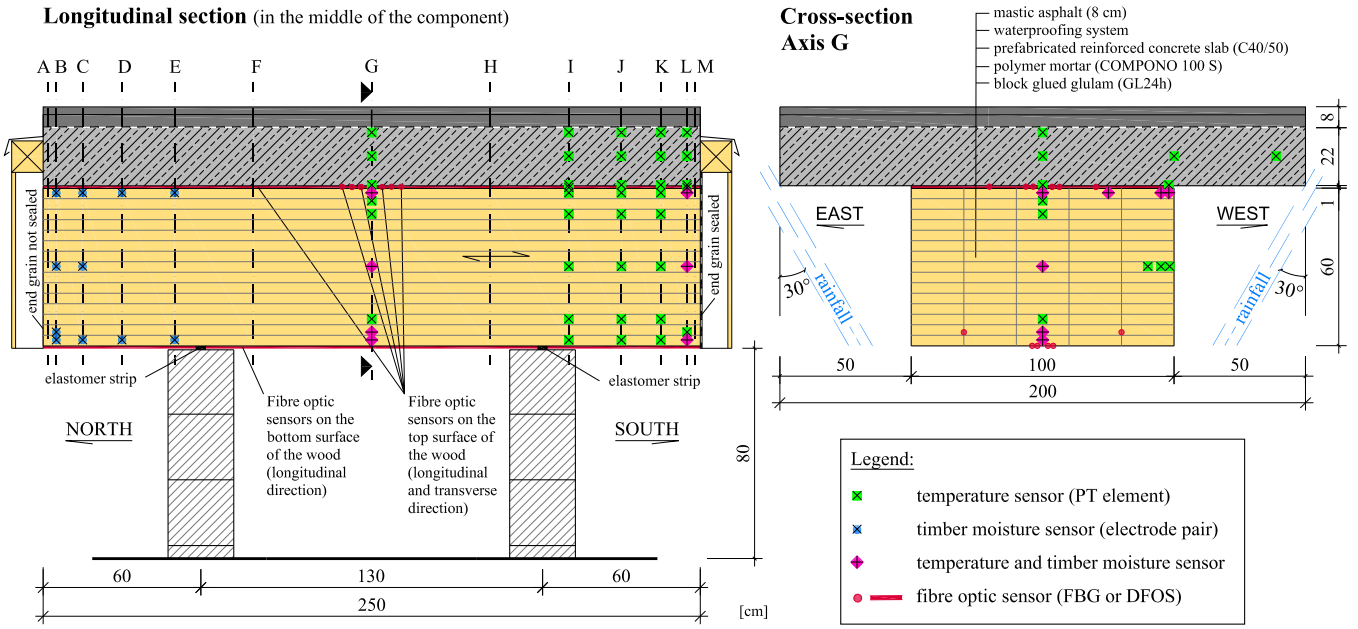

Figure 3. Superstructure segment: geometry, measuring planes and locations of the different sensors in the cross-section

The measurement of the FBG sensors has been continuously recorded while the DFOS measurement has been only recorded intermittently for a few days or weeks because of the massive amount of data and the availability of the measuring device. The FBG fibres and DFOS were placed lengthwise and cross-directionally on top of the timber girder in the adhesive joint as well as lengthwise on the bottom. Furthermore, some DFOS were integrated lengthwise within the glulam beams before they were block glued. Results of the fibre optic measurements are given in [11].

The timber moisture content (TMC) was measured using the electrical resistance method which is standardised in EN 13183-2 [12]. The measurement method is based on the correlation between electrical resistance and TMC. As temperature changes influence the electrical resistance, compensation is needed to correctly determine the TMC. Therefore, the temperature measurements with the PT elements are used for the compensation.

32 pairs of electrodes were integrated in the measurement planes B, C, D, E, G and L. Few of them were installed before the glulam beams were block glued, but most were installed after. The electrodes were made of stainless-steel screws partly insulated with a shrinking tube to define specific measurement depths. They were inserted into pre-drilled holes which were partly filled with epoxy putty. This filling material served as a sealing against the ambient climate in order to avoid changes in TMC within the drill hole. Furthermore, the epoxy putty fixed the screws along their entire length within the drill hole. This is important because earlier studies [13] showed that the screws could loosen due to swelling and shrinkage caused by the seasonal climate changes over time. Preliminary pull-out tests demonstrated that the pull-out strength of samples with a bonding length of approx. 5 cm is three times as high as those of samples without epoxy putty. The exposed tips were screwed into the wood without pre-drilling through the epoxy putty. Plastic washers between wood and screw heads as well as epoxy putty around the screw heads were used to decouple the screw heads from the wood to prevent creepage currents on the wood surface. The measuring equipment employed was produced by Scanntronik Mugrauer GmbH, Germany. A similar measurement setup has already been applied in several other studies [14][15][16].

Furthermore, a meteorological station near the superstructure segment was used to record the ambient climate conditions. The air temperature and relative humidity measured were used to calculate the equilibrium moisture content (EMC) using the Hailwood-Horrobin sorption model [17] with material specific parameters for Sitka spruce (*Picea sitchensis*) [18].

3 RESULTS OF MOISTURE MONITORING

3.1 Initial TMC and moisture equalisation

The timber girder was fabricated with lamellas conditioned to approximately 15 % moisture content. A few days after block gluing, the timber girder was transported to the technical centre of the BUW and stored there in an indoor climate until the final bonding. The girder was stored two months in indoor climate and nearly two months outdoor before the measurement started end of July 2023.

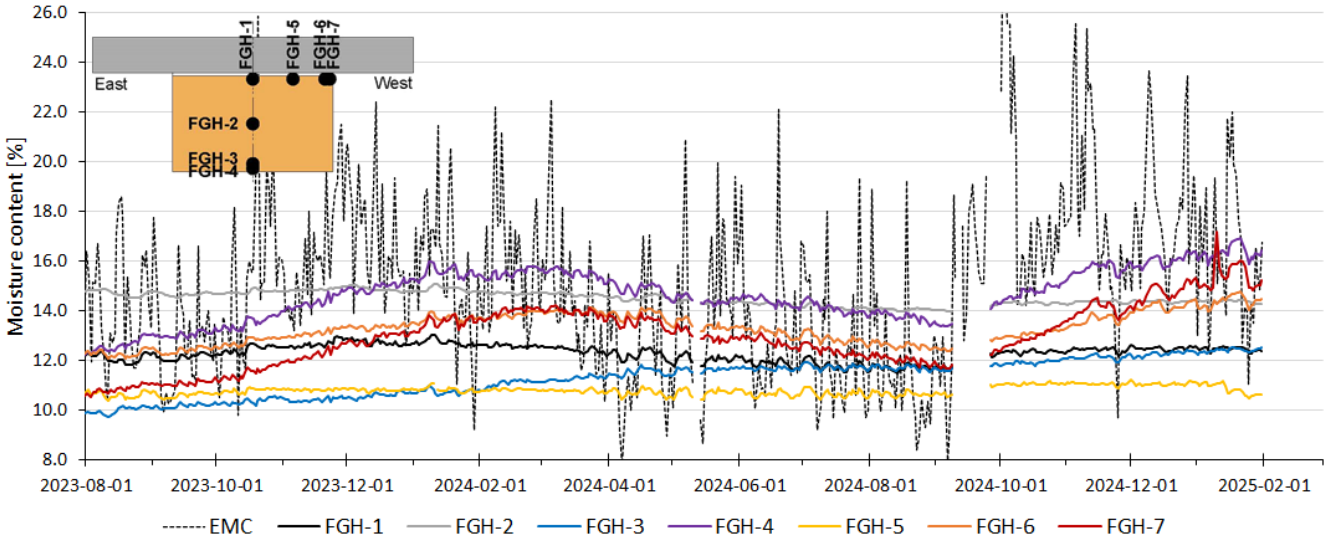

Figure 4. Daily mean values of equilibrium moisture content (EMC) and timber moisture content at several positions in measurement plane G (middle of the superstructure segment)

Figure 4 shows that the moisture content in the middle of the cross-section (FGH-2) amounted to 15 % at the beginning of the measurements. After the summer 2024 it decreased to approximately 14 % but increased on nearly 15 % in the following winter again. Due to the large dimensions of the girder, this small range was expected.

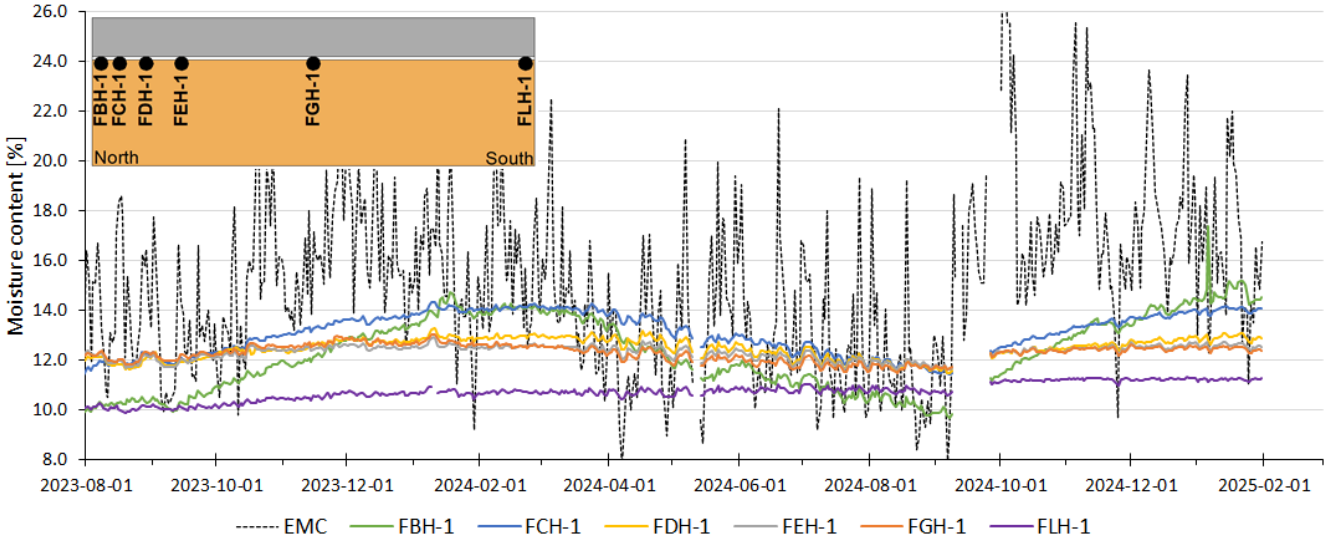

Figure 5. Daily mean values of equilibrium moisture content (EMC) and timber moisture content at several positions in the longitudinal section close to the adhesive joint

As shown in Figure 4, the moisture distribution in the inner part of the cross-section equalises. However, due to the large dimensions of the girder, the TMC in the inner part of the cross-section has not already adapted to the climate conditions at the testing site as can be seen in Figure 5. It shows the development of TMC near the adhesive joint in the longitudinal section. The moisture content in axis L (FLH-1) started on 10 % as a result of drying as described above. It increases more and more to the level of the moisture contents in axis D, E and G, which is an ongoing process even 18 months after the measurements began.

The outer zone of the cross-section dried form April to end of July 2023, to approximately 10 to 12 % moisture content, which matches the indoor climate and summer weather of this period of time. This is the TMC of the measuring points when the measurement started as can be seen in Figure 4. Comparable TMC's of the outer zone of the cross-section were obtained in the other measurement planes. The difference between 10 and 12 % moisture content indicates that the lamellas were not all perfectly conditioned on 15 %. This is plausible because they were stored in outdoor conditions to increase the moisture content. The varying climate conditions could have caused a light heterogeneous moisture distribution in the block glued girder in the initial state.

3.2 End grain sealing

In Figure 6, the moisture measurement results are displayed in the sealed end grain area (axis L). It can be seen that the sealing works well. The moisture content of FLH-1, FLH-2 and FLH-4, which are located in the inner part of the cross-section, increases very slowly from 10 to 11 % to 11 to 12 % over the course of 18 months. As expected, the measuring points close to the surface (FLH-3 and FLH-5) mirror seasonal climatic changes.

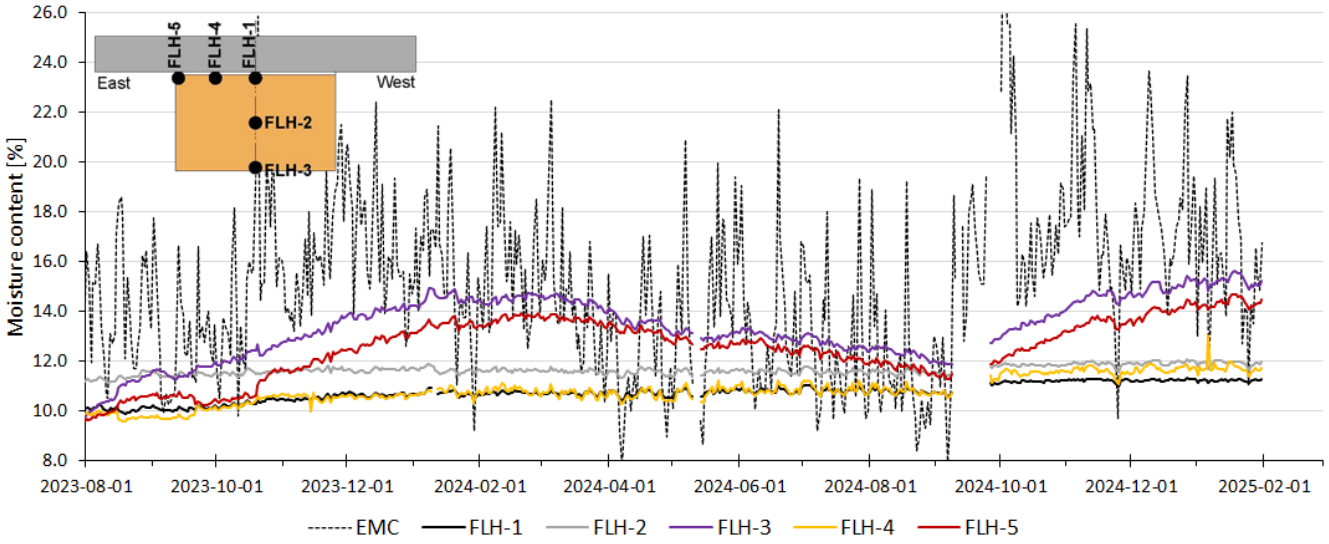

Figure 6. Daily mean values of equilibrium moisture content (EMC) and timber moisture content at several positions in measurement plane L (sealed end grain)

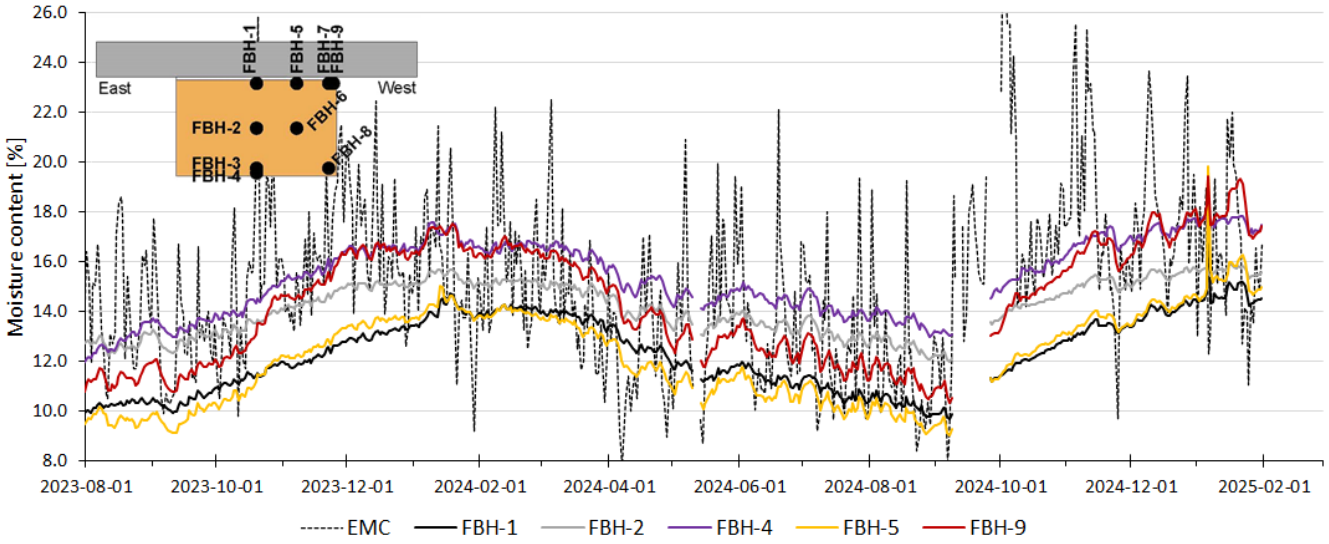

Figure 7. Daily mean values of equilibrium moisture content (EMC) and timber moisture content at five positions in measurement plane B (not sealed end grain)

Figure 7 shows the reverse situation at the other end grain zone, which has not been sealed. It can be seen that the measuring points near the surfaces show the same strong moisture variation of approximately 4 to

5 % as in axis L. However, the measuring points in the inner zone of the cross-section shows a similar development of moisture content due to the short distance to the end grain of 50 mm in a longitudinal direction. This moisture variation results in lots of small cracks due to swelling and shrinkage.

3.3 Durability

In the draft of "Eurocode 5 - Design of Timber Structures - Part 2: Bridges" [19], it is recommended that the TMC should not exceed 20 % due to prevent fungal attack. This becomes of even greater importance considering that spruce is categorised in Durability Class 4 [20]. The monitoring data showed that the daily mean values of TMC never exceeded 20 % (see the dotted red line in Figure 8) except for at one measuring point (FBH-8 in Figure 8). Therefore, fungal decay is not to be expected generally and the structure should be durable. The overhang of the concrete deck slab well protects the wooden girder which generally is a great advantage of the TCC construction method.

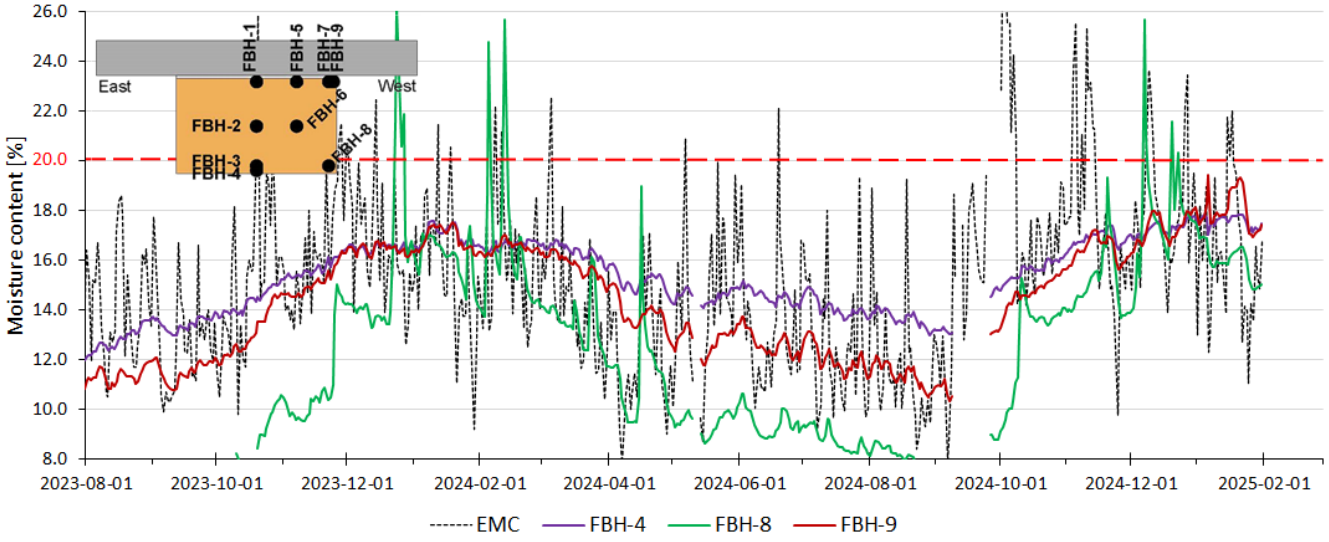

Figure 8. Daily mean values of equilibrium moisture content (EMC) and timber moisture content at three positions in measurement plane B (not sealed end grain)

A weakness in the wood protection concept was identified at the unsealed end grain area (see Figure 9 left). As shown in Figure 8, sensor FBH-8 located at the corner of the cross-section recorded moisture levels of up to 26 %. Inspections confirmed rainwater ingress. In Figure 9 right, water marks close to FBH-8 are clearly visible. This is a short conceptual flaw in the wood protection concept of the superstructure segment. However, in practice, this should not be a problem, as the expansion joints of wooden bridges should be preferably waterproof [21].

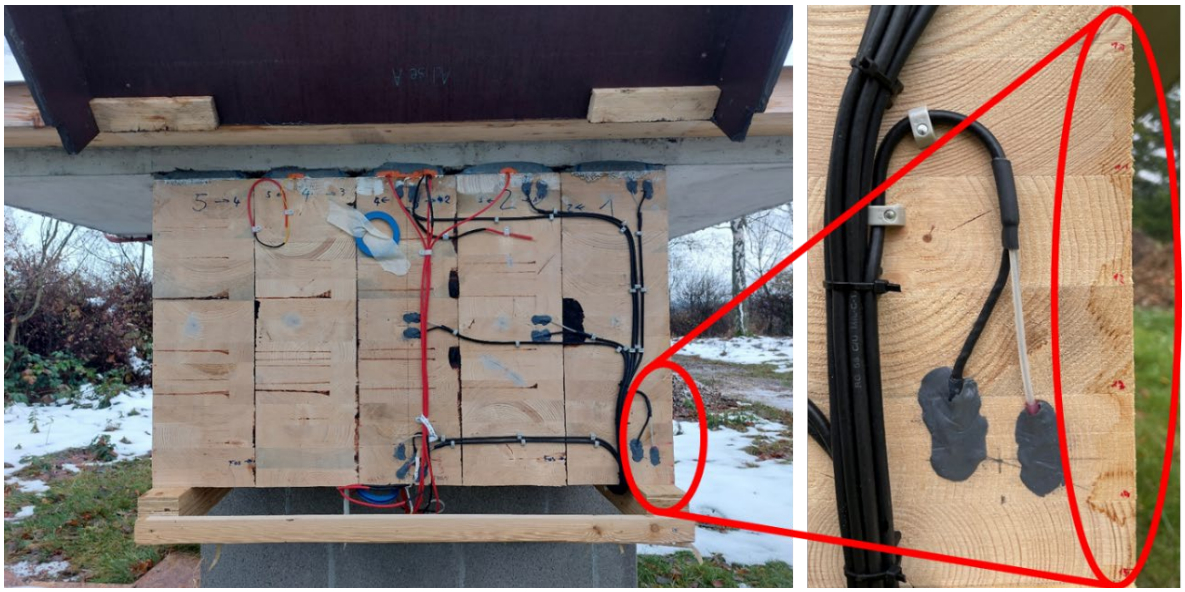

Figure 9. left: North-facing, unsealed end grain of the superstructure segment;
right: Water marks close to measuring point FBH-8

3.4 Visualisation in a digital model

For the illustration of the measurement data in the several measurement planes, a digital model has been created. The moisture content was logged once per hour and the wood temperature was logged six times per hour. The raw data was processed in Microsoft Excel to temperature compensated daily mean values of the TMC. That was the basis for the diagrams shown above but also for the digital model (see Figure 10 left). In addition, the temperature data has also been integrated so that it can also be displayed (see Figure 10 right). For visualisation, the program Autodesk Revit was used. Programming was performed with the Dynamo player Add-In.

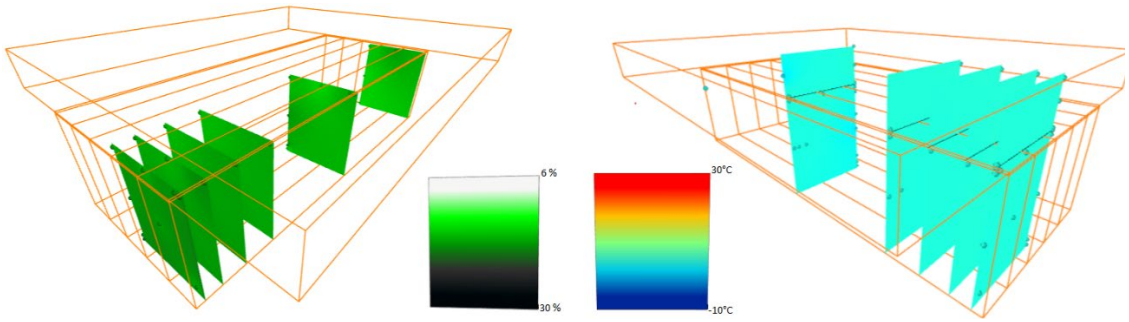

Figure 10. Visualisation of the measurement data in a digital model; left: Timber moisture distribution; right: Material temperature distribution

4 CONCLUSIONS AND OUTLINE

The experimental investigation of an ATCC superstructure segment in outdoor conditions focuses on the analysis of moisture, temperature and strain distributions within the components and the adhesive joint. For this purpose, a sensor network including temperature sensors, wood moisture sensors and fibre optic sensors (FBG and DFOS) for strain and temperature monitoring was implemented. Additionally, a meteorological station recorded the climate conditions facilitating a comprehensive understanding of environmental effects on the superstructure segment.

As a result, a comprehensive profile of the moisture distribution in the wooden girder was generated. The initial moisture distribution was not fully homogeneous but within the expected range. Due to the large dimensions of the girder in height and width, the TMC in the inner part of the cross-section had not already adapted to the climate conditions at the testing site.

One of the end grain zones was sealed vapour tight using an end grain sealing paste and also a self-adhesive vapour barrier. The sealing reliably prevented a moisture diffusion between ambient air and the end grain area of the girder.

The overhanging concrete deck slab protects the timber girder against weathering. Therefore, TCC bridges are expected to show a high durability and a long service life. The measurement results confirm a TMC mostly far below 20 % which is the limit that should not be exceeded for durable structures.

To illustrate the moisture and temperature distribution, a digital model was created in Autodesk Revit using the Dynamo player Add-In.

Future work aims to use the measurement results for the calibration of a simulation model to investigate several climate conditions on ATCC structures with varying dimensions.

ACKNOWLEDGEMENT

Thanks go to the Fachagentur Nachwachsende Rohstoffe e.V. (FNR) and to the Federal Ministry of Food and Agriculture (BMEL) of Germany for funding the ongoing research project “HBVSens” (FNR-project no.: 2221HV097). Special thanks go to partners from industry Bennert GmbH, STRAB Ingenieurholzbau Hermsdorf GmbH, Beton Fertigteilbau Erfurt GmbH, HEBAU GmbH, STRABAG AG, Sika Deutschland GmbH, Riwega GmbH, FBGS GmbH, AOS GmbH and Polytec GmbH for strong support and fruitful discussion during the project. Thanks also go to the staff of the testing facility “Versuchstechnische Einrichtung” at the Bauhaus-University Weimar and the MFPA for their support in the fabrication of the ATCC segment and for preparation and help during testing.

REFERENCES

1. Simon, A., 2008. Analyse zum Trag- und Verformungsverhalten von Straßenbrücken in Holz-Beton-Verbundbauweise. Doctoral Thesis. Bauhaus-Universität Weimar.
2. Kästner, M., 2019. Zum Tragverhalten von Polymermörtel-Klebverbindungen für die Anwendung bei Straßenbrücken in Holz-Beton-Verbundbauweise. Doctoral Thesis. Bauhaus-Universität Weimar.
3. Kirchner, A., Kästner, M., Paetow, H., Ganß, M., Kraus, M., 2025. Investigations on adhesively bonded TCC-specimens under tensile, cyclic temperature and shear loading. In: Proceedings of the World Conference on Timber Engineering (WCTE 2025), Brisbane, Australia.
4. Koch, J., Simon, A., Schumann, P., 2025. Analysis of the durability of the adhesive joint of timber-concrete composite bridges. In: Proceedings of the World Conference on Timber Engineering (WCTE 2025), Brisbane, Australia.
5. Jahreis, M. G., 2019. Zur Entwicklung von Polymerverguss-Kopplungselementen für den Holzbau. Doctoral Thesis. Bauhaus-Universität Weimar.
6. Kästner, M., Hädicke, W., Jahreis, M., Rautenstrauch, K., 2014. High-Tech Timber Beam – a high-performance hybrid beam system made of composites and timber. In: Proceedings of the World Conference on Timber Engineering (WCTE 2014), Quebec City, Canada.
7. Deutsches Institut für Bautechnik, 2021. Allgemeine bauaufsichtliche Zulassung Nr. Z-10.7-282: Polymerverguss zur Verstärkung von Holzbauteilen. Bennert GmbH, Klettbach.
8. BASt - Bundesanstalt für Straßenwesen, 2022. Zusätzliche technische Vertragsbedingungen und Richtlinien für Ingenieurbauten – ZTV-ING, Teil 6 – Bauwerksausstattung, Bergisch Gladbach.
9. Kästner, M., Ganß, M., Kirchner, A., Paetow, H., Koch, J., Simon, A., Kraus, M., 2025. Adhesively bonded timber-concrete composite bridges – Analysis of thermal actions on the superstructure. In: Proceedings of the World Conference on Timber Engineering (WCTE 2025), Brisbane, Australia.
10. Koch, J., Ganß, M., Kästner, M., Simon, A., 2023. A promising approach of linear timber structural health monitoring. In: Proceedings of the World Conference on Timber Engineering (WCTE 2023), Oslo, Norway.
11. Martin G., Andreas K., Henri P., Martin K., Johannes K., Antje S., Matthias K., 2025. Investigations on ATCC components using fiber-optical sensors for structural analysis. In: Proceedings of the 5th International Conference on Timber Bridges (ICTB 2025), Rotorua, New Zealand.
12. EN 13183-2, 2002. Moisture content of a piece of sawn timber - Part 2: Estimation by electrical resistance method.
13. Koch, J., Simon, A., Jahreis, M.G., 2022. Effectiveness of structural protection measures for timber bridges – Results of long-term moisture monitoring. In: Proceedings of the 4th International Conference on Timber Bridges (ICTB 2021 PLUS), Biel/Bienne, Switzerland.
14. Gamper, A., Dietsch, P., Merk, M., 2015. Gebäudeklima - Langzeitmessung zur Bestimmung der Auswirkungen auf Feuchtegradienten in Holzbauteilen – Schlussbericht F 2962. Fraunhofer-IRB-Verlag, Stuttgart.
15. Franke, B., Müller, A., Vogel, M., Tannert, T., 2012. Holzfeuchte-Langzeitmessung – Langzeitmessung der Holzfeuchte und Dimensionsänderung an Brücken aus blockverleimtem Brettschichtholz - Forschungsbericht 2775-SB-01. Fachhochschule Architektur, Holz und Bau, Biel.
16. Brischke, C., 2007. Untersuchung abbaubestimmender Faktoren zur Vorhersage der Gebrauchsdauer feuchtebeanspruchter Holzbauteile. Doctoral Thesis, University of Hamburg.
17. Hailwood, A.J., Horrobin, S., 1946. Absorption of water by polymers: analysis in terms of a simple model. Transactions of the Faraday Society, Volume 42B, pp. 84-92.
18. Simpson, W.T., 1973. Prediction of equilibrium moisture content of wood by mathematical model. Wood and Fiber, Volume 5, No. 1, pp. 41-49.
19. FprEN 1995-2, 2025 Eurocode 5 - Design of timber structures - Part 2: Bridges. (Document date 2025-02-05).
20. EN 350, 2016. Durability of wood and wood-based products - Testing and classification of the durability to biological agents of wood and wood-based materials.
21. Simon, A., Arndt, R. W., Jahreis, M. G., Koch, J., 2018. MuZ-HolzBr – Musterzeichnungen für Holzbrücken, Forschungsprojekt ProTimB, Fachhochschule Erfurt.

ICTB 2025. 5th International Conference Timber Bridges
Rotorua, New Zealand, 29 June to 2 July 2025.

THE REHABILITATION DESIGN OF THE WEST MONTROSE COVERED BRIDGE

Andrew Lehan[1], David Moses[2]

ABSTRACT

The West Montrose Covered Bridge is the only remaining covered bridge in Ontario to carry vehicular traffic. Built in 1881, the bridge carries a single lane of traffic along two 28.9m spans over the Grand River in West Montrose, Ontario. The bridge has been designated as a heritage structure under the Ontario Heritage Act. A major rehabilitation was recently completed for the bridge. It followed a detailed visual inspection with non-destructive testing, a Schedule 'C' Class Environmental Assessment, and a preliminary design that was approved by Regional Council of the Region of Waterloo (the Owner). A major feat of the rehabilitation design is the strengthening of the existing wood trusses to carry all gravity loads. The bridge was retrofitted circa 1965 with steel Bailey trusses to augment its capacity. These Bailey trusses will be removed, reverting the bridge back to being a bridge where wood is the primary load carrying material. Other rehabilitation actions include replacement of the roof structure, exterior cladding, nail-laminated timber deck, stringers, floor beams, needle beams, truss end diagonals, truss bottom chords, and bottom lateral bracing. A new top lateral bracing system is also being introduced to stabilize the top chords and brace them against wind loads. The bridge is proceeding to construction at the time of writing this paper.

1 INTRODUCTION

1.1 Overview

The West Montrose Covered Bridge is a wood truss covered bridge carrying a single lane of traffic across the Grand River in the community of West Montrose, Ontario (see Figure 1). The bridge has two equal simply-supported spans of approximately 28.9m. The bridge is the only remaining wood covered bridge in Ontario to carry vehicular traffic. It was designated to be of cultural heritage value pursuant to the Ontario Heritage Act. It is currently owned and maintained by the Region of Waterloo (Region).

Figure 1. Aerial view of bridge looking west (left) and view of bridge at north end portal (right).

The Region engaged our consulting team in 2022 to design a major rehabilitation of the bridge superstructure. The assignment was to inspect the bridge to determine its existing condition, perform a structural evaluation to determine its load-carrying capacity, develop and evaluate rehabilitation design alternatives, complete an environmental assessment, and complete the preliminary and detailed designs.

1.2 History of Structure & Local Significance

The bridge was designed by John Bear in 1880. It was built in 1881 by John and his brother, Benjamin Bear. The bridge has undergone numerous documented and undocumented repairs since then.

[1] Associate, Entuitive,
e-mail: andrew.lehan@entuitive.com,
[2] Founding Principal, Moses Structural Engineers

The wood trusses were augmented by the installation of steel Bailey trusses within the bridge circa 1965 (see Figure 2). The Bailey trusses are concealed behind white-coloured interior wood cladding. Local sections of Bailey truss at the pier were replaced by stronger Mabey-Johnson truss panels in 1999. On-going downward deflections of the wood trusses suggest that the bridge self-weight is being shed to the steel trusses. The deflections are thought to be the product of wood creep, connection slip, occasional passage of overweight vehicles, and on-going decay of the bottom chords. The steel trusses have been identified by others as not being strong enough to support the total vertical load demand of the bridge.

Figure 2. Steel Bailey trusses (left) and interior white wood cladding concealing steel trusses (right).

The local community has been key to the continued preservation and celebration of the bridge. The West Montrose Residents Association (the "Bridge Keepers") are advocates for preserving the bridge. They hold annual events that celebrate the bridge, such as an annual Christmas caroling event inside the bridge.

Since at least the 1930's, the bridge has been posted for various live load limits between 2 and 5 tonnes [1]. The bridge is currently posted for a 3t live load limit, regulating its use to cars and pick-up trucks. The local Mennonite community also regularly cross the bridge in horse-drawn carriages.

1.3 Structural System

The original superstructure is a wood through-truss structure comprised of two planes of trusses. The wood truss members are oriented in a rare, if not unique, "hybrid Howe" configuration (see Figure 3). Each truss is comprised of a king post within a queen post truss within a larger queen post truss.

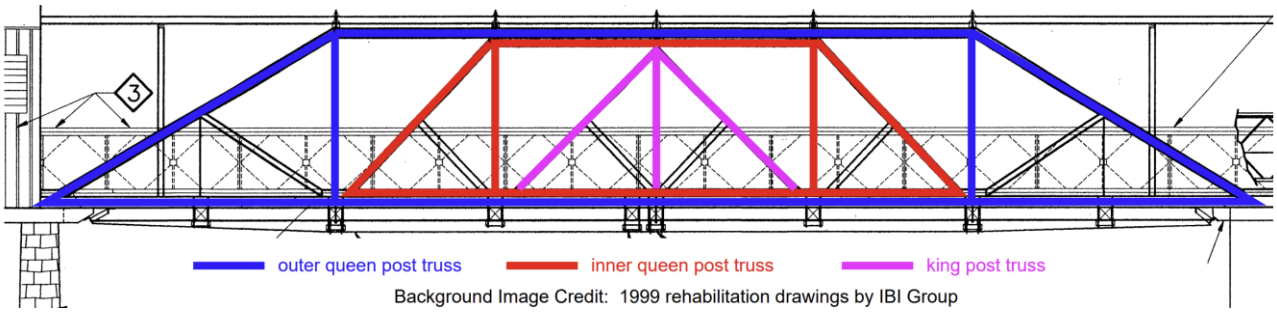

Figure 3. "Hybrid Howe" wood truss configuration of original wood trusses

The truss diagonal and chord members large solid sawn timbers. Hardwood "squash blocks" space apart the top chord and lower top chord members. The truss vertical members are comprised of pairs of steel tension rods (see Figure 4). These rod are fastened to resist tension only [4].

The gable roof has a slope of approximately 2:1. The rafters terminate at a central ridge board. Their bottom ends are supported by rafter plates that have been referred to as "edge beams" by others. The edge beams span between the truss top chord nodes. They are supported by solid sawn wood vertical posts outside the limits of the top chord members. The rafters are connected to the edge beams using a birdsmouth joint. Rafter thrust is restrained by transverse tie beams referred to as "cross beams" (see Figure 4).

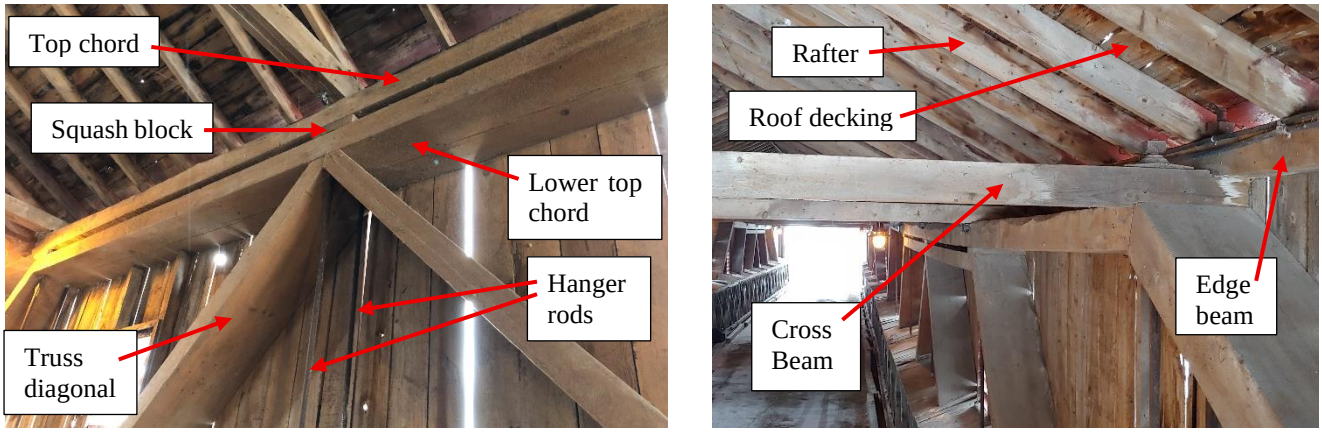

Figure 4. Wood truss members (left) and interior view of roof structure (right).

The connections between the diagonals and top chord members are bearing connections, relying on the direct bearing of mitred joints for load transfer. The connections between the diagonals and bottom chords are notched bearing connections, with the notches acting as the lateral force transfer mechanism. (see Figure 5). The pairs of vertical steel tension rods pass through holes drilled in the chord and diagonal members. They are anchored above the top chords, thereby compressing the nodal connections and providing a clamping force for force transfer by friction in the wood connections.

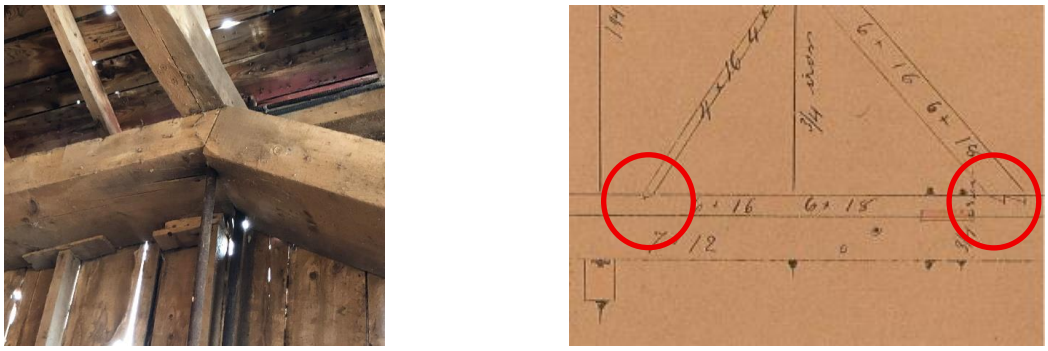

Figure 5. Typical truss node bearing connection (left) and typical truss node notched connection (right).

The floor system consists of a nail-laminated timber (NLT) deck supported on solid sawn wood stringers, which are in turn supported on solid sawn wood floor beams and needle beams (see Figure 6). Every other floor beam extends outward beyond the plan limits of the floor system and is called a needle beam. Both the floor beams and needle beams are positioned below the bottom chords. This configuration is rare for covered bridges. They are usually positioned on top of the bottom chords.

Figure 6. Typical floor system (left) and typical sway bracing at needle beam (right).

In addition to performing the same role as the shorter floor beams, the needle beams also anchor the diagonal sway bracing. This bracing stiffens the superstructure against cross-sectional distortions and provides a load path for transmitting lateral loads from the top chords of the wood trusses down to the bottom chords and bottom lateral bracing. The sway bracing consists of steel tension rods with turnbuckle tensioning assemblies. They are anchored to the ends of the needle beams at their lower ends and to the edge beams (i.e. rafter plates) at their upper ends.

The wood superstructure is supported on concrete abutments and a masonry pier.

2 INSPECTIONS & NON-DESTRUCTIVE TESTING

2.1 Inspection & NDT Methodology

Our team undertook two arm's length visual inspections of the bridge (see Figure 7). The interior of the bridge was inspected in February 2023 from deck level. Extension ladders and a scissor lift were used for access. The scissor lift was carefully selected to respect the 3-tonne load limit currently applied to the bridge. A second inspection was conducted from a floating platform in June 2023 to inspect the underside of the bridge. A baker's scaffold was used to gain arm's length access to the underside of the deck [2].

Figure 7. Wood truss inspection from deck level (left) and floating work platform for on-water inspection (right).

The arm's length visual inspections examined the wood members, connections, and steel rods. Resistance drilling measurements of the wood members were taken using a 400mm long drilling rod to assess the likelihood of decay within a member. Moisture content measurements were taken for the wood members to assess the likelihood of decay within a member. All moisture content and resistance drilling measurements were taken at at least three locations along each member. Small samples of the wood elements were removed for species identification under microscope in a laboratory. In-situ visual grading was estimated for the wood members.

2.2 Key Inspection & NDT Findings

The original truss members were found to be comprised of Eastern Hemlock, Red Pine, and White Pine wood species. All members were estimated to be Select Structural grade [2].

The inspections and non-destructive testing yielded the following key findings [2]:

- The top chords, lower top chords, interior diagonals, and lower diagonals in good to fair condition
- The east bottom chord is in poor condition and the west bottom chord is in fair condition
- The NLT deck, stringers, floor beams, and needle beams were in fair to poor condition
- The exterior cladding and roof were in poor condition

3 STRUCTURAL EVALUATION

3.1 Evaluation Methodology

A structural evaluation was conducted in accordance with the CAN S6:19 Canadian Highway Bridge Design Code (CHBDC) [3]. The evaluation examined the existing wood structure acting without the steel Bailey trusses present. The intent was to determine the capacity of the original wood structure and to inform the development of the rehabilitation alternatives by identifying the weaker parts of the bridge.

The bridge was analyzed using CSiBridge structural analysis software. A 2D model was created for a single line of wood trusses (see Figure 8). All truss members were modelled using frame elements. All truss members were released of their end moments to behave as pin-ended members. A 3D model was later created for the detailed design to better capture structural behaviour under lateral and torsional loading.

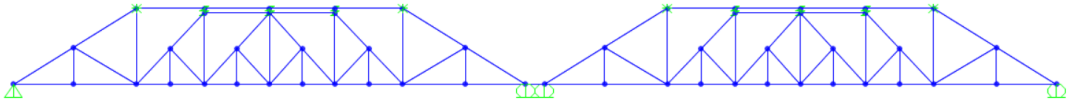

Figure 8. CSiBridge structural analysis model for structural evaluation

The structural evaluation was conducted for design live loads on a 1t incremental basis ranging from 3t to 15t, inclusive. The CL3-625-ONT was assumed for the design live load geometry and axle weight

distribution. This approach allowed the design team to understand the "fuse points" within the system; that is, the design live load above which further intervention to the wood trusses would be necessary [2].

3.2 Key Evaluation Findings

The structural evaluation yielded the following key findings [2]:

- The bottom chords become overstressed for a 10-tonne design live load
- The end diagonals become overstressed for a 4-tonne design live load
- Member design should be limited to 75%-80% utilization to account for section loss at connections

4 PRELIMINARY DESIGN

4.1 Value Engineering Workshop

A Value Engineering (VE) workshop was undertaken early in the project in March 2023 "to analyze functional requirements of the project, as well as generate, evaluate, and develop ideas for alternative value enhancements to move forward with this project" [4]. A quality modelling exercise was undertaken "to identify the areas of greatest concern and their relative priorities" [4]. The conclusions from the VE workshop were used to help develop the rehabilitation alternatives.

4.2 Development of Rehabilitation Alternatives

The following rehabilitation alternatives were developed based on the inspection findings, structural evaluation findings, and VE workshop:

- Alternative A – Replace steel Bailey trusses with new steel box girders
- Alternative B – Reinforce wood trusses using surface-bonded fibre-reinforced polymer (FRP) strips
- Alternative C – Remove steel Bailey trusses and strengthen wood trusses in kind

Other works such as replacing the roof, exterior cladding, and floor system were understood to be common to all rehabilitation alternatives.

4.3 Evaluation of Rehabilitation Alternatives

The "Multi-Attribute Trade-Off System" (MATS) was used to evaluate the rehabilitation alternatives. This system makes use of the "weighted additive method", which is a double-weighted quantitative method of evaluation [4]. The evaluation was based on four global factors (heritage, structural, social environment, and cost) determined by the Technical Advisory Committee (TAC) (i.e. key project staff and the Region), The TAC also identified numerous sub-factors for the evaluation. Weights were assigned to both global factors and sub-factors by each member of the TAC (see Figure 9).

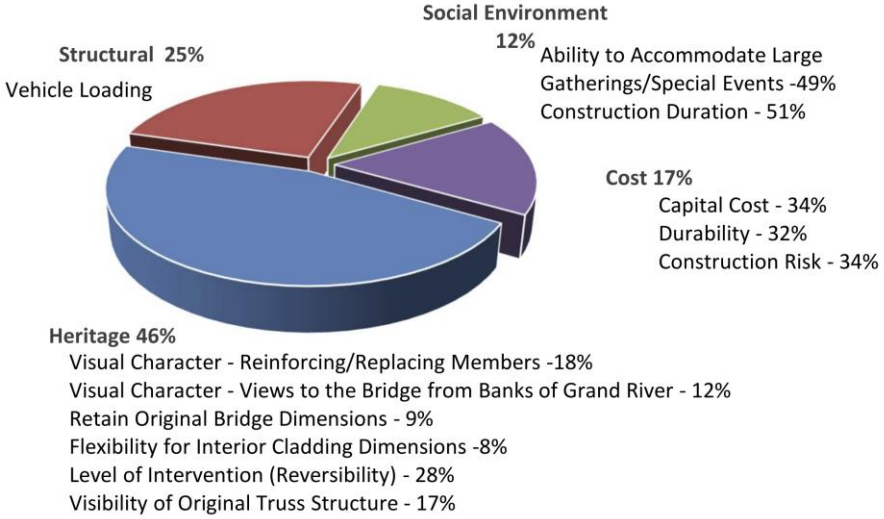

Figure 9. Average Global Factor and Sub-Factor Weightings

The MATS evaluation found Alternative C2 to have the highest scoring. Alternative C2 was a sub-option of Alternative C, wherein the design vehicular live load was 10 tonnes. A sensitivity analysis was undertaken to confirm the outcome of the MATS evaluation. The sensitivity analysis did not alter the

outcome. For this reason, the TAC recommended that Alternative C2 be adopted as the preferred rehabilitation alternative [4].

4.4 Environmental Assessment

A Schedule 'C' Class Environmental Assessment (EA) was completed upon identifying Alternative C2 as the preferred rehabilitation alternative. A Public Information Centre was held in November 2023 to present the preferred alternative to the public and to solicit their feedback for refinement of the preferred alternative. An online survey was subsequently posted by the Region to solicit further feedback. This feedback and the EA process was documented in an Environmental Study Report that was filed in winter 2024 [4].

4.5 Alternative C2 – The Preferred Rehabilitation Concept

The preferred rehabilitation concept was Alternative C2. It involves the replacement of the wood truss bottom chords, the steel rod truss verticals, the wood floor system, the exterior wood cladding, the wood roof, and the steel rod bottom lateral bracing. It also involves the addition of a wood top lateral bracing system, a robust steel bottom lateral bracing system, and strengthening of some of the wood truss diagonals and truss connections. The rehabilitation will permanently remove the steel Bailey trusses and revert the bridge back to a true wood bridge where wood is the primary load-carrying material (see Figure 10).

Figure 10. Rendering of Alternative C2

5 DETAILED DESIGN

This section of the paper explains the notable detailed design features. All replacement members will be solid sawn wood to reflect the original construction. The public strongly indicated this preference versus engineered wood materials like glued-laminated timber. All new steel connection plates, rods, and fasteners will be hot-dip galvanized for protection against corrosion.

5.1 Design Loads

Design loads were adopted per Section 3 of the CSA S6:19 Canadian Highway Bridge Design Code [3].

The CHBDC prescribes a pedestrian design load of 4.0kPa applied over the entire travelable deck surface. Reductions are possible for spans greater than 30m, which does not apply here. This loading was deemed too conservative because the bridge carries a low-volume local road and because high density foot-traffic events are unlikely for the bridge. Instead, the project team worked with the Region to develop a site-specific pedestrian design load of 4.0kPa applied across the full travelable deck width for a 2.5m length. This loading was intended to represent a large tourist bus of 70 persons stopping at the bridge and all

persons congregating for a group photo. This loading was also intended to cover the effects of the annual Christmas caroling event held on the bridge by the Bridge Keepers.

A 10-tonne design live load vehicle comprised of a scaled-down version of the CL3-625-ONT design truck was adopted in lieu of the CL-625-ONT design truck. This loading was developed in collaboration with the Region as part of the preliminary design (see Figure 11). A wheel footprint of 600mm wide by 250mm long was adopted per typical CHBDC assumptions. The bridge will remain posted for a 3t load limit. The choice to design for a 10t truck was made to protect against the passage of overweight vehicles, which is something that is known to have occurred periodically at this site.

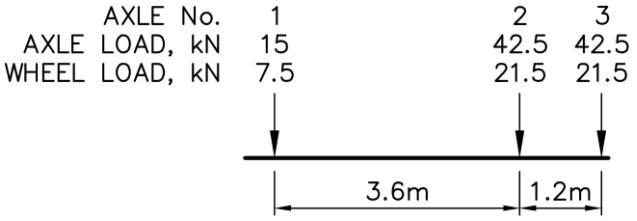

Figure 11. 10-tonne design live load vehicle

The bridge experiences frequent loading by horse-drawn carriages from the local Mennonite community. The most significant loading was determined to occur on Sundays when a local church service is held. Dozens of horse-drawn carriages are known to cross the bridge back-to-back to get to and from this church service. The project team studied this loading and adopted a design load of 2.4kPa over the entire deck surface to account for this loading condition. This area load was adopted in lieu of the CHBDC lane load.

The effect of a horse's hoof was designed for by assuming a 5kN load applied over a 100mm wide by 100mm long footprint. This loading was adopted from the recently published CSA S7:23 Pedestrian, Cycling, and Multiuse Bridge Design Guideline that is recommended but not yet normative in Canada [5].

Horizontal wind loads were calculated assuming a drag coefficient of 1.3 to reflect the lower aspect ratio of the covered bridge frontal area relative to typical, higher aspect ratios for girder bridges, wherein the drag coefficient is usually taken as 2.0. All other wind loads and their application were per the CHBDC.

Site-specific snow loads acting on the roof were determined by others via a previous study commissioned by the Region [4]. The study found the uniform design snow load to be 1.6kPa. It also identified a non-uniform snow load of 2.1kPa on the windward half of the roof and 0.5kPa on the leeward half of the roof.

Hydraulic analysis found the bridge likely to be partially inundated in the 100-year and Regional storm events. The already steep approaches and neighbouring properties made it prohibitively difficult to justify raising the structure to be entirely above the flood waters. Therefore, it was recommended to design the bridge for the flood loading commensurate with the Regional storm event. This flood loading is quite significant. It is uncommon to design for but is understandable given the "priceless" nature of the bridge. Lateral hydrostatic and hydrodynamic drag forces were found by hydraulic analysis to be 6.4kN/m and 11.4kN/m, respectively. Similarly, vertical hydrostatic and hydrodynamic forces were found to be 22.5kN/m (uplift) and -0.14kN/m (downward), respectively. Ice floes were found to clear the bridge soffit.

All load combinations were per the CHBDC. Special consideration was given to snow acting on the roof simultaneously with heavy live load acting on the deck. The CHBDC does not cover this situation. The "Covered Bridges Manual" published by the US Federal Highway Administration [6] suggests simultaneous full snow and design live loading is highly unlikely. Consequently, snow was considered to act simultaneously with full design live load for the ULS 2 and ULS 3 load combinations, assuming a ULS load factor of 0.50 for the snow load. This approach is consistent with the MTO Structural Manual's recommendations for pedestrian bridges (2020 edition and previous) [7]. An additional load combination was considered assuming a ULS load factor of 1.5 for the snow load, no live load on the bridge, and full ULS factored dead loads. This combination satisfies the National Building Code of Canada [8].

5.2 Wood Trusses

The steel Bailey trusses are going to be removed from the bridge. The gravity load-carrying system will be the original wood trusses. The trusses are being strengthened, including some member replacements, to accommodate the design loading. The bottom chord members are being replaced because of their poor

condition and inability to carry the design loading. The new bottom chords will be comprised two parallel 203mm wide by 318mm deep (8in x 12-1/2in) solid sawn timbers spaced 51mm apart. Each member will be comprised of three segments per span due to length limitations for solid sawn timbers. Field splices will be comprised of steel splice plates with bolted shear plate connectors (see Figure 12).

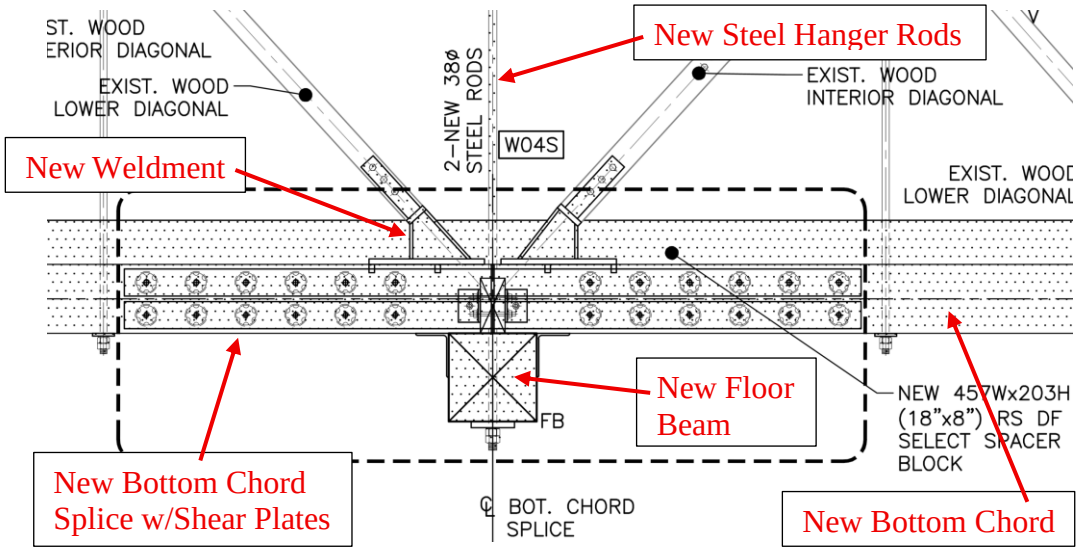

Figure 12. Typical rehabilitated wood truss details at bottom chord splice

The uplift from the design hydraulic loading is significant and will result in a stress reversal in the wood trusses. The existing truss nodal connections do not have any provision for transferring tensile forces. They also do not have any provision for transferring shear forces, beyond what can be transferred by friction. Therefore, all truss nodal connections required strengthening to enable tensile and shear force transfer. Steel connection plates, fasteners, and weldments were used for this purpose (see Figure 13).

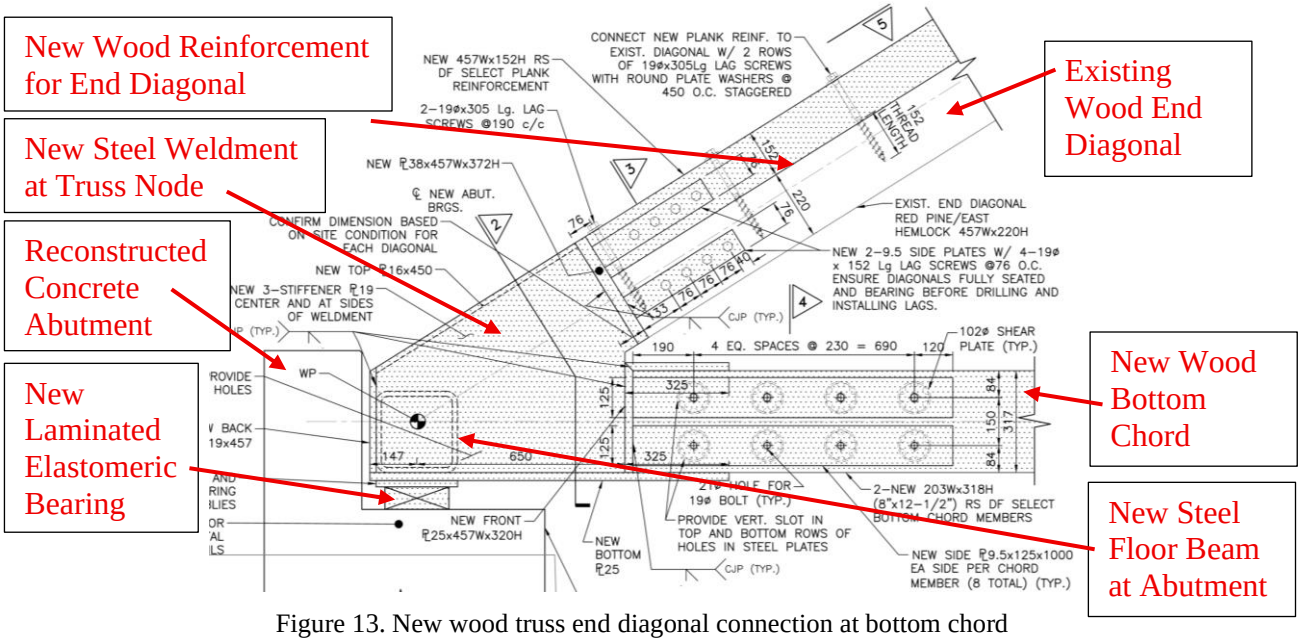

Figure 13. New wood truss end diagonal connection at bottom chord

The existing wood trusses are supported on large wood bolsters. These bolsters are in a severe environment and have decayed in the past. They are being replaced in the new design by laminated elastomeric bearing assemblies, which are much more durable. These assemblies will be fastened to the bottom chord weldments at the abutments.

5.3 Lateral System

New top lateral bracing was designed for the bridge. The existing bridge does not have top lateral bracing. The new bracing will stiffen the bridge against lateral wind loading and brace the top chords and lower top chords against buckling. The new top lateral bracing will be 178mm wide by 203mm deep (7in

x 8”) sawn timbers positioned in an X-bracing arrangement (see Figure 14). The bracing will act with the cross-beams, edge beams, and gravity truss top chords to form a lateral truss in plan.

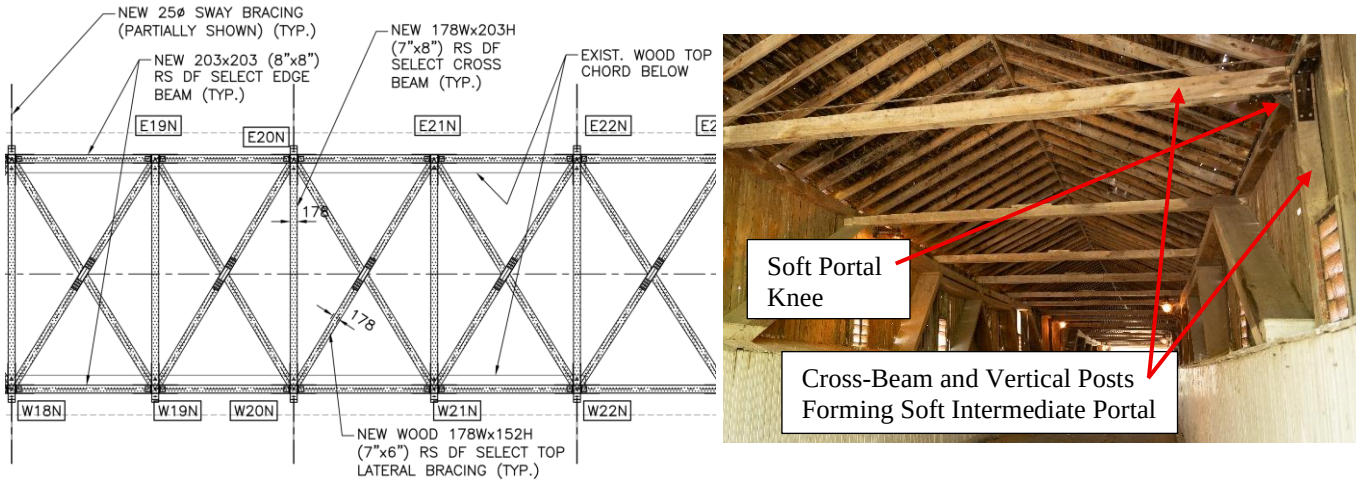

Figure 14. Excerpt of new wood top lateral bracing system (left) and intermediate portal frame in existing condition (right)

The bridge has intermediate wood portal frames at every floor beam and needle beam. The portals at the needle beams feature diagonal steel sway bracing rods on the outside of the bridge (see Figure 6). The portal at the pier does not feature sway bracing rods. The intermediate portals and pier portal are not laterally stiff relative to the top lateral truss, even where sway bracing rods are present. So, lateral forces tend to accumulate in the top lateral trusses and span all the way to the abutments, where they are transferred out of the top lateral truss via stiffened end portals. These end portals are wood frames with diagonal steel sway bracing rods that are anchored into the concrete abutments. Anchoring the rods into the abutments significantly stiffens these frames relative to the intermediate portals and pier portal.

The bottom lateral system is being replaced. The existing system featured a bottom lateral truss formed by the gravity truss bottom chords, steel rods in an X-bracing arrangement, and the floor/needle beams. The new system was governed by the very large lateral flood forces, which required shifting the new lateral bracing rods upwards so that their lines of action were nearly coincident with the gravity truss bottom chords. The connection eccentricity would have otherwise been prohibitive to design for. The large lateral flood forces were also overstressing the bottom chords in a state of combined tension and biaxial bending, so the new bottom lateral bracing members were anchored to the exterior stringers instead of the bottom chords. These exterior stringers were upsized as a result. The bottom chords were blocked against the exterior stringers at discrete intervals to allow the flood forces to transfer to the new bottom lateral truss formed by the exterior stringers, the new lateral bracing, and the floor/needle beams (see Figure 15).

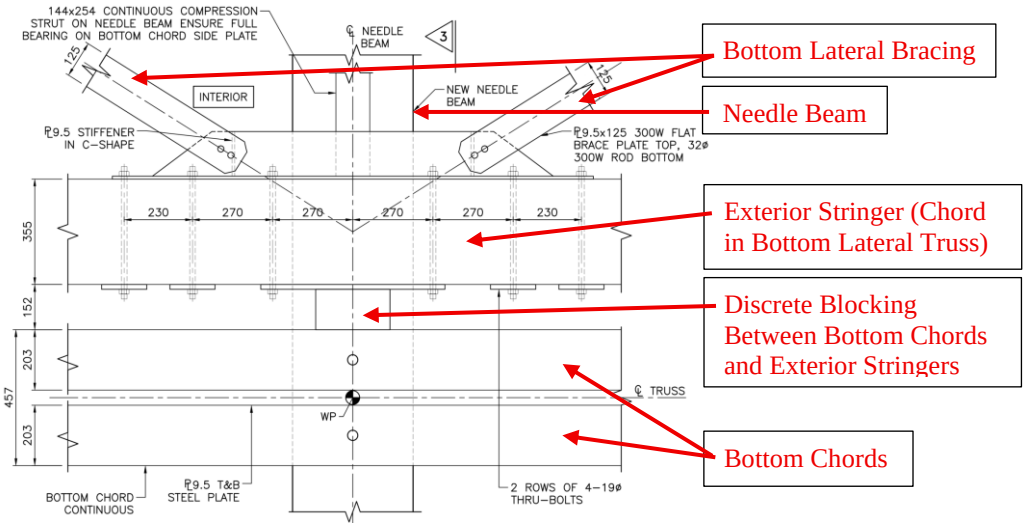

Figure 15. Excerpt of bottom lateral truss details.

Steel floor beams comprised of HSS 254x254x16 members were necessary at the abutments and pier to anchor the large forces in the bottom lateral bracing due to lateral flood loading (see Figure 13). Hold-down anchorages and lateral guides were detailed between these steel floor beams and the abutments and pier. The steel floor beams also provide jacking points for future bearing replacement. The wood stringers frame into custom steel hangers that project off the side face of these floor beams.

5.4 Exterior Cladding

The new exterior cladding with be 22mm thick by 203mm wide (1in x 8") boards. They will be constructed in the board-and-batten style, with 19mm thick by 64mm thick (1in x 3in) batten boards closing the gaps between the main cladding boards. The existing cladding was nailed directly to the outside faces of the wood truss members. The new details feature a spacer block to offset the cladding from the truss members, which should improve durability by limiting moisture transfer to the wood truss members. The existing louvre windows will be replicated within the new cladding.

5.5 Roof

The existing roof structure has insufficient strength to carry the design snow loading. The new rafters are being upsized from the original 44mm by 152mm (2in x 6in) members to 76mm by 152mm (3" x 6") members. The 610mm (2ft) on-centre spacing is being maintained. The 19mm (3/4in) thick roof plank decking is being replaced with new 38mm (1-1/2") thick planking decking with 12.5mm (1/2") plywood sheathing. The new roof envelope will consist of No. 1 400mm western red cedar shingles with an underlayment and breather layer.

5.6 Deck Wearing Surface

The existing NLT deck has a tar-and-chip wearing surface, which was observed to have a short, roughly 2-year service life. It did not perform well under the action of horses' hooves. The new wearing surface will be an epoxy-and-chip wearing surface, which will be harder and more durable. The deck will be waterproofed with a polyurethane membrane, which will further increase durability. Sheet metal flashing will be installed along the end grain faces of the deck laminations to protect them from surface runoff.

6 CONCLUSIONS

The West Montrose Covered Bridge has successfully functioned for the past 144 years. The current major rehabilitation is expected to enable another 75+ years of service. The bridge is proceeding to construction at the time of writing this paper.

REFERENCES

1. IBI Group, 2014. West Montrose Covered Bridge Preservation Plan (pp 5-6, B-1). IBI Group, Toronto, Canada.
2. Entuitive, 2023. West Montrose Covered Bridge Field Inspection Summary Report (pp 3-10, 15-32). Entuitive, Toronto, Canada.
3. CSA Group, 2019. CSA S6:19 Canadian Highway Bridge Design Code. CSA Group, Toronto, Canada.
4. BT Engineering Inc., 2024. West Montrose Covered Bridge Rehabilitation, Schedule C Environmental Assessment Study. BT Engineering Inc., London, Canada.
5. CSA Group, 2023. CSA S7:23 Pedestrian, Cycling, and Multiuse Bridge Design Guideline. CSA Group, Toronto, Canada.
6. Pierce, P.C., Brungraber, R.L., Lichtenstein, A., and Sabol, S., 2005. Covered Bridge Manual, Publication No. FHWA-HRT-04-098. United States Department of Transportation, Federal Highway Administration, Turner-Fairbank Highway Research Center, McLean, Virginia, United States.
7. Ministry of Transportation Ontario (MTO), 2021. Structural Manual. MTO, Transportation Infrastructure Management Division, Standards and Contracts Branch, Structures Office, St. Catharines, Canada.
8. National Research Council, 2020. National Building Code of Canada 2020 Volume I. National Research Council, Ottawa, Canada.

ICTB 2025. 5th International Conference Timber Bridges
Rotorua, New Zealand, 29 June to 2 July 2025.

DOWEL-TYPE CONNECTION BEHAVIOUR OF HIGH-DENSITY NATURALLY DURABLE HARDWOOD

Milad Lezgi[1], Hyungsuk Thomas Lim[2]

ABSTRACT

This study investigates the connection behaviour of *Eucalyptus bosistoana*, a naturally durable, high-density hardwood, suitable for outdoor structural applications, such as timber bridges. The performance of dowel-type joints under tensile loading was evaluated by varying end distance (3d, 5d, 7d), edge distance (1d, 2d, 3d), and dowel spacing (3d, 4d, 5d), where d represents a 12 mm dowel diameter. Results showed that increasing the end distance from 3d to 5d improved load-bearing capacity by 50% and ductility by 100%, while further increasing it to 7d provided negligible additional benefits. Similarly, increasing edge distance from 1d to 2d enhanced capacity by 17% and ductility by 72%, while 3d provided greater stiffness (49%) and ductility (57%) with no significant capacity increase compared to 2d. Dowel spacing significantly affected joint performance, with 4d and 5d increasing the mean load-bearing capacity by 11.6% and 19%, respectively. Among the analytical models, the mechanical model showed the best prediction of the dowel connection capacity. On the contrary, NZS/AS 1720.1 underestimated the capacity by 51% and overestimated the connection stiffness by more than 100%. These findings highlight the need for design adjustments to ensure the safe and efficient use of high-density hardwoods in connections.

Keywords: dowel-type connections, high-density hardwoods, *Eucalyptus bosistoana*, dowel spacing, end and edge distance, analytical prediction models, timber connection design

1 INTRODUCTION AND BACKGROUND

The emerging naturally durable eucalypt industry in New Zealand presents a significant opportunity to utilize the high mechanical properties of these species in structural applications. Among the species developed by New Zealand Dryland Forests Innovation (NZDFI), *Eucalyptus bosistoana* stands out with a modulus of elasticity of 21 GPa, a bending strength of 163 MPa, and class 1 ground-durability [1]. Its natural resistance to decay without chemical treatment makes it an ideal candidate for timber bridge construction. While *E. bosistoana* offers exceptional strength and stiffness, understanding its connection behaviour is crucial for effective structural implementation.

Dowel connections, particularly those incorporating steel plates and dowels to join timber elements, are widely used in timber bridges, such as in truss node connections [2]. The lateral behaviour and force-displacement response of dowelled joints primarily depend on wood and dowel material properties, as well as geometric parameters, including end distance, edge distance, and dowel spacing [3]. Previous studies [4] have demonstrated that timber density and splitting strength significantly influence dowel connection performance. Given that *E. bosistoana* exhibits high density and internal stresses, it may be more prone to splitting, necessitating further investigation [5].

Design standards such as NZS/AS 1720.1[6] establish minimum spacing criteria to prevent splitting and promote ductile failure modes, primarily based on Johansen's yield theory [7]. They provide formulas for predicting the strength and elastic stiffness of dowelled connections

[1] PhD Candidate, School of Forestry, University of Canterbury, Christchurch, New Zealand
e-mail: milad.lezgi@pg.canterbury.ac.nz,
[2] Senior lecturer above bar, School of Forestry, University of Canterbury, Christchurch, New Zealand

when spacing requirements are met. However, hardwood species are not typically included in these standards; for instance, species with an average modulus of elasticity exceeding 15.2 GPa are not covered by NZS/AS 1720.1[6], requiring special consideration when designing with these species. Beyond design standards, analytical models have been developed, many of which build upon Jorissen's beam-on-elastic-foundation model [8]. Studies such as Liu et al. [9] incorporate parallel-to-grain stiffness of substrate wood in a mechanical model for predicting the behaviour of timber joints with steel bolts or dowels. Jensen [10] took another approach and applied fracture mechanics to capture the response of single-bolt connections subjected to parallel-to-grain loading. This study aims to, firstly, assess the effect of geometric parameters of end distance, edge distance, and dowel spacing on the hardwood joints performance. Secondly, it evaluates the accuracy of analytical models and NZS/AS 1720.1 provisions [6] in predicting hardwood connection performance.

1.1 Mechanical modelling method

Liu et al. [9] proposed an empirical formula to predict the force-displacement (P -Δ) behaviour of single-bolted joints up to their peak load. Their approach is based on two critical parameters: load-bearing capacity (P_P) and elastic stiffness (k_e) of the bolted joints. This formula provides a reasonably accurate representation of the joint's response until it reaches its maximum load:

$$P = P_P \left[1 - exp\left(-\frac{k_e}{P_P}\Delta\right)\right] \quad (1)$$

They theoretically determined the load-bearing capacity and elastic stiffness of timber joints with slotted-in steel plates, based on failure modes. Three yield models were proposed: yield model I: crushing of wood, yield model III: partial wood crushing with one plastic hinge in the bolt, and yield model IV: partial wood crushing with two plastic hinges in the bolt.

$$P_P = f_{e,u}.d.l \quad \text{Yield Model I} \quad (2)$$

$$P_P = f_{e,u}.d.l\left(\sqrt{2 + \frac{16M_u}{f_{e,u}.d.l^2}} - 1\right) \quad \text{Yield Model III} \quad (3)$$

$$P_P = 4\sqrt{M_u.f_{e,u}.d} \quad \text{Yield Model IV} \quad (4)$$

where $f_{e,u}$ is the ultimate bearing strength of wood (MPa), d is the dowel diameter (mm), l is the bolt embedment length in wood (mm), and M_u represents the ultimate bending moment of the bolt (N.mm). To determine the elastic stiffness (k_e), they developed an analytical model based on the Bernoulli beam on an elastic foundation, incorporating Winkler foundation stiffness to represent the dowel bearing stiffness of wood. By solving the resulting differential equations, they derived the stiffness of bolts embedded in wood (Eq. (5)).

$$k_e = \frac{P}{\Delta} = \beta\left(k_s \sqrt[4]{\frac{4EI}{k_s}}\right) \quad (5)$$

Here, β is the rotational factor, equal to 2 for a fully constrained bolt, k_s represents the dowel bearing stiffness of the wood, and EI denotes the bending stiffness of the embedded bolt. Based on these parameters, the force-displacement response of a single bolt embedded in wood can be represented as shown in Figure 1.

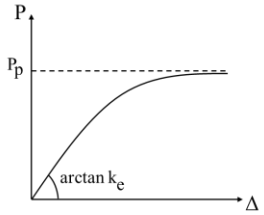

Figure 1. Mechanical model of the embedded bolt in wood [9].

1.2 Fracture mechanics-based method

Brittle failure in single-bolt timber connections primarily occurs through two failure modes: splitting (mode I) and row shear (mode II), as illustrated in Figure 2. Jensen [10] applied the Timoshenko beam theory to account for shear deformations and analyse their effects on dowel-embedded wood. Under parallel-to-grain loading, the wood is modelled as resisting splitting through two types of springs, each representing a distinct stiffness component: a spring for fracture layer stiffness (k_f) and two symmetrical springs modelling elastic stiffness perpendicular to the grain (k_s) (Figure 2a). The foundation stiffness and the contributing parameters are defined in Eqs. (6) - (8).

$$k = \frac{2\ k_f\ k_s}{k_f + k_s} \tag{6}$$

$$k_f = \frac{f_t^2}{2G_{f,I}} \tag{7}$$

$$k_s = \frac{E_{90}}{h} \tag{8}$$

Here, f_t is the tensile strength perpendicular to the grain, $G_{f,I}$ is the fracture energy associated with failure mode I, E_{90} denotes the elastic modulus perpendicular to the grain, and h is the beam depth in the Timoshenko beam model, equivalent to half the timber width, as shown in Figure 2a. According to Figure 2, failure mode I occurs when the tensile stress perpendicular to the grain exceeds its strength, resulting in splitting failure.

Failure mode II, attributed to row shear, involves a timber segment being pulled out. This failure occurs when the shear stress induced by the dowelled connection surpasses the shear strength parallel to the grain. The shear stiffness of the fracture layer (Γ) is expressed as:

$$\Gamma = \frac{f_v^2}{2G_{f,II}} \tag{9}$$

where f_v is the shear strength parallel to the grain and $G_{f,II}$ is the fracture energy of mode II.

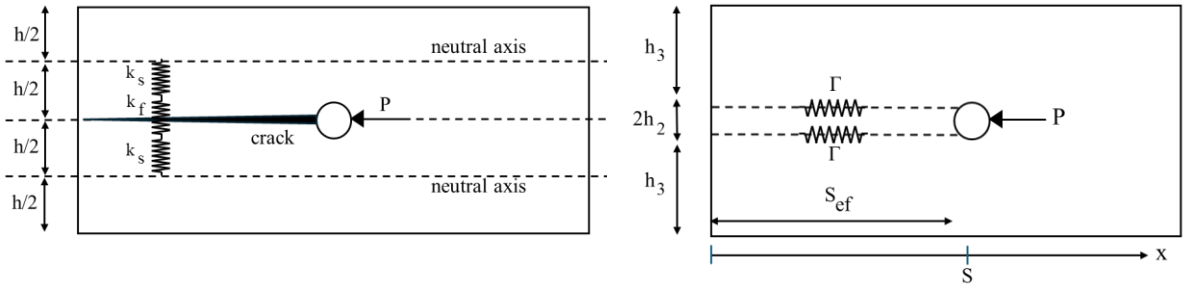

Figure 2. (a) Failure mode I: Splitting of the single-bolt connection loaded parallel to the grain. (b) Failure mode II: Row shear parallel in a single-bolt connection loaded parallel to the grain [11].

However, a mixed-mode failure usually happens, necessitating an interaction between perpendicular-to-grain tensile stress and parallel-to-grain shear stress (10). Hanhijärvi and Kevarinmäki [12] introduced an empirical formula (Eq. (11)) to account for this interaction. Using Eqs. (11), (12) and (14), based on experimental investigations on row shear and splitting in bolted connections, as well as Eqs. (13) and (15), derived from fracture mechanics analysis of row shear failure in dowelled timber connections, the capacity of the dowel connection can be determined [11].

$$\left[\frac{\sigma(x)}{f_t}\right]^2 + \left[\frac{\tau(x)}{f_v}\right]^2 < 1 \tag{10}$$

$$P_u = \begin{cases} P_{u,II}\left(1 - k_{interaction}\frac{P_{u,II}}{P_{u,I}}\right) & if\ P_{u,II} \le P_{u,I} \\ P_{u,I}\left(1 - k_{interaction}\frac{P_{u,I}}{P_{u,II}}\right) & if\ P_{u,I} \le P_{u,II} \end{cases} \tag{11}$$

$$P_{u,I} = \frac{k_{conc}}{\beta}\frac{1}{\mu} f_t s b \tag{12}$$

$$P_{u,II} = 2bs_{ef} f_v \frac{\tanh\omega}{\omega} \tag{13}$$

$$\mu = \begin{cases} \dfrac{2.7}{\cosh[(s/h) - 1.4]} & for\ x = 0 \\ max[1\,;\, 0.65(s/h)] & for\ x = s \end{cases} \tag{14}$$

$$\alpha = \frac{h_3}{h_2}\ ,\ \omega = \frac{s_{ef} f_v}{\sqrt{2h_2 E G_{f,II}}}\sqrt{\frac{1+\alpha}{\alpha}} \tag{15}$$

where $k_{interaction}$ and k_{conc} are considered to be 0.3 and 0.7 by Hanhijärvi and Kevarinmäki [12]. The wedging effect factor of β is taken 0.1 by Jorissen [8], b is the thickness of the specimens, x is the distance from the end of the plate, s is the end distance, h is the edge distance, and s_{ef} is the effective shear length. The parameters h_2 and h_3 are shown in Figure 2-b.

1.3 NZS/AS 1720.1:2022

The design load-carrying capacity of a dowel or bolt connection is determined based on brittle failure modes and yielding failure mechanisms. For connections loaded parallel to the grain ($\alpha = 0$), the applied load (N^*) must be less than both the ultimate yielding strength of the fastener group ($N_{\alpha,y}$) and the design strength of the fastener group ($N_{0,w}$).

$$N^* \le \min(N_{\alpha,y}, N_{0,w}) \tag{16}$$

$$N_{\alpha,y} = n_{\alpha,y} n_s n \tag{17}$$

$$N_{0,w} = \min(N_{0,rs}, N_{0,t}) \tag{18}$$

where $n_{\alpha,y}$ is determined by the failure mode, n_s is the number of shear planes, and n denotes the total number of fasteners. In a double-shear plane joint, assuming failure occurs in the main member, which is timber in this study, the yielding strength of the fastener is given by Eq. (19):

$$n_{\alpha,y} = 0.5 f_{2,\alpha} d t_2 \tag{19}$$

where $f_{2\alpha}$ is the design embedment strength of timber, d is the dowel diameter and t_2 is the thickness of the main member, which is timber here. The design embedment strength of timber loaded parallel to the grain ($\alpha = 0$) under normal service conditions and static loading is:

$$f_{2,0} = \varphi_y f'_{2,0} \tag{20}$$

where φ_y is the material capacity factor for yielding failure of timber (0.8) and $f'_{2,0}$ is the characteristic embedment strength of timber, calculated as: $f'_{2,0} = 0.082\ \rho'\ (1 - 0.01d)$. ρ' is the 5th percentile characteristic density of wood at 12% moisture content (kg/m^3) and d is the dowel diameter (mm). Based on the connection type in this study, $N_{0,w}$ is determined as the minimum of the row shear strength ($N_{0,rs}$) and net tensile strength ($N_{0,t}$).

$$N_{0,rs} = \varphi_w\ RS_1 = 0.7\ (0.75\ f'_s\ n_f\ a_{cr}\ t_{net}) \tag{21}$$

$$N_{0,t} = 0.8\ f'_t\ A_n \tag{22}$$

where φ_w is the material capacity factor for brittle failure of timber (0.7), f_s' and f_t' represent the characteristic shear and tensile strength parallel to the grain, respectively, n_f is the number of fasteners in a row, a_{cr} is the minimum of the spacing between fasteners in a row and the end distance, t_{net} is the net thickness of the member, and A_n is the member's net cross-section area.

Additionally, the connection stiffness (K_{ser}) can be determined using the empirical relationship provided by the standard between the average lateral deformation of a dowel connection (Δ_l) in mm, number of dowels (n), and the applied load (N_a) in newtons (23). The lateral stiffness of a dowel depends on the characteristic timber density (kg/m^3) and the dowel diameter (d).

$$K_{ser} = \frac{N_a}{n\,\Delta_l} = \rho^{'}\frac{d}{12.6} \tag{23}$$

2 MATERIALS AND METHODS

E. bosistoana boards, sawn from over 100-year-old trees in New Zealand, were used in this study. Density measurements of 233 samples yielded a mean air-dry and oven-dry density of 1088 kg/m³ and 1043 kg/m³, with coefficients of variation (COV) of 3.25% and 3.24%, respectively. Having shown a normal distribution through statistical tests, the characteristic air-dry density required for NZS/AS 1720.1 was determined to be 1086.94 kg/m³ following [13]. Knot-free 24 mm thick boards were selected for double-shear joint tests with steel side plates. The bottom side of the specimens was fixed using 16 mm high-strength steel dowels (class 12.9), while 12 mm steel dowels of the same class were used to pull up the specimens. 10 mm thick steel plates were attached to the load cell for tensile load application, with two additional steel plates securing the specimen to the base, as shown in Figure 3. The high-strength steel dowels ensured that failure modes and capacities were determined solely by the timber.

To investigate the effects of geometric parameters, three end distances (2d, 4d, and 5d), three edge distances, and three fastener spacings were tested, as detailed in Table 1. Five replicates of each configuration were prepared following ASTM D1761 [14]. The test speed was set to 0.4 mm/min, ensuring the maximum load was reached within approximately 10 minutes.

For experimental analysis, the average force-displacement curves resulting from five curves were first derived to visualise the effect of the spacing on connection performance. The elastic stiffness (k_e) was determined based on 10% and 40% of the peak load (F_p). The yield load (F_y) was defined using an offset line equal to 5% of the dowel diameter from the proportional line. As per ASTM D5652 [15], the ultimate point (F_u) was identified as the point where force reached 80% of the peak load after passing the maximum load. The ductility of the connection (D) was calculated as the ratio of ultimate displacement (Δ_u) to yield displacement (Δ_y). Based on this classification, five failure regions were identified in the force-displacement curves (Figure 4). The results were then presented in terms of mean and COV.

Table 1. Test Series

Series	End distance	Edge distance	Dowel spacing	Parameter studied
1	3d	2d	-	End distance
2	5d	2d	-	Edge and edge distance
3	7d	2d	-	End distance
4	7d	1d	-	Edge distance
5	7d	3d	-	Edge distance
6	7d	2d	3d	Dowel spacing
7	7d	2d	4d	Dowel spacing
8	7d	2d	5d	Dowel spacing

The embedment properties of *E. bosistoana*, necessary input for the mechanical model, were determined using the half-hole embedment test (ASTM D5764-24 [16]). Thirty specimens (40 mm thick, 55 mm wide, and 55 mm long) were prepared with 12 mm diameter half-holes to evaluate embedment strength and stiffness parallel to the grain (Figure 5). Shear parallel-to-grain and tension perpendicular-to-grain tests were conducted following ASTM D143 [17] to provide input for the fracture mechanics-based model. $G_{f,II}$ was determined from the area under the stress-deformation curve of the shear test. Additionally, NZS/AS 1720.1 requires tensile strength parallel to the grain, necessitating a tensile test in this direction (Figure 5).

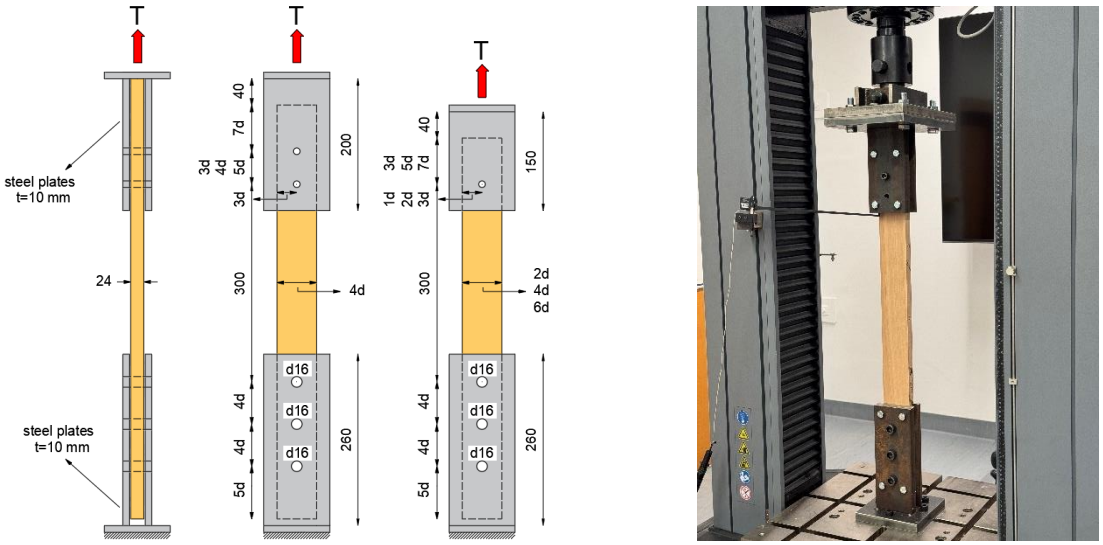

Figure 3. Details of the connection test setup (units: mm)

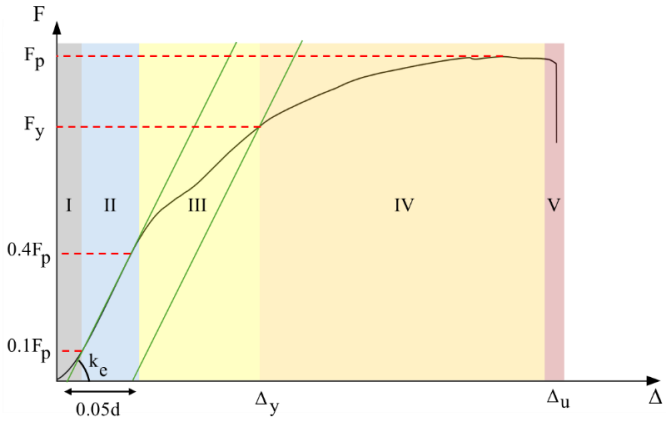

Figure 4. Typical force-displacement curve resulting from connection test containing five regions: (I) initial slip, (II) elastic region, (III) stiffness degradation, (IV) yield plateau, and (V) failure.

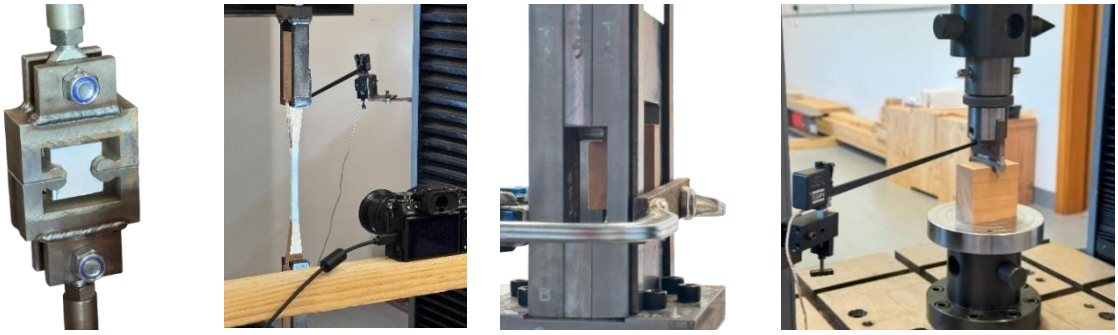

Figure 5. Mechanical tests on small clear samples from left to right: tension perpendicular to the grain, tension parallel to the grain, shear parallel to the grain, and dowel embedment test.

3 RESULTS

3.1 Material Test Results

The material properties of *E. bosistoana* required for the analytical and standards-based methods are presented in Table 2. They include dowel bearing strength (f_{eu}), dowel stiffness (k_s), tensile strength parallel to the grain ($f_{t,0}$) and perpendicular to the grain ($f_{t,90}$), shear strength (f_v) and mode II fracture energy ($G_{f,II}$). The characteristic values were determined according to method 4 of AS/NZS 4063.2 [13] based on the method given by ASTM D2915 [18], except from k_s which followed the method prescribed for the modulus of elasticity. The modulus of elasticity of the bolt is 2.06×10^5 MPa, and the dowel diameter is 12mm.

Table 2. Material properties of *E. bosistoana* under embedment, tensile, and shear tests.

Property	f_{eu} (MPa)	k_s (MPa)	$f_{t,0}$ (MPa)	$f_{t,90}$ (MPa)	f_v (MPa)	$G_{f,II}$ (N/mm)
Mean	85.9	1785.4	204.4	8.59	18.29	7.75
characteristic	69.96	1570.29	98.89	3.66	14.66	4.26
COV (%)	11	23.3	27	33	14	28.1

3.2 Connection Test Results

The influence of end distance, edge distance, and spacing between the dowels on the force-displacement curves are illustrated in Figure 6. Each graph represents the average force-displacement response derived from five replicates per configuration. Additionally, from each tests sample, the important connection performance parameters, including load-bearing capacity, elastic stiffness, ultimate displacement, and ductility coefficient, were taken for statistics and the results from 5 samples for each series are summarized in Table 3.

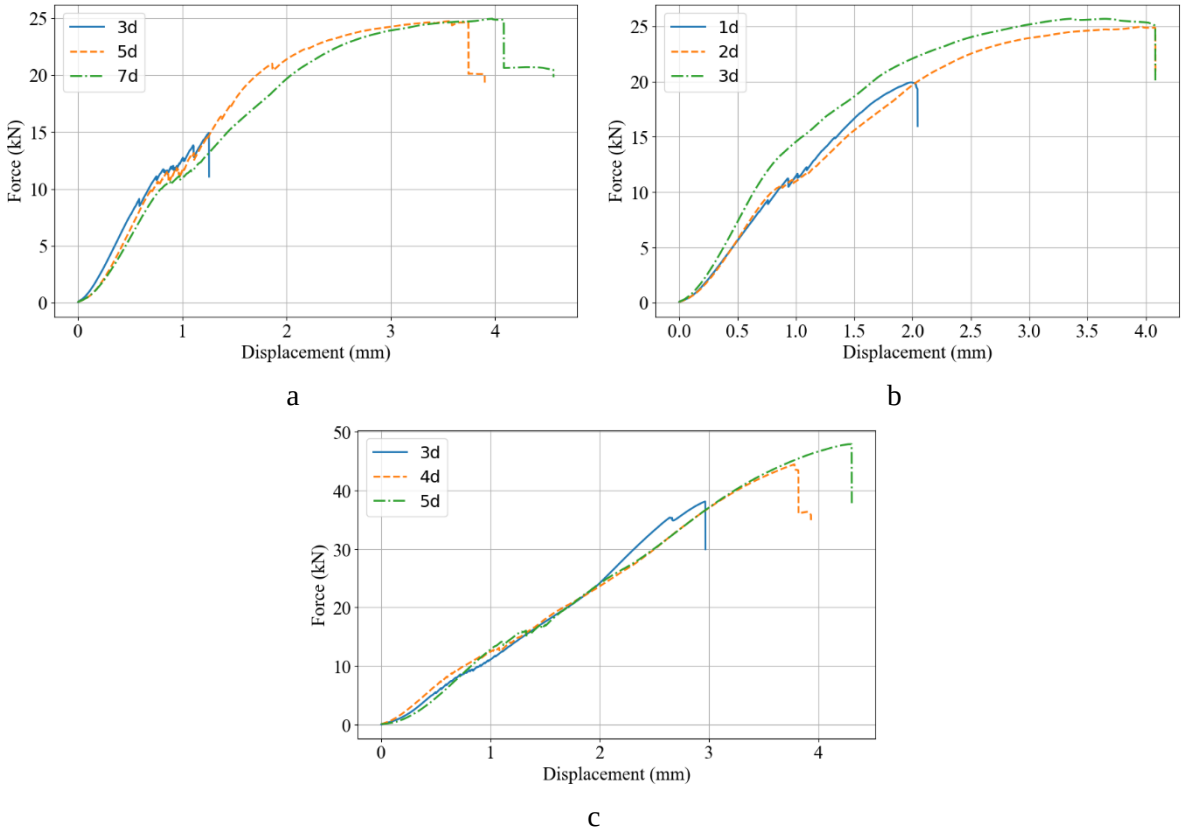

Figure 6. Average force-displacement curves showing the effect of (a) end distance (3d, 5d, 7d), (b) edge distance (1d, 2d, 3d), and (c) dowel spacing (3d, 4d, 5d) on connection performance.

Table 3. Mean bearing capacity, stiffness, ultimate displacement, and ductility coefficient for varying end distance, edge distance, and dowel spacing, with their COV in parentheses.

End distance	Edge distance	Dowel spacing	F_p(kN)	k_e(kN/mm)	Δ_u(mm)	D
3d	2d	-	16.47 (18.5%)	17.23 (7.5%)	1.38 (6%)	1.00 (0.3%)
5d	**2d**	**-**	**24.78 (3.7%)**	**16.55 (14.3%)**	**4.15 (8.4%)**	**2.00 (8.7%)**
7d	2d	-	25.66 (6.9%)	12.71 (22.9%)	4.81 (9.8%)	1.91 (15%)
7d	1d	-	22.03 (4.1%)	13.54 (14.5%)	2.46 (12.8%)	1.11 (0.9%)
7d	2d	-	25.66 (6.9%)	12.71 (22.9%)	4.81 (9.8%)	1.91 (15%)
7d	3d	-	26.17 (4.7%)	18.98 (5.7%)	4.87 (14.9%)	2.67 (17.1%)
7d	2d	3d	41.45 (6%)	11.87 (19.5%)	3.22 (6.3%)	1.04 (7.3%)
7d	2d	4d	46.26 (7.6%)	12.54 (24.4%)	4.11 (6.4%)	1.10 (16.7%)
7d	2d	5d	49.34 (2.8%)	12.68 (9.7%)	4.89 (10.1%)	1.06 (3.6%)

3.3 Analytical Methods Results

The bearing capacity and elastic stiffness of a single-dowel connection with an end distance of 5d and an edge distance of 2d predicted by the mechanical model, fracture-based approach, and AS/NZS 1720.1 are presented in Table 4. The experimental characteristic capacity and stiffness obtained following Sections B2.2 and B3 of AS/NZS 4063.2 [13], respectively, assuming a lognormal data distribution, are presented in the same table for comparison. Given the small sample size of five, the standard sampling factors may be less valid, potentially affecting the accuracy of the characteristic values.

Table 4. Analytical predictions and characteristic experimental results for a single-dowel connection with end and edge distances of 5d and 2d.

Parameter	Mechanical Model	Fracture Energy	NZS/AS 1720.1	Experiment
F_p(kN)	20.15	17.63	11.08	22.56
k_e(kN/mm)	84.90	-	34.13	15.72

4 DISCUSSION

Figure 6 illustrates how variations in end distance, edge distance, and dowel spacing impact the performance of dowel connections, while Table 3 provides insights into their effects on bearing capacity, stiffness, ultimate displacement, and the ductility coefficient.

Increasing the end distance from 3d to 5d and 7d resulted in a substantial improvement in the mean bearing capacity from 16.47 kN to 25.66 kN. This indicates that larger end distances help prevent premature failure modes. However, the mean stiffness decreased from 17.23 kN/mm at 3d to 12.71 kN/mm at 7d, with a high COV of 22.9%, suggesting that increased end distance allows for greater deformation but introduces higher variability in connection rigidity. The mean ultimate displacement increased from 1.38 mm at 3d to 4.81 mm at 7d. The mean ductility coefficient increased from 1.00 at 3d to 1.91 at 7d, with a high COV of 15%, indicating greater energy dissipation before failure. The recommended end distance of 5d aligns with the observed performance, as both strength and ductility improved significantly compared to 3d. However, increasing the end distance to 7d neither significantly enhanced bearing capacity nor improved stiffness and ductility. This suggests that 5d is the optimal end distance for *E. bosistoana*, balancing load-bearing capacity, stiffness, and ductility.

Edge distance plays a key role in the ductility of a connection. Beyond increasing the mean capacity from 22.03 kN to 26.17 kN, the mean ductility experienced a significant increase from

1.11 to 2.67 when the edge distance increased from 1d to 3d. Mean stiffness reached its highest value at 3d (18.98 kN/mm) with the lowest COV (5.7%), suggesting that this configuration provides a balance between strength and rigidity. Similarly, the mean ultimate displacement increased significantly to 4.87 mm at 3d, showing that 3d enhances all the performance criteria. The recommended edge distance of 2d is supported by the results, as it provides substantial strength improvement compared to 1d. However, 3d further enhanced stiffness and ductility, which may be more suitable for high-density hardwoods that require additional edge distance. Further research is needed to confirm this finding.

Dowel spacing significantly affected load-sharing efficiency and stress distribution between the dowels. The mean bearing capacity increased consistently from 41.45 kN at 3d to 49.34 kN at 5d, with a very low COV (2.8%) at 5d, indicating more stable and reliable performance. While mean stiffness did not exhibit significant changes with increasing dowel spacing, the COV values indicate greater stability and consistency when spacing increased from 3d to 5d. Similarly, ductility did not change significantly, but the lowest COV was observed at 5d, suggesting that this spacing provides the most consistent ductility performance. Considering the mean bearing capacity of a single dowel (25.66 kN), two dowels should bear 51.32 kN if sufficient spacing is provided. However, the bearing capacities recorded for 3d, 4d, and 5d dowel spacings resulted in reductions of 19%, 9.8%, and 3.8%, respectively, from 51.32 kN. These findings indicate that the recommended dowel spacing of 4d may not provide sufficient spacing for high-density hardwood, whereas 5d shows additional improvement in load-bearing capacity and performance consistency.

Among the analytical methods, the mechanical modelling approach most accurately predicted connection capacity while requiring only embedment strength and stiffness as inputs. However, it overestimated the stiffness by 440%. The fracture mechanics-based method was highly sensitive to the specified coefficients, such as β. The capacity in Table 4 was derived using the recommended values of $k_{interaction}$ = 0.3, $k_{conc} = 0.7$, and $\beta = 0.1$.

The NZS/AS 1720.1 design standard provided a conservative estimate of connection capacity. For a single-dowel connection, the predicted capacity was 51% lower than the experimental value, primarily due to the application of material capacity factors (φ_y and φ_w). When the number of fasteners was doubled, the predicted capacities were 13.30 kN, 17.73 kN, and 22.17 kN for dowel spacings of 3d, 4d, and 5d, respectively. In comparison, the corresponding characteristic experimental capacities were significantly higher: 40.86 kN, 42.35 kN, and 47.67 kN. In terms of stiffness, NZS/AS 1720.1 predictions aligned more closely with the experimental results than other methods. However, stiffness was still overestimated by more than 100%, highlighting the need for further investigation across different timber species.

5 CONCLUSIONS

Eucalyptus bosistoana, a naturally durable hardwood with high mechanical properties, is well-suited for outdoor structural applications such as timber bridges. However, as existing design standards are primarily developed for softwoods, their applicability to high-density hardwoods requires more investigation. This study examined the influence of key geometric parameters on the performance of double-shear joints with steel side plates.

Experimental findings indicate that an end distance of 5d is optimal, as increasing it to 7d provides minimal additional capacity without improving stiffness or ductility. An edge distance of 2d enhances capacity by 17% and ductility by 72% compared to 1d, while increasing it to 3d offers marginal capacity gains but significantly improves stiffness (49%) and ductility (57%), making it preferable for greater rigidity and energy dissipation. Dowel spacing below 5d reduces load-sharing efficiency, leading to lower-than-expected capacities. Experimental results suggest that a minimum spacing of 5d is preferable for optimal performance, though further research is needed to validate these findings under different loading conditions.

Among the analytical models, the mechanical model provided more accurate connection capacity, whereas NZS/AS 1720.1 underestimated the capacity by 51.7% and overestimated the stiffness by more than 100%. These discrepancies highlight the need for modifications to the standard, to better reflect the behaviour of high-density hardwood dowel connections.

6 ACKNOWLEDGMENT

The authors wish to acknowledge the support provided by New Zealand Timber Design Society (NZTDS) and New Zealand Dryland Forests Innovation (NZDFI). Any opinions, findings, conclusions, or recommendations expressed in this publication are those of the author(s) and do not necessarily reflect the views of the funding organisations. This publication is a contribution of the School of Forestry, University of Canterbury.

7 REFERENCES

[1] Keith R. Bootle, *Wood in Australia Types, Properties and Uses*, 2nd ed. Sydney: McGraw-Hill, 2010.

[2] P. C. Pierce, R. L. Brungraber, A. Lichtenstein, and S. Sabol, "Covered bridge manual," Turner-Fairbank Highway Research Center, 2005.

[3] K. Sawata, "Strength of bolted timber joints subjected to lateral force," *Journal of Wood Science*, vol. 61, no. 3, pp. 221–229, 2015, doi: 10.1007/s10086-015-1469-8.

[4] C. Sandhaas and J. W. G. van de Kuilen, "Strength and stiffness of timber joints with very high strength steel dowels," *Engineering Structures*, vol. 131, pp. 394–404, 2017, doi: 10.1016/j.engstruct.2016.10.046.

[5] S. M. Dijkstra, "Investigating the mechanisms of the formation of spiral grain and interlocked grain in wood," *University of Canterbury*, 2020.

[6] Standards New Zealand, "NZS AS 1720.1:2022 Timber Structures Part 1: Design Methods".

[7] K. W. Johansen, "Theory of timber connections," *International Assoc. of Bridge and Structural Engineering Publication*, vol. 9, pp. 249–262, 1949.

[8] A.J.M. Jorissen, "Double shear timber connections with dowel type fasteners," TU Delft, 1998.

[9] Y. Liu, Y. Wang, Y. Zhang, M. Chen, and X. Nie, "Force–displacement relations of bolted timber joints with slotted-in steel plates parallel to the grain," *Journal of Wood Science*, vol. 66, no. 1, 2020, doi: 10.1186/s10086-020-01931-x.

[10] J. L. Jensen, "Quasi-non-linear fracture mechanics analysis of the double cantilever beam specimen," *Journal of Wood Science*, vol. 51, no. 6, pp. 566–571, 2005, doi: 10.1007/s10086-005-0700-4.

[11] J. L. Jensen, U. A. Girhammar, and P. Quenneville, "Brittle failure in timber connections loaded parallel to the grain," *Proceedings of the Institution of Civil Engineers: Structures and Buildings*, vol. 168, no. 10, pp. 760–770, 2015, doi: 10.1680/stbu.14.00108.

[12] A. Hanhijärvi and A. Kevarinmäki, *Timber failure mechanisms in high-capacity dowelled connections of timber to steel. Experimental results and design.* 2008.

[13] AS/NZS 4063.2:2010, "Australian/New Zealand Standard Characterization of structural timber Part 2: Determination of characteristic values."

[14] ASTM D1761, "Standard Test Methods for Mechanical Fasteners in Wood and Wood-Based Materials," 2020.

[15] ASTM D5652, "Standard Test Methods for Single-Bolt Connections in Wood and Wood-Based Products," *ASTM International*, 2021.

[16] ASTM D5764, "Standard Test Method for Evaluating Dowel-Bearing Strength of Wood and Wood-Based Products," *ASTM International*, 2024.

[17] ASTM D143, "Standard Test Methods for Small Clear Specimens of Timber," *ASTM International*, 2022.

[18] ASTM D2915, "Standard Practice for Sampling and Data-Analysis for Structural Wood and Wood-Based Products," *ASTM International*, no. Reapproved 2022, 2017.

ICTB 2025. 5th International Conference Timber Bridges
Rotorua, New Zealand, 29 June to 2 July 2025.

DEVELOPMENT OF THE COMPOSITE HYBRID BRIDGE – A NOVEL SOLUTION FOR A LOW CARBON FUTURE

Dr Royce Liu[1], Raed El Sarraf[2], Lowri Swygart[3] and Hanna Davidson[4]

ABSTRACT

The use of structural timber in new bridges will be critical in reducing their carbon emissions contribution. In addition to sustainability targets, a well-designed bridge must also meet economic, structural, and durability requirements. This paper investigates a proposed novel type of bridge superstructure system dubbed steel/concrete composite timber hybrid bridge system, or CHB. This system maximises the advantages of the different construction materials in order to satisfy all of the aforementioned design requirements. This paper presents the design philosophy and assumptions, the proposed solution, and a discussion on the carbon life cycle comparison between the different bridge systems.

1 INTRODUCTION

Addressing the climate challenge provides an excellent opportunity for innovation, especially in the construction sector that contributes ~40% of the global greenhouse emissions. One of those sectors is bridges, which is still dominated by the use of carbon intensive materials, mainly structural steel and concrete. The New Zealand Transport Agency Waka Kotahi, have previously indicated their interest in shifting towards the widespread adoption of timber bridge superstructures for spans up to 30m [1]. However, significant challenges currently exist and have hampered its adoption to date in New Zealand. Three design challenges that are yet to be addressed for fully timber bridges are: 1) durability of the structural components to last 100 years and/or have an understanding of the maintenance requirements over that period, 2) having adequate toughness and strength to withstand extreme loading (such as flood debris) with minimal damage, and 3) adhesion with surfacing materials that can withstand the wear and impact loading from an increasing frequency of heavy vehicles.

Alternatives to fully timber bridges are partially timber bridges, such as conventional steel girders with timber decking (Figure 1, left), which were commonly used by Local Authorities throughout New Zealand in the past, and timber-concrete composite (TCC) bridges [2] (Figure 1, right). TCC bridges were developed in the United States, with examples over 80 years in existence [3], where timber can be used to reduce the amount of concrete required, thus supporting the goal of reducing the amount of embodied carbon in the structure (albeit not to the same extent as for a fully timber bridge), whilst retaining the benefits provided by a concrete deck. However, TCC is limited to short span lengths (without compromising on structural depth) and the current design environment is focussed on maximising span lengths of the order of 25m+. Hence, our challenge was exploring how else timber could be used to reduce the embodied carbon of new bridges, whilst satisfying current design requirements and constraints.

[1] Bridge Engineer, WSP. Email: Royce.Liu@wsp.com

[2] Technical Principal – Asset Integrity Management, WSP.

[3] Consultant, Swygart Sustainability.

[4] Bridge Engineer, WSP.

Figure 1. Left, typical New Zealand steel girder bridge with timber deck, Tukemokihi Bridge in Hawkes Bay. Right, timber concrete composite Quiaios Bridge, Portugal [4].

2 COMPOSITE HYBRID BRIDGE SYSTEM

2.1 Concept

One such solution, is to utilise the inherent advantages of structural steel, concrete and timber; into a steel/concrete composite timber hybrid bridge system, or CHB, first proposed by Swygart and El Sarraf [5] where the case for a steel, concrete and timber bridge superstructure was given, with the aim to reduce the overall embodied carbon of conventional bridge systems through the use of structural timber. This was later developed further into the bridge configuration shown in Figure 2, which takes a conventional steel/concrete multi-girder bridge, and replaces the typical steel cross-girders and partial depth precast decking with a timber concrete composite (TCC) deck (Figure 2).

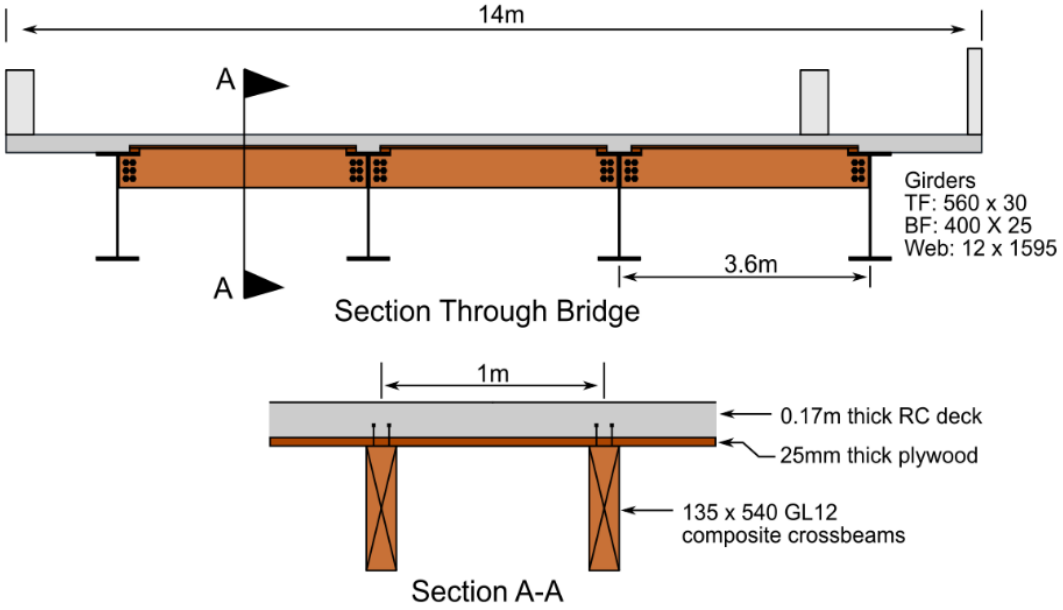

Figure 2. Proposed Composite Hybrid Bridge (CHB) Concept, showing a cross section through the bridge at midspan (top) and partial transverse section (bottom). Dimensions shown result from preliminary design.

The TCC deck (Section A-A in Figure 2) spanning transverse to the bridge, comprises stay-in-place plywood formwork with glulam beams and a composite concrete slab. Composite action between the glulam and concrete is achieved with shear connectors such as screws. The glulam cross beam ends are supported by bolted connections to the girders it spans between. Thus, the steel/timber hybrid portion of the concept name arises from the combination of steel-concrete composite action in the longitudinal direction and timber-concrete composite action in the transverse direction. The benefits of using timber this way is a reduction in deck thickness and

hence concrete related carbon, and the timber components being sheltered from direct exposure to sunlight and rain making it likely (in addition to chemical treatment) that the 100-year durability requirement can be met.

2.2 Benefits of combining steel, concrete and timber

As mentioned above, the aim was to fully utilise the inherent advantages of structural steel, concrete and timber, which are:

- Steel's high strength to weight ratio that allows for longer spans, with multi-girder superstructures spanning up to 68m, using Grade 350 MPa steel. This could be further extended when higher strength steel is used.
- Concrete's ability to act compositely with both steel and timber, thus maximising the total structural capacity of both materials, while providing a robust, durable pavement substrate.
- Timber's lighter weight, lower embodied carbon and sequestration ability, allows for the reduction of the concrete deck weight by up to 20% (as discussed in Section 4). Thus, reducing the superstructure overall deadload by over 40%, which will have corresponding substructure savings.

3 SUPERSTRUCTURE DESIGN COMPARISON STUDY

To assess the benefits and efficacy of the CHB system, a desktop numerical study was undertaken, that compares four different superstructure configurations (Figures 2 & 3) for a simply supported 30m bridge. These are:

- Concrete super-tee, selected from NZTA *Standard Precast Concrete Bridge Beams* [6]; taken as being the "reference design" because it is currently the most commonly used superstructure configuration.
- Steel-concrete composite multi-girder bridge, designed to AS/NZS 5100.6 [7].
- A timber bridge, designed to the draft *New Zealand Timber Bridge Design Guide* [8] NZS3603-1993 [9] and Eurocode 5-Part 1 [10].
- Proposed CHB system (Figure 2), as discussed herein.

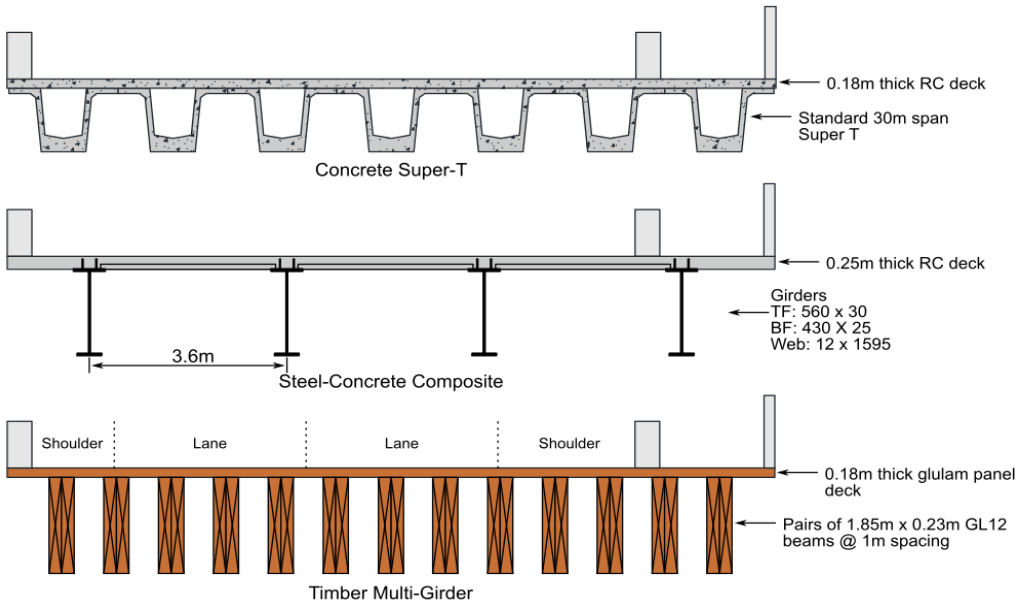

Figure 3: Cross section of conventional construction materials bridge configurations with dimensions from preliminary design.

The quantitative metrics compared were superstructure weight per unit length and life-cycle carbon emissions. While the qualitative metrics compared include compliance pathway risks, peer review risks, constructability, durability and in-service risks.

3.1 Assumptions and Methodology

A high level of care was taken to ensure that the comparison between the different designs was made as fair as possible. The assumptions and methodologies used to undertake this study are outlined in this subsection.

3.1.1 Superstructure geometry and design

The following parameters were used for superstructure design:

- The superstructure has a span of 30m.
- The overall deck is 14m wide, comprising of two 3.5m wide traffic lanes, two lane shoulders (1.5m and 2.5m), and a footway.
- For the designs with concrete decks, the thickness of the deck cantilevers was assumed to be 250mm. The reason for this was to ensure that deck could sustain the loads from vehicle collision with TL4 barriers without requiring additional design.

The superstructures underwent preliminary design considering SLS and ULS HN-HO-72 traffic and dead loads. Load combinations considered were taken from [11]. To undertake the design of the TCC cross beams and deck, Eurocode Part 5 [10] was used in conjunction with proprietary fasteners designed to be used as shear studs [12], as shown in Figure 4. Currently the New Zealand timber design standard, NZS 3603, does not cover the design of timber-concrete composite construction; while the draft *New Zealand Timber Bridge Design Guide* [8], mentions the TCC system and refers to [10] for design guidance. As only preliminary design was undertaken, in order to approximate the quantity of fasteners and brackets used for the timber bridge option, the Mistissini Bridge in Quebec [13] was used to estimate this, which was taken as a volume of stainless steel fasteners and brackets equal to 0.45% the total volume of timber used for the bridge.

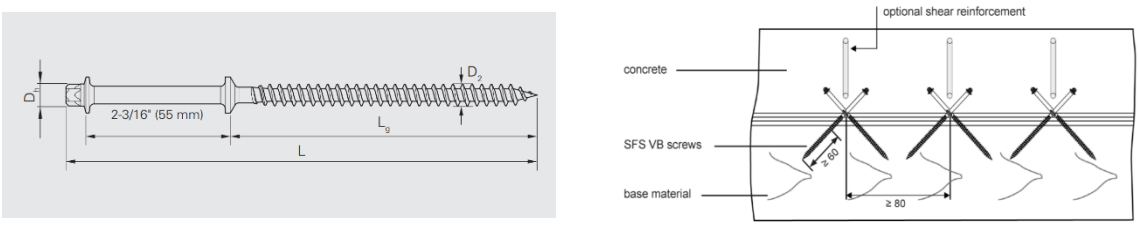

Figure 4: Example of the proprietary fastener shear stud. SFS VB screws [10]

Finally, commercially available materials and section sizes satisfying current New Zealand design standards were used where possible. For example, structural steel was taken as WR350 weathering steel to AS/NZS 3678 [14], concrete was assumed to be 40MPa except for the precast Super-T which was 50MPa andye to NZS 3101 [15], and reinforcing steel was assumed to be grade 500 to AS/NZS 4671 [16]. Glulam was assumed to be NZS 3603 [9] grade GL12, structural plywood was assumed to be AS/NZS 2269.0 [17] grade F11, and lumber was assumed to be NZS 3603 [9] grade SG8. Minimum concrete cover was assumed to be 40mm to exposed faces and 25mm elsewhere, as per NZS 3101 [15].

3.1.2 Carbon Assessment

A carbon assessment was carried out to compare the carbon impacts of the four bridge superstructure configurations investigated. The assumptions made within the carbon assessments are outlined below:

- The carbon assessment was undertaken in accordance with IStructE *Carbon Calculation Methodology* [18] and BS EN 15978:2011 [19]
- One Click, as the LCA calculator was used; with the given Environmental Product Declarations (EPD's) outlined below
    - Reinforced concrete, cast-in-situ, 5800 psi, 40 MPa, 2590 kg/m3, 100kg/m3 steel reinforcing [20]
    - Hot-rolled structural steel sections [21] and Xlerplate steel, Alloyed Steel [22]
    - Glulam Radiata Pine H5 CCA [23]
    - Structural plywood from radiata pine, kiln-dried, untreated, 593 kg/m3, 12% moisture content, ECOPLY [24]
    - Cold rolled stainless steel for austenitic 316 stainless steel [25]
- Only the superstructure has been considered within this carbon assessment to allow for a simplistic comparative study. No pavement or surfacing has been included.
- The included modules are A1-A3 (with biogenic carbon reported separately), A4, A5w, C, and D.
- Module A covers the construction phase. For this assessment, values within the mentioned EPDs above have been used for A1-A3. Module A4 which accounts for the transport of construction materials to site has assumed supply of structural steel from South Korea, imported to Napier, timber from Levin, and concrete from Ashburton, with all delivered to the same site location in Clutha District. Module A5w which considers construction site emissions only considers material wastage, using default wastage rates provided within OneClick LCA.
- Module B covers the use phase. For this assessment, module B has been excluded as there is not sufficient information to accurately account for it.
- Module C covers the demolition and deconstruction of the structure, default values calculated within OneClick LCA for each material.
- Module D covers the benefits beyond the system boundary from the materials within the structure options. Default assumptions have been used from within OneClick LCA for each material, with concrete assumed to be crushed, timber assumed to be burned and reinforcing steel and steel assumed to be recycled.
- Biogenic carbon from the wood has been reported within the results separately, as per MBIE *Whole-of-Life Embodied Carbon Assessment: Technical Methodology* [26].

Furthermore, the effects of site location, construction activities, and substructure design were excluded. Although these are important factors when designing a bridge, the purpose of this exercise was to focus on the carbon inherent in given superstructure option.

4 RESULTS

4.1 Geometry and Quantities from Design

Table 1 outlines the resulting superstructure structural geometry for the four different superstructure types investigated (Figures 2 and 3). In terms of structural depth, it can be seen that the traditional composite, fully timber and proposed CHB options have similar structural depths for a 30m span, However, this is likely to drastically change if larger span lengths were

examined. Another point to note from Table 1 is that the fully timber superstructure requires far more main girders than the other options (Figure 3). If the fully timber superstructure became overtopped in a flood, the buoyant force from the volume of the superstructure may be quite significant and require careful consideration for the design of both the hold-downs and the superstructure itself.

Table 1: Superstructure design parameters.

Item	Concrete Super-T	Steel/Concrete Composite	Timber Bridge	CHB
Beam spacing, m	1.99	3.6	1	3.6
Overall superstructure depth, m	1.41	1.9	2.03	1.9
Deck depth, m	0.18	0.25	0.18	0.195*
Beam depth, m	1.23	1.65	1.85	1.65

* Including timber plywood formwork thickness. Deck cantilevers remain at 0.25m thick

Table 2 outlines the superstructure weight comparison between the different considered systems (Figure 2 and 3). Unsurprisingly, the fully timber superstructure is the lightest at under half the lineal weight of a concrete Super-T superstructure. However, the proposed CHB option demonstrates significant weight savings as well and improves upon the conventional composite design by 13.9%. These weight savings have the potential to reduce foundation costs related to both vertical and seismic load cases.

Table 2: Superstructure weight comparison

Item	Concrete Super-T	Steel/Concrete Composite	Timber Bridge	CHB
Superstructure weight per unit length (kN/m)	157	102	69	88
Percent reduction in superstructure weight relative to Super-T	-	35%	56%	44%

4.2 LCA Comparison Results

The material quantities used to conduct the LCA are summarised in Table 3. Results of the carbon assessments for all the bridge superstructure configurations are outlined in Table 4 below. Comparisons have been made against the concrete Super-T reference bridge to understand the potential carbon reduction for each option, while considering the different scopes of LCA modules included and how these impact the total carbon reduction. From Table 4, it is clear that the lowest carbon option depends on what modules are counted and if biogenic carbon is included in the assessment. Looking at only modules A – C, excluding biogenic carbon, the fully timber bridge option has the highest reduction in carbon at 38%; followed by the CHB system at 12%. However, when assessing modules A to D, excluding biogenic carbon, the CHB system (at 83%) has a slighter higher reduction in carbon than the timber bridge (at 82%) by 1%.

An interesting observation from the assessment calculations was that for the timber option, ~80% of the 116 tCO2eq, is attributed to the stainless-steel fasteners and brackets even though they comprise only 0.45% by volume of the total bridge (Table 3). Therefore, an opportunity for improvement has been identified, to reduce that embodied carbon of the timber bridge in Module A, by reducing the use of metallic components and using more timber joinery techniques for example.

The inclusion of the effect of biogenic carbon (BC) sequestration is generally a point of contention due to the uncertainty related to the end-of life use of the timber. That is, the carbon is technically only able to be sequestered if the timber is not burnt or decomposed at its end-of

life. One can argue that recycling and reuse (Module D), for any material, may have a similar level of uncertainty. Therefore, assuming that BC and Module D have similar levels of uncertainty and comparing the proposed CHB option and timber bridge on this basis, it can be seen that the proposed CHB option has the second highest carbon reduction with a 12% improvement over a traditional composite superstructure.

Table 3: Superstructure material quantities used for LCA calculation

Material EPD	Concrete Super-Tee	Steel/Concrete Composite	Timber Bridge	CHB
Reinforced Concrete [17]	188.7m^3	105m^3	-	81.9m^3
Structural Steel Hot Rolled [18,19]	-	5,61m^3	-	5.52m^3
Structural Timber [20]	-	-	409.5m^3	23.4m^3
Timber formwork [21]	-	-	-	7.2m^3
Stainless Steel [23]	-	-	1.83m^3	-

Table 4: Superstructure Configuration LCA Comparison Results.

Modules	Total Embodied Carbon (tCO_2eq)			
	Concrete Super-Tee	Steel/Concrete Composite	Timber Bridge	CHB
A1-A3	243	220	116	200
A4	40	50	46	42
A5w	0	9	5	5
C	3	5	8	5
D	-43	-221	-133	-210
Biogenic Carbon (BC)	0	0	-329	-12
A-C Excl BC	286	284	175	252
% Reduction from Reference	-	0.7%	38%	12%
A-C Incl BC	286	284	-154	240
% Reduction from Reference	-	0.7%	146%	16%
A-D Excl BC	243	63	42	42
% Reduction from Reference	-	74%	82%	83%
A-D Incl BC	243	63	-287	30
% Reduction from Reference	-	74%	218%	88%

5 DISCUSSION

The LCA calculations undertaken in the previous section were for conventional carbon intensive concrete and steel, with additional carbon savings could be realised for the CHB option (as well as the conventional steel and concrete bridge examples), when low carbon steel [28] and concrete (e.g. Allied Ecrete) are used when assessing Module A.

Another aspect where additional carbon savings could be made for the CHB option (in addition to the other options using concrete) is the use of galvanized reinforcing. This would allow the concrete cover to reduce from 40mm to 25mm, thus for the proposed CHB option this could mean an additional weight saving of around 5%.

Although, the results show that a fully timber bridge has both the highest embodied carbon saving (Table 4) and lowest superstructure deadload (Table 2), these are only two of the many considerations which a Bridge Engineer would need to evaluate when designing a new bridge. That is, the “best” solution may not necessarily be the one with the best score for only one design metric (i.e. embodied carbon) when other design metrics (such as durability) may have much lower scores. The proposed CHB option in this study appears to provide a viable solution,

when accounting for all the considerations for a structurally optimised low carbon superstructure solution.

6 BRIDGE ENGINEERS CONSIDERATIONS

As previously mentioned, a number of design considerations needs to be evaluated by a Bridge Engineer when selecting a superstructure type. In this section, a number of these considerations will be discussed and related to the superstructure options evaluated in this study.

6.1 Efficient Design

The main duty of a Bridge Engineer (and Building Structures Engineers for that matter) is to design a structure that meets the structural, durability, economic and performance requirements for the given national standards. In this case, for bridges as outlined in the NZTA *Bridge Manual* [11] and relevant clauses of the NZ *Building Code* [27]. Therefore, a design is deemed to be efficient when it inherently satisfies all of these requirements. As such, embodied carbon should be treated in the same manner as the other requirements being considered.

It is in the Authors view, that when a Bridge Engineer assesses the embodied carbon of a structural option, they should primarily focus on Modules A to C, and initially ignore both biogenic carbon sequestration and Module D. The primary focus is to design the most structural efficient and durable structure, with the least amount of in-service maintenance (i.e. Module B), while meeting the above requirements. Based on this discussion, Table 6 below compares a number of considerations, that a Bridge Engineer should consider when comparing the given bridge configurations discussed herein.

6.2 Durability

The durability of any bridge structure is governed by the durability of the surfacing to deck bond and the durability of the structural components. Resurfacing a bridge typically results in significant downtime and major disruption to bridge users. Current experience from WSP's bridge asset management of timber decked road bridges indicates frequent surfacing maintenance being required (less than 10 years [28]) irrespective of the speed limit of the carriageway (Figure 5). In terms of durability of the timber structural components, it is in the authors' opinion that the greatest challenge will be the sealing of any deck joints and perforations to prevent water ingress onto timber members. With the bridge examples shown in Figure 5, the timber deck was found to require replacement around every 25 years [28] due to its deterioration from vehicular impact damage. A cast-in-place concrete deck would resolve both of these issues, giving the proposed CHB option a significant advantage for these aspects.

Figure 5: Surfacing distress on a timber deck state highway bridge (left) and suburban road bridge (right).

Table 6: Comparing different the superstructure options based on a Bridge Engineers considerations.

Considerations	Concrete Super-Tee (Reference)	Steel/Concrete Composite	Timber Bridge	CHB
Weight reduction potential	Heaviest overall superstructure.	Has moderate weight reduction potential.	Highest weight reduction potential.	Has moderate weight reduction potential approx. 10%-15%
Constraints controlling preliminary design	SLS of main girders. Deck capacity for barrier loads. Deck capacity for wheel loads.	ULS capacity of main girders. SLS rebar fatigue and cracking (min deck thickness). Deck cantilever thickness.	SLS overall deflection. ULS Capacity of main girders. Deck capacity for barrier loads. Deck capacity for wheel loads.	ULS capacity of main girders. Load sharing in composite action: stiffness of cross-girder and shear fasteners. Edge distances of shear fasteners. Deck cantilever thickness. SLS rebar fatigue and cracking (min deck thickness).
NZBC compliance pathway risks	Low risk.	Low risk.	High risk, pathway needs to be determined.	Medium risk, pathway needs to be determined.
Main peer review risks	Vertical seismic due to eccentric tendons. Impact damage.	Impact damage.	Fire resistance. Durability. Flood debris impact. Diaphragm action. Vibration resistance of fastener connections. Beam splice connections. Impact damage.	Timber fire resistance. Fatigue of TCC composite shear connection. Timber Durability Impact damage.
Constructability	Conventional construction methods.	Conventional construction methods.	Smaller cranes required. Design may require higher onsite labour for structural connections. Number of beam splices will be governed by beam lengths.	Higher amount of onsite labour required: installation of cross-girders and plywood formwork.
Durability	Provided by concrete cover.	Provided by concrete cover. Girders are either painted or utilise weathering steel.	Higher level of durability detailing is required to prevent water ingress at joints and weathering reducing deck capacity and/or main girder capacity.	Higher level of durability is required for the timber components, as the transverse deck capacity is reliant on composite action.

6.3 Module B: Maintenance

As discussed above, the embodied carbon relating to maintaining the different bridge superstructure is currently excluded from this investigation, as there is a significant uncertainty

around the actual maintenance that will be required for a fully timber bridge, and the timber components in the CHB system as both are highly dependent on the efficacy of the durability detailing selected.

Maintenance for the proposed CHB option is foreseen to be low as the timber components are sheltered by both the deck and steel girders, from direct exposure to both sunlight and water from the rain. Moreover, commercial products are readily available for the waterproofing of concrete surfaces to prevent ingress through potential cracks in the deck; as well as the potential to overcoat the timber components to fully encapsulate them from the weather.

On this basis, the embodied carbon for a fully timber bridge has the risk of being significantly higher than estimated if its performance falls below its design expectation. As previously discussed, simple timber deck road bridges constructed to date in New Zealand have been found to require deck replacement approximately every 25 years due to vehicular impact damage, which falls far below the target life of 100 years.

7 CONCLUSION AND RECOMMENDATIONS

In conclusion, a new bridge superstructure was proposed by this paper, that utilises a steel girder acting compositely with a concrete deck in the longitudinal direction, combined with a timber cross girder acting compositely with the same concrete deck in the transverse direction, with the timber cross girders bolted to the steel girders. This Composite Hybrid Bridge system (CHB) combines the advantages of these conventional construction materials, to provide an optimised low carbon bridge superstructure solution.

A comparison of this system was made against a reference Super-T, traditional composite, and fully timber superstructure in terms geometry, weight, and embodied carbon based on the outcome of preliminary structural design.

A case was made for the selection of the optimal superstructure system based on satisfying multiple criteria requirements. For embodied carbon calculation it was argued that the focus should be on Module A to C, excluding biogenic carbon sequestration and reuse/recycling Module D, and that embodied carbon should not be weighted more than the other design and performance requirements.

A short discussion was made around the current challenges faced by fully timber bridges with some evidence given from asset management experience of timber decked road bridges. Based on which it was found that the proposed CHB system has the potential to be a viable low carbon alternative to conventional bridge structures.

Further work is recommended to understand the effects of both Maintenance (Module B) and the substructure when considering the whole of life-embodied carbon and investigating the mitigation of the risk of fire to timber components, to reduce their vulnerability from either accidental or intentional fires.

REFERENCES

1. Netley, J., 2022, Engineered Timber Bridges for Highways in New Zealand, Austroads Bridge Conference, Adelaide Australia
2. Rodrigues J.N., Dias A.M.P.G., & Providencia P., 2013, Review of TCC bridges, BioResources, 8(4), pg 6630-6649
3. Wacker, J.P., Dias, A.M.P.G., and Hosteng, T.K., 2020, 100 year performance of Timber-Concrete Composite Bridges in the United States, Journal of Bridge Engineering, 25(3)
4. Rodrigues J., Providencia, P., Dias, A., 2010, Use of composite timber-concrete bridges solutions in Portugal, International Conference on Timber Bridges, Norway
5. Swygart L., & El Sarraf R., 2024, Carbon Caveats, Bridge Design and Engineering Magazine, Issue 114, www.bridgeweb.com

6. Beca & Opus, Standard precast concrete bridge beams, NZ Transport Agency Research Report 364
7. Standards Australia Ltd & New Zealand Standards Executive, 2017, AS/NZS 5100.6 Steel and Composite Construction
8. PTL Structural & Fire, 2024, DRAFT NZ Timber Bridges Design Guide
9. Standards New Zealand, 1993, NZS3603 Timber Structures Standard A1&2&4
10. European Standard, 2014, EN 1995-1-1:2004+A2:2014 Eurocode 5: Design of Timber Structures Part 1-1
11. Waka Kotahi NZ Transport Agency, 2022, Bridge Manual 3rd Ed. Amdt. 4 SP/M/022, Wellington NZ
12. DIBT, 2018, European Technical Assessment of SFS VB Screws ETA-13/0699, https://us.sfs.com/products/fasteners-connections/timber-connections/vb-special-head-timber-concrete-composite-floor-152452 accessed 26/03/25
13. Lefebvre, D., Richard, G., 2014, Design and Construction of a 160-Metre-Long Wood Bridge in Mistissini, Quebec, Internationales Holzbau-Forum.
14. Standards Australia & Standards New Zealand, 2016, AS/NZS 3678 Structural steel - Hot-rolled plates, floorplates and slabs
15. Standards New Zealand, 2006, NZS 3101 Concrete Structures Standard Part 1 –The Design of Concrete Structures
16. Standards Australia & Standards New Zealand, 2019, AS/NZS 4671 Steel for the reinforcement of concrete
17. Standards Australia & Standards New Zealand, 2012 AS/NZS 2269.0 Plywood - Structural
18. Gibbons, O.P., Orr, J.J., & Arnold W., 2022, How to Calculate Embodied Carbon (Second Edition), London, The Institution of Structural Engineers
19. British Standards Institute, 2011, BS/EN 15978: Sustainability of Construction Works. Assessment of Environmental Performance of Buildings. Calculation Method.
20. BRANZ, 2019, CO_2NSTRUCT Embodied Carbon Database
21. EPD Australia, 2022, Environmental Product Declaration - Liberty Primary Steel: Hot rolled Structural and Rail
22. Bluescope, 2020, Xlerplate Steel Environmental Product Declaration Version 2.0, EPD Australasia
23. Wood Processors and Manufacturers Association of New Zealand Inc., 2021, Environmental Product Declaration for solid, finger-jointed and laminated timber products including timber preservation options, EPD Australasia
24. EPD Australasia, 2023, Environmental Product Declaration – Carter Holt Harvey: Plywood
25. EPiC, 2019, ecoinvent database, Cold rolled stainless steel
26. Ministry of Business Innovation and Employment, 2022, Whole-of-life embodied carbon assessment technical methodology
27. Ministry of Business Innovation and Employment, 2014, New Zealand Building Code Handbook
28. WSP Internal Communication
29. HERA, How to specify low-caron steel. 2025. https://hera.org.nz/resource-specify-low-carbon-steel/

ICTB 2025. 5th International Conference Timber Bridges
Rotorua, New Zealand, 29 June to 2 July 2025.

ANALYSIS OF THE COLLAPSE OF THE TIMBER BRIDGE OVER THE DURATÓN RIVER, IN PEÑAFIEL (SPAIN)

Alfonso Lozano[1], Julio Vivas[2], David Lorenzo[3], Felipe Álvarez[1]

ABSTRACT

In 2012, the construction of a pedestrian GL timber bridge over the Duratón River (Valladolid-Spain) was completed. This structure connected the urban center of Peñafiel with its famous castle area.

Shortly after its inauguration, some deformations and inclinations of its arches were detected, as well as other defects such as cracks, distortions and failures in the glued of the laminates

Over the following years, the deflections increased; and also other problems in the arches and beams appeared. Additionally, under certain loads, vibrations began to be worrying.

Given this situation of insecurity, in 2018 the Peñafiel City Council ordered the shoring up of the structure; and a few months later, it was dismantled.

In 2020 a new bridge was built, with similar characteristics, but appropriate design and calculation to support the loads foreseen in the project.

This paper describes the original bridge, exposes the progressive deterioration it suffered over the five years following its assembly, and analyzes the causes that forced the removal of this structure.

1 INTRODUCTION

Ribera del Duero is a famous appellation that includes vineyards located in Castilla y León (Spain), within the Duero River basin, about 115 km long and 35 km wide, located at the confluence of four Spanish provinces: Soria, Burgos, Segovia and Valladolid. One of the most important villages of this area is Peñafiel, located in Valladolid.

In 2010, the works that were intended to be carried out in this area around the Duero River in Peñafiel were publicly presented. The overall amount of the action, which included the reconstruction of the old pedestrian path that ran parallel to that river, was 5.28 million euros.

This action had the purpose of recovering an old fishing path that existed between several small villages in the area, with the double objective of facilitating the connection between said villages and, at the same time, promoting sustainable development and tourism in that region, famous for the quality of its vineyards.

Among the items of that ambitious plan, were included the adaptation of the aforementioned pedestrian path of approximately 40 km in total length, the environmental recovery of the banks of the rivers that flow through the area, with the planting of various native species and especially the construction of four bridges, made of laminated timber.

The first bridge would be located in the centre of Peñafiel, as the main village of this wine region; the second one was very close to this small town; and the last two in Pesquera and Quintanilla, both villages located a few kilometres from the Peñafiel itself.

[1] Industrial engineer, university of Oviedo,
e-mail: alozano@uniovi.es,
[2] Civil engineer, Media Madera Ingenieros Consultores
[3]Forestry engineer, university of Vigo

In 2012, the construction on the first one of these four structures, the most visible of all of them, was completed. This pedestrian timber bridge connected the urban area of Peñafiel with the castle hill. Figure 1 and 2 shows the bridge, with the castle in the background, on the top of the hill.


Figures 1 and 2. The timber bridge of Peñafiel, with its famous castle at the top of the hill.

The other three bridges, which, unlike the first, had been designed and calculated by the engineer Julio Vivas and manufactured entirely in Asturias by the company Media Madera Ingenieros Consultores S.L., were assembled on site a few months later, and were very different to the first one.

With a proximately 100 m long and 3 m width, its original geometry, defined by its designer, was based on the monsters of Asturian mythology, similar to dragons and fearsome guardians of treasures (Figures 3, 4 and 5).



Figures 4, 5 and 6. Timber bridges in Peñafiel, Pesquera de Duero and Quintanilla, by engineer Julio Vivas.

2 DESCRIPTION OF THE TIMBER BRIDGE OF PEÑAFIEL

The pedestrian bridge analyzed in this paper was designed in two sections, both of them of 2.00 m width: one resolved by a two hinge arch of 50 m spam, responsible for receiving the loads of the deck plate through timber and steel hangers (Figure 7), plus another straight section, arranged after the previous one, supported by concrete piles (Figure 8).


Figures 7 and 8. Both parts of the Peñafiel timber bridge.

Focusing the attention on the arches part, it was a quite traditional design: cross beams hanged from the arches, supporting the main beams; over them, floor springers and the plank deck. Bracing systems of the arches was achieved by means of horizontal trusses; in the case of the deck, bracing beams and diagonal elements, disposed between the main beams. In the following pictures some of the connections between the main elements of the structure and the bracing systems, can be seen (Figures 9, 10, 11 and 12).




Figures 9, 10, 11 and 12. Different structural components and bracing systems.

Both types of trusses should absorb the wind loads and also restrain the beams and arches against lateral buckling.

In theory, wooden laminates, of 35 mm thickness, would be made of Scots Pine (*Pinus sylvestris*, M.), Strength Class GL28c.

3 PATHOLOGICAL PROCESSES AND CHRONOLOGY

Shortly after its inauguration, the first pathological processes were detected in the part of the bridge corresponding to the arches.

Specifically, in the month of April 2013, obvious deformations and inclinations of its arches were observed (Figure 13), as well as smaller defects, such as delaminations and cracks (Figure 14) in the laminates that constitute the main elements of the structure.

On the contrary, the straight section of the bridge, of the same length, did not present distortions or deformations of any kind.

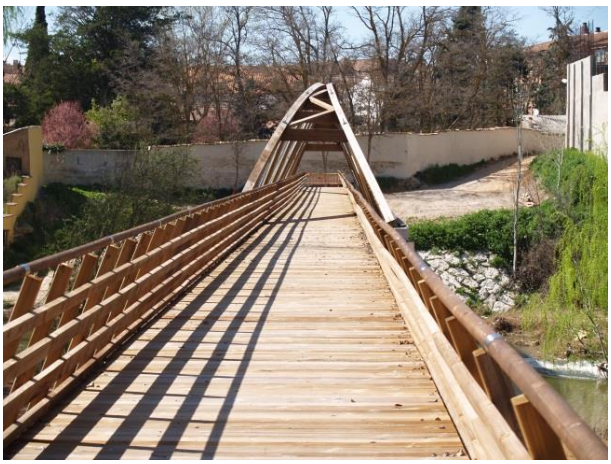
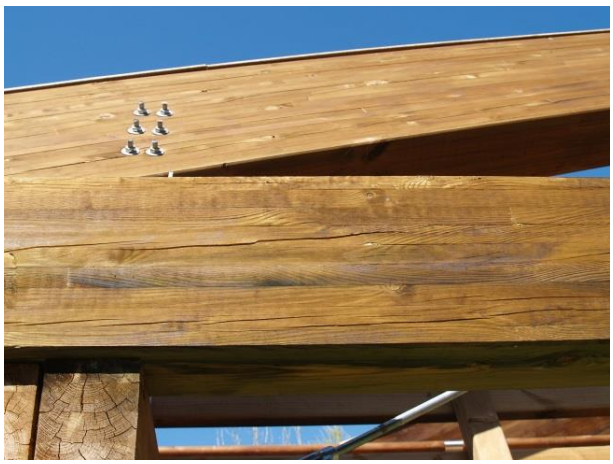

Figures 13 and 14. Deflections of the arches and cracks in the main beams.

During the following months, the number of laminates affected by delaminations grew up significantly; and the same applies to the width and depth of the cracks.

This problem was especially noticeable in the arches, where defects were practically observed throughout the entire section (figures 15 and 16).


Figures 15 and 16: Delaminations in arches and beams.

In August 2013, new tie rods of steel were connected between the keystone of each arch and the structural elements of the deck on the opposite side, in addition to reinforcing the initial bracing system of the arches.

Although some of these rods may be seen in Figure 17, the buckling of the arches did not stop. At this point, the company that built and assembled the bridge, decided to increase the section of some of the tying beams and the number of rods.

Two years later, in the month of May 2017, despite the specific reinforcements that the company periodically carried out, the deformations and losses of verticality continued to increase in the arches (Figure 18).

Furthermore, the problem was extended to the main beams, which also suffered very obvious deformations, even to the naked eye (figure 19).

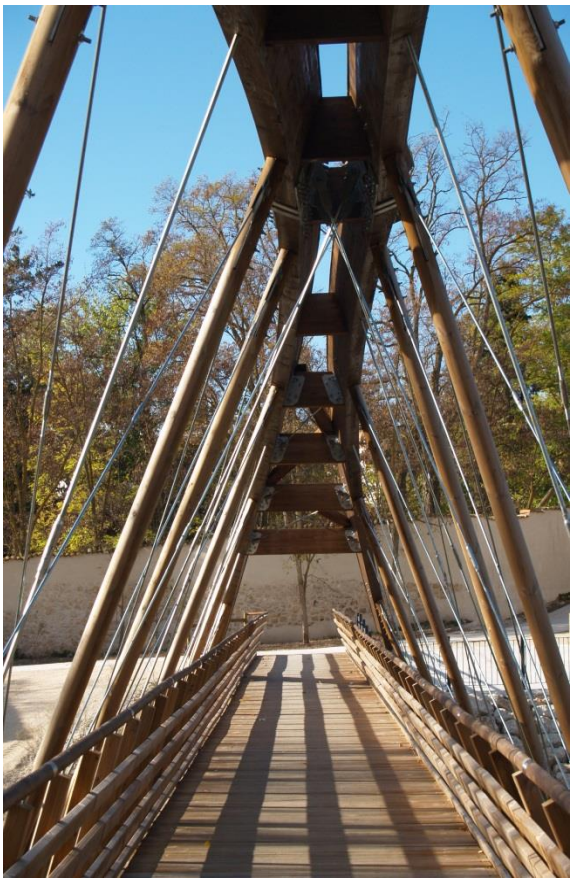

Figures 17, 18 and 19. New tie rods in august 2013, but distortions were really important in the month of May 2017.

Given this situation of insecurity, at the beginning of 2018, the Peñafiel City Council ordered the shoring up of the structure of the arches (Figure 20); and a few months later, this part of the bridge was dismantled.

Figure 20: Shoring up the arches and deck, just before been dismantled.

4 STRUCTURAL ANALYSIS OF THE PROBLEM

Regardless of the opening of cracks and delaminations, due to the sudden thermal changes that occur throughout the year in that area, combined with the environmental humidity related to the river (Figures 21 and 22), the really important question was to determine the origin of the deformations and overturning of the arches.

Figures 21 and 22. Big differences in the moisture content of the timber elements.

On the other hand, without analysing whether or not the wooden sections were well dimensioned, or whether the laminated wood actually reached a Strength Class GL28c, there is no doubt that the type of failure of the arches corresponds to one of the buckling modes (Figures 23 and 24).

Figures 23 and 24. Failure mode due to buckling.

Furthermore, there were noticeable differences between the initial design that originally appeared in the project (Picture 25), compared to the one that was finally built.

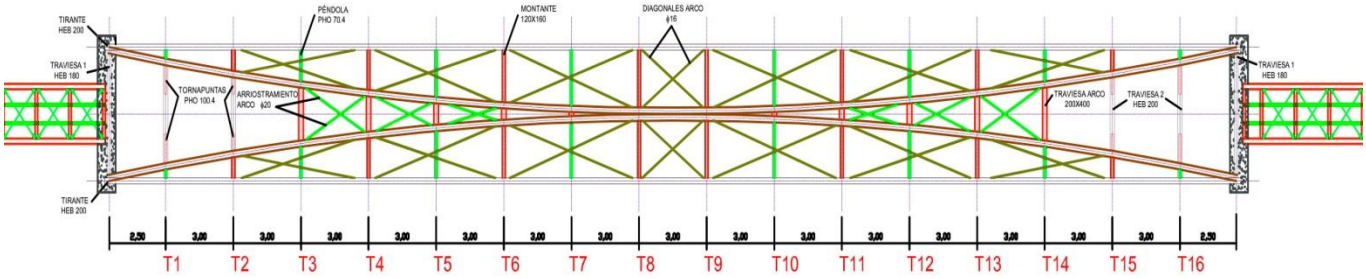

Figure 25. Original design of the bridge.

Among other small variations, the most important ones were the following:

1. Bracing system of the arches (Figure 26).
2. Diagonals of the deck plate (Figure 27).
3. Smaller diameter for the timber hangers.

Anyway, it is obvious that the bracing system of the arches was not effective at all, even after the reinforcement applied in the keystone of the arch, during the month of august of 2013 (Picture 28), and the main reason is that some connections, that had been considered like rigid joints in the project, they really were not.

This is possibly the main mistake that was made in this project, and the reason of its collapse.

Figures 26, 27 and 28: Changes in the initial design of the bridge (left), and new rods (right)

Fortunately, in this occasion, authorities decided to replace the collapsed structure by another bridge, also built in GL timber, with similar characteristics like the old one, but with a proper design and calculation, able to support the loads foreseen in the project.

Their decision was based on the good condition of the other three bridges that had been built by Media Madera Ingenieros Consultores S.L., at the same time as the damaged one, and the good acceptance by the local population and tourists who frequent that area.

The new structure, now built by this same company, included some steel beams to avoid buckling and guarantee the bracing, and was assembled on site in 2020 (Figure 29).

Figure 29. The new bridge was built in 2020.

5 CONCLUSIONS

As is well known, arch bridges work by transferring the self weight and imposed loads to the abutments or pillars, by compressing the arch. In these supports, they are transformed into a horizontal thrust and a vertical load [1].

In general, it can be stated that arch bridges with suspended deck are the more stable, the more load is applied to the arches.

If we talk about mechanical properties and structural behaviour, the strength resistance of glulam timber, combined with its low self-weight and ability to absorb energy, makes it a perfectly valid material for the assembly of bridges [2].

However, for the same reason, the stability of this type of structures against overturning and buckling effects, must be analysed more carefully. That is, bracing systems must be perfectly designed and calculated for each particular situation [3].

These systems serve to stabilize the main elements (beams and/or arches) during the construction, contribute to the distribution of the effects of the load and, as is the case at hand, restrict the movement of the compression chords where, otherwise, they could suffer lateral buckling.

On the other hand, it is very difficult to get the connections in bridges of this type to really work as rigid joints. Hence it must always be considered that the system is articulated; and design the bracing system in this sense, to avoid unacceptable deformations.

In the bridge of Peñafiel, over the Duratón River, regardless of the more or less correct calculation of the sections of its structural elements, or the quality and mechanical properties of the wood, the failure has occurred precisely due to mistakes in the design of the joints and the bracing systems, which have not been able to prevent the displacements of the arches, almost since their assembly.

REFERENCES

1. Ritter, M.A. 1990. Timber Bridges: Design, Construction, Inspection, and Maintenance. Washington, DC: 944 p.
2. Crocetti, R. 1990. Timber bridges: general issues, with particular emphasis on Swedish typologies. 20. International Holzbau-Forum IHF 2014.
3. Bendsoe, M.P. 1989. Optimal shape design as a material distribution problem. Structural optimization 1(4). pp.: 193-202.

ICTB 2025. 5th International Conference Timber Bridges
Rotorua, New Zealand, 29 June to 2 July 2025.

EXTENDED DESIGN RULES TO IMPROVE THE DURABILITY OF TIMBER STRUCTURES

Roland Maderebner[1], Thomas Stieb[2], Julian Gahbauer[3], Christoph Niederegger[4]

ABSTRACT

In recent years, damage to timber bridges has been documented in Austria. The damage was so extensive, particularly in the case of truss bridges, that some had to be demolished. The majority of these timber bridges were subsequently replaced with steel structures. In Austria, around 23 $kg \cdot m^{-2} \cdot a^{-1}$ of road salt is used to prevent ice formation on bridge pavements during winter. While the salt solutions do not affect the durability of timber structures, they are carried into the structure with other particles. Knife sheets are typically milled to fit precisely for adequate stiffness. The gaps between the metal sheets and the timber surfaces, which are only a few millimetres wide, accumulate dust particles. Combined with the salts, this can create a substrate that absorbs moisture from the ambient air, leading to latent dammed-up water or can help to absorb water. This study illustrates the influence of the moisture content of adjacent timber components on slotted-in steel plates with clogged gaps and the role of salts within this context. Based on these findings, recommendations for detailing these connections are presented.

1 INTRODUCTION

The construction and maintenance of timber bridges presents a particular challenge. Timber protection must be carefully planned, especially in countries like Austria, where climatic conditions and the use of road salt significantly impact the service life of such structures. The article does not study the chemical processes that salt can cause in wood, including the interaction between salt and cellulose, lignin, and other wood components [e.g. 1,2,3,4]. This article aims to present the most important protective measures, risks, and influences on timber bridges with slotted-in (knife) steel plates, as well as the influence of NaCl in combination with contaminations in the gaps between steel parts and timber members.

The design life T_{lf} for timber bridges must be established based on EN 1990:2023 [5], and the design specifics should be chosen accordingly. During the design phase, it is crucial to consider various load scenarios influenced by climate, usage patterns, and maintenance intervals. In general, a distinction is made between organisational, structural, and chemical wood preservation. In Austria, structural wood preservation is preferred over chemical wood preservation. Organisational wood preservation includes regular inspections, timely maintenance, and well-planned use and structural design. An additional roof structure is often typical for bridges if closed panelling does not fully protect the structural timber parts. The principles for designing the roof structure are outlined in EN 1995-2 [6]. An angle of 30° to the vertical is recommended to prevent a direct rainwater ingress. A good drainage concept is also crucial in this regard, and additional protective layers, water noses, gutters, etc., need to be planned.

Chemical wood preservatives can complement structural wood preservation, but are controversial in many areas. Their use is limited, particularly on bridges in contact with water or in environmentally sensitive locations. In addition, many products lose their effectiveness over time and require regular re-treatment, which can be challenging to manage and costly in practice.

[1] Prof. Dipl.-Ing. Dr. Roland Maderebner, University of Innsbruck – Timber Engineering Unit (Austria), e-mail: roland.maderebner@uibk.ac.at
[2] Dipl.-Ing. Thomas Stieb, University of Innsbruck – Timber Engineering Unit (Austria)
[3] Bac. Johannes Gahbauer, University of Innsbruck – Tragwerkspartner GmbH, Innsbruck (Austria)
[4] Dipl.-Ing. Dr. Christoph Niederegger – ZT GmbH Niederegger, Neustift / Stubai (Austria)

The implementation of monitoring systems is becoming more prevalent in the prevention of damage. Critical points in the construction and durability of many bridges occur particularly at joints consisting of dowel connectors, slotted-in steel plates and timber-to-timber connections (contact joints). In Tyrol/Austria, several timber bridges have been dismantled in recent years, although the structural timber protection was designed according to standards. In all damage cases, insufficient attention was paid to water management in the detailed design of the joints. Scientific investigations of the damage cases revealed that the accumulation of dirt (including trees' needles, leaves, tyre debris and other materials) was significant in some cases. Moisture measurements confirmed permanent moisture ingress in these areas. The ingress of moisture or contamination is mainly from the inside rather than the outside.

The authors posit that structural engineers have not given the issue sufficient attention. This has led to considerable failures of load-bearing structures, although the above-mentioned principles of structural timber protection were in principle fulfilled. This is also why these damage mechanisms were not always recognised at an early stage. This necessitates additional sensitisation in the planning and inspection of bridge structures.

2 CASE STUDIES

After damage to bridges in Tyrol was observed within a comparatively short service life, more detailed investigations were initiated as part of an accompanying master's thesis. The two bridge structures presented in this study are both truss bridges (see Fig. 1):

The first, known as the *Klimm-Bridge*, is located near Reutte and spans the Lech River, a largely natural and unregulated alpine river. It is a heavy-duty traffic bridge designed to withstand loads of 650 kN and was constructed in 2002.

The second bridge examined is the *Notburga-Bridge*, a pedestrian and bicycle bridge that is also used for cattle drives. It is located in North Tyrol, in the municipalities of Jenbach and Rotholz, and spans the Inn River across three fields, completed in 2005.

Both bridges are equipped with a roof structure that, by the 30° rule of EN 1995-2 [6], provides substantial protection for the substructure. However, at the Notburga-Bridge, this roof overhang could not be consistently maintained in the area of the raised roof sections. In addition, both bridges feature smaller roof elements designed to offer further protection to the lower chord against environmental exposure.

2.1 Klimm-Bridge

At the Klimm-Bridge, the lower chord was already so severely damaged that a tensile failure occurred, directly in the area of a construction joint in the lower chord (see Fig. 2). The diagonals were connected to the upper and lower chords using knife plates. As part of the evaluation of possible maintenance measures for the bridge structure, the adjacent joints were also closely examined. Initial measurements of the moisture content [7] at depths between 15 and 60 mm revealed values of approximately 19.5 %, indicating a critical moisture condition. Using drilling resistance – Resistograph - measurements and core sampling, a far-advanced internal brown rot was detected in large portions of the investigated areas, in some cases affecting up to one-third of the cross-sectional width (see Fig. 3). These damages were not visible from the outside and were therefore likely not identified during prior bridge inspections. In the innermost third of the cross-section, only a completely degraded wood matrix and humus-like material could be extracted. The findings were confirmed by drilling resistance tests. Additionally, significant contamination was found in all joints, particularly in areas near the riverbanks and between the steel plates and timber members, which likely contributed to moisture accumulation and subsequent damage.

Figure 1. Notburga-Bridge, river Inn (left) and Klimm-Bridge, river Lech (right) [8]

Figure 2. Klimm-Bridge, tension failure at the lower chord [9]

2.2 Notburga-Bridge

Following the damage observed at the Klimm-Bridge, the responsible municipalities also initiated a detailed investigation of the Notburga-Bridge. In particular, the design of the knife plates in the areas of the steel portal frames at the intermediate concrete supports, as well as at the raised ridge section, leads to increased moisture ingress.

Similar to the previous case, the moisture content [7] of approximately 19 % was measured in the affected components. However, measurements using a Resistograph have so far shown no apparent signs of internal wood decay in the beam cross-sections. Nevertheless, the heavy moss growth and already advanced surface deterioration suggest that insufficient bridge inspections have occurred in the past. Additionally, significant contamination of the joints was observed in several areas.

2.3 Additional information on bridge use and maintenance

Following consultations with the responsible road maintenance departments, the following additional information was documented:

- Bridge cleaning using high-pressure cleaners is carried out as needed, on a case-by-case basis
- Salt spreading is performed both manually and mechanically, though not on a regular schedule

During inspections of both bridge structures, it was found that the joints between the slotted-in steel plates and the timber elements were, in some cases, completely clogged, raising concerns about persistent moisture accumulation (water retention). As a result, substrate samples were collected and subsequently analysed in detail at the University of Innsbruck's laboratory.

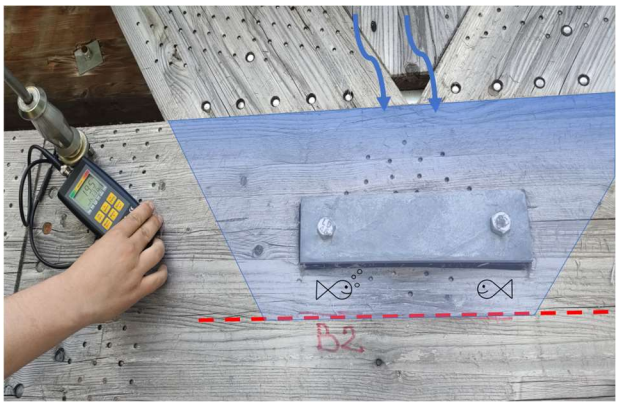

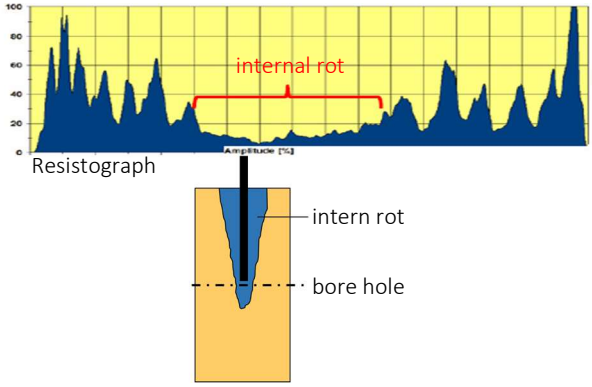

Figure 3. Klimm-Bridge: Joint with knife plates: Measurement of the moisture content (left) and drilling resistance at the bottom of the slotted-in steel plates (right)

Figure 4. Notburga-Bridge: Resistograph measurements and details of the knife plate (top), moisture content and contact joints to the steel portal frame (bottom)

Figure 5. Selected substrates/contamination from the bridges

3 APPLIED METHODS

3.1 Composition of substrates in the gaps of the joints

The material sampled from the bridge structures predominantly consists of organic and mineral substances such as soil and humus, undecomposed small branches, leaves, plastic contaminants (e.g., tire wear particles), and animal fibres. Elevated salt concentrations were also detected, particularly near the bridge portals. The particle sizes of the mineral components range from a few millimetres, while leaves and branches can reach larger sizes. A homogeneous mixture reflecting the on-site contamination was required to ensure a consistent and representative distribution of contamination in the experimental series. Following compositional analysis and consultation with chemists, a commercially available plant culture substrate (see Fig. 5) was selected, as its composition closely resembles the sampled materials. This substrate comprises bark humus, various plant fibres (including wood fibres), and compost. The pH value ranges from 5.0 to 7.0, aligning with the measured values of the bridge contaminants.
The substrate's density in the undried state is 0.34 g/cm³ at a mass-based moisture content of 114 %. To match the measured salt contents, the substrate was adjusted in the test series to investigate its influence on wood moisture content, with a standard salt concentration set at 1.5 g/l.
Since the effect of contamination on wood durability, especially related to salt content, is strongly influenced by local conditions, climate data from the relevant sites were also analysed concurrently.

3.2 Climate data at the locations

Climate data for the study sites were sourced from the GeoSphere Austria Data Hub [10] (https://data.hub.geosphere.at/) and selected from weather stations located close to the bridge structures:

- *Jenbach* (Weather Station ID: 11901), sea level 563 m
- *Holzgau* (Weather Station ID: 11401), sea level 1080 m

Data were averaged over five years from January 2016 to December 2020. Monthly mean values were calculated and further aggregated by season: winter (Dec–Feb), spring (Mar–May), summer (Jun–Aug), and autumn (Sep–Nov). This seasonal aggregation provides a robust basis for assessing climate-induced stresses, including periods of moisture exposure, temperature variability, and freeze-thaw cycles. Figure 6 illustrates the averaged monthly temperature and relative humidity values. Based on this climatic data, the expected moisture content (EMC) of the wooden structural components was estimated using Keylwerth's diagrams.

3.3 Experimental Setup for Measuring Wood Moisture Content

Four test series were conducted, each consisting of four specimens. The aim was to systematically investigate the influence of contamination on the moisture content of timber components. In each setup, two spruce wood specimens with an average density of 435 kg/m³ were placed 10 mm apart, with their side surfaces facing each other (see Fig. 7) with a randomised annual ring orientation. The gap between the wood elements was filled with the substrate described in chapter 3.1, either in its pure form or with the addition of sodium chloride (NaCl). The test setups were then subjected to three different climate conditions (see Tab. 1). To continuously monitor the moisture content levels, moisture electrodes [11] were inserted at depths of 10 mm and 40 mm into each wood sample and measured for several weeks.

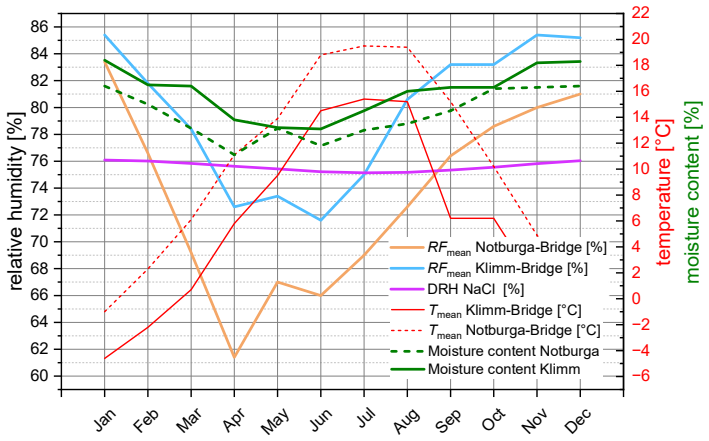

Figure 6. Climate Conditions and estimated moisture content of timber members at the locations of the Bridges

Table 1. Test series with varying relative humidities, temperatures and substrates

series	specimen no.	relative humidity	temperature	substrate
1	P01-P04	65 %	20 °C	without NaCl, wet substrate
2	P05-P06	65 %	20 °C	with NaCl, wet substrate
	P07-P08			without NaCl, wet substrate
3	P05-P06	85 %	20 °C	with NaCl, dry substrate
	P07-P08			without NaCl, dry substrate
4	P05-P06	variable	variable	with NaCl, dry substrate
	P07-P08			without NaCl, dry substrate

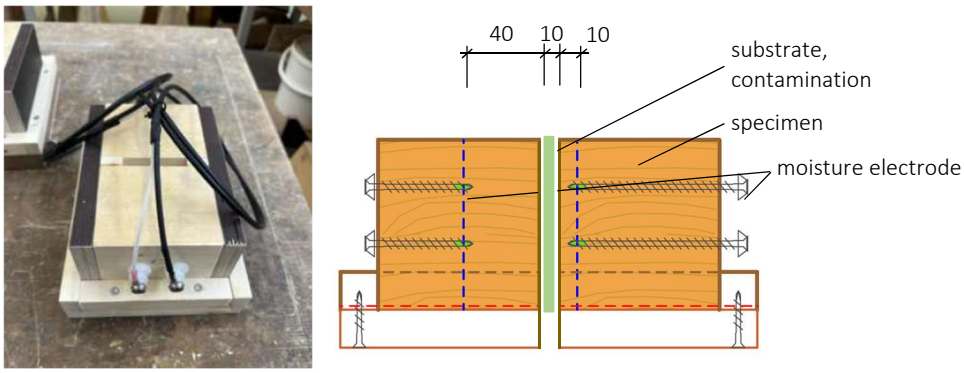

Figure 7. Test setup to measure the moisture content: two spruce wood specimens (435 kg/m³) placed 10 mm apart, with a substrate in between. Moisture sensors were installed at two depths (10 mm and 40 mm) in each specimen

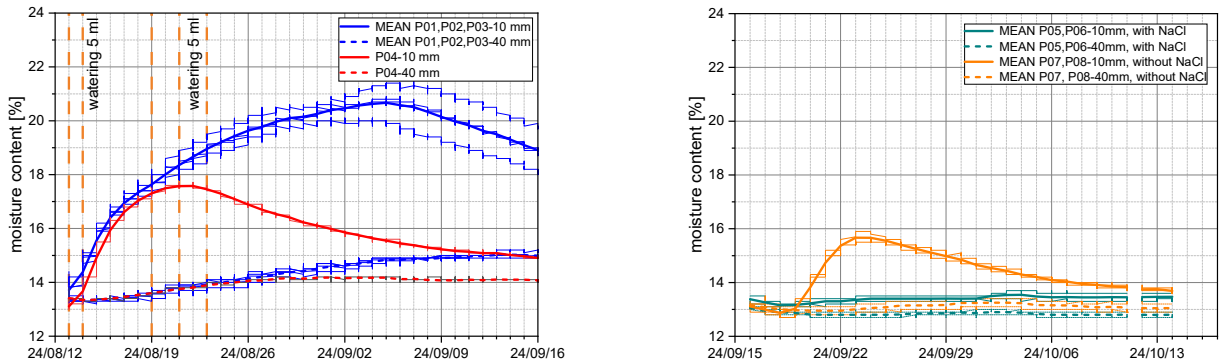

Figure 8. Influence on the moisture content of timber members, series 1 (left): wet substrate without additional NaCl, 20/65 and series 2 (right): wet substrate with/without additional NaCl, 20/65

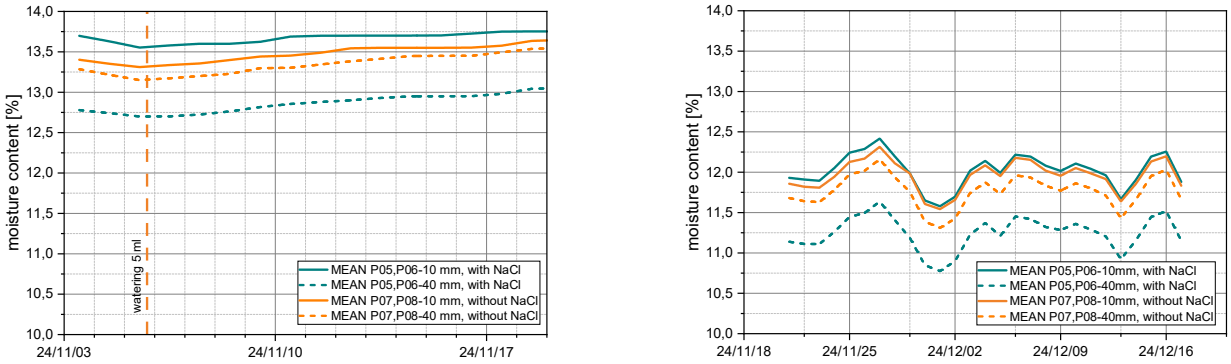

Figure 9: Influence on the moisture content of timber members, series 3 (left): dry substrate with/without NaCl and series 4 (right), 20/85: dry substrate with/without additional NaCl, variabel

4 RESULTS

4.1 Influence of Contamination on Wood Moisture Content

The first experimental series investigated the influence of a substrate without additional NaCl on the moisture content of spruce wood. Initial measurements indicated a baseline average wood moisture content of approximately 13.5% (see Fig. 8, left). A controlled addition of 5 ml of water into the substrate-filled joint between the specimens markedly increased the moisture content. In specimens P01, P02, and P03, four additional water applications were performed throughout the experiment, timed by precipitation events at the corresponding bridge locations. At a sensor depth of 10 mm, a gradual but significant increase in moisture content was observed, with peak values of approximately 20.5 % reached after three weeks. Following this peak, a slow decrease in moisture levels was recorded. Specimen P04, which received only one water application, exhibited a maximum moisture content of 17.5 %, reached approximately one week after the initial application. In contrast, at the deeper measurement depth of 40 mm, moisture uptake occurred more slowly and to a lesser extent across all specimens, indicating limited moisture transport into the specimen's core under the tested boundary conditions. These results suggest that contaminant accumulation in construction joints, especially under repeated exposure to moisture, can lead to a gradual but significant increase in the wood moisture content near the surface.

Following the completion of series 1, the second experimental series, with specimens P05 to P08, was conducted using a substrate with a gravimetric moisture content of 114 %. In specimens P05 and P06, NaCl was admixed into the substrate, while P07 and P08 were conducted without NaCl.

Under controlled climatic conditions of 20 °C and 65 % relative humidity, the presence of NaCl exerted a hygroscopic buffering effect (see Fig. 8, right), attributable to its deliquescence relative humidity (DRH) of approximately 75 %. As a result, moisture uptake in the adjacent timber elements progressed more slowly than in specimens without added salt.

Furthermore, changes in substrate mass were monitored over the test duration. The initial substrate weight before insertion was 15 g. After 14 days, specimens without NaCl exhibited a mass reduction of approximately 50 %, while those containing NaCl showed a decrease of only 38%. This differential supports the conclusion that the salt-treated substrate retained moisture for extended periods, thereby delaying moisture transfer to the wood.

In test series 3, the only modification compared to series 2 was an increase in relative humidity to 85%, which exceeded the deliquescence relative humidity (DRH) of sodium chloride, thereby initiating potential moisture release. Specimens P05 and P06 were filled with previously dried substrate containing NaCl, while P07 and P08 received dried substrate without salt. All substrates were oven-dried until no further mass change was observed, and then tested. At a relative humidity of 65 %, neither the salt-contaminated nor the uncontaminated samples showed any notable increase in wood moisture content (see Fig. 9, left). However, after increasing the relative humidity to 85%, a delayed increase in moisture content was observed at a depth of 40 mm. In contrast, at a depth of 10 mm, moisture levels rose almost immediately.

In the final part of the experiment, series 4, the specimens were stored in an open but sheltered outdoor environment, exposing them to natural fluctuations in temperature and humidity. These storage conditions correspond to Service Class 3, as specified in EN 1995-1-1. Following the laboratory phase, the specimens were subjected to varying environmental conditions (see Fig. 9, right). Similar to the observations from the controlled tests, no significant differences in moisture behaviour were observed between the salt-contaminated and uncontaminated specimens. While moisture levels in the salt-contaminated samples were slightly higher, the differences remained marginal. Fluctuations in wood moisture content were nearly identical at both measurement depths (10 mm and 40 mm), with an amplitude of approximately 1%.

5 SUMMARY

Structural wood preservation

Despite adherence to the standard 30° roof inclination, timber bridges frequently exhibit premature damage and necessitate deconstruction. This is primarily attributable to excessive clearance between the roofing and the protected structure, enabling moisture ingress even under wind exposure. Crucially, moisture input also comes from sources like cleaning activities and vehicular traffic. Furthermore, horizontal surfaces prone to water accumulation contribute to moisture retention when adequate drainage is not ensured. A decisive factor is the inadequate detailed design of water management at critical connections. Joints such as timber-to-timber interfaces, dowel connections, and slotted steel plate connections are particularly susceptible to contamination ingress. This ingress leads to waterlogging and subsequent timber decay, significantly compromising the structural integrity of the bridge.

Snow-related effects on moisture exposure

In Austrian road maintenance, sodium chloride (NaCl) is the primary de-icing agent. Calcium chloride ($CaCl_2$) and magnesium chloride ($MgCl_2$) are used less frequently due to their higher cost and strong hygroscopic nature. $MgCl_2$ notably retains its hygroscopic properties under most ambient conditions, while NaCl only exhibits deliquescence above approximately 75 % relative humidity, a threshold that decreases with rising temperature. Salt spreading methods encompass dry and wet applications, with manual spreading common on pedestrian and cycle bridges. The maximum recommended salt dosage is 40 g/m². Salt solutions can deeply penetrate wood cracks and joints, retaining moisture due to their hygroscopic characteristics. However, preliminary findings from this study suggest that while salts influence wood moisture content, their effect is overshadowed mainly by moisture retention caused by clogged joints and contaminant deposits. These deposits impede effective drainage and act as significant moisture reservoirs, thereby exacerbating waterlogging in timber elements.

Influence of contamination and joint design

Contamination in steel-to-wood connections without sufficient protective detailing results in rapid increases in wood moisture content, exceeding the critical threshold of 20 %. Contaminants function as moisture buffers during drying cycles, preventing wood from reaching equilibrium moisture contents typical for in-service timber bridges (approximately 18 to 20 %). In natural exposure scenarios, moisture ingress may be even more pronounced than observed in controlled experiments, where moisture was applied locally. To prevent clogging and moisture accumulation, design recommendations include implementing dust protection screens and increased joint clearances adapted to the site's surrounding vegetation and environmental conditions. Given the fine particle sizes observed in contamination, enlarging joint gaps is generally advisable to reduce debris buildup.

Conclusions and Recommendations

Many documented timber bridge failures in alpine regions can be attributed to insufficient joint detailing, inadequate water management, and moisture ingress exacerbated by de-icing salts. Future timber bridge designs must prioritise detailed drainage and contamination prevention planning. Incorporating monitoring systems, leveraging site-specific climatic data and salt exposure assessments, is essential for proactive maintenance.

Enhanced training for engineers and inspectors regarding salt-induced hygroscopic effects and vulnerability analysis of timber joints is strongly recommended. Long-term, the adoption of adaptive digital maintenance frameworks, supported by sensor data, has the potential to significantly reduce preservation costs and extend the service life of timber bridge structures.

In high-altitude regions, such as Elmen, where winter periods are prolonged and freeze-thaw cycles frequent, the mechanical and moisture stresses on timber components are elevated. These conditions necessitate careful material selection, robust detailing, and tailored maintenance strategies to mitigate damage risks associated with salt exposure and climatic factors.

To prevent contamination within the joints between steel plates and timber elements, two primary strategies can be considered:

i) Integration of fine grates over the slots: These grates are designed to prevent debris ingress while allowing for adequate ventilation. Crucially, they should be easily removable for inspection and cleaning, facilitating the removal of accumulated contaminants to prevent waterlogging.

ii) Designing very wide slots: An alternative approach involves increasing the width of the slots significantly. This aims to prevent the accumulation of contamination within the joint altogether. However, this design choice introduces greater compliance, as the fasteners are subjected to additional bending stresses.

Influence of gap widths at slotted steel plates on the mechanical properties of the connection

Numerical preliminary investigations were performed to quantify the influence of the gap width between slotted steel plates and adjacent timber members on the mechanical behaviour of the connection. A single dowel with a diameter d=12 mm was analysed using a *Beam on Foundation* model (see Fig. 10). The numerical model was developed in Ansys Workbench following the approach outlined by Hochreiner and Schweigler [12,13].

The connection considered was a double-shear type featuring an internally positioned steel plate with a thickness of t=10 mm. The gap between the steel plate and the timber side member, herein referred to as the clearance, was systematically varied. The timber member width was set to t=90 mm to promote a failure mechanism characterised by the formation of two plastic hinges, following the European Yield Model (EYM).

Fig. 10 shows the investigated connection's geometry and corresponding numerical model. The steel cross-section was assigned a multilinear isotropic material model calibrated from tensile tests of S355 steel dowels. Contact springs between the steel plate and the dowel were modelled as linear-elastic springs with a bedding modulus of 2500 N/mm^3. The springs representing the interaction between the timber members and dowels were assigned bilinear load-displacement behaviour based on parameters reported by Schweigler. Frictional effects between timber and dowel were neglected.

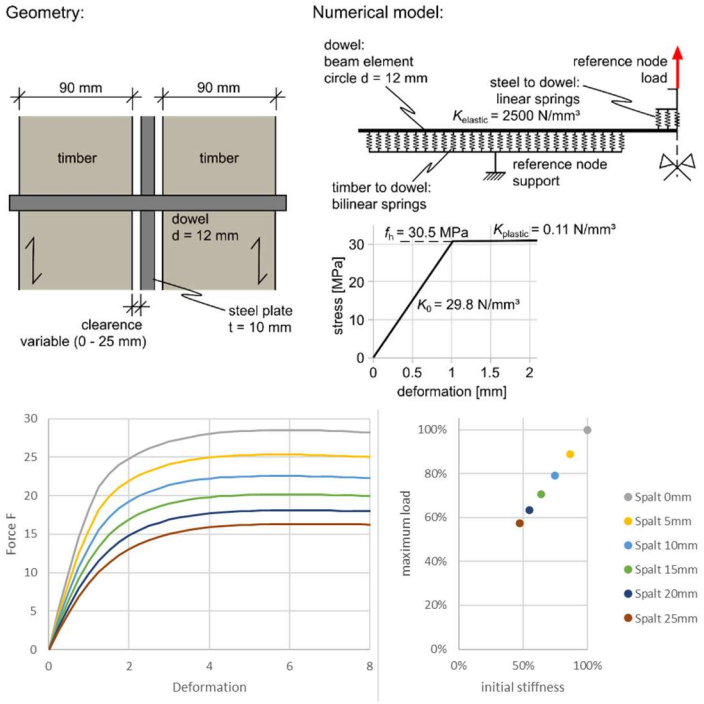

Figure 10. Numerical model setup of the knife plate connection with a single dowel embedded in timber with increasing gaps, load-deformation graphs (left) and slip modules (right)

6 REFERENCES

1. Kirker, G. T.; Brischke, C.; Passarini, L.; Zelinka, S. L. (2020): *Salt damage in wood: controlled laboratory exposures and mechanical property measurements*; Wood and Fiber Science, 52(1), 2020, pp. 44-52, Society of Wood Science and Technology
2. Stadlmann, A.; Pramreiter, M.; Stingl, R.; Kurzböck, C.; Jost, T.; Müller, U. (2020): *Durability of Wood Exposed to Alternating Climate Test and Natural Weathering*. Forests, 11 (9), article 953, MDPI, https://doi.org/10.3390/f11090953
3. Zelinka, S. L.; Kirker, G. T. (2018): *Assessment of fastener corrosion and salt damage in the bilge of the Eureka*. Forest Products Laboratory Research Note FPL-RN-0356. U.S. Department of Agriculture, Forest Service, Forest Products Laboratory, https://doi.org/10.2737/FPL-RN-356
4. Krzysik, M.; Jastrzębski, R.; Sadowska, D.; Krystofiak, T.; Szczerba, K. (2023): *Effect of Seawater with Average Salinity on the Moisture Content, Ash Content and Tensile Strength of Some Coniferous Wood*. Forests, 14 (5), article 1011. MDPI, https://doi.org/10.3390/f14051011.
5. EN 1990 (2013): *Eurocode – Basis of structural design*
6. EN 1995-2 (2023): *Eurocode – Design of timber structures – Part 3: Execution*
7. EN 13183-2 (2002): *Moisture content of a piece of sawn timber - Part 2: Estimation by electrical resistance method*
8. Hofer , R. (2022): *Brücke über Lech droht Einsturz*, survey date: 2024/04/24, https://tirol.orf.at/stories
9. Gotsch, K.; Brückenbilder Lechtal, survey date 20.04.2024, in https://www.karl-gotsch.de
10. GeoSphere Austria – Bundesanstalt für Geologie, Geophysik, Klimatologie und Meteorologie, survey date: 2022, Vienna (GeoNames ID 2761369), Austria, https://data.hub.geosphere.at/
11. Scanntronik Mugrauer GmbH, Material Moisture Gigamodul, https://www.scanntronik.
12. Hochreiner, G. et al. (2013): Stiftförmige Verbindungsmittel im EC5 und baustatische Modellbildung mittels kommerzieller Statiksoftware. In: Bauingenieur, 88, pp. 275 – 289
13. Schweigler, M. (2018): Nonlinear modelling of reinforced dowel joints in timber structures – a combined experimental-numerical study. Dissertation, Vienna University of Technology.

ICTB 2025. 5th International Conference Timber Bridges
Rotorua, New Zealand, 29 June to 2 July 2025.

FEASIBILITY OF NEW ZEALAND CROSS-LAMINATED TIMBER PANEL FOR BRIDGES APPLICATION: PRELIMINARY EXPERIMENTAL, NUMERICAL AND ANALYTICAL STUDY

Reza Masoudnia[1]

ABSTRACT

The application of Cross Laminated Timber (CLT) in both structural and non-structural elements of bridges has increased globally in recent years. The CLT panel comprises several layers of timber boards, which are stacked crosswise at 90 degrees and glued together on the wider face of the timber boards. Although the CLT panel, as a high-performance, massive engineered wood product (EWP) , has played a significant role in the current progress of timber mass construction in New Zealand, there is not even one notable CLT bridge project. Therefore, this paper investigates the feasibility of using CLT panels, made from New Zealand materials, in bridge applications. This research examines the structural performance of CLT panels experimentally, numerically, and analytically. Experimental results for a five-layer CLT panel with 210 mm thickness, 600 mm width, and 5040 mm length demonstrate that the panels are sufficiently strong to carry structural loads for a wide range of structural applications. A numerical parametric study, based on an experimentally verified ABAQUS model, confirmed that a bare CLT panel and CLT composite double T-beam fabricated from New Zealand Radiata Pine are structurally ideal for short- and intermediate-span bridge applications. The parametric study on CLT composite double T-beams discloses that the effective flange width increases as the ratio of the transverse layer depth to the longitudinal layer depth of the CLT flange rises. Additionally, using a CLT flange with a higher modulus of elasticity slightly improves the effective flange width. This study also revealed that the CLT panel has great potential for factory prefabrication in a controlled environment, to make site assembly significantly faster. Additionally, an optimization study indicated that a majority of the non-structural bridge elements could be supplied from waste CLT material. This prefabrication potential could also enhance the speed and safety of bridge repair or replacement processes. Ultimately, the CLT bridge is an excellent, environmentally friendly alternative to concrete bridges, with a lower environmental impact on the surrounding environment during construction.

Keywords: CLT, EWP, double T-beams, EFW, short- and intermediate-span bridge

1 INTRODUCTION

Cross Laminated Timber (CLT) panels have the potential for use in various structural applications, including timber bridges. Although CLT is a relatively new material for bridge structures, it has gained widespread popularity in residential and commercial building construction [1–6].

CLT is a high-performance, massive engineered wood product typically made from low-grade softwood species such as Radiata Pine, which are glued together in a cross-layered fashion. It typically features a symmetric layup with a standard thickness ranging from 126 mm to 420 mm and consists of three to eleven

[1] CPEng, PhD in Timber Structural Engineering, Senior Timber Structural Engineer at Red Stag, Honorary Lecturer at the University of Waikato,
e-mail: reza.masoudniaa@gmail.com, rmas551@aucklanduni.ac.nz, reza.masoudnia@redstag.co.nz,

layers (refer to Figure 1) [1–6]. New Zealand produces a large volume of timber per year, of which Radiata Pine is the primary plantation species; around 90 percent of production forests are Radiata Pine. The popularity of the species is largely due to its short harvest time (25–30 years) and high timber yields. A good site can achieve high-quality timber at 30 m³/ha/year, or up to 50 m³/ha/year [5,11]. The benefits of CLT panels, such as design flexibility, fast installation, and excellent seismic performance, have led to their widespread application in various types of structures, including buildings and bridges. Additionally, a cost-effectiveness estimation study in the USA has shown that CLT structures are practically cost-competitive compared to concrete, masonry, and steel materials [7–9].

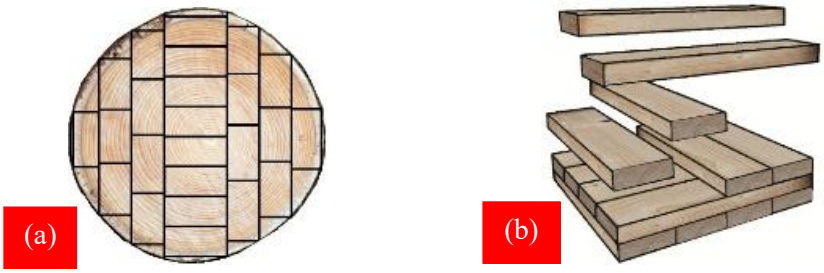

Figure 1. CLT production process; (a) Sawing log, (b) Arranging boards and final CLT product.

Despite the large number of studies regarding concrete-steel composite bridges, comprehensive comparative research has not been conducted on timber, specifically CLT bridges. Therefore, the objective of this study is to verify the applicability of using CLT panels made from locally grown New Zealand Radiata Pine for bridge structures. Figure 2 illustrates a couple of examples of CLT panel usage in bridge applications. The CLT panels were analyzed and found to be capable of withstanding a load of 707 kg/m², which is sufficient for bridges intended for pedestrian or bicycle traffic and robust enough to support the weight of a passing vehicle. Figure 3 presents the loading configurations on CLT bridges.

Figure 2. CLT panel application for short-span bridges.

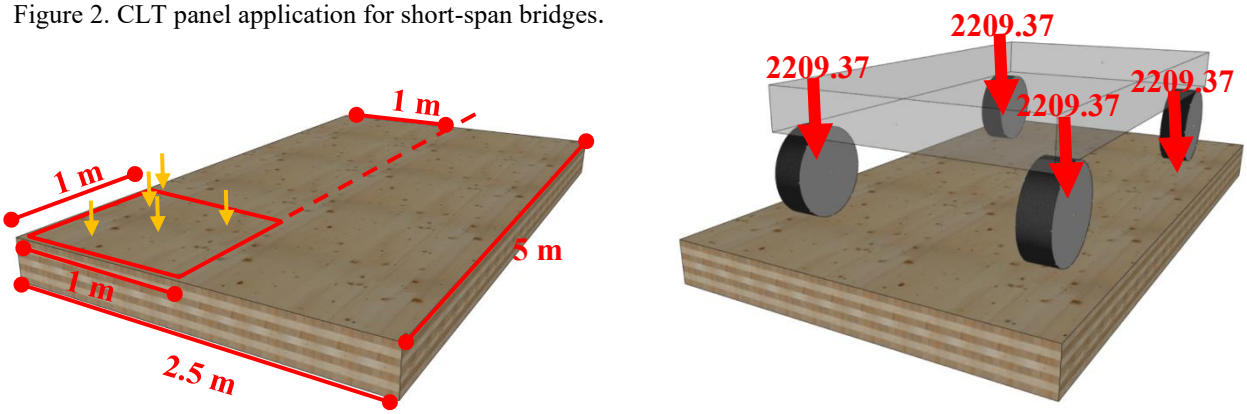

Figure 3. Uniformly loaded CLT bridge and equivalent loading for vehicle load configuration.

Additionally, the lighter weight of CLT bridges and the advantages of factory prefabrication can significantly enhance efficiency. In contrast to concrete-steel composite bridges, CLT serves as a renewable

alternative that sequesters carbon throughout its life cycle. The CLT bridge is lighter, stronger, and more environmentally sustainable than concrete-steel composite bridges, thereby reducing transportation time and increasing construction speed (refer to Figure 4). Moreover, it is possible to supply the majority of the non-structural elements of the CLT bridge using leftover CLT material through optimized prefabrication in the controlled environment of a CLT factory.

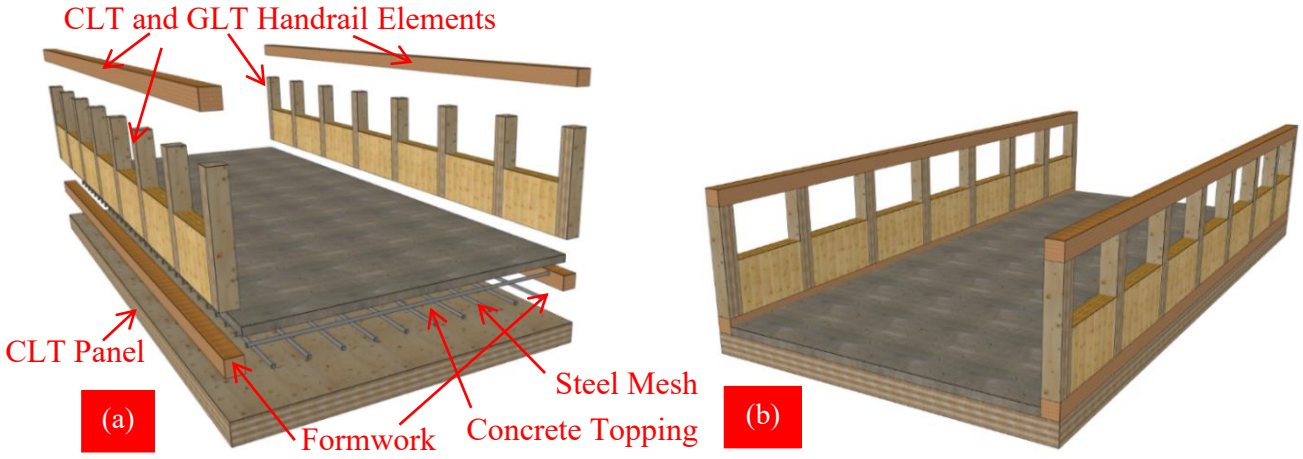

Figure 4. Prefabricated CLT bridge; a) before assembly, b) after assembly.

Current research on CLT panels indicates that CLT emits 75% less carbon dioxide—the primary greenhouse gas responsible for anthropogenic climate change—compared to reinforced concrete under various conditions. In contrast, timber-concrete composites emit 65% less CO_2, and their environmental impact decreases as the span increases [7].

The lightweight nature and prefabrication potential of the CLT bridge can make the process of repairing or replacing the bridge much faster and safer. As shown in Figure 5, the bridge can remain semi-operational during the repair or replacement construction process. The damaged part of the CLT bridge can be quickly replaced by a new prefabricated part. Even the concrete topping and handrails can be cast and pre-assembled before replacement, which makes reopening the bridge much faster and allows it to become fully operational more quickly. An upside-down wide spline joint could make the reassembly process significantly easier, faster, and safer without disturbing traffic flow.

Large-scale fire testing of CLT panels on existing products in the New Zealand market demonstrates that these panels are reliable for application in vehicle bridges. The CLT panels will remain structurally stable for more than 60 minutes under structural loads during a fire event at 900 degrees Celsius (refer to Figure 6). All existing fire test results are based on the test setups for CLT building applications and the fire event occurs on the underside of the CLT panel [10]. Although no fire test results are available for CLT panels with a fire event on the top surface to simulate fire resistance of the panel for bridge application, it is expected that the CLT panel will perform notably better when the fire is on the top surface, due to a notably lower charring rate. This major difference in the charring rate of CLT panels is highlighted in Figure 6, which presents a seven-layer CLT panel as an example.

2 EXPERIMINTAL TETST SET-UP

A real-scale four-point bending test has been conducted on a single five-layer CLT panel with a width of 2000 mm, a thickness of 200 mm, and a length of 6000 mm using a Material Testing Systems (MTS) actuator testing machine to verify the structural performance of the panel (refer to Figure 7) [15]. The data acquisition system has the ability to record load data from the MTS, and three LVDTs were located on top of each of the two end supports and under the mid-span of the CLT panel at the same time, as shown in Figure 8.

The same test set-up has been used for testing CLT composite beam. The CLT panel is attached as top flange to the top of a LVL girder. The external top, bottom, and middle layers of the CLT panel were oriented in the longitudinal direction of the LVL beam assembly which was 302 mm wide, 610 mm deep and 7 meter long (refer to Figure 9).

The CLT slab was predrilled, and the two parts were mechanically fastened using 550-mm screws with a diameter of 11 mm. A total of 48 screws were used in the test to provide composite action between CLT slab and LVL beam. The screws penetrated the 200-mm CLT slab and entered the supporting LVL beam at a 45° angle to a depth of approximately 276 mm.

Figure 6. Red Stag CLT fire test.

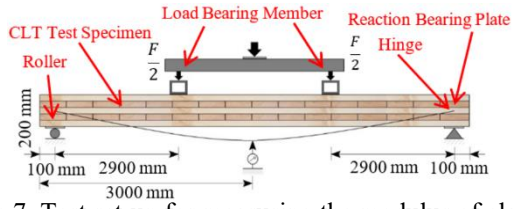

Figure 7. Test set-up for measuring the modulus of elasticity [15].

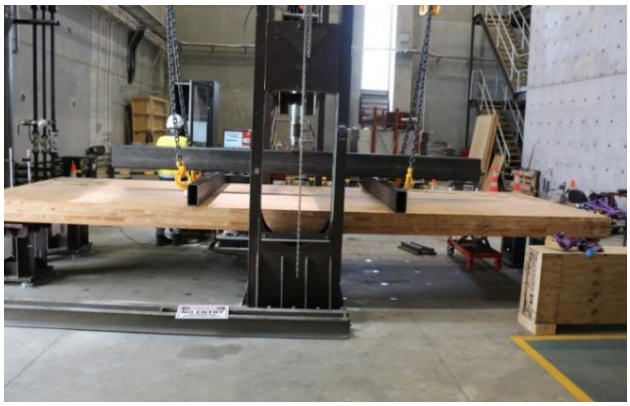

Figure 8. 500 kN MTS testing machine configured for four-point bending test [15].

3 NUMERICAL ANALYSIS

The finite element package ABAQUS version 6.13-3 was chosen for the analysis and simulation of a simply supported CLT panel in bending. The detailed numerical modelling and convergence study confirmed the accuracy of the developed numerical model (refer to Figures 10 and 11). An eight-node element (C3D8R), which is a linear three-dimensional solid element, was used for the analysis of the CLT panel [12-15]. The CLT properties specified in this study are for timber boards made from Radiata Pine trees grown commercially in New Zealand (refer to table 1). The coordinate system used is based on the principal axes of the wood, as shown in Figure 12.

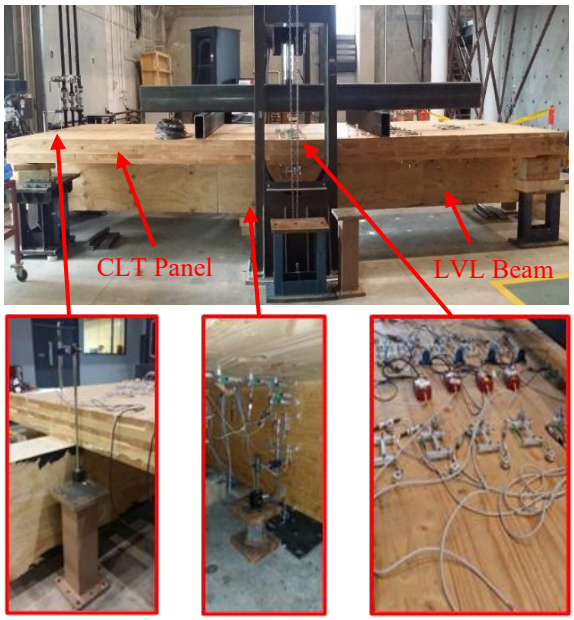

Figure 9. Experimental test set-up. (a) LVDT, (d) MTS Machine, (e) Roller Support, (f) Hinge Support, (g) Load Bearing Plate, and (h) Data Acquisition System [15].

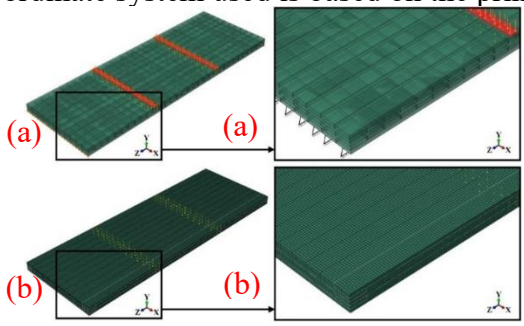

Figure 10. Typical boundary conditions and finite element mesh used in this study. (a) FE model boundary conditions (Load and support), (b) Finite element mesh.

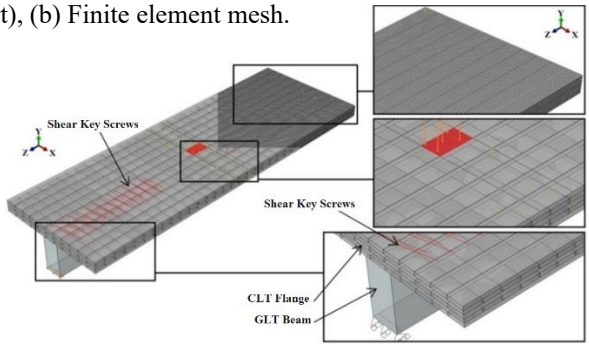

Figure 11. General arrangement of the numerical model to show boundary conditions and mesh.

Table 1. Material Properties of the CLT's boards [12-15].

Component	E_L	E_R	E_T	ν_{LT}	ν_{TL}	ν_{LR}	ν_{RL}	ν_{TR}	ν_{RT}
MSG 8 boards	8000	363	363	0.2	0.018	0.15	0.018	0.21	0.18
MSG 6 boards	6000	272	272	0.15	0.013	0.11	0.013	0.09	0.13

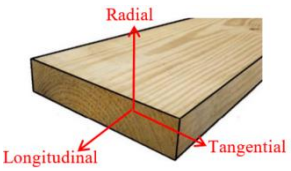

Figure 12. Principal axes of wood

3.1 Convergence study

Convergence studies were carried out on the 6-meter CLT panel to find a suitable finite element mesh to increase the accuracy of the analysis. Figures 13 and 14 illustrate the mid- span deflection of the CLT panel that is plotted against the corresponding number of elements for ten different mesh sizes [15].

Table 2. Comparison of the mid-span deflection results.

Specimen	CLT's Lamella $W^1 \times T^2 \times L^3$ (mm)	Deflection Experimental	Deflection Numeical
CLT Panel	2030×200×6000	18 mm*	17.9 mm*

W=Width, T=Thickness, L=Length of the CLT panel
* Deflections under 50 kN four points loading test.

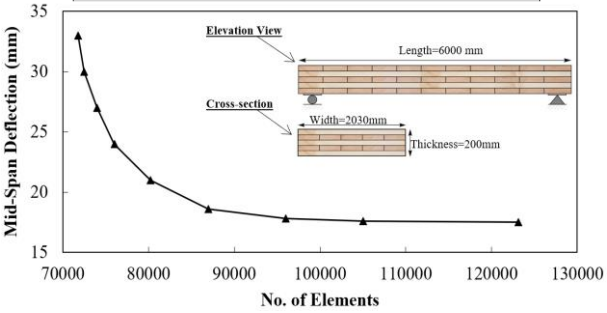

Figure 13. Convergence study numerical results.

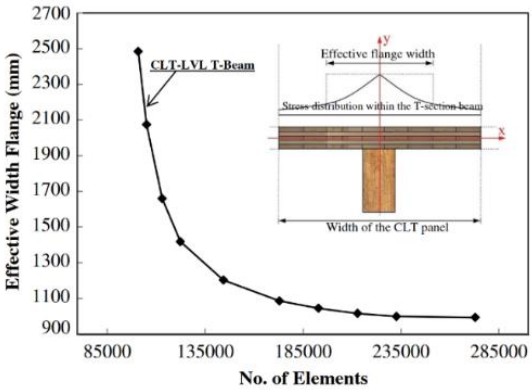

Figure 14. Convergence study result of EWF of CLT composite beam versus number of mesh elements.

4 PARAMETRIC STUDY AND DISCSSION OF RESULTS

The experimentally verified numerical model has been used to study the capability of various panel thicknesses for bridge applications (refer to Table 1). The mid-span deflection measurements show that the model is sufficiently accurate to predict the behaviour of the CLT panel.

Numerical analysis and analytical calculations have confirmed the structural capability of the CLT panels made from commercially grown New Zealand Radiata Pine trees for bridge applications. Specifications, shear, and moment capacity of various cross-section sizes of the CLT panel for bridge application are summarised in Table 3 to Table 4 [16-17].

The construction industry (including buildings and other types of structures) is a large contributor to greenhouse gas emissions and a massive consumer of natural resources. Therefore, even small improvements in construction technologies are important to reduce greenhouse gas emissions and thereby attain national goals to mitigate climate change. Table 5 presents long-term locked-up carbon for six CLT bridge configurations and their serviceability performance under 707 kg/m^2 [20]. The comparison between numerical and analytical calculations shows that the analytical calcination results are by 10% over design and conservative (refer to table 6).

Table 3. Specifications of the CLT panels specimen.

Specimen Number	CLT's Lamella $W^1 \times T^2 \times L^3$	CLT's Lamella E_{longi} E_{trans}
1	1000 mm×210 mm×4000 mm	8 GPa 6 GPa
2	1000 mm ×210 mm×4000 mm	8 GPa 8 GPa
3	1000 mm×228 mm×5000 mm	8 GPa 6 GPa
4	1000 mm×228 mm×5000 mm	8 GPa 8 GPa
5	1000 mm×228 mm×5500 mm	8 GPa 6 GPa
6	1000 mm×228 mm×6000 mm	8 GPa 8 GPa

W=Width, T=Thickness, L=Length of the CLT panel
E_{longi}=MoE of longitudinal layers, E_{trans}=MoE of transverse layers

Table 4. The capacity of the CLT Panels.

Specimen Number	CLT's Panel Weight	Vn (kN)	Mn (kNm)
1	420 kg	55.42	421.3
2	420 kg	55.42	421.3
3	570 kg	141.21	69.47
4	570 kg	141.21	69.47
5	808 kg	188,73	97.56
6	882 kg	188.73	97.56

Factors: Ø=0.85, k_1=0.8, k_4=1, k_6=1, k_9=1, k_{12}=1 Refer to NZSAS 1720.
Load Case: 1.2 Dead Load + 1.5 Live Load.

Table 5. The serviceability performance and estimated carbon dioxide of the CLT Panels.

Specimen Number	Mid-span Deflection	Estimated Carbon	Sequestered Carbon Dioxide
1	9.9 mm	168 tons	727 tons
2	9.4 mm	168 tons	727 tons
3	16.2 mm	228 tons	1048 tons
4	15.8 mm	228 tons	1048 tons
5	14.8 mm	323 tons	1487 tons
6	5.7 mm	352 tons	1622 tons

Mid-Span Deflection: Long-Term Deflection: $(G+\Psi_1 Q)\times j2+(\Psi_s+\Psi_1)Q$.

Table 6. Mid-span deflection result based on experimentally verified numerical analysis.

Specimen Number	CLT's Lamella $W^1\times T^2\times L^3$ (mm)	CLT's Lamella $E_{longitudinal}$ $E_{transverse}$	Deflection Numeical
1	1000×210×4000	8 GPa 6 GPa	8.9 mm*
2	1000×210×4000	8 GPa 8 GPa	8.9 mm*
3	1000×228×5000	8 GPa 6 GPa	15.6 mm*
4	1000×228×5000	8 GPa 8 GPa	14.3 mm*
5	1000×228×5500	8 GPa 6 GPa	13.3 mm*
6	1000×228×6000	8 GPa 8 GPa	5.1 mm*

W=Width, T=Thickness, L=Length of the CLT panel
$E_{longitudinal}$=MoE of longitudinal layers, $E_{transverse}$=MoE of transverse layers
* Deflections under 50 kN four points loading test.

5 NUMERICAL PARAMETRIC OF CLT COMPOSITE BEAMS

The main focus of study is investigation of various CLT panel configurations on the EFW of single and double CLT composite T-beams.

5.1 Eeffect of CLT panel layer configuration

Two groups of single and double CLT composite beams with various CLT layers configurations were analysed to investigate the effect of layer thickness on the EFW. As seen from table 7 and Figure 13 (Specimens 2 to 1), an increase in the transverse layer thickness enhances the EFW. Again, numerical analysis result shows that similar increase in the transverse layer thickness over longitudinal layer enhances the EFW in double CLT composite beams (refer to table 8, Specimens 14 vs 13 and 12).

In the first series of analysis of CLT composite single T-beams, when 20 mm transverse boards in 166 thick CLT panel are replaced by 40-mm-thick boards, and the 20 mm thick, EFW increased 210 mm (Configuration 2 and 1 in Table 3). Moreover, when the 40-mm longitudinal layers and 20-mm transverse layers in Configurations 3 were replaced by boards with a thickness of 40 mm and 20 mm (Configurations 1 in table 7), the EFW increased more than 4 times. The similar change in CLT composite double T-beam increasing the CLT slab effective width noticeably more than 4.7 times (Configuration 14 and 15 in table 8). Therefore, the space between two LVL girders in the CLT composite double T-beam could be increased by 1500 mm based on the predicted EFW of the CLT composite double T-beam.

5.2 Effect of CLT material properties

The effect of the elastic modulus of the CLT panels on the EFW are provided in Figure 15, 16, Table 7 and 8. In general, increasing the modulus of elasticity of the CLT panels increased the EFW of Single and double CLT composite T-beams. For example, as shown in Figure 15, when the modulus of elasticity of the CLT panel increased from 6 GPa (Configuration 5 in Table 7) to 8 GPa (Configuration 1 in Table 7), the EFW increased from 760 to 790 mm, thus increasing by 5 and 30%, respectively.

In addition, the comparison indicates when the 6 GPa transverse boards in 210 mm thick CLT panels in single and double CLT composite beams replaced with 8-GPa boards, EFW enhances 85 mm and 180 mm respectively. The numerical parametric analysis showed that higher ratio of longitudinal thickness over transverse layer has higher improvement effect on EFW compared to higher ratio of longitudinal MoE over transverse layer MoE.

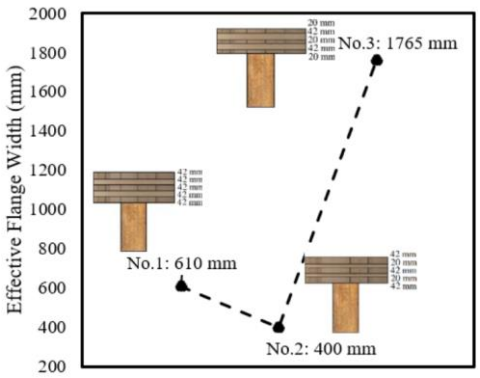

Figure 13. Effect of the layer's configuration change on the effective flange width for Configurations 1, 2, 3.

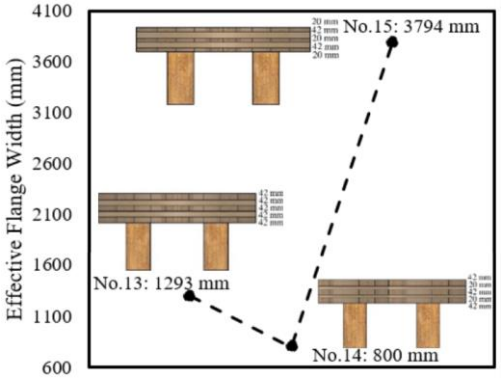

Figure 14. Effect of the layer's configuration change on the effective flange width for Configurations 13, 14, 15.

It is really important to note all these numerical analyses are only practicing the EFW of single or double CLT composite beams and the CLT slab required further deign and investigation based on structural application. For instance, the 3-layer central layers of 5-layer CLT panel in CLT composite double T-beam should be design as simply supported CLT panel to ensure the system can perform structurally safe for bridge application (Figure 17 & 18). The Figure 18 and Table 8 shows that how high loads due to heavy vehicle weights on CLT panel between side-by-side girders lead to reduction girders spacing in CLT composite double T-beams.

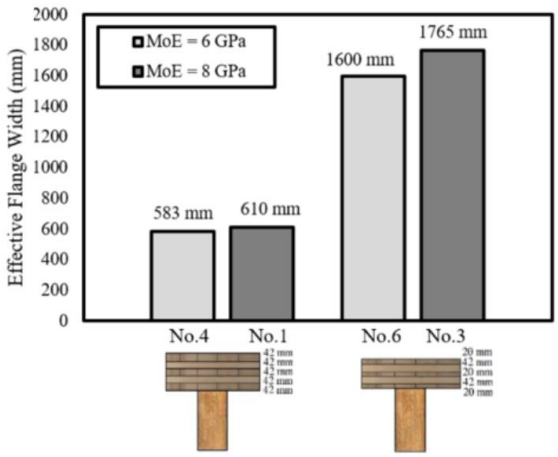

Figure 15. Effect of CLT material properties on effective flange width of CLT composite single T-beams.

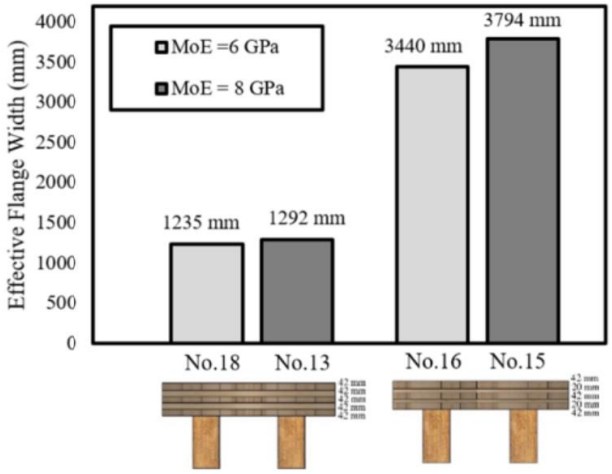

Figure 16. Effect of CLT material properties on effective flange width of CLT composite double T-beams.

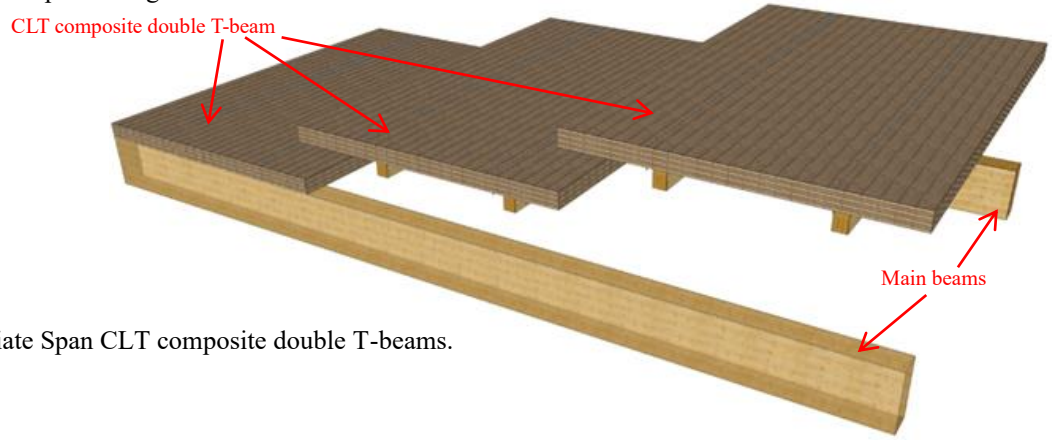

Figure 17. Intermediate Span CLT composite double T-beams.

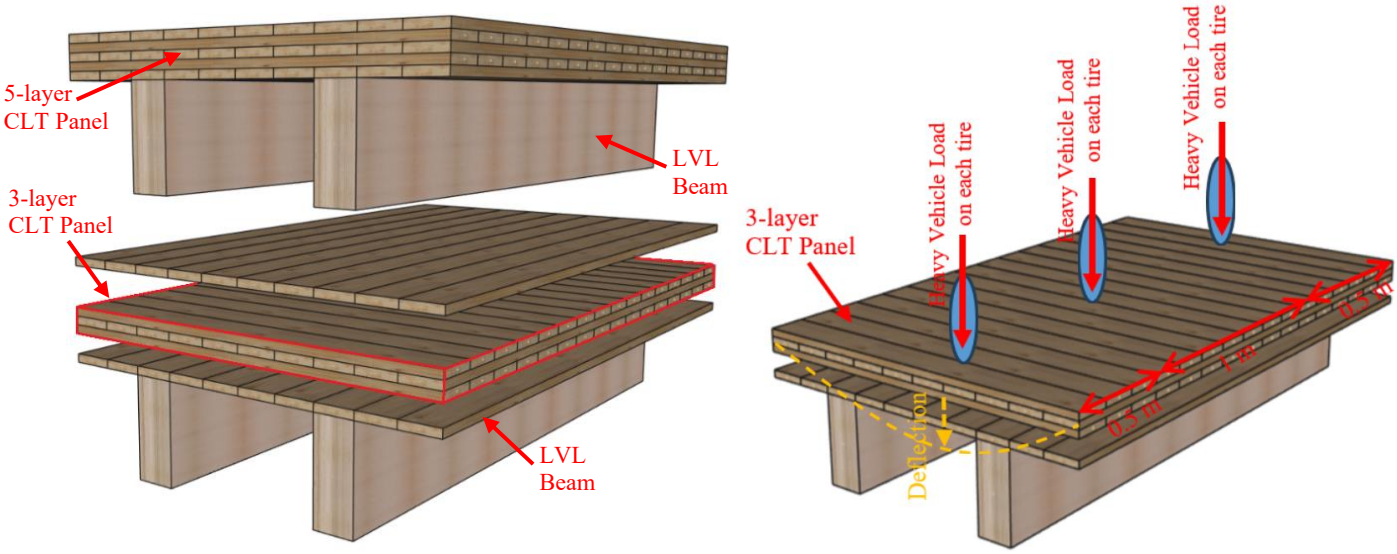

Figure 18. CLT composite double T-beam structural design concept for bridge application.

Table 7. CLT composite T-beam specifications and EFW result.

Specimen Number	CLT		LVL		Predicted effective width flange (mm)
	W×T×L (mm)	MoE of Layers (GPa)	W×T×L (mm)	MoE (GPa)	
1	2000×210×6000 2000×(42+42+42+42+42)[a]×6000	8,8,8,8,8 [b]	350×600×6000	11	610
2	2000×166×6000 2000×(42+20+42+20+42)[a]×6000	8,8,8,8,8 [b]	350×600×6000	11	400
3	2000×166×6000 2000×(20+42+20+42+20)[a]×6000	8,8,8,8,8 [b]	350×600×6000	11	1765
4	2000×210×6000 2000×(42+42+42+42+42)[a]×6000	6,6,6,6,6 [b]	350×600×6000	11	583
5	2000×166×6000 2000×(42+20+42+20+42)[a]×6000	6,6,6,6,6 [b]	350×600×6000	11	380
6	2000×166×6000 2000×(20+42+20+42+20)[a]×6000	6,6,6,6,6 [b]	350×600×6000	11	1600
7	2000×210×6000 2000×(42+42+42+42+42)[a]×6000	8,6,8,6,8 [b]	350×600×6000	11	570
8	2000×166×6000 2000×(42+20+42+20+42)[a]×6000	8,6,8,6,8 [b]	350×600×6000	11	365
9	2000×166×6000 2000×(20+42+20+42+20)[a]×6000	8,6,8,6,8 [b]	350×600×6000	11	1660
10	2000×210×6000 2000×(42+42+42+42+42)[a]×6000	6,8,6,8,6 [b]	350×600×6000	11	623
11	2000×166×6000 2000×(42+20+42+20+42)[a]×6000	6,8,6,8,6 [b]	350×600×6000	11	407
12	2000×166×6000 2000×(20+42+20+42+20)[a]×6000	6,8,6,8,6 [b]	350×600×6000	11	1810

Note: MoE = modulus of elasticity (units of GPa).
[a] Numbers in parentheses are the thickness of individual CLT layers (units of mm).
[b] The five numbers are the modulus of elasticity of each layer (units of GPa).
W: Width, T: Thickness, L: Length (units of mm).

Table 8. CLT composite double T-beam specifications and EFW result.

Specimen Number	CLT		LVL		Predicted EFW (mm)	Practical EFW for Bridge Application
	W×T×L (mm)	MoE of Layers (GPa)	W×T×L (mm)	MoE (GPa)		
13	4000×210×6000 4000×(42+42+42+42+42)[a]×6000	8,8,8,8,8 [b]	Two 350×600×6000	11	1293	798 mm
14	4000×166×6000 4000×(42+20+42+20+42)[a]×6000	8,8,8,8,8 [b]	Two 350×600×6000	11	800	Not Applicable
15	4000×166×6000 4000×(20+42+20+42+20)[a]×6000	8,8,8,8,8 [b]	Two 350×600×6000	11	3794	683 mm
16	4000×210×6000 4000×(42+42+42+42+42)[a]×6000	6,6,6,6,6 [b]	Two 350×600×6000	11	1235	700 mm
17	4000×166×6000 4000×(42+20+42+20+42)[a]×6000	6,6,6,6,6 [b]	Two 350×600×6000	11	760	Not Applicable
18	4000×166×6000 4000×(20+42+20+42+20)[a]×6000	6,6,6,6,6 [b]	Two 350×600×6000	11	3440	632 mm
19	4000×210×6000 4000×(42+42+42+42+42)[a]×6000	8,6,8,6,8 [b]	Two 350×600×6000	11	1208	704 mm
20	4000×166×6000 4000×(42+20+42+20+42)[a]×6000	8,6,8,6,8 [b]	Two 350×600×6000	11	730	Not Applicable
21	4000×166×6000 4000×(20+42+20+42+20)[a]×6000	8,6,8,6,8 [b]	Two 350×600×6000	11	3569	697 mm
22	4000×210×6000 4000×(42+42+42+42+42)[a]×6000	6,8,6,8,6 [b]	Two 350×600×6000	11	1410	797 mm
23	4000×166×6000 4000×(42+20+42+20+42)[a]×6000	6,8,6,8,6 [b]	Two 350×600×6000	11	814	Not Applicable
24	4000×166×6000 4000×(20+42+20+42+20)[a]×6000	6,8,6,8,6 [b]	Two 350×600×6000	11	3891	699 mm

Note: MoE = modulus of elasticity (units of GPa).
[a] Numbers in parentheses are the thickness of individual CLT layers (units of mm).
[b] The five numbers are the modulus of elasticity of each layer (units of GPa).
W: Width, T: Thickness, L: Length (units of mm).

6 CONCLUSIONS

An accurate numerical model has been developed, which has been experimentally verified. The numerical parametric study and analytical calculations show that the bare CLT panel and CLT composite double T-beams are sufficiently strong to carry structural loads for various bridge applications. This study demonstrates that the high strength-to-weight ratio of CLT panels provides a lightweight, sturdy bridging solution for short-span bridges. In addition to their exceptional strength, CLT panels, as a mass timber material, also exhibit high dimensional stability. This ensures that bridges constructed from seven layers or thicker CLT panels, comprised of treated timber boards and protected with a waterproof membrane and concrete topping, can resist distortion even in extreme weather conditions, further improving their service life.

ACKNOWLEDGEMENT

The author thanks graphic designer Nariman Valizadeh and Navid Masoudnia for providing excellent photos and figures. I would also like to thank Red Stag for financially sponsoring this research paper.

This technical paper has been developed to demonstrate the significant structural potential of CLT panels and CLT composite double T-beams constructed from Red Stag CLT panels for bridge applications. Please note that it is the responsibility of the bridge engineer or designer to ensure that the presented results are appropriate for their specific project and not to rely solely on the numerical analyses.

REFERENCES

1. A. Fortune, P. Quenneville. Feasibility study of New Zealand radiata pine cross-laminated timber, New Zealand Timber Design Journal, 2011.
2. M. Mohammad, S. Gagnon. Introduction to Cross-Laminated Timber, Wood Design Focus, Volume 22, Number 2, pp. 13-21; 2012
3. B. Yeh, S. Gagnon, T. Williamson, C. Pirvu, C. Lum, D. Kretschmann, The North American Product Standard for Cross-Laminated Timber, Wood Design Focus, Volume 22, Number 2, pp. 13-21; 2012.
4. M. Jelec, D. Varevac, V. Rajcic, Cross-laminated timber (CLT) - A state of the art report, GRADEVINAR, 70 (2), 75-95.
5. R. Brandner, G. Flatscher, A. Ringhofer, G. Schickhofer, A. Thiel, Cross laminated timber (CLT): overview and development, Wood and Wood Products, Volume 74, pages 331–351, (2016).
6. K. Lewis, R. Shrestha, K.I. Crews, Introduction to cross-laminated timber and development of design procedures for Australia and New Zealand, 23rd Australasian Conference on the Mechanics of Structures and Materials (ACMSM23), 2014.
7. M. F. Laguarda Mallo, O, Espinoza, Cross-laminated timber vs. Concrete/steel: cost comparison using a case study, World Conference on Timber Engineering 2016, Vienna, Austria.
8. S. Ahmed, I. Arocho, Analysis of cost comparison and effects of change orders during construction: Study of a mass timber and a concrete building project, Volume 33, Journal of Building Engineering January 2021, 101856.
9. M. F. Laguarda Mallo, O, Espinoza, Outlook for Cross-Laminated Timber in the United States, bioresources 2014, 10.15376/biores.9.4.7427-7443.
10. Red Stag CLT Design Guide V1.5, September 2024.
11. P. Maclaren. Radiata Pine Growers Manual. New Zealand Forest Research Institute, Rotorua, New Zealand, 1993.
12. R. Masoudnia, A. Hashemi, and P. Quenneville. “Predicting the effective flange width of a CLT slab in timber composite beams.” In: Journal of Structural Engineering 144.7 (2018), pp. 04018084.
13. R. Masoudnia, A. Hashemi, and P. Quenneville. “Evaluation of effective flange width in timber composite beams.” In: New Zealand Timber Design Journal 26.2 (2018), pp. 14–24.
14. R. Masoudnia and S. Masoudnia. “Numerical investigation of effective flange width in CLT-GLT composite T-beams.” In: New Zealand Timber Design Journal 27.3 (2019), pp. 7–16.
15. R. Masoudnia. “State of the art of the effective flange width for composite T-beams.” In: Construction and Building Materials 244 (2020), Art. 118303.

ICTB 2025. 5th International Conference Timber Bridges
Rotorua, New Zealand, 29 June to 2 July 2025.

FEASIBILITY OF NEW ZEALAND CROSS-LAMINATED TIMBER PANEL FOR BRIDGES APPLICATION: PRELIMINARY EXPERIMENTAL, NUMERICAL AND ANALYTICAL STUDY

Reza Masoudnia[1]

ABSTRACT

The application of Cross Laminated Timber (CLT) in both structural and non-structural elements of bridges has increased globally in recent years. The CLT panel comprises several layers of timber boards, which are stacked crosswise at 90 degrees and glued together on the wider face of the timber boards. Although the CLT panel, as a high-performance, massive engineered wood product (EWP) , has played a significant role in the current progress of timber mass construction in New Zealand, there is not even one notable CLT bridge project. Therefore, this paper investigates the feasibility of using CLT panels, made from New Zealand materials, in bridge applications. This research examines the structural performance of CLT panels experimentally, numerically, and analytically. Experimental results for a five-layer CLT panel with 210 mm thickness, 600 mm width, and 5040 mm length demonstrate that the panels are sufficiently strong to carry structural loads for a wide range of structural applications. A numerical parametric study, based on an experimentally verified ABAQUS model, confirmed that a bare CLT panel and CLT composite double T-beam fabricated from New Zealand Radiata Pine are structurally ideal for short- and intermediate-span bridge applications. The parametric study on CLT composite double T-beams discloses that the effective flange width increases as the ratio of the transverse layer depth to the longitudinal layer depth of the CLT flange rises. Additionally, using a CLT flange with a higher modulus of elasticity slightly improves the effective flange width. This study also revealed that the CLT panel has great potential for factory prefabrication in a controlled environment, to make site assembly significantly faster. Additionally, an optimization study indicated that a majority of the non-structural bridge elements could be supplied from waste CLT material. This prefabrication potential could also enhance the speed and safety of bridge repair or replacement processes. Ultimately, the CLT bridge is an excellent, environmentally friendly alternative to concrete bridges, with a lower environmental impact on the surrounding environment during construction.

Keywords: CLT, EWP, double T-beams, EFW, short- and intermediate-span bridge

1 INTRODUCTION

Cross Laminated Timber (CLT) panels have the potential for use in various structural applications, including timber bridges. Although CLT is a relatively new material for bridge structures, it has gained widespread popularity in residential and commercial building construction [1–6].

CLT is a high-performance, massive engineered wood product typically made from low-grade softwood species such as Radiata Pine, which are glued together in a cross-

[1] PhD in Timber Structural Engineering, Senior Timber Structural Engineer at Red Stag, Honorary Lecturer at the University of Waikato
e-mail: reza.masoudniaa@gmail.com, rmas551@aucklanduni.ac.nz ,and reza.masoudnia@redstag.co.nz

layered fashion. It typically features a symmetric layup with a standard thickness ranging from 126 mm to 420 mm and consists of three to eleven layers (refer to Figure 1) [1–6]. New Zealand produces a large volume of timber per year, of which Radiata Pine is the primary plantation species; around 90 percent of production forests are Radiata Pine. The popularity of the species is largely due to its short harvest time (25–30 years) and high timber yields. A good site can achieve high-quality timber at 30 m³/ha/year, or up to 50 m³/ha/year [5,11]. The benefits of CLT panels, such as design flexibility, fast installation, and excellent seismic performance, have led to their widespread application in various types of structures, including buildings and bridges. Additionally, a cost-effectiveness estimation study in the USA has shown that CLT structures are practically cost-competitive compared to concrete, masonry, and steel materials [7–9].

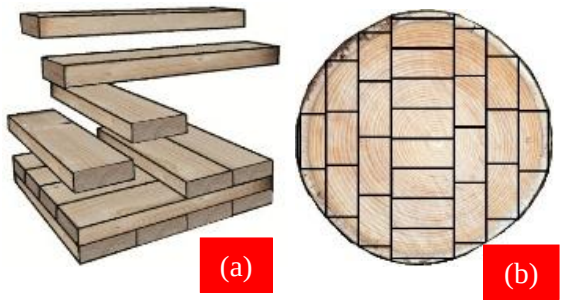

Figure 1. CLT production process; (a) Sawing log, (b) Arranging boards and final CLT product.

Despite the large number of studies regarding concrete-steel composite bridges, comprehensive comparative research has not been conducted on timber, specifically CLT bridges. Therefore, the objective of this study is to verify the applicability of using CLT panels made from locally grown New Zealand Radiata Pine for bridge structures. Figure 2 illustrates a couple of examples of CLT panel usage in bridge applications. The CLT panels were analyzed and found to be capable of withstanding a load of 707 kg/m², which is sufficient for bridges intended for pedestrian or bicycle traffic and robust enough to support the weight of a passing vehicle. Figure 3 presents the loading configurations on CLT bridges.

Figure 2. CLT panel application for short-span bridges.

Additionally, the lighter weight of CLT bridges and the advantages of factory prefabrication can significantly enhance efficiency. In contrast to concrete-steel composite bridges, CLT serves as a renewable alternative that sequesters carbon throughout its life cycle. The CLT bridge is lighter, stronger, and more environmentally sustainable than concrete-steel composite bridges, thereby reducing transportation time and increasing construction speed (refer to Figure 4). Moreover, it is possible to supply the majority of the non-structural elements of the CLT bridge using leftover CLT material through optimized prefabrication in the controlled environment of a CLT factory.

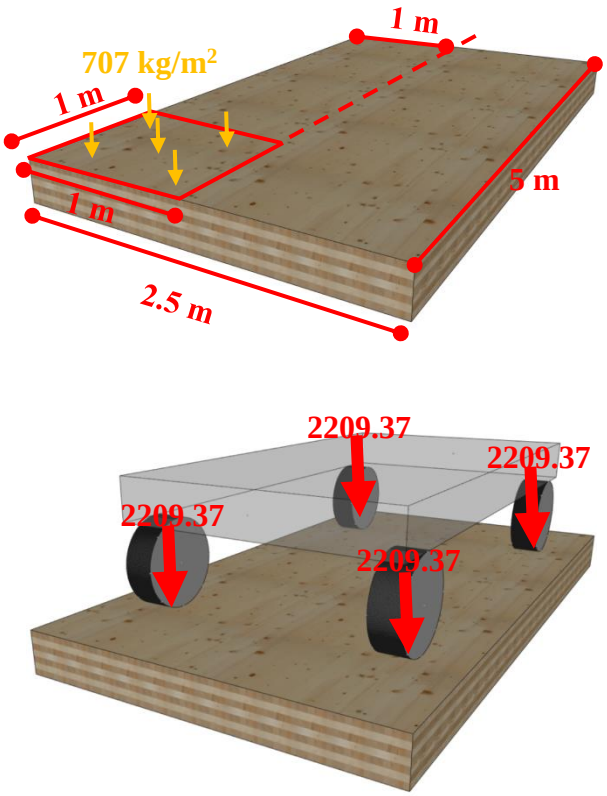

Figure 3. Uniformly loaded CLT bridge and equivalent loading for vehicle load configuration.

Current research on CLT panels indicates that CLT emits 75% less carbon dioxide—the primary greenhouse gas responsible for anthropogenic climate change—compared to reinforced concrete under various conditions. In contrast, timber-concrete composites emit 65% less CO_2, and their environmental impact decreases as the span increases [7].

The lightweight nature and prefabrication potential of the CLT bridge can make the process of repairing or replacing the bridge much faster and safer. As shown in Figure 5, the bridge can remain semi-operational during the repair or replacement construction process. The damaged part of the CLT bridge can be quickly replaced by a new prefabricated part. Even the concrete topping and handrails can be cast and pre-assembled before replacement, which makes reopening the bridge much faster and allows it to become fully operational more quickly. An upside-down wide spline joint could make the reassembly process significantly easier, faster, and safer without disturbing traffic flow.

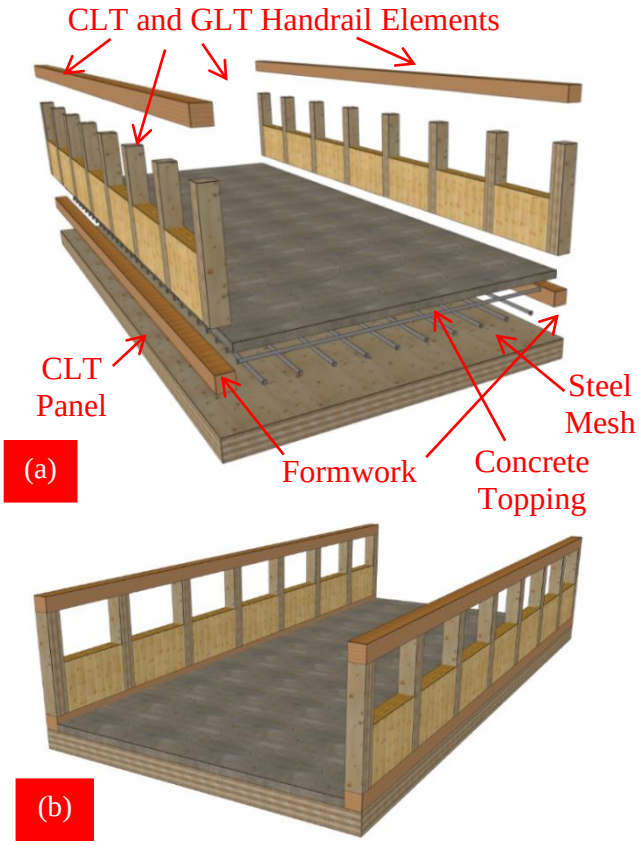

Figure 4. Prefabricated CLT bridge; a) before assembly, b) after assembly.

Large-scale fire testing of CLT panels on existing products in the New Zealand market demonstrates that these panels are reliable for application in vehicle bridges. The CLT panels will remain structurally stable for more than 60 minutes under structural loads during a fire event at 900 degrees Celsius (refer to Figure 6). All existing fire test results are based on the test setups for CLT building applications and the fire event occurs on the underside of the CLT panel [10]. Although no fire test results are available for CLT panels with a fire event on the top surface to simulate fire resistance of the panel for bridge application, it is expected that the CLT panel will perform notably better when the fire is on the top surface, due to a notably lower charring rate. This major difference in the charring rate of CLT panels is highlighted in Figure 6, which presents a seven-layer CLT panel as an example.

2 EXPERIMINTAL TETST SET-UP

A real-scale four-point bending test has been conducted on a single five-layer CLT panel

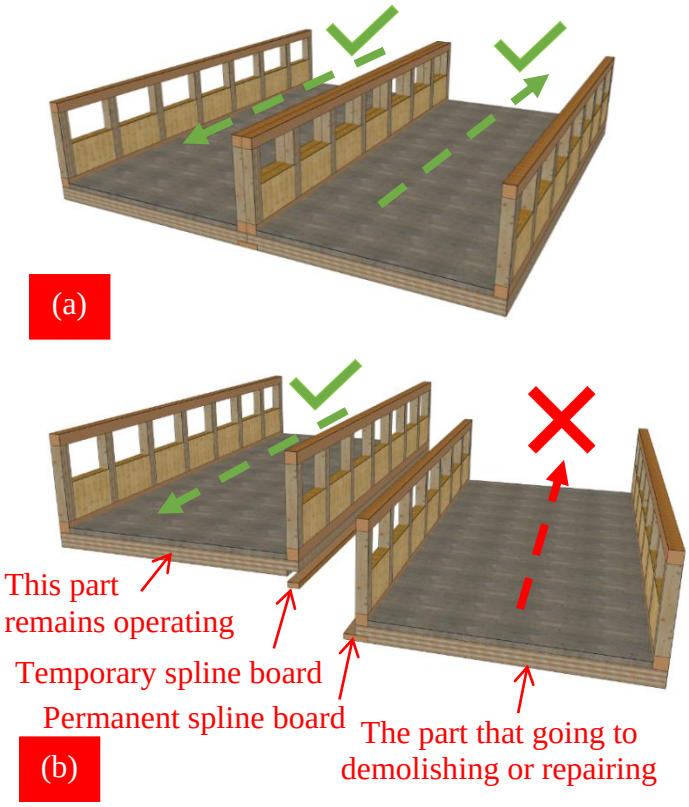

Figure 5. CLT bridge can remain semi-operational during the replacement of the old or damaged part of the bridge. a) fully operational, b) partially disassembled, and semi-operational.

Figure 6. Red Stag CLT fire test.

with a width of 2000 mm, a thickness of 200 mm, and a length of 6000 mm using a Material Testing Systems (MTS) actuator testing machine to verify the structural performance of the panel (refer to Figure 7) [15]. The data acquisition system has the ability to record load data from the MTS, and three LVDTs were located on top of each of the two end supports and under the mid-span of the CLT panel at the same time, as shown in Figure 8.

The same test set-up has been used for testing CLT composite beam. The CLT panel is attached as top flange to the top of a LVL girder. The external top, bottom, and middle layers of the CLT panel were oriented in the longitudinal direction of the LVL beam assembly which was 302 mm wide, 610 mm deep and 7 meter long (refer to Figure 9).

The CLT slab was predrilled, and the two parts were mechanically fastened using 550-mm screws with a diameter of 11 mm. A total of 48 screws were used in the test to provide composite action between CLT slab and LVL beam. The screws penetrated the 200-mm CLT slab and entered the supporting LVL beam at a 45° angle to a depth of approximately 276 mm.

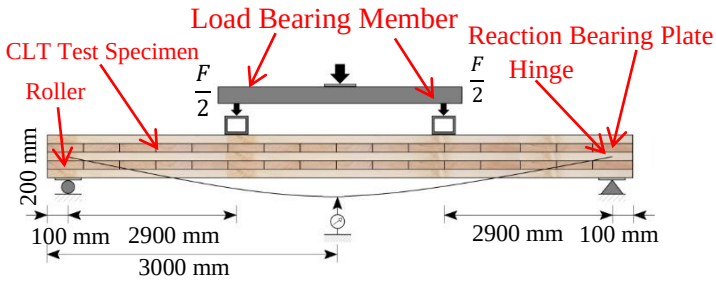

Figure 7. Test set-up for measuring the modulus of elasticity [15].

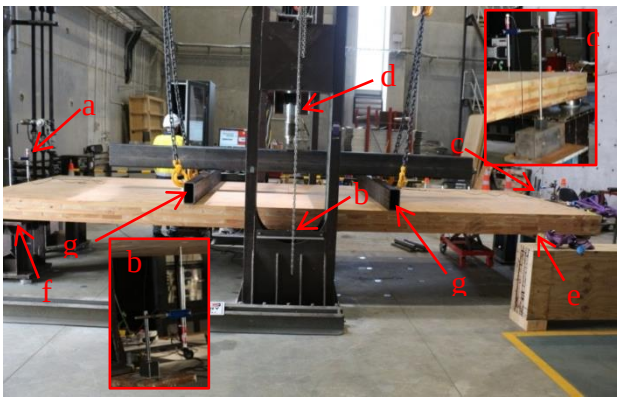

Figure 8. 500 kN MTS testing machine configured for four-point bending test. (a) LVDT 1, (d) MTS Machine, (e) Roller Support, (f) Hinge Support, (g) Load Bearing Plate, and (h) Data Acquisition System [15].

3 NUMERICAL ANALYSIS

The finite element package ABAQUS version 6.13-3 was chosen for the analysis and

simulation of a simply supported CLT panel in bending. The detailed numerical modelling and convergence study confirmed the accuracy of the developed numerical model (refer to Figures 10 and 11). An eight-node element (C3D8R), which is a linear three-dimensional solid element, was used for the analysis of the CLT panel [12-15]. The CLT properties specified in this study are for timber boards made from Radiata Pine trees grown commercially in New Zealand (refer to table 1). The coordinate system used is based on the principal axes of the wood , as shown in Figure 12.

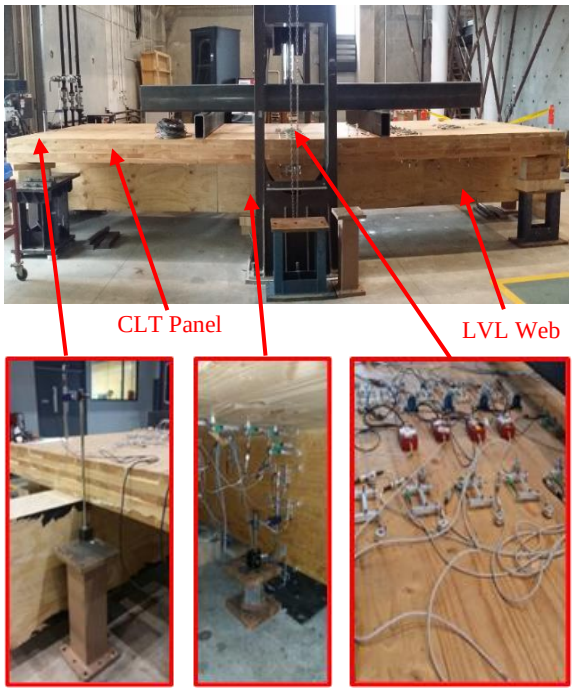

Figure 9. Experimental test set-up. (a) LVDT , (d) MTS Machine, (e) Roller Support, (f) Hinge Support, (g) Load Bearing Plate, and (h) Data Acquisition System [15].

Table 1. Material Properties of the CLT's boards [12-15].

Component	E_L	E_R	E_T	ν_{LT}	ν_{TL}	ν_{LR}	ν_{RL}	ν_{TR}	ν_{RT}
MSG 8 boards	8000	363	363	0.2	0.018	0.15	0.018	0.21	0.18
MSG 6 boards	6000	272	272	0.15	0.013	0.11	0.013	0.09	0.13

E=Modulus of Elasticity (N/mm2 for all modulus for CLT's boards).

ν=Poison's ratio, L=Longitudinal, R=Redial, T=Tangential

3.1 CONVERGENCE STUDY

Convergence studies were carried out on the 6-meter CLT panel to find a suitable finite element mesh to increase the accuracy of the analysis. Figure 13 and 14 illustrate the mid-span deflection of the CLT panel that is plotted against the corresponding number of elements for ten different mesh sizes [15].

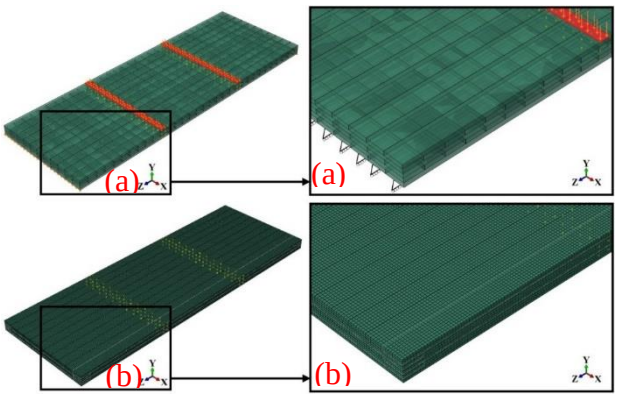

Figure 10. Typical boundary conditions and finite element mesh used in this study. (a) FE model boundary conditions (Load and support), (b) Finite element mesh.

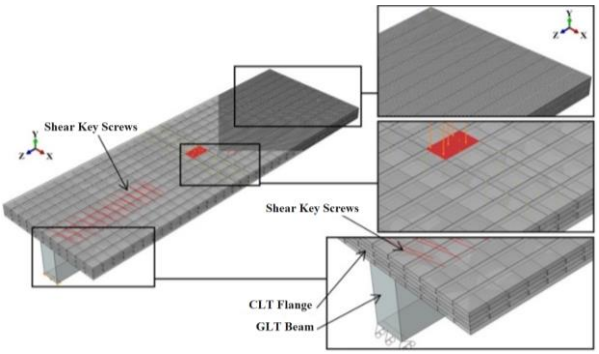

Figure 11. General arrangement of the numerical model to show boundary conditions and mesh.

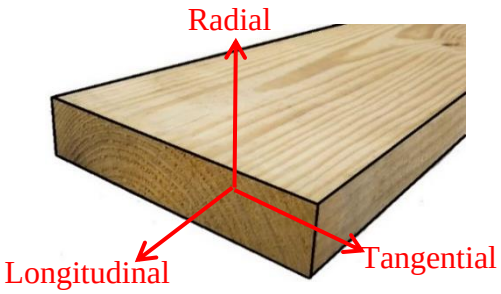

Figure 12. Principal axes of wood.

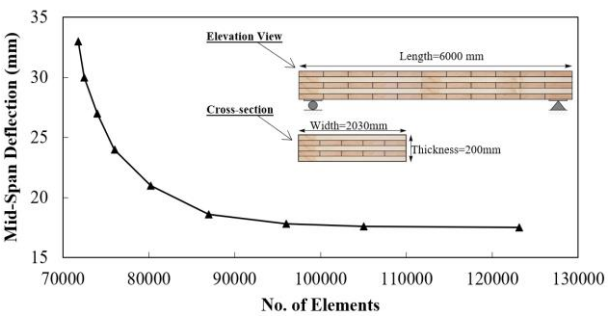

Figure 13. Convergence study numerical result.

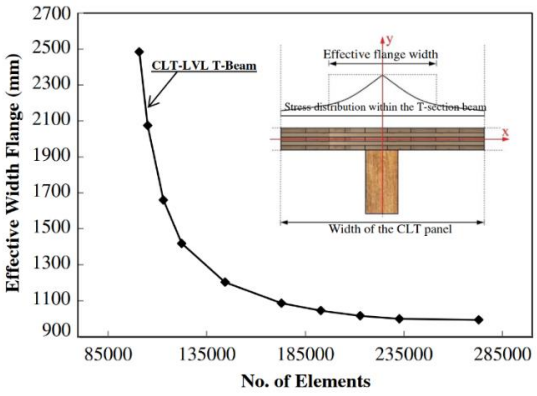

Figure 14. Convergence study result of EWF of CLT composite beam versus number of mesh elements.

4 PARAMETRIC STUDY AND RESULT DISCUSSION

The experimentally verified numerical model has been used to study the capability of various panel thicknesses for bridge applications (refer to Table 1). The mid-span deflection measurements show that the model is sufficiently accurate to predict the behaviour of the CLT panel.

Numerical analysis and analytical calculations have confirmed the structural capability of the CLT panels made from commercially grown New Zealand Radiata Pine trees for bridge applications. Specifications, shear, and moment capacity of various cross-section sizes of the CLT panel for bridge application are summarised in Table 3 to Table 4 [16-17].

The construction industry (including buildings and other types of structures) is a large contributor to greenhouse gas emissions and a massive consumer of natural resources. Therefore, even small improvements in construction technologies are important to reduce greenhouse gas emissions and thereby attain national goals to mitigate climate change. Table 5 presents long-term locked-up carbon for six CLT bridge configurations and their serviceability performance under 707 kg/m^2 [20]. The comparison between numerical and analytical calculations shows that the analytical calcination results are by 10% over design and conservative (refer to table 6).

Table 2. Comparison of the mid-span deflection results.

Specimen	CLT's Lamella $W^1 \times T^2 \times L^3$ (mm)	Deflection Experimental	Deflection Numeical
CLT Panel	2030×200×6000	18 mm*	17.9 mm*
W=Width, T=Thickness, L=Length of the CLT panel * Deflections under 50 kN four points loading test.			

Table 3. Specifications of the CLT panels specimen.

Specimen Number	CLT's Lamella $W^1 \times T^2 \times L^3$	CLT's Lamella E_{longi} E_{trans}
1	1000 mm×210 mm×4000 mm	8 GPa 6 GPa
2	1000 mm ×210 mm×4000 mm	8 GPa 8 GPa
3	1000 mm×228 mm×5000 mm	8 GPa 6 GPa
4	1000 mm×228 mm×5000 mm	8 GPa 8 GPa
5	1000 mm×228 mm×5500 mm	8 GPa 6 GPa
6	1000 mm×228 mm×6000 mm	8 GPa 8 GPa
W=Width, T=Thickness, L=Length of the CLT panel E_{longi}=MoE of longitudinal layers, E_{trans}=MoE of transverse layers		

Table 4. The capacity of the CLT Panels.

Specimen Number	CLT's Panel Weight	Vn (kN)	Mn (kNm)
1	420 kg	55.42	421.3
2	420 kg	55.42	421.3
3	570 kg	141.21	69.47
4	570 kg	141.21	69.47
5	808 kg	188,73	97.56
6	882 kg	188.73	97.56
Factors: Ø=0.85, k_1=0.8, k_4=1, k_6=1, k_9=1, k_{12}=1 Refer to NZSAS 1720. Load Case: 1.2 Dead Load + 1.5 Live Load.			

Table 5. The serviceability performance and estimated carbon dioxide of the CLT Panels.

Specimen Number	Mid-span Deflection	Estimated Carbon	Sequestered Carbon Dioxide
1	9.9 mm	168 tons	727 tons
2	9.4 mm	168 tons	727 tons
3	16.2 mm	228 tons	1048 tons
4	15.8 mm	228 tons	1048 tons
5	14.8 mm	323 tons	1487 tons
6	5.7 mm	352 tons	1622 tons
Mid-Span Deflection: Long-Term Deflection: (G+Ψl Q)×j2+(Ψs+Ψl)Q.			

Table 6. Mid-span deflection result based on experimentally verified numerical analysis.

Specimen Number	CLT's Lamella $W^1 \times T^2 \times L^3$ (mm)	CLT's Lamella $E_{longitudinal}$ $E_{transverse}$	Deflection Numeical
1	1000×210×4000	8 GPa 6 GPa	8.9 mm*
2	1000×210×4000	8 GPa 8 GPa	8.9 mm*
3	1000×228×5000	8 GPa 6 GPa	15.6 mm*
4	1000×228×5000	8 GPa 8 GPa	14.3 mm*
5	1000×228×5500	8 GPa 6 GPa	13.3 mm*
6	1000×228×6000	8 GPa 8 GPa	5.1 mm*
W=Width, T=Thickness, L=Length of the CLT panel $E_{longitudinal}$=MoE of longitudinal layers, $E_{transverse}$=MoE of transverse layers * Deflections under 50 kN four points loading test.			

5 NUMERICAL PARAMETRIC STUDY

The main focus of study is investigation of various CLT panel configurations on the EFW of single and CLT composite double T-beams.

5.1 EFFECT OF CLT PANEL LAYER CONFIGURATION

Two groups of single and double CLT composite beams with various CLT layers configurations were analysed to investigate the effect of layer thickness on the EFW. As seen from table 7 and Figure 13 (Specimens 2 to 1), an increase in the transverse layer thickness enhances the EFW. Again, numerical analysis result shows that similar increase in the transverse layer thickness over longitudinal layer enhances the EFW in double CLT composite beams (refer to table 8, Specimens 14 vs 13 and 12).

In the first series of analysis of CLT composite single T-beams, when 20 mm transverse boards in 166 thick CLT panel are replaced by 40-mm-thick boards, and the 20 mm thick, EFW increased 210 mm (Configuration 2 and 1 in Table 3). Moreover, when the 40-mm longitudinal layers and 20-mm transverse layers in Configurations 3 were replaced by boards with a thickness of 40 mm and 20 mm (Configurations 1 in table 7), the EFW increased more than 4 times. The similar change in CLT composite double T-beam increasing the CLT slab effective width noticeably more than 4.7 times (Configuration 14 and 15 in table 8). Therefore, the space between two LVL girders in the CLT composite double T-beam could be increased by 1500 mm based on the predicted EFW of the CLT composite double T-beam.

5.2 EFFECT OF CLT MATERIAL PROPERTIES

The effect of the elastic modulus of the CLT panels on the EFW are provided in Figure 15, 16, Table 7 and 8. In general, increasing the modulus of elasticity of the CLT panels increased the EFW of Single and double CLT composite T-beams. For example, as shown in Figure 15, when the modulus of elasticity of the CLT panel increased from 6 GPa (Configuration 5 in Table 7) to 8 GPa (Configuration 1 in Table 7), the EFW increased from 760 to 790 mm, thus increasing by 5 and 30%, respectively.

In addition, the comparison indicates when the 6 GPa transverse boards in 210 mm thick CLT panels in single and double CLT composite beams replaced with 8-GPa boards, EFW enhances 85 mm and 180 mm respectively. The numerical parametric analysis showed that higher ratio of longitudinal thickness over transverse layer has higher improvement effect on EFW compared to higher ratio of longitudinal MoE over transverse layer MoE.

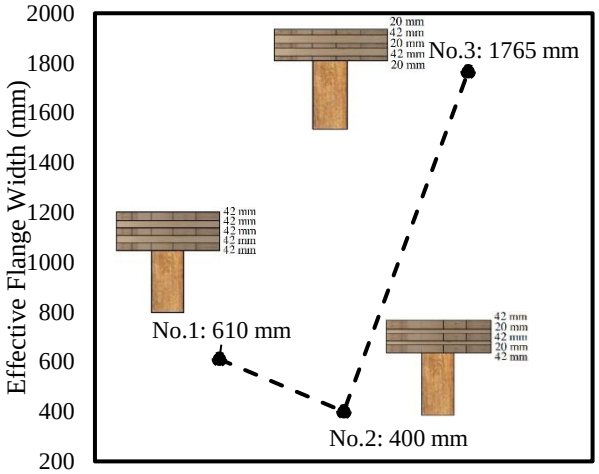

Figure 13. Effect of the layer's configuration change on the effective flange width for Configurations 1, 2, 3.

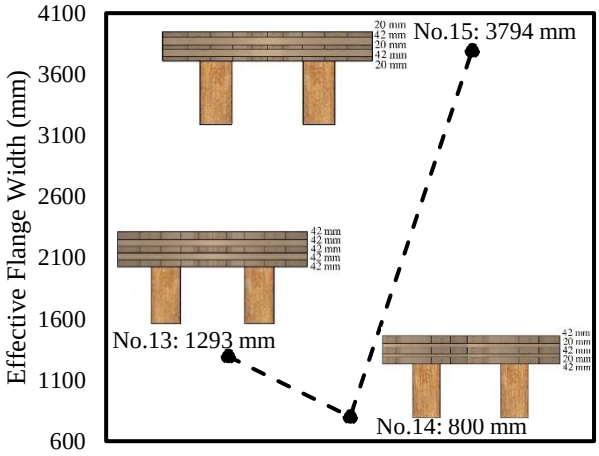

Figure 14. Effect of the layer's configuration change on the effective flange width for Configurations 13, 14, 15.

It is really important to note all these numerical analyses are only practicing the EFW of single or double CLT composite beams and the CLT slab required further deign and investigation based on structural application. For instance, the 3-layer central layers of 5-layer CLT panel in CLT composite double T-beam should be design as simply supported CLT panel to ensure the system can perform structurally safe

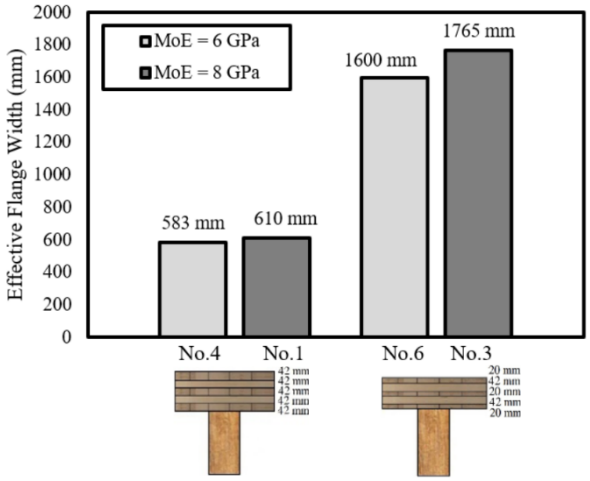

Figure 15. Effect of CLT material properties on effective flange width of CLT composite single T-beams.

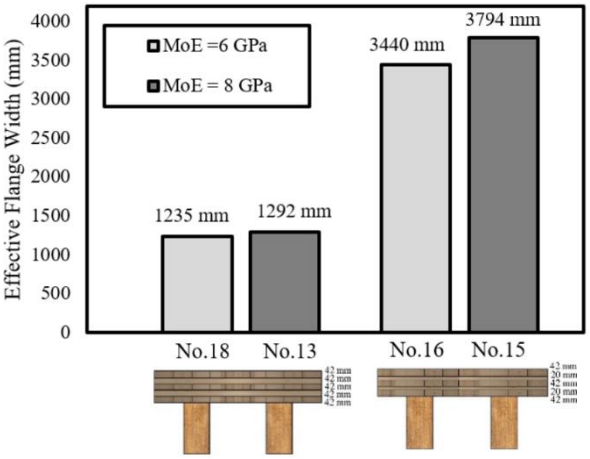

Figure 16. Effect of CLT material properties on effective flange width of CLT composite double T-beams.

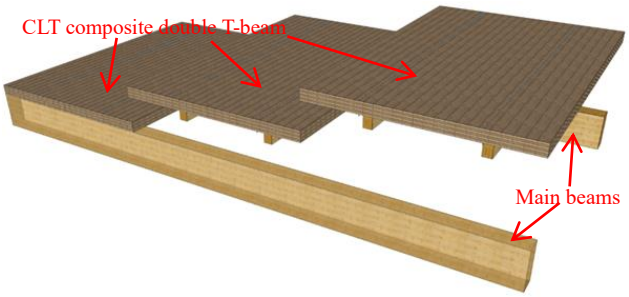

Figure 17. Intermediate Span CLT composite double T-beams.

for floor application. The Figure 18 and Table 8 shows that how high loads due to heavy vehicle weights on CLT panel between side-by-side girders lead to reduction girders spacing in CLT composite double T-beams.

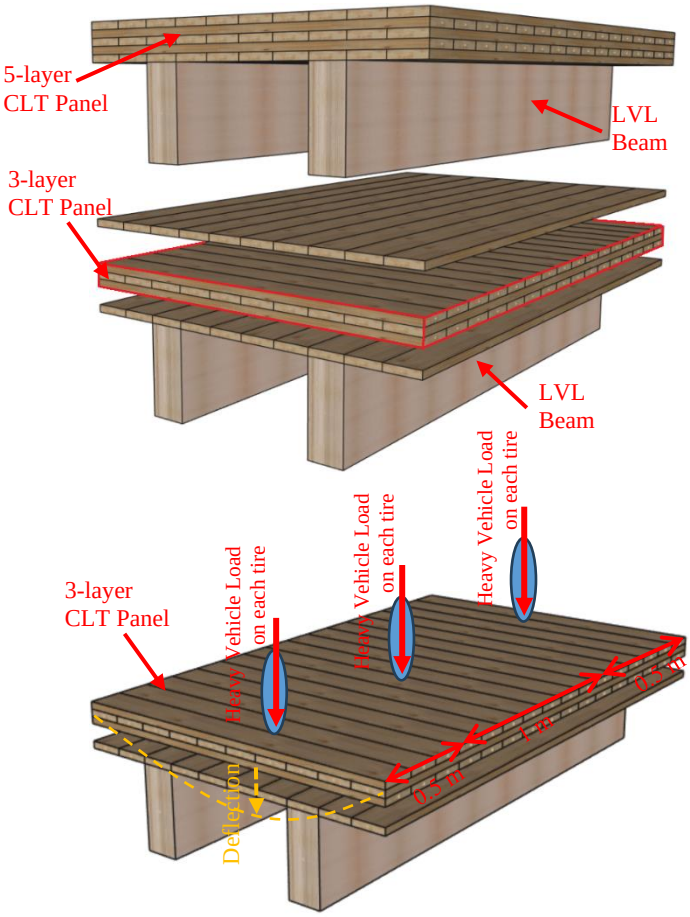

Figure 18. CLT composite double T-beam structural design concept for bridge application.

6 CONCLUSIONS

An accurate numerical model has been developed, which has been experimentally verified. The numerical parametric study and analytical calculations show that the bare CLT panel and CLT composite double T- beams are sufficiently strong to carry structural loads for various bridge applications. This study demonstrates that the high strength-to-weight ratio of CLT panels provides a lightweight, sturdy bridging solution for short-span bridges. In addition to their exceptional strength, CLT panels, as a mass timber material, also exhibit high dimensional stability. This ensures that bridges constructed from seven layers or thicker CLT panels, comprised of treated timber boards and protected with a waterproof membrane and concrete topping, can resist distortion even in extreme weather conditions, further improving their service life.

Table 7. CLT composite T-beam specifications and EFW result.

Specimen Number	CLT		LVL		Predicted effective width flange (mm)
	W×T×L (mm)	MoE of Layers (GPa)	W×T×L (mm)	MoE (GPa)	
1	2000×210×6000 2000×(42+42+42+42+42)[a]×6000	8,8,8,8,8 [b]	350×600×6000	11	610
2	2000×166×6000 2000×(42+20+42+20+42)[a]×6000	8,8,8,8,8 [b]	350×600×6000	11	400
3	2000×166×6000 2000×(20+42+20+42+20)[a]×6000	8,8,8,8,8 [b]	350×600×6000	11	1765
4	2000×210×6000 2000×(42+42+42+42+42)[a]×6000	6,6,6,6,6 [b]	350×600×6000	11	583
5	2000×166×6000 2000×(42+20+42+20+42)[a]×6000	6,6,6,6,6 [b]	350×600×6000	11	380
6	2000×166×6000 2000×(20+42+20+42+20)[a]×6000	6,6,6,6,6 [b]	350×600×6000	11	1600
7	2000×210×6000 2000×(42+42+42+42+42)[a]×6000	8,6,8,6,8 [b]	350×600×6000	11	570
8	2000×166×6000 2000×(42+20+42+20+42)[a]×6000	8,6,8,6,8 [b]	350×600×6000	11	365
9	2000×166×6000 2000×(20+42+20+42+20)[a]×6000	8,6,8,6,8 [b]	350×600×6000	11	1660
10	2000×210×6000 2000×(42+42+42+42+42)[a]×6000	6,8,6,8,6 [b]	350×600×6000	11	623
11	2000×166×6000 2000×(42+20+42+20+42)[a]×6000	6,8,6,8,6 [b]	350×600×6000	11	407
12	2000×166×6000 2000×(20+42+20+42+20)[a]×6000	6,8,6,8,6 [b]	350×600×6000	11	1810

Note: MoE = modulus of elasticity (units of GPa).
[a] Numbers in parentheses are the thickness of individual CLT layers (units of mm).
[b] The five numbers are the modulus of elasticity of each layer (units of GPa).
W: Width, T: Thickness, L: Length (units of mm).

Table 8. CLT composite double T-beam specifications and EFW result.

Specimen Number	CLT		LVL		Predicted EFW (mm)	Practical EFW for Bridge Application
	W×T×L (mm)	MoE of Layers (GPa)	W×T×L (mm)	MoE (GPa)		
13	4000×210×6000 4000×(42+42+42+42+42)[a]×6000	8,8,8,8,8 [b]	Two 350×600×6000	11	1293	798 mm
14	4000×166×6000 4000×(42+20+42+20+42)[a]×6000	8,8,8,8,8 [b]	Two 350×600×6000	11	800	Not Applicable
15	4000×166×6000 4000×(20+42+20+42+20)[a]×6000	8,8,8,8,8 [b]	Two 350×600×6000	11	3794	683 mm
16	4000×210×6000 4000×(42+42+42+42+42)[a]×6000	6,6,6,6,6 [b]	Two 350×600×6000	11	1235	700 mm
17	4000×166×6000 4000×(42+20+42+20+42)[a]×6000	6,6,6,6,6 [b]	Two 350×600×6000	11	760	Not Applicable
18	4000×166×6000 4000×(20+42+20+42+20)[a]×6000	6,6,6,6,6 [b]	Two 350×600×6000	11	3440	632 mm
19	4000×210×6000 4000×(42+42+42+42+42)[a]×6000	8,6,8,6,8 [b]	Two 350×600×6000	11	1208	704 mm
20	4000×166×6000 4000×(42+20+42+20+42)[a]×6000	8,6,8,6,8 [b]	Two 350×600×6000	11	730	Not Applicable
21	4000×166×6000 4000×(20+42+20+42+20)[a]×6000	8,6,8,6,8 [b]	Two 350×600×6000	11	3569	697 mm
22	4000×210×6000 4000×(42+42+42+42+42)[a]×6000	6,8,6,8,6 [b]	Two 350×600×6000	11	1410	797 mm
23	4000×166×6000 4000×(42+20+42+20+42)[a]×6000	6,8,6,8,6 [b]	Two 350×600×6000	11	814	Not Applicable
24	4000×166×6000 4000×(20+42+20+42+20)[a]×6000	6,8,6,8,6 [b]	Two 350×600×6000	11	3891	699 mm

Note: MoE = modulus of elasticity (units of GPa).
[a] Numbers in parentheses are the thickness of individual CLT layers (units of mm).
[b] The five numbers are the modulus of elasticity of each layer (units of GPa).
W: Width, T: Thickness, L: Length (units of mm).

The numerical parametric study of single and double CLT composite T-beams shows that the EFW increases with any change that increases the ratio of transverse layer depth to longitudinal layer depth.

Moreover, using thicker longitudinal layers in CLT slabs of similar thickness decreased the effective flange width. Furthermore, stiffer transverse layers in CLT panels with a higher modulus of elasticity slightly improved the EFW. structural design performance check of the CLT panel perpendicular to LVL Girder reveals the spacing restrictions of LVL girders due to high loads of heavy vehicles weight. Finally, the installation of a CLT bridge is much faster due to its lighter weight, making it a great substitute for a concrete bridge. This helps replace a carbon-intensive material with a renewable, low-carbon alternative.

ACKNOWLEDGEMENT

The author thanks graphic designer Nariman Valizadeh and Navid Masoudnia for providing excellent photos and figures. I would also like to thank Red Stag for financially sponsoring this research paper.

This technical paper has been developed to demonstrate the significant structural potential of CLT panels and CLT composite double T-beams constructed from Red Stag CLT panels for bridge applications. Please note that it is the responsibility of the bridge engineer or designer to ensure that the presented results are appropriate for their specific project and not to rely solely on the numerical analyses.

REFERENCES

[1] A. Fortune, P. Quenneville. Feasibility study of New Zealand radiata pine cross-laminated timber, New Zealand Timber Design Journal, 2011.

[2] M. Mohammad, S. Gagnon. Introduction to Cross-Laminated Timber, Wood Design Focus, Volume 22, Number 2, pp. 13-21; 2012

[3] B. Yeh, S. Gagnon, T. Williamson, C. Pirvu, C. Lum, D. Kretschmann, The North American Product Standard for Cross-Laminated Timber, Wood Design Focus, Volume 22, Number 2, pp. 13-21; 2012.

[4] M. Jelec, D. Varevac, V. Rajcic, Cross-laminated timber (CLT) - A state of the art report, GRADEVINAR, 70 (2), 75-95.

[5] R. Brandner, G. Flatscher, A. Ringhofer, G. Schickhofer, A. Thiel, Cross laminated timber (CLT): overview and development, Wood and Wood Products, Volume 74, pages 331–351, (2016).

[6] K. Lewis, R. Shrestha, K.I. Crews, Introduction to cross-laminated timber and development of design procedures for Australia and New Zealand, 23rd Australasian Conference on the Mechanics of Structures and Materials (ACMSM23), 2014.

[7] M. F. Laguarda Mallo, O, Espinoza, Cross-laminated timber vs. Concrete/steel: cost comparison using a case study, World Conference on Timber Engineering 2016, Vienna, Austria.

[8] S. Ahmed, I. Arocho, Analysis of cost comparison and effects of change orders during construction: Study of a mass timber and a concrete building project, Volume 33, Journal of Building Engineering January 2021, 101856.

[9] M. F. Laguarda Mallo, O, Espinoza, Outlook for Cross-Laminated Timber in the United States, bioresources 2014, 10.15376/biores.9.4.7427-7443.

[10] Red Stag CLT Design Guide V1.5, September 2024.

[11] P. Maclaren. Radiata Pine Growers Manual. New Zealand Forest Research Institute, Rotorua, New Zealand, 1993.

[12] R. Masoudnia, A. Hashemi, and P. Quenneville. “Predicting the effective flange width of a CLT slab in timber composite beams.” In: Journal of Structural Engineering 144.7 (2018), pp. 04018084.

[13] R. Masoudnia, A. Hashemi, and P. Quenneville. “Evaluation of effective flange width in timber composite beams.” In: New Zealand Timber Design Journal 26.2 (2018), pp. 14–24.

[14] R. Masoudnia and S. Masoudnia. “Numerical investigation of effective flange width in CLT-GLT composite T-beams.” In: New Zealand Timber Design Journal 27.3 (2019), pp. 7–16.

[15] R. Masoudnia. “State of the art of the effective flange width for composite T-beams.” In: Construction and Building Materials 244 (2020), Art. 118303.

5TH INTERNATIONAL CONFERENCE ON
Timber Bridges
EFFECTIVE • EFFICIENT • RESILIENT
Rotorua, New Zealand · 29 June – 2 July 2025

AUSTENITIC STAINLESS-STEEL SELF-TAPPING SCREWS IN TIMBER BRIDGE DESIGN: A PRELIMINARY PERFORMANCE ANALYSIS

Rodrigo Adolfo Benitez Mendes[1], Ömer Asim Şişman[2], Musaab Ahmed Mahjoub[3]

ABSTRACT

Bridges are engineered structures designed to have a lifespan extending over several decades, often approaching a century. Historically, there has been a misconception regarding the durability of timber bridges compared to their concrete and steel counterparts. However, recent advances in timber engineering research, along with the development of innovative structural wood products and connection materials, are shifting this perspective. In this context, the quality of fastener materials is particularly critical to the durability of timber bridges. An optimal fastener must exhibit resilience to the typical demands placed on a bridge, including fatigue and dynamic loads, as well as resistance to harsh chemical conditions. This paper presents a preliminary analysis of the suitability of A4 austenitic stainless steel self-tapping screws as a superior fastening and reinforcing solution for timber bridge design, in comparison to traditional galvanized carbon steel screws. The evaluation involved monotonic and cyclic bending tests conducted in accordance with European standards, along with an analytical beam reinforcement calculation utilizing a web-based tool. Results, supported by existing literature, indicate that the improved static and cyclic ductility of A4 stainless steel screws, combined with their exceptional corrosion resistance, make them a compelling fastener choice for timber bridge design. Additionally, its reinforcement performance can match that of a carbon steel screw, contingent upon the beam's geometry.

1 INTRODUCTION

For many decades, wood has been underestimated and not considered a primary construction material choice in essential urban projects. However, advancements in scientific research and industry enabled increasing reliability in wood as a structural material, which can be noted in the ease of building code regulations worldwide and the expansion of its application in areas where steel and concrete were historically preferred. Structures built in seismic hazard zones, subjected to fatigue loads and completely exposed to weathering, such as bridges, are notable examples of this (Figure 1).

A commonly held belief is that timber bridges have a shorter service life than steel or concrete bridges [1,2]. As a case in point, out of the 4,200 road bridges in service in New Zealand, only 14 are made of timber [3]. This scenario is progressing towards a change since, as of early 2025, the construction of the new 9 m span Onetai bridge became the first state highway bridge built from timber in 50 years. With proper maintenance, the bridge is designed for a service life of at least 100 years [4].

The durability and longevity of these structures primarily depend on the quality of materials used in their construction. Apart from the correct selection of the preservative treatment applied on wood components, the steel type of connectors and fasteners are also a key factor for effective long-term performance and maintenance costs. Special attention is given to dowel-type fasteners, which are primarily responsible for transferring static and dynamic loads between the big-sized glued laminated timber girders typically used and reinforcing them [5]. Additionally, in earthquake-prone regions such as New Zealand and Australia,

[1] MSc. Structural Engineer, Global Technical Advisor, Eurotec GmbH
e-mail: r.mendes@eurotec.team,
[2] MSc. Structural Engineer, Global Technical Advisor, Eurotec GmbH
[3] MSc. Structural Engineer, Global Technical Advisor, Eurotec GmbH

both ductility and energy dissipation through repeated plastic deformation of metal fasteners must be guaranteed under seismic loading [6,7,8]. Moreover, given the high-humidity service conditions of bridges and the heavy treatments used on wood for protection against weathering and biological deterioration [1], metallic fasteners adopted need to withstand such corrosive conditions [9].

Being aware that modern hardened carbon steel wood screws with electrogalvanized coating are the usual choice for most timber projects, the novel variant made of A4 austenitic stainless steel may potentially be a better option in the case of timber bridges due to the overall good mechanical properties and excellent corrosion resistance. While there is a small number of studies on the seismic performance of carbon steel screws assessed following the new test method from EN 14592:2022 Annex E [10,11,12], the current literature lacks any information about stainless-steel screws. This is also the case for test data according to EN 409 [13], with which fasteners' yield moment and static ductility are determined. Therefore, a comparative analysis is necessary to evaluate more effectively the differences in ductility and structural performance between the two alternatives.

This article aims to carry out a preliminary analysis of the suitability of A4 stainless steel wood screws as a superior fastener alternative for the design and construction of timber bridges. To this end, comparisons with both carbon steel and A4 stainless steel screws are made experimentally through quasi-static monotonic and cyclic bending tests according to EN 409 and EN 14592. Additionally, an analytical comparison of a static reinforcement calculation is performed with the aid of a web tool. Finally, considerations are made towards the durability of timber bridges in relation to the choice of screw material.

Figure 1. Te awa Cycleway truss bridge, Hamilton, New Zealand [courtesy of Techlam].

2 MODERN SELF-TAPPING WOOD SCREWS

The manufacturing technology of self-tapping wood screws has evolved alongside advancements in engineered wood products (EWP). Key innovations include the introduction of new lengths and diameters of sufficient size for the joints required in large-scale timber projects, as well as an appropriate level of steel hardness to ensure safe installation. This combination, along with reduced minor-to-major diameter ratios, enables superior withdrawal forces and allows for installation without pre-drilling in most cases. In the European market, these screws meet the requirements outlined in EN 14592 [10] and are utilized by practitioners in accordance with the guidelines provided in the European Technical Approval (ETA) [14] issued for each fastening system in agreement with the European Assessment Document (EAD) [15].

Self-tapping screws are generally divided into partially threaded and fully threaded categories. Partially threaded screws, also called assembly screws, have both threaded and smooth shank portions along their length and are specially designed for pulling wood members together. Aside from promoting the rope effect by creating a firm bearing surface between wood components, they are predominantly used to transfer lateral forces with the shear plane perpendicular to its axis (Figure 2e). Fully threaded screws are engineered to resist high axial loading, taking advantage of the coarse threads running along its entire length with a smaller pitch compared to partially threaded screws. This characteristic makes them the most appropriate screw to reinforce wood components subjected to perpendicular to grain stresses [5] (Figure 2 a-d). Regarding laterally loaded joints, although fully threaded screws are primarily installed with an inclined orientation to the shear plane to exploit the high withdrawal resistance, they have demonstrated enhanced ductility and stiffness when fully loaded in shear perpendicular to its axis [16].

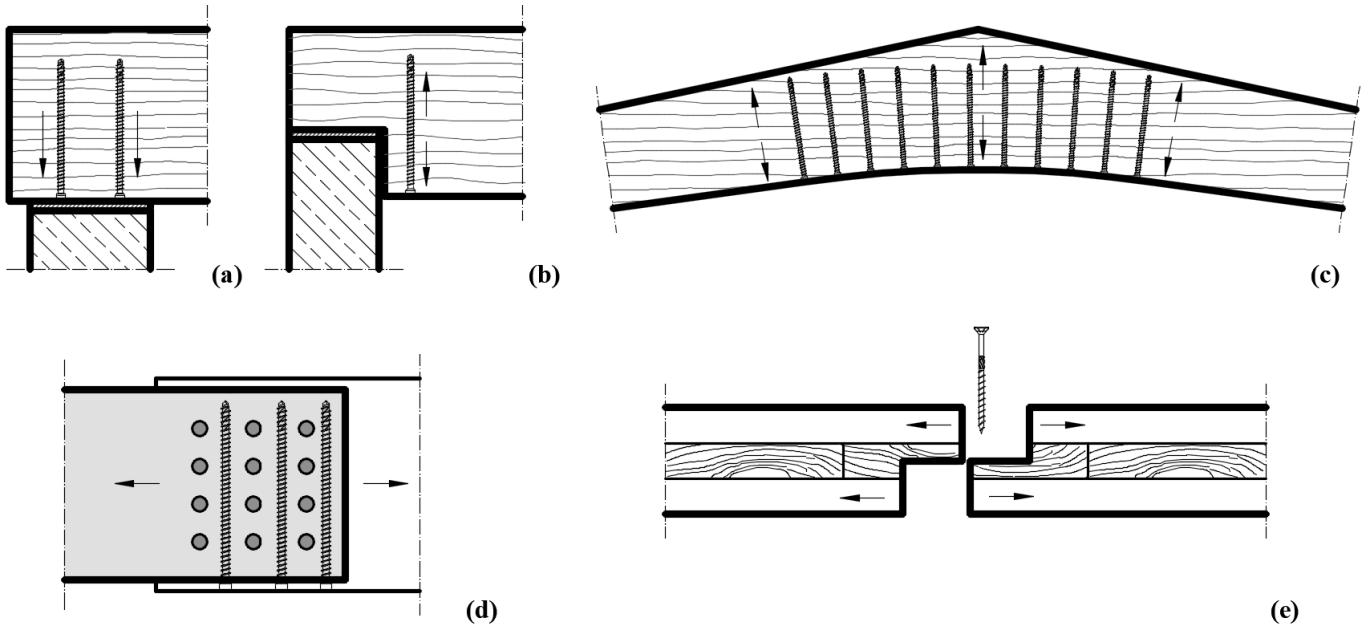

Figure 2. Application examples of modern wood screws: (a) compression reinforcement of support areas, (b) tension reinforcement of notched beams, (c) apex tension reinforcement of pitch cambered beams, (d) reinforcement of dowel-type connections, (e) half-lap joint of CLT panel

The application of self-tapping screws also varies depending on the type of steel used for its manufacture. One of the most common steel alloys used to manufacture these screws, and the one chosen for the carbon steel group of this article, is SAE 10B21. This low-carbon steel grade contains a small percentage of boron, making it particularly suitable for applications requiring good hardenability and strength. Its typical composition comprises carbon (0.18-0.23%), boron (0.0003-0.0005%), and manganese (0.60-0.90%) [17]. The other group analyzed consists of screws made of A4 austenitic stainless steel, which is composed primarily of chromium (16.5-18.5%), nickel (10-13%), molybdenum (2-2.5%), and carbon (0.07%) [18]. The smaller carbon quantity of the A4 stainless steel accounts for its higher ductility but lower strength compared to SAE 10B21. The presence of molybdenum further enhances its corrosion resistance, especially in chloride environments. As the torsion resistance of stainless-steel screws is lower compared to conventional carbon steel screws, most of the commercially available screws need pre-drilling for installation, but there are variants that feature a drill tip, allowing for direct installation without the risk of fracture (Figure 3) [14].

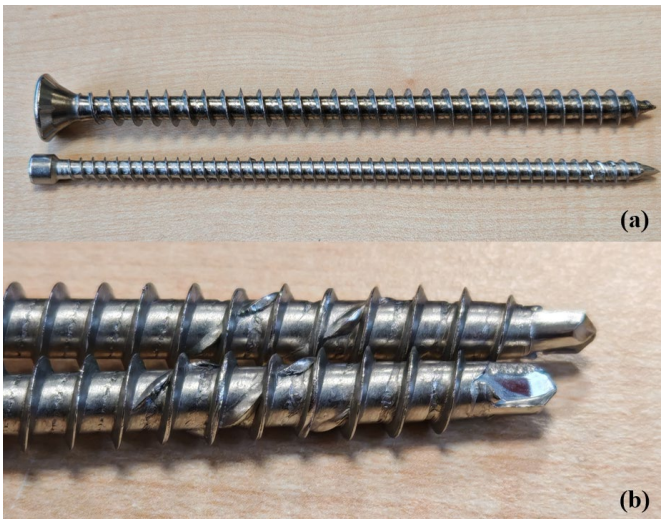

Figure 3. Fully threaded screws made of A4 austenitic stainless steel: (a) complete length of the screws with needle tip type, (b) close-up on the drill tip type variant of these screws.

3 MATERIALS AND METHODS

3.1 Materials

For the experimental investigation, self-tapping screws from manufacturer Eurotec GmbH (Hagen, Germany) made of carbon steel SAE 10B21 and A4 austenitic stainless steel with the same diameter and thread type were selected for comparison. The monotonic tests' sampling comprised fully threaded screws KonstruX ST ZK with 6.5 mm and 8 mm of nominal diameter (d). The specimens for the cyclic tests were partially threaded screws Paneltwistec SK with 5 mm and 6 mm of nominal diameter.

For the analytical comparison using the web tool, fully threaded KonstruX screws with a nominal diameter of 10 mm and a length of 400 mm, made of the two specified steel types, were evaluated. The complete geometric and mechanical properties of these screws are shown in the ETA-11/0024 [14].

3.2 Methods

3.2.1 Monotonic bending moment and low cycle ductility tests

The maximum bending moment of the screws was determined based on EN 409 [13]. This test consists of a 4-point bending test that produces a pure moment on the fastener itself (Figure 4a). During the test, both the moment and the bending angle are measured, and the maximum recorded plastic moment was determined, limited to a bending angle of 45°. However, the test continued up to approximately 60°. The screw's free bending length l_2 is set to $2d$. Ten specimens each were tested for screws with both materials.

The cyclic 3-point bending tests were carried out classify the screws according to the low-cycle ductility classes defined in EN 14592 [10]. To this end, three tests under cyclic load and three tests under monotonic load are required, where only the screw itself is bent (Figure 4b). The cyclic test comprises three fully reversed cycles up to a bending angle α_c and a final monotonic loading to determine the residual bending moment capacity of the screw. The bending angles α_c are defined in accordance with the three low cycle ductility classes established in the standard, wherein each succeeding class number denotes a higher energy dissipation capacity, thereby requiring larger bending angles α_c to be achieved. Hence, α_c is defined as follows: for low-cycle ductility class S1, α_c is defined as α; for class S2, α_c is defined as 1.5α; and for class S3, α_c is defined as 2α, where α corresponds to equation (1): $45°/d^{0,7}$, where d is in mm. During the test, two criteria must be fulfilled for a screw to be classified into the previously chosen low cycle ductility class. For criterion 1, screws must reach (without breaking into two pieces) a minimum bending angle of at least 45° for diameters up to 8 mm or 30° for screws with larger diameters, respectively. In this work, this criterion is observed for both the monotonic and cyclic curves. For criterion 2, if the moment capacity under cyclic load after three fully reversed cycles (residual bending moment capacity) reaches at least 80 % of the moment capacity under monotonic load, the screw passes the test. It is important to note that for this article, only low cycle ductility class S_3 was considered in the experiments.

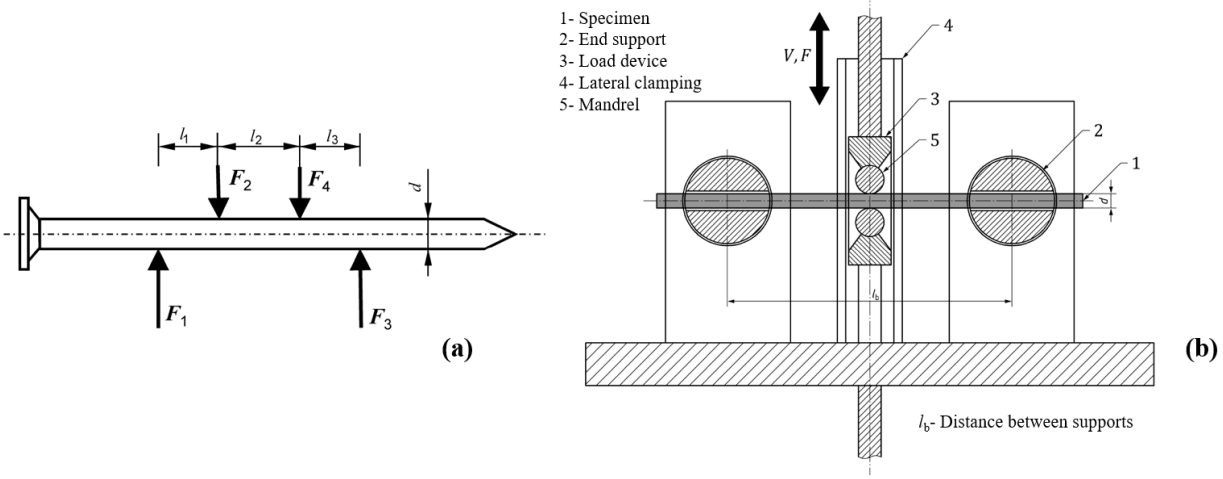

Figure 4. Bending tests of dowel-type fasteners: (a) free body diagram of monotonic test according to EN 409 [13], (b) setup of cyclic loading test according to EN 14592 [10].

As in EN 409, the screw is also tested on its threaded part. The test setup must comply with a maximum distance between supports l_b of 16d. This distance is established as 15.8d for this article. The end supports must allow axial displacements and free rotations of the sample. The sample must also be laterally restrained to prevent out-of-plane rotations.

3.2.2 Beam notch reinforcement example with analytical web tool

CLT Toolbox is a new commercial web-based structural timber design software (web tool) that supports many international design codes [19]. The software includes several member design calculators such as cross-laminated timber (CLT) floor, timber beam, and connection design. The program is fully parametric, allowing to change dimensions and properties of the timber members, input of load and its duration, and the manufacturer and type of screws used in the connections and timber reinforcement modules.

Being aware that large-size notched girders are usual in timber bridge design, this article uses the beam notch calculator with screw reinforcement as an example. The beam dimensions and characteristics are based on the glued laminated timber girders of the new Onetai bridge [4], having 675 mm of depth, 225 mm of width, and a notch depth of 195 mm. As the dimensions of the abutment were not provided, the support dimensions were selected to be 300 mm in length, with a width equal to that of the girder. The strength grade of the girder is set as GL24h, which is the equivalent European grade to the local GL10 specified on the project, considering its bending strength [20]. The reinforcement comprises one row of three screws installed 100 mm away from the notch's edge, meeting the spacing and distance requirements.

The selected design code for the analysis is prEN 1995-1-1:2023 [7], and the reinforcement analytical method is explained in detail in section 8.3.5.2. As the actual support load is unknown, it is arbitrarily set as 110 kN, considering a short load duration. Service class 3 condition is selected. All other concerning factors and coefficients are set following the code. The reinforcement performance between both fully threaded screws of different steel types is compared and discussed.

4 RESULTS AND DISCUSSION

The monotonic moment-bending angle curves according to EN 409 for screws with nominal diameters 6.5 mm and 8 mm are shown in Figure 5 and Figure 6, respectively. The average maximum bending moments for d= 6.5 mm were 13.9 Nm (0.86) and 24.6 Nm (0.64) for A4 stainless steel and carbon steel materials, respectively, showing the coefficient of variation (COV) between parentheses. The average maximum bending moments for d= 8 mm were 21.3 Nm (3.30) and 36.0 Nm (1.25) for A4 stainless steel and carbon steel materials, respectively. It can be seen for both diameter sizes that the moment-bending angle curves have different behavior for carbon steel and A4 stainless steel. The stainless-steel curves show almost an ideally elastic-plastic behavior with a constant slight hardening from 15° onwards. The carbon steel curves exhibit much stiffer behaviors. They are characterized by minimal hardening and a gradual decline after reaching a maximum, ultimately leading to failure before attaining 60°. Finally, average maximum bending angles are around 70% higher for carbon steel screws.

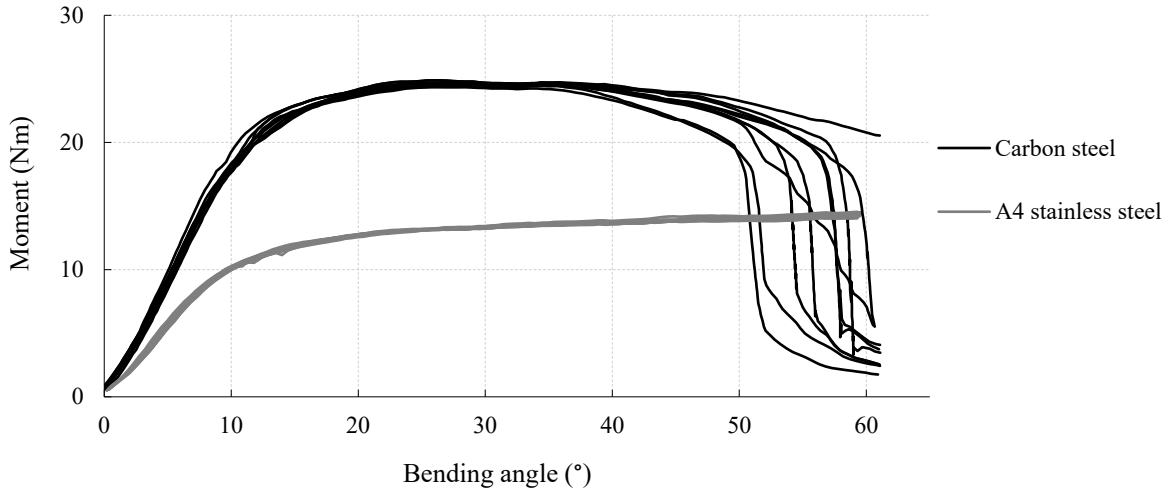

Figure 5. Monotonic bending test according to EN 409 of fully threaded screws with d= 6.5 mm and different material.

These differences are naturally attributed to the carbon composition of both steel types, added to the carburizing and hardening processes after screw manufacturing. Even though tempering retrieves some ductility to carbon steel screws, their response can be qualified as quite brittle compared to A4 stainless steel screws. Correlating with Steiler *et al*. [21], screws with moment-bending angle curves shaped as the ones determined for A4 stainless steel are more likely to reach higher low-cycle ductility classes and, therefore, to form plastic hinges through repeated loading while enduring large deformations.

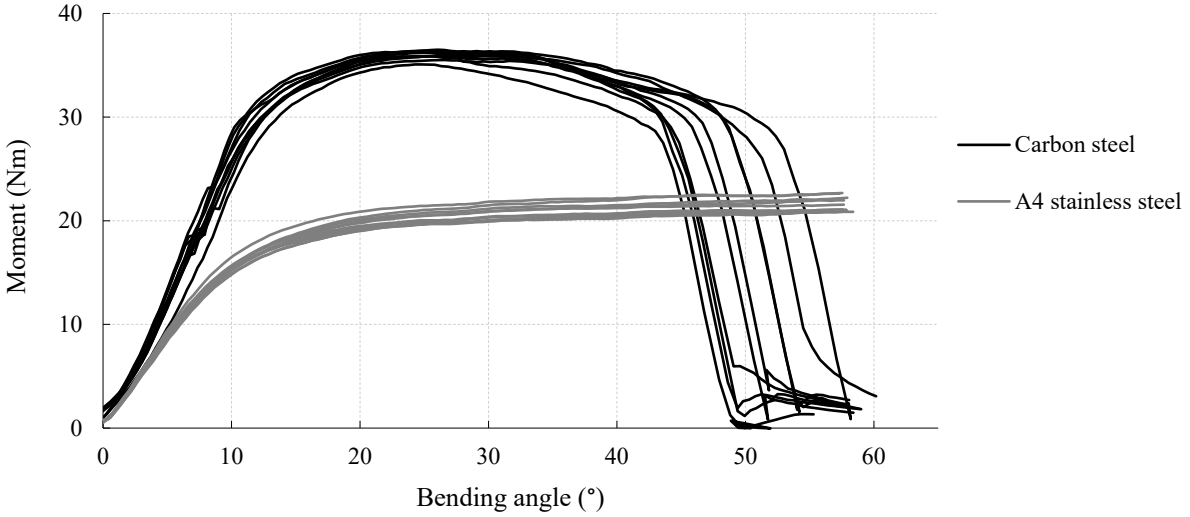

Figure 6. Monotonic bending test according to EN 409 of fully threaded screws with d= 8.0 mm and different material.

Figure 7 and Figure 8 show the moment-bending angle curves for the monotonic and cyclic loading tests according to EN 14592 for partially threaded screws with nominal diameters of 5 mm and 6 mm, respectively. α_c for low-cycle ductility class S3 is equal to 29.2° for d= 5 mm and to 25.7° for d= 6 mm. It can be observed that two of the three carbon steel specimens of d= 5 mm endured the three fully reversed load cycles but reached rupture before finishing the final monotonic ramp, failing to meet criterion 2 and not classifying as S3. On the other hand, A4 stainless steel screws with the same nominal diameter passed the test for S3 class. Regarding screws with d= 6 mm, both different materials could be classified as S3. The residual bending moment capacities of the carbon steel and A4 stainless steel specimens exceeded criterion 2 with around 10% and 15% margins, respectively.

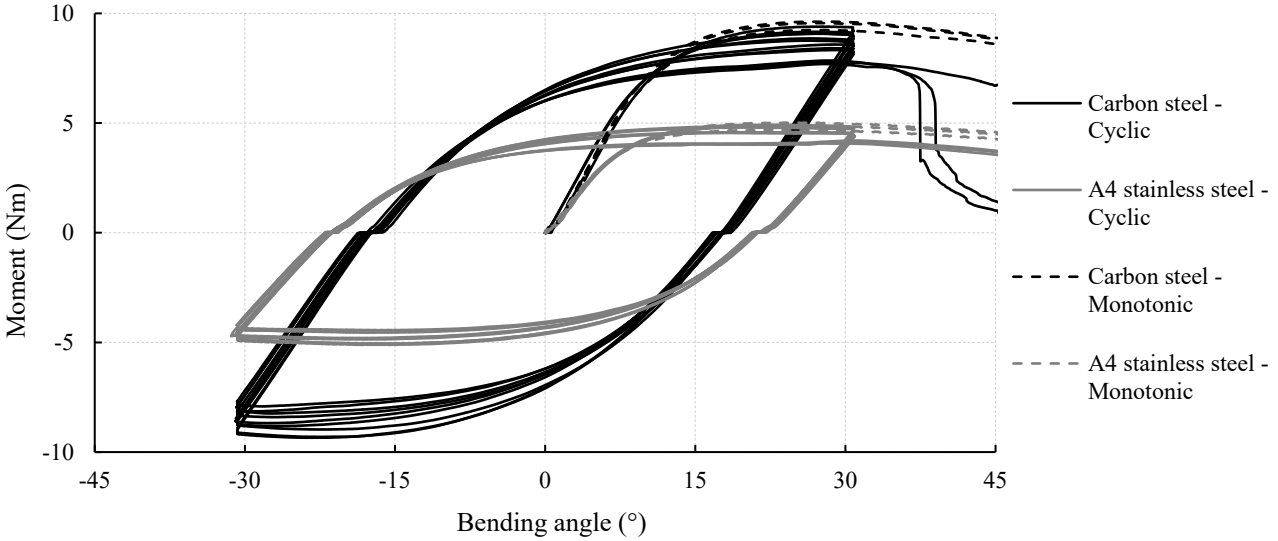

Figure 7. Cyclic bending test of partially threaded screws with nominal diameter d= 5.0 mm and different material, carried out by assuming a low cycle ductility class S3.

Although the sampling of this work is considerably small, some observations can be drawn that contrast with other authors' results. Izzi and Polastri [11] obtained mixed results by only achieving class S3 for carbon steel SAE 10B21 screws with nominal diameters 8 mm and 10 mm but not for 6 mm. Screws with d= 8 mm made of carbon steel 17 B2 did not pass S3 test. Blaß [22] tested screws of six different diameters made of carbon steel and of three different diameters made of A2 austenitic stainless steel. Only one diameter size of the carbon steel group achieved class S3, while two diameter sizes of the stainless steel group achieved the highest ductility class. Summarizing, even though the cyclic test results of this work and of other authors don't bring a fully consistent outcome, there is a higher tendency for austenitic stainless-steel screws to achieve greater low cycle ductility classes.

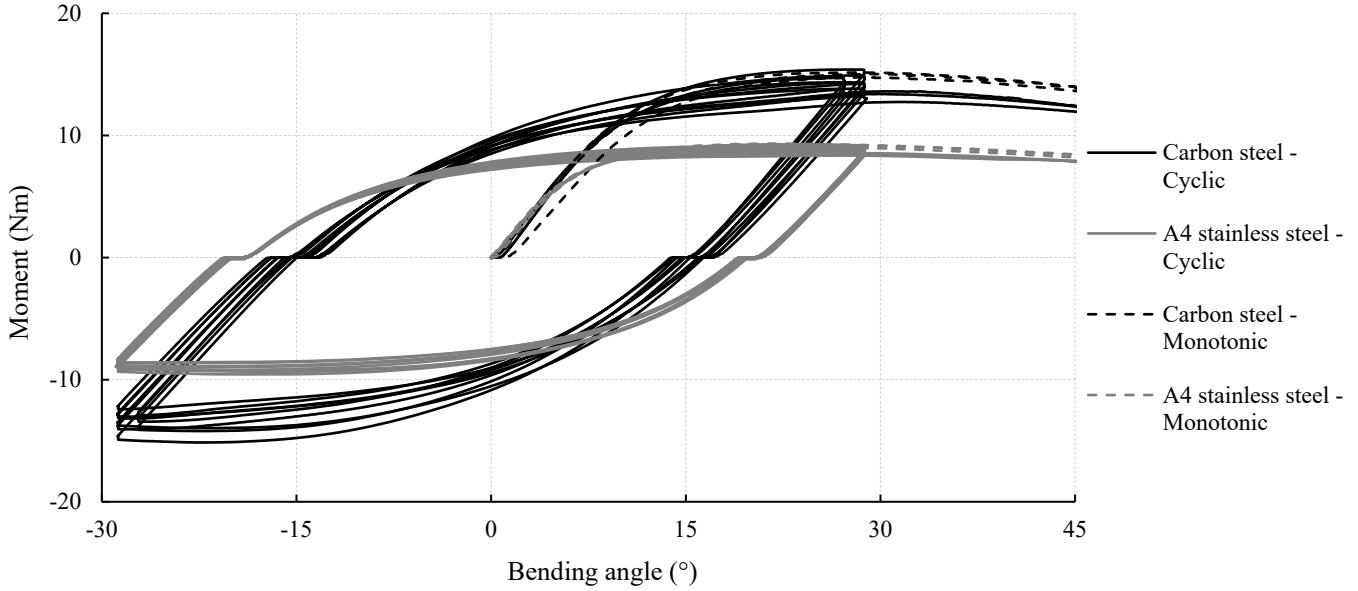

Figure 8. Cyclic bending test of partially threaded screws with nominal diameter d= 6.0 mm and different material, carried out by assuming a low cycle ductility class S3.

Figure 9 shows the CLT Toolbox 2D model of the notched beam reinforced with A4 stainless steel screws, where all relevant dimensions and screw positions are visible. Figure 10 presents a summary of the corresponding necessary verifications, displayed as demand-resistance ratios in percentage. A comprehensive step-by-step calculation report can be printed on the software [19]. It is noted on the shear stress check at the notched area without reinforcement that the demand is more than twice the resistance of the timber member. Hence, a reinforcement measure is needed. In accordance with the method, the minimum reinforcement length $l_{r,u}$, which is the screw's threaded length above the horizontal notch's face (possible crack line), is the minimum value between the notch's depth (195 mm) and 1.5 times the distance of the support load to the vertical notch's face (240 mm). For this example, a screw's length of 400 mm suffices, and a longer one would produce the same structural benefit.

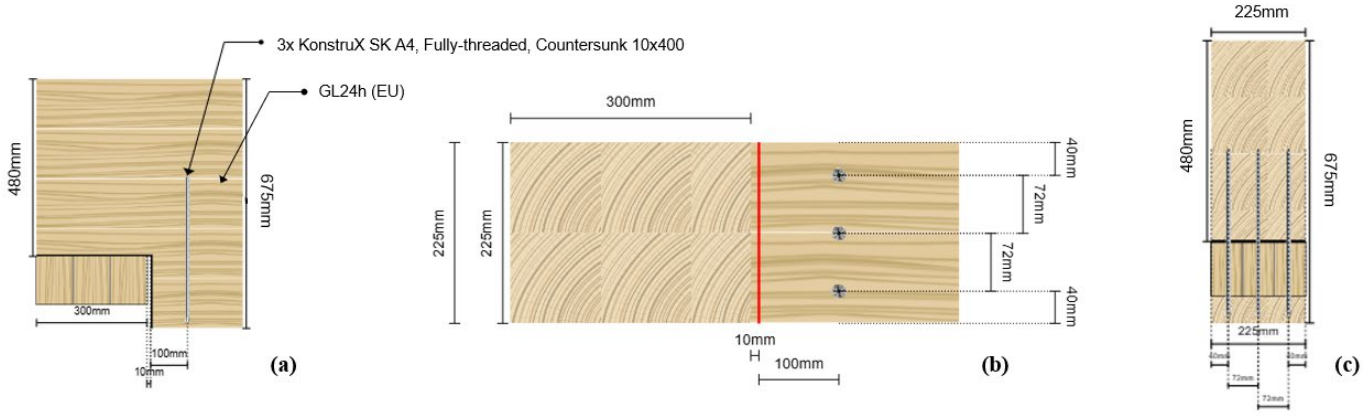

Figure 9. Reinforcement of notched beam with CLT Toolbox webtool: (a) section view, (b) bottom view, (c) side view.

After applying the reinforcement with the A4 stainless screws, the shear stress check is verified with a ratio of 91%, and the reinforcement of tensile stresses perpendicular to the grain is verified with a 94% ratio. Upon conducting the same verification with carbon steel screws, the results obtained are almost identical. It is important to note that both screw types share the same characteristic withdrawal parameter since this mechanical property is not material-dependent, and the geometry of both screws is essentially the same. Even though the tensile strength of the carbon steel screw is 65% higher compared to the A4 stainless steel screw [14], for this example, its axial capacity is governed by the withdrawal resistance of the threaded part below the possible crack line. Conversely, in the case of A4 stainless steel screws, the tensile strength governs, which in this case is very similar to the withdrawal resistance of the lower threaded part mentioned.

These results show that, depending on the geometry of the girders of a timber bridge and its notch dimensions, A4 stainless steel fully threaded screws can provide the same reinforcement resistance as equivalent carbon steel screws. Although its tensile strength is significantly lower and may become a limiting factor for larger girders with deeper notches, the capacity of the reinforcement increases by 33% with each new added screw when the tensile strength is governing.

In this example, prEN 1995-1-1:2023 penalizes the shear stress check of the notched girder by a factor of 0.4 when a reinforcement is not implemented [7]. For this reason, it is recommended to apply reinforcement whenever possible to mitigate cracks and long-term deformations of timber girders.

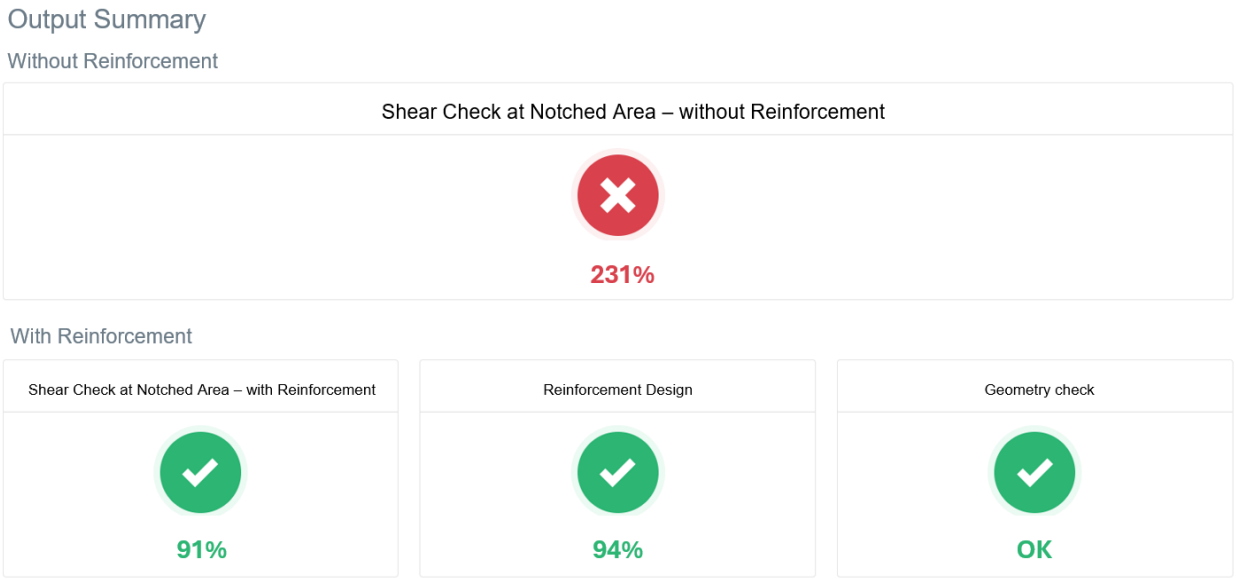

Figure 10. CLT Toolbox summary of verifications.

5 IMPLICATIONS OF FASTENER MATERIAL SELECTION FOR DURABILITY

Bridges, in general, are structures designed to have a lifespan of many decades or even a century. The steel type of the metallic connections employed, including fasteners, plays a crucial role in achieving the desired durability and serviceability of timber bridges. In this sense, it is important to point out that the use of preservative-treated timber is frequent or even mandatory. These preservatives usually contain components such as copper, such as the traditional Copper Chrome Arsenate (CCA), which is strongly corrosive to metal fasteners [9]. As timber bridges are in service class 3 conditions, moisture increases the corrosion rate of fasteners embedded in treated timber. Thus, experts recommend the use of stainless-steel fasteners, specifically those made of A4 austenitic stainless steel, to enhance the durability of such bridges [23].

Another consequence of timber bridges being exposed to the weather is the continuous swelling and shrinkage of wood due to the big variations in the surrounding humidity. These repeated movements along the service life of a bridge may cause fatigue failure on the more brittle carbon steel screws. The higher ductility and resilience of A4 austenitic stainless-steel screws may pose an advantage for resolving this issue, especially on the bridge decking [4].

6 CONCLUSIONS

This paper provided a preliminary examination of A4 austenitic screws as a better-suited structural fastener alternative for the design of timber bridges in comparison to traditional galvanized carbon steel screws. Monotonic and cyclic bending tests were conducted as per EN 409 and EN 14592 using partially threaded and fully threaded self-tapping screws of both materials and of varying diameters between 5 mm and 8 mm. Moreover, an analytical comparison between the screws of both materials was carried out using the beam notch reinforcement calculator of a structural design web tool. Finally, considerations were made regarding the relationship between fastener material and the durability of timber bridges.

The monotonic test results highlighted the enhanced static ductility of the A4 stainless steel screws towards the carbon steel ones for all diameters analysed. Average maximum bending angles are around 70% higher for carbon steel screw. No bending moment degradation was observed for the A4 stainless-steel specimens until the test end, whereas carbon steel specimens experimented post-peak softening until reaching rupture before finishing the test, suggesting a more brittle response.

The cyclic experiments yielded a primary insight into the low-cycle ductility class of screws made with both materials. Screws with 5 mm of diameter made of carbon steel did not pass the test for S3 ductility class because they broke before the final monotonic ramp finished. In contrast, A4 stainless steel screws passed the same test without issues. Contrary the initial result, screws with 6 mm of diameter of both materials were assigned to the low cycle ductility class S3. Given that this study involved a limited sample size, additional tests are necessary to draw more conclusive observations. Additionally, whole joint shear tests are strongly suggested to be carried out to be able to correlate their results with EN 14592 cyclic test.

The analytical comparison showed that, depending on the size of the beam and the dimensions of the notch, A4 stainless steel fully threaded screws are equivalent in performance to carbon steel fully threaded screws regarding shear and tension perpendicular to grain reinforcement of notched beams. If the lower mechanical strength and stiffness of A4 austenitic steel becomes a limiting factor in the design, it is recommended to study the possibility of adding more screws to benefit from its excellent long-term corrosion resistance.

To summarize, A4 austenitic stainless-steel screws might be a better fastener option than carbon steel screws for the design of timber bridges for the following reasons: superior corrosion resistance to (i) the most common preservative treatments used in timber bridges (also recommended by experts in the field) and (ii) the high-humidity related to service class 3 conditions and high-chloride content of coastal areas such as Australia and New Zealand; (iii) elevated static ductility and also possibly low-cycle ductility class. This enhanced property is crucial to endure the fatigue cycles of load and unload that a bridge is subjected throughout its service life. This is particularly important in earthquake-prone regions, where ductile connections are essential for dissipating as much energy as possible to preserve the integrity of the structure during seismic loading. The higher plasticity of A4 stainless steel screws gives more reliability when designing a lateral connection assuming dual-hinge failure modes of the Johansen formulas.

Finally, despite the higher initial cost involved, the potential long-term financial benefits of using A4 austenitic stainless-steel screws make a compelling case for their adoption.

ACKNOWLEDGMENTS

The authors gratefully acknowledge Daniel Moroder for providing relevant information for this article about the Onetai bridge project. The authors also thank Carmen Sandhaas and Henning Kunkel for facilitating key research information for curating this article.

REFERENCES

1. Rashidi, M., Hoshyar, A.N., Smith, L, Samali, B., Siddique, R., 2021. A comprehensive taxonomy for structure and material deficiencies, preventions and remedies of timber bridges. Journal of Building Engineering, v. 34, 101624. Elsevier, Amsterdam, Netherlands.
2. Singh, T. and Page D., 2018. Case studies on the history and use of timber bridges in New Zealand. Wood Material Science and Engineering, v. 13, no. 3, pp 159-166. Taylor & Francis, Abingdon, England.
3. NZTA, 2025. Bridges and structures. Retrieved from the New Zealand Transport Agency official website, https://www.nzta.govt.nz/roads-and-rail/bridges-and-structures/. Wellington, New Zealand.
4. Douglas, C., Moroder, D., Edwards, L., Buchanan, A., 2025. SH 26 Onetai stream bridge - The first modern timber bridge on a state highway in New Zealand in decades. Conference Proceedings 5th ICTB, Rotorua, New Zealand.
5. Dietsch, P. and Brandner, R., 2015. Self-tapping screws and threaded rods as reinforcement for structural timber elements – A state-of-the-art report. Construction and Building Materials, v. 97, pp 78-89. Elsevier, Amsterdam, Netherlands.
6. SNZ, 2022. NZS AS 1720:2022 Part 1: Design methods. Standards New Zealand, Wellington, New Zealand.
7. CEN, 2023. prEN 1995-1-1:2023, Eurocode 5: Design of Timber Structures. Part 1-1: General. Common rules and rules for buildings. European Committee for Standardization, Brussels, Belgium.
8. CEN, 2023. prEN 1995-2:2023, Eurocode 5: Design of Timber Structures. Part 2: Bridges. European Committee for Standardization, Brussels, Belgium.
9. Zelinka, S.L., Glass, S.V., Derome, D., 2014. The effect of moisture content on the corrosion of fasteners embedded in wood subjected to alkaline copper quaternary treatment. Corrosion Science, v.83, pp 67-74. Elsevier, Amsterdam, Netherlands.
10. CEN, 2022. EN 14592:2022, Timber structures. Dowel-type fasteners. Requirements. European Committee for Standardization, Brussels, Belgium.
11. Izzi, M. and Polastri, A., 2019. Low cycle ductile performance of screws used in timber structures. Construction and Building Materials, v. 217, pp 416-426. Elsevier, Amsterdam, Netherlands.
12. Cervio, M. and Muciaccia, G., 2018. Low-cycle behavior of wood screws under alternating bending. European Journal of Wood and Wood Products, v. 78, pp 41-52. Springer, Heidelberg, Germany.
13. CEN, 2009. EN 409:2009, Timber structures. Test methods – Determination of the yield moment of dowel type fasteners. European Committee for Standardization, Brussels, Belgium.
14. ETA, 2024. ETA-11/0024, EuroTec screws. Screws for use in timber constructions. European Technical Assessment, Copenhagen, Denmark.
15. EOTA, 2019. EAD 130118-00-0603, Screws for use in Timber Constructions. European Organisation for Technical Assessment, Brussel, Belgium.
16. Hossain, A., Danzig, I., Tannert, T., 2016. Cross-Laminated Timber Shear Connections with Double-Angled Self-Tapping Screw Assemblies. Journal of Structural Engineering, v. 142, 16. ASCE, Reston, USA.
17. Carbon And Alloy Steels Committee, 2014. SAE J403. Chemical compositions of SAE carbon steels. SAE International, Troy, USA.
18. CEN, 2014. EN 1088-1:2014, Stainless steels. Part 1: List of Stainless Steels. European Committee for Standardization, Brussels, Belgium.
19. CLT Toolbox, 2025. Structural timber design software. Accessible from https://clttoolbox.com/ Melbourne, Australia.
20. ASH, 2019. Glulam AU/NZ vs Europe. Retrieved from the Australian Sustainable Hardwoods website, https://ash.com.au/blog/gl-au-nz-vs-europe/. Heyfield, Australia.
21. Steilner, M., Kunkel, H., Sandhaas, C., 2022. Low cycle ductility of self-tapping screws. Conference Proceedings 10th International Network on Timber Engineering Research: Meeting 55, Paper 55-7-5. Bad Aibling, Germany.
22. Blaß, H.J., 2024. Expert's Report. Low cycle ductility classes for Würth screws. KIT, Karlsruhe, Germany.
23. Li, Z., 2009. Corrosion of fasteners. Build Magazine, August/September, pp 47-48. BRANZ, Porirua, New Zealand.

ICTB 2025. 5th International Conference Timber Bridges
Rotorua, New Zealand, 29 June to 2 July 2025.

SUSTAINABLE SPANS - TIMBER'S ROLE IN NEW EUROPEAN PEDESTRIAN AND CYCLING NETWORKS

Frank Miebach[1], Lukas Osterloff[2]

ABSTRACT

Modern timber bridges represent a groundbreaking lever for CO2 reduction in the infrastructure sector. The capabilities and benefits of these innovative structures will be demonstrated through three current examples of modern timber bridge projects in Europe.

1 INTRODUCTION

The transport sector plays a significant role in global CO2 emissions. Worldwide, increasing measures are being implemented to promote cycling and pedestrian traffic to reduce CO2 emissions caused by motorized individual transport. One of the most effective measures is the creation and improvement of cycling paths in the daily lives of citizens. In this context, crossings in the form of bridges are often constructed. The construction of these bridges using modern timber construction represents a particularly consistent and sustainable measure for reducing CO2 emissions in the slow traffic sector. Three projects of modern timber bridges illustrate the architectural and technical possibilities of modern timber bridge construction in Europe: three pedestrian and cycling bridges as nodes of a new cycling network, a new pedestrian and cycling bridge over a highway for the 2024 Paris Olympics, and a greened railway station bridge in the centre of Zwolle in the Netherlands.

2 MODERN TIMBER BRIDGES IN EUROPE – DETAILING TO LONGIVITY

The construction of timber bridges in Europe is currently on the rise. Many countries have set the goal of reducing CO2 emissions in infrastructure projects and are increasingly using timber as a building material. To achieve truly sustainable timber bridges, the lifespan of the structures must be the focus. With the next generation of Eurocode 5, the design life of a protected timber bridge is set at 100 years.

To meet these requirements and adequately consider aspects such as maintenance and inspection, the constructively protected "block beam bridge" type has proven to be particularly suitable. For the load-bearing structure, one or more block-glued laminated timber beams are used. For permanent protection, a ventilated, water-bearing deck construction made of prefabricated panels is used, which reliably protects the timber structure through a combination of lateral overhang and a manufacturing-related gradation of the timber beams and at least 60° and allows classification in use class II.

These measures ensure that the load-bearing timber structure is permanently protected and a service life of 100 years is achievable. The bridge decks can be made of precast concrete elements, natural stone slabs, or timber-based materials with an additional sealing and covering layer. The prefabricated construction method also considers the dismantling and reuse of the individual components for other purposes, making subsequent uses possible compared to other construction methods. With these approaches, a new generation of timber bridges is emerging, reinterpreting insights from several centuries of timber bridge construction to meet current needs for resource-efficient infrastructure.

[1] Dipl. – Ing. (FH) Frank Miebach, IB-Miebach,
e-mail: frank.miebach@ib-miebach.de
[2] B.-Ing. Lukas Osterloff

Figure 1 Neckarbrücke Wernau, left 1989 after erection (Schaffitzel), right 2025 (Miebach)

The concept of the block beam bridge with a water-bearing deck dates back to the 1980s in Germany. One of the oldest constructions of this type spans the Neckar River in the city of Wernau. This bridge demonstrates that this type of construction stands the test of time and serves as a model for sustainable solutions and was design by Milbrand/Sengler. Further evidence is provided by research projects from the Bern University of Applied Sciences in Switzerland, the University of Applied Sciences Erfurt, and the FH Aachen. Various research projects[3,4,5] have proven that the assumptions about the moisture behaviour of protected timber bridges consistently align with the assumptions of use class II, ensuring an average equilibrium moisture content of the timber components below 20%, thereby eliminating the risk of wood-destroying fungi.

3 MODERN TIMBER BRIDGES IN EUROPE – A RECENT SELECTION

3.1 New cycling bridges in Frankenberg (Eder), Germany

In the town of Frankenberg (Eder), Germany, three large cycle bridges spanning the River Eder have been constructed using modern timber construction techniques, ranging in length from 60 to 95 meters. These bridges have created a completely new cycling network, connecting various neighbourhoods in innovative ways. Each bridge features a dynamic cross-section that enhances slenderness over the river. The primary structure comprises two curved glulam beams with a trapezoidal cross-section, supporting decks made of large precast concrete slabs on a wooden substructure. A 1.0% side slope ensures effective drainage, and an epoxy resin coating provides a non-slip surface.

Figure 2 Brücke Wehrweide, Frankenberg (Eder) by Peter Beckmann

[3] Müller, Franke, Franke (2014): Langzeit-Monitoring von Holzbrücken – Erkenntnisse zum Feuchteverhalten im Tragquerschnitt

[4] Simon, Jahreis, Arndt, Koch (2019): Development of unified guidelines for design, construction, maintenance and inspection for structurally protected timber bridges

[5] Uibel, Moorkamp, Peterson (2022): Nachhaltige Holzbrücken für Geh- und Radwege

3.1.1 Concept

As part of the comprehensive modernization program "Frankenberg 2020," the 60-meter-long block beam bridge "Wehrweide" represents the central core element of the new cycling traffic concept and was the initial spark for an entire family of bridges. As a hub of the new attractive cycling traffic axis, it creates – now completed by the two sister bridges "Ederdorf" and "Wildpark" of the same construction type with lengths of 80 and 90 meters – short, safe, and nature-oriented connections between living, working, and leisure.

Always focusing on sustainability: the two-span and multi-span structures of the bridges are climate-friendly constructions due to their timber construction, as the total of 700 m³ of laminated timber used stores approximately 700 m³ of CO_2, making the bridges virtually "climate-neutral." Where the bridge and path construction intervened in the natural environment, it had a positive impact: with the renaturation of Eder tributaries and streams, the creation of perennial beds, nesting aids for waterfowl, accompanying flood protection, and much more. The integration of local mobility, urban development, sustainability, nature experience, environmental and species protection has been successful.

3.1.2 Design

The bridge layout of the designs follows the direction of the planned cycling connections in an arc shape, creating a harmonious route. The natural material of the structure is highlighted by the elegant design with stepped side surfaces and dynamic cross-sections. Due to the curvature of the bridge body, appealing views from different perspectives are created, and the bridges gain increased visibility. A crucial requirement for the planning and construction of the bridges was their accessibility.

3.1.3 Structure/Construction

The superstructure consists of two symmetrical block beams of quality GL28h (Si) with dynamic cross-section height. The geometries of the individual beams were developed with regard to manufacturability and transportability. A longitudinally movable Gerber joint in the foreland field limits the component lengths to standard transport dimensions. The coupling of the cross-sections is done via steel frames with head plate joints. The frames are connected to the timber beams with fully threaded screws. It was considered in the planning that only steel-to-steel connections need to be made on-site, and the complete timber beam assembly could be carried out in the factory. Overall, the construction has a tolerance of ± 15 mm, requiring high precision in the manufacture of the substructures and superstructures.

3.1.4 Laminated Timber Beams

The symmetrical spans result from the arrangement of the bridge piers. The laminated timber beams themselves are biaxially curved and stepped. The precise block gluing of the two beams in different lengths and widths results in dynamic cross-section heights between 50 cm and 1.84 cm, with the greatest expansion over the piers. This manufacturing method guarantees minimal waste with optimal material utilization.

Figure 3 Single elements before block lamination by Schaffitzel

3.1.5 Abutments and Bearings

To achieve particularly robust and durable abutments at the bridge ends while also implementing a design-corresponding element, the foundations were designed with a 45° inclined surface. This guarantees timber construction-appropriate safety against waterlogging and vertically picks up the tapered bridge beam shape. The bridge is supported on the piers with classic elastomer bearings. At the abutments, steel bearings with hinge bolts were used, integrated into the beam structure. Underside maintenance openings allow for easy inspection.

3.1.6 Deck and Parapet

The railings consist of V-shaped flat steel posts with a filling of horizontal stainless steel cables. Accoya laminated timber was chosen for the upper railing finish. An additional stainless steel round tube complements the railing for barrier-free use. LED spots were arranged within the tube to illuminate the bridges at night. Through intelligent control, this lighting is reduced to a minimum and dimmed together with the street lighting. To ensure a non-slip surface, the concrete slabs were coated with epoxy resin and fine gravel. This method was also applied to the adjacent asphalt surfaces, increasing their durability and achieving the appearance of a bound gravel surface that blends subtly into the floodplain landscape. The resulting low surface temperatures in winter provide an additional advantage for the fauna.^

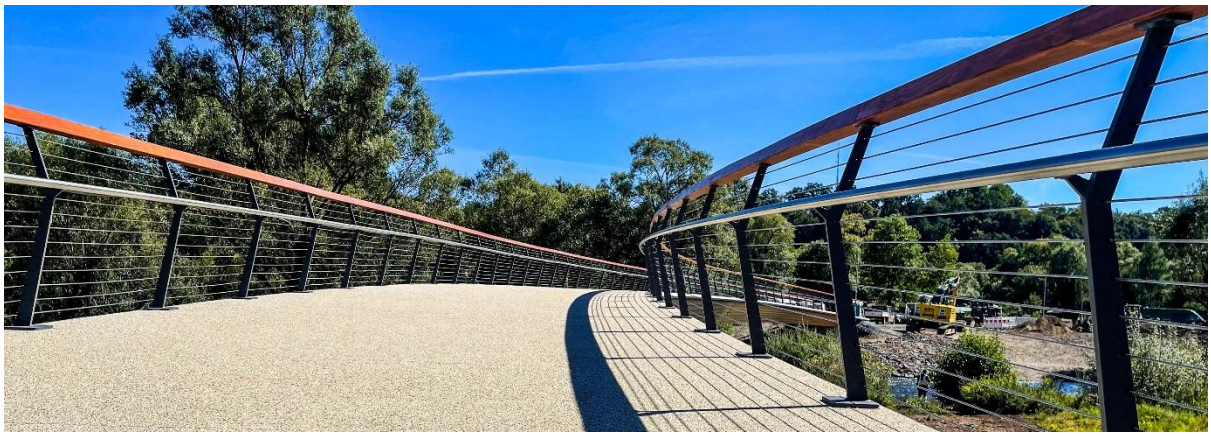

Figure 4 Bridge Deck Wildpark by Peter Beckmann

3.1.7 Timber Protection Concept

The execution as a protected timber bridge according to DIN EN 1995-2 is achieved through the use of a water-bearing deck made of prefabricated concrete elements of quality C50/60 with easily transportable dimensions. The deck slabs, which can bear loads of up to 12 tons, are placed on a ventilation layer made of construction timber and underlaid with corrosion-resistant channels in the joint areas. A vapor-permeable membrane on the timber beams provides additional safety. The deck width increasing towards the center ensures sufficient splash protection, even in the area of the increased structure height over the pier. These measures allow for the complete avoidance of chemical wood preservatives.

3.1.8 Lifespan

As a result, the timber remains visible as the defining material but is sustainably protected and low-maintenance. The assumed high lifespan of the bridges is thus comparable to that of a structure made of steel, reinforced concrete, or prestressed concrete. In the event of the bridge's dismantling, non-destructive disassembly is also ensured, making all components suitable for reuse.

3.1.9 Bridge Family

The "Wehrweide" bridge set the precedent for the construction type of the three nodes of the local mobility traffic concept. With lengths of 60, 80, and 95 meters, they now form the core of the measures

of the modernization program to connect the city and nature, creating a sustainable effect for the local mobility of the region and simultaneously being a novelty in Hesse's cycling infrastructure. Until now, funding for timber bridges through the local mobility program was not permitted, as conventional timber bridges had too short lifespans. With the constructively protected design realized here, the client HessenMobil was able to fully convince and thus make an important contribution to sustainable infrastructure construction in Hesse.

3.1.10 Wehrweide

The timber bridge "Wehrweide," planned as a replacement for a non-renovatable predecessor bridge, was the beginning and guarantees equivalence in its lifespan with steel or concrete bridges with the protected construction according to DIN EN 1995-2.

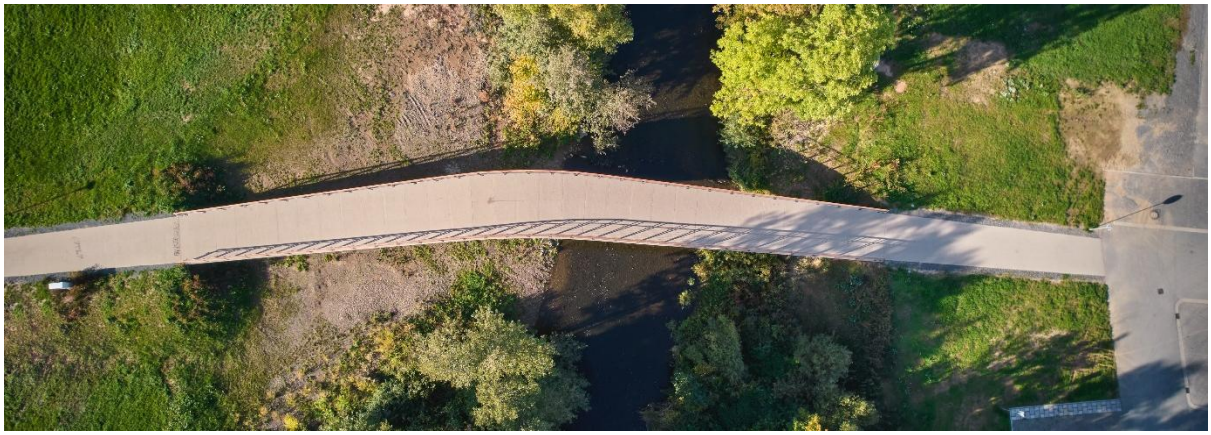

Figure 5 Airal View Bridge Wehrweide by Peter Beckmann

3.1.11 Wildpark

With a span of 80 meters over two fields, this "sister structure" is 20 meters longer than the Wehrweide bridge. Its cross-section follows the same principle: two doubly curved block beams, covered with a concrete deck, create a generous crossing aid. Due to the larger individual spans, the beams were connected with rigid joints.

Figure 6 Underside Bridge Wildpark by IB Miebach

3.1.12 Ederdorf

The largest of the three bridges is named "Ederdorf" and is approximately 95 meters long. It spans two fields and, thanks to its particularly strongly curved course, provides a flood-optimized connection of the paths with a ramp arranged parallel to the Eder.

Figure 7 Sideview Bridge Ederdorf by Peter Beckmann

3.2 New cycling and pedestrian bridge in Paris, France for the Olympic games 2024

Figure 8 Rendering Exploration Architecture

Following a successful competition entry with our French partners Exploration Architecture and AIA Life designers for a "Design and build" project of a bicycle and pedestrian bridge for the Paris 2024 Olympics, this bridge has been realized as part of infrastructure improvements in 2023 and 2024. Spanning the French A1 highway, the bridge connects the Media Village and Sports Complex in Le Bourget. It is based on a simple and cost-effective but iconic design that ensures durability and low maintenance due to thoughtful structural wood protection. Specific requirements included fire resistance capabilities of up to 2 hours to meet fire safety standards.

3.2.1 The challenge of planning and implementation

The requirement for a 100m long bridge spanning more than 50m freely over the motorway made the choice of a suitable design challenging. Such spans are rare in timber bridge construction. Initial considerations with an overhead supporting structure in the form of an arch or pylon construction were postponed in favour of a block girder construction, as the solid and compact design has advantages: The structural timber protection can be easily ensured by the watertight decking, which is sufficiently cantilevered on the upper side. In addition, the cross-section of the bridge was designed in such a way that it tapers downwards in a 30° line from the vertical. This means that the structure is considered a protected structure in accordance with EC1995-2. Chemical wood protection is irrelevant.

Furthermore, the high fire protection requirement for stability after a 2-hour fire event can be easily met with such a full cross-section. With a burn-off rate of 1.2 mm/min, this results in a circumferential cross-section loss of 144 mm after 120 minutes. (Special tests by the CERIB laboratory) This must therefore be added during production.

The two-part support structure, consisting of French Douglas fir wood in GL24h, was manufactured by the Simonin company in eastern France.

The waterproof concrete decking with asphalt covering lies on cross battens made of Douglas fir wood and is ventilated. Two additional empty conduits were integrated in the centre of the bridge.

Figure 9 Detail Ridges Joint

The favoured short transport lengths of the beams to the cramped construction site next to the motorway posed a particular challenge. The 100 metre long construction was divided into five segments in the longitudinal direction and the cross-section was divided into two in the transverse direction. The connection of the components by means of glued-in threaded rods and steel brackets proved to be very easy to assemble. This connection, which the Simonin company has patented under the name "Resix", allows blunt component joints that can be quickly assembled on site using a steel-to-steel connection.

To ensure fire protection, the connection areas were subsequently sealed with wooden inserts and 2x 20 mm "Weather Defence" Gypsum board.

3.2.2 The Result

Figure 10 Bridge Mounting by IB Miebach

The wooden supporting structure was installed on schedule at the beginning of August 2023 in six nightly shutdowns of 6 hours each. The decking followed at the end of 2023, well secured by protective scaffolding above the flowing traffic.

The two inclined intermediate pillars in prefabricated reinforced concrete construction are a special design feature. Pre-assembly took place on site in vertical alignment. After striking the formwork, the piers were lowered into their inclined position. The inclination of the piers has the advantage that the span width was reduced and the foundations could be laid in the undisturbed area.

The resulting geometry creates a design dynamic that figuratively emphasises the compact supporting structure towards the growing intermediate supports.


Figure 11 Completion March 2024

3.3 An elevated street for the trans station Zwolle in the Netherlands


Figure 12 Rendering Bridge Concept by Karres en Brands

One of the largest timber bridges in Europe is currently being constructed in the Dutch city of Zwolle. The bridge features a deck area of over 1,200 m² and will have a park-like surface combining greenery with paved walkways and recreational areas. The main structure consists of four parallel glued laminated timber beams, which support the decking designed as a green roof on a cross-laminated timber base. All exposed components are made of steel or concrete to ensure a lifespan exceeding 80 years in an urban setting. Access to the bridge is provided through staircases on three sides and elevators, with their carrying structures also made of timber. The bridge will be opened for the public in 2025.

3.3.1 Planning community and vision

The planning team consisting of landscape architects Karres en Brands from Hilversum (NL) and urban design specialists IPV Delft (NL) was put together with the support of Wouter Kolijn and commissioned to plan the bridge in 2020. The work was carried out in close collaboration, which was also characterised by the Covid pandemic. In order to enable good visual cooperation, more use was made of tools such as virtual reality and a large number of live visualisations during the planning phase.

Together, the vision of an "Elevated Street" was developed. A bridge that meanders over the railway tracks like an elevated street with lush greenery. The result is a bridge with a length of approx. 130 metres with stairs on both sides, which is characterised by a park-like design that, in addition to being used by pedestrians, allows sufficient space for intensive greening over a width of 10 metres.

3.3.2 Planning challenge

In addition to the technical and design requirements, a long-term schedule with pre-determined closure times for the tracks to be bridged had to be taken into account when developing the initial sketches. The

assembly of the main structure had to be completed within 100 hours so as not to obstruct the important transport hub in the north of the Netherlands any longer.

In addition, the existing structures in the construction area had to be handled with great care, so that the route of the bridge had to be optimised over several stages.

In addition to the span widths of over 34.0 metres and the short assembly time, the development of a cross-section with a planned service life of 100 years in timber construction with the inclusion of a deck structure as a green roof was also a priority. In order to fulfil these requirements, a redundant system consisting of four solid block-bonded timber beams made of GL28h (spruce) was chosen. The beams are coupled via steel frames and covered with a ventilated cross laminated timber decking structure. The cross laminated timber layer is only used to absorb the loads from the superstructure, so that it can be replaced at any time. A full-surface monitoring system had to be integrated to enable monitoring of the two-layer EPDM seal on the CLT layer.

Figure 13 Rendering Bridge Concept by Karres en Brands

As part of the structural design, special requirements had to be checked at an early stage. For example, the bridge was designed for a train fire scenario, which posed a particular challenge for the steel couplings. By carefully positioning these elements and protecting some of the steel parts with timber panelling, a redundant system was developed that could also meet the requirements for progressive failure.

Due to the high complexity of the structure, the structural design of the timber superstructure was supervised by IB-Miebach until realisation and transferred in parallel to a BIM model, which now represents the digital twin of the almost completed bridge.

3.3.3 Challenges of structural realisation

Figure 14 Test Mounting by Schmees und Lühn

The Dutch company Dura Vermeer was entrusted with the realisation of the project together with the North German timber bridge specialists from Schmees and Lühn.

The massive dimensions and complex geometries of the bridge alone presented a particular challenge for all the companies involved. Thanks to highly detailed planning, test assembly and precise production - also by the suppliers of the glulam beams, Schaffitzel Holzindustrie and Wiedmann Holzleimbau - assembly could be realised within the given time frame.

It needs to be emphasised that the precision required during production far exceeded the normative requirements. Tolerances of just a few millimetres had to be sufficient for the assembly of a length of over 130 metres. To ensure this, the main structure was already assembled in the factory for testing, taking into account the exact position of the supporting structures. With the knowledge gained from this, the assembly could be realised within the tight time frame without any major obstacles, whereby the transport and the dimensioning of the mobile cranes had to be carried out close to the limits of feasibility.

3.3.4 Result

The overall structure of the bridge is currently still under construction, although the timber structure and the superstructure have already been completed apart from the bridge deck. The bridge is accessed by three staircases - which were designed in steel for reasons of durability - and three lifts, which are characterised by a shaft construction in timber.

Figure 15 Completion by Schmees und Lühn

4 CONCLUSIONS FOR THE USE OF TIMBER IN LARGE SCALE INFRASTRUCTURE PROJECTS

Timber is becoming an increasingly crucial component of infrastructure projects due to its significant advantages in reducing CO2 emissions, speeding up construction, and enhancing aesthetics and user identification. The three examples showcased illustrate what is already achievable with timber and provide a glimpse into the future of timber in infrastructure projects.

These European examples should be an important inspiration for infrastructure buildings around the world, as they fulfil complex new infrastructure tasks by using the resource-saving building material wood, which in itself already makes an important contribution to a sustainable transport transition through new user behaviour. It should be emphasized that wood is not only becoming more interesting for cycle path bridges, but also for road bridges.

ICTB 2025. 5th International Conference Timber Bridges
Rotorua, New Zealand, 29 June to 2 July 2025.

EFFECTS OF BROWN-ROT DECAY AND CORROSION ON POLYMER COMPOSITION OF RADIATA PINE CONNECTORS

Camilo Montoya[1], Lisa-Mareike Ottenhaus[2], Tripti Singh[3] , Jeffrey J Morrell[4], Luis Yermán [5]

ABSTRACT: Moisture and associated deterioration affect the performance of timber joints which in turn can affect the integrity of timber bridges. High levels of moisture promote fastener corrosion altering the chemical environment in wood. This modified environment can promote fungal growth which leads to significant changes in connector performance, even during early decay stages. However, the role of the metal (corrosion) in decayed connectors remains poorly understood. This study investigated the localized effects around galvanized and stainless steel nails on brown-rot (*Fomitopsis ostreiformis*) degradation of radiata pine (*Pinus radiata*) sapwood during early decay stages (up to 10% mass loss). Fourier Transform Infrared (FT-IR) spectroscopy was used to compare chemical changes at the wood-metal interface with those away from the metal. Both fastener types accelerated carbohydrate degradation, likely due to metal ion release (Zn and Cr, respectively). Lignin modification was minimal, consistent with brown-rot decay. Although stainless steel influenced the wood chemical environment, the impact was more pronounced in galvanized specimens due to available corrosion products for fungal growth. These findings highlight the critical, localized role of the fastener material in wood decay which could be useful for developing more durable timber structures, including timber bridges. Further investigations using complementary techniques (pH measurement, chemical analysis, microscopy) are recommended to explain the underlying mechanisms.

KEYWORDS: Wood connections, fungal decay, FT-IR, corrosion.

1 INTRODUCTION

Timber connectors play a crucial role in bridges, by connecting elements and transmitting forces. One common connector type is the nail, especially for fastening bridge decking. Nails can be made from steel, iron or aluminium [1], and can be coated with other metals (zinc or chromium) to protect the nail against environmental factors [2]. Fasteners can be differentiated by the way the force is transmitted between the fastener and the wood. For example, wood fibres are compressed once a nail is driven into the wood. The capacity of this connection is often attributed to the compression of wood at the wood-metal interphase (Figure 1) [3].

Timber bridges are exposed outdoors to variable environmental conditions which can limit their lifespan [4]. There are numerous mechanisms deteriorating timber bridges, but moisture is the most important as it subsequently impacts other deterioration mechanisms [5]. Wood is an orthotropic and hygroscopic material whose strength properties are highly dependent on moisture content [6]. This is also applicable to timber connectors, as metal fasteners can create localized conditions for moisture accumulation.

Moisture accumulation around metal fasteners can trigger corrosion [7]. This process causes a gradual deterioration of the connection due to degradation of the metals [8]. The acidic nature of most woods also affects corrosion, changing the chemical environment of the adjacent wood [9]. Corrosion is categorized as atmospheric or crevice corrosion [10]. Although having different mechanisms, both affect the wood chemical environment. Atmospheric corrosion is localized in the fastener area exposed to the air as oxygen is the primary oxidant. This oxidation leads to accumulation of metal ions at the wood surface which can

[1] Camilo Montoya, The University of Queensland, Australia, https://orcid.org/0000-0003-3226-736X
[2] Dr Lisa-Mareike Ottenhaus, The University of Queensland, Australia
[3] Prof Tripti Sign, National Centre for Timber Durability & Design Life, Australia
[4] Prof Jeffrey J Morrell, Oregon State University, United States of America
[5] Dr Luis Yermán, The University of Queensland, Australia

migrate into the wood around the embedded fastener, causing crevice corrosion. However, crevice corrosion inside the gap between the fastener and wood can occur without atmospheric corrosion. A key attribute of crevice corrosion is the quick oxygen depletion occurring at the wood-metal interphase, leading to changes in the corrosion process as the environment becomes more acidic, degrading the metal much faster than regular atmospheric corrosion.

The impact on the wood chemical environment also varies with the fastener material [11]. For instance, galvanized nails protected by a zinc coating release zinc ions when wetted. Stainless steel, with its high chromium content and passive oxide layer (more corrosion-resistant) can still degrade when wet and release chromium. Both metals react differently with the acidic environment in the wood depending on exposure time [12]. The zinc layer corrodes easily, but does not directly degrade wood; instead, it promotes degradation by other mechanisms as it provides metals ions that accelerate growth by bacteria or fungi. The chromium layer is corrosion resistant and requires more exposure time to be degraded in similar wet environments. Chromium ions can react with wood components, altering and degrading the chemical structure, potentially creating an easier path for fungal degradation.

Fungal growth requires specific conditions including high moisture levels, and acidic environments [13]. Fungi produce enzymes that lower the pH of the wood for easier depolymerisation of components. In some instances, both corrosion and decay can occur simultaneously in timber joints. The modified chemical environment created by the corroded fastener can promote fungal growth [14]. These conditions might also affect growth patterns [15], connector performance [16] and, accelerate both decay rates and fastener corrosion [17]. A 50% loss in mechanical performance can occur even in early, visually undetectable decay stages [18]. This reduction is often attributed to the fungal degradation of wood components (cellulose, hemicellulose and lignin). Despite this, studies evaluating effects of decay on timber connections are limited.

While the general effects of fungal decay on wood chemistry are well-studied [18], the localized impacts of different fastener materials at the wood-metal interface in decayed wood are less understood. This study used Fourier Transform Infrared (FT-IR) spectroscopy to analyse the effects of galvanized and stainless steel fasteners on brown-rot degradation of timber connectors.

2 EXPERIMENTAL

2.1 Sample preparation and fungal exposure

Smooth shank (2.8 mm diameter) stainless steel (non-corrosive) and hot-dip galvanized (corrosive) nails were driven across the grain into pre-drilled holes in *Pinus radiata* sapwood blocks (440 ± 50 kg/m³, 30 x 35 x 70 mm³). A total of 180 blocks were prepared. Specimens were exposed to the brown-rot fungus *Fomitopsis ostreiformis* following the incubation and inoculation processes described in Montoya et al. [16]. Control specimens (without fasteners) were used to determine sampling points (35, 70, 105, and 140 days) based on targeted mass losses (approx. 0.51%, 2.85%, 6.96%, and 10.57%, respectively). FT-IR analysis was performed on a subset of 24 specimens (3 per exposure period per fastener type).

Figure 1. Subject specimens depicting wood-metal interphase.

2.2 Sample collection and measurement

For FT-IR analysis, thin wood sections (~1 cm^2) were extracted from the wood-metal interface ("near" zone) and a location 1-2 cm distant ("away" zone) (Figure 1). Three points per section were analysed by FT-IR, and the spectra were averaged and normalized for comparison of relative peak intensities. Due to the small sample size (n=3 per group), statistical analysis was not performed; results are presented as observed trends. The reproducibility of spectral trends across replicates enabled the presentation of a single representative spectrum for each condition presented in Figures 2 to 5. The objective was to identify subtle chemical changes in the early stages of fungal decay for each type of fastener material.

2.3 FT-IR analysis

FT-IR spectroscopy is a useful technique for investigating the chemical alterations occurring in wood during fungal biodegradation [19]. The spectra region between 800-1800 cm^{-1} is known as the "fingerprint" of wood [20]; it shows alterations in the intensity and position of peaks, indicating the breakdown of wood components due to decay and corrosion byproducts. The existing literature on radiata pine [21] was used to segment the spectral data into three regions (Table 1) for targeted analysis.

Table 1. Analysed FT-IR spectra regions

Assignment	Spectra region (cm^{-1})
Carbohydrates (cellulose and hemicellulose)	985 - 1160
Lignin	1510 - 1660
Water/Oxidation	1660 - 1800

3 RESULTS AND DISCUSSION

3.1 Carbohydrate Regions

The carbohydrate region is mainly composed of cellulose and hemicellulose. Cellulose provides strength to the wood [22]. Analysis of the carbohydrate region, reflecting cellulose and hemicellulose degradation, revealed distinct trends related to fungal exposure and fastener material. Carbohydrate degradation was observed after 35 days of exposure, despite minimal mass loss. Both fastener types enhanced early carbohydrate degradation at the near zone compared to away zone, but the effect was more pronounced in galvanized specimens, especially after 35 and 70 days. At this stage, significant loss of connector performance has been reported [16]. The greater spectral differences between wood near and away from galvanized fasteners suggest that corrosion products [8] accelerated carbohydrate breakdown [20]. While stainless steel experienced minimal corrosion, results still indicated an influence on decay, likely via metal-fungus-wood interactions [14].

The intensity differences between near/away zones from galvanized fasteners diminished after 105 days. This suggests either propagation of the initially localized accelerated degradation or migration of metal ions/reaction influence on wood chemistry further away from the fastener. In contrast, stainless steel samples showed increased near/away differences after 105 days, reinforcing the role of metal ions in accelerating decay, even without corrosion [9].

3.2 Lignin Regions

Lignin provides stiffness to the wood and a barrier against decay [22]. Minimal changes were observed in this region, indicating that lignin was largely unaffected, consistent with brown-rot fungi's preference for degrading carbohydrates over lignin [23].

Lignin near the water/oxidation region exhibited minor differences between near/away zones for galvanized specimens after 70 days of exposure. However, the lack of marked intensity or wavenumber shifting suggests these variations were not primarily due to lignin modification but from decay-associated oxidation [13] or interactions with metal-related ions [12]. In contrast, differences were evident in the stainless steel in the near/away zone after 140 days exposure, further supporting the different effects or pathways affecting wood environment.

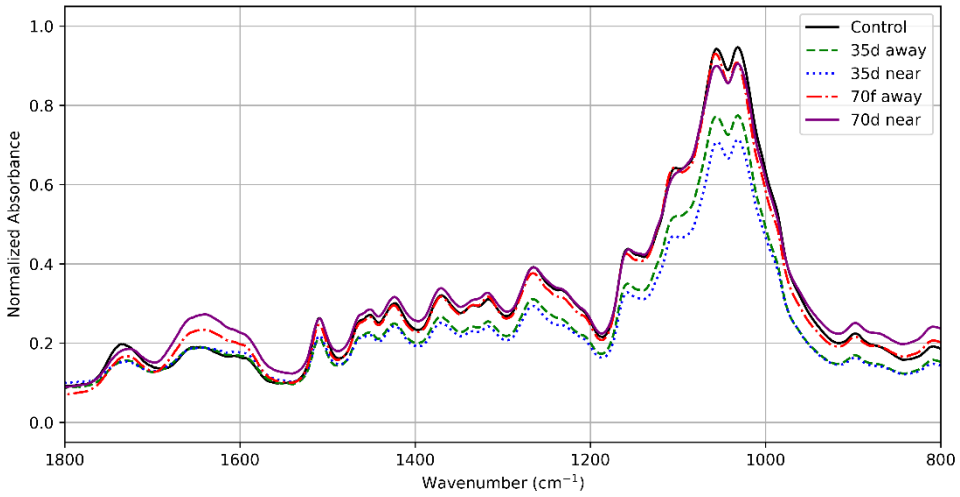

Figure 2. FT-IR spectra of wood adjacent to and 1-2 cm away from a galvanized connector exposed to a brown-rot fungus for 35 days (35d) and 70 days (70d)

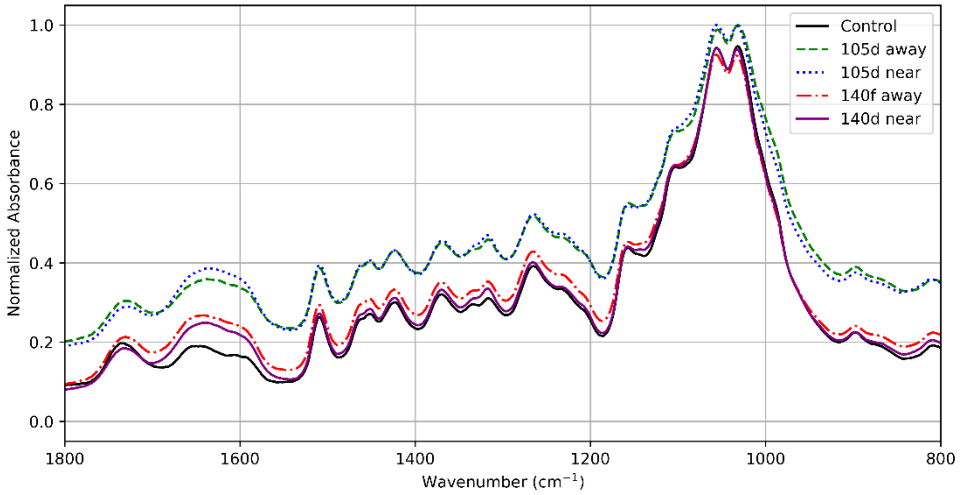

Figure 3. FT-IR spectra of wood adjacent to and 1 to 2 cm away from a galvanized connector exposed to a brown-rot fungus for 105 days (105d) and 140 days (140d)

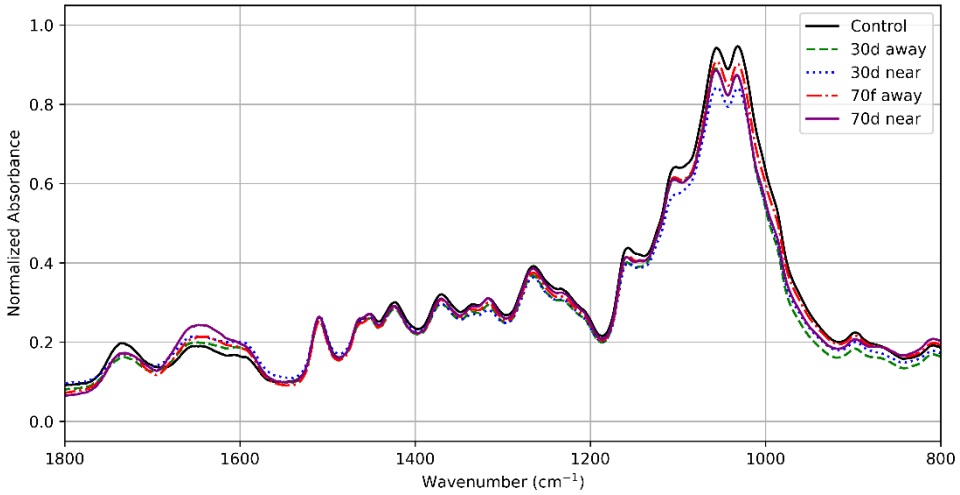

Figure 4. FT-IR spectra of wood adjacent to or 1 to 2 cm away from a stainless steel connector exposed to a brown-rot fungus for 35 days (35d) and 70 days (70d)

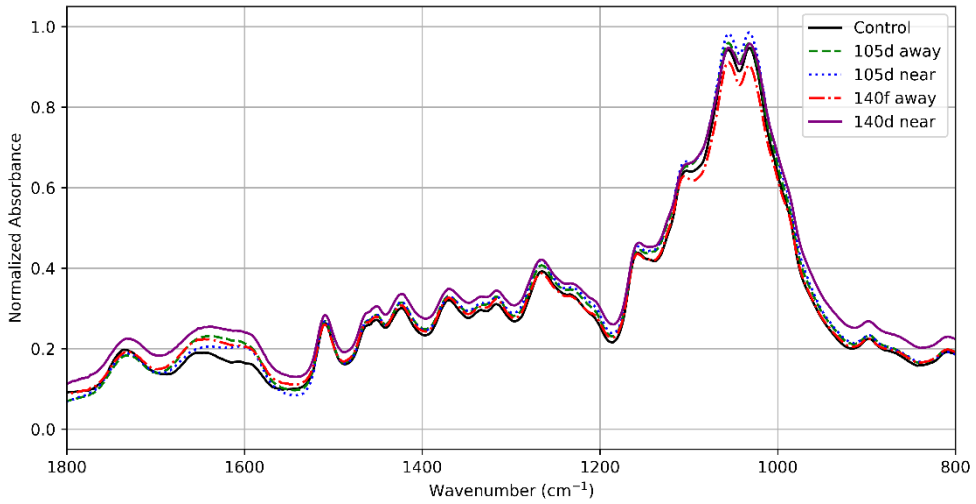

Figure 5. FT-IR spectra of wood adjacent to or 1 to 2 cm away from a stainless steel connector exposed to a brown-rot fungus for 105 days (105d) and 140 days (140d)

3.3 Water/Oxidation Regions

Moisture plays a crucial role in wood strength and decay. Moisture-induced corrosion of timber connectors significantly affects withdrawal performance [7]. Both specimen types showed spectral changes in this region, in both band shape and intensity, from the early stages of exposure, with curve shape deformations becoming more pronounced over time. While water interactions may have contributed to these alterations, the increased intensity relative to the control suggests metal ion accumulation (Zn and Cr) [14].

Absorbance values later in the fungal exposure converged between areas near/away from the fasteners, indicating a homogenization of chemical changes. While initial differences diminished over time, the distinct influence of corroded galvanized over stainless steel fasteners remained evident. These changes were linked to increased connector performance [16], contradicting previous findings [7].

These contrasting, time-dependent, and location-dependent behaviours highlight a complex interaction between the wood, the presence of metal fasteners, and fungal activity. The underlying chemical processes were clearly influenced by both spatial proximity to the fasteners and the duration of exposure.

4 CONCLUSION

This study revealed that both galvanized and stainless steel fasteners impacted the early stages of brown-rot decay in radiata pine, creating localized chemical changes at the wood-metal interface. Both fastener types accelerated the degradation of wood carbohydrates, a key factor in timber strength reduction. However, galvanized fasteners, due to their corrosion byproducts, exhibited a greater and more direct acceleration of wood degradation

Future research should employ complementary techniques (e.g., chemical analysis, microscopy, pH measurements) to explain the mechanisms linking wood degradation and connector performance. The use of corrosion-resistant materials may effectively delay fungal activity in the early stages in comparison to corrosive materials, thus enhancing the durability and longevity of timber bridges.

5 ACKNOWLEDGEMENT

This research was supported by the National Centre for Timber Durability and Design Life (Professor Dr. Tripti Singh, Director), a collaborative research program at the University of the Sunshine Coast, The University of Queensland, and the Queensland Department of Primary Industry.

6 REFERENCES

1. C. Brischke and G. Alfredsen, *Mechanical Connections in Wood Structures*, 84th ed. New York: American Society of Civil Engineers, 1996.

2. N. Kip and J. A. van Veen, “The dual role of microbes in corrosion,” *ISME J*, vol. 9, no. 3, pp. 542–551, Mar. 2015, doi: 10.1038/ismej.2014.169.
3. T. Claus, W. Seim, and J. Küllmer, “Force distribution in self-tapping screws: experimental investigations with fibre Bragg grating measurement screws,” *European Journal of Wood and Wood Products*, vol. 80, no. 1, pp. 183–197, Feb. 2022, doi: 10.1007/s00107-021-01740-z.
4. D. Goodman and D. Tingley, “Timber Bridges in Local Government-Part of the Solution not the Problem,” in *2017 IPWEAQ Annual Conference Proceedings*, Institute of Public Works Engineering Australasia Queensland, Oct. 2017.
5. F. Abdoli, M. Rashidi, J. Wang, R. Siddique, and V. Nasir, “Structural health monitoring of timber bridges – A review,” Dec. 01, 2024, *Elsevier B.V.* doi: 10.1016/j.rineng.2024.103084.
6. D. R. Rammer and S. G. Winistorfer, “Effect of Moisture Content on Dowel-bearing Strength,” *Wood and Fiber Science*, vol. 33, no. 1, pp. 126–139, 2001.
7. L. Yermán, Y. Zhang, J. He, M. Xiao, L. M. Ottenhaus, and J. J. Morrell, “Effect of wetting and fungal degradation on performance of nailed timber connections,” *Constr Build Mater*, vol. 353, Oct. 2022, doi: 10.1016/j.conbuildmat.2022.129113
8. S. L. Zelinka, “Corrosion of Metals in Wood Products,” in *Developments in Corrosion Protection*, InTech, 2014, pp. 567–592. doi: 10.5772/57296.
9. R. H. Farmer, “Corrosion of Metals in Association with Wood,” in *Chemistry in the Utilization of Wood*, Elsevier, 1967, pp. 92–108. doi: 10.1016/B978-0-08-012137-6.50012-7.
10. A. J. Baker, “Degradation of wood by products of metal corrosion,” 1974.
11. A. Wahyudianto, A. Fernandes, Erwin, and Wajilan, “Metal corrosion in wood joint products and structures: a review,” *International Journal of Corrosion and Scale Inhibition*, vol. 11, no. 3, pp. 1269–1281, 2022, doi: 10.17675/2305-6894-2022-11-3-21.
12. R. D. Graham, M. M. Wilson, and A. Oteng-Amoako, “Wood-Metal Corrosion: An Annotated Survey,” 1976.
13. Winandy. J.E. and J. J. Morrell, “Relationship Between Incipient Decay, Strength, and Chemical Composition of Douglas-fir Heartwood,” *Wood and Fiber Science*, vol. 25, no. 3, pp. 278–288, 1993.
14. J. W. Koenigs, “Hydrogen Peroxide and Iron: A proposed System For Decomposition of Wood by Brown-rot Basidiomycetes,” *Wood and Fiber*, vol. 6, no. 1, pp. 66–80, 1974.
15. K. P. Noetzli, B. Albert, B. Frey, F. Graf, S. Thomas, and O. Holdenrieder, “Release of iron from bonding nails in torrent control check dams and its effect on wood decomposition by *Fomitopsis pinicola*,” *Wood Research*, vol. 52, no. 4, pp. 47–60, 2007.
16. C. Montoya, L.-M. Ottenhaus, T. Singh, J. J. Morrell, and L. Yermán, “Effect of fungal decay on withdrawal capacity of timber nail connections in radiata pine,” in *2025 WCTE Conference Proceedings*, Brisbane, 2025.
17. S. S. Djarwanto and W. M. Arsyad, “Fungal decay resistance of 16 tropical wood species embedded with metal screws,” *Source: Journal of Tropical Forest Science*, vol. 31, no. 4, pp. 443–451, 2019, doi: 10.2307/26804395.
18. R. A. Zabel and J. J. Morrell, *Wood Microbiology*. Elsevier, 2020. doi: 10.1016/C2018-0-05117-8.
19. C. Pozo, J. Díaz-Visurraga, D. Contreras, J. Freer, and J. Rodríguez, “Characterization of temporal biodegradation of radiata pine by *Gloeophyllum trabeum* through principal component analysis-based two-dimensional correlation FTIR spectroscopy,” *Journal of the Chilean Chemical Society*, vol. 61, no. 2, pp. 2878–2883, Jun. 2016, doi: 10.4067/S0717-97072016000200006.
20. K. K. Pandey and A. J. Pitman, “FTIR studies of the changes in wood chemistry following decay by brown-rot and white-rot fungi,” *Int Biodeterior Biodegradation*, vol. 52, no. 3, pp. 151–160, 2003, doi: 10.1016/S0964-8305(03)00052-0.
21. M. Traoré, J. Kaal, and A. Martínez Cortizas, “Differentiation between pine woods according to species and growing location using FTIR-ATR,” *Wood Sci Technol*, vol. 52, no. 2, pp. 487–504, Mar. 2018, doi: 10.1007/s00226-017-0967-9.
22. B. Goodell, J. E. Winandy, and J. J. Morrell, “Fungal degradation of wood: Emerging data, new insights and changing perceptions,” *Coatings*, vol. 10, no. 12, pp. 1–19, Dec. 2020, doi: 10.3390/coatings10121210.
23. V. Arantes and B. Goodell, “Current Understanding of Brown-Rot Fungal Biodegradation Mechanisms: A Review,” 2014, pp. 3–21. doi: 10.1021/bk-2014-1158.ch001.

ICTB 2025. 5th International Conference Timber Bridges
Rotorua, New Zealand, 29 June to 2 July 2025.

SH1 PAPAKURA TO DRURY PROPOSED SHARED USE PATH TIMBER BRIDGE

Tony Pham[1], Richard Nutton[2], Tea Blazic[3]

ABSTRACT

This paper presents the design and engineering analysis of the SH1 Papakura to Drury project's proposed Shared Use Path (SUP) timber bridge, a significant infrastructure project undertaken by NZ Transport Agency Waka Kotahi. The proposed bridge emphasised sustainable construction through the use of glued laminated timber (glulam), which would have reduced carbon emissions by approximately 30% compared to steel alternatives. Additionally, the proposed bridge integrated cultural narratives from local Mana Whenua, which would strengthen community engagement and identity. Advanced structural modelling techniques were employed to evaluate loading conditions and seismic performance, which would ensure resilience against environmental factors. A comprehensive maintenance strategy was also developed to enhance the longevity of the proposed timber structure. While the bridge has been fully designed, financial constraints have prevented its construction at this stage. Nevertheless, the design serves as a model for sustainable infrastructure, blending ecological responsibility with cultural significance. It is also noted that the overall Papakura to Drury project design does not preclude the reintroduction of the timber bridge in future should further funding become available.

1 INTRODUCTION

The urgency of sustainable infrastructure development in response to climate change has accelerated the exploration of environmentally friendly construction materials. Timber, a renewable resource, offers a low carbon footprint and exceptional structural versatility. The Papakura to Drury (P2D) project, led by the NZ Transport Agency Waka Kotahi (NZTA), embodied this innovative approach by designing a timber truss bridge for a Shared Use Path (SUP) at the Papakura Interchange. This initiative would enhance transport connectivity, promotes active transport modes, and would preserve cultural heritage through the incorporation of local Mana Whenua narratives.

At the project's inception, a concept design of a utilitarian truss was developed to meet the functional requirement of carrying the SUP over a motorway on-ramp. As shown in Figure 1, the initial design featured a single-span 40m truss with glulam top and diagonal chords, while the bottom and vertical chords were either steel or heavily reinforced with steel. The deck comprised of a Stress Laminated Timber (SLT) plate with an asphalt topping, supported on a concrete pile foundation behind vertical retaining walls.

[1] Lead Structural Engineer, Aurecon,
e-mail: tony.pham@aurecongroup.com,
[2] Technical Director, Aurecon
[3] Lead Consultant, Aurecon

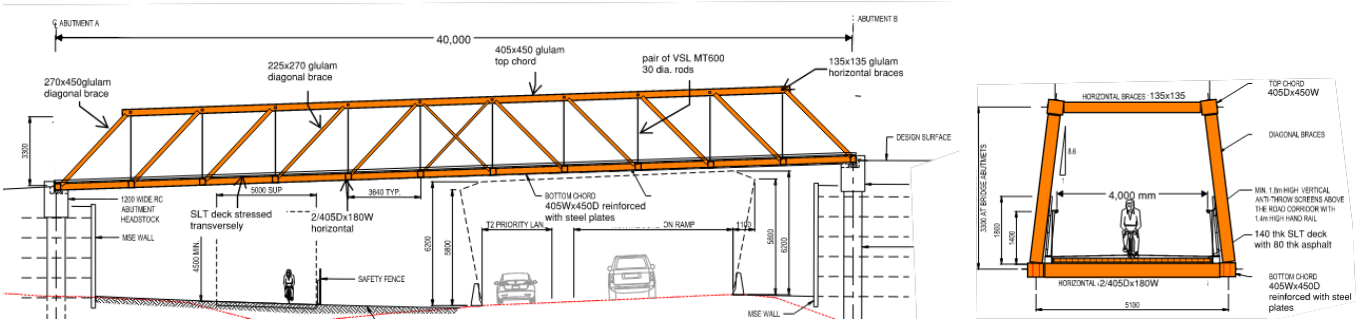

Figure 1 Initial concept design – elevation and cross section

The proposed bridge employed a hybrid material strategy, maximizing the inherent strengths of timber in compression and steel in tension. This approach would prevent brittle failure in timber while optimising structural performance. A parallel concept design of a simple steel truss bridge was developed for comparison, but the assessment found no significant cost premium for the timber option. Given the broader project benefits and NZTA's climate initiatives, the timber truss was advanced to detailed design.

During the subsequent design phase, the primary objectives that guided the SUP bridge design encompassed the following important aspects:

- Sustainability and environmental stewardship: Utilising low carbon materials and reducing overall carbon emissions compared to conventional construction methods.
- Cultural integration and community engagement: Collaboratively working with Mana Whenua to ensure the bridge reflected cultural significance and community values.
- Enhanced connectivity and accessibility: Creating a bridge that would facilitate safe transit for pedestrians and cyclists, thereby encouraging active transport usage.
- Resilience and durability: Designing the structure to withstand environmental factors and potential natural disasters, particularly concerning New Zealand's seismic activity.
- Aesthetic integration: architectural input from Warren and Mahoney ensuring that the bridge design would harmonise with the surrounding landscape while reflecting unique cultural and environmental aspects.

Extensive consultations with Mana Whenua representatives facilitated the incorporation of culturally significant elements into the bridge design. The proposed final bridge form evolved into a distinctive modern timber truss with a multi-span configuration, featuring a sinuous alignment and a gentle curve for improved aesthetics and functionality (Figure 2 and Figure 3). The main span measured 30m, with two 15m approach spans. The opened and inclined trusses would reach a height of 3.5m above the deck at the midspan. A 3.75m spacing between glulam cross-girders would optimise deck span configuration, with deck widths of 4m at the main span and 5m at curved approaches to ensure clear sightlines for cyclists.

Figure 2 Final proposed bridge design – isometric view

Figure 3 Final proposed bridge design – truss view (render courtesy of Warren & Mahoney Architects)

2 SUSTAINABILITY AND COST ASSESSMENT

As the proposed bridge form evolved, a comparative life cycle assessment (LCA) was conducted to quantify the embodied carbon of the timber bridge against three steel footbridges of similar architectural form. The LCA followed the 'Procurement Guide to reducing carbon emissions in building and construction' [1], utilising Infrastructure Sustainability Council emission factors. Superstructure emissions were assessed, excluding secondary elements like barriers and safety screens. A conservative assumption of a 75-year lifespan for the timber bridge (versus 100 years for steel) was applied.

Figure 4 presents the estimated greenhouse gas emissions per square meter of bridge deck. The results confirmed that the use of glulam would significantly reduce the carbon footprint - by 30% compared to a fully steel bridge. However, a timber structure would exhibit higher operational and maintenance emissions due to more frequent repairs and replacements.

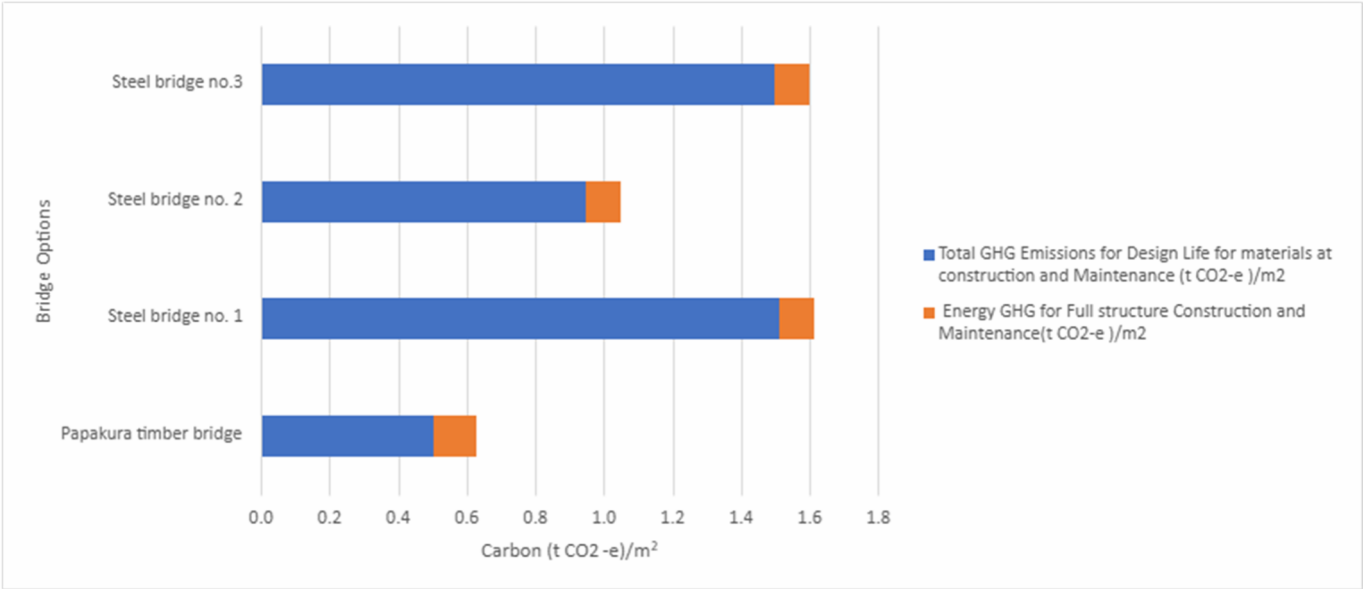

Figure 4 Greenhouse gas emission for each bridge assessed

Cost comparisons also revealed that the timber bridge would be more expensive to construct than a steel equivalent. Additionally, maintenance costs were projected to be higher. Despite these findings, the project proceeded with the detailed design phase. However, financial constraints ultimately led to the decision not to proceed with construction of any bridge after the design was fully completed, though a bridge may be reintroduced in future should further funding become available. Nevertheless, the design remains a valuable case study in sustainable bridge engineering.

3 SUPERSTRUCTURE DESIGN

The bridge was designed to accommodate a 5 kPa uniform distributed load for crowd loading and a 40 kN axle load, representing an ambulance vehicle. Advanced computational analysis using Midas Civil ensured the structural integrity of the timber truss under various conditions. Key assessments included:

- Static Analysis: Evaluated the bridge's ability to support dead loads, including self-weight, as well as pedestrian and cyclist live loads.
- Dynamic Load Assessment: Considered environmental forces such as wind and seismic effects to refine the design and enhance performance.
- Pedestrian-Induced Vibrations: Assessed in accordance with Eurocode 1 [3], confirming that the structure would not experience excessive lateral movements under crowd loading.

Glulam truss members were designed to balance strength, material efficiency, and aesthetics, ensuring compliance with NZS AS 1720.1 Timber Structures [2]. Member sizing took into account the width and thickness of commonly available sawn timber laminates in New Zealand. Key glulam member dimensions include:

- Top chord = 450mm × 450mm
- Diagonal = 270mm × 270mm (increased to 360mm at end principals)
- Cross-girder = twin 180mm × 495mm (increased to 270mmx585mm at curved spans)
- Sway brace = 180mm x 180mm (increased to 225mm x 225mm at curved spans)

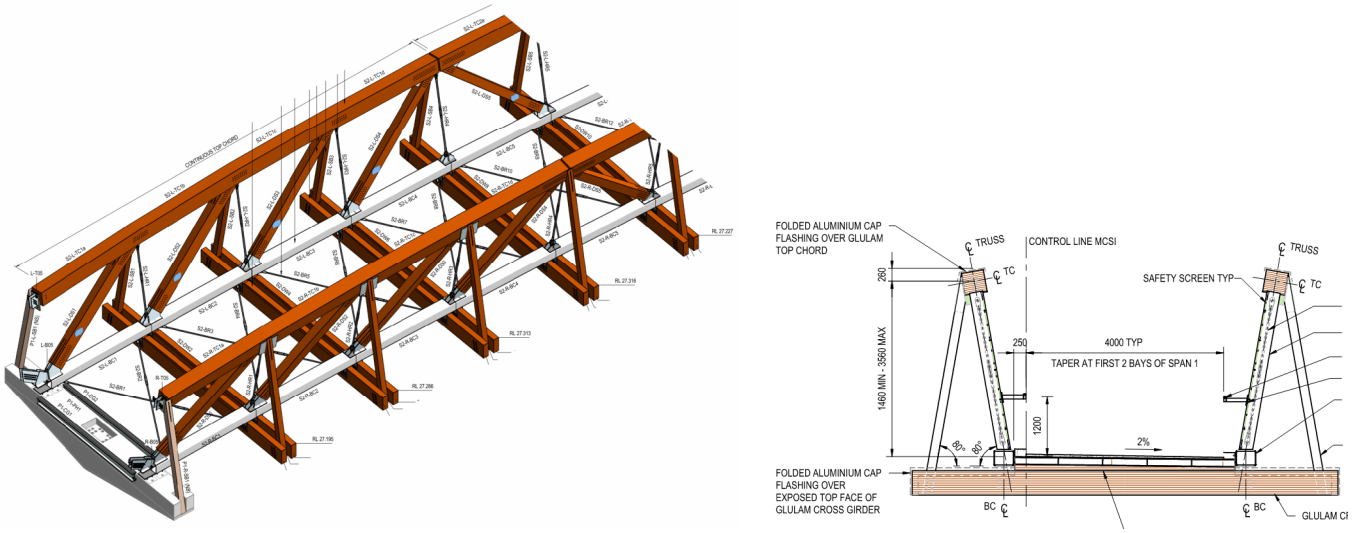

Figure 5 Half span truss isometric view and typical cross section

As shown in Figure 5, vertical steel rods suspend the truss bottom chord and cross-girders between truss joints. The cross-girders extend beyond the truss to support lateral sway braces, ensuring a fully open truss configuration. At curved approach spans, these elements also provide a torsional load path to counteract vertical load eccentricities.

To simplify load distribution and minimize tensile stress in glulam members, the truss spans were designed as simply supported. Top chord segments between spans were non-structural and were detailed to slide,

preserving the simply supported span arrangement. For seismic resilience and pedestrian stability, diagonal steel rods were integrated along the bridge length.

4 CONNECTIONS DESIGN

Glulam truss members were primarily designed as simple compression members. However, directly butting glulam members against each other to transfer compression forces would be unreliable due to potential deterioration of the timber end grain. Therefore, a steel-timber joint was necessary to transfer the compression force across the glulam members. For optimal aesthetics, the truss connections were designed as dowelled internal slotted steel plate joints, commonly used in European designs.

As shown in Figure 6, each top truss joint would consist of stainless-steel dowels passing through two slotted stainless steel fin plates that extend outside the members, acting as gusset plates for the steel hanger rods. The dowels would resist the compression forces from the truss members through the embedment strength of the dowel in the wood fibre. The dowelled connection was designed according to NZS AS 1720.1 and supplemented with Eurocode 5 [4], capable of transferring compression forces up to 800kN. Typically, 12mm diameter stainless dowels were used in the connection, except at the ends where 10mm diameter stainless screws provided clamping force across the glulam slots.

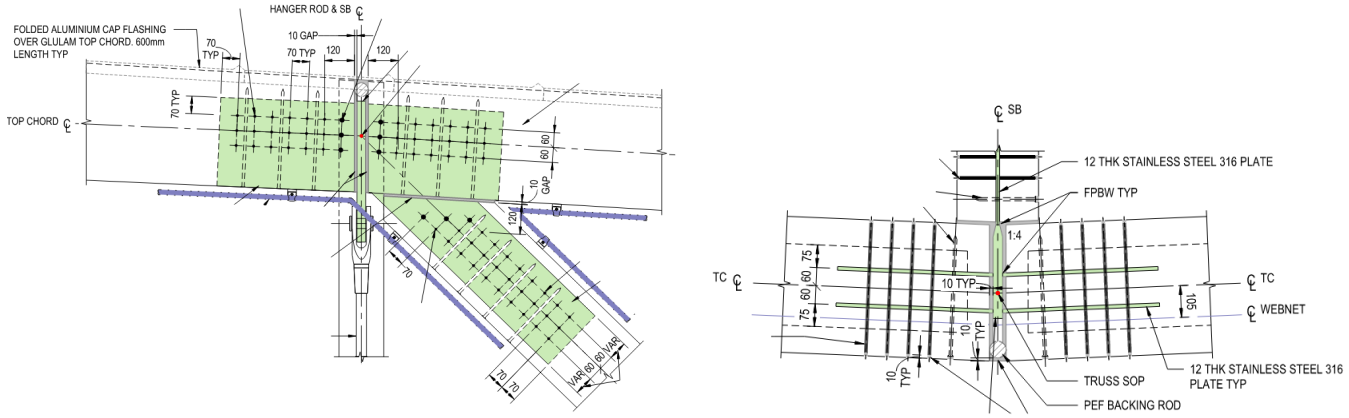

Figure 6 Typical top chord connection – elevation and plan view

At the bottom of the diagonal struts, the slotted stainless steel plates would extend from the glulam struts and would be bolted to steel bottom chord gusset plates, as shown in Figure 7, The glulam cross-girders were designed to be supported below the truss steel bottom chord by a bolted connection through steel gusset plates. This cross-girders connection was the only location where potential brittle timber failure due to splitting perpendicular-to-grain from vertical shear force needed to be evaluated. Consequently, 12mm diameter stainless screws were used to reinforce deeply into the cross-girders above the potential split plane along the bolt lines.

Various measures were employed to improve the durability of the connections. Firstly, all gaps at the member end faces would be sealed with caulking compound to prevent moisture ingress into the timber end-grains. Secondly, the glulam joints would be reinforced with stainless screws to minimize the risk of perpendicular-to-grain splitting along the dowel lines. Finally, cap flashing would be added on the top face of exposed members such as truss top chords and cross-girders.

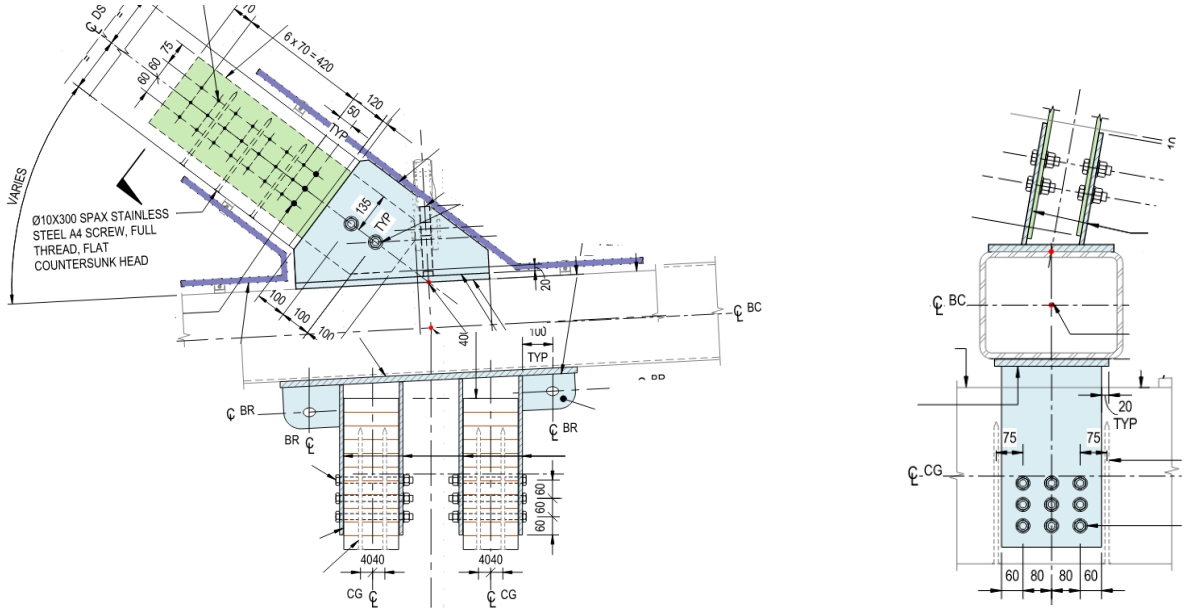

Figure 7 Typical bottom chord connection - elevation and cross section

5 BRIDGE DECK

Instead of the SLT deck in the initial concept design, interconnected glulam panels were adopted for the proposed bridge deck to facilitate future maintenance, allowing individual panels to be replaced if necessary. These glulam panels would typically be 135mm deep and 0.9m wide and would be simply supported between cross-girders. The panels would be interconnected by continuous steel stiffener plates to effectively distribute wheel loads, in accordance with the AASHTO LRFD Bridge Design Specification [5]. The steel plates would feature slotted holes to accommodate moisture-induced movement within the panels.

As shown in Figure 8, the glulam panels would be overlaid with a layer of sacrificial plywood, a waterproofing membrane, and finally an asphalt surface. The plywood layer would serve to separate the asphalt surface from the moisture-induced movement within the glulam panels, enhancing the durability of both the asphalt layer and the glulam deck. At the abutment, where the glulam deck required an expansion joint, a steel capping plate would be provided to protect the timber end grain. The glulam deck was designed to be elevated above the abutment concrete to aid natural ventilation.

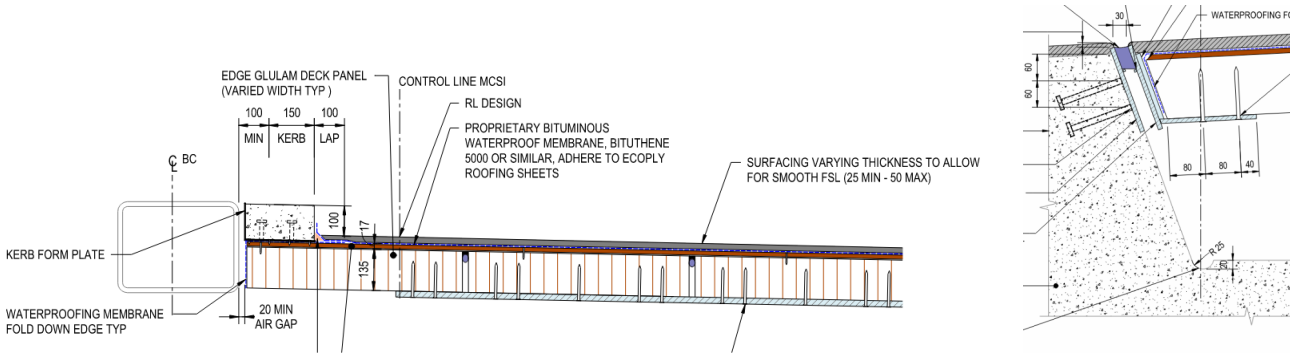

Figure 8 Glulam deck plate – typical cross section and expansion joint detail

6 SUBSTRUCTURE

The trusses would be supported by concrete piers and abutments, which would effectively separate ground moisture from the superstructure, enhancing the durability of the timber elements. All piers and abutments would be founded on bored piles to ensure resilience during extreme events such as earthquakes or collisions from road traffic.

As shown in Figure 9, a significant effort was made to integrate the substructure elements with the superstructure for a cohesive aesthetic outcome. The pier heads would be sculpted to match the end faces of the glulam cross-girders and would include non-structural sway braces to align with the truss spans. Similarly, the abutment wing walls were designed to extend the shallow slope angle of the truss top chord down to ground level.

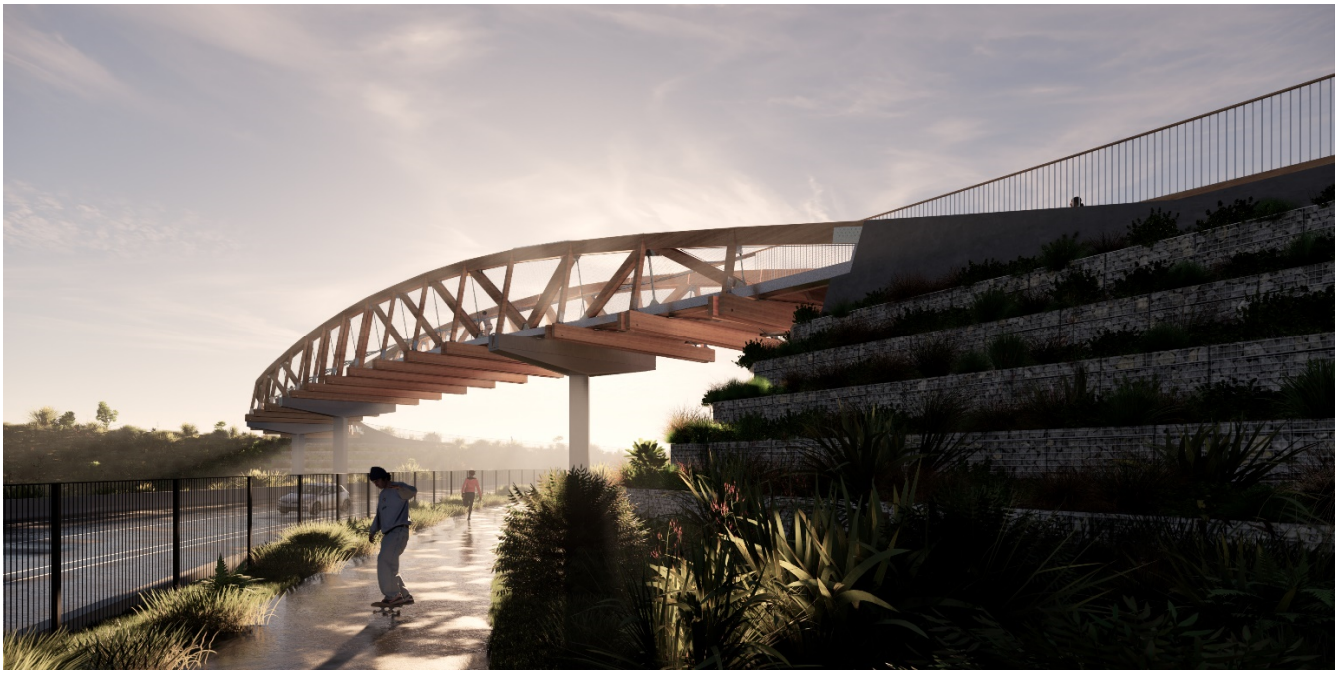

Figure 9 Pier and abutment blend into superstructure (render courtesy of Warren & Mahoney Architects)

7 DURABILITY, OPERATION AND MAINTENANCE

All concrete substructure elements were designed to last 100 years without major renovation. The primary superstructure elements, including the timber truss, deck, and replaceable components, were designed to last over 50 years with regular maintenance.

Key durability enhancements were implemented to ensure the longevity of the timber components:

- H5 Preservative Treatment: This is the highest level of chemical treatment available for glulam in New Zealand. The Copper Chromium Arsenate (CCA) treatment protects against biological threats and decay.
- Pigmented Oil-Based Stain Finishes: This finish would not only enhance aesthetic qualities but also provide UV protection and moisture resistance, effectively limiting weather-related degradation.
- Design for Longevity: The bridge design prioritised moisture management. Various detailing techniques, as discussed in previous sections, were incorporated into the connection design to mitigate risks associated with rot and decay.
- Integration of Sensors for Monitoring: Moisture sensors were proposed for the glulam deck and truss joints near abutments. These sensors would provide real-time data on moisture levels and structural integrity, enabling proactive maintenance strategies to extend the lifespan of the timber components

A robust maintenance regime would be essential for preserving the longevity and integrity of the proposed timber bridge. The design included a proposed plan focusing on:

- Regular Inspections: Scheduled inspections were proposed to assess both structural performance and surface conditions, ensuring the prompt identification of any deterioration related to moisture or insect infestation.

- Repair Protocols: Timely and effective repair protocols included guidelines for inspecting and maintaining timber connections, joint sealing, and treatments to prevent moisture ingress.
- Training for Maintenance Personnel: Enhancing the knowledge of maintenance teams regarding the specific requirements of timber structures and their degradation processes would be crucial. Workshops and training would focus on identifying early symptoms of damage, effective treatment methods, and sustainable practices.
- Use of Technology in Maintenance: The integration of smart devices for monitoring structural health would offer real-time insights, enabling proactive maintenance decisions and preventing issues before they result in significant damage or endanger safety.

8 CONCLUSIONS

The Papakura to Drury project's proposed SUP Timber Bridge emphasized the incredible potential of timber to serve as a primary construction material in modern infrastructure projects. By integrating sustainable design principles, rigorous engineering analyses, and engaging local cultural narratives, this project could stand as a model for future timber bridges in New Zealand and beyond. The innovative use of glulam, coupled with a collaborative approach to community engagement, would foster environmental responsibility while reflecting local identity.

Through meticulous engineering and effective maintenance strategies, the proposed bridge would be poised to serve as a resilient, functional, and beloved part of the infrastructure landscape for future generations. This project exemplified how infrastructure can be constructed to reflect the values of sustainability and community, transitioning towards more environmentally responsible building practices in the civil engineering field.

ACKNOWLEDGEMENT

The authors would like to acknowledge the numerous and continuing support of the NZ Transport Agency Waka Kotahi, Mana Whenua representatives on the Southern Iwi Integration Group, Warren & Mahoney Architects and the local suppliers in the development of the proposed SUP Timber Bridge.

REFERENCES

1. New Zealand Government Procurement, 2022. Procurement guide to reducing carbon emissions in building and construction: A practical guide
2. Standards New Zealand, 2022. NZS AS 1720.1: Timber structures Part 1: Design methods
3. British Standards, 2008. NA to BS EN 1991-2: UK National Annex to Eurocode 1: Actions on structures – Part 2: traffic loads on bridges
4. European Standard, 2008. EN 1995-1-1: Eurocode 5: Design of timber structures – Part 1-1: General – Common rules and rules for buildings
5. American Association of State Highway and Transportation Officials, 2007. LRFD bridge design specifications SI units.

ICTB 2025. 5th International Conference Timber Bridges
Rotorua, New Zealand, 29 June to 2 July 2025.

THARWA BRIDGE RESTORATION AND MAINTENANCE

Marcia Prelog[1]

ABSTRACT

Tharwa Bridge is a 4 span Allan truss bridge located 30km to the south of Australia's capital city, Canberra, serving as the main thoroughfare for the community and local business whilst providing safe, high-level access for the town during flood occurrences. It is of exceptional national heritage significance due it to being one of the oldest surviving Allan truss bridges in service.

Following significant deterioration over the years, the bridge was fully reconstructed between 2008 and 2011 with collaboration from Roads ACT, Transport for NSW (formerly RMS) and Aurecon. The restoration to the superstructure comprised new timber trusses and a stress laminated timber deck, with detailing to improve the durability of timbers and reduce long term maintenance.

Restoration of this historically significant timber truss bridge utilised a combination of modern techniques in construction and design, whilst adhering to conservation management plan requirements. The design features provided a more sustainable use of timber, improving durability and thus reducing maintenance costs.

Following construction, Aurecon was commissioned to prepare a bespoke maintenance plan and oversee the maintenance tasks for 10 years post-restoration, ensuring the bridge's continued serviceability. The inspections provided key insights into the effectiveness of the design detailing and Aurecon's innovative truss recambering methodology was demonstrated to be effective and adopted as part of the maintenance plan.

1 INTRODUCTION

1.1 History of Timber Truss Construction

Early bridge construction in New South Wales made use of the abundant natural resources available. The first bridge was constructed of timber logs, over the Tank Stream in Sydney in 1788, most likely using hardwoods sourced from eucalypts that are common for the Sydney region [1].

Timber bridges were cheap and fast to construct, establishing themselves as the most dominant type of construction in the 1800's. The Government directive in 1861 to use local materials such as stone and timber, in preference to the more expensive wrought iron, further bolstered the construction of timber on bridges.

The majority of truss bridges between 1788 and 1850 were constructed in the forms common to those found in US and Britain; this commonly was the Howe and Pratt truss designs.

[1] Technical Director, Aurecon,
e-mail: Marcia.Prelog@aurecongroup.com,

The key disadvantage using timber was the difficulty in the maintenance and replacement of timber components. Developments to improve truss design and maintainability ensued in following years.

In the 1890's Percy Allan, a prominent engineer in the Department of Public Works, created his version of a timber truss using twin elements similar to that found within the Howe truss form. The diagonals slope toward the centre with twin vertical rods at each truss bay connecting the top and bottom chords (Figure 1).

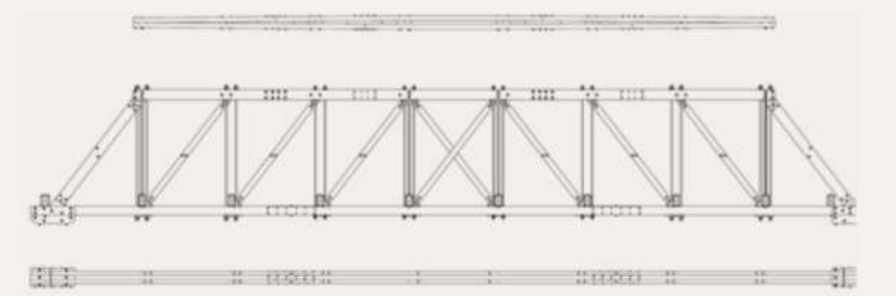

Figure 1. Typical Allan truss design [2]

Ongoing maintenance was facilitated by the use of twin members which could be replaced individually without closing the bridge. The smaller timber sections spliced together for the top and bottom chords could also be replaced individually. It reduced the need to use large sections of timber, with smaller sections being more easily sourced. The smaller contact faces at steel interfaces were also less subject to rot.

The twin steel vertical rods allowed for tightening of the truss following timber shrinkage and facilitated the replacement of timber cross girders supporting the deck.

2 THARWA BRIDGE DESIGN

Tharwa bridge was constructed as a 90-foot Allan truss with timber top and bottom chords and diagonal members carrying the compressive forces and steel rods carrying the tension. The truss bottom chords supported timber cross girders, which in turn supported a 5m wide deck, which consisted of multiple stringers and transverse timber decking bolted into place.

Figure 2. Image of the original Tharwa bridge circa 1895 [3]

The main spans were originally supported on timber pier trestles supported on timber piles (Figure 2). Concrete piers replaced the timber trestles in 1934, whilst the timber trusses were the original construction from 1895 [4]. Concrete approach spans frame each side of the four main truss spans.

2.1 Deterioration of Tharwa Bridge

After being in service for over 110 years, Tharwa bridge suffered significant deterioration of the timber sections as a result of environmental influences. Weathering under harsh weather extremes and the presence of white ants accelerated the deterioration of the timber sections (particularly the bottom chord), which required the installation of temporary Bailey trusses in 2005 to offer additional structural support.

However, as a result of further degradation of the timber and loss of structural stability, the Bailey trusses were required to be laterally braced in 2006, resulting in the full closure of the bridge.

2.2 Truss Restoration Objectives

In 2007, Roads ACT proposed the $26m upgrade of the Allan truss bridge in preference to full replacement. This approach was taken in response to community support for the original bridge to be restored, due to its historical significance in terms of local heritage and an example of Allan's innovative technical design of the time.

Specific requirements in the use, repair and restoration of the structure need to be defined to meet key conservation values.

A detailed Conservation Management Plan (CMP) was developed and adhered to in both the design and maintenance stages for Tharwa bridge [4]. The intent of the CMP was to ensure the longevity of Tharwa Bridge as an historic road bridge remaining in service [5].

Roads A.C.T., A.C.T. Heritage, and a peer review group consisting of eminent engineers Ray Wedgwood, Brian Pearson and Gary Barker worked closely with Aurecon to achieve the desired outcomes.

Discussions were made on each innovative modification to ensure the bridge's historical value was maintained, including adherence to the conservation management plan, whilst achieving the sustainable use of timber.

2.3 Truss Design Innovations

The following innovative developments in the truss design and timber deck were adopted to more effectively utilise timber:

- Camber was incorporated into the truss design by modifying the length of the timber elements, where the truss top chord segments are longer than the respective bottom chord.
- Tightening of the tension rods produced the profile of a parabolic curve correlating with the expected deflection, whereas the original design followed a radial camber profile. The final truss camber was 22mm with the deck in place.
- Secondary diagonals were increased in size to cater for the increased traffic loading of 44 tonnes. All diagonals were cut at different lengths to support the installed camber, which allowed stresses in the timber to be evenly balanced under its own self weight.
- Sway braces were installed on all cross girders to provide additional lateral stability to the truss frame under increased traffic loads by reducing the top chord effective length.
- The timber bottom chord of the truss was replaced by two parallel steel plates to carry the full tensile load, noting that timber performs better long term under compression.

This was a departure from the original design. The improvement to durability justified this change with the addition of timber fascia panels affixed along the steel face, maintaining the bridge's traditional appearance but not providing any structural support.

- The interface between steel and timber were limited by the use of nylon spacers between the elements, limiting degradation effects in these areas.

2.4 Connection Configuration

Modifications to connections improved the durability of timber and steel interfaces.

Each diagonal is connected by steel shoes at the top and bottom chords. Cast iron was historically adopted for the connections, which were often subject to fatigue. Cast iron had particularly been known to fracture at low temperatures, noting that Tharwa experienced sub-zero temperatures during Winter months.

All critical steel elements were replaced with low temperature, high strength grade steel (300L15 and 350L15) suited to the environment, limiting possible failure through brittle fracture. This replaced the original cast iron shoe design with little aesthetic impact.

The bottom chord shoes were modified to become a simple pinned steel connector through the bottom chord plates (Figure 3). This ensured correct truss behaviour through free rotation at the lower connections and allowed free drainage.

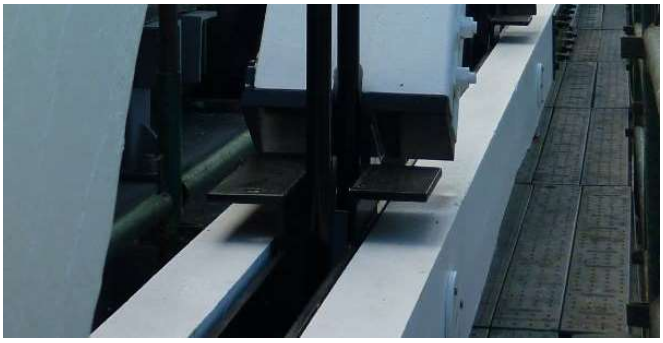

Figure 3. Pinned diagonal shoes connected at bottom chord steel plates

Truss supports were constructed as independent rather than shared elements to facilitate individual truss placement during construction and for future works. Exposed elastomeric bearings on steel bearing plates facilitated inspection and general cleaning as part of maintenance (Figure 4).

Figure 4. Truss bearings

2.5 Deck and Cross Girder Design Innovation

Rather than use a multitude of timber elements for the new deck and supports which require frequent maintenance, the adopted deck design consisted of timber laminates compressed together using high strength strands to form one monolithic element. The stress laminated timber (SLT) deck was fixed directly to the cross girders (Figure 5).

Timber cross girders are typically one of the earliest components to deteriorate and are one of the most frequently replaced elements due to the rate of degradation at deck connections. They are known to be one of the first modes of failure in a timber truss and deck support system.

The new cross girder design adopted steel box sections of a similar form to the original timber section. This design solution was rationalised through the improved durability, reduced maintenance and benefit to structural capacity.

A thin bearing strip also offers a degree of spacing between the steel/SLT timber interface, another potential area of degradation due to moisture.

Figure 5. SLT deck and cross girder support

The deck has been constructed in one piece 110 metres long, allowing a reduction in joints from a possible five to just one at each end.

Deck joints in timber suffer under repeated traffic impact, resulting in high localised damage. This justified the adoption of a full length deck and required significant changes to the fixity of the overall bridge to allow differential movement between the deck and the trusses. This movement was able to be taken through the elastomeric bearings under each cross girder. The timber deck was finally surfaced with a 7mm spray seal to provide a wearing surface that mitigates water ingress.

Provision of a variety of timber lengths for the SLT deck had to be addressed at design and construction phase. The timber elements adopted standardised, readily available sizes to reduce off cuts and waste.

2.6 Sustainability and Resilience

The removal of the existing truss presented an opportunity for the reuse of some of the materials available. The existing steel top chord splice plates were slightly modified and repainted for use on the new bridge structure. The majority of washer plates that supported the tension rods at the bottom and top chords were retained for reuse (Figure 6).

Additional washer plates were sourced from previous TfNSW Allan truss rehabilitation projects to supplement the quantity, thus ensuring a high level of quality by replacement of any items in poor condition.

Figure 6. Reuse of existing washer plates

New requirements in traffic barrier design to AS5100 were merged with maintaining the aesthetics of the original design. The traffic barriers were shaped to match the original design drawings but were constructed of more durable and stronger steel hollow sections.

Carefully managed timber selection and procurement practices aided in sourcing and maintaining sustainable sections of timber with minimal waste, as detailed in the following section.

2.7 Quality Control in Procurement and Construction

The quality management of timber sourcing and the seasoning process was a key factor in ensuring the level of timber strength and quality was achieved and maintained through adequate storage.

TfNSW procured the truss timber in December 2008 and seasoned the timbers for 12 months in their workshop. However, during inspection of the timber, several pieces were identified to have excessive checking as a result of seasoning through the hot & dry summer.

One of the several controls implemented to limit checking of the timber was through "reconditioning" of the timber, and the subsequent paint system. "Reconditioning" involved the application of controlled wetting cycles while seasoning the timber. This aimed to reinstate the natural moisture content of the timber, close up excessive checks and then allow timber to season in a controlled environment to prevent checks reappearing.

This process had not been carried out on such large section timbers before. The success of this process was demonstrated by the larger checks closing up over time and the moisture content of the timber increasing from 8% at the surface to 20%.

2.8 Protective Coating System

To limit timber deterioration through repeated exposure to water, UV and thermal fluctuations, steel flashing was introduced at the top of the truss top chords, end diagonals and bottom chords (Figure 7). All timber elements were painted white, a simple yet effective method of sustaining the life of the timber elements through reflection of light energy.

Figure 7. Flashing above top chord

The interfaces between steel and timber elements were also fully painted to reduce rot occurrence.

Due to the Tharwa bridge truss timber being reconditioned by regular watering in Wagga, the design required a paint coating system that complimented this process by allowing water diffusion. The final paint coating system required a primer that could be applied to timber and remain breathable / permeable, allowing the moisture to continue to diffuse from the timber.

The system would also need to avoid the formation of moisture bubbles blowing out paint and have gap filling characteristics to fill any large checks. The paint coating system ultimately selected specifies two acrylic primer coats, then two acrylic paint finish coats, to reduce the time between paint coats and allow paint application as soon as possible after planing, cutting and shaping timber. This was to reduce the risk of checks opening up between paint coats.

2.9 Construction

The design was refined to improve constructability, as in the following examples:

- All steelwork was fabricated and painted off-site and transported for on-site assembly.
- Steel barriers were designed in panels for easier installation.
- Timber truss elements were fabricated, painted and disassembled in the Wagga workshop, maintaining quality standards with final onsite assembly removing transportation difficulties.
- The SLT deck was constructed North of the bridge site and rolled out in one section

3 MAINTENANCE PHASE

Aurecon was commissioned by the client to prepare a bespoke maintenance plan and oversee maintenance tasks for the following 10 years after restoration. This has provided the client with 10 years of specialist knowledge, giving a better understanding of the efficacy of the design innovations and maintenance regime adopted.

3.1 Maintenance Manual

The Tharwa Bridge Maintenance Manual provided a “systematic methodology for the maintenance of the bridge, both in the long and short term, compliant with the Conservation Management Plan [4],[6].

Inspection and maintenance actions on the timber elements were undertaken in accordance with the TfNSW Bridge inspection and Timber Bridge Manual in the first instance. This has now been amended to align with the client’s asset management system for both inspection and maintenance tasks.

3.2 Inspection Findings

Inspections were undertaken between 2010 and 2018 in accordance with the procedures. A number of TfNSW staff members were familiar with truss maintenance and were part of the designated team for the contracted maintenance period following construction. The inspections

involved reporting on truss camber, truss and deck condition under various weather conditions during both Summer and Winter times, since temperature and moisture influence timber properties and behaviour.

Maintenance tasks are typically allocated by the presence, severity and consequence of defects visually observed within the inspection process. Defects are typically due to material deterioration, but timber is also subject to ongoing creep and shrinkage effects, requiring maintenance to address these aspects over time.

Creep effects on camber

Creep is dependent on the load applied and how long it is applied for, as well as the initial moisture content (MC) of the timber. Creep effects decline over time; this plateaus after one year under self-weight loading. The maximum creep effects occur with a MC greater than 25%.

A review was undertaken of the original design to assess the creep expected in each member under its own self weight. Most timbers which were used at Tharwa had greater than 25% average MC when they were placed into the truss, following the seasoning process. Regular tightening of the vertical rods would be required to maintain the design camber as timber elements shortened under compression.

The effect of timber creep shortening is difficult to predict when working with a number of different timber species, each truss piece being a unique section of timber as well as being subject to unknown environmental fluctuations and loading data. Significant deflection of the trusses was observed over the years, which was attributed to not only the moisture content but the different timber species behaving differently and the cumulative effect of vehicle loads.

Consequential effects were observed on some timber elements, where gaps formed along the contact area with the shoe. In turn, the truss camber was diminished. At the design stage the predicted loss of camber was calculated to be within the range of 12-21mm, depending on the assumed moisture content and the method of analysis. The observed loss of 14mm fit within this range for the majority of trusses by 2014 (Figure 8).

However, by 2016 all trusses were experiencing reverse camber (sag), instigating the need for further repair actions comprising re-tensioning of the tie rods.

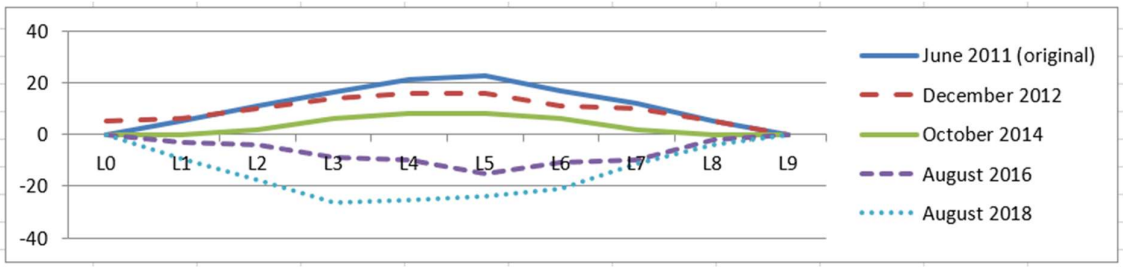

Figure 8. Truss deflection survey data along the truss span at each node

Deck

Areas of minor seepage were observed through the deck, which correlated with the localised loss of spray seal. The timber elements were in very good condition overall. The constant compressive force on the timber laminates induced a reduction of the deck width due to creep and subsequent loss of prestress at individual strands.

Strand anchorages were covered with grease and nylon protective caps. By 2017 several nylon caps were cracking, due to continuous UV exposure coupled with temperature and moisture fluctuations.

Timber truss

The protective paint systems performed well throughout the truss. Some bubbling or cracking of the paint occurred in some local areas where checks had formed in the timber and moisture was being emitted as the part of the timber seasoning process The flashing provided excellent protection on the top surfaces with the paint system fully intact.

3.3 Repairs

The majority of defects were addressed in accordance with the TfNSW guidelines and specifications for timber truss repair, SLT deck restressing, resealing of the deck, reinstatement of protective coatings and tightening of bolted connections. The nylon caps which cover the SLT strand anchorages degraded due to a combination of thermal and/or UV effects. Hydrolysis may also have contributed to the deterioration as the caps were exposed to water, condensation and thermal fluctuations. The replacement material chosen for the cap was HPDE, a UV and temperature stable material. Strength was of minor importance, as the cap was simply a form of protection for the strand end.

3.4 Truss Re-cambering

Re-cambering of the four spans was required to reinstate the 22mm design profile. A number of TfNSW Allan truss restorations have adopted a square and level truss using even element lengths, which is then tightened to achieve the camber required. The TfNSW Specifications TS 02178 Timber Truss Repairs- Construction and TS 03383 Timber Truss Repairs – Temporary Support and Minor Design detail the procedures for re-cambering these trusses [7].

The initial truss camber under the Specification is set as zero, since that is the design layout of the truss with equal top and bottom chord segment lengths. As the cambering process changes the shape, the load distribution and stresses in the truss, this specification subsequently requires an extensive list of checks to be undertaken to ensure the truss is not locally overstressed or damaged. This zero camber methodology does not hold true for Tharwa bridge, which has an in-built profile.

Aurecon developed an alternative staged tightening procedure based on the TFNSW Specification, without the need for a Bailey truss temporary support system. It was noted that Percy Allan also designed the Allan truss for the replacement of elements without the need for additional support. This new re-cambering procedure stayed true to the original intent.

The developed procedure for Tharwa involved cyclical jacking of the tension rods working from the outer nodes to the centre of the truss. A hydraulic jack was placed at the top chord node points to lift the tension rods incrementally and allow the nut to be tightened in its new position on both rods at the same time, until the desired camber was achieved.

This process was undertaken for each span consecutively. The incremental load redistribution induced by the tightening was checked to confirm overstressing did not occur. An unexpected benefit resulted from jacking at the two outer nodes at the same time, which allowed tightening of the tension rods along the span with a wrench without the need for jacking. This accelerated the cambering process, resulting in works being completed within a single week closure.

4 CONCLUSIONS

The Tharwa Bridge restoration successfully preserved a historically significant structure while incorporating modern engineering techniques and innovations in the use of timber. The choice of materials, timber detailing and use of modern features such as a stress laminated timber deck, enhanced the bridge's durability and reduced maintenance needs while achieving the desired conservation objectives.

The collaborative efforts of Roads ACT, Heritage ACT, and TfNSW were crucial in achieving the project's goals.

The maintenance phase demonstrated the effectiveness of the design innovation, with the majority of maintenance repair tasks being minor in nature. This is a testament to the quality of workmanship and choice of materials used, coupled with details that have prevented timber deterioration. The unique re-cambering process resulted in minimal interference to the community and subsequently at a reduced cost.

Overall, the Tharwa Bridge restoration serves as a model for balancing historical preservation of timber truss bridges with the service needs of the community.

5 REFERENCES

1. Ariyaratne, W. et al, Roads and Maritime Authority (now TfNSW), date, "Timber Truss Bridge Book", accessed 12 March 2025, <https://ttb.transport.nsw.gov.au/index.html>
2. Ariyaratne, W. et al, Roads and Maritime Authority (now TfNSW), date, "Timber Truss Bridge Book", Chapter 2, accessed 12 March 2025, <https://ttb.transport.nsw.gov.au/chapter-2.html>
3. 1895, [Tharwa Bridge with two unidentified men standing on left riverbank, Australian Capital Territory] [picture], <http://nla.gov.au/nla.obj-136964186>
4. Phillip Leeson Architects, 2008, "Tharwa Bridge Conservation Management Plan", < Tharwa Bridge Conservation Management Plan 2009>
5. ACT Government Heritage register, <https://www.act.gov.au/__data/assets/pdf_file/0006/148506/tharwa-bridge-entry-to-the-heritage-register.pdf>
6. Aurecon / Roads A.C.T., 2020, "Tharwa Bridge Maintenance Manual" Revision 6
7. TfNSW, 2020, "TS 02178 Timber Truss Repairs- Construction, "TS 03383 Timber Truss Repairs – Temporary Support and Minor Design", accessed 12 March 2025, <https://standards.transport.nsw.gov.au/>

6 ACKNOWLEDGEMENTS

This project's success is attributed to the collaborative efforts of Roads A.C.T., Heritage A.C.T. and TfNSW's Wagga Wagga maintenance team.

ICTB 2025. 5th International Conference Timber Bridges
Rotorua, New Zealand, 29 June to 2 July 2025.

MONITORING TECHNOLOGIES FOR THE LONG-TERM EVALUATION OF TIMBER BRIDGES

Andreas Rödel[1]

ABSTRACT

Timber bridges are gaining importance in modern civil engineering due to their sustainability, high load-bearing capacity, and aesthetic appeal. However, wood's sensitivity to moisture requires specific considerations in design, construction, and maintenance. Moisture, fungal infestation, and structural damage can significantly impact durability, making innovative monitoring systems essential for long-term preservation. Modern monitoring technologies enable precise tracking of critical parameters such as wood moisture, structural movements, and sealing integrity. Point, linear, and full-surface measurement systems address different application needs. Successful implementations in Germany, Belgium, and the Netherlands demonstrate how targeted monitoring extends service life, reduces maintenance costs, and enhances safety. Real-time monitoring surpasses traditional inspection methods by providing continuous data collection and early damage detection. Advancements in sensor technology, automated data analysis, and remote access will further improve timber bridge monitoring and ensure long-term functionality.

1 INTRODUCTION

Timber bridges are experiencing a renaissance due to increasing interest in sustainable construction. Wood’s high load-bearing capacity, low dead weight, and environmental benefits make it an attractive alternative to steel and concrete. Additionally, its natural aesthetics enhance both rural and urban landscapes. Despite these advantages, wood's organic nature presents challenges in bridge construction and maintenance. Moisture absorption can lead to swelling, shrinkage, fungal infestation, and structural damage. As timber bridges are exposed to environmental influences, effective moisture control and sealing measures are crucial. Innovative monitoring solutions are essential for cost-efficient maintenance and long-term functionality.

This paper presents modern moisture and seal monitoring technologies that have proven effective in practice. Various measurement methods, including point, linear, and full-surface systems, address different structural requirements [1]. Practical projects demonstrate how combining multiple monitoring systems enables comprehensive condition assessments, enhancing service life and safety. A systematic analysis of long-term measurements offers valuable insights into timber bridge behavior, optimizing maintenance strategies and advancing timber construction techniques [2]. Three case studies illustrate key considerations for implementing effective monitoring solutions to ensure durability without com-promising aesthetics.

2 IMPORTANCE OF MONITORING WOODEN BRIDGES

2.1 Influence of Environmental Factors

Timber bridge durability is affected by various environmental factors, particularly moisture from precipitation, spray water, or humidity. Prolonged exposure promotes biological degradation, including fungal infestation, compromising structural integrity. Fluctuations in moisture content cause swelling and

[1] Andreas Rödel, Dipl.-Ing. VDI, affiliation, ProGeo Monitoring Systeme und Services GmbH & Co KG, e-mail: roedel@progeo.com

shrinkage, leading to mechanical stresses and cracking. Additional influences such as temperature changes, UV radiation, and pollutants contribute to material fatigue. Continuous monitoring is essential for early intervention and preventive maintenance.

2.2 Risks Due To Moisture

Moisture-related risks include material fatigue, fungal attack, and structural damage. Wood moisture above 20 % accelerates enzymatic decomposition, weakening load-bearing components. Repeated moisture fluctuations increase mechanical stress, promoting cracks that allow deeper water penetration and further deterioration. Unchecked moisture damage can result in severe structural failure.

2.3 Advantages of Continuous Monitoring

Early Damage Detection

Modern sensor technologies detect minor changes in material moisture and structural behavior, identifying potential damage before it becomes severe. This is especially important for wooden bridges, where issues often develop beneath the surface. Real-time data enables proactive maintenance decisions.

Reduction of Maintenance Costs

Traditional inspections occur at fixed intervals or in response to visible damage, leading to either unnecessary maintenance or costly late-stage repairs. Continuous monitoring optimizes maintenance schedules, reducing expenses and minimizing service disruptions.

Increased Safety

Permanent monitoring improves safety by detecting excessive moisture, structural weakening, or load changes early. Preventive measures can be implemented before critical failures occur, ensuring the long-term stability of timber bridges.

3 SECTION HEADINGS AND TEXT STYLE

Depending on the structural conditions of the object to be monitored and the monitoring objectives to be ensured, different approaches can be taken for the project-specific monitoring concept [3].

3.1 Spot Moisture Measurement

Spot measurements use sensors at predefined locations to monitor moisture content. This method provides precise absolute values but is limited to known critical areas. Resistance and capacitive sensors detect moisture changes, while equilibrium humidity sensors measure moisture indirectly through sealed air pockets within the wood. Spot measurements are effective when combined with broader monitoring methods.

3.2 Linear Moisture Measurement

Linear sensors detect moisture trends over extended areas, improving reliability. These sensors measure electrical resistance along a sensor strip, detecting changes over time. They are particularly useful for joints, component transitions, and high-risk areas. Although they do not provide absolute moisture values, they help track moisture accumulation patterns.

3.3 Full-Surface Leak and Moisture Monitoring

Comprehensive monitoring systems detect moisture ingress across large areas, ensuring early detection of leaks. These systems use conductive layers beneath waterproofing materials to measure voltage changes caused by water penetration. Full-surface monitoring is especially valuable for concealed areas where visual inspection is impractical [4].

4 PRACTICABLE EXAMPLES

4.1 Argen Bridges, Wangen/Allgäu, Germany

Two integral timber-concrete composite bridges were built over the River Argen, forming part of new infrastructure for the local development project. Each bridge comprises two block beams made of glued plank stacks with a superstructure of in-situ concrete and block foundations on either side. Figure 1 shows one of the bridges over the river Argen, Figure 2 the design plan. To ensure the longevity of these timber elements, special attention was paid to potential moisture ingress at the critical interface zones.

Figure 1: Integral Bridge over River Argen Wangen Allgäu, Germany

To monitor this moisture ingress, the block beam end faces of each bridge were equipped with a total of 24 resistive wood moisture sensors. Figure 3 shows the position of the sensors and the cavities for the cabling in principle. These sensors are designed to measure the wood's moisture content at regular intervals, providing data on whether the end faces absorb excessive moisture from rain or groundwater. The sensors were embedded in flush-mounted plastic boxes, preventing direct contact with concrete slurry during the casting of the block foundations and offering protection against physical damage.

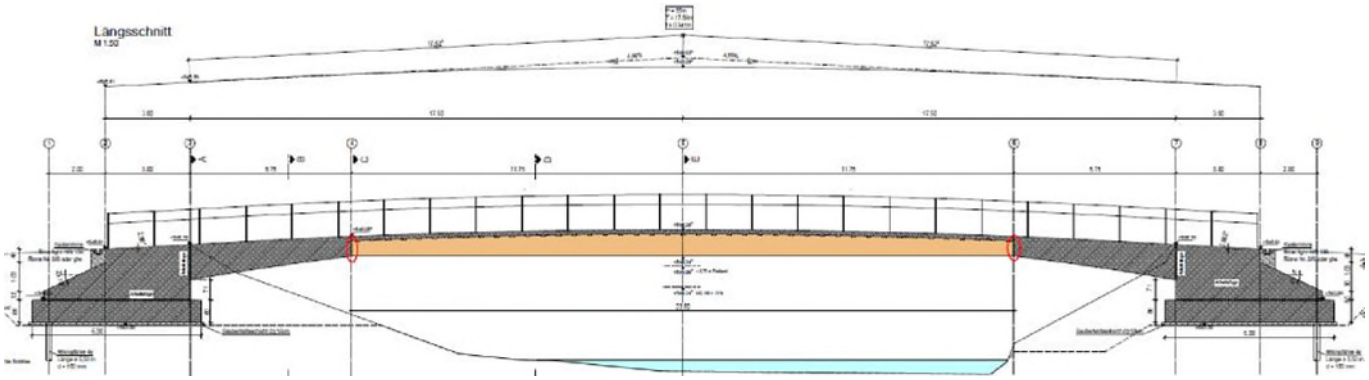

Figure 2: Design plan of the bridge

Sensor cables run through concealed cavities within the block beams and terminate at an external electrical cabinet placed along the riverbank. This setup allows authorized personnel to easily connect a standard wood moisture meter to each sensor point, enabling quick, on-site assessments. Monthly control measurements have been carried out since the project's completion in early 2024. So far, no significant moisture accumulations or critical values have been detected, indicating that the sealing and drainage measures are performing as expected. An additional benefit of placing sensors at the block beam end faces is the ability to

isolate localized moisture issues before they spread deeper into the structure. If a sensor reading indicates a rise in moisture, maintenance crews can focus on resealing or repairing only the affected area. This targeted approach reduces downtime and avoids unnecessary costs. Early detection through this system helps maintain the aesthetic and structural qualities of the timber, ensuring the bridges remain functional for many years. Figure 4 shows one Sensor installed in protection housing, Figure 5 the measuring cabinet with handheld moisture measurement device.

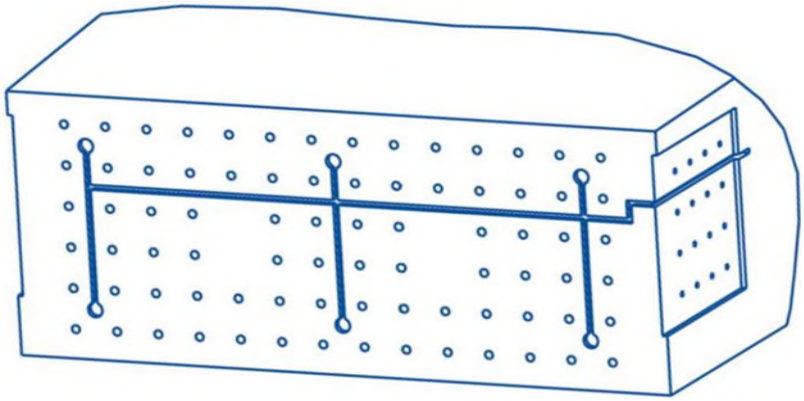

Figure 3: Position of resistive moisture sensor in principal

Figure 4: Resistive Sensor with protection housing

Figure 5: Measuring cabinet

4.2 Tervuren Bicycle Bridge, Belgium

Located east of Brussels, this architecturally distinctive laminated veneer lumber (LVL) bridge spans a busy road junction as part of a trans-Belgian bicycle route. The curved timber box girder design not only provides aesthetic appeal but also demonstrates the versatility of engineered wood products in large-scale infrastructure. Figure 6 shows the bridge in its final position above the crossing. During the planning stages, the client and engineering team identified several key risk areas, including potential leaks at the roof sheeting seams and moisture infiltration in the underside beams caused by road spray. To address these concerns, an extensive array of sensors was installed.

Linear Moisture Sensors: A total of eight linear sensors were placed along the ridges and eaves of the metal roof. By monitoring changes in electrical resistance, these sensors detect moisture that slips beneath the metal sheeting. If rainwater or condensation breaches the primary waterproofing layer, the sensors record the event and trigger alerts for further investigation.

Figure 6: Cycle Bridge Tervuren. Belgium

Resistive Wood Moisture Sensors: Sixteen resistive wood moisture measuring points were installed from the bottom of the box girder into the LVL beams. These sensors focus specifically on areas vulnerable to splash water from passing vehicles. Concealed channels were milled into the underside of the beams to protect sensor wiring, and stainless steel plates were added to safeguard cables during the final construction stages. Figure 7 shows the installation of the sensors from the inside of the bridge.

Figure 7: Drilling the holes for the wood moisture measuring points

Full-Surface EPDM Monitoring: In addition to the roof sensors, the structure features a comprehensive EPDM waterproofing layer on certain sections. The system is equipped with integrated sensor technology to detect any compromise in the seal. This ensures that if water penetrates the EPDM membrane, maintenance teams can identify the exact location.

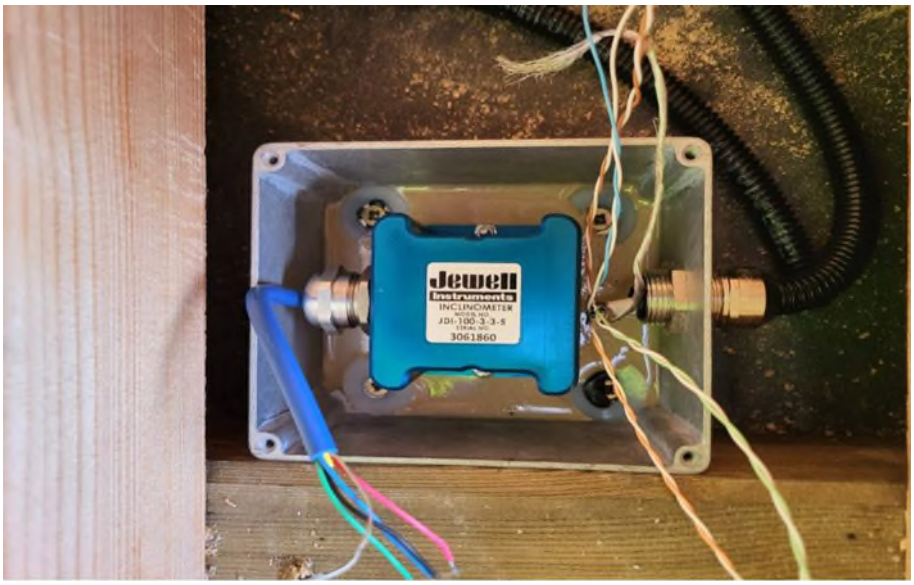

Figure 8: High-precision inclinometer for measuring the subsidence in the middle of the bridge

Inclinometers for Structural Monitoring: Four high-precision inclinometers, with a resolution of 0.01 mRad, are strategically placed near the bridge supports, Figure 8. These measure even slight angular variations that may indicate differential settlements, changes in load distribution, or other structural shifts over time. By comparing data from the inclinometers with moisture readings, engineers can determine whether anomalies in structural behavior correlate with moisture penetration.

All sensor data is transmitted via an LTE modem to a central monitoring platform, where long-term data storage, trend analyses, and automated threshold alarms are managed. Construction was completed in late 2024, and the full monitoring system is scheduled to go live by March 2025. Anticipated benefits include reduced maintenance costs, timely leak detection, and enhanced structural safety for cyclists and pedestrians.

4.3 Passarelle Green Bridge, Zwolle, Netherlands

Spanning approximately 125 meters, the Passarelle Green Bridge forms part of a broader urban development in Zwolle aimed at connecting neighborhoods across a four-track railway line, figure 9. Each segment of the bridge rests on steel supports and features four parallel board-stacking block girders. On top, a cross-laminated timber (CLT) slab provides a continuous deck approximately 10 cm thick, which is sealed with a two-layer EPDM membrane.

The bridge's design accommodates a landscaped park with planters for trees, flower beds, and green areas, alongside a pedestrian walkway and a small artificial watercourse. These design elements create an inviting public space but also introduce substantial moisture risks. Soil in planters and irrigation systems, plus the presence of standing water, can challenge the waterproofing over time. Consequently, the project incorporates a full-surface smartex® mx real-time monitoring system, specifically configured for EPDM seals, Figure 10. This system consists of a three-layer PP felt combination sensor placed directly beneath the EPDM seal. The top and bottom felt layers act as electrical insulation when dry, while the middle conductive layer, connected to approximately 170 measurement points, provides continuous voltage mapping. The measurement points are integrated into special flat cables that connect to a data acquisition unit.

Figure 9: Passarelle Zwolle, Netherlands

Figure 10: Installation of waterproofing with integrated full area leak monitoring

By applying a low-voltage signal to the wet outer surface (via a counter-electrode in the overlying substrate), the system measures voltage distribution beneath the EPDM. Any breach in the seal that allows water to pass creates a conductive bridge, causing localized voltage spikes. Figure 12 shows the timeline of one data point taken during the integrity test, figure 13 the spatial distribution of data with leak and wet spot in red, figure 14 an instantly found leak in the membrane.

Figure 11: Flooded deck for integrity test

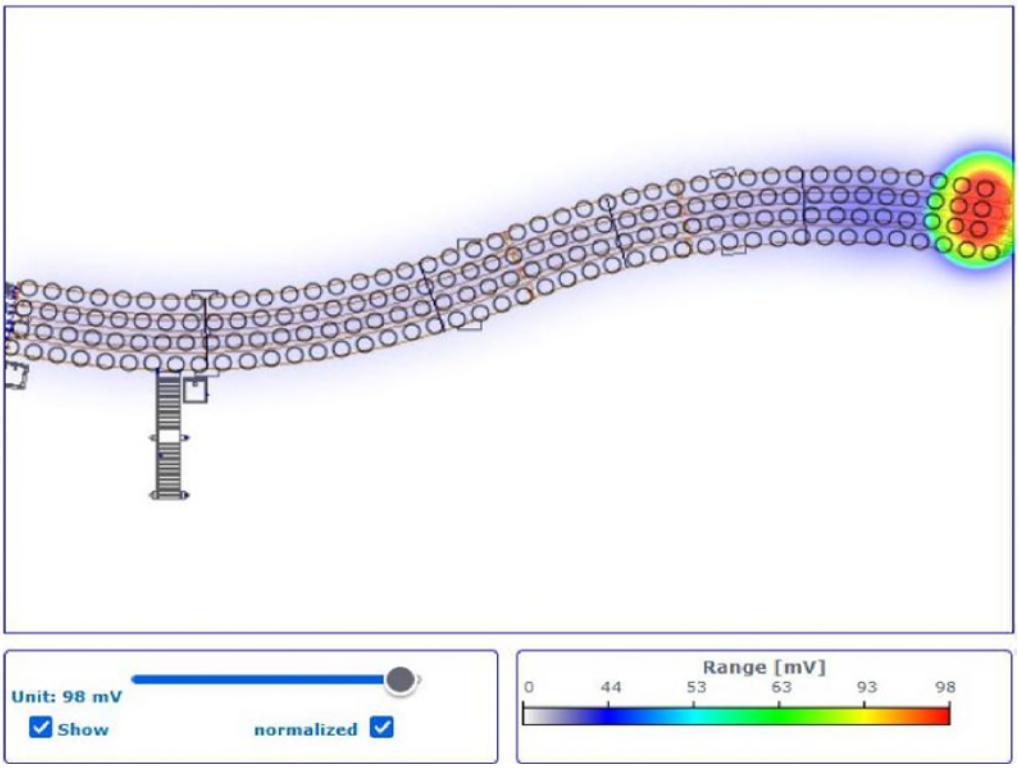

Figure 12: Visualization of online integrity test

A distinguishing feature of this setup is its capacity for highly precise leak localization, to within decimeters. Facility managers can quickly identify where water infiltration occurs and schedule targeted repairs, often without the need for large-scale dismantling of the overlying landscape. Since the monitoring system came online in summer 2024, it has logged real-time data on the structural waterproofing. The data are continuously transmitted to an internet-based ProGeo monitoring portal, which integrates with the City of Zwolle’s control systems.

Figure 14: membrane leak identified and found with the installed full areal real-time monitoring system

The monitoring approach also includes layered redundancy: in addition to the real-time leak detection, spot checks are performed in critical areas such as penetration points for planters or edges near structural joints. Because the system immediately flags any changes in voltage, these on-site checks can confirm the extent of water intrusion. By merging local inspections with automated alerts, the city's maintenance team can protect the bridge's structural timber components and preserve the intended aesthetic of the landscaped pedestrian environment.

5 CONCLUSIONS

Timber bridges require effective moisture monitoring to ensure long-term functionality and efficient maintenance. Real-time monitoring systems with automated data collection and analysis offer significant advantages over manual inspections, including early detection of leaks or structural weakening, reduced maintenance costs, and improved public safety. As sensor and communication technologies continue to evolve, integrating them into timber bridge designs becomes increasingly feasible in diverse settings.

Expert planning remains essential for selecting the most appropriate monitoring strategy, taking into account site-specific conditions, potential damage scenarios, and budgetary constraints. In areas prone to unpredictable failure points - such as extensive waterproof surfaces - full-surface monitoring offers a reliable means to detect and localize water ingress rapidly. Meanwhile, point and linear sensors can be strategically placed to capture local variations and support targeted maintenance efforts.

Overall, a well-designed monitoring system contributes to the longevity and reliability of timber bridges, aligning with sustainability goals by reducing material consumption and extending the life cycle of these structures. As demonstrated in Germany, Belgium, and the Netherlands, integrating advanced monitoring solutions not only safeguards structural integrity but also preserves the aesthetic and ecological benefits of timber construction. By investing in state-of-the-art sensor networks and data analysis platforms, bridge owners and engineers can anticipate issues before they escalate, ensuring safe passage and cost-effective asset management over the decades to come.

REFERENCES

[1] Bauphysikkalender 2002. Ernst & Sohn Verlag, Berlin, Part C6, Seite 607-632. Andreas Rödel: Leckagen-ortung an Bauwerksabdichtungen

[2] Bautechnik. Sonderheft Flachdächer 2022. Ernst & Sohn Verlag, Berlin. Seite 10-13. Andreas Rödel: Mon-itoringsysteme richtig planen und betreiben.

[3] Bautechnik. Sonderheft Holzbau Ausgabe 2, 2021. Ernst & Sohn Verlag, Berlin. Seite A20-A21. Andreas Rödel: Echtzeitmonitoring schützt vor unbemerkten Langzeitschäden

[4] Cost Action CA20139, 2022. holistic design of taller timber building (HELEN). Sustainability and Durability of Taller Timber Buildings: A State of the Art Report. Part 4 Moisture Impact. WG4.SG4.03 Andreas Rödel: Full-Area covering leakage and wetness monitoring on big timer structures using real time monitoring. Page 55-58.

ICTB 2025. 5th International Conference Timber Bridges
Rotorua, New Zealand, 29 June to 2 July 2025.

ADDING BROADER VALUE TO AOTEAROA NEW ZEALAND – HOW TIMBER BRIDGES CAN CREATE REGIONAL ECONOMIC GROWTH WHILE REDUCING CARBON EMISSIONS.

Liz Root[1], Jack Manners[2], Jonathan Chambers[3], Oliver De Lautour[4]

ABSTRACT

Concrete bridges are well proven in New Zealand, however their continued use locks in high carbon construction techniques and does not provide an opportunity for more diverse supply chain participation. Although the concrete sector is making in-roads to reducing embodied carbon, this is largely through Supplementary Cementitious Materials (SCMs), which are predominantly produced offshore, and the decarbonisation roadmap for the concrete industry in NZ[1] shows that the industry will be relying heavily on offsets.

What if we could drive a true step-change in embodied carbon reduction on transport projects, while unlocking broader value for Aotearoa New Zealand? Timber bridges produced at scale could drive a genuine transformation in embodied carbon reduction, while enabling growth in the engineered timber sector, in turn creating associated high-value, high-salary jobs - particularly in the regions, where forestry/wood production is centred (Rotorua, Nelson, Northland, East Coast, West Coast, Canterbury). This has the potential to drive economic and GDP growth,

1 INTRODUCTION

Embodied carbon associated with the delivery of roading infrastructure is a result of the construction materials utilised – e.g. the asphalt, the aggregates, concrete, cement and reinforcing steel – and the fuel consumed to power construction vehicles, both on site (plant and equipment) and for haulage of materials and waste transported to and from site. Carbon hotspots (those areas of a road being constructed that have proportionally higher carbon than average) for roading infrastructure are known to typically be tunnels and bridges.

This paper focuses on the opportunity to reduce the embodied carbon of road bridges through adoption of engineered timber superstructures. It will stay silent on tunnels, apart from acknowledging that decarbonisation of road tunnels is likely best suited to alignment with the concrete and steel sectors' decarbonisation pathways, rather than the adoption of alternate materials and supply chains.

2 CONCRETE, STEEL AND CARBON

Road bridges in New Zealand are typically of reinforced concrete construction. Cement, concrete and steel are widely acknowledged to be the most significant contributors to the carbon footprint of infrastructure

[1] Director, Sustainability and Climate Change, Aurecon,
e-mail: liz.root@aurecongroup.com,
[2] Lead Engineer, Bridges and Civil Structures, Aurecon,
e-mail: jack.manners@aurecongroup.com,
[3] Manager, Sustainability and Climate Change, Aurecon,
e-mail: jonathan.chambers@aurecongroup.com,
[4] Technical Director, Bridges and Civil Structures, Aurecon,
e-mail: oliver.delautor@aurecongroup.com,
[5] whilst some other materials have higher carbon footprints per weight, such as aluminium, the quantities of such materials used are typically negligible to that of steel and concrete

carbon[5]. Global cement manufacturing alone produced 1.6 billion metric tonnes of CO_2 in 2022, approximately 8% of the world's total CO_2 emissions [2].

The concrete and steel sector in NZ acknowledge their impact and are making progress to reduce carbon emissions. The Government partnership with NZ Steel in 2023 to co-fund an electric arc furnace at their facility in Glenbrook has been reported widely. This will enable NZ Steel to produce lower-carbon steel by melting scrap steel using electricity instead of coal, cutting greenhouse gas emissions at their facility by up to one million tonnes per annum [3 & 4]. Concrete NZ published their Roadmap to 2050, net zero carbon pathway in 2023 [1] aligning with the Global Cement and Concrete Association's (GCCA) Cement and Concrete Industry Roadmap for Net Zero Concrete.

3 OPPORTUNITY

Whilst the concrete and steel industries are walking a pathway to decarbonise, there is a high reliance on SCMs in the short to medium term. The currently available and proven SCMs in the NZ context (fly ash and ground granulated blast furnace slag) are globally traded commodities in demand for those trying to reduce the carbon of their concrete products or construction. These SCMs are also bi-products from high carbon activities, such as burning coal, that are being transitioned away from. As such there can be cost barriers and or availability challenges for their use.

Consequently, it is our hypothesis that if we are to decarbonise the delivery of infrastructure in NZ, these SCMs should be reserved for where there are no alternatives (or currently none) to concrete, such as for road tunnels or long span road bridges. A natural flow on from this hypothesis is to identify those assets currently constructed from concrete, that could feasibly be built from an alternate, lower carbon material, whilst still fulfilling the same function. In this paper, the option to construct local road bridges over state highways is considered.

It should be noted that this paper does not cover the technical feasibility and or technical barriers to engineered timber bridge design and construction. This subject is covered well by others. Instead, we are taking a carbon and economic lens to the opportunity.

3.1 Timber bridges and carbon

Local road bridges with an engineered timber superstructure are being constructed in Europe, with an example of a pinned arch bridge shown in Figure 1.

A comparison of construction carbon between a 'typical' concrete Super-T bridge and this engineered timber pinned arch construction type has been undertaken on a like for like span (figure 2).

Preliminary calculations suggest using structural timber can reduce materials' embodied carbon for a bridge superstructure by 40-50%. When considering the carbon associated with both the superstructure and substructure, carbon reductions remain significant at approximately 30-35%. This carbon reduction has been calculated to be an approx. 215 to 240 tCO_2e reduction per bridge. Refer figure 3.

Figure 1. Pinned arch timber bridge in Norway

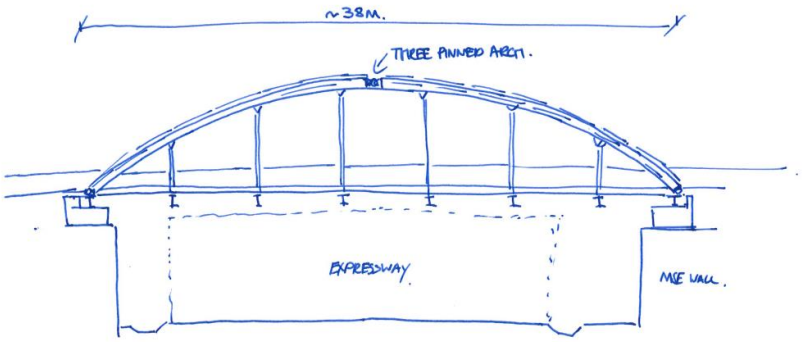

Figure 2. Sketch of engineered timber bridge considered in carbon calculations

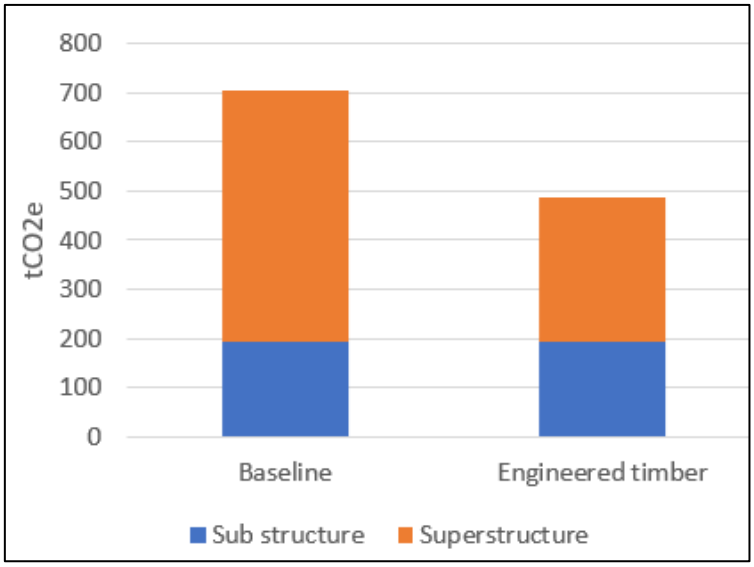

Figure 3. Graph showing carbon associated with the sub structure and super structure of a base line (Super Tee) bridge with an Engineered timber pinned arch bridge.

This initial estimate of carbon did not consider transport or on-site construction emissions, the concrete option has excluded the benefit of SCMs and reinforcing steel adopted an environmental product declaration from Pacific Steel. It was also noted that emissions savings would depend on the type of timber product and specific supplier.

When considering a 24km stretch of NZs state highway network it would not be uncommon to have up to 10-12 local road crossings. In this instance, if all bridges were of a similar span to the example calculated here and were of an engineered timber design, construction of the highway and associated bridges could have avoided circa 2,150 to 2,880 tCO_2e.

3.2 Timber and the economy

Demand for timber products is falling. Before Covid, wood product manufacturing was valued at $6 billion, with 35% of logs and 18% of other products exported. A slow-down in residential building activity in two key markets (NZ and China) is suppressing demand for NZ wood products. Construction costs are increasing by 8% annually [5]. At the same time, sawmills are closing around the country. Marginal increases in wood product manufacturing output has been shown to induce economic activity across the country [6]. Wood & wood product manufacturing is a significant employer in the regions (East Coast, Northland, Nelson), and in large population centres (Bay of Plenty & Auckland) [7].

Creating increased demand for mass engineered timber products in NZ could provide an opportunity to help to supplant reduced demand for timber products. Growing domestic wood production could also serve as a low-cost, supply-chain resilient option for NZ.

4 THE CHALLENGES AND THE MITIGATIONS

Whilst considering the following hypotheses, there are challenges and barriers to overcome.

1. Building a pipeline of timber bridge construction and renewal projects will create regional economic growth through job creation and industry expansion.
2. This pipeline can boost domestic demand for the Forestry and Wood Processing sector, building resilience against a slow-down in global demand for NZ timber products.

Anecdotally, we have heard price premiums stated as circa 35% for an engineered timber super structure. Cost premiums can be understood to be associated with materials, manufacture, construction and the risk of the new, but additionally beauty. Bespoke architectural bridges are breathtaking. A bespoke architectural timber bridge will knock your socks off, however, will it be built? A low carbon bridge that is never built, does not decarbonise our infrastructure delivery and it does not contribute to the required step change.

The NZ engineered timber manufacturers are currently geared up to support the building sector, not infrastructure. Their economy of scales comes from mass customisation of elements. To supplement items 1 and 2 of our hypotheses above, we are introducing item 3:

3. By developing standardised & repeatable approach to engineered timber construction, this can become a viable and affordable option for delivering low carbon road bridges.

The beauty and elegance of the pinned arch bridge used in our example above is acknowledged, but this construction typology may not be the solution to reducing our infrastructure carbon, where the design may be considered too bespoke to suite mass customisation. However, at circa 350m^3 of glulam per bridge (based on Figure 2), and with a significant forward pipeline of roading infrastructure projects, construction of 50-100 engineered timber bridges a year could trigger the threshold for volumes that appeal to the New Zealand wood processing sector.

4.1 Mitigations

Until we have an early adopter, questions remain about actual cost impacts, genuine opportunities for standardisation and interest from the wood processors. Below we have framed some potential research opportunities and next steps to support in resolving these questions, Figure 4.

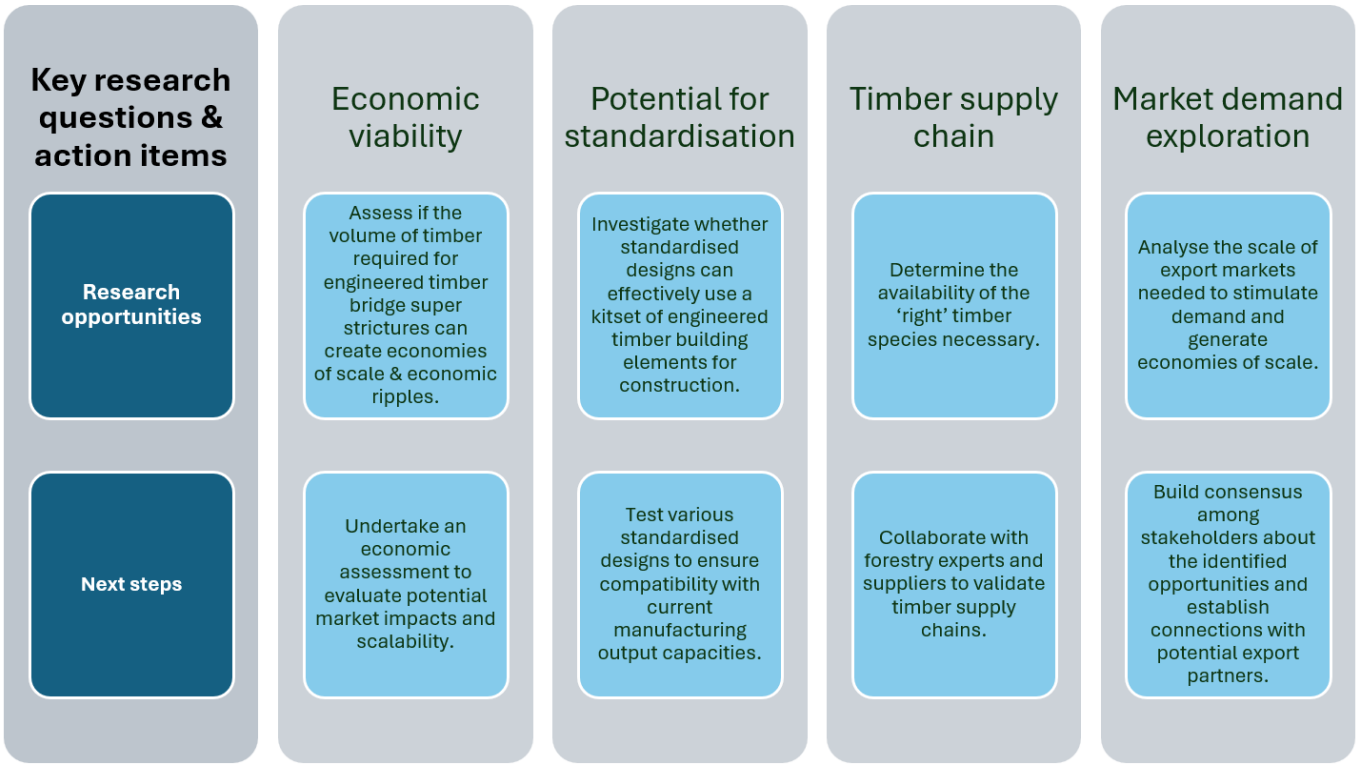

Figure 4. Potential research opportunities and next steps to understand economic impact and viability of widely adopting standardised timber bridge design.

5 CONCLUSIONS

Whilst we are not currently in a position to state matter of fact that the adoption of engineered timber bridges will add broader value to New Zealand, we have shown potential carbon savings associated with this 'alternate' material and have identified a potential scale that could contribute to interest from manufacturers. Understanding of the manufacturers desire for mass customisation, repeated elements, should drive design of low carbon bridges that can be built and will contribute to lower carbon infrastructure.

REFERENCES

1. BRANZ, BIP, ConcreteNZ, 2023. A Net-Zero Carbon Concrete Industry for Aotearoa New Zealand: Roadmap to 2050 https://cdn.ymaws.com/concretenz.org.nz/resource/resmgr/docs/cnz/c_roadmap_concrete.pdf
2. Purton, M., 2024. Cement is a big problem for the environment. Here's how to make it more sustainable: https://www.weforum.org/stories/2024/09/cement-production-sustainable-concrete-co2-emissions/#:~:text=Global%20cement%20manufacturing%20produced%201.6,to%20achieving%20global%20climate%20targets.
3. NZ Steel. Transition to lower emissions steel making can go further, faster. https://www.nzsteel.co.nz/news-and-media/securing-the-future-of-steelmaking-in-nz/
4. MfE, 2023. Government partnership with NZ Steel set to unlock massive emissions reductions https://environment.govt.nz/news/government-partnership-with-nz-steel-set-to-unlock-massive-emissions-reductions/
5. CoreLogic 2024. Cordell Construction Cost Index https://www.corelogic.co.nz/news-research/reports/cordell-construction-cost-index
6. Stats NZ, March 2020. National Input Output Tables https://www.stats.govt.nz/information-releases/national-accounts-input-output-tables-year-ended-march-2020/
7. Stats NZ, February 2023. Business Demography Statistics https://www.stats.govt.nz/information-releases/new-zealand-business-demography-statistics-at-february-2023/

ICTB 2025. 5th International Conference Timber Bridges
Rotorua, New Zealand, 29 June to 2 July 2025.

BEST PRACTICES IN TIMBER RAILWAY OVERBRIDGE ASSET MANAGEMENT: QUEENSLAND CASE STUDIES

Dan Schneider[1], Daniel Anstice[2], David Crump[3]

ABSTRACT

Timber railway overbridges have long been a vital part of Queensland's transport infrastructure, supporting freight and passenger movement across challenging landscapes. However, with many of these bridges exceeding their design life, they now face significant challenges, including structural deterioration, increased load demands, and environmental exposure. This paper presents case studies of three timber overbridges—Drayton Bridge, Wallangarra Bridge, and Hopes Road Bridge—each exhibiting unique structural issues such as deck failure, bushfire damage, and settlement-related instability.

Through detailed inspections, structural assessments, and rehabilitation strategies, these case studies highlight the importance of proactive asset management, cost-effective repairs, and adherence to established maintenance frameworks such as those presented within the TMR *Timber Bridge Maintenance Manual*. The findings emphasise the need for routine monitoring, load capacity evaluations, and strategic investments to ensure the long-term viability of these heritage structures. By leveraging proven rehabilitation techniques, engineers and policymakers can extend the service life of timber bridges while balancing heritage conservation with modern infrastructure demands.

Figure 1. Timber rail overbridge at Hopes Road

[1] Schneider, Dan, GHD
e-mail: dan.schneider@ghd.com,
[2] Anstice, Daniel, GHD
[3] Crump, David, GHD

1 INTRODUCTION

Timber bridges have historically played a crucial role in the railway network around Queensland, which is the second largest state in Australia by geographical area. These timber bridges have served as vital links across roads, railways, rivers, valleys, and challenging terrain. The extensive use of timber bridges was particularly prominent in regional and rural areas of Queensland, where alternative materials like steel or concrete were either too expensive or logistically difficult to transport and construct [1].

Queensland's railway network, spanning thousands of kilometres, relies on many timber bridges to support freight and passenger transport, particularly in remote areas. These structures have been essential in facilitating economic activities by enabling a reliable means of transport across difficult landscapes.

However, as these timber bridges remain in service, they face significant challenges related to ageing, environmental exposure, and increasing operational demands. This has led to concerns regarding their structural resilience and long-term sustainability.

2 BACKGROUND OF TIMBER BRIDGES IN QUEENSLAND

2.1 History of Timber Bridges in Queensland

Due to early plentiful supplies of very strong and durable hardwoods, such as ironbark and spotted gum trees, timber initially became the traditional form of bridging used in Queensland from the early 1800s to the early 1900s. Layouts and details of Queensland timber bridges were standardised by 1925 and no changes to basic structure and member sizes have been made to the present time – refer to Figure 1 for a typical timber road bridge over rail.

The Queensland state road authority, Department of Transport Main Roads (TMR), typically required girder logs which were 9 m long and 480 mm in diameter, while piles were often 400 mm diameter and 10 to 15 m in length. Such timber sizes have simply become difficult to source, requiring much longer lead times for supply. However, timber bridges were built into the early 1960s, and these now form an ageing population with a mean age of some 60 years, showcasing their historical significance and resilience.

In terms of timber railway bridges, in Queensland alone it was estimated in 2004 that there were over 100 kms of rail bridges, consisting of more than 17,000 spans [1]. In terms of timber road bridges, available records indicate that between 1925 and 1970, some 1,300 timber bridges were built by TMR in Queensland [2]. It is estimated that less than 500 TMR timber bridges are still in service, with the largest population on the lesser class roads. In addition, local government authorities have responsibility for many timber road bridges that are deteriorating. In 2024, AU$1,400 million worth of concrete and timber bridges under local council management in Australia were reported in poor condition or worse. In fact, 18% of all timber bridges under local council management in Australia are in poor condition, which have an estimated replacement cost of AU$365 million [3]. At the current rate of replacement, it is apparent that there will be an ongoing need for large-scale timber bridge management in Queensland for at least another 20 years.

2.2 Unique Features of Queensland Timber Bridges

Timber bridges in Queensland also offer distinctive design features. A design feature considered unique to Queensland timber bridges is the use of a spiking plank, which is a timber member placed atop the outer girders to which the decking is fastened. Notably, the decking is not directly connected to the inner girders. Instead, cambering – the jacking up of internal girders – is employed to maintain a tight deck-to-girder system, which serves to minimise movement and reduce rattling of the bridge deck in service [2].

Queensland's hot and humid climate poses significant challenges to these structures. Despite their historical significance and continued use, timber bridges in Queensland are increasingly susceptible to:

- Material degradation: Timber is prone to rot, insect infestation, and moisture-induced deterioration.
- Increased load demands: Modern rail and road traffic often exceed the capacities of aging timber bridges, causing additional stresses and failures. Many lack the redundancy of concrete bridges.
- Environmental exposure: Bushfires, floods, cyclones, and severe weather events pose a continual threat.
- Maintenance: Timber bridges need frequent inspections, interventions, and occasional replacement.

Given these unique challenges faced by timber bridges in Queensland, it is essential to examine how these issues impact timber rail overbridges, which are critical to the state's rail network. The study presented in this paper focuses on addressing these concerns through detailed case studies, aiming at providing asset managers with practical insights for extending the service life of timber rail overbridges.

2.3 Maintenance and Rehabilitation Practices

To manage the abovementioned challenges, rail and road authorities in Queensland implement routine inspections using non-destructive testing techniques.

Despite these efforts, a trend towards replacing timber bridges with concrete or steel alternatives is evident, especially in high-traffic areas where safety and durability are paramount. Nonetheless, heritage timber bridges are often preserved due to their historical value, balancing modernisation with conservation.

These combined strategies reflect a pragmatic approach to extending the service life of Queensland's timber bridges while addressing their inherent vulnerabilities.

3 EXPERTISE AND BEST PRACTICES IN TIMBER BRIDGE MANAGEMENT

Timber bridges, like all infrastructure, require diligent inspection, assessment, and rehabilitation to ensure their longevity and safety. The unique properties of timber, such as its susceptibility to moisture, pests, and environmental conditions, necessitate a deep understanding of the material and its behaviour over time. Experienced professionals who are well-versed in timber bridge design and maintenance play a crucial role in conducting thorough inspections and evaluations. These specialists, armed with industry-specific knowledge and tools, are essential to identifying early signs of deterioration, assessing load-bearing capacities, and recommending appropriate rehabilitation measures. By adhering to industry best practices, including the use of standardised guidelines and protocols, these professionals can ensure that timber bridges continue to perform safely and effectively throughout their lifespan, thus extending their operational life and minimising the risk of failure.

4 CASE STUDY 1: DRAYTON RAIL OVERBRIDGE

4.1 Background

GHD received an emergency call from the bridge authority to attend the site of a rail overbridge at Drayton, Queensland, citing localised failure of the bridge deck. The bridge is a three span timber road overbridge on Brisbane Street. The superstructure features five girders with plywood decking and an asphalt overlay. The bridge accommodates a two-way carriageway with a footpath on the northern side of the deck.

4.2 Site Inspection

Prior to undertaking any site work, GHD undertook a job safety and environment analysis (JSEA) to ensure that the inspection could be carried with an acceptable safety risk. In addition to GHD's prior experience on similar projects, the JSEA helped to determine that the bridge inspectors were required to hold various qualifications and accreditations that are mandated by federal and state regulators, operators, asset owners, and clients. The qualifications and accreditations required for this project included: Rail Industry Worker certification, Construction Safety White Card, Registered Professional Engineer of Queensland accreditation, Work Safely at Heights certification, Safely Access the Rail Corridor certification, and Working in Electrified Territory qualifications. Regardless of these project details, it is incumbent upon all practitioners involved with timber bridge site works to ensure that they have undertaken site-specific risk assessments and determined the relevant accreditations needed to undertake works safely and competently.

No special access provisions were utilised during this inspection and thus all observations were made from safely accessible areas in and around the existing bridge that were accessible by foot. The inspections involved a visual and hammer tap structural inspection only, i.e., no timber drilling, sampling, or laboratory testing. Due to the short notice in the lead up to the inspection, the urgent need to inspect, and the limited timeframe on site, the inspection scope was generally limited to the superstructure components.

4.3 Assessment of Defects

The primary inspection issue observed, as shown in Figure 2 below, was deck failure that seemed to be due to punching failure of the plywood decking material over Pier 3. Other key findings from the inspection included moisture ingress accelerating rot and decay in the affected decking area – see Figure 3.

Figure 2. Drayton Rail Overbridge elevation and deck issues

Figure 3. Rotten plywood deck sheeting at Drayton Rail Overbridge

4.4 Rehabilitation Recommendations

Based on GHD's site inspection and following a desktop assessment of the observed defects, GHD suggested that the root cause of the observed localised shear failure of the plywood deck was likely due to a combination of: plywood deck rotting due to water ingress, delamination between plywood deck sheets due to water ingress, and the wheel load effect (taken as being at 600 mm from the inside kerb).

GHD suggested to the bridge authority that the proposed rehabilitation approach in the short term be to locally restore the damaged plywood deck. Reference was made to Part Two of the TMR *Timber Bridge Maintenance Manual* (refer to Figure 5), where an example of a temporary deck repair is illustrated.

Rather than replacing temporary deck plank sections, a replacement plywood section was recommended. The decking was recommended to be cut locally at the girders. The timber blocking under the deck was recommended to be continued approximately 600 mm across each of the adjacent 1200 mm wide transverse plywood deck panels, i.e., each timber blocking plank is to be approximately 2400 mm in length. Further, it was recommended that a polyurethane elastomer joint filler be applied at the transverse butt joints between the repair section and the existing adjacent sheets, and that a waterproofing layer be provided on top of the replacement plywood decking. A longitudinal steel channel distributor was also recommended to be installed centrally between the girders adjacent to the temporary repair, throughout Span 2.

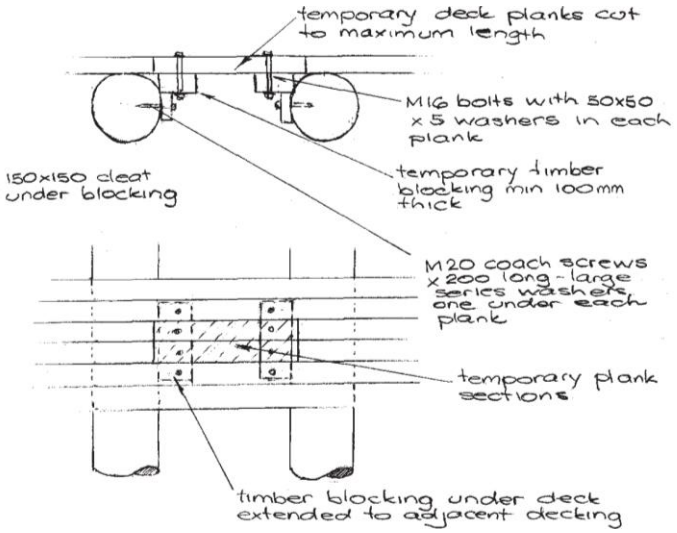

Figure 4. Indicative emporary deck repair for Drayton Rail Overbridge (Source: TMR TBMM [2])

In light of the observed plywood deck deterioration, GHD also provided long-term recommendations regarding replacement of the entire decking at all three spans of the bridge, as follows (refer Figure 5):

- Replace all plywood decks of the bridge with like for like decks. Consideration given to more durable materials, such as hardwood planks or other materials.
- Where bridge decking is replaced with like-for-like plywood deck sheets, apply a polyurethane elastomer joint filler at the transverse butt joints between sheets, and provide a waterproofing layer on top of the plywood decking.
- If the bridge decking is replaced with like-for-like plywood deck sheets, install longitudinal steel channel distributors centrally between each line of girders to help prevent differential edge deflections in the sheets and install longitudinal steel channel distributors under the barrier posts to control distortions in the plywood deck sheets induced by post impacts.

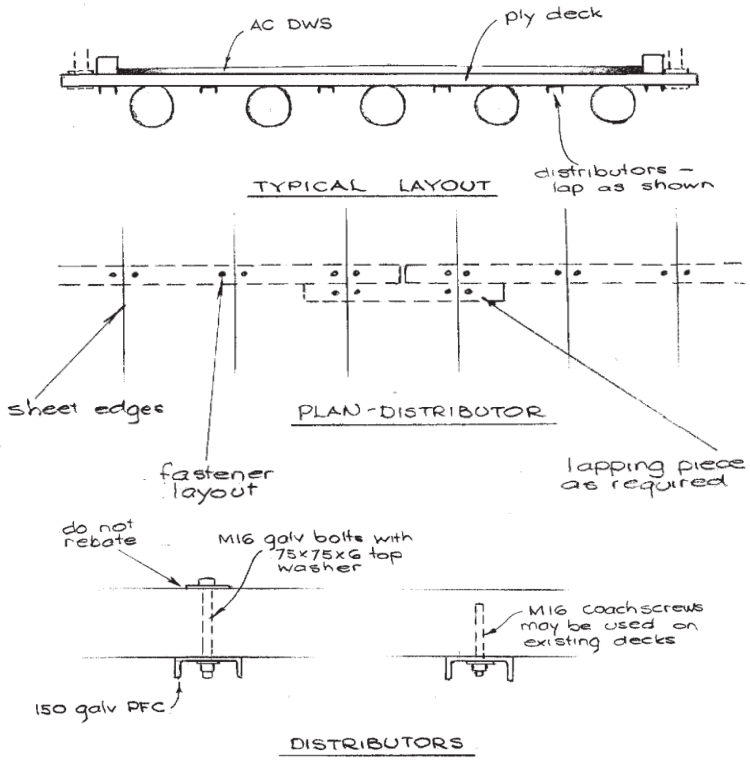

Figure 5 Indicative replacement decking layout of Drayton Rail Overbridge (Source: TMR TBMM [2])

4.5 Risk Management

Prior to GHD's mobilisation to site, the bridge authority had their own risk and safety measures, including implementation of traffic management at the bridge site, involving closing one lane adjacent the deck failure while keeping the other lane open to traffic.

GHD identified two key risks for the bridge authority to manage during remediation works:

- Partial bridge collapse due to road traffic loading, posing risks to road users and pedestrians.
- Partial bridge collapse leading to debris dropping onto railway users below the bridge.

GHD recommended for the bridge authority to maintain the traffic control measures (i.e., keep traffic lane with deck failure closed) until the recommended repairs were completed to mitigate risks to bridge users.

5 CASE STUDY 2: WALLANGARRA BRIDGE

5.1 Background

This structure is a five span timber rail overbridge on Bridge Link Drive at Wallangarra, Queensland. The superstructure features five girders with plywood decking and asphalt overlay. The bridge accommodates a one lane of road traffic with a footpath on the northern side of the deck. Prior to the inspection, the bridge authority advised GHD that the bridge had suffered bushfire damage to multiple structural elements, raising concerns about the integrity of its decking, girders, and piles, and thus the operational safety of the bridge.

5.2 Site Inspection

A small mobile crane was used to provide access to the soffit of the plywood bridge deck during the inspection. Only a visual and hammer tap structural inspection was carried out, i.e., no timber drilling, sampling, or laboratory testing. The inspection focussed on fire-affected areas, as shown in Figure 6 below.

Figure 6. Fire damage (Mid Span Girder left, Pile right) at Wallangarra Rail Overbridge

5.3 Assessment of Defects

Key findings from the inspection were as follows:

- The fire damage at Span 3 Girder 1 had burnt a nominal 300 mm diameter hole through the 350 mm diameter girder at near mid span. Zero remaining section was observed at the deteriorated mid-span section.
- The 145 mm thick plywood deck sheets directly above the Span 3 Girder 1 had suffered damage over an area of approximately 1200 mm x 1200 mm (confined to the one 1200 mm plywood deck sheet). The damage was measured to a depth of maximum 110 mm.
- Varying fire damage evident at multiple piles and bracing elements.
- Absence of longitudinal steel channel distributors between girders, which are typically placed centrally between each line of girders to help prevent differential edge deflections of plywood deck sheets.

5.4 Rehabilitation Recommendations

Following the site inspection, GHD proposed the following rehabilitation approach to the bridge authority:

- Replace the affected girder in its entirety and carry out a plywood deck repair of the fire damaged area directly above the girder (the latter employing the solution detailed above (Figure 4) for the Drayton Rail Overbridge) as a long-term repair due to the localised damage only at the Wallangarra Bridge.
- Providing remediation recommendations to the fire damaged bracing elements and piles were out of scope for this commission. Notwithstanding, GHD's recommendation would be to replace those bracing elements and for pile splicing to be installed to replace fire damaged pile portions. Pile splicing is considered a suitable solution here, where the pile portion above the ground has defects which severely reduce load carrying ability, but the lower pile portion in ground is sound and there is adequate ground support. The pile portion at and above the damage is propped, removed and replaced, and a splice connection is provided to ensure load transfer between existing and new piles portions (refer Figure 7).

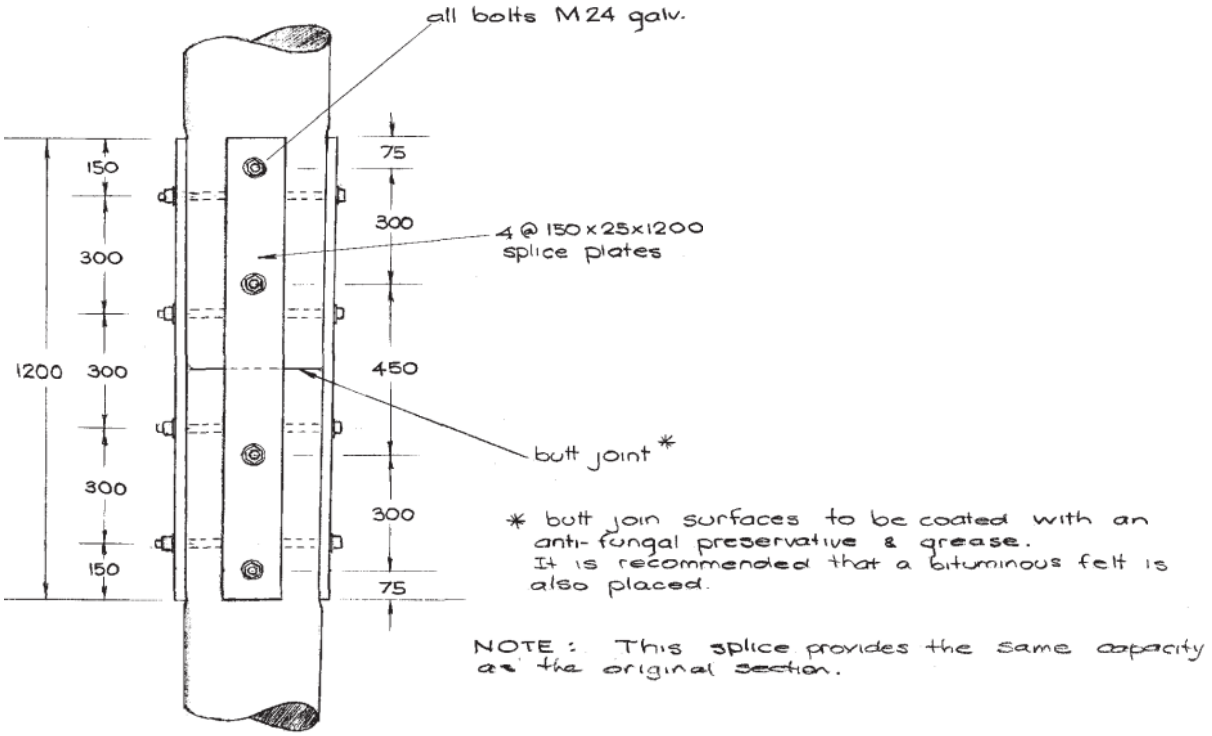

Figure 7. Pile Splice Connection Detail (Source: TMR TBMM [2])

5.5 Risk Management

Prior to GHD's commissioning, the bridge authority had closed the Wallangarra rail overbridge to the public. GHD recommended maintaining this measure until repairs were completed to mitigate safety risks. The bridge authority also noted that the railway track below was temporarily not in use due to the bushfires.

In addition, GHD identified two key risks for bridge authority to manage during remediation works:

- Partial bridge collapse leading to debris dropping onto railway maintenance staff below the bridge.
- Potential bridge collapse due to road traffic loading, posing risks to road users and pedestrians.

6 CASE STUDY 3: HOPES ROAD RAIL OVERBRIDGE

6.1 Introduction

GHD was commissioned by the bridge authority to undertake a structural inspection and then a desktop load rating assessment and concept repair design for the rail overbridge on Hopes Road (also referred to as Hopfs Road), located at Kuttabul, Queensland. Compared to the reactive inspections of the abovementioned bridges, the inspection of the Hopes Road rail overbridge was a planned inspection following the observed settlement at the western bank approach/abutment. This bridge is a three span timber girder bridge catering for one lane of road traffic. The superstructure features five girders that support timber plank decking.

6.2 Site Inspection

A ‘Level 2’ type of structural inspection and associated reporting was undertaken for this bridge in accordance with the TMR *Structures Inspection Manual* (SIM) [4]. This Level 2 inspection, in accordance with the TMR SIM, consisted of a visual and drilling inspection that was carried out utilising a ladder and rail-mounted elevated working platform during a network shutdown. The drilling investigation of the primary structural components was carried out using a 12 mm diameter bit, which bored holes into the timber components at critical and suspect locations, as determined by the experienced inspectors. The extent and severity of any piping or rot within the component was assessed by the inspectors based, in part, on the resistance to drilling. This method relies on the experience and subjective judgement of the inspector. All test holes were then plugged with wooden dowels, which had been treated with an approved preservative.

6.3 Assessment of Defects

The overall structure was assessed based on the classification system from the TMR SIM as Condition State 3, i.e., ‘poor’ condition. The settlement-affected approach was rated as being in Condition State 4 (i.e., ‘very poor’ condition). The bridge was observed to have experienced major settlement and localised failure of the abutment sheeting at the western approach (refer Figure 8), leading to structural instability. Other issues observed were over-sniping, minor piping and rot in multiple girder, column, and corbel members.

Figure 8. Approach settlement and abutment sheeting failure at Hopes Road Rail Overbridge

6.4 Desktop Structural Load Rating Assessment

Following the site inspection and detailed dimensional analysis, a load rating assessment was carried out. GHD and the road authority agreed upon adopting an Ultimate Limit State (ULS) approach for this assessment. (Other load rating approaches for timber bridges in Queensland include using the Serviceability Limit State (SLS) and ISO 13822. The bridge was assessed in accordance with the TMR *Tier 1 Bridge Heavy Load Assessment Criteria* (T1BHLAC) [5], which is based on the ULS approach. The load rating assessment was undertaken to quantify load effects due to vertical loading from dead loads and live loads, as well as horizontal loads from earth pressure at the abutments. Consistent with the T1BHLAC, specific load exclusions from the load rating assessment were train collision loads, road traffic barrier impact loads, wind loads, flood loads, temperature loads, road traffic braking loads, and earthquake loads.

This assessment was completed by experienced bridge engineers in conjunction with the relevant Australian Standards for bridge design. The abovementioned industry recognised bridge assessment guidelines were used to estimate the bridge’s ability to carry road traffic live loads. The assessment considered component defects from the Level 2 Inspection Report, which impacted some member stiffnesses and capacities.

Through consultation with the bridge authority, the bridge was load rated using a 42.5 tonne mass semi-trailer assessment vehicle. Given the width of the bridge, only one ‘reference vehicle’ could traffic the bridge and there were no ‘accompanying vehicles’. The structure was modelled using *SpaceGass* structural analysis software as a 3D space frame model subject to a linear-elastic analysis.

6.5 Rehabilitation Options

To conclude the scope of work, GHD undertook the repair concept design and a Safety in Design (SiD) workshop for the deteriorating approach/abutment in close collaboration with the bridge authority. Cost-effective repair options were devised with a minimalist approach, noting the bridge authority's desire to extend the service life of the structure by nominally 10 years, before a replacement bridge is planned.

The methodology for the repair concept design included:

- Assessment of deterioration mechanisms.
- Identification of three repair concept design options.
- Comparison of the three options using a multiple criteria assessment (MCA), with criteria, scoring, and weighting that was discussed with and agreed by the bridge authority.
- Preparation of a memorandum that summarised the above process.

The final repair concept design involved a shotcrete facing, new deck headstock and piles in a soldier pile wall, shown in Figure 9, aimed to minimise rail track and road closure time, addresses approach pavement failures and produces a cost-effective and appropriate solution to the dilapidated bank end.

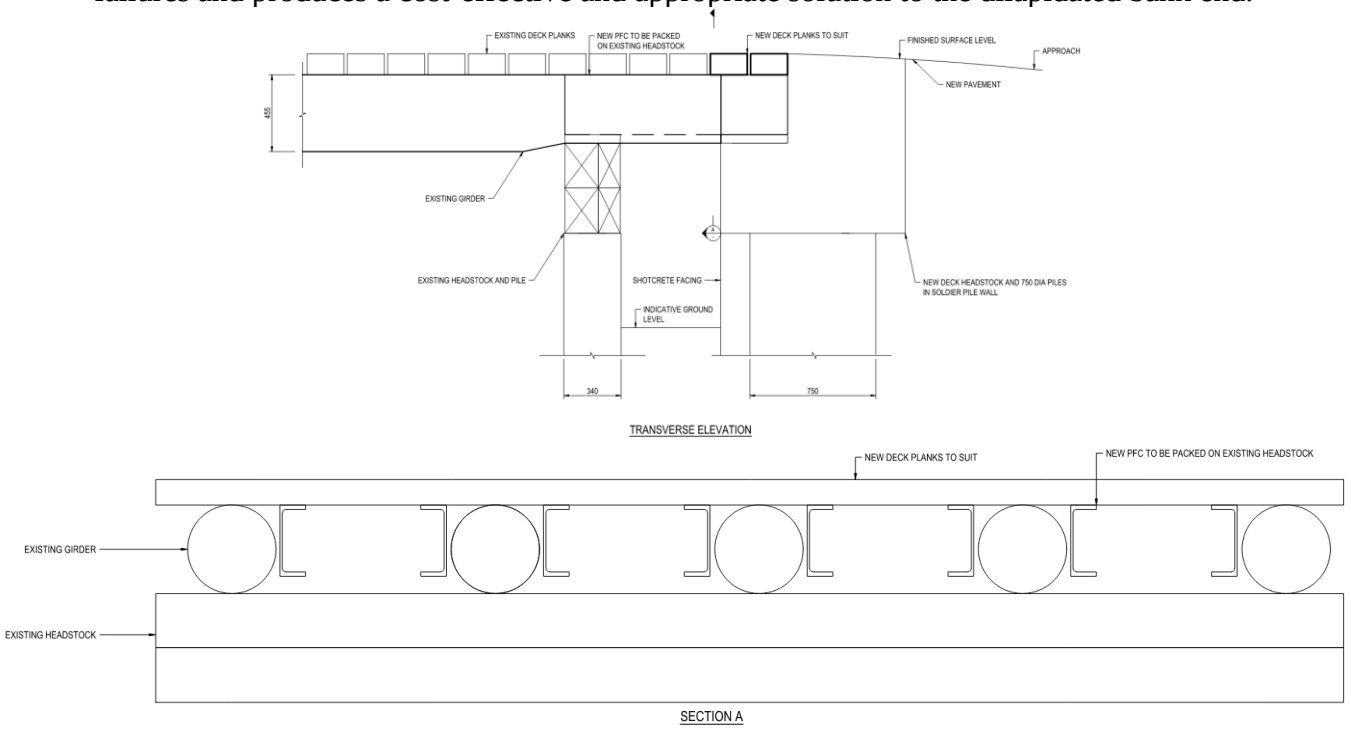

Figure 9. Bank end repair concept design at Hopes Road Rail Overbridge.

6.6 Risk Management

Informed by the collective outcomes from the structural inspection, load rating assessment, and repair concept design, GHD recommended the following measures to the bridge authority:

- Restrict road traffic across the bridge to small vehicles such as a sedan, utility, two-axle rigid trucks up to 15 tonnes gross vehicle mass, and emergency services vehicles
- Add 15 tonne maximum posted load limit signage to both approaches of the bridge to mitigate overload.
- Add 10 km/hr posted speed limit signage to both approaches of the bridge to mitigate overload.
- Replace or strengthen critical bridge elements in poor condition using similar timber or steel elements.
- Concept design for the western abutment embankment repair was provided to inform construction planning and cost estimating for these works, which included transferring a Safety in Design register.

Keep the abovementioned load and speed restriction signage in place until bridge element strengthening or replacement justifies reducing the above traffic restrictions to permit heavier vehicles to traffic the bridge.

7 DISCUSSION AND RECOMMENDATIONS

Key points from the case studies provide critical insights into timber bridge asset management:

- Proactive inspection and monitoring: Implement early defect detection techniques to prevent failures and reduce long-term maintenance costs by adhering to regular inspection and routine maintenance.
- Cost-effective rehabilitation: Utilise the resources like the TMR *Timber Bridge Maintenance Manual* (or local comparable equivalent), and other proven strategies to extend the service life of timber bridges.
- Policy considerations: Prioritise long-term resilience to ensure sustainable timber bridge management.
- Load capacity considerations: Where increased traffic loads exceed original design parameters, reinforcement strategies must be investigated and implemented to mitigate unacceptable risks.

Timber bridges will always present maintenance challenges. Effective management relies on proactive monitoring by experienced practitioners, adherence to best practices, and sustained investment in maintenance. Groundbreaking innovation unnecessary – instead, follow established methods like the TMR *Timber Bridge Maintenance Manual*. Regular inspections and maintenance will extend the service life of timber bridges in Queensland. A collaborative approach involving experienced timber bridge inspectors, designers, and structural analysts, is essential for effective asset management. The case studies highlight common failure mechanisms in timber railway overbridges and reinforce the need for proactive assessment and rehabilitation strategies.

8 CONCLUSION

The case studies in this paper highlight the challenges and key considerations in assessing and rehabilitating timber railway overbridges in Queensland. The Drayton Rail Overbridge, Wallangarra Rail Overbridge, and Hopes Road Rail Overbridge each had unique issues, including plywood decking failure, bushfire damage, and abutment settlement. Through targeted investigations and rehabilitation strategies, these case studies underscore the importance of regular inspections, timely interventions, and adherence to established maintenance frameworks such as the TMR *Timber Bridge Maintenance Manual*.

The findings emphasise the need for proactive asset management to ensure timber bridge longevity and safety. Load assessments and traffic restrictions are critical when structural integrity is compromised.

Timber bridges are vital to Queensland's railway infrastructure, but their continued use depends on diligent maintenance, strategic investments, and balancing heritage conservation with modernisation. By applying best practices in timber bridge management, asset owners can extend their service life, ensuring ongoing functionality and reliability. The case studies serve as a resource for engineers, inspectors, and policymakers in making informed decisions about the future of timber railway overbridges in Queensland.

REFERENCES

1. Humphreys, M. F., & Francey, K. L., 2004. An investigation into the rehabilitation of timber structures with fibre composite materials. *Queensland University of Technology*.
2. Queensland Government, 2005. *Timber Bridge Maintenance Manual*. Department of Transport and Main Roads. Available at: https://www.tmr.qld.gov.au/business-industry/technical-standards-publications/timber-bridge-maintenance-manual [Accessed 7 February 2025].
3. Australian Local Government Association, 2024. *2024 National State of the Assets Report*. Institute of Public Works Engineering Australasia. Available at: https://alga.com.au/app/uploads/ALGA-2024-National-State-of-the-Assets-Technical-Report.pdf [Accessed 7 February 2025].
4. Queensland Government, 2016. *Structures Inspection Manual*. Department of Transport and Main Roads. Available at: https://www.tmr.qld.gov.au/business-industry/Technical-standards-publications/Structures-Inspection-Manual [Accessed 7 February 2025].
5. Queensland Government, 2013. *Tier 1 Bridge Heavy Load Assessment Criteria*. Queensland Department of Transport and Main Roads.

ICTB 2025. 5th International Conference Timber Bridges
Rotorua, New Zealand, 29 June to 2 July 2025.

EMERGING TECHNOLOGY IN TIMBER BRIDGE DECK REPLACEMENT: RECENT USE OF ENGINEERED PLYWOOD PANELS IN NEW ZEALAND

Jeremiah Shaw,[1] John van Rij[2]

ABSTRACT

This paper discusses the use of engineered plywood panels (EPPs) for timber bridge deck replacement in New Zealand. This technology is in its early stages of adoption locally, providing opportunities for learning and improvement with each project. EPPs are particularly suitable for timber deck replacement and situations where reinforced concrete decks would require substructure changes. The paper highlights the limitations of existing nail laminated decks, and how EPPs offer a solution that can extend the life of aging bridge assets. One of the key challenges for the use of EPPs is surfacing performance that also impacts the durability of the panels. The aim of this paper is to inform asset owners, designers, and contractors about the potential benefits and challenges of using EPPs for future deck replacement projects.

1 INTRODUCTION

Timber bridges and bridge decks have been used for centuries in different parts of the world, including New Zealand. Over time, timber elements were gradually removed from New Zealand bridges as reinforced concrete and structural steel became more widely used. Typical legacy timber elements remaining on road network bridges include nail laminated timber bridge decks. Many of these are reaching the end of their usable life and have performance and maintenance problems. Replacement with concrete decks in these situations is often not feasible. In this paper, we will explore how engineered plywood panels (EPPs) can address these problems, extending the life of the asset and providing a more sustainable solution for bridge deck replacement. Drawing on recent deck replacement projects in New Zealand we will highlight the benefits and challenges of this approach together with some lessons learned.

2 LIMITATIONS OF EXISTING TIMBER BRIDGE DECKS

Overtime timber elements have gradually been removed from bridges in New Zealand as other materials have become more readily available. Hardwood decks that reach the end of their useful life are difficult to replace with hardwoods due to limitations of supply. One of the common timber legacy elements that remain on road bridges are nail laminated bridge decks. These are made up of timber battens typically 200 to 250mm deep and 50 or 75mm wide usually nailed together. The typical arrangement is to span transversely over longitudinal steel beams.

Four of the more common problems with existing nail laminated bridge decks are:

- Failure of individual battens in conjunction with the failure of nails in shear
- Local failure of the battens at the location of barrier posts under barrier impact
- Delamination of surfacing under wheel loads due to excessive movement between adjacent battens

[1] Technical Director, Beca Limited,
e-mail: jeremiah.shaw@beca.com ,
[2] Structural Engineer, Beca Limited.

- Wet rot of timber

Figure 1 Delamination of surfacing on nail laminated bridge deck

Figure 2 Failure of laminated bridge deck

A solution is required that addresses these problems and that also accounts for other design and constructability challenges. Within the last ten years, Engineered plywood panels (EPP) have emerged as an option for increasing numbers of deck replacement projects in New Zealand.

3 MANUFACTURING

Engineered plywood panels are made from softwood veneers that are cross laminated and bonded together with an adhesive. It is called an 'engineered' panel because it is manufactured to meet structural performance criteria. Current availability to the New Zealand market consists of imported EPPs from Australia or Papua New Guinea. At the time of writing the authors of this paper are not aware of any projects that have used New Zealand manufactured options. The standard EPP width is 1200mm and this can be varied larger or smaller according to design requirements. The lengths vary up to a maximum of about 12m in length. Longer panels can be provided but is limited in New Zealand by shipping container size. Thicknesses can vary up to 251mm to suit design requirements, with 198mm often being used.

Some EPPs have each veneer preservative treated before they are bonded together to maximise penetration and provide a standard H4 treatment to NZS 1601.1:2021, or H5 on request [1]. The veneers are then bonded together with phenolic resin, (also known as phenol-formaldehyde resign) with what is called a structural "A" bond.

Other products on the market are deep envelope treated rather than veneer treated. The suppliers indicate they achieve an H5 treatment to NZS 1601.1:2021[2]. A concern with this approach is whether full penetration through the depth of the section is achieved. Full penetration is required to provide treatment

in the middle of thick sections, especially since drill holes and cut faces can provide a path for moisture into the internal veneers.

EPPs are treated with Alkaline Copper Quaternary (ACQ) to protect against decay, rot and insects. ACQ treatment is now preferred over the older Chromated Copper Arsenate (CCA) treatment, for environmental and safety reasons. ACQ contains higher levels of copper than CCA making it more effective as a preservative, though this means the timber is more corrosive to ferrous metals. Because of the ACQ treatment in the EPPs, stainless steel fixings are typically used to reduce corrosion risk.

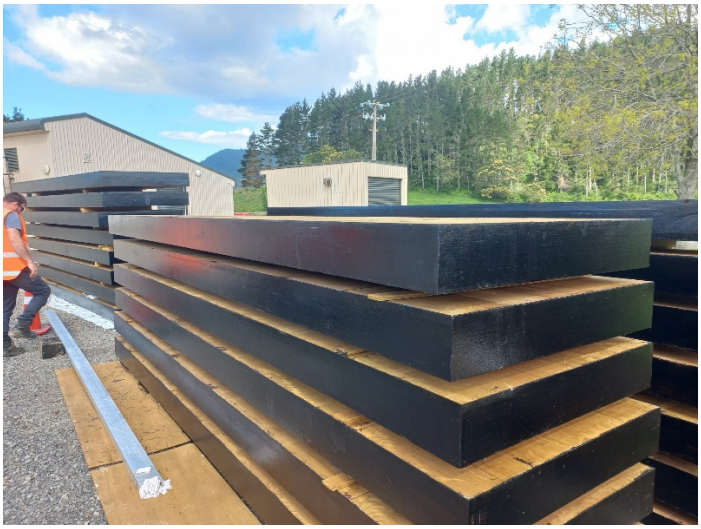

Figure 3 Engineered plywood panels ready for installation

There are several key performance requirements of EPPs for use in bridge deck replacements. What is required is a new bridge deck that is lightweight, simple to install, durable, sustainable, and able to accommodate barrier impacts and wheel loads. These performance requirements are discussed under the headings below.

4 WEIGHT

The primary reason that EPPs are considered as an option for bridge deck replacement is that they are a similar weight to existing timber decks. Existing timber decks are generally replaced with timber for the following reasons:

- A timber deck is approximately 25% the weight of a concrete alternative
- Typically, these bridges are located on an existing foundation of unknown capacity
- A heavier deck option (concrete) may decrease the seismic resilience of the structure without further strengthening

An increase in seismic mass increases the risk profile of the bridge and it is usually uneconomic to strengthen the substructure or foundations. When a concrete deck is not a practical or economical solution due to its weight, a lightweight EPP can provide a feasible alternative.

5 SIMPLE INSTALLATION

Simple installation is an important performance criterion when considering timber deck replacement. Bridges selected for deck replacements are commonly single laned and often the only detours available add considerable travel time. Night closures or compressed programs are often used to minimise road closures and community disruptions. EPPs can be installed relatively simply and rapidly allowing re-opening of the bridge after overnight closures with only some sections of deck replaced. The panels are lifted into place with small cranes that can often be accommodated on the existing bridge structure. See Figure 4 and Figure 5 below for pictures of installation of panels.

Figure 4 Installation of engineered plywood panels for a recent deck replacement project

Figure 5 Engineered plywood panels soon after installation.

There are design decisions that can influence the ease of placement of the panels. Standard panels have a width of 1.2m, though custom orders can accommodate wider sizes up to about 3.6m. Using wider panels has the benefit of reducing the number of panels to be installed, reducing the number of joints in the deck. This also allows the panels to be aligned with standard barrier post spacing, though there is a trade-off with larger panels to transport and handle. Recent jobs have used 2.0m panels to match standard barrier post spacing.

Detailing of hold down bolts to attach the panels to the superstructure is a continued area of improvement. A good connection will be easily constructable and give confidence that the connections will be robust and durable under long term live load. Some connection details that have been used on recent projects include:

- Clamping action with hold down bolts onto the top flange of underlying steel beams though this carries the risk of loosening under repeated live load. See Figure 6 below.
- Coach bolts or bolts attached through holes drilled into the top flange, which may be acceptable if the beam has sufficient capacity to accommodate loss of flange due to the holes. See Figure 7 below.
- Welded tabs on the top flange. This requires accurate site welding and extends site time during panel installation, but does provide a reliable connection . See Figure 8 below.

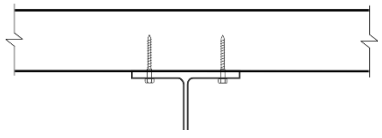

Figure 6 Sketch of Coach bolts through top flange

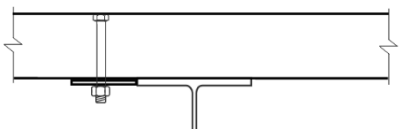

Figure 7 Sketch of Tab welded to flange, bolted to EPP

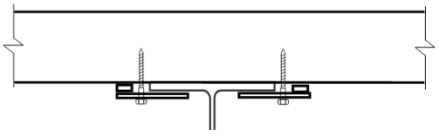

Figure 8 Sketch of coach bolts clamping EPP to top flange

6 DURABILITY

Product manufacturers advise EPPs have a 50-year design life. However, these panels have only recently been introduced to NZ conditions, which are considered to be damper than reference performance examples suggested by the product manufacturers. Further, maintenance and use alterations (such as attaching services) may have an influence on achieved service life. In addition to treatment, good design and construction practices that keep the timber protected from moisture will be vital for durability.

The panels usually come with edges pre-painted from the supplier, but cuts made on site should be repainted. The main protection for the deck from moisture is the surfacing. Good surfacing practices that prevent water getting into the panels will extend the EPPs useful life. Surfacing in the summer months when it is dry increases the probability of a more durable bridge deck. Some instances of veneer delamination have been observed where the top surface of the timber deck has been left exposed to the weather beneath the guardrail. Suppliers have investigated these instances and now recommend that in addition to all surfaces of the EPP being painted, the surfacing treatment should extend to the deck edge. See Figure 9 for an example of a bridge deck with this detail.

Figure 9 Chipseal extended to the edge of to prevent water pooling

7 SUSTAINABILITY

7.1 Production and Installation

At the beginning of the panel life cycle, these timber panels are inherently a more sustainable option than many other materials since they come from a renewable resource. In addition to this, the panels coming out of Papua New Guinea are processed using hydro power and a wood-based boiler, which has obvious environmental benefits, although the shipping to New Zealand has its associated environmental costs. Improvements in the future would be the production and use of local products to limit transportation, though the current locally available radiata pine would have lower strength compared with hoop pine.

7.2 Useful life

The durability and sustainability of these panels are closely linked, since longer lasting panels will be replaced less often. Keeping the panels as dry as possible in the damp New Zealand climate will increase their life. As construction and design practices improve with increased use in New Zealand it is hoped that the useful life of the bridge decks will increase, making EPPs an increasingly sustainable option.

7.3 Disposal

Consideration of the safe disposal and reuse of these products is required, given the chemical compounds used to treat them. Phenolic resin combined with timber is not suitable for incineration and is difficult to recycle. While ACQ treatment is an improvement on the older CCA from an environmental point of view, it still renders the panels difficult to dispose of. It appears likely that bridge decks installed now will be disposed of in landfill. This presents an opportunity in the future to move towards a circular economy with timber bridge construction, if a material could be sourced that is durable without requiring chemical treatment. One possibility would be the production and use of local hardwoods or resinous softwoods. This would require a programme of development similar to that which has taken place to reduce the harvest time for our current softwood production but could prove an invaluable resource for generations to come. A durable timber that doesn't require extensive chemical treatment could be more easily disposed of.

8 STRUCTURAL PERFORMANCE

8.1 Barrier impact

Engineered plywood panels can take larger barrier impact loads than the previously used nail laminated decks due to their higher characteristic strength and wider load spread. Especially if larger width panels are selected and weak post systems are used, damage from barrier impact should be limited to the barriers.

Figure 10 Local failure of laminated bridge deck under barrier impact

EPPs are likely to continue to be limited to deck replacements on existing structures due in part to the vehicle barrier requirements on new bridges. The standard acceptable solution for new state highway bridges in New Zealand are rigid (usually concrete) barriers. Proprietary semi rigid barriers on new State Highway structures generally represent a departure from the recommendations.[3] EPPs are unlikely to be able to accommodate both the additional weight of concrete barriers and the larger rigid barrier impact loads. This means that currently the more common application of EPPs is bridge deck replacements, rather than new bridges.

8.2 Live Loads

EPPs on bridge decks in New Zealand need to be designed for the standard NZ Bridge Manual Wheel loads (HN-HO 72). The bearing strength of the panels is usually comfortably able to accommodate the required design wheel loads. We can illustrate the relative flexural strength of the various options by showing the thickness of deck that would be required to achieve a similar flexural strength as shown in Table 1. The larger reliable bending capacity of Hoop Pine EPPs is primarily due to higher strength of Hoop Pine, as well as the benefits of randomising defects section and cross lamination.

Table 1 Comparison of products and flexural strength [1] &[4].

Product	**Grade**	**Characteristic Bending Strength (f'_b, *MPa*)**	**Equivalent Thickness of Panel Required for the Approximately Equivalent Flexural Capacity (mm)**
Hoop Pine EPP	F14*	36	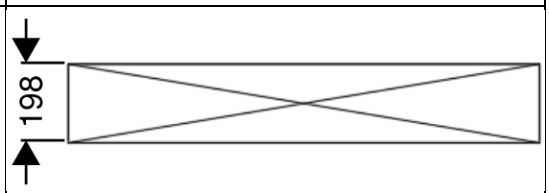
Radiata Pine EPP	F8	25	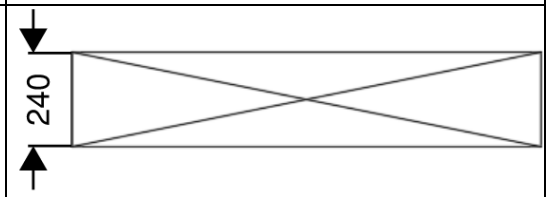
Nail Laminated Radiata Pine Battens**	SG8	14	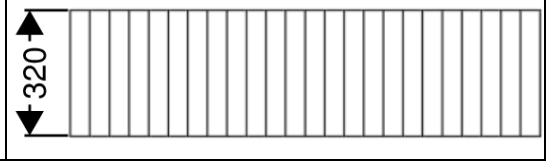

*Grade F17 with f'_b=MPa can be provided if each panel is stress graded.
**Assumes full composite action of the nail laminations.

The critical live load case for the design of the panels is often the case where a vehicle has knocked off the guardrail, and an HN wheel load is placed on the edge of the deck, cantilevering outside longitudinal steel beams. An iterative optimisation of the design is required here, as larger carriageways and offsets behind the barrier are preferred, provided both the EPP and the outer supporting beam can accommodate this load case.

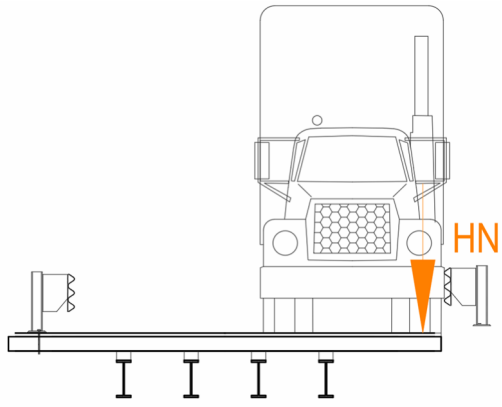

Figure 11 Sketch of load case when barrier has been knocked off

9 SURFACING

Adhesion of surfacing to timber presents a well-known challenge on New Zealand timber road bridges. Factors influencing outcomes include adverse temperatures and weather conditions, surfacing design, applicator quality control, traffic volume and loadings, and any differential movements occurring between timber elements. EPP panels reduce the incidence of joints between timber elements but share the same risk factors as traditional nail laminated timber decks. Great care is required to optimise the durability and performance of the surfacing.

10 CONCLUSION

With the technology in the early stages of adoption in New Zealand each project is an opportunity to learn from and improve on the last. EPPs can be an ideal solution for extending the life of aging bridge assets. They are particularly suited where rapid or incremental deck replacement is required, and where reinforced concrete decks would dictate strengthening the substructure. At this early-stage of adoption, low-volume roads are preferred due to surfacing performance risks, though further development of surfacing solutions may alleviate these concerns. We hope that this paper informs asset owners, designers and contractors about the potential of using engineered plywood panels on their next deck replacement project.

11 NOMINATED THEMES

Structural design of timber bridges.

REFERENCES

1. PNG Forestry Products. (March 2023). *Construction Manual- Niubridge & Niudeck.* https://nzwoodproducts.co.nz/media/products/files/2024/NiuBridge_Construction_Manual_300_Compress_IBUILT.pdf

2. Big River Group. (n.d.). https://www.bigrivergroup.com.au/product/engineered-plywood-bridge-decking/. Retrieved from Engineered Plywood Bridge Decking: https://www.bigrivergroup.com.au/product/engineered-plywood-bridge-decking/

3. NZ Transport Agency Waka Kotahi. (31 July 2024). NZTA M23:2022, *Appendix B: Rigid and bridge barrier systems Version 5.*

4. Standards New Zealand, *NZS AS 1720.1:2022 - Timber structures Standard. 2022.*

ICTB 2025. 5th International Conference Timber Bridges
Rotorua, New Zealand, 29 June to 2 July 2025.

DURABILITY OF WOODEN BRIDGES: INSIGHTS FROM HISTORICAL SERVICE TEST DATA IN NEW ZEALAND

Tripti Singh[1] and Dave Page[2]

ABSTRACT

Wooden bridges have historically played a crucial role in New Zealand's road and rail networks. Although concrete and steel have largely replaced wooden structures on major routes, timber bridges remain valuable for lightweight, easily assembled structures, especially on roads with relatively low traffic loads. Over the past decade, there has been a resurgence in the use of engineer-designed wooden structures. Unlike traditional construction methods, these prefabricated components are manufactured in factories and assembled on-site with minimal cutting and drilling. Wood offers certain design features that are difficult to achieve with other materials, enhancing architectural and engineering possibilities.

This presentation will summarise the history and use of timber bridges in New Zealand. Many older bridges were built with Australian hardwood and native New Zealand timber. During the 1950s and 1960s, preservative-treated timber, particularly glue-laminated bridges, became popular. Using some specific case studies based on our historical service test data, we looked at the durability of wooden bridges in New Zealand.

1 INTRODUCTION

In the late 1950s, the Forest Research Institute (now Scion) initiated an in-service, long-term testing program for wooden products [1]. This program included various types of wooden products and components, mainly preservative-treated and used in external environments such as timber bridge components [2]. The other tested items encompassed poles and piles, railway sleepers, building components, and specialised timbers like those used in cooling towers. These were generally commercially produced wood products in typical use across the country. Test sites were revisited every 3-5 years, and the results were used to determine whether naturally durable and preservative-treated wood met consumer durability expectations. The inspection program was somewhat abandoned in the 1990s, but many test sites still exist and are periodically assessed.

This document provides a summary of the history and use of timber bridges in New Zealand. Many older bridges were constructed using Australian hardwoods and durable native New Zealand timbers [3]. During the 1950s and 1960s, preservative-treated timber, particularly glue-laminated bridges, became more common. Today, few bridges are built entirely from wood; however, treated timber is still widely used for superstructures and decking in smaller bridges [4]. Drawing on historical service test data, we examine specific case studies to assess the durability and maintenance requirements of wooden bridges in New Zealand.

[1] Dr Tripti Singh, Scion Research, Rotorua New Zealand
e-mail: tripti.singh@scionresearch.com
[2] Mr Dave Page, Scion Research, Rotorua New Zealand

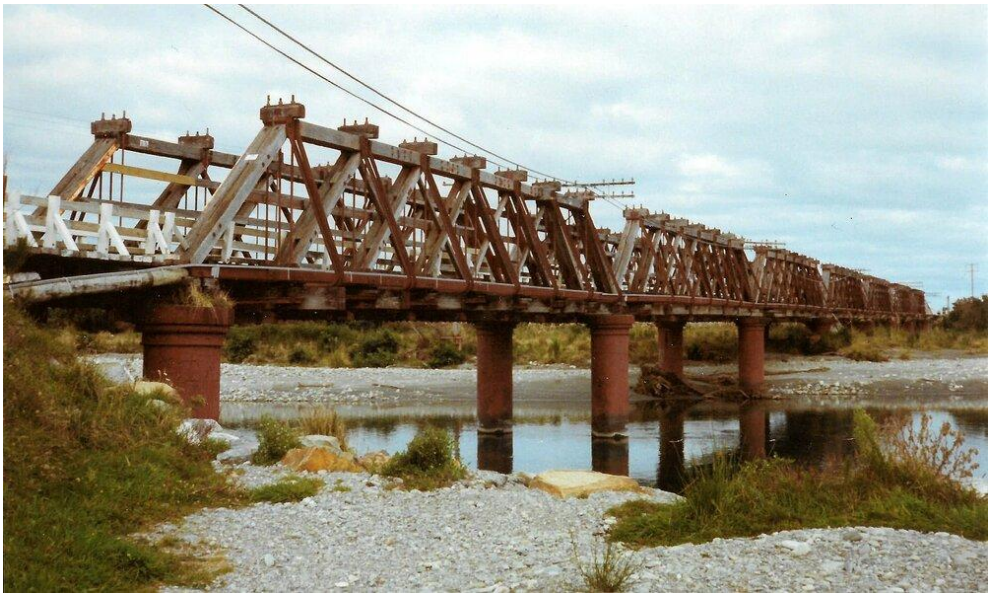

Figure 1 – A Howe-Truss bridge built from durable Australian hardwood typical of those which were common throughout the New Zealand road and rail networks in the first half of the 20th century.

2 THE EVOLUTION OF WOODEN BRIDGES

During the 19th century and up until the Second World War, New Zealand constructed numerous substantial timber bridges (Figure 1)[4]. In the 1940s and 1950s, preservative-treated radiata pine (*Pinus radiata*) and, occasionally, Douglas-fir (*Pseudotsuga menziesii*) began replacing naturally durable local and imported species in outdoor structures. During this time, advancements in synthetic adhesives enabled the use of laminated preservative-treated pine in large structures such as bridges. Timber bridges were favoured for their ability to be prefabricated and installed quickly (Figure 2), as well as their lower cost compared to reinforced concrete. Recognizing these advantages, the New Zealand Forest Service, through its timber production facility near Rotorua, developed bridge designs and manufacturing processes for roads within its forests.

Figure 2 - Panmure basin footbridge, a 60 m long, CCA treated pine structure installed in 1984. Once site works and foundations were in place the wooden bridge structure was completed within a week.

Initially, timber used in outdoor applications was treated with oil-based preservatives such as creosote or pentachlorophenol (PCP). However, by the 1950s, waterborne multi-salt preservatives, including copper-chrome arsenate (CCA) and copper-zinc-chrome arsenate (CZCA), became the preferred options. Oil-

based treatments required lamination before preservation, often leading to limited penetration and effectively providing only an envelope treatment. In contrast, waterborne preservatives were applied before lamination, but this necessitated costly re-drying after treatment. When applied to previously laminated components, waterborne preservatives caused differential swelling of laminates and variable penetration, though they did not significantly compromise glue line integrity. Table 1 presents a summary of the bridge components and preservatives used in the service test conducted at Scion.

For most structural bridge components, CCA retention levels were comparable to New Zealand's current H4 specification (0.72% TAE, NZS 3640) [5], while CZCA retention was approximately 4.06 kg/m³ TAE. All structural timber components treated with waterborne preservatives underwent full-cell treatment before lamination, followed by re-drying, machining, and assembly.

Table 1: Summary of In-Service Tests of Preservative Treated Laminated Pine Bridges

Location	Type	Components	Preservative	Installed
Kaingaroa	Forest access	Decking etc	Creosote, CZCA	1957
Shannon	Highway	Decking	CCA	1960
Whakarewarewa	School access	Decking etc	CZCA	1961
Rangitaiki	Farm access	Decking etc	PCP in Oil	1961
Waimakariri	Highway	Decking	CCA, CZCA	1963*
Lyell	Highway	Decking	CCA, CZCA	1962
Kaingaroa	Forest access	Beams, decking	PCP in Oil	1962
Ngongotaha	Footbridge	All	CCA, D-fir	1962*
TePuke	Highway	All	PCP, CCA	1965
FRI Rotorua	Campus access	Decking etc	CCA	1968*
Harihari	Forest access	Beams	CZCA	1968
Waitahanui	Footbridge	All	PCP, CCA	1968*
Pakuranga	Footbridge	All	CCA	1975*
Taneatua	Highway	Decking	CCA	1978
Okarito	Forest access	Beams, decking	CCA	1977
Whakarewarewa	Village access	All	CCA	1980*

*Bridges that were still in use in 2024.

3 OBSERVATIONS FROM BRIDGE SERVICE TESTS

The assessment of the service testing programme is not very frequent, it was largely discontinued in 1990s. However, many of the test sites still exist and few have been visited recently and reported [1, 2]. This output covers the recent assessment (May 2022-July 2022) information and images.

Generally, bridge beams that were treated with PCP-in-oil after lamination are still in good condition here after 55 years in service. These beams were all made from pine species that are easily penetrated by preservatives and expected to have deep but variable envelopes. Beams made up of laminates that have been treated with CCA before assembly have also shown good durability.

The Waititi Stream footbridge at Ngongotaha, Rotorua:

This bridge was assessed in June 2022 (Figures 3A-C). This bridge has been in place for almost 60 years.

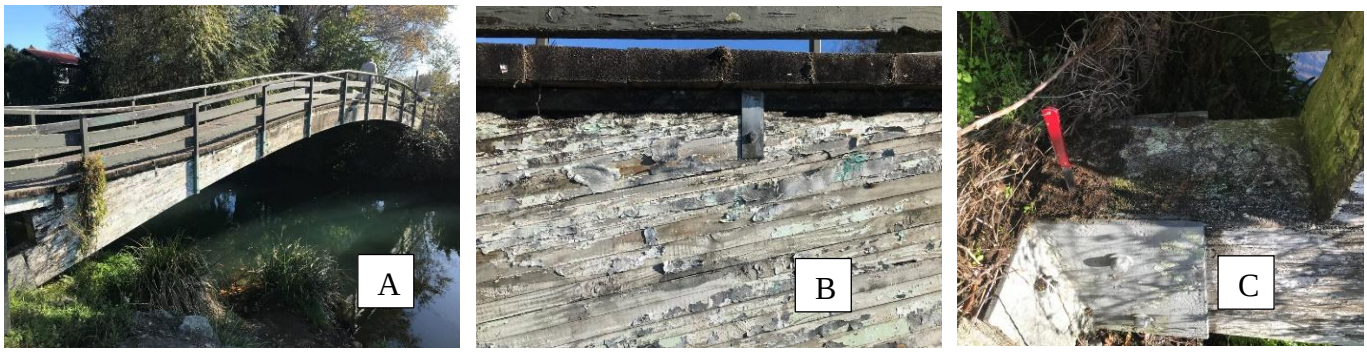

Figure 3. Waititi Stream footbridge, installed 1962 (Ngongotaha, Rotorua), current condition.

There is decay in angle pieces attached to the upper sides of the arches, close to the ends, to reduce the gradient. These pieces have ends cut on a sharp angle with the end grain facing upwards allowing deep water penetration (Figure 3A). Otherwise, there is only minor surface soft rot. There are small pockets of decay at the ends of the beams where the beams are partly buried in soil and decaying vegetation (Figure 3C).

Handrails posts and rails were originally Douglas-fir but were replaced with steel and treated pine when they decayed within 20 years. Recent assessments showed that the paint on the Glulam is in poor condition, however, timber in the arches was sound with minor cracking and delamination (Figure 3C).

The two Scion's old entry bridges:

These two bridges have been in place for more than 50 years (Figures 4 & 5). While the south entry bridge has PCP-in-oil treated glulam beams with CCA treated deck and glulam superstructure the north entry only has CCA treated decking and superstructure. Apart from minor soft rot in the superstructure where paint has failed and in the ends of decking both are still in good condition. Delamination and cracking of glulam footpath buffers were partly associated with treatment after lamination.


Figure 4. The Scion North entry bridge was installed 1968.


Figure 5. The Scion South entry bridge was installed 1965.

The Pakuranga footbridge in Auckland:

The Pakuranga footbridge was visited in July 2022 (figure 6). It has been in place for 47 years and unlike the Waititi stream bridge, was not painted and has received little maintenance since installation. All timber is CCA treated.

Figure 6. Pakuranga (Auckland) footbridge, installed 1975.

There is minor, occasional checking and delamination on the exposed northern side, small soft rot pockets at the ends where there is contact with soil and debris plus extensive surface soft rot 2-3 mm deep, and a small pocket of decay at one of the metal post brackets on the continually damp south side (Figure 6B). Based on current condition, it appears that the decking has been replaced in the past decades. The downstream (exposed) side of the beam is showing minor delamination, weathering, and extensive algal growth but no visible decay (Figure 6C).

Whakarewarewa, Rotorua entrance Bridge:

The Puarenga stream bridge at Whakarewarewa (Figure 7) has been in place for 42 years. This structure is all CCA treated, Glu-laminated. This is exposed to constant steam from the surrounding geothermal area and surface degradation a few millimetres deep on the beams and underside of the decking is associated with delignification caused by the constant exposure to geothermal steam (Figure 7B). The beams on this bridge contained delamination that became obvious shortly after the bridge was constructed and surface checking developed on the more exposed north-western side of the outside beam. The outer faces of the outside beams were coated with a soft waxy substance “Goldseal”, more often used for protection on steel structures. This has largely gone from the north-western facing upstream beam but remains, along with dust and debris sticking to it, on the outside of the sheltered downstream beam. While there is significant decay in the unprotected ends of the decking there is no obvious decay in any of the beams. Minor soft rot at join-in laminated handrail was observed where paint coatings had failed (Figure 7C).

Figure 7. Whakarewarewa (Rotorua) entrance bridge was installed in 1980.

Footbridge at Hamurana, Rotorua:

Hamurana footbridge was installed in 1985. The main beams are laminated, CCA treated pine uncoated for part of their life then coated with oil based stain but poorly maintained more recently. Some of the components in this bridge may have been preservative treated to the lower H3.2 specification, rather than the H4 specification normally recommended for bridge components. The upper edge of the beams are fully exposed. Severe checking and decay have developed in the upper laminate (Figure 8B). The stain coating has done little to prevent deterioration. Delamination and cracking on the upper section of the beam is observed also, the ends of the decking have significant softrot as has the side of the beam where it is in contact with the decking and debris (Figure 8C).

Figure 8. Hamurana footbridge's current condition.

The Panmure Basin footbridge, Auckland:

The Panmure Basin footbridge (Figure 9), constructed in 1984, features laminated support beams and arches, with all timber composed of CCA-treated radiata pine. A July 2022 assessment identified a few minor areas of soft rot where paint coatings have cracked at component intersections (Figure 9B). However, the glue-laminated beams and arches were found to be in good condition overall.

The H3 treated plywood roof section was in poor condition but the structure of the beams appeared sound (Figure 9C).

Figure 9. The Panmure Basin footbridge in Auckland.

We were recently informed that the bridge has been replaced due to health and safety concerns, unrelated to any timber structural failure (Figure 10) The project manager confirmed that “timber is in surprisingly good condition despite the bridge being closed last year due to safety concerns”.

We are currently in the process of collecting timber samples from the old bridge for further close examination.

Figure 10. The replacement of the Panmure Basin timber Bridge (March 2025) with a steel structure.

Results from service testing indicate that the use of film-forming surface coatings to protect glue laminated components may have some benefits providing coatings are well maintained. The Waititi stream footbridge, the Scion north entry bridge, and a footbridge near the Panmure basin, installed in 1984 all have large glue laminated components that have been painted. At Panmure and Scion, the paint coatings have been maintained but on the Waititi stream bridge, repainting of the beams has not been done this century. Where the paint coatings have been well maintained it is difficult to determine whether the components have been laminated, i.e. there is little or no delamination. On the Waititi stream beams the paint coatings have largely disintegrated and while there is minor delamination there is very little surface cracking. By comparison, beams on a footbridge at Hamurana, which were uncoated for a period and then coated with an oil-based stain, are severely cracked in the fully exposed upper laminate and show more delamination and decay than other bridges.

While physical protection systems such as sacrificial fascia panels or metal cappings were not installed on any of the test bridges, protection of the beams from the weather will extend the life of timber structures. This is evidenced on the bridges where partial protection by the decking and road surfacing bitumen has largely prevented deterioration of the supporting beams whereas the ends of some decking boards, beyond the bitumen surfacing, have significant decay. Exposed end grain particularly upward facing as on the Waitete Stream footbridge is particularly prone to water ingress and soft rot. While this bridge has treated wooden decking and there appears to be little decay in the upper edge of the arches, the upper facing end grain in the slope reduction pieces at each end of the arches contains significant soft rot.

4 CONCLUSIONS

Based on history and evidence from the service tests at Scion, the following conclusions can be drawn;

- Preservative-treated radiata pine laminated bridge beams have been in service for 60 years in New Zealand and have shown few problems with durability associated with decay particularly if glue laminated beams are not in direct contact with soil and decaying vegetation.
- Biological decay resistance of H5 is better than H4 but H4 treatment has given reasonable service in our test bridges and it presents fewer problems than H5 treated timber with glues. If a 100-year life is expected, logically the H5 treatment would be desirable [6].
- Only resorcinol-formaldehyde (RF) or phenol-formaldehyde (PF) glues have shown long-term durability in Scion test bridges. More recent PU (Polyurethane) and PUR (polyurethane

reactive) glues have not been included in long-term exposure trials at Scion Hence, to get a better understanding and confidence, long-term exposure trials should be set up using PU and PUR glues in the local New Zealand conditions.

- Design and maintenance are the key elements of timber bridge durability. Laminated beams that are on the exterior of the structure and fully exposed to weather, particularly where the upper edge is exposed, are likely to deteriorate more rapidly than those that are partly protected by decking
- Treatment with water-based CCA formulations before lamination has proven just as effective as using oil-based formulations after lamination. Pre-lamination treatment offers the advantage of preservative penetration throughout the entire component, whereas post-lamination treatment tends to result in uneven, envelope-type protection. However, a potential drawback of using CCA-treated timber at very high retention levels is that it can impair the effectiveness of gluing
- Evidence from service testing indicates that the use of film-forming surface coatings to protect glue laminated components have some benefits in extending the service life providing coatings are well maintained.

ACKNOWLEDGEMENTS

The authors wish to acknowledge Ian Simpson for his assistance in inspecting some of the bridges. All other present and past wood preservation group members are also acknowledged.

REFERENCES

1. Singh, T. and Page D., 2018. Case studies on the history and use of timber bridges in New Zealand. Wood Material Science and Engineering 13 (3): 159-166.
2. Page, D. and Durbin, G., 2000. In-service Wood Preservative Test on the Howe Truss Railway Bridge, Waikino. Conservation Advisory Science Notes No. 299, Department of Conservation, Wellington.
3. Roche, M. (1990) History of New Zealand Forestry (Wellington: GP Print Ltd). ISBN 0-477-00004-5.
4. Thornton, G. (2001) Bridging the Gap. Early Bridges in New Zealand 1830–1039 (Auckland: Reed Publishing Ltd). ISBN 0 7900.
5. New Zealand Standard NZS, 3640: 2003. Chemical preservation of round and sawn timber.
6. Singh, T. and Page D., 2016. CCA treated wood, will it last 100 years? International Research Group on Wood Protection, IRG/WP 16-20575.

ICTB 2025. 5th International Conference Timber Bridges
Rotorua, New Zealand, 29 June to 2 July 2025.

TIMBER CIRCULARITY: SUSTAINABLE WOOD RESOURCE MANAGEMENT IN AUSTRALIA

Tripti Singh [1], Penelope Mitchell[2], Martin Strandgard[3]

ABSTRACT

Engineered Wood Products (EWPs) used in timber bridges are particularly attractive due to their long service life, versatility, and sustainability. However, the end-of-life disposal of preservative-treated timber presents a significant challenge. At this stage, these materials can become a liability, often requiring special and more costly disposal options.

The initiative led by the National Centre for Timber Durability and Design Life (NCTDDL) in collaboration with Forest and Wood Products Australia (FWPA) and a consortium of industry stakeholders, focuses on integrating timber into the circular economy by addressing the challenges of reusing, repurposing, and recycling chemically treated materials. The project is organised around seven key tasks designed to tackle these challenges and develop practical solutions.

1 INTRODUCTION

In recent years, there has been a global resurgence of interest in the bioeconomy. The bioeconomy relies on renewable, biological resources to replace carbon-intensive materials such as steel, concrete, and plastics with fossil-free alternatives like forest and wood products [1]. A circular bioeconomy offers a pathway to reducing fossil fuel dependency, addressing supply chain challenges, and mitigating climate change, contributing to a more sustainable future [2].

To achieve climate neutrality by 2050, adopting a circular economy (CE) and transitioning to a regenerative, bioeconomic model are essential. This shift toward a low-carbon, circular framework presents an opportunity to tackle resource scarcity, waste, and emissions while enhancing economic security. In line with these goals, the Australian Government has set a target for implementing a circular economy by 2030 to address global challenges such as climate change, biodiversity loss, waste, and pollution while advancing net-zero commitments [3].

[1] Professor Tripti Singh, National Centre for Timber Durability and Deign Life (NCTDDL), University of the Sunshine Coast (USC), Queensland, Australia, tsingh1@usc.edu.au

[2] Dr. Penelope Mitchell, National Centre for Timber Durability and Deign Life (NCTDDL), University of the Sunshine Coast (USC), Queensland, Australia, pmitche2@usc.edu.au

[3] Dr. Martin Strandgard, NCTDDL, USC, Queensland, Australia, mstrandg@usc.edu.au

The timber circularity enables resources to re-enter the supply chain, circulating products and materials through multiple lives at their highest value and then cascading through reuse, recycling and recovery [4].

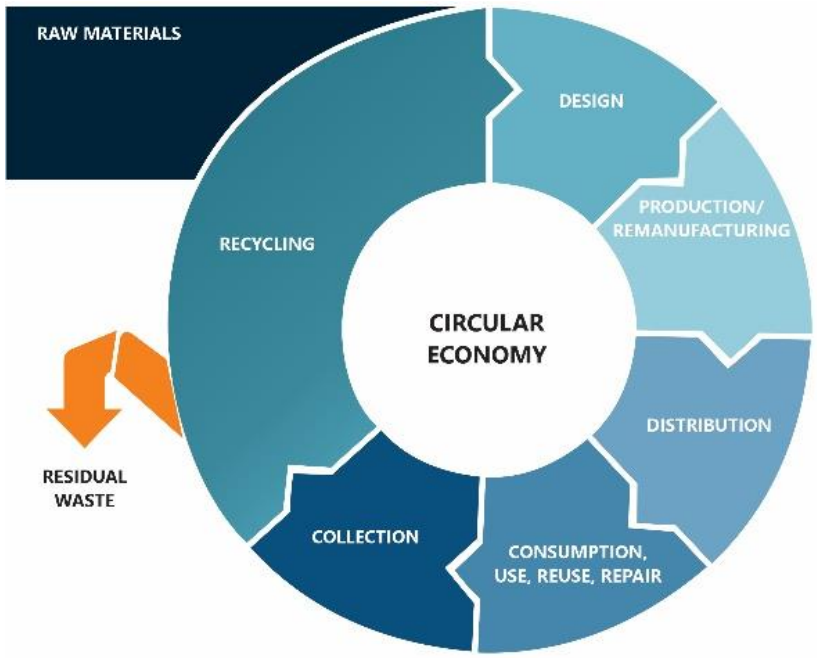

Figure 1. *Circular Economy Diagram (based on 2018 National Waste Policy CE Diagram).*

Using timber over multiple life cycles ensures long-term carbon sequestration and increased resource efficiency. Preservative treated timber and engineered wood products (EWP) provide significant advantages; the life of the products is extended by many folds [5]. Chemical treatments and adhesives however become problematic when timber products reach end-of-life. With the Australian government, pushing for a circular economy by 2030, it is timely for the forest and wood products industry to address the challenges associated with the recycling and reuse of timber [2].

The Timber Circularity Project is a three-year, industry-funded national initiative aimed at developing strategies and solutions to retain wood fibre within the supply chain under a circular economy (CE). Led by the National Centre for Timber Durability and Design Life (NCTDDL), the project is supported by Forest and Wood Products Australia (FWPA) alongside a consortium of timber manufacturers and producers (such as AFPA, EWPAA, FTMA) chemical and glue suppliers (Koppers Performance Chemicals, Azelis), and timber users (Wine Australia).

The project focuses on preservative-treated timber and engineered wood products (EWP), which present end-of-life (EOL) challenges due to chemical treatments and adhesives. Key products under investigation include treated vineyard posts, frame and truss (F&T) timber, and EWPs. The reuse and recycling opportunities for these materials remain poorly understood within a CE framework. Currently, all EOL treated timber and EWPs are classified as controlled or priority waste by Australian state environmental protection authorities (EPAs), despite variations in treatment and adhesive compositions.

The project's primary goal is to identify circular pathways for treated wood and EWP in Australia, enabling more sustainable resource management and reducing waste.

2 PROJECT TASKS

The project is organised around seven key tasks (Figure 2) designed to tackle these challenges and develop practical solutions.

1. **Identification of Regulatory Hurdles**: This task involves identifying local, state, and federal regulatory barriers that impact the transport and reuse of treated timber and engineered wood products (EWPs). Understanding these regulations is crucial for developing compliant and effective reuse and recycling strategies.

2. **Development of Transport Cost Models**: This task focuses on creating models to estimate transport costs for specific timber products across the country. Accurate cost estimation is essential for assessing the economic viability of reuse and recycling programs.

3. **Program for Identifying Attractive Reuse Options**: This involves developing a program that uses material characteristics, volumes, and location data to identify the most attractive reuse options for a given treated timber/EWP in a specific geographic area. By leveraging data on material properties and availability, the program aims to optimize reuse opportunities.

4. **Small-Scale Reuse/Recycling Program Development**: This task aims to develop a small-scale reuse and recycling program for one type of treated timber/EWP. The goal is to assess the feasibility of the approach and identify logistical challenges, providing insights for scaling up the program.

5. **Assessment of Resource Availability and Condition**: Understanding where treated timber resources are located and their volumes and conditions will aid in determining regional solutions. This task involves creating a comprehensive database to inform strategic decision-making.

6. **Stakeholder Collaboration**: By engaging timber producers, chemical suppliers, and timber users, this task ensures that the solutions developed are practical and economically viable.

7. **Development of Recycling and Repurposing Technologies**: This task focuses on advancing technologies and methods to recycle and repurpose chemically treated timber safely. Innovations in this area are critical for mitigating environmental and health risks associated with treated timber.

Figure 2. Schematic diagram showing all different tasks undertaken.

Quantifying current and projected volumes of end-of-life treated wood and EWP **resources available and their distribution** is crucial. With the use of surveys, site-visits, and discussion resources availability information is generated. These information sources have provided a snapshot of resources and their geographic distribution so that appropriate End of life solutions can be determined. Understanding where resources are located, what currently happens with these resources, costs associated with current end of life options, including landfill costs for treated timber disposal on a state basis, is important in determining costs for future circular options. For example, there are 273 unique F&T facilities processing around 2.5 million cubic metres framing timber annually. Unused resources generated by F&T facilities vary over the course of the year, but on average, small facilities (21% of all facilities) produce around 6m^3 of clean offcuts and sawdust per month (medium (40%) 16m^3; large (18%) 32m^3; extra-large (21%) 81m^3) [6].

Conditions of the resources have been assessed at end-of-life to evaluate their potential for reuse and recycling. This analysis includes determining the retained treatment levels in preservative-treated timber for continued durability, assessing strength for reuse applications, and identifying contaminants such as nails and other debris. Data collection involved visual inspections during site visits, sample collection, laboratory analysis, and strength testing to inform future application opportunities. For example, analysis of treatment levels in end-of-life vineyard posts—typically removed due to mechanical damage after 17–26 years in service—revealed that stockpiled posts generally retained chromated copper arsenate (CCA) levels meeting the minimum requirements specified in the Australian Standard (AS/NZS 1604) for in-ground use [7]. This suggests that reuse options requiring durability, such as agricultural fence posts, are viable. Additionally, strength testing confirmed that end-of-life vineyard posts retained sufficient structural integrity and consistency for repurposing in low-stress outdoor applications [8]. This suggests that reuse options requiring durability, such as agricultural fence posts, are viable. Furthermore, visual inspections and sorting assessments at frame and truss (F&T) and engineered wood product (EWP) facilities indicated that timber offcuts and sawdust are typically uncontaminated and effectively separated from other waste streams, such as nails, nail plates, plastics, and food waste. This enhances their potential for circular reuse and recycling within a circular economy framework.

Australia's unique geographic challenges, particularly the vast distances between cities, make it essential to analyse collection, transport, and infrastructure to ensure the practical implementation of a circular economy. The costs and emissions associated with processing, loading/unloading, and transporting resources must be carefully considered. Understanding **transport logistics**, including available truck types and their characteristics, will help identify the most efficient CE strategies. A case study conducted by the project team demonstrated that chipping biomass before transport could lower costs and emissions. However, on-site chipping at each facility was found to be more expensive overall, as the added cost of moving a chipper between locations outweighed the benefits of reduced transport expenses [9]. Further case studies are being developed to assess logistic efficiencies, including the advantages of backloading, to refine strategies for cost and emission reductions. These findings will contribute valuable insights into optimizing transport logistics and reducing costs, ultimately supporting emissions reductions and enhancing CE outcomes. Additionally, the analysis will help identify suitable locations for regional recycling and processing hubs, aiding government efforts in infrastructure planning and development.

As part of the Timber Circularity Project, national, state, and territory **regulations and policies** have been reviewed [10] to identify barriers and enablers for a timber circular economy (CE). In most Australian states, end-of-life treated timber and EWP are classified by environmental protection authorities (EPAs) as controlled or priority waste, regardless of the specific treatment or adhesive types used. This classification typically requires disposal at licensed facilities with advanced leachate management systems, leading to significantly higher disposal costs compared to general waste. The inconsistent approaches across Australian states present a significant barrier to landfill alternatives. While some policies remain deliberately vague to allow for case-by-case risk assessments, most state regulations do not adequately support the reuse and recovery of treated timber within a CE model. Aligning regulatory provisions with circular economy principles could enhance resource recovery, reduce landfill reliance, and contribute to both climate change mitigation and economic development in Australia.

A geospatial map has been developed to provide a visual representation of end-of-life treated timber and EWPs resources, potential solutions, and supporting infrastructure, including licensed landfills and transfer stations. The newly developed **Timber Circularity Resource Map** (*timbercircularity.com.au*) serves as a comprehensive reference for an Australian timber circular economy as illustrated in Figure 3. The map displays available resources, potential solutions, and relevant infrastructure, including councils with CE or zero-waste strategies, as well as landfills and transfer stations licensed to accept treated timer. Additionally, the map provides state-by-state regulatory guidance on the potential use of End of life treated timber in new products, ensuring solution providers have access to relevant compliance information. Councils with CE or zero-waste initiatives have also been mapped, with details on their specific plans and strategies. For licensed landfills and transfer stations, the platform offers information on current disposal costs, including waste levies, and notes on their acceptance policies for treated timber.

Built-in features enhance usability, including search tools that allow users to locate resources or solutions within a specified radius and the ability to download spreadsheets of resource data for a given location. These functionalities enable stakeholders to analyze resource availability, logistics, and proximity to infrastructure.

It is envisioned that the Timber Circularity Resource Map will become the go-to reference for the entire timber industry, supporting CE initiatives and guiding decisions on optimal locations for upcoming pilot demonstrations.

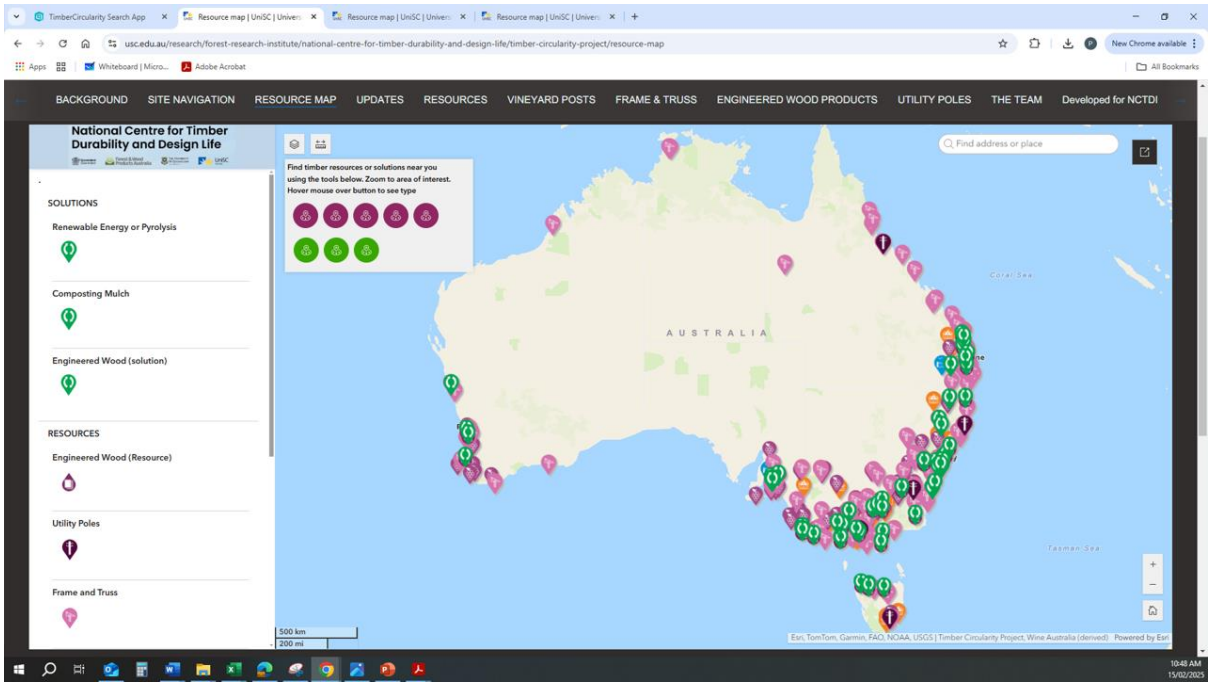

Figure 3. Timber Circularity Project Geospatial Mapping (screenshort)

The **pilot demonstration** is a critical component of the Timber Circularity Project (TCP), focusing on end-of-life treated timber and EWPs. The preparatory tasks outlined above have helped shape key considerations for the pilot, including resource availability in different regions, material condition, logistical factors affecting site selection, and potential locations based on state regulatory requirements. While these insights provide a foundation, identifying viable solutions remains essential. A national and international solutions analysis has been conducted to better understand potential stakeholders, such as demonstration partners, transport companies, and contractors. This analysis examines factors including the volume of material needed for the trial, costs, required timelines, market opportunities for new products, and associated challenges.

By integrating these insights, the pilot aims to demonstrate scalable solutions for managing end-of-life treated timber and EWPs, paving the way for sustainable material recovery, regulatory alignment, and the broader adoption of CE practices within the timber industry.

3 CONCLUSIONS

The **Timber Circularity Project** is playing a pivotal role in addressing the challenges associated with end-of-life treated timber and EWP in Australia. Through extensive analysis of resource availability, regulatory frameworks, logistics, and potential solutions, the project is laying the foundation for a more sustainable and circular approach to timber use.

Key findings highlight the barriers posed by inconsistent state regulations, the economic and environmental costs of current disposal methods, and the logistical challenges of collection and transport. However, the development of the Timber Circularity Resource Map provides a vital tool to visualize available resources, infrastructure, and circular solutions, offering a strategic reference for industry stakeholders.

The upcoming pilot demonstration will be instrumental in identifying scalable solutions for material recovery and reuse. By integrating insights from national and international best practices, the pilot will explore viable pathways for processing, reusing, or recycling these materials while considering logistical efficiencies, regulatory compliance, and market demand.

A transition towards a circular bioeconomy requires a whole-of-supply-chain approach, incorporating strategies such as design for disassembly, waste minimization, regional processing hubs, and service-based business models. By leveraging these principles, the project aims to establish long-term circular pathways for timber, reducing reliance on landfilling and incineration while promoting sustainability, economic security, and climate resilience.

Ultimately, the success of this project will depend on industry collaboration, regulatory adaptation, and investment in circular infrastructure. The findings and pilot outcomes from the project will provide a blueprint for a national timber circular economy, ensuring that wood resources remain in use for as long as possible, supporting both environmental and economic objectives.

REFERENCES

1. Muscat, A. de Olde, E.M. Ripoll-Bosch, R. et al. “Principles, drivers and opportunities of a circular bioeconomy.” Nat Food 2, 561–566 (2021).
2. Hassegawa, M. Van Brusselen, J. Cramm, M. and Verkerk, P.J. “Wood-Based Products in the Circular Bioeconomy: Status and Opportunities towards Environmental Sustainability.” Land 2022, 11, 2131.
3. Muscat, A. de Olde, E.M. Ripoll-Bosch, R. et al. “Principles, drivers and opportunities of a circular bioeconomy.” Nat Food 2, 561–566 (2021).
4. European Union. “Circular Economy Action Plan: For a cleaner and more competitive Europe”, European Commission, 2020
5. Stirling, R. et al. Global survey on durability variation – on the effect of the reference species. IRG/WP 16-20573 (2016).
6. Strandgard, M. Mitchell, P., & Singh, T. “Frame and Truss Unused Resources Survey, Report V4.0 October 2024, Timber Circularity Project, NCTDDL & FWPA, 2024
7. Singh, T., Yi, T., Mitchell, P. and Norton, J. “Levels of chromated copper arsenate in aged radiata pine vineyard posts”. IRG/WP 24-50389, 2023
8. Yan, Z. & Yerman, L. “Performance Assessment of New and Aged Vineyard CCA-Treated Timber Posts, UQ & NCTDDL, Nov. 2024
9. Strandgard, M. Mitchell, P., & Singh, T. “Frame and Truss Offcut Utilisation Case Study, Report V4.0 October 2024, Timber Circularity Project, NCTDDL & FWPA, 2024.
10. Martin, R. “Policies and Regulations Affecting or Restricting the Circularity of Treated Timber and Engineered Wood Products”, NCTDDL & FWPA, 2024.

ICTB 2025. 5th International Conference Timber Bridges
Rotorua, New Zealand, 29 June to 2 July 2025.

METHODS OF LIFE CYCLE ASSESSMENT OF BRIDGE CONSTRUCTIONS AND EXEMPLARY INVESTIGATION OF DIFFERENT BRIDGE CONSTRUCTIONS OF PEDESTRIAN AND CYCLE BRIDGES

Sven Steinbach[1], Christoph Kunde[2], Jan-Mathis Borchers[3], Antje Simon[4],

ABSTRACT

This paper presents a comparative life cycle assessment (LCA) of five pedestrian and bicycle bridge variants based on real planning data provided by Autobahn GmbH. The study applies the LCA.inf tool to evaluate the environmental impacts of a carbon concrete trough bridge, a reinforced concrete bridge, two timber-concrete composite designs, and a steel bridge. A "cradle-to-gate with options" approach was used, including modules A1–A3, B4, C3–C4, and D1–D2. The timber-concrete bridges demonstrated the lowest global warming potential (GWP), benefitting from CO_2 storage and material efficiency. The carbon concrete variant showed advantages in material reduction but faced data uncertainties. The steel bridge scored positively due to high recycling rates. Different recycling scenarios for timber were modeled and revealed significant end-of-life benefits. A comparison with One-Click-LCA confirmed the validity of LCA.inf for early-stage planning. The paper concludes with recommendations to enhance infrastructure LCA practice and promote sustainable bridge design.

1 INTRODUCTION

Background and motivation

According to the German Federal Environment Agency, the construction industry is responsible for more than 35 percent of total waste in the European Union. Of this, 200 million tons of mineral construction waste can be attributed to Germany (Umweltbundesamt, 2021). The environmental impact is not only caused by disposal but also by carbon dioxide emissions from new construction in both building construction and infrastructure sectors.

Bridges represent an important component in German transport infrastructure, enabling the crossing of waters, elevation differences, or other infrastructure components. Pedestrian and cycle bridges are particularly significant as they promote climate-friendly local transportation. However, certification and sustainability assessment usually do not take place in public procurement as there are no direct specifications. Here, costs typically remain the primary focus (Zinke et al., 2021, p. 262). Life cycle assessment, which is at the center of this study, offers one possibility for sustainability evaluation of bridges.

Research objectives

This paper aims to:

- Create and derive requirements for a life cycle assessment system for pedestrian and cycle bridges from existing literature, considering different construction variants

[1] Prof. Dr.-Ing., Erfurt University of Applied Science,
e-mail: sven.steinbach@fh-erfurt.de,
[2] M.Sc., Erfurt University of Applied Science
[3] B.Sc., Erfurt University of Applied Science
[4] Prof. Dr.-Ing., Erfurt University of Applied Science

- Analyze existing assessment tools for bridge life cycle assessment and evaluate their applicability to pedestrian and cycle bridges, while considering current research in the field of life cycle assessment
- Further development of the LCA.inf assessment tool developed by Erfurt University of Applied Sciences for practical application on pedestrian and cycle bridges and exemplary investigation and assessment of the life cycle assessment of various bridge structures

Scope of the study

The study examines five alternative pedestrian and cycle bridges from a real project provided by the German Autobahn GmbH: a carbon concrete trough bridge, a reinforced concrete bridge, two timber-concrete composite bridges (with block girders and fish belly design), and a steel bridge. The planning documents were made available by Autobahn GmbH, who planned five alternative pedestrian and cycle bridges for a real project (Borchers, 2024).

The investigation follows the life-cycle approach "from cradle to gate with options" (DIN EN 15804, 2022, p. 16). The analysis includes modules A1-3, module B4, modules C3 and 4, as well as modules D1 and 2, covering production, replacement, disposal, and recycling. This approach is used because sufficient information for other modules is not yet available at the preliminary planning stage.

2 THEORETICAL BACKGROUND

Life cycle assessment fundamentals

Life cycle assessment (LCA) according to DIN EN ISO 14040 (2020) has gained increasing importance due to growing environmental concerns and the need to evaluate environmental impacts associated with products and systems. It provides a methodology to improve environmental performance throughout a product's life cycle by supporting decision-making processes and quantifying environmental impacts.

The assessment follows a structured approach consisting of four interconnected phases: definition of goal and scope, life cycle inventory analysis, impact assessment, and interpretation. Within the first phase, system boundaries, functional units and cut-off criteria are determined. During the inventory analysis phase, data is collected and calculated. The results are then evaluated in the impact assessment before being interpreted in the final phase.

The framework conditions for life cycle assessments are defined in various standards. DIN EN ISO 14040 (2020) and DIN EN ISO 14044 (2021) establish the general requirements and principles for conducting LCAs. Building upon these, DIN EN 15643 (2021) outlines the basis for sustainability assessment of buildings and engineering works. While DIN EN 15804 (2022) specifies calculation rules for Environmental Product Declarations, DIN EN 17472 (2022) defines the fundamentals for life cycle assessment of engineering structures.

Various environmental impact categories and indicators can be used in LCA. One of the most significant is the Global Warming Potential (GWP), expressed in CO2 equivalents. The importance of GWP has grown considerably due to international climate protection goals, as exemplified by the Paris Agreement's target to limit global temperature rise to well below 2°C compared to pre-industrial levels. The calculation of GWP involves collecting emissions data for different greenhouse gases, applying characterization factors to convert emissions into CO2 equivalents, and summing all contributions to determine total GWP. Some greenhouse gases can have a warming effect up to 15,000 times greater than CO2 (IPCC, 2021).

Current state of research

The development of sustainability assessment systems began with the first officially usable system BREEAM in the United Kingdom in 1990. The first life cycle assessments of bridges emerged in the late 1990s (Zinke et al., 2021, p. 260). This was followed by various national developments of building assessment systems, including DGNB in Germany and similar initiatives in other countries.

Life cycle assessment has grown significantly in importance in the building sector over recent years. This development can be attributed to several factors. Globally, the construction and operation of buildings account for a substantial portion of greenhouse gas emissions. This has led to increasing political pressure worldwide to reduce CO2 emissions in the building sector.

Well-established building assessment systems have integrated life cycle assessment as a core component of sustainability evaluation. Many countries have developed their own certification systems and standards. Economic incentives through various funding programs and green building certifications have further driven the adoption of LCA in the building sector. Additionally, the data foundation was significantly improved through the development of national and international databases for Environmental Product Declarations (EPDs).

According to Zinke et al. (2021), there is currently no widely established assessment system for comprehensive consideration of infrastructure. Nevertheless, valuable expertise has emerged from studies conducted in recent years that provides frameworks for bridge assessment (p. 262). The absence of mandatory evaluation systems and the fact that bridge certification, unlike in building construction, provides limited financial benefits since the structures are often publicly owned, has restricted the widespread adoption of LCA in infrastructure projects.

This development is particularly relevant as pedestrian and cycle bridges play an important role in sustainable transport infrastructure by promoting climate-friendly local mobility. A systematic assessment and optimization of their environmental impacts over the entire life cycle is therefore becoming increasingly important.

3 METHODOLOGY

System boundaries and functional unit

The assessment follows the approach "from cradle to gate with options". Within this scope, the following modules are considered:

- Modules A1-A3: Production phase
- Module B4: Refurbishment
- Modules C3 and C4: Waste processing and disposal
- Modules D1 and D2: Reuse/recycling potential and exported energy

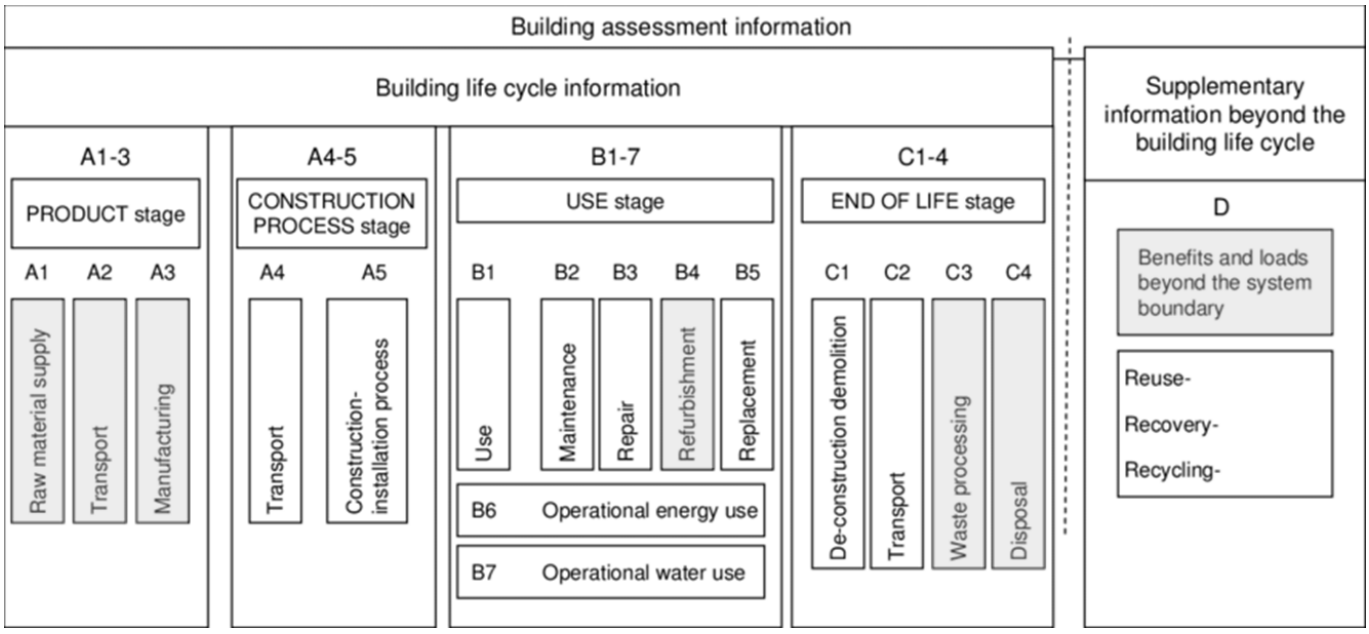

Table 1: diagram of modular information for the various phases of the assessment of engineering structures; DIN EN 17472

Transport phases (A4), construction processes (A5), and modules B1, B3-B8 are excluded due to insufficient data availability in the preliminary planning stage.

The functional unit is defined as square meters [m²] of bridge deck area, enabling direct comparison between different bridge variants. This unit was chosen based on common practice in German infrastructure assessment.

In contrast to buildings, for which a reference service life of 50 years is usually used in life cycle assessments in accordance with EN 15978, there is currently no harmonised guideline for the assessment period of bridges. In this study, a service life of 100 years was assumed for all bridge variants. This is based on the specifications of the German ABBV - which considers 80-100 years to be the typical service life for bridge structures - and the planning service life assumptions for the bridge structures analysed. This assumption reflects the intended long-term use of the infrastructure and enables an assessment of the environmental impacts over the realistic service life of such structures. This choice is also consistent with the academic and engineering literature, which recommends a hundred-year service life for new bridge structures.

Assessment tools comparison

As part of the work, three different life cycle assessment tools were analysed and compared with regard to their suitability for the assessment of footpath and cycle path bridges: LCA.inf, RENI-LCA and One-Click-LCA.

LCA.inf is an Excel-based tool developed by the Institute for Quality Assessment in Building Physics (IBQS) at Erfurt University of Applied Sciences. It is characterised in particular by its high level of transparency and traceability of the calculation steps. All calculation formulae are openly accessible and can be customised if necessary, which allows flexible integration of project-specific assumptions. Due to the table format, however, there may be an increased manual processing effort, especially when entering data and preparing results. The user interface is functional, but comparatively simple.

RENI-LCA was developed as part of a dissertation at the University of Bochum specifically for footbridges and cycle bridges. It is also based on Excel, but offers a more user-friendly interface and also takes into account aspects of maintenance, in particular module B2. RENI-LCA is particularly focussed on the requirements of small infrastructure structures. However, the tool was still undergoing further development at the time of the study, which is why it could not be fully utilised for this work.

One-Click-LCA is a commercial, web-based life cycle assessment tool with a comprehensive material database, including the ÖKOBAUDAT database for environmental impact data of materials. It supports modern planning approaches such as Building Information Modelling (BIM) and enables the automatic assignment of materials from digital planning documents. The calculations are largely automated. However, the biggest limitation is the lack of traceability of the internal calculation logic and the limited ability to carry out individual module adjustments or variant comparisons in detail.

After analysing all the tools mentioned, LCA.inf was selected as the main tool for the present work. The decision was based on the possibility to fully view and customise the calculation paths, the direct connection to ÖKOBAUDAT and the suitability for use in the early planning phase of bridge structures, when complete digital data models are usually not yet available. One-Click-LCA was also used to validate the results of a comparison of variants. The deviation between both tools was less than 5 %, which confirms the applicability of LCA.inf in the infrastructure sector.

Data sources and assumptions

The analysis uses the following primary data sources:

- Preliminary planning documents providing quantities and specifications
- ÖKOBAUDAT database for environmental impact data of materials
- ABBV (German ordinance) for service life and replacement cycles
- DIN standards and technical guidelines

For carbon concrete, for which no ÖKOBAUDAT data was available, manufacturer data was used that indicates 20 tonnes of CO2 equivalent per tonne of carbon fibre. Special assumptions therefore had to be made for the service life of carbon concrete, whereby 100 years was also assumed due to the non-corrosive properties.

Calculation methods

The assessment follows these steps:

1. Definition of functional unit and study period
2. Component categorization according to AKVS system
3. Material quantity determination from planning documents
4. Assignment of environmental impact data from ÖKOBAUDAT
5. Calculation of impacts for each life cycle module
6. Consideration of replacement cycles
7. Integration of recycling potentials
8. Result compilation and visualization

Special consideration was given to different recycling scenarios for timber components, analyzing both energetic and material recycling pathways.

4 CASE STUDY ANALYSIS

The study examines five alternative pedestrian and cycle bridge designs developed for a real infrastructure project provided by the German Autobahn GmbH. The project's primary objective was to enable non-

motorized traffic—specifically pedestrians and cyclists—to safely cross over a motorway section while ensuring sufficient vertical clearance and structural reliability for long-term use. These bridges serve the vital function of promoting environmentally sustainable mobility by closing gaps in active transportation networks.

All five bridge variants were designed to fulfill identical boundary conditions and functional requirements. Each structure spans a clear width of 10.0 meters with a total bridge width of 3.0 meters and a minimum clearance height of 4.5 meters to accommodate traffic passing underneath. These geometric constraints were derived from national technical guidelines for highway overpasses and safety clearances. The life cycle assessment (LCA) of each bridge followed the modular approach "from cradle to gate with options" in accordance with DIN EN 15804 (2022), incorporating modules A1-A3 (product stage), B4 (replacement), C3-C4 (end-of-life processing and disposal), and D1-D2 (benefits and loads beyond the system boundary, such as recycling and reuse). Transport to site (A4), construction activities (A5), and use-phase impacts (B1, B3-B8) were excluded due to the preliminary planning status and lack of available data.

Carbon Concrete Trough Bridge

The carbon concrete trough bridge is designed as an integral structure, meaning the superstructure and substructure are monolithically connected without the use of bearings or joints. This construction method increases long-term durability by eliminating vulnerable interface points. The bridge deck is cast as a trough-shaped cross-section, providing both geometric stiffness and structural efficiency. The use of carbon fiber reinforcement—a non-corrosive material—allows for a significantly reduced concrete cover, which in turn reduces the overall material volume and dead load. The superstructure contains 51.5 m³ of concrete, 472.6 kg of carbon fiber, and 912.0 kg of conventional steel reinforcement. The innovative use of carbon fiber provides increased tensile strength while resisting corrosion-induced degradation, making the structure highly durable. However, life cycle data for carbon fiber remains limited, requiring assumptions for end-of-life modeling.

Reinforced Concrete Bridge

The reinforced concrete bridge follows a conventional *integral design*, widely used in infrastructure applications for its simplicity and robustness. The superstructure and abutments are rigidly connected, eliminating the need for bearings and reducing maintenance requirements. This variant utilizes 15.8 m³ of concrete in the deck and contains a substantial amount of reinforcement steel, with 1,895.4 kg in the substructure and 6,178.8 kg in the superstructure. The design complies with standard durability and loading criteria outlined in German engineering codes. Its traditional construction method makes it a reliable baseline for comparison with the more novel bridge variants examined in the study.

Timber-Concrete Composite Bridge with Block Girders

This bridge type utilizes a hybrid structural system, where timber block girders act as the primary load-bearing elements and a concrete deck slab provides additional rigidity and environmental protection. The composite system balances sustainability and mechanical performance. The superstructure consists of 15.8 m³ of concrete, 1,895.4 kg of steel reinforcement, and 15.7 m³ of laminated timber. The use of timber allows for carbon sequestration during the use phase, while the concrete slab ensures adequate load distribution and weather resistance. The design includes mechanical connectors between timber and concrete to ensure composite action. Both material and energetic recycling scenarios for timber were modeled to assess end-of-life benefits.

Timber-Concrete Composite Bridge with Fish Belly Girders

This variation represents an optimization of the block girder concept by implementing fish belly-shaped timber beams with a variable cross-section height. This geometry allows for efficient material usage while maintaining structural integrity and aesthetic appeal. The bridge maintains the same concrete and reinforcement steel quantities as the previous variant (15.8 m³ concrete, 1,895.4 kg steel) but reduces the timber volume to 14.0 m³ due to the optimized shape. The arched profile improves moment distribution, resulting in reduced bending stresses and minimizing timber mass. As with the block girder variant, both energetic and material recycling were considered in the assessment.

Steel Bridge

The steel bridge is a conventionally supported structure, where the superstructure is separated from the substructure using bearings, allowing for thermal expansion and easing maintenance operations. The bridge deck includes 2.4 m³ of concrete, but the structural frame is dominated by 18,589 kg of structural steel, complemented by 8,284 kg of reinforcement steel. Steel offers excellent recyclability, with well-documented end-of-life reuse rates and established environmental product declarations. The use of bearings reduces internal restraint forces but introduces potential maintenance needs. Due to its heavy reliance on steel, the bridge exhibits high embodied energy during production, yet performs well in the recycling phase (Module D).

An overview of material quantities is provided in Table 2.

Bridge Type	Concrete Volume [m³]	Steel Reinforcement [kg]	Timber Volume [m³]	Carbon Fiber [kg]	Main Steel Structure [kg]
Carbon Concrete Trough	51.5	912.0	–	472.6	–
Reinforced Concrete	15.8	8,074.2	–	–	–
Timber-Concrete (Block Girders)	15.8	1,895.4	15.7	–	–
Timber-Concrete (Fish Belly)	15.8	1,895.4	14.0	–	–
Steel Bridge	2.4	8,284.0	–	–	18,589

Table 2: Summary of key characteristics and material quantities for all bridge variants

5 RESULTS AND DISCUSSION

Life Cycle Phase Comparison

Figure 1 shows the Global Warming Potential (GWP) of each bridge type over the defined life cycle. The timber variants exhibit the lowest GWP, followed by the steel and reinforced concrete bridges. The carbon bridge shows higher GWP due to high emissions from carbon fiber production.

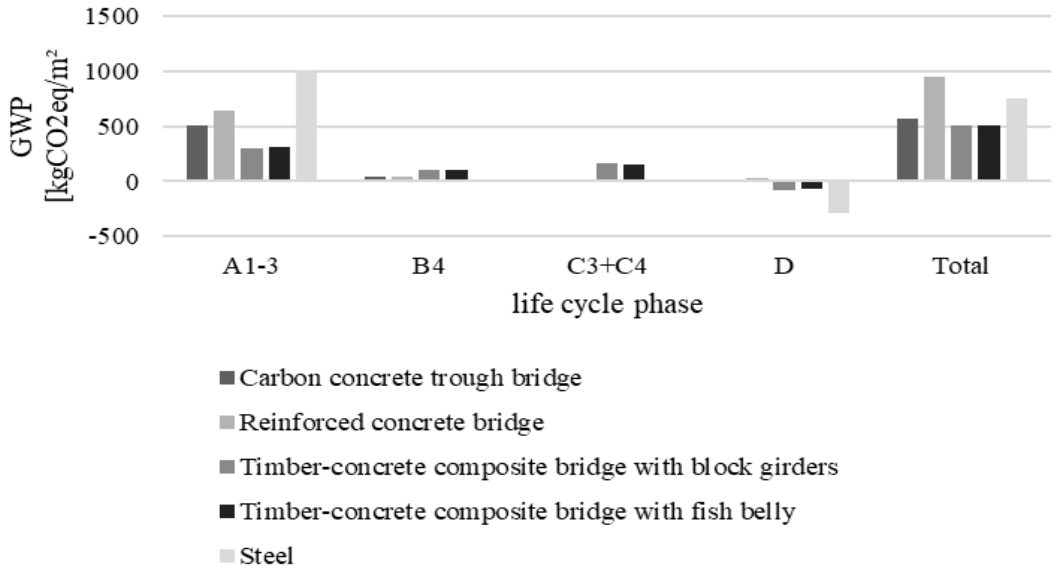

Figure 1: Comparison of the GWP results of the life cycle phases of the investigated bridge structures

Material Influence Analysis

Material choice significantly impacts overall environmental performance of the bridge variants. For the carbon concrete variant, the reduced concrete volume due to thinner cover contributes to lower emissions in the concrete portion. However, this advantage is partially offset by the high production emissions from carbon fiber, estimated at 20t CO2eq per ton. The assessment of this innovative material is limited by the lack of comprehensive environmental product declaration data.

The timber variants demonstrate notable benefits through CO2 storage during the use phase. Their environmental impact is substantially influenced by the chosen end-of-life scenario, with significant differences between energetic and material recycling approaches. Additionally, these variants require less concrete volume compared to the conventional concrete bridge, further reducing their environmental impact.

Recycling Potential Assessment

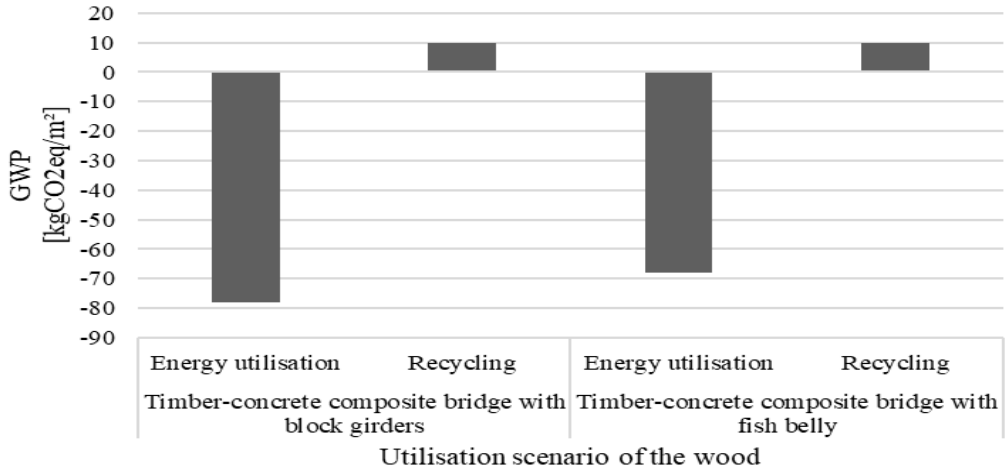

Figure 2: Recycling Potential Assessment of the two investigated timber bridge constructions

The two timber-concrete composite bridge designs demonstrate considerable advantages regarding end-of-life recovery. Timber elements used in both the block girder and fish belly variants can be recycled through both energetic recovery (e.g., incineration with energy capture) and material recycling (e.g., reprocessing into wood-based products). In the assessment, both scenarios were modeled to reflect realistic end-of-life pathways. Energetic recycling contributes to substitution effects in Module D2, where fossil fuels can be replaced. Material recycling supports resource efficiency and closed-loop material cycles. The environmental benefits of these recovery processes are reflected in negative emissions contributions within Module D, which considerably improve the overall life cycle performance of the timber bridge variants.

Critical Evaluation of Results

Several uncertainties and limitations must be considered when interpreting these results. The lack of environmental product declaration data for carbon fiber reinforcement necessitated the use of manufacturer data, potentially affecting result accuracy. Assumptions regarding the service life of innovative materials, particularly carbon concrete, add uncertainty to the long-term impact assessment.

Comparison with other studies

The results of this analysis generally align with previous research findings in the field of bridge life cycle assessment. The benefits of timber construction for GWP reduction are consistent with other studies, as is the observation of high production impacts but good recycling potential for steel structures.

The analysis clearly demonstrates the complexity of environmental impact assessment for bridge structures and highlights the necessity of considering multiple life cycle phases when comparing different construction variants. The results provide valuable insights for future bridge design decisions, particularly in the context of pedestrian and cycle bridges.

6 CONCLUSIONS

The detailed life cycle assessment analysis of five different pedestrian and cycle bridge variants provides valuable insights into their environmental performance across different life cycle phases.

Key findings

Based on the presented analysis, several important conclusions can be drawn. The timber-concrete composite variants and the carbon concrete bridge design show the lowest overall CO2 emissions. For the timber variants, this can be attributed to the CO2 storage effect and reduced concrete volume in the superstructure. The carbon concrete variant achieves low emissions through minimized concrete cover requirements, though uncertainties remain due to limited environmental data availability for carbon fiber reinforcement.
The steel bridge variant demonstrates excellent recycling potential, performing better than the reinforced concrete bridge when considering the complete life cycle. Energy requirements for steel production and recycling significantly influence the CO2 emissions. Future changes in the energy mix, particularly a reduction in fossil fuel usage, would directly affect these results.

Recommendations

To support sustainable bridge planning and improve LCA practice in infrastructure projects, the following recommendations are made:

- Encourage the early-stage use of timber-concrete hybrid designs for pedestrian and cycle bridges.
- Promote the inclusion of end-of-life scenarios, especially recycling options, in infrastructure LCA methodology.

- Improve data availability for innovative materials like carbon fiber through dedicated environmental product declarations.
- Enhance LCA tool functionality for infrastructure through BIM integration and user-oriented interfaces.
- Carbon bridges, while innovative, require further LCA data.
- LCA.inf proves suitable for early-stage infrastructure planning.
- Further harmonization of LCA practices in civil engineering is needed.

Study Limitations

The interpretation of our results must consider several important limitations. The most significant constraint was the limited availability of environmental product declaration data for carbon fiber reinforcement, which required the use of manufacturer data and introduced uncertainty into the assessment. Additionally, service life assumptions for innovative materials had to be based on theoretical considerations rather than long-term experience.

The early planning stage of the project necessitated the exclusion of transport emissions and the use of simplified replacement scenarios. This may lead to some deviation from actual life cycle impacts. Furthermore, the manual processing of data required due to lacking standardization in bridge life cycle assessment introduces potential for inconsistencies in the evaluation process.

Key Findings	Timber-concrete bridges show lowest GWP due to CO_2 storage and reduced material use.
	Carbon concrete reduces concrete usage but is limited by uncertain EPD data.
	Steel bridges benefit from high recycling potential in Module D.
Recommendations	Prioritize timber-concrete bridges in early-stage planning.
	Incorporate end-of-life recycling scenarios into LCA evaluations.
	Develop standardized EPDs for innovative materials like carbon fiber.
	Enhance LCA tools with BIM integration and infrastructure-specific features.
Limitations	Missing EPD data for carbon fiber leads to higher uncertainty.
	Exclusion of transport and construction modules due to planning phase constraints.
	Manual processing due to lacking standardization in bridge LCA introduces inconsistencies.

Table 3: Summary of key findings, recommendations, and limitations

The study demonstrates that life cycle assessment provides valuable decision support for bridge design, while also highlighting areas requiring further research and standardization.

REFERENCES

[1] DIN EN ISO 14040. (2020). Environmental management – Life cycle assessment – Principles and framework.
[2] DIN EN 17472. (2022). Sustainability of construction works – Environmental product declarations – Infrastructure works.
[3] DIN EN 15643. (2021). Sustainability of construction works – Assessment of buildings.
[4] DIN EN 15804. (2022). Sustainability of construction works – Environmental product declarations – Core rules.
[5] EN 15978. (2011). Sustainability of construction works – Assessment of environmental performance of buildings – Calculation method.
[6] ABBV. (2010). Verordnung zur Berechnung von Ablösungsbeträgen.
[7] Özdemir, M. (2022). Life cycle assessment for pedestrian bridges.
[8] Müller, F. (2024). Application of BIM in LCA for infrastructure projects.
[9] Zinke, A. et al. (2021). Sustainability assessment of infrastructure.

ICTB 2025. 5th International Conference Timber Bridges
Rotorua, New Zealand, 29 June to 2 July 2025.

131 M SPAN TIMBER CYCLE-PEDESTRIAN BRIDGE: STRUCTURAL DESIGN AND CALCULATION, WIND TUNNEL TESTING AND IMPLEMENTATION OF VIBRATION CONTROL SYSTEM

Mario Suárez Álvarez[1], Pelayo Fernández Fernández[2], Antonio Navarro-Manso[2], Juan José del Coz Díaz[2], Julio Vivas Padilla[1], Andrea Fernández Chavarría[2]

ABSTRACT

In today's world, sustainability has become a cornerstone of design and construction. This paper presents the design and analysis of a 131-m span wooden pedestrian bridge prototype that demonstrates the potential of wood as an optimal material in engineering applications. The project combines traditional materials with modern technology to address structural, environmental, and economic demands. Key aspects include an in-depth structural calculation, wind tunnel testing, computational fluid dynamics simulations, and the implementation of a tuned mass damper to control vibrations. The bridge's innovative design, featuring a double inclined arch with an intermediate deck, integrates concrete elements to prevent wood–water contact and steel profiles for enhanced lateral stability. Experimental and numerical analyses confirm that the bridge meets performance criteria under variable loads, dynamic pedestrian interaction, and adverse wind conditions. This work not only showcases the potential of wooden bridges but also provides a reference framework for future sustainable civil engineering projects.

1 INTRODUCTION

Figure 1 – General view

[1]Media Madera Ingenieros Consultores S.L.
[2]University Of Oviedo, Spain
e-mail: mariosuareez@gmail.com

There is no material that is inherently superior to another; rather, each has its optimal application according to the project's needs. Steel, concrete, and wood coexist, each contributing with its particular advantages based on the structural, environmental, and economic demands of the project.

In this context, the 131-meter span timber cycle-pedestrian bridge prototype represents a clear example of the potential that this material offers in contemporary civil engineering works. To ensure its stability and safety, the project has included an exhaustive structural analysis, wind tunnel tests to evaluate the behavior under aerodynamic and aeroelastic forces, and the implementation of a vibration control system using tuned mass dampers. This combination of advanced technology and traditional material positions this bridge as a benchmark in the integration of sustainability and high-performance structural design.

2 DEFINITION OF THE ADOPTED SOLUTION

The bridge is located in the Ría de Villaviciosa, connecting El Puntal with Rodiles in Asturias, Spain. It is constructed with pine wood chemically treated to obtain acetylated wood. In the treatment, the free –OH groups in the wood are transformed into acetyl groups; that is, the groups responsible for water absorption in the wood are converted into groups that no longer absorb water.

In the case of the bridge, the main timber elements are protected from rain by coverings (zinc sheets or wooden canopies) that function as secondary sacrificial elements which must be replaced periodically (every 50 years). This ensures that the primary elements are not directly exposed to rain, thereby greatly increasing their durability and meeting the minimum service life requirement of 100 years. The bridge features a 131-meter span and a 5-meter clear width, and it displays a double inclined arch typology with an intermediate deck.

Figure 2 – General view of the area

The first segment of the arch is constructed in concrete to prevent contact between the wood and the river water. In the initial designs, the arch was projected onto the deck plan. However, given the high forces near the supports and the structure's limited lateral stability, the arch was opened by increasing the number of chords and introducing arches in both the vertical and horizontal planes, following the principle of "form follows function."

Figure 3 – Elevation view of the bridge

Figure 4 – Plan view of the bridge

The arches are composed of four chords (two upper and two lower), which in turn are made up of double beams. The arch's lattice is closed with inclined struts following a Warren truss typology in the plane. Lateral stability is provided by circular-section stainless steel tubular profiles placed transversely. Steel is used to increase rigidity in the transverse plane and to avoid aesthetically overloading the arches with an excessive amount of wood.

Figure 5 – General view of the arch

The bridge deck is connected to the arch through crossed tie-rods that provide greater vertical rigidity. It consists of two double beams on which a prestressed laminated deck of acetylated wood is mounted. The bracing of the beams is completed by the installation of struts and wooden diagonals in the plane perpendicular to the beams.

Figure 6 – General view of the deck

The guardrail, also made of wood, is composed of curved posts arranged in such a way as to prevent climbing, along with intermediate stainless steel cables.

Figure 7 – Cross-sectional view

To mitigate high accelerations due to pedestrian traffic, a 6-ton tuned mass damper (TMD) is installed, supported by four tie-rods at the center of the span. With proper tuning, it is possible to almost entirely mitigate the vibrations produced when the pedestrian traffic's step frequency coincides with the bridge's first natural vertical and horizontal frequencies.

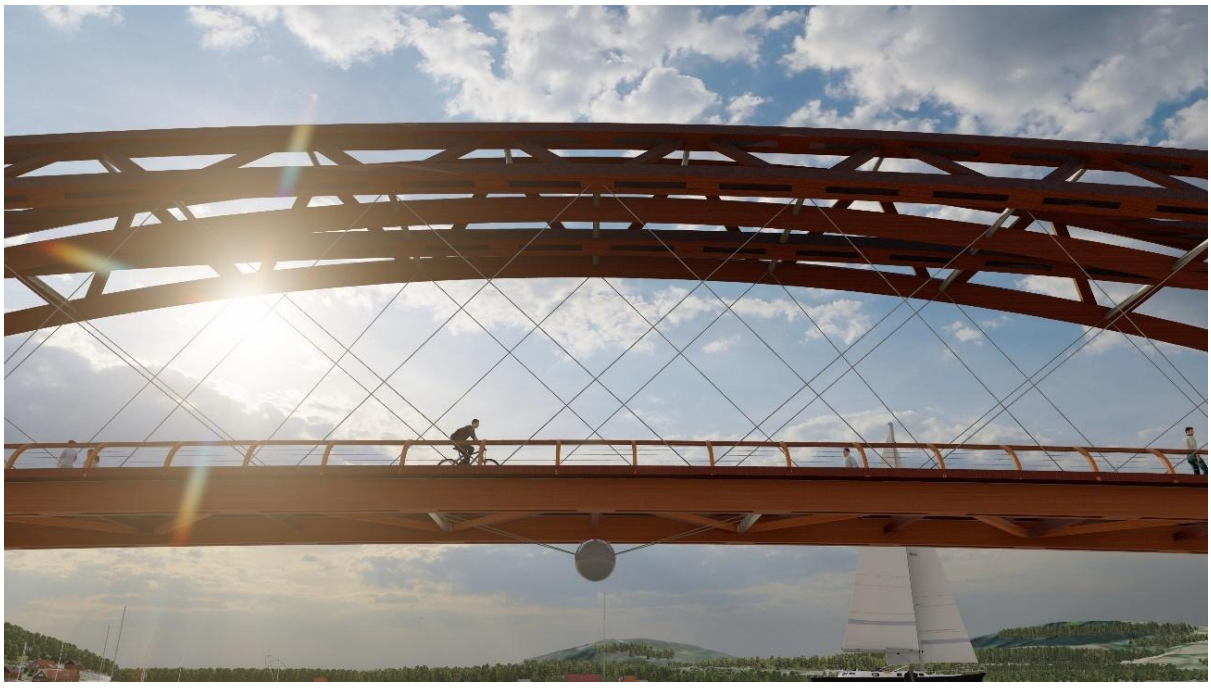

Figure 8 – TMD implementation

The structure is part of a larger project aimed at connecting the two banks of the river. It is of vital importance to intervene as little as possible in the river's channel, which is why a solution without intermediate supports was chosen. In this project, in addition to installing the footbridge as a major milestone, the current dikes must be adapted for pedestrian access and another wooden footbridge installed along the promenade.

3 STRUCTURAL ANALYSIS METHODS

With respect to structural analysis, engineers face the challenge of modeling the various time-dependent loads that affect the structure. Therefore, they must quantify a load that is, by definition, stochastic. The number of people crossing the bridge varies over time in terms of quantity, distribution on the deck, load, speed, and step frequency… all of which means that the load applied at each point of the bridge varies in a non-periodic manner.

In the case of wind, it exhibits an even more difficult-to-quantify movement. The standard establishes various guidelines that allow for an estimation of the effects that may be generated. It should be noted that, for special structures (as is the case with this bridge), aeroelastic phenomena may occur that could cause the structure to collapse even at wind speeds much lower than those specified in the design [1, 2].

Therefore, conservative simplifications must be made to model the various hypotheses and verify the structure's strength and stability. Depending on the complexity of the structure, these can be expressed in two ways. Both types of calculations are explored in detail through the following procedure:

- Quasi-static approximations
- Dynamic calculations

4 SECOND-ORDER STATIC STRUCTURAL ANALYSIS

Static analysis focuses on the examination of structures subjected to constant or slowly varying loads over time. This type of analysis determines the internal forces, stresses, deformations, and displacements in the components under static loads, ensuring that the structure can support the applied loads without failing, thereby guaranteeing its strength and stability [3].

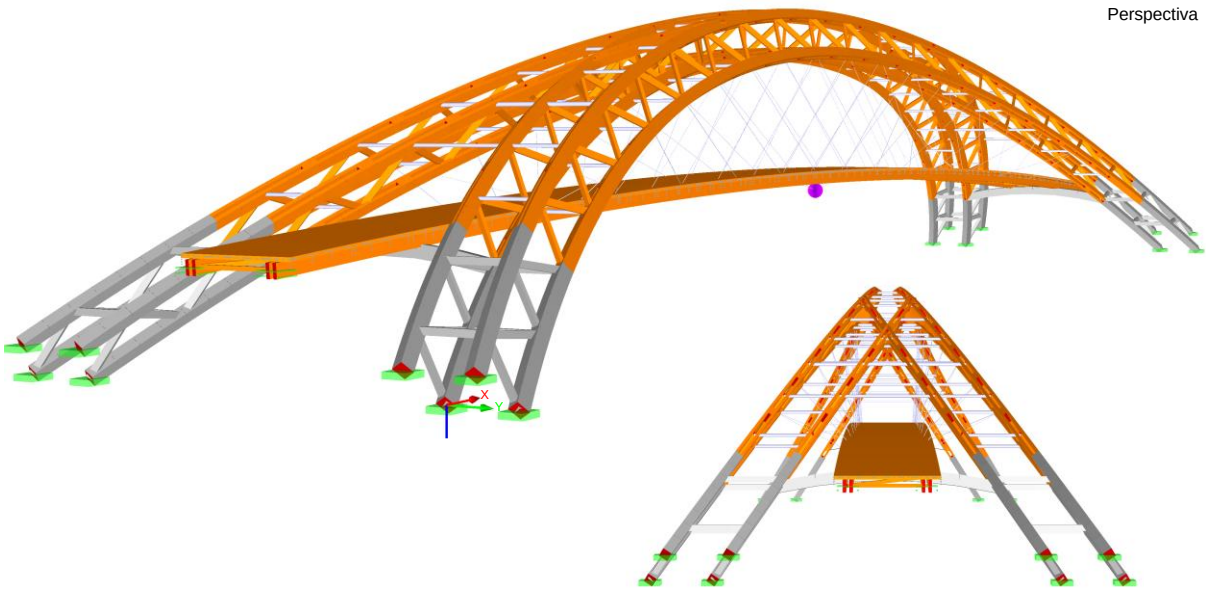

Figure 9 – Static analysis model

5 GLOBAL BUCKLING ANALYSIS USING THE PROGRESSIVE NONLINEAR METHOD WITH EIGENVALUE ANALYSIS

Global buckling analysis is a nonlinear calculation that considers second-order effects through an iterative process, applying the load in incremental steps and recalculating the structure at each step. Initial imperfections are included. The critical load factor, which indicates the ratio between the critical buckling load and the applied load, is 2.81. This means that the most

unfavourable load combination must be multiplied by this value for the structure to fail due to buckling.

$\lambda = 2.81 > 1$ ✓

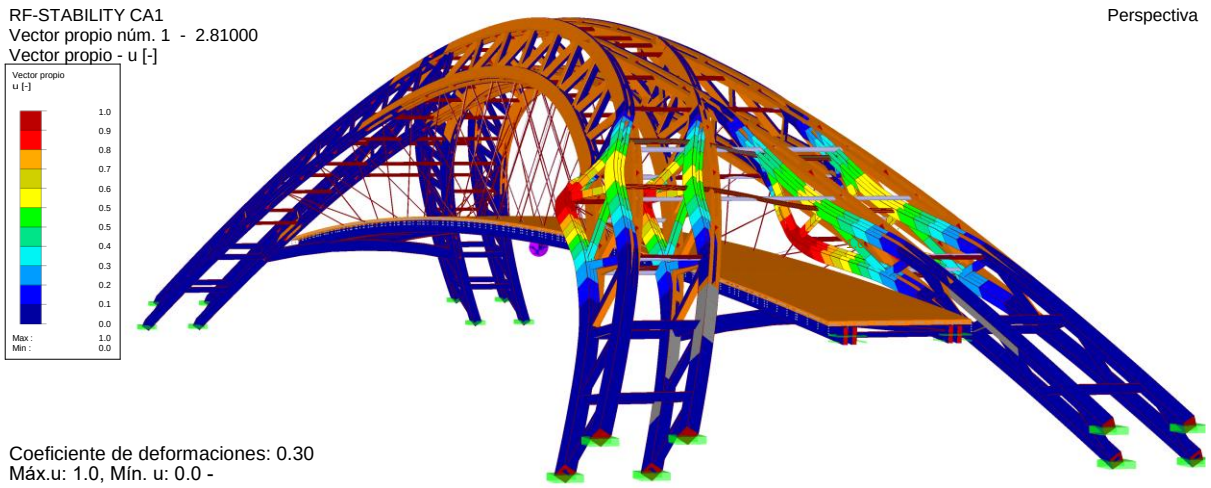

Figure 10 – Buckling calculation

6 DYNAMIC PEDESTRIAN-STRUCTURE INTERACTION ANALYSIS

Dynamic analysis of pedestrian-structure interaction is an essential aspect in the design of pedestrian bridges. The objective is to ensure that the vibrations induced by the movement of people do not compromise structural safety or generate excessive discomfort. A key aspect is the coincidence between the pedestrians' step frequency and the natural frequency of the bridge, which can cause resonance and amplify the vibrations [4].

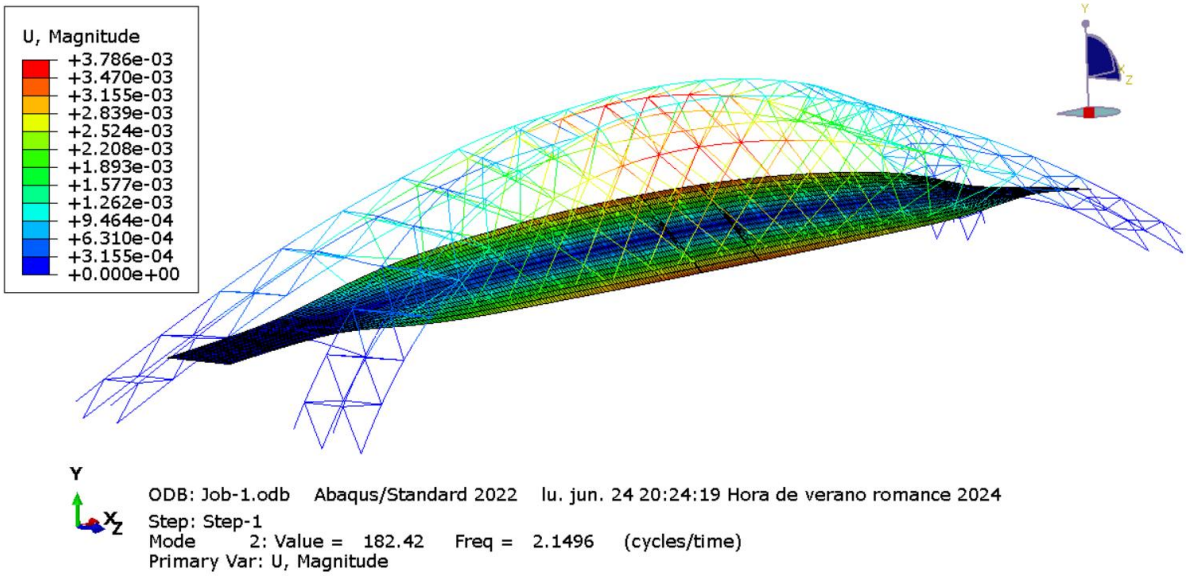

Figure 11 – Natural frequency with the highest likelihood of resonance

To address this phenomenon, analytical and numerical models, as well as computational simulations, are used to evaluate different load and movement scenarios. After analysing all the frequencies within critical ranges, it is determined that the maximum accelerations obtained fall within the medium comfort range (below the purple band). This implies that the vibrations generated will be merely perceptible to users but will never become uncomfortable.

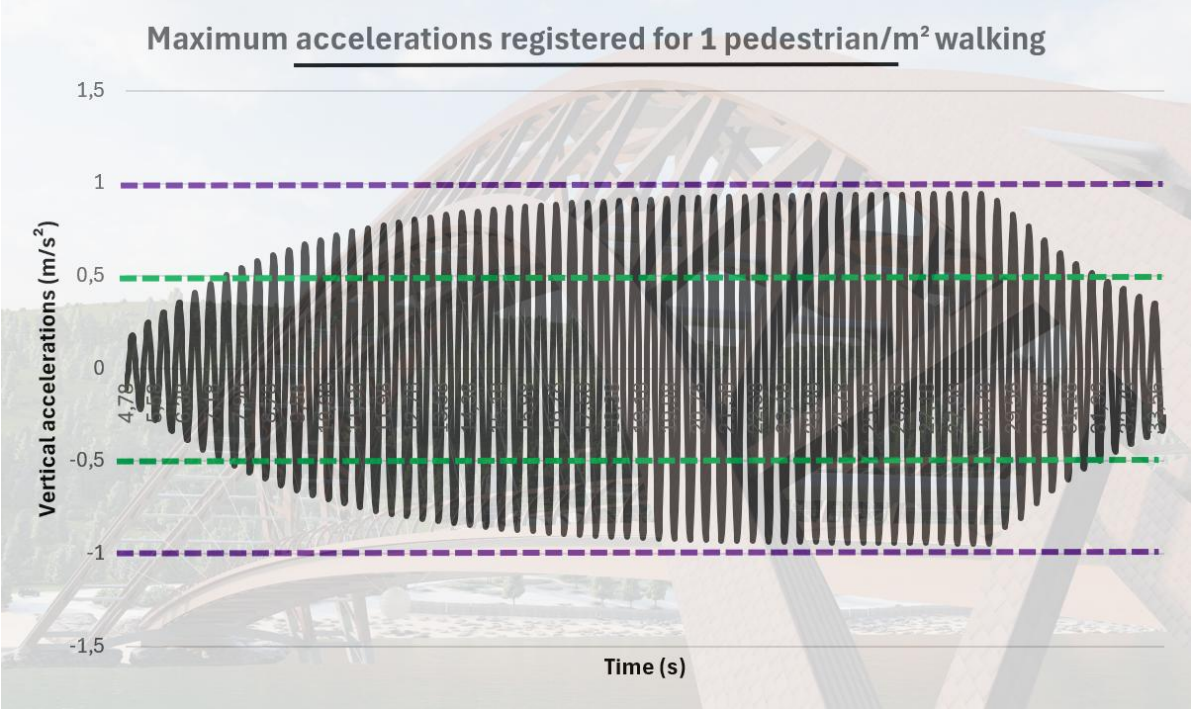

Figure 12 – Maximum recorded accelerations

Although not strictly necessary, the implementation of a tuned mass damper (TMD) is ultimately chosen to reduce vibrations in both bending and lateral modes. For solving the problem of obtaining the TMD parameters, the equations formulated by Warburton are adopted and optimized for a structure with natural damping.

Figure 13 – TMD design

7 STUDY OF WIND EFFECTS

In this study on wind effects in wooden bridges, an exhaustive analysis has been conducted using wind tunnel tests and computational fluid dynamics (CFD) simulations to evaluate the structure's stability under aerodynamic loads [5].

Figure 14 – Scaled model of the bridge

First, a 1:100 scale model of the complete bridge was constructed and tested in the wind tunnel of the Polytechnic School of Mieres. Subsequently, a CFD model calibrated with the experimental results was developed to obtain the pressure distribution and validate its reliability against current standards.

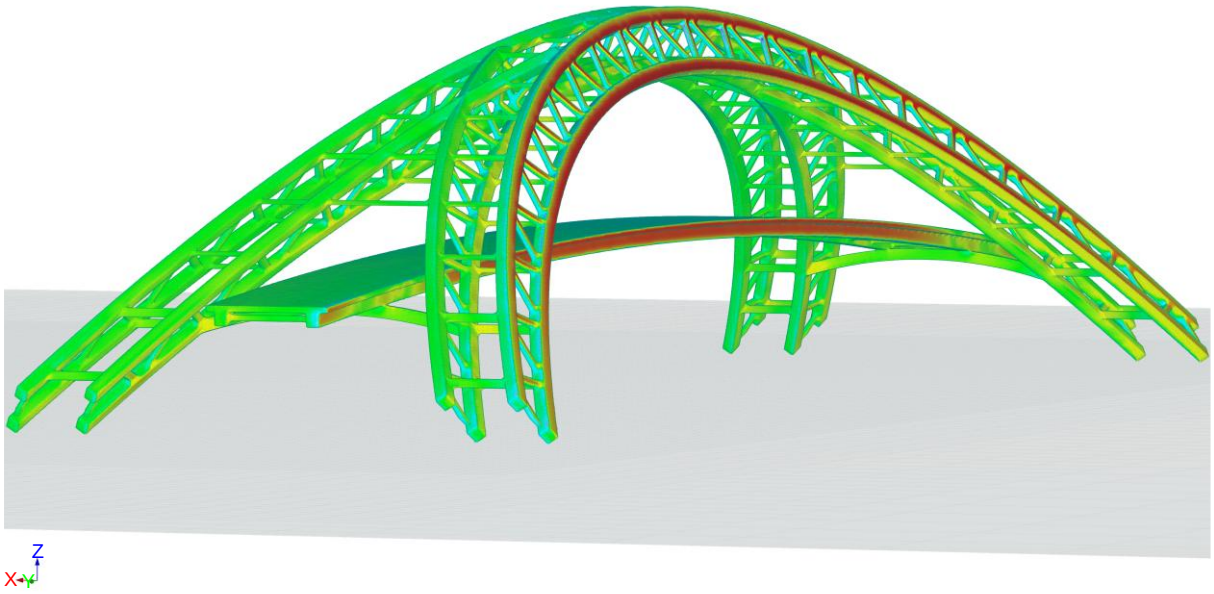

Figure 15 – CFD simulation of the complete bridge

The work also included a simplified study of some aeroelastic instabilities such as vortex shedding, galloping, flutter, and torsional divergence. For this purpose, a 1:30 scale model of the bridge deck was constructed and subsequently tested in free vibration. Finally, additional checks on joints, seismic response, fatigue, and construction phase calculations were also carried out.

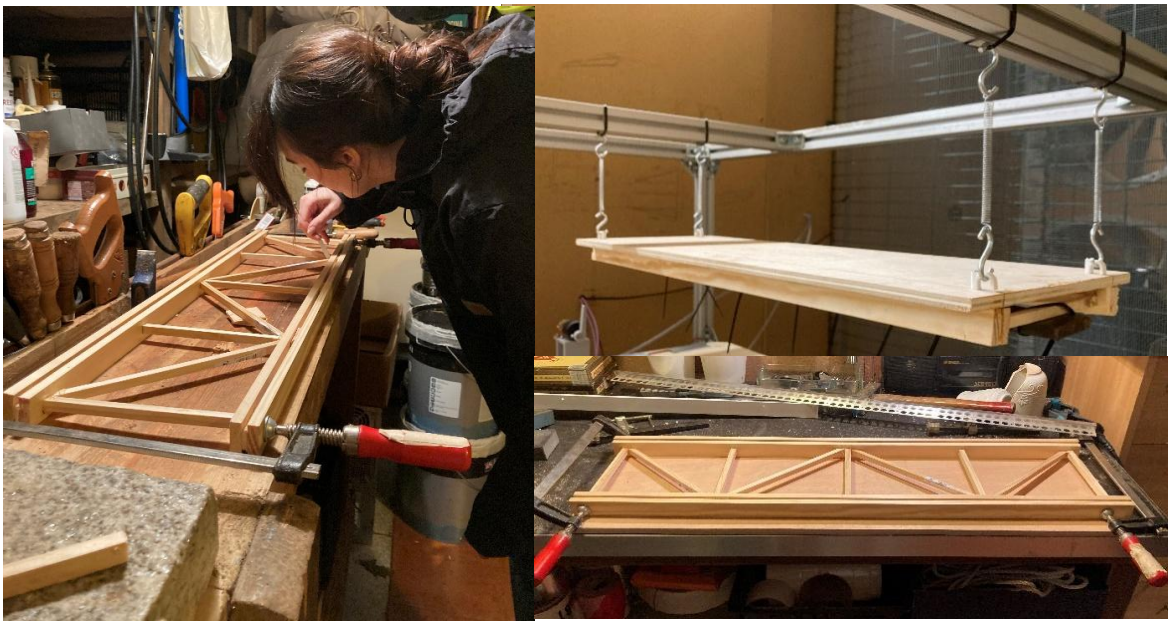

Figure 16 – Sectional model of the deck

8 CONCLUSIONS

The 131-meter timber cycle-pedestrian bridge is a significant step forward in wooden bridge engineering. Key conclusions include:

- **Longevity:** The bridge's longevity is largely due to the meticulous attention to construction details, ensuring a service life of at least 100 years and making it a sustainable long-term solution.
- **Vibration Mitigation:** A tuned mass damper effectively reduces pedestrian-induced vibrations, enhancing both comfort and safety.
- **Stability Verification:** Wind tunnel tests and CFD simulations have been crucial for understanding wind effects and confirming the structure's stability.
- **Future Applications:** This project paves the way for the broader use of wood in large bridges, potentially expanding into road bridges and innovative structural designs.

Overall, the bridge not only proves structurally viable but also sets a precedent for future sustainable infrastructure projects.

REFERENCES

1. European Committee for Standardization (CEN), 2019. Eurocode 0: Basis of Structural Design. Brussels, Belgium.
2. European Committee for Standardization (CEN), 2019. Eurocode 1: Actions on Structures. Brussels, Belgium.
3. European Committee for Standardization (CEN), 2016. Eurocode 5: Design of Timber Structures – Part 2: Bridges. Brussels, Belgium.
4. SETRA, 2006. Assessment of Vibrational Behaviour of Footbridges Under Pedestrian Loading. SETRA, Paris, France.
5. ASCE/SEI 49-21, 2021. ASCE Standards and Commentary. American Society of Civil Engineers, Reston, VA, USA.

ICTB 2025. 5th International Conference Timber Bridges
Rotorua, New Zealand, 29 June to 2 July 2025.

LONGEVITY AND SERVICE LIFE CONSIDERATIONS FOR VEHICLE TIMBER BRIDGES IN NEW ZEALAND

Hanshen Wang[1], Gary M. Raftery[2]

ABSTRACT

Timber is a sustainable material, being a renewable resource with a low carbon footprint. From a civil and transportation engineering perspective, vehicle timber bridges represent a unique intersection of sustainability and engineering, offering an eco-friendly alternative to conventional materials like concrete and steel. However, the adoption of such infrastructure in New Zealand has been hindered by concerns over durability, service life, and maintenance requirements. This research seeks to address these challenges by developing a framework for the inspection, and maintenance of timber bridges, tailored to the environmental and operational conditions specific to New Zealand. The study identifies key deterioration mechanisms specific to New Zealand, including mechanical wear, biological decay, and environmental weathering, and proposes innovative inspection techniques, including non-destructive, semi-destructive methods, and advanced remote monitoring systems. A structured inspection schedule is outlined to enhance the performance of timber bridges. By combining international practices and adapting them to the local context, this research aims to establish a foundational document that supports the wider adoption of timber as a sustainable and durable material for vehicle bridges in New Zealand. The findings are expected to contribute to the development of more resilient infrastructure while aligning with global sustainability goals.

1 INTRODUCTION

Timber has long been recognised as a sustainable and renewable material, offering significant environmental benefits over conventional construction materials such as concrete and steel. Its low carbon footprint, coupled with its renewability, has made it a favourable choice for infrastructure projects, particularly in bridge construction. Historically, older timber bridges in New Zealand were primarily built using a combination of Australian hardwood and native New Zealand timber. By the mid-20th century, preservative-treated timber became more common in bridge construction. However, fully timber-built bridges are now rare [1].

With the Net Zero goal by 2050, greenhouse gas emissions reduction has become an essential sector. The timber-based and engineered wood can be used as alternatives to steel and concrete because of the sustainability attributes associated with the material with a lower greenhouse gas emission [2].

In some previous decades, a trend has developed in which the replacement of timber bridges with less sustainable materials, such as concrete and steel, has become a common practice

[1] Civil Engineer, Andy O'Sullivan Geotechnical Engineering, Auckland, New Zealand
e-mail: wangwhs99@gmail.com,
[2] CIRCUIT Research Centre Co-Director/Senior Lecturer, Department of Civil and Environmental Engineering, The University of Auckland.

globally, despite the higher embodied carbon associated with these materials [3]. This trend has also been evident in New Zealand, where many ageing timber bridges have been replaced by concrete, steel or composite systems of cush materials. However, with a growing emphasis on sustainable infrastructure and the urgent need to reduce carbon emissions, there is a renewed interest in timber as a primary material for vehicle bridges.

In recent years, advancements in technology and automation in engineered wood manufacturing have enabled the production of larger and longer timber members, making it possible to achieve the spans and load capacities required for full-scale vehicle timber bridge construction. Glued laminated timber, composed of layers of laminated wood bonded together, has emerged as a high-performance material for modern timber bridges [4]. The adoption of glued laminated timber for such applications produced from domestically sourced Radiata pine plantation forests presents an attractive solution. The elements can be produced in versatile configurations with optimisation of the structural mechanical properties easily being achieved during manufacture. Radiata pine grown in New Zealand is a fast-growing and abundantly available resource that achieves good strength and stiffness characteristics, and the species is particularly receptive to preservative treatment such as chromate copper arsenic. This treatment is widely used in the domestic timber industry when being exposed to higher hazard risk classes such as outdoor exterior environments [5]. These engineered wood products require adequate durability and satisfactory adhesive bond line integrity, especially when exposed to exterior high humidity environments [7, 6].

Despite advancements in such engineered wood technology, the use of timber structural elements in New Zealand's vehicle bridges remains limited due to concerns over durability, service life, and maintenance. Ensuring the long-term performance of timber bridges requires addressing key challenges, including mechanical wear from heavy vehicle loads, biological decay from fungi and insects, and environmental weathering caused by ultraviolet radiation (UV) exposure. These deterioration mechanisms are further intensified by New Zealand's unique environmental and operational conditions, making effective maintenance strategies essential for wider adoption.

The current knowledge void in New Zealand lies in achieving the required service life of 100 years for structural timber and engineered wood elements being used in vehicle bridges. Such a service life can be achieved with steel and concrete elements in bridges. The use of clever detailing techniques during the design phase and impregnation of the timber with chemical preservatives is essential to achieve such a target. However, the adoption of modern technologies for monitoring and maintaining timber bridges in the transportation network to identify deterioration at an early stage is also critical. Internationally, advanced inspection and monitoring technologies, such as non-destructive testing (NDT), semi-destructive testing (SDT), and remote health monitoring systems, have proven highly effective in efforts to achieve long-term durability issues in timber structures.

2 DETERIORATION MECHANISMS

Timber bridges in New Zealand are exposed to a range of deterioration mechanisms that are influenced by the country's unique environmental and operational conditions. Understanding these mechanisms is critical to developing effective inspection, monitoring, and maintenance strategies that can enhance the longevity and design service life of the structures. This section

outlines three primary deterioration mechanisms for timber vehicle bridges in New Zealand, including: mechanical wear, insect attacks, decay, UV exposure and geothermal weathering. The relevant case study example for each deterioration mechanism will also be presented.

2.1 Mechanical Wear

Mechanical wear is one of the most significant challenges facing timber bridges in New Zealand, particularly in rural and industrial areas where heavy agricultural and logging vehicles are prevalent. These vehicles, which often exceed standard weight limits, place substantial stress on timber bridge components such as decks, beams, and joints. Over time, this repeated loading leads to surface failure, fatigue cracking, and pile deformation, all of which compromise the structural integrity of the bridge.

Surface failure occurs as vehicle tyres and heavy loads grind against the timber or other face layer material, wearing down the surface and exposing the underlying layers to further damage. Fatigue cracking develops due to the cyclic loading of heavy vehicles, creating small cracks that gradually expand and weaken the timber. Deformation, such as bending or warping, occurs when timber elements are subjected to sustained heavy loads, leading to permanent changes in shape that can affect the overall stability of the structure.

According to Farm Forestry New Zealand, 7% of New Zealand's land area is used for forest plantation [8]. In 2014, the forestry sector contributed 3.20% towards the total New Zealand GDP. In regions like Tauranga and Whangarei where major exporting ports are located, logging and transportation activities are intensive, timber bridges are frequently subjected to heavy loads from trucks carrying logs, agricultural equipment [9]. For example, a timber bridge in a rural logging area may experience accelerated mechanical wear due to the constant passage of heavily laden logging trucks. This shortens the bridge's service life and increases the risk of sudden failures if wear and tear are not detected and addressed early.

The TePuke timber bridge as shown in Figure 1, located 20km southwest of Tauranga, New Zealand, experienced significant mechanical deterioration due to heavy traffic loads. With 6,000 vehicles daily, including 15% heavy vehicles, the bridge suffered decking failure after just 13 years of service. Key factors contributing to the failure included beam deflection from high-speed heavy traffic, inadequate fastening between decking and beams, and insufficient nail length. Damaged sections were replaced with stronger fastenings, extending the bridge’s service life by 19 years. However, the structure was eventually replaced as the ageing decking could no longer sustain heavy traffic loads [1].

Figure 1. TePuke timber bridge exterior condition [10].

2.2 Insect Attacks

Biological decay caused by wood-boring insects is a major threat to timber bridges in New Zealand, particularly in coastal and humid environments. Native insects, such as the Puriri moth, pose a significant risk, as their larvae tunnel into the wood, creating extensive networks of cavities that weaken the structural integrity over time [11]. Another example is the Teredo worm, a non-indigenous marine borer that thrives in seawater and attacks timber bridges at the interface between wood and water. These worms burrow into the timber, causing internal damage that can go unnoticed until significant deterioration has occurred [12].

The Nuhuka rail bridge, located 50km southwest of Gisborne in the Hawkes Bay region, was built in 1922 and spanned 110m with six spans supported by hardwood timber piers. Situated 1.5km from the coast, the bridge collapsed on 6th May 2005 when Train 60 crossed, causing a 60-tonne rail crane to fall into the river. The collapse was primarily due to insect attacks, specifically Teredo worms, which tunnelled into the timber piers between 300mm to 600mm above and below the low tide level. These worms created 10mm diameter holes, significantly weakening the structure [13].

2.3 Decay

In New Zealand, the combination of high humidity and frequent rainfall in many regions creates ideal conditions for biological decay in timber bridges. Fungal growth, which grows in damp and shaded areas, accelerates the decay process, significantly reducing the service life of these structures. Fungi typically begin to grow when the moisture content in timber remains consistently above 20%, leading to the breakdown of the internal timber elements, which are essential for the wood's structural integrity [14].

The Waimakariri Gorge Bridge, a single-lane structure in inland Canterbury, South Island, New Zealand, is still currently in use. Its primary deterioration issue stems from the region's cool climate and high annual rainfall of 750 mm, creating a consistently moist and humid environment. After 30 years, decay was observed in exposed areas of the decking [1]. To extend the bridge's service life, the local district council engaged contractors to replace the decking in 2024 [16]. Refer to Figure 2 for the detailed information.

Figure 2. Waimakariri Gorge Bridge (a) Side view [15]. (b) Decking replacement 2024 [16].

2.4 UV Exposure

UV radiation is a critical form of environmental weathering that needs to be carefully considered in relation to achieving the required design service life for full scall vehicle timber bridges in New Zealand. New Zealand experiences 40% higher UV radiation than countries at similar latitudes in North America due to Earth's elliptical orbit, which brings the southern hemisphere closer to the sun during summer [17]. Prolonged exposure to UV rays degrades the timber surface, leading to cracking and splintering. To mitigate this, protective measures such as paint and surface coatings can be applied to shield the timber from UV damage. However,

these coatings deteriorate over time, necessitating regular inspection and maintenance to ensure continued protection. An example picture is shown in Figure 3 for the timber bridge condition after constant exposure to UV radiation.

Figure 3. Example bridge section after long term UV radiation [14]

2.5 Geothermal Weathering

Geothermal weathering is a unique deterioration mechanism that affects timber bridges in regions with significant geothermal activity, such as parts of New Zealand's North Island. In these areas, the combination of heat, steam, and mineral-rich groundwater can accelerate the degradation of timber structures. As a hygroscopic material, timber absorbs and releases moisture based on environmental conditions. When it reaches its fibre saturation point, swelling occurs due to moisture accumulation, with excess water confined to the cell cavities, leading to timber member deformation [14].

The Whakarewarewa Village Bridge, located in Rotorua, New Zealand, was built in 1980 using CCA-treated Radiata pine glue-laminated beams and decking. The continuous exposure to hydrogen sulphide-rich geothermal steam made the bridge highly susceptible to moisture accumulation. After 35 years in service, inspections revealed that the protective coating on the upstream beams had deteriorated due to prolonged steam exposure, leading to surface delignification by several millimetres [1]. Figure 4 reveals the Whakarewarewa Village Bridge site environment.

Figure 4. Whakarewarewa Village Bridge plan view [18]

3 DURABILITY CONSIDERATIONS AND TECHNIQUES

After summarising the challenges and deterioration issues for timber vehicle bridges specifically related to New Zealand, some considerations and techniques to enhance the longevity and service life are indicated in this section. To ensure the design life is achieved, advanced inspection and monitoring techniques are essential. These methods enable early

detection of deterioration, allowing for the prevention of deterioration expansion. This section explores Non-Destructive Testing (NDT), Semi-Destructive Testing (SDT), and Long-Term Health Monitoring techniques that could be used in New Zealand timber bridge maintenance sector, highlighting their applications and benefits in enhancing the durability of timber bridges in New Zealand.

NDT encompasses a range of testing methods used to assess materials, components, or structures without causing actual damage to the bridge body. In contrast, SDT typically involves removing small samples from timber members for further analysis to evaluate their strength properties.

3.1 Visual Inspection

Visual inspection is a fundamental NDT method used to assess the external condition of timber vehicle bridges. This technique involves systematic examinations to identify visible defects such as surface cracks, displacement, deformation, fungal growth, and signs of moisture infiltration. Regular visual inspections help detect early signs of deterioration, allowing for timely maintenance interventions. While cost-effective and straightforward, visual inspection has limitations, as it may not reveal internal defects or subsurface degradation. To enhance accuracy, visual assessments are often complemented by other NDT techniques, such as stress wave timing testing and ultrasonic testing, to enable a more comprehensive evaluation.

Unmanned aerial vehicle (UAV) such as drones can also be utilised to inspect the condition of timber vehicle bridges, particularly in areas that are difficult to access [19]. Drones equipped with high-resolution cameras can capture detailed visual data, identifying surface defects and signs of deterioration. This method enhances safety by reducing the need for manual inspections in hazardous locations while improving efficiency by covering large areas in a short time. Additionally, UAVs can be integrated with advanced software for image analysis over a certain period of time and structural assessments, providing valuable insights for maintenance planning and long-term bridge monitoring.

3.2 X-Ray

X-ray and Computed Tomography (CT) are also NDT techniques used for assessing the internal condition of timber bridge components. These methods provide detailed imaging of internal defects such as voids, cracks, and decay that may not be visible through surface inspections. The recorded images are processed with an optical system that functions similarly to human vision, making them effective for identifying surface defects that differ in colour or pattern from sound wood [20]. Figure 5 shows the X-ray cross-section and associated images.

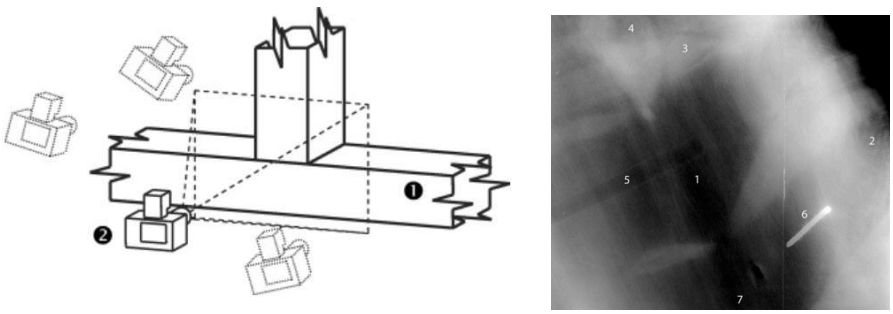

Figure 5. V-ray (a) Image taking [20]. (b) Processed image with cracks [21]

3.3 Stress Wave Timing

The stress-wave timing method is a non-destructive testing (NDT) technique that assesses internal deterioration without causing damage to the bridge structure. It is particularly useful for detecting hidden defects that are not visible on the surface. This test is typically performed in damp areas, where timber is more susceptible to decay.

The first transmitter, the transmitting transducer, emits shear waves through the timber member and the signal is picked up by the receiving transducer. The time taken for the signal to propagate between the two transmitters is recorded by a microsecond timer [22].

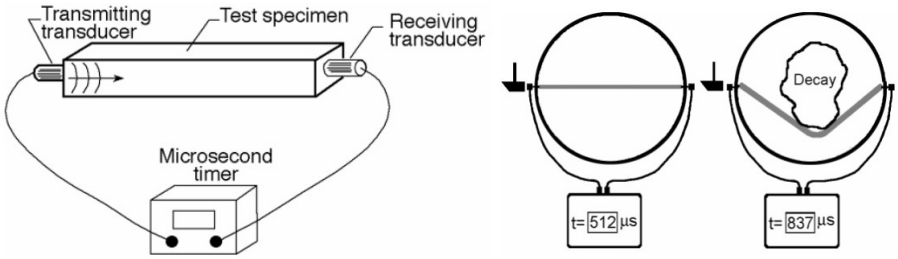

Figure 5. Stress wave timing (a) Test set-up [22]. (b) Reading comparison showing internal decay [23]

It can also be utilised in testing the decaying level of the deteriorated timber from visual inspections. This method is a relatively easy way to effectively measure and identify the condition of the structural elements, along with measuring the modulus of elasticity (MOE) in one dimension [24]. From the measured transmission timing, the dynamic modulus of elastic (MOE_{sw}) can be determined from equation (1).

$$MOE_{sw} = \left(\frac{d}{t}\right)^2 \left(\frac{W}{V}\right) \frac{1}{g} \quad (1)$$

Where d is the timber member's length, W is the weight, V is the volume, t is the tested transmission time and g is the acceleration of gravity [25]. The mean MOE_{sw} of a timber member tested under non-decay, white-rot (medium decay) and brown-rot (advance decay) scenarios are summarised in Table 1.

Table 1. MOEsw values indicating decay levels

	Non-decay	White-rot (medium decay)	Brown-rot (advanced decay)
MOE_{sw} (GPa)	6.35	6.22	5.87

3.4 Resistance Drilling

Micro-drilling as an inspection tool for timber bridges is a semi-destructive testing technique used to assess the internal condition of timber bridge members. Micro-drilling specifically involves drilling small-diameter holes into timber members while measuring resistance during drilling. The tool features a steel drilling bit with a small diameter (0.06 to 0.12 inches) that penetrates the wooden structure at a uniform speed. During drilling, resistance is measured and recorded as data points on a relative 0–100% scale [26].

According to the United States Department of Agriculture (USDA) Wood Condition Assessment Manual, the deterioration index for classifying timber condition levels can be divided into three categories: Sound Wood (>25% resistance), Moderate Decay (10–25% resistance), and Advanced Decay (0–10% resistance) [26].

Figure 6. Resistance drilling method has been used for assessing timber internal condition [23]

3.5 Moisture Content Monitoring

In countries such as the USA, Norway, and Sweden, remote health monitoring is commonly used for timber bridges. These systems gather and store real-time data, allowing for continuous assessment of bridge structural performance [27]. As summarised in Section 2, the moisture content fluctuation within the timber members can lead to splits and associated decay and geothermal weathering, can result in timber deterioration. The structural members can experience swelling and shrinkage with changes in the surrounding humidity, a scenario particularly applicable to the New Zealand environment, which can compromise the integrity of structural members in the bridge over the intended service design life.

Remote moisture content monitoring systems can track the fluctuation in timber moisture content, allowing for early detection of potential issues and decay. These systems often operate by embedding chrome-steel screw electrodes at varying depths within timber piles and structural members. These electrodes are driven perpendicular to the timber elements, which measure both surface and internal moisture variations, providing critical data for assessing the bridge's condition and informing timely maintenance [28]. The data is collected by a real-time data reading device and sent to a main control centre for further analysis.

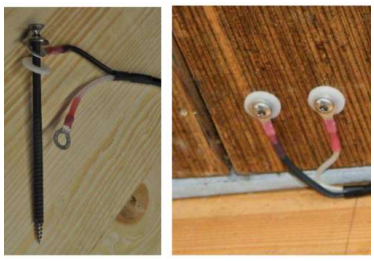

Figure 7. Chrome-steel electrodes installed into timber members [26]

When the moisture content consistently exceeds 20%, conditions become favourable for mould growth, posing a risk to the timber [29]. Once the moisture level passes 25%, decay and fungal activity can be initiated, further challenging structural integrity [30]. To mitigate these risks, predefined alert and alarm thresholds can be established for moisture content monitoring. When these thresholds are exceeded, it is recommended that immediate attention and intervention be undertaken to prevent further deterioration.

3.6 Loading Monitoring

The Forest Products Laboratory (FPL) in the United States have conducted specialised research to assess the load and deflection behaviour of timber bridge decking. This study utilised load cells to track variations in forces exerted by traffic, monitoring the stress distribution on both the bridge decking and supporting pile over time [31]. Similar to the moisture content

monitoring, it is recommended that alert and alarm threshold levels are established and set. Relevant procedures are followed once triggered.

3.7 Temperature and Relative Humidity Monitoring

Environmental factors such as temperature and humidity fluctuations play a critical role in the long-term performance of timber bridges, particularly in influencing creep deflection [32]. Advanced sensor technology is employed to effectively monitor these changes. Sensors with 1 cm diameter probes can be embedded within timber support members at depths of 100–200 mm, ensuring accurate internal readings while minimising external disturbances [33]. Additionally, a transmitter connected to multiple wired sensors is recommended for simultaneously recording temperature and humidity, providing a more comprehensive assessment of environmental impacts [34]. The collected data is continuously transmitted to a remote-control centre, enabling real-time analysis and facilitating maintenance strategies. Refer to Figure 8 for the detailed sensor arrangement.

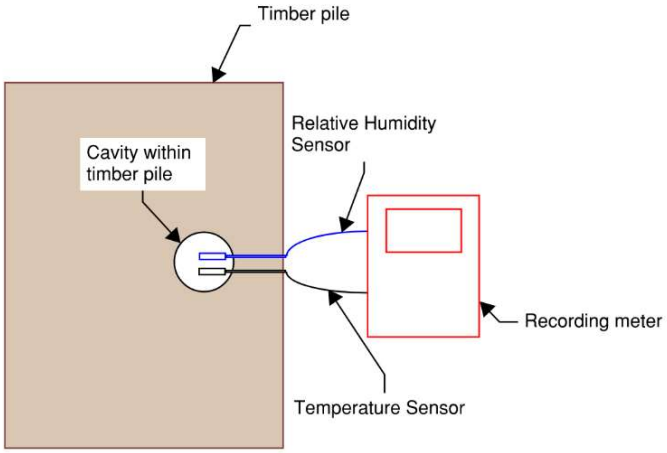

Figure 8. General arrangement of sensor installation

3.8 Displacement Monitoring

Linear variable differential transformers (LVDTs) are highly precise and durable inductive transducers used for measuring displacement, position, and level. The devices consist of a primary winding, two secondary windings, and a movable core. The secondary windings are connected in opposition, producing a differential signal based on the core's position. Due to their high resolution and reliability, LVDTs are widely applied in structural monitoring to track deformations and movements in timber bridge components, providing critical data for assessing long-term performance [35].

4 RECOMMENDED INSPECTION TIMELINE

The inspection methods stated in Section 3 are recommended to be carried out regularly to detect any deterioration and defects at an early stage. These inspections are categorised into two types: one involves on-site assessments by specialised bridge engineers, who perform detailed inspections and testing, while the other utilises remote monitoring systems to detect unexpected issues in real time. Refer to Figure 9 for the inspection schedules summary.

4.1 Visual and Testing

Sections 3.1 to 3.4 involve in-person assessments, primarily consisting of visual inspections. After identifying any surface defects, further testing methods such as stress-wave timing, X-

ray, CT or resistance drilling can be applied to evaluate internal deterioration. These inspections are recommended to be conducted at regular intervals by qualified bridge engineers to ensure early detection of potential issues. The recommended inspection interval is every 3-6 months [36]. However, the frequency of inspections may vary depending on factors such as environmental conditions, bridge age, and traffic loads.

4.2 Health Monitoring

Health monitoring involves the continuous or periodic assessment of a timber bridge's structural condition using remote sensing technologies and automated data collection systems. As stated in Sections 3.5 to 3.8, sensors embedded in critical bridge components can track parameters such as moisture content, relative humidity fluctuations, load responses, and deflection movements, providing real-time insights into potential deterioration.

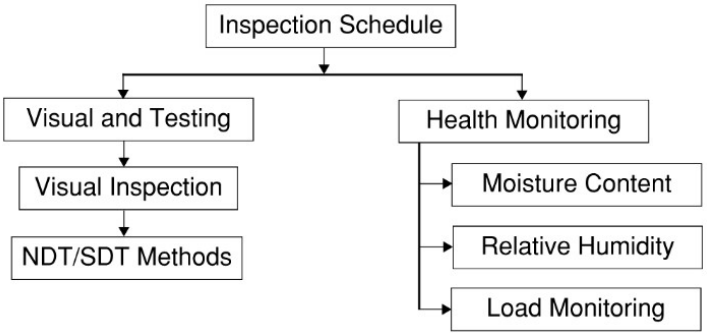

Figure 9. Inspection schedules summary

5 CONCLUSIONS

The adoption of timber vehicle bridges is confronted by significant longevity challenges primarily because of environmental factors. Specifically in New Zealand, critical questions exist regarding the longevity of engineered wood when subject to high humidity and high UV exposure. Fluctuating moisture content cycles, and extreme weather conditions can create additional issues. Prolonged exposure to such an environment for these elements can lead to deterioration, including decay, weathering, deformation, mechanical issues and insect attacks. To enhance the service life of timber bridges, as well as adopting clever detailing techniques during the design phase and the use of impregnated softwood with chemical preservation, a combination of advanced inspection and monitoring techniques is essential.

Regular in-person inspections, including visual assessments and various NDT/SDT methods, allow for early detection of deterioration. Techniques such as stress-wave timing, unmanned aerial vehicle (UAV) inspections, X-ray and resistance drilling enable proactive maintenance, reducing the risk of unexpected failures. Additionally, remote health monitoring systems provide continuous real-time data on critical factors such as moisture content, temperature, humidity, and structural movement. Instruments like linear variable differential transformers (LVDTs) offer precise displacement measurements which can aid in long-term structural performance assessments.

By integrating these advanced inspection and monitoring strategies, timber vehicle bridges in such environments could be effectively maintained which would extend the service life of the primary structural elements and ensure structural reliability. Implementing a systematic maintenance approach is critical to assist in the mitigation of environmental impacts, improve resilience, and support the adoption and development of timber and engineered wood in core bridge infrastructure in New Zealand.

REFERENCES

1. Singh, T., & Page, D. (2018). Case studies on the history and use of timber bridges in New Zealand. *Wood Material Science & Engineering, 13(3), 159-166.*
2. Tupenaite, L., Kanapeckiene, L., Naimaviciene, J., Kaklauskas, A., & Gecys, T. (2023). Timber construction as a solution to climate change: A systematic literature review. *Buildings*, *13*(4), 976.
3. Skullestad, J. L., Bohne, R. A., & Lohne, J. (2016). High-rise timber buildings as a climate change mitigation measure–A comparative LCA of structural system alternatives. *Energy Procedia, 96*, 112-123.
4. Thelandersson, S., & Larsen, H. J. (Eds.). (2003). Timber engineering. John Wiley & Sons.
5. Standards Association of New Zealand. (2003). NZS 3602: Timber and wood-based products for use in building. Wellington, New Zealand.
6. Raftery, G. M., Karami, Z., Pizzi, A., & Nicholson, C. L. (2024a). Durability assessment of one-component polyurethane adhesives for bonding of preservative treated wood subject to artificial ageing. *International Journal of Adhesion and Adhesives, 129*, 103594.
7. Raftery, G. M., Karami, Z., & Nicholson, C. L. (2024b). Natural ageing of one-component polyurethane bonded preservative treated wood evaluated using fracture energy tests. *International Journal of Adhesion and Adhesives, 132*, 103681.
8. Visser, R. (2016). Timber Harvesting in New Zealand: A Guide for Small Scale Forest Landowners. NZFFA, Wellington, New Zealand.
9. NZ Forest Owners Association. (2014). 2014 Facts & Figures New Zealand Plantation Forest Industry. NZFFA, Wellington, New Zealand.
10. Yalde., P., Guild., Ben. (2012). Te Puke rail bridge. Te Puke, New Zealand.
11. Tobi, D. R., Grehan, J. R., & Parker, B. L. (1993). Review of the ecological and economic significance of forest Hepialidae (Insecta: Lepidoptera). *Forest ecology and management, 56(1-4),* 1-12.
12. Rayes, C. A. (2014). Marine wood borers in New Zealand: an interdisciplinary study of their origins, impacts and management. PhD Thesis, University of Waikato, Hamilton, New Zealand.
13. Jeffries, H. W. P. (2007). Collapse of Bridge 256 over Nuhaka River, Palmerston North-Gisborne Line, New Zealand. *Transport Accident Investigation Commission Report 05-116.*
14. Rashidi, M., Hoshyar, A. N., Smith, L., Samali, B., & Siddique, R. (2021). A comprehensive taxonomy for structure and material deficiencies, preventions and remedies of timber bridges. *Journal of Building Engineering*, *34*, 101624.
15. Heritage New Zealand. (n.d.). Waimakariri Gorge Bridge. Canterbury, New Zealand.
16. Selwyn District Council. (2024). Waimakariri Gorge Bridge Deck Replacement. Canterbury, New Zealand.
17. McKenzie, R., Bodeker, G., Scott, G., Slusser, J., & Lantz, K. (2006). Geographical differences in erythemally-weighted UV measured at mid-latitude USDA sites. *Photochemical & Photobiological Sciences, 5*, 343-352.
18. The MacDiarmid Institute for Advanced Materials and Nanotechnology. (2023). Whakarewarewa Living Village and the MacDiarmid Institute to restore the health of culturally significant stream. Rotorua, New Zealand.
19. Seo, J., Duque, L., & Wacker, J. (2018). Drone-enabled bridge inspection methodology and application. *Automation in construction*, *94*, 112-126.
20. Riggio, M., Sandak, J., & Franke, S. (2015). Application of imaging techniques for detection of defects, damage and decay in timber structures on-site. *Construction and Building Materials*, *101*, 1241-1252.
21. Wedvik, B., Stein, M., Stornes, J. M., & Mattsson, J. (2016). On-site radioscopic qualitative assessment of historic timber structures: identification and mapping of biological deterioration of wood. *International Journal of Architectural Heritage, 10(5),* 646-662.
22. Ross, R. J. (2000). Stress wave timing nondestructive evaluation tools for inspecting historic structures: a guide for use and interpretation (Vol. 119). US Department of Agriculture, Forest Service, Forest Products Laboratory.
23. Wang, Xiping, et al. "Assessment of decay in standing timber using stress wave timing nondestructive evaluation tools." *US Department of Agriculture. Forest Products Laboratory, Technical Report* 147 (2004).

24. Honfi, D., Lechner, T., & Köhler, J. (2017). Rational maintenance of timber bridges. In *3rd International Conference on Timber Bridges*. Skelleftea, Sweden.
25. Yang, Z., Jiang, Z., Hse, C. Y., & Liu, R. (2017). Assessing the impact of wood decay fungi on the modulus of elasticity of slash pine (Pinus elliottii) by stress wave non-destructive testing. *International Biodeterioration & Biodegradation, 117*, 123-127.
26. Brashaw, B. K. (2005). Condition assessment of timber bridges (No. 160). US Department of Agriculture, Forest Service, Forest Products Laboratory.
27. Brownjohn, J. M. (2007). Structural health monitoring of civil infrastructure. Philosophical Transactions of the Royal Society A: Mathematical, Physical and Engineering Sciences, 365(1851), 589-622.
28. Tannert, T., Berger, R., Vogel, M., & Müller, A. (2011). Remote moisture monitoring of timber bridges: a case study. In *Proceeding of the 5th International Conference on Structural Health Monitoring of Intelligent Infrastructure (SHMII-5)* (pp. 11-15). Cancun, Mexico.
29. Björngrim, N., Myronycheva, O., & Fjellström, P. A. (2022). The use of large-scale X-ray computed tomography for the evaluation of damaged structural elements from an old timber bridge. *Wood Material Science & Engineering, 17(6),* 1028-1029.
30. Viitanen, H. (1994). Factors affecting the development of biodeterioration in wooden constructions, *Materials and Structures 27(8),* 483-493.
31. Ritter, M. A., Geske, E. A., McCutcheon, W. J., Moody, R. C., Wacker, J. P., & Mason, L. E. (1991). Methods for assessing the field performance of stress-laminated timber bridges. In *Proceedings of the 1991 International Conference on Timber Engineering.* London, England.
32. Mårtensson, A. (1994). Creep behavior of structural timber under varying humidity conditions. *Journal of Structural Engineering*, *120*(9), 2565-2582.
33. Palma, P., & Steiger, R. (2020). Structural health monitoring of timber structures–Review of available methods and case studies. *Construction and Building Materials*, *248*, 118528.
34. Wacker, J. P., & Calil, C. (2004). Pennsylvania hardwood timber bridges: field performance after 10 years. In *Proceedings of the Structural Materials Technology VI.* Buffalo, New York, USA. American Society for Nondestructive Testing. pp 222-227.
35. Petchmaneelumka, W., Koodtalang, W., & Riewruja, V. (2019). Simple technique for linear-range extension of linear variable differential transformer. *IEEE Sensors Journal*, *19*(13), 5045-5052.
36. Simon, A., Jahreis, M., & Koch, J. (2023). Improvement of the durability of timber bridges by intelligent design and responsible maintenance. In Proceeding of the *World Conference on Timber Engineering*. Oslo, Norway.

ICTB 2025. 5th International Conference Timber Bridges
Rotorua, New Zealand, 29 June to 2 July 2025.

TIMBER BRIDGES ASSET MANAGEMENT

Gang Yu[1], Cam Gordon[2]

ABSTRACT

Auckland Transport (AT) manages numerous bridges in Auckland, using timber, concrete, and steel as key materials. Timber bridges present several management challenges, including lifespan, durability, maintenance, repair, load management, environmental impact, and emergency preparedness. This paper examines AT's approach to managing timber bridge assets and provides insights on this topic.

Timber bridges offer benefits such as visual appeal and the potential for sustainable resource use. However, they require strict inspection and maintenance to prevent wood decay and ensure structural integrity. Proper asset management is essential to keep these bridges safe and operational, integrating environmental benefits with modern engineering practices. This paper discusses observations and lessons learned from several completed timber bridge repair projects.

It is anticipated that modern timber bridge design could enhance user experience and reduce maintenance requirements.

1 INTRODUCTION

Auckland Transport (AT) manages 45 timber bridges, and more than 60 steel timber composite bridges for transport service, while Auckland Council Park has about 120 timber bridges. Figure 1 provides an overview of AT bridges made from various materials. With changes in designation, AT frequently assumes responsibility for additional timber bridges for Auckland Council. Additionally, there are numerous other structural timber elements exist in these bridges. The number of timber bridges is expected to increase with the growth of greater Auckland.

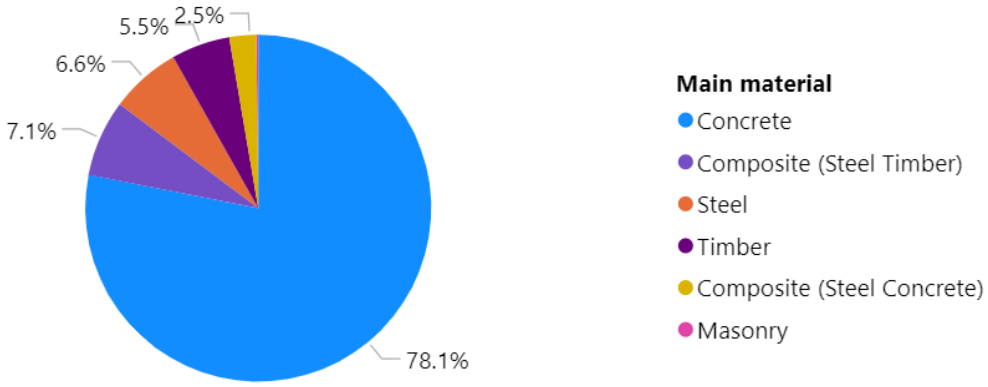

Figure 1. Summary of AT Bridges Constructed with Various Materials

As the custodian of numerous timber bridges, AT promotes structural timber use to support the nation's carbon-neutral goal.

Timber, alongside concrete and steel, is one of the primary materials for bridge construction. However, timber has a significantly lower unit carbon emission factor of 0.015 ($kgCO_2$-e)/kg compared to concrete at 0.203 and steel at 2.85 [1]. Therefore, timber options should be actively considered where appropriate. While how to define “appropriate” will be discussed in the later sections.

[1] Principal Asset Engineer, Auckland Transport,
e-mail: gang.yu@at.govt.nz,
[2] Strategic Asset Manager, Auckland Transport

Table 1. Embedded carbon emission factors

Items	Materials		
	Concrete	Steel	Timber
Unit	kg	kg	kg
Carbon emissions ($kgCO_2$-e/kg)	0.203	2.85	0.015

Efforts to reduce carbon emissions should encompass the entire lifecycle of structures, from decision-making through asset creation to the end of service life. This was discussed in detail in another paper presented at the 2021 Decarbonising Transport Conference [2].

Beyond evaluating carbon emissions, it is advantageous for asset owners to consider the merits of options throughout the entire lifecycle of a bridge, ensuring a thorough assessment. We encourage the broader engineering community, including consultants and contractors, to adopt this holistic approach.

2 TYPICAL AT MANAGED TIMBER BRIDGES AND ISSUES

A significant number of bridges managed by AT are timber deck-steel girder structures constructed between 1940 and 1970 (refer to Figure 2). That serves vehicles transport. Typical issues associated with these bridges include:

- Frequent reapplication of wearing surfaces for friction.
- Lack of composite action between timber and steel, limiting load capacity.
- Poorly treated interactions with roads, causing settlements and gaps.
- Timber elements are not durable due to loading impact and environmental corrosion.
- Bridge barriers fail to meet modern standards and cannot effectively transfer impact loads.

Figure 2. Timber deck - Steel girder Bridges distribution

Some bridges face significant capacity issues; 12 out of 19 weight-restricted bridges in AT network fall into this category. While quick construction might have been practical in the past, it is not ideal for modern bridges.

Another portion is full timber superstructure, some have timber substructure, bridges, mainly for pedestrians and cyclists. Typical issues include:

- Slippery surfaces due to insufficient friction, especially in wet and cold weather.
- Substandard barriers.

- Failure of steel connect elements, like bolts, nuts, or brackets.
- Corrosion of timber and steel elements.

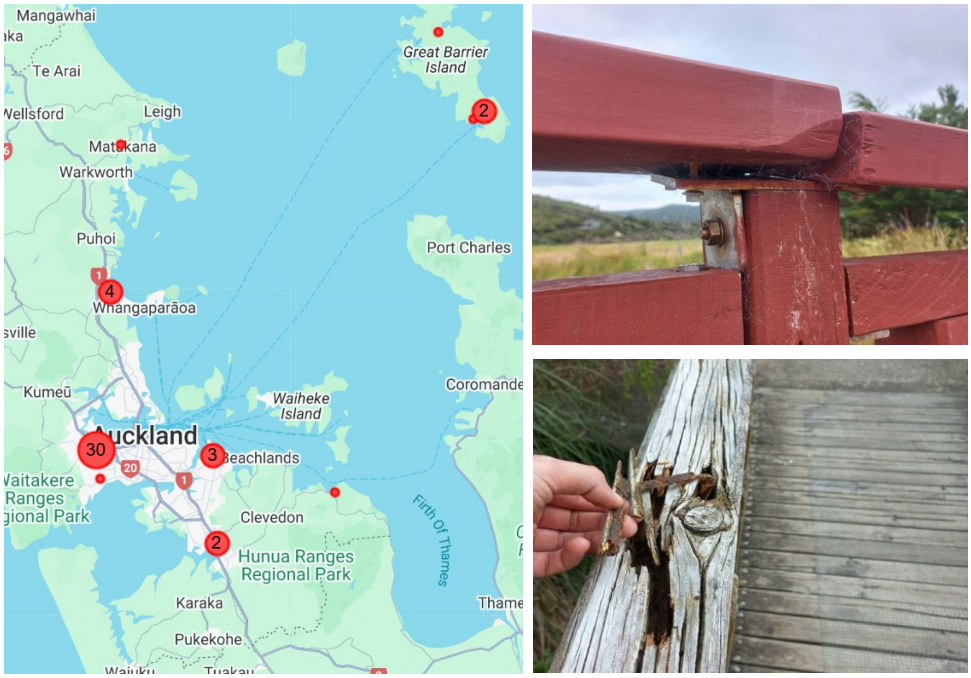

Figure 3. Full-timber Bridges distribution

AT has managed several timber bridge repairs and anticipates more projects in the next decade. Based on completed work, the following notes may serve as valuable references for ongoing projects:

- **Component inspection**
  Timber bridges consist of numerous small-scale components. Certain elements can only be inspected once the surrounding parts are uncovered, increasing uncertainties during repairs.
- **On-site Labour**
  The high number of connection points among elements necessitates intensive on-site labour. It is advisable to explore pre-assembly of small elements in a factory setting to reduce on-site installation and minimize traffic disruptions.
- **Temperature-Sensitive Bonding**
  For bridges that support vehicular transport, it is crucial to note that the bonding primer for the wearing surface and timber deck must be applied at specific temperatures. This requirement can significantly impact the construction schedule and should be considered during program development and cost estimation.
- **Steel Component Durability**
  Timber bridges often include significant steel components, which may fail before the timber elements. Therefore, it is advisable to consider high durability requirements for steel elements holding timber elements, as the tight space makes a lot of connectors replacement and/or recoating protection difficult after construction.
- **Interface Details**
  The interface details need to be developed at the timber bridge and approaching roads. The existing timber bridge often has a natural connection without many details. However, gaps tend to get larger over time, creating dents when driving through. This can cause more damage to the timber elements at abutments due to high dynamic impact from vehicles. Ultimately, leads to more frequent repairs.

AT manages bridges using a whole-of-lifetime approach, employing Net Present Value (NPV) analysis to determine the optimal timing for repairs or replacements. The next section outlines the factors involved in managing timber bridges.

3 MULTI CRITERIA CONSIDERATION IN MANAGING THE TIMBER BRIDGES

It is acknowledged that timber, as a material, is merit at carbon emission compared to concrete and steel, however, any final solution is the combination of multi factors. That can be illustrated in Figure 3 as an example.

In Figure 3:

- Each criterion (Cost, Sustainability, Availability, Durability, Aesthetics) is connected to each option (Timber, Concrete, Steel) with edges that have weights representing the importance of each criterion for each alternative.
- For example, Timber has a high weight for Sustainability (0.9) and Aesthetics (0.8), while Concrete has a high weight for Durability (0.9) and Availability (0.8).
- This is the quantitative way we often use to evaluate the new bridges development options, for example, the timber bridge carbon emission merit is reflected under "sustainability" criterion.

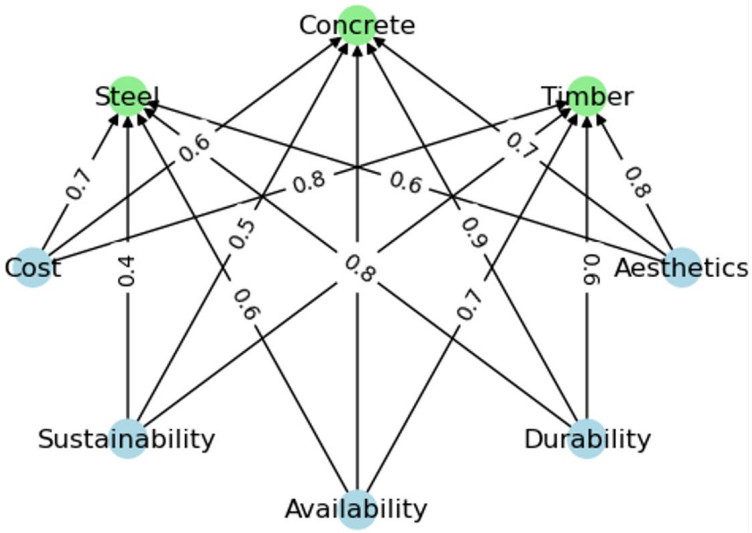

Figure 4. Mult-factors assessment of options illustration

3.1 Whole of life considerations

Figure 5 shows the lifecycle of a bridge, which includes construction, multiple repairs, and eventual demolition. Each stage requires investment.

- For example, a timber bridge might be less expensive than concrete bridge to build, but more costly during the operation stage.
- While some timber bridges have lasted over a century, their generally accepted service life is 50 years with proper treatment. This means that when comparing costs between timber and concrete bridges, one should account for building two timber bridges to match the 100-year lifespan of a typical concrete bridge.
- The carbon emission calculations of an option can also refer to this diaphragm, as each stage will generate the carbon emission, the overall carbon emission can be calculated by summing of carbon emission of all stages [2].

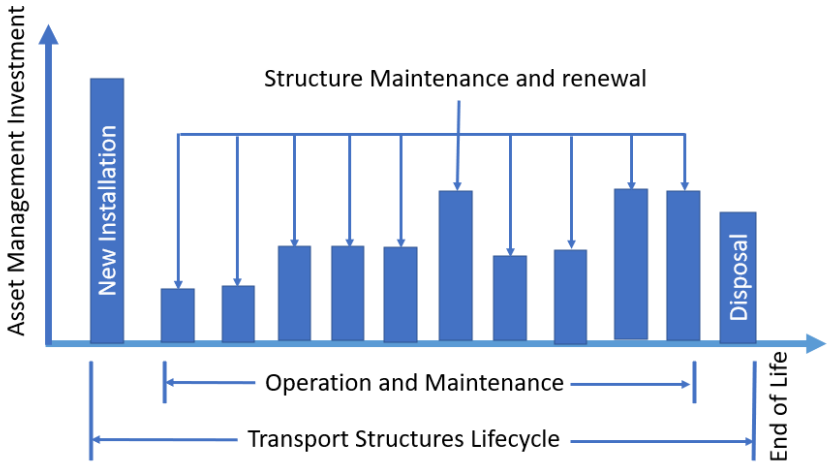

Figure 5. Lifecycle of a bridge

3.2 Giving more consideration to operation and maintenance

The initial construction of a timber bridge is only a small part of its total lifespan and cost. Maintenance, repairs, and eventual demolition are significant factors. It is essential to design access and space for future repairs.

As noted previously, some projects reveal hidden problems in timber elements and steel connectors when surrounding elements are removed. Recommendations include:

- Provide maintenance-free protection during construction if space and access are impractical.
- Factor in future maintenance/repair costs when estimating overall options.
- Considering modular replacement concepts for isolated repairs from the design stage minimizes traffic flow disruption.
- Run maintenance and repair scenarios during design to ensure adequate space and access and include these in the asset owner's manual [3][4].

3.3 The indirect cost estimation because of the traffic disruptions

In many projects, the indirect costs resulting from traffic disruption are often not adequately accounted for, which can significantly impact the overall cost assessment. Although some rapid construction options may appear more expensive, a comprehensive calculation of both direct and indirect costs reveals that these indirect costs can be pivotal in evaluating the total societal cost. Guidance on calculating these indirect costs is available in NZTA Research Report 670 [5].

Timber bridge on-site fabrication is time-consuming and labour-intensive. Considering both direct and indirect costs together suggests the need to develop modular and pre-assembled construction methodologies to minimize on-site work duration.

4 CONCLUSIONS

This paper provides an overview of AT managed timber bridges and summarizes several discussion points based on our past projects. Some of these points may not be exclusive to timber bridges but also cover common features of all types of bridges.

When discussing timber bridges, it is important to consider the heavy steel elements used for connections. The durability of these steel elements contributes significantly to the overall performance of the timber bridge. Notably, certain steel components should be maintenance-free in areas where space for maintenance and repair is limited.

Timber bridges are notable for their carbon emission savings. However, at the optioneering stage, a whole-of-life approach is recommended to assess both carbon emissions and cost estimates.

Efforts to reduce onsite labour for timber bridge fabrication can promote the use of timber bridges and minimize traffic disruption, particularly for road bridges.

Fast construction can benefit the overall economy, that can be tested through an indirect cost calculation per NZTA guidance. This is especially crucial when constructing a bridge in urban areas.

REFERENCES

1. MBIE, 2020. Whole-of-Life Embodied Carbon Emissions Reduction Framework, online resource: Ministry of Business, Innovation and Employment (MBIE).
2. Matiul, K., Gang, Y., 2021. Integrated Carbon Emissions Control in Decision-Making. Decarbonising Transport, Transportation Group Conference, New Zealand.
3. NZ Transport Agency, Minimum Standard Z/15 - Asset Owner's Manual, New Zealand.
4. NZ Transport Agency, Standard Professional Services Guideline – PSG/15 – Asset Owner's Manual, New Zealand.
5. NZ Transport Agency research report 670, Better measurement of the direct and indirect costs and benefits of resilience, New Zealand.

ICTB 2025. 5th International Conference Timber Bridges
Rotorua, New Zealand, 29 June to 2 July 2025.

SMOOTH-SHANK NAIL WITHDRAWAL CAPACITY: EFFECTS OF WOOD RELAXATION AND MOISUTRE CONTENT

Yuhao Zhang[1], Lisa-M. Ottenhaus[2], Jeffrey J. Morrell[3], Tripti Singh[4], Luis Yermán[5]

ABSTRACT

Nails are primary fasteners in timber structures. One important mechanical property of nails is their ability to resist withdrawal, also known as nail withdrawal capacity (NWC). Extensive studies have investigated NWC changes under different factors (e.g., moisture, biodeterioration), but the wood relaxation impact was often neglected. Wood relaxation is an important factor affecting NWC and neglecting it can compromise NWC assessment, potentially leading to biased conclusions for structure design. This study assessed the effects of wood relaxation on NWC in radiata pine at 9%, 12% and 18% moisture contents (MC) over 28 days. NWC decreased by 40% at 9% and 12% MC, whereas a slight improvement (10%) occurred at 18% MC. Stress relaxation tests demonstrated gradual stress loss in all conditions. The NWC improvement at 18% MC may be owed to an increased friction coefficient at the wood-nail interface.

1 INTRODUCTION

Connections are vital in timber structures, as they are typically designed to be the weakest link [1,2]. Various types of connectors and fasteners are engineered to connect wood elements, with the most commonly employed fastener being nails [3]. The mechanical performance of nails has been extensively investigated, with nail withdrawal capacity (NWC) being the most extensively studied parameter. Smooth-shank nails derive their NWC from friction, governed by Coulomb's Law of Friction (Equation 1), dictated by three factors: compressive stress around the nail shank created during driving, wood-nail contact area and friction coefficient at the wood-nail interface [4].

$$NWC = Friction = Stress \times Contact\ Area \times Friction\ Coefficient \quad \text{Eq.1}$$

Prior research has studied NWC changes under varying factors. Nail corrosion under high humidity can temporary increase NWC [5,6]. Significant reductions in NWC have also been documented due to changes in wood moisture content (MC) [7,8,9]. The effect of fungal degradation on NWC has also been studied [10,11]. Most studies exposed nailed wood samples to an influencing factor (e.g., moisture or fungi) over weeks or months and then assessed NWC loss.

While perceptions of NWC vary, moisture-induced losses were primarily driven by corrosion, wood cracks, nail backout and wood relaxation [5,12,13,14].

Metal fasteners can corrode if exposed to high humidities [15]. Corrosion initially generates rust on fasteners, increasing their volume, surface roughness and enhancing NWC. However, the rust become loose over time, resulting in significant NWC loss [5].

Moisture-induced internal stresses create wood cracks [16]. These cracks can reduce stress around the nail if developed immediately adjacent to the fastener, leading to a significant decline in NWC [9,12].

[1] PhD Candidate, School of Civil Engineering, The University of Queensland, Brisbane, Australia, yuhao.zhang@uq.edu.au
[2] Senior Lecturer, School of Civil Engineering, The University of Queensland, Brisbane, Australia, l.ottenhaus@uq.edu.au
[3] Professor Emeritus, Department of Wood Science and Engineering, Oregon State University, Corvallis, USA, jeff.morrell@oregonstate.edu
[4] Professor, National Centre for Timber Durability and Design Life, University of the Sunshine Coast, Sunshine Coast, Australia, tsingh1@usc.edu.au
[5] Research Fellow, School of Civil Engineering, The University of Queensland, Brisbane, Australia, l.yerman@uq.edu.au

Nail backout describes the progressive outward movement of nails caused by cyclic wood swelling and shrinkage due to MC changes [17]. The cyclic movement can reduce the contact area at the wood-nail interface and potentially reduce NWC [18].

Wood relaxation refers to time-dependent stress loss in wood and this process reduces compressive stress around the nail shanks and consequently leads to NWC loss, causing up to 70% NWC loss for smooth-shank nails [14,19].

Lhuede [20]documented a 26% loss in NWC in mountain ash and a 12% loss in radiata pine with 3.15 mm smooth-shank nails, although the relaxation duration and moisture conditions were not clearly stated. Zhao et al. [21] observed a 7% NWC loss over 7 days on 2.82 mm diameter smooth-shank nails driven into Chinese fir side grain at 20°C and 65% relative humidity (RH).

Wood relaxation intensifies with increased MC [22]. Pina et al. [23] observed a 200% higher bending relaxation in radiata pine at 28°C and 81% RH versus 28°C and 45% RH. Similarly, Saifouni et al. [19] observed increased tension relaxation in silver fir at 21°C and 70% RH compared to 21°C and 30% RH. This occurs because absorbed water molecules interact with hydroxyl groups on cellulose microfibrils, increasing intermolecular distance of wood polymers and reducing the physical and mechanical properties of wood [24,25].

Research confirmed wood relaxation results in NWC loss by introducing gradual stress loss, whereas increased MC levels significantly amplify wood relaxation. However, current studies are unclear about the magnitude and temporal progression of NWC loss linked with wood relaxation. Furthermore, wood MC impact on NWC was poorly characterized. Understanding these parameters is critical to quantify wood relaxation impact on NWC and enable more precise NWC assessment with external factors.

Most existing NWC studies on smooth-shank nails did not consider wood relaxation, potentially leading to biased results. A comprehensive investigation into relaxation is essential to develop strategies for mitigating relaxation-related errors.

This study investigated the influence of wood relaxation on NWC of smooth-shank nails and quantified both NWC loss and stabilization time. These results deliver actionable strategies to improve the precision of NWC assessments when studying the impact of external factors.

2 MATERIALS AND METHODS

Coulomb's Law of Friction identifies stress as one critical factor governing NWC. This stress can be reduced by wood relaxation, causing significant NWC loss. Hence, the experiment incorporated stress relaxation tests alongside standard nail withdrawal tests to study the stress changes around the nail and validate the results of nail withdrawal tests.

2.1 Nail withdrawal test

Deflect-free MGP12 radiata pine boards (45 mm x 90 mm x 2400 mm) graded with AS/NZS standard 1748 [26] with densities ranging from 500 to 650 kg/m^3 were cut into 126 blocks each with 320 mm in length. These blocks were conditioned at 23°C and 65% RH, their dimensions and masses were measured to determine density, then divided into three groups of 42 samples with similar density distributions. The three groups were then conditioned to three target MCs (9%, 12% and 18%) termed as DRY, SERVICE and WET using the temperatures and relative humidities specified in Table 1. Actual MCs were determined using the oven-dry method following ASTM standard D4442-20 [27].

Table 1. Temperatures and relative humidities for DRY, SERVICE and WET. Brackets contain standard deviations.

Conditions	DRY	SERVICE	WET
Temperature (°C)	23	23	32
Relative Humidity (%)	45	65	90
Target wood MC (%)	9	12	18
Actual wood MC (%)	9.0 (0.3)	12.2 (1.5)	17.7 (0.9)

Nail withdrawal samples were fabricated following the ASTM standard D1761-12 [28] using conditioned wood blocks and smooth-shank 316-stainless-steel nails that were 2.8 mm in diameter and 50 mm long. All nails were cleaned using isopropyl alcohol wipes and manually hammered into the side grain of the wood blocks to a consistent depth of 36 mm. Five nails were driven into each wood block, positioned apart to avoid cracking and splitting (Figure 1). After nail driving, 18 assemblies (6 assemblies per condition) were immediately tested, while the other assemblies were returned to their respective conditioning environments and tested on the designated dates.

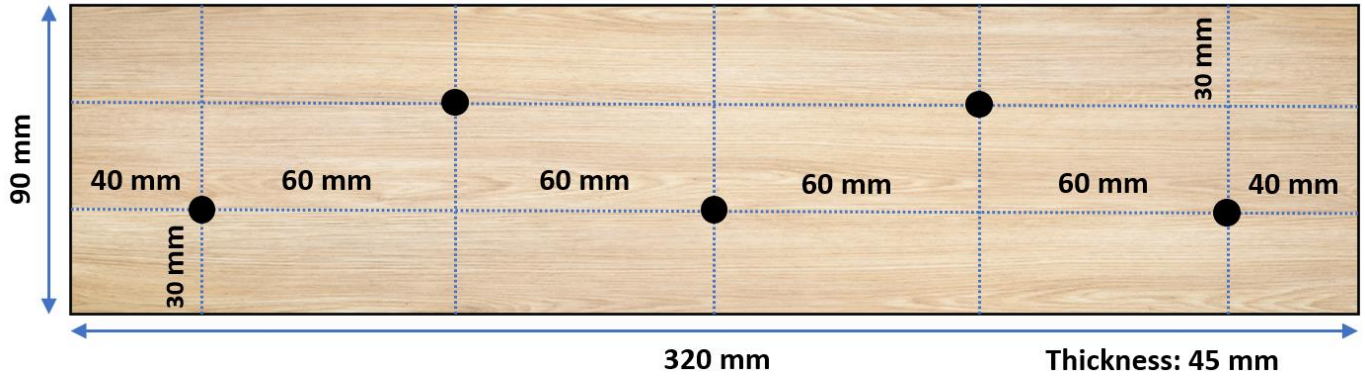

Figure 1. Configuration of a nailed assembly for nail withdrawal tests. Black dots represent the driving positions of nails.

NWC was tested after 0 (immediately after driving), 1, 2, 3, 7, 14, and 28 days of driving in wood conditioned at DRY, SERVICE or WET. Each time step included 30 repetitions, totalling 630 tests. Nails were withdrawn by gripping the nail head using a metal rig that was further attached to a universal testing machine (UTM, Instron 3400) as demonstrated in Figure 2a, while the wood was held stationary at the base of the UTM by steel frames (Figure 2b). Withdrawal was performed following BS EN 1382 standard [29] using a constant speed of 0.4 mm/min while recording load-displacement curves. The highest load of each curve was determined as the NWC.

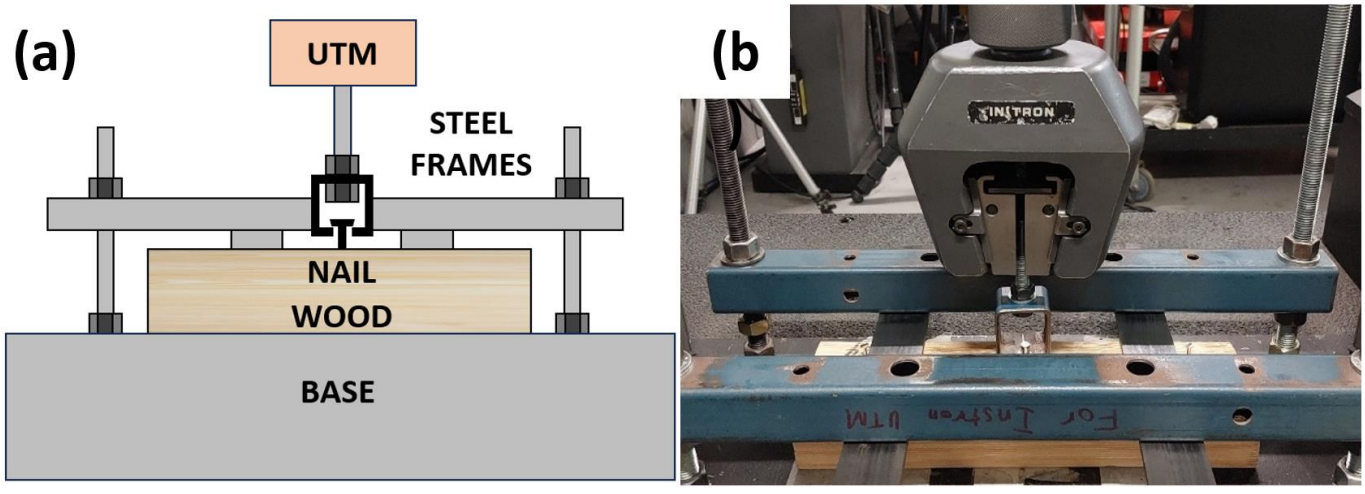

Figure 2. (a) Configuration of nail withdrawal setup and (b) a photo of the nailed assembly held by steel frames.

2.2 Stress relaxation test

Stress measurements around the nail shank can be technically complex, because the nail driving process physically obscures the wood-nail interface, while artificially exposing this interface can disrupt stress. A customized setup was designed to replicate stress dynamics around the nail shank, enabling continuous stress assessment. A nail shank (48 mm in length, head removed using a hack saw) was horizontally placed on the end grain of wood blocks (45 mm x 90 mm x 100 mm) conditioned to DRY, SERVICE or WET levels, and wrapped using thin PVC film to prevent MC changes (Figure 3a).

The nail shank was compressed vertically into the wood by a press attached to the UTM (Figure 3b) using a compression rate of 0.5 mm/min and a target depth of 1.4 mm (the nail radius), simulating the stress condition around a driven nail shank. Once target depth was reached, the press remained stationary for at least 62 hours and load was continuously recorded. Mass changes of PVC-wrapped wood were less than 0.1% mass during test period, confirming its effectiveness in preventing moisture exchange. Four repetitions were tested per moisture condition (DRY, SERVICE and WET), totalling 12 repetitions.

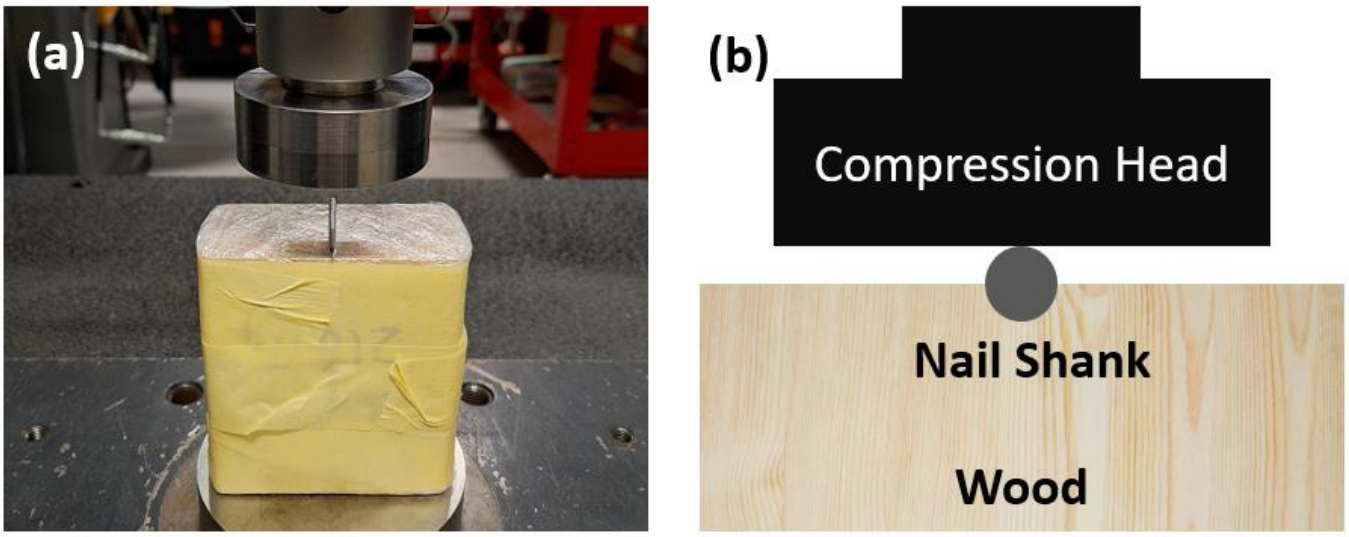

Figure 3. (a) Setup of stress relaxation tests and (b) illustration of nail shank compressed for 1.4 mm (the nail radius) into the wood block.

2.3 Statistical analysis

Nail withdrawal results were subjected to an Analysis of Variance (ANOVA, $\alpha = 0.05$). Normal distribution was checked by Q-Q plots, while Levene's Tests verified the equality of variance. Parametric results underwent Tukey's post-hoc tests, whereas nonparametric data was evaluated using Kruskal-Wallis tests with Dunn's post-hoc comparisons.

3 RESULTS AND DISCUSSION

3.1 Nail withdrawal test

The load-displacement curves showed divergent behaviours (Figure 4), reflecting differences in natural wood structures. Most curves displayed steady increases in load, while others showed significant slips before developing sustained loading.

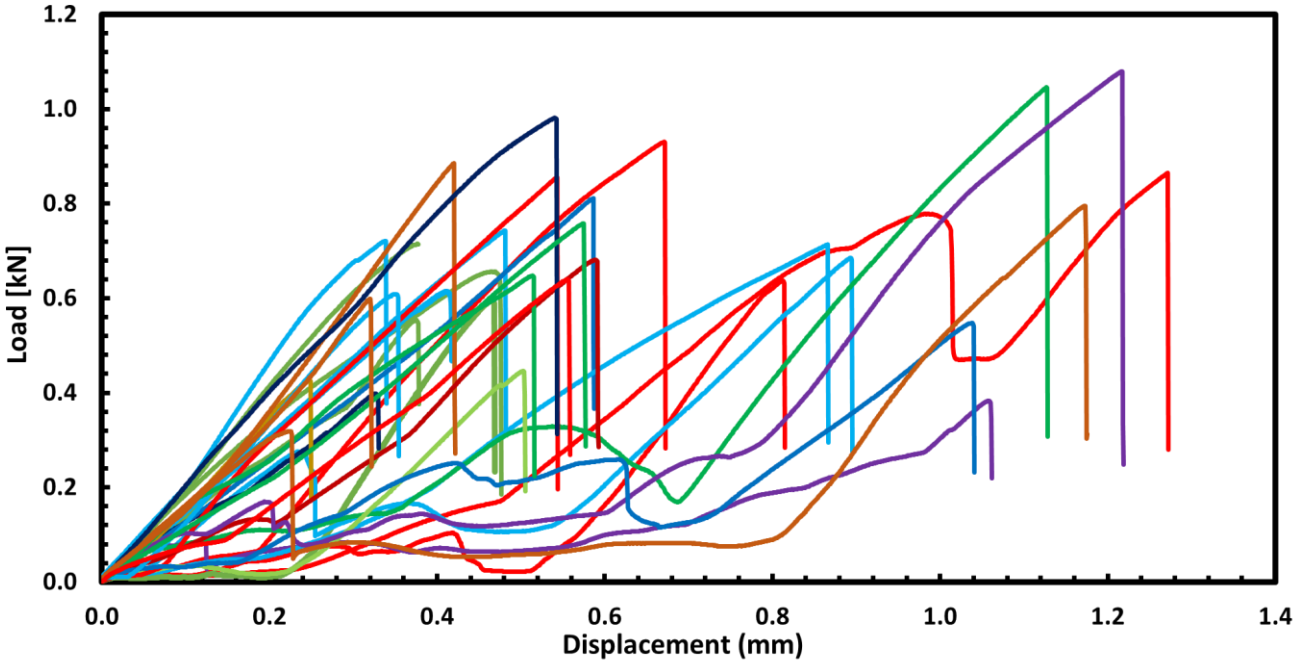

Figure 4. Load-displacement curves derived from day 0, DRY.

Figure 5 illustrates average NWC changes for wood at DRY, SERVICE, and WET levels. NWC under DRY conditions experienced 41% loss 28 days after driving, with significant loss occurring between days 1 and 2, then remained statistically stable throughout the following days. NWC loss in SERVICE was similar (44 %) to DRY, with significant loss occurring between 7 and 14 days. In contrast, NWC in WET sample increased 10% after 28 days compared to initial (day 0) NWC.

The significant impact of wood relaxation on NWC was confirmed by the nail withdrawal tests. However, test results also showed an unexpected NWC increase in the WET condition. According to Coulomb's Law of Friction and the fact that contact areas (driving depth) were consistent for all moisture conditions, the unexpected NWC increases were likely due to differences in stress or friction coefficient at different MCs. Higher wood MC increases friction coefficients at the wood-metal interface [30]. This increased friction coefficient may counteract additional stress loss at higher MC, ultimately increasing NWC.

In addition, the initial (day 0) NWC of DRY samples was 16% lower compared to SERVICE samples, which may also be attributed to higher friction coefficients in the wetter wood. While lower MC in DRY was associated with improved compressive strength and consequently created higher stress at wood-nail interfaces, a higher friction coefficient in SERVICE appeared to provide more improvement of NWC [31].

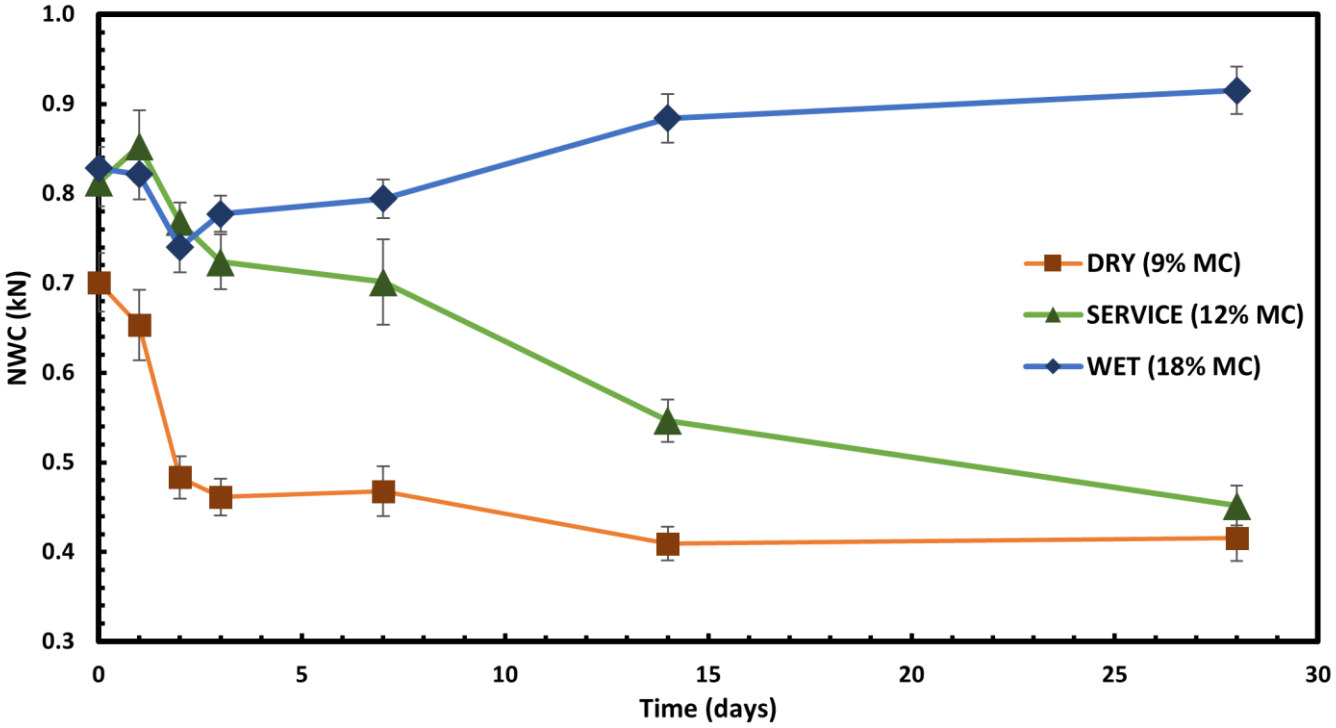

Figure 5. Average NWC changes from 0 to 28 days in DRY, SERVICE or WET. Error bars indicate standard errors.

3.2 Stress relaxation test

Stress around the nail shank sharply decreased and gradually stabilized with time (Figure 6). Most stress loss occurred within five hours after compression, then the loss steadied to less than 1% stress loss in the last ten hours.

Stress losses at 60 hours were 40%, 44%, and 52% for DRY, SERVICE and WET conditions, respectively. Higher wood MC resulted in higher stress loss and was consistent with previous findings [19,23]. The magnitude of stress loss was reasonable, as similar stress losses have been reported [32] with a 30% loss in the first hours of 1.2 mm-compression in Scots pine at 9% MC.

The stress relaxation tests indirectly showed that the increased friction coefficients were likely the main cause for NWC increase in WET samples. We recommend further investigation into the mechanisms behind the increased friction coefficients.

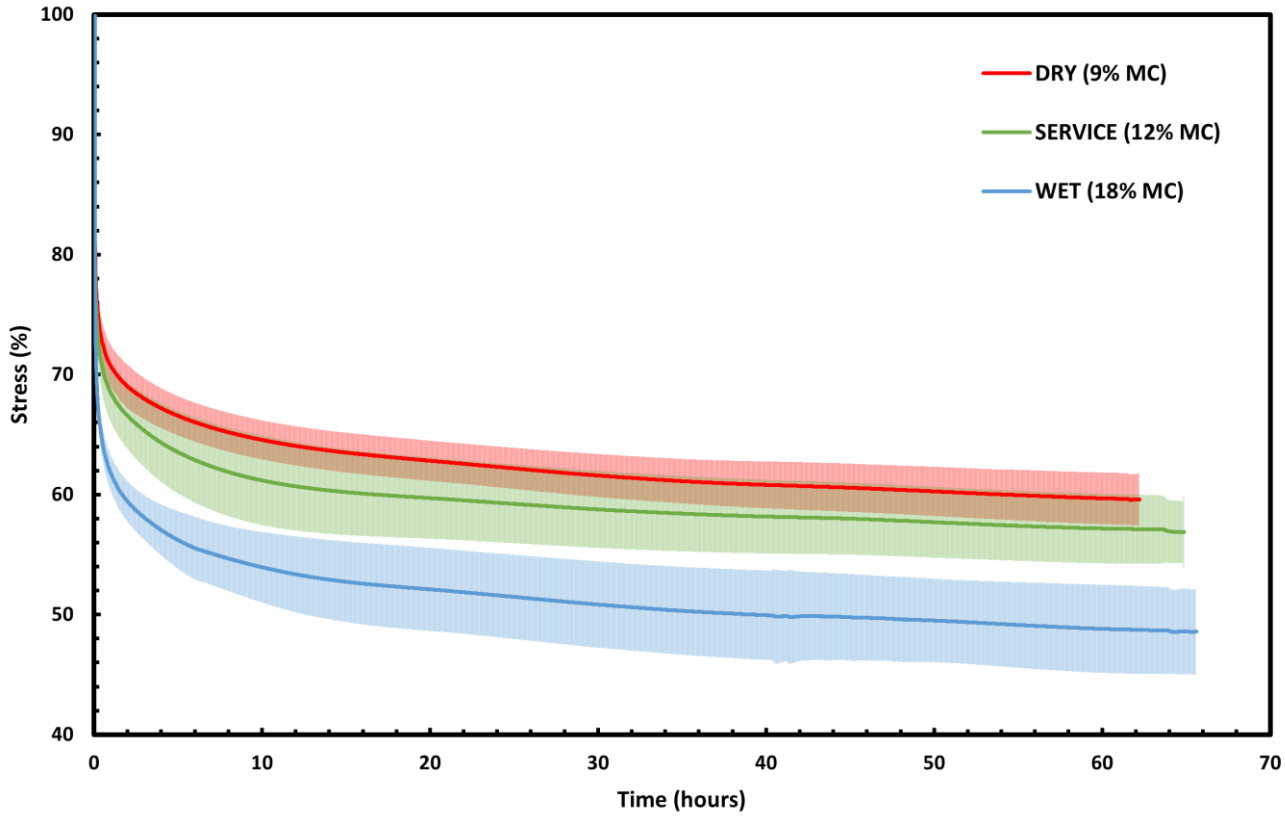

Figure 6. Average stress retention curves from 0 to 62 hours in DRY, SERVICE and WET. Shaded areas indicate standard deviation.

4 CONCLUSIONS

Major findings from this study were as follows:

- Wood relaxation significantly impacted NWC, causing up to 40% NWC loss.
- NWC stabilized 14 days after driving in all moisture conditions.
- Higher moisture content increased NWC, potentially introducing higher friction coefficients at the wood-nail interface.

This study provided two important guidelines for future NWC studies on smooth-shank nails:

- Existing studies on the NWC of smooth-shank nails may produce less accurate results and biased conclusions if relaxation was not properly considered.
- Future NWC research must consider wood relaxation. Specifically, procedures should allow at least 14 days of relaxation after driving if immediate NWC testing is not feasible for all conditions.

REFERENCES

[1] R. Jockwer, G. Fink, and J. Köhler, "Assessment of the failure behaviour and reliability of timber connections with multiple dowel-type fasteners," *Eng. Struct.*, vol. 172, no. December 2017, pp. 76–84, 2018, doi: 10.1016/j.engstruct.2018.05.081.

[2] Australian Standard, *AS 1720.1 - Timber structures Part 1 : Design methods*. GPO Box 476, Sydney, NSW 2001: Standards AUstralia Limited, 2010.

[3] Task Committee on Fasteners, *Mechanical Connections in Wood Structures*. American Society of Civil Engineers, 1996. [Online]. Available: https://ascelibrary.org/doi/book/10.1061/9780784401101

[4] Y. Wang and S. H. Lee, "A theoretical model developed for predicting nail withdrawal load from wood by mechanics," *Eur. J. Wood Wood Prod.*, vol. 76, no. 3, pp. 973–978, 2018, doi: 10.1007/s00107-017-1227-2.

[5] J. F. Senft and S. K. Suddarth, "Withdrawal resistance of plain and galvanized-steel nails during changing moisture content conditions," *For. Prod. J.*, vol. 21, no. 4, pp. 19–24, 1971.

[6] S. Wang, F. Wang, F. Kong, P. Ma, Z. Chen, and Z. Que, "Influence of repeated wetting and drying on withdrawal capacity of wooden nails and metal nails," *Constr. Build. Mater.*, vol. 409, no. November, p. 133991, 2023, doi: 10.1016/j.conbuildmat.2023.133991.

[7] R. H. Perkins, "Nail withdrawal resistance in plantation red pine grown in Indiana," *For. Prod. J.*, vol. 21, no. 6, pp. 29–32, 1971.

[8] Z. Que, L. Yang, F. Wang, X. Zhu, Y. Wang, and T. Mori, "Effects of salinity on the nail-holding power of dimension lumber used in light-frame wood building," *J. For. Res.*, vol. 26, no. 3, pp. 765–770, 2015, doi: 10.1007/s11676-015-0118-9.

[9] L. Yermán, L. M. Ottenhaus, C. Montoya, and J. J. Morrell, "Effect of repeated wetting and drying on withdrawal capacity and corrosion of nails in treated and untreated timber," *Constr. Build. Mater.*, vol. 284, pp. 1–9, 2021, doi: 10.1016/j.conbuildmat.2021.122878.

[10] Y. Gao, S. Mei, X. Ma, and X. Meng, "Effects of decay on the mechanical properties of nailed joints in light wood frame structure," *For. Prod. J.*, vol. 71, no. 1, pp. 46–57, 2021, doi: 10.13073/FPJ-D-20-00054.

[11] L. Yermán, Y. Zhang, J. He, M. Xiao, L. M. Ottenhaus, and J. J. Morrell, "Effect of wetting and fungal degradation on performance of nailed timber connections," *Constr. Build. Mater.*, vol. 353, no. September, 2022, doi: 10.1016/j.conbuildmat.2022.129113.

[12] P. Dietsch, "Effect of reinforcement on shrinkage stresses in timber members," *Constr. Build. Mater.*, vol. 150, pp. 903–915, 2017, doi: 10.1016/j.conbuildmat.2017.06.033.

[13] A. Mainey, B. P. Gilbert, H. Bailleres, S. Gunalan, and M. Smith, "Solutions to reduce moisture driven backout and improve withdrawal strength of nailplates: experimental investigations," *Eur. J. Wood Wood Prod.*, vol. 77, no. 2, pp. 257–269, 2019, doi: 10.1007/s00107-019-01386-y.

[14] T. E. McLain, "Design axial withdrawal strength from wood: II. Plain-shank common wire nails," *For. Prod. J.*, vol. 47, no. 6, pp. 103–109, 1997.

[15] A. Wahyudianto, A. Fernandes, Erwin, and Wajilan, "Metal corrosion in wood joint products and structures: a review," *Int. J. Corros. Scale Inhib.*, vol. 11, no. 3, pp. 1269–1281, 2022, doi: 10.17675/2305-6894-2022-11-3-21.

[16] W. T. Simpson, *Dry kiln operator's manual*. Madison, Wisconsin, 1991. [Online]. Available: https://www.fpl.fs.usda.gov/documnts/usda/ah188/ah188.htm

[17] L. H. Groom, "Effect of Moisture Cycling On truss-plate joint behaviour," *For. Prod. J.*, vol. 44, no. March 1993, pp. 21–29, 1994.

[18] A. Mainey, B. P. Gilbert, A. Redman, S. Gunalan, and H. Bailleres, "Time dependent moisture driven backout of nailplates: experimental investigations and numerical predictions," *Eur. J. Wood Wood Prod.*, vol. 79, no. 6, pp. 1589–1605, 2021, doi: 10.1007/s00107-021-01735-w.

[19] O. Saifouni, J. F. Destrebecq, J. Froidevaux, and P. Navi, "Experimental study of the mechanosorptive behaviour of softwood in relaxation," *Wood Sci. Technol.*, vol. 50, no. 4, pp. 789–805, 2016, doi: 10.1007/s00226-016-0816-2.

[20] E. P. Lhuede, *Side and end grain withdrawal loads for single nails in Australian timber species*. Highett, Melbourne, Victoria: Commonwealth Scientific and Industrial Research Organization, Division of Building Research, 1985. [Online]. Available: https://catalogue.nla.gov.au/catalog/1690809

[21] R. J. Zhao, B. H. Fei, E. L. Chen, W. Guo, and H. Bin Zhou, “Nail withdrawal strength of Chinese fir dimension lumbers,” *Jianzhu Cailiao Xuebao/Journal Build. Mater.*, vol. 13, no. 4, pp. 463–467, 2010, doi: 10.3969/j.issn.1007-9629.2010.04.009.

[22] P. Navi and S. Stanzl-Tschegg, “Micromechanics of creep and relaxation of wood. A review. COST Action E35 2004-2008: Wood machining - Micromechanics and fracture,” *Holzforschung*, vol. 63, no. 2, pp. 186–195, 2009, doi: 10.1515/HF.2009.013.

[23] J. C. Pina *et al.*, “Experimental study on the short-term stress relaxation response of Chilean radiata pine,” *Wood Sci. Technol.*, vol. 56, no. 3, pp. 833–850, 2022, doi: 10.1007/s00226-022-01380-3.

[24] X. Arzola-Villegas, R. Lakes, N. Z. Plaza, and J. E. Jakes, “Wood moisture-induced swelling at the cellular scale-Ab intra,” *Forests*, vol. 10, no. 11, 2019, doi: 10.3390/f10110996.

[25] P. U. A. Grossman, “Requirements for a model that exhibits mechano-sorptive behaviour,” *Wood Sci. Technol.*, vol. 10, no. 3, pp. 163–168, 1976, doi: 10.1007/BF00355737.

[26] Standards Australia, “AS/NZS 1748.1 Timber - Solid - Stress-graded for structural purposes,” Sydney, NSW, 2011. [Online]. Available: https://au.i2.saiglobal.com/management/display/index/0/894876/-/81465c14dec07f659b4a4d5fcb8c916a

[27] ASTM International, “Standard test methods for direct moisture content measurement of wood and wood-base materials - D4442-20,” vol. 92, no. December, pp. 1–6, 2007, doi: 10.1520/D4442-20.

[28] ASTM International, “Standard Test Methods for Mechanical Fasteners in Wood and Wood-Based Materials,” Conshohocken, USA, 2020. doi: 10.1520/D1761-20.

[29] British Standards Institution, “Timber Structures — Test methods — Withdrawal capacity of timber fasteners BS EN 1382:2016,” 2016. [Online]. Available: https://bsol-bsigroup-com.ap1.proxy.openathens.net/Bibliographic/BibliographicInfoData/000000000030297196

[30] Y. Murase, “Friction of Wood Sliding on Various Materials,” *J. Fac. Agric. Kyushu Univ.*, vol. 28, no. 4, pp. 147–160, 1984, doi: 10.5109/23785.

[31] Forest Products Laboratory, “Wood Handbook: Wood as an Engineering Material,” Madison, Wisconsin, USA, 2010. doi: 10.2737/FPL-GTR-190.

[32] S. Huč, T. Hozjan, and S. Svensson, “Rheological behavior of wood in stress relaxation under compression,” *Wood Sci. Technol.*, vol. 52, no. 3, pp. 793–808, 2018, doi: 10.1007/s00226-018-0993-2.

ICTB 2025. 5th International Conference Timber Bridges
Rotorua, New Zealand, 29 June to 2 July 2025.

BRIDGES IN SWITZERLAND - EXPERIENCE OF BRIDGES FOR PEDESTRIANS, TRAFFIC AND WILDLIFE OVERPASS

Stefan Zöllig[1], Bettina Franke[2], Lukas Rüegsegger[3], Andreas Burgherr[4]

ABSTRACT

The contemporary use of timber in bridge construction in Switzerland includes the growing trend of integrating sustainable materials into modern infrastructures. The study reviews the recent advancements and applications of timber in various bridge types, with a focus on replacement and wildlife animal bridges. The paper discusses the design, emphasizing the need for innovative solutions that balance durability, environmental impact, and structural performance. The findings suggest that timber, when properly designed and maintained, offers a viable alternative to conventional materials, aligning with sustainability goals while meeting the demands of modern infrastructure.

Keywords: Timber Bridges, advancements, heavy traffic bridges, wildlife overpass, durability

1 INTRODUCTION

Timber bridges have been an integral part of infrastructure for centuries, valued for their natural aesthetic, sustainability, and adaptability. In recent years, there has been a renewed interest in timber as a primary material for bridge construction, driven by advancements in engineering techniques and a growing emphasis on environmentally friendly building practices, [1]. The construction of timber bridges encompasses a variety of structural designs, each suited to different environmental conditions and load requirements. Suspension bridges, known for their flexibility and ability to span long distances, truss bridges, which offer strength and rigidity through a framework of interconnected elements, and arch bridges, celebrated for their classic form and efficient load distribution, are all common in timber construction. Additionally, block glued glulam beam bridges, which utilize solid timber beams, provide a straightforward yet effective solution for shorter spans.

The historical development of bridges is summarized in Figure 1. The green-shaded area illustrates bridge types already realized in timber construction – ranging from pedestrian and road bridges to wildlife overpasses. The diversity of structural designs and performance capabilities is described, among others, by [2], [3]. The examples shown in the figure are taken from Switzerland and serve as representative case studies. The grey-shaded area of the figure outlines visionary concepts for heavy traffic | motorway bridges with up to three traffic lanes in one direction. Engineers are currently working on innovative solutions to realize such large-scale timber bridges. Initial studies demonstrate both the technical feasibility and the potential of these concepts, [4], [5], [6]. Each of these designs leverages the unique properties of timber – such as its high strength-to-weight ratio, fast er and ease of handling – while also presenting specific challenges related to durability, maintenance, and long-term performance. This paper addresses the potential for durable timber bridges through the use of structurally protected wood. Insights gained from planning processes and bridge inspections are summarized and discussed.

[1] Stefan Zöllig, Timbatec Holzbauingenieure Schweiz AG, Switzerland, e-mail: stefan.zoellig@timbatec.ch
[2] Dr. Bettina Franke, Timbagroup Holding AG, Switzerland, e-mail: bettina.franke@timbatec.ch
[3] Lukas Rüegsegger, Timbatec Holzbauingenieure Schweiz AG, Switzerland, e-mail: lukas.ruegsegger@timbatec.ch
[4] Andreas Burgherr, Timbatec Holzbauingenieure Schweiz AG, Switzerland, e-mail: andreas.burgherr@timbatec.ch

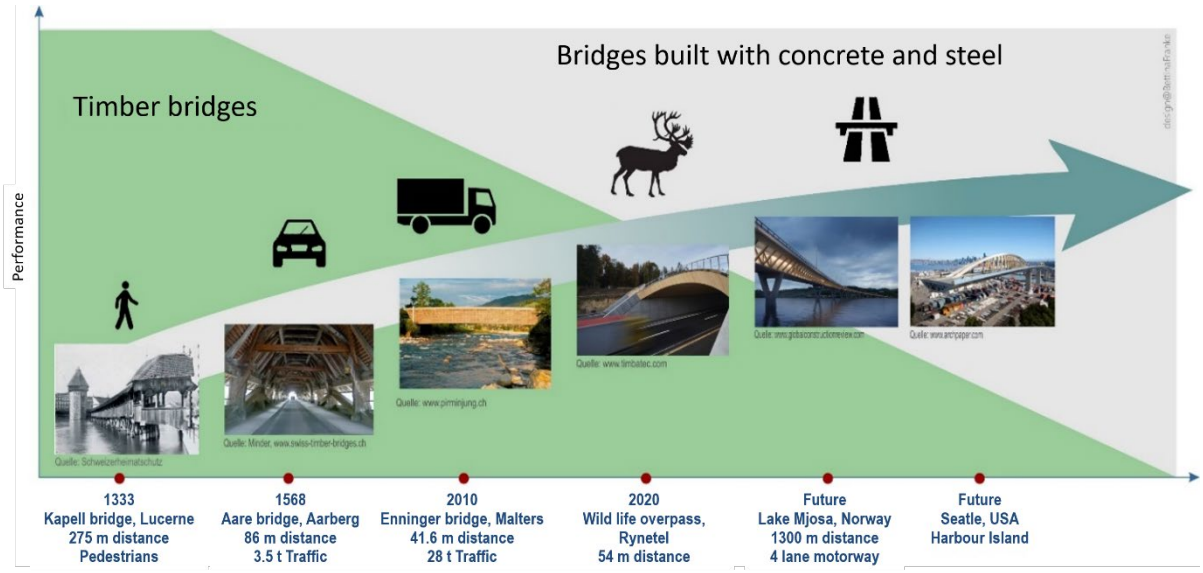

Figure 1. Timber bridge construction technologies with different performances and vision for the future, source: [4], [5], [6]

2 PRESERVATION OF WOOD VERSUS MOISTURE CONTENT

Bridges are part of the infrastructure and, according to EN 1990:2010, must be designed for a service life of 100 years. Historical examples such as the timber bridge in Aarberg, which serves for traffic up to 3.5 tonnes for more than 450 years, demonstrate the long-term performance potential of timber as a structural material, [7]. Timber can perform sustainably if it remains dry or has the ability to dry out after wetting. As an organic and hygroscopic material, wood naturally adjusts its moisture content in response to ambient climatic conditions. Increased humidity or direct exposure to the elements results in increased moisture content in the wood. This has been confirmed by studies carried out as part of a monitoring campaign on timber bridges.

Seasonal climate variations cause cyclic changes in the moisture content of the wood, particularly in the outer layers to a depth of approximately 5 cm. These moisture variations create moisture gradients over the cross section that lead to internal stresses, particularly tensile stresses perpendicular to the grain in the wetting zone, [8]. These stresses are not negligible and must be carefully considered in structural design and durability assessments. Increasing moisture increases the risk of infestation by wood-destroying insects or fungi. Infestation is favoured by prolonged contact of the timber structure with leaves, soil, grit and snow. The timber structure must therefore be protected in such a way that the moisture content of the material remains below 20 M% on an annual average and the structure is not damaged by direct contact with dirt, [9], DIN 68800-1.

In general, timber bridges can be classified in service class 2 according to EN 1995-1:2004. During a monitoring campaign, representative bridge projects were investigated and the climate and moisture content were recorded. The average values measured were compared to the theoretical equilibrium moisture content calculated from the climate data of a nearby meteorological station, as shown in Figure 2. Both results confirm, that timber bridges can be generally classified in service class 2 according to EN 1995-1:2004. In Switzerland and throughout middle Europe (Germany, Austria and Switzerland), timber bridges are typically designed without the use of chemical wood preservatives ([9], [10]. Instead, wood protection is integrated into the overall bridge design by structural protection measures. These include roofs, cladding elements or, in the case of open bridges, the use of durable deck systems such as sealed surfaces, [11], [12], [13], [14], [15], [16]. Additionally, monitoring systems can be used for prevention and warning systems, [17]. This approach represents an important step towards climate-

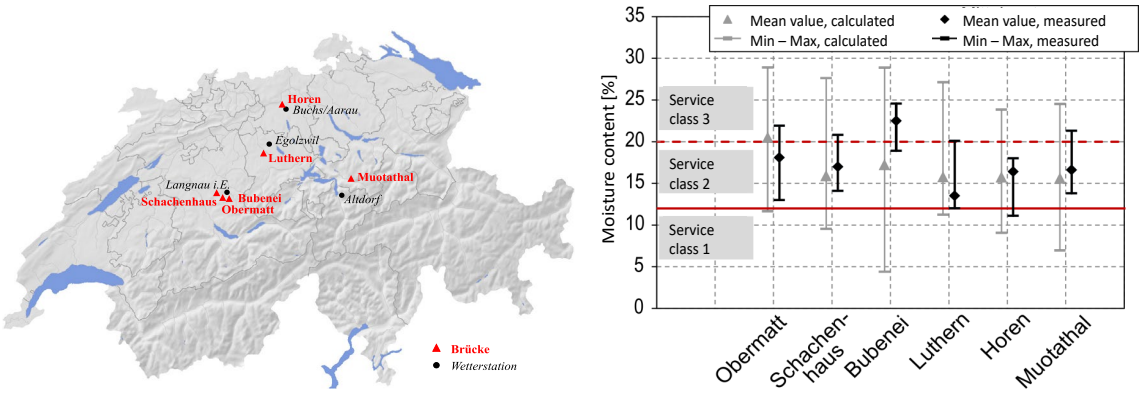

Figure 2. Map of Switzerland with monitored bridges marked (left) and classification of moisture content measured compared to service classes according to EN 1995-1:2004, source: [16]

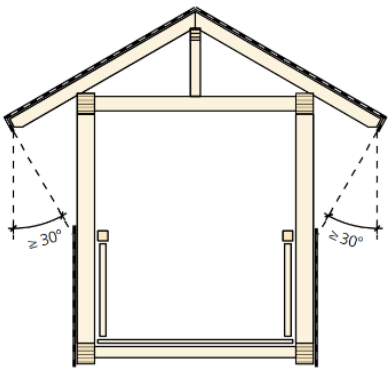

Figure 3. Covered roof bridges with gladding against driving rain, source: [9]

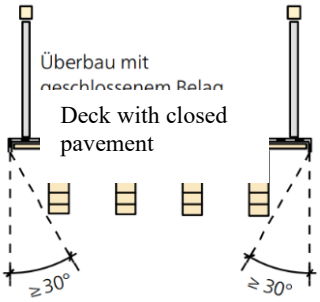

Figure 4. Open bridges, dense coverings to protect the construction, source: [9]

friendly and sustainable constructions, based on the principles of material recycling and long service life. By eliminating chemical treatments and relying on intelligent design strategies, timber bridges can meet modern durability requirements while supporting environmental goals.

3 REPLACEMENT OF OLD BRIDGES WITH MODERN TIMBER BRIDGES

3.1 Le Tirage – Open bridge type

The renovation project of the "Le Tirage" bridge in Valangin, Switzerland, involved the replacement of a historic bridge originally constructed in 1913. Due to significant deterioration, the old bridge was no longer capable of safely handling modern traffic loads. The new timber bridge, designed and built to withstand loads up to 40 tons. The primary structure consists of glued laminated spruce beams. Solid larch boards are installed transversely to the main beams. They are manufactured with an integrated slope from the centre of the deck to the longitudinal edges, as shown in Figure 6, intended to prevent the formation of black ice. The rainwater is channelled via a longitudinal slope of the bridge to the road transition. The transition joint is a closed solution for the protection of the timber structure.

This reconstruction demonstrates the ability of modern timber engineering to provide durable, high-capacity infrastructure while respecting the historic context of the site. The bridge was prefabricated, allowing for a fast and efficient construction process. By assembling large structural elements off-site and installing the bridge as a single lifted unit, site works were minimised, significantly reducing construction time and traffic disruption. This approach demonstrates the benefits of industrialised timber construction, combining precision fabrication with accelerated project delivery.

Figure 5. Le Tirage bridge, side view, lifting of bridge deck element, cross section, source: Timbatec Holzbauingenieure Schweiz AG.

3.2 Wühribach Bridge – Covered bridge

The ravages of time had clearly taken their toll and the concrete bridge over the Wühribach was falling apart. For this reason, the two local authorities decided to demolish the existing concrete structure and build a new timber bridge. The deciding factor for timber was that in a heavily forested area, a timber bridge is a commitment to local timber. The demands on the bridge over the Wühribach are high. Forestry vehicles regularly transport logs across the stream. The bridge is therefore approved for 32 tonnes. The wooden bridge has a span of 13.5 metres, the clearance profile is 4 metres wide and 4.50 metres high. The side walls have been designed as trussed girders. The new bridge is covered, partly for structural reasons and partly to protect the wooden bridge structure from the weather, thus ensuring a long service life for the structure.

A distinctive feature of this covered bridge is its timber deck, which consists solely of solid oak planks. A conscious decision was made to omit any asphalt layer, relying instead on the proven durability of oak in this type of bridge and its intended use. Experience has shown that oak decking performs reliably, even under regular traffic loads. After seven years in service, no significant signs of deterioration have been observed. This finding is supported by studies on comparable reference projects, where oak decking has been in use for several decades and subjected to regular inspections. Aside from minor surface wear in the wheel tracks, oak has proven to be a robust and sustainable material, offering long-term performance without the need for additional protective layers.

Figure 6. Wühribach bridge, views and flooring with oak planks, source: Timbatec Holzbauingenieure Schweiz AG

4 WILDLIFE OVERPASSES IN SWITZERLAND

Wildlife overpasses, also known as ecoducts, wildlife or green bridges, play a crucial role in maintaining ecological connectivity in fragmented landscapes. As transportation infrastructure expands, natural habitats are increasingly divided, posing significant risks to biodiversity and leading to wildlife-vehicle collisions. Wildlife overpasses are specifically designed to enable safe crossing for animals, thereby reconnecting habitats, supporting migration routes, and contributing to the conservation of species. While such structures are traditionally built using concrete, timber has emerged as a viable and sustainable alternative. Timber overpasses offer several advantages: they are carbon-storing, renewable, and visually well-integrated into natural landscapes. Moreover, modern timber engineering enables the realization of robust and durable structures in a short time.

Figure 7. Rynetel wildlife overpass, source: Timbatec Holzbauingenieure Schweiz AG

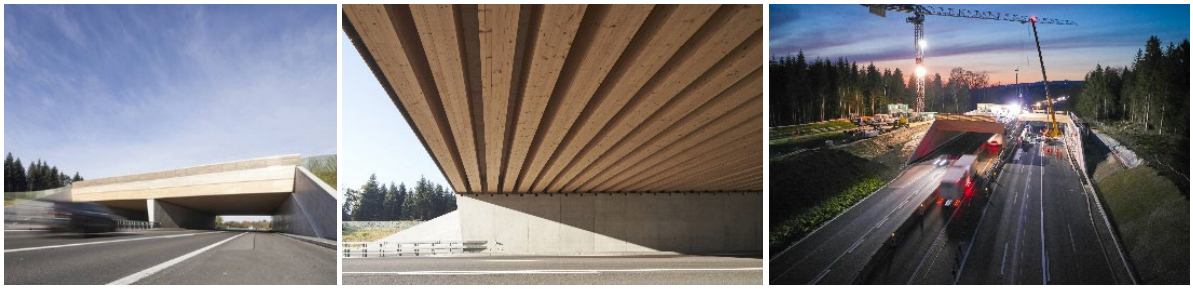

Figure 8. Wildlife overpass Neuenkirch, Lucerne, view from outside and underneath; construction during night, source: Timbatec Holzbauingeneure Schweiz AG

In Rynetel, Neuenkirch, and Biberlikopf wildlife overpasses are built in the national road network of Switzerland. The Rynetel wildlife overpass, located along the A1 motorway in the canton of Aargau (Switzerland), is one of Switzerland most prominent examples of timber-based ecological infrastructures, [19]. Commissioned in 2011, it was the first large wildlife overpass constructed entirely using timber as the primary load-bearing material. The overpass spans approximately 50 meters along the road axes and has a total width of 2 x 18 meters, enabling safe passage for a wide range of animal species from small mammals to deer. The structural concept is based on a two-hinged arch system, realized with glued-laminated timber (glulam) elements. The arch ribs support a timber deck system that forms the base of the overpass, covered with layers of soil, vegetation, and natural substrates, recreating a habitat corridor across the motorway.

The second wildlife overpass with a structural system of timber was Neuenkirch. The wildlife overpass in the canton of Lucerne has a width of 50 metres and a length of around 36 metres. The clear height is 4.80 metres. The overpass is a girder bridge with two spans. The beams have a height of 1.24 metres and are closely spaced. During the design phase, the spacing between the beams was assessed using a building physics simulation to ensure sufficient air circulation in the upper areas where the deck joins. The 2- and 3-year inspections confirm that the spacing is sufficient and that air circulation is good, as the beams do not have elevated wood moisture levels. The challenge during the construction phase was that traffic continued to flow even while the girders were being installed. During around 30 nights, traffic was restricted to one lane in two-way traffic. During the day, two lanes were always available in each direction.

To restore ecological corridors across major transport routes, the "Biberlikopf" wildlife crossing will be another timber eco-duct in Switzerland. Currently at an advanced design stage, it will be constructed as a 57-metre-wide timber arch bridge spanning the A3 motorway. The design follows the successful approach of using engineered wood as the primary structural material, ensuring a combination of sustainability, durability and harmonious integration into the surrounding landscape. Due to the specific ground conditions, concrete rammed piles will

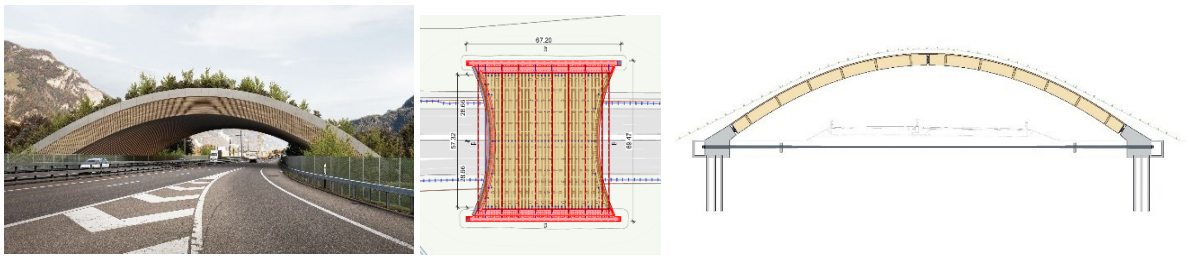

Figure 9. Wild life overpass «Biberlikopf», visualization and timber arch planned, source: Nightnurse Images, Zürich, dsp Ingenieure + Planer AG, Timbatec Holzbauingenieure Schweiz AG

be used instead of large foundations to support the lightweight and delicate timber arch structure. The arch will span both directions of traffic, and steel tie rods will be installed below the road surface to effectively transfer the tensile forces and ensure the stability of the bridge.

For all three wildlife overpasses, in addition to the structural challenges, the issue of durability due to of traffic spray was a key concern. These bridges span distances of up to 50 metres, raising several questions about the drying potential of the supporting structure, the effects of freeze-thaw salt exchange and the need for chemical wood preservatives. The answers to these questions are provided by the monitoring results from the Rynetel wildlife overpass. Continuous measurements of wood moisture content were taken at various locations, including the entrance and exit arches and the centre of the bridge, as shown in Figure 10. The results indicate that there is no significant threat to the wood, [20]. The average moisture content values were consistently well below the critical threshold of 20 % moisture content - the point at which the wood is at risk of deterioration.

The three wildlife overpasses show also the development in terms of avoiding or reducing the use of chemical wood preservatives. In the case of the first wildlife overpass Rynetel, there was still uncertainty of the building owner, so that chemical wood preservatives were used in the support structure. For the construction of the second wildlife bridge in Neuenkirch, the amount of chemical wood protection was reduced. Only the top 4 lamellas of the structural beams were chemically protected, as increased wood moisture was expected due to the anticipated limited air circulation during the planning phase. For the third Biberlikopf wildlife overpass, chemical wood preservatives have been completely eliminated from the load-bearing structure. This is a positive development based on experience and the results of monitoring the moisture content on the timber structure caused by the traffic flow.

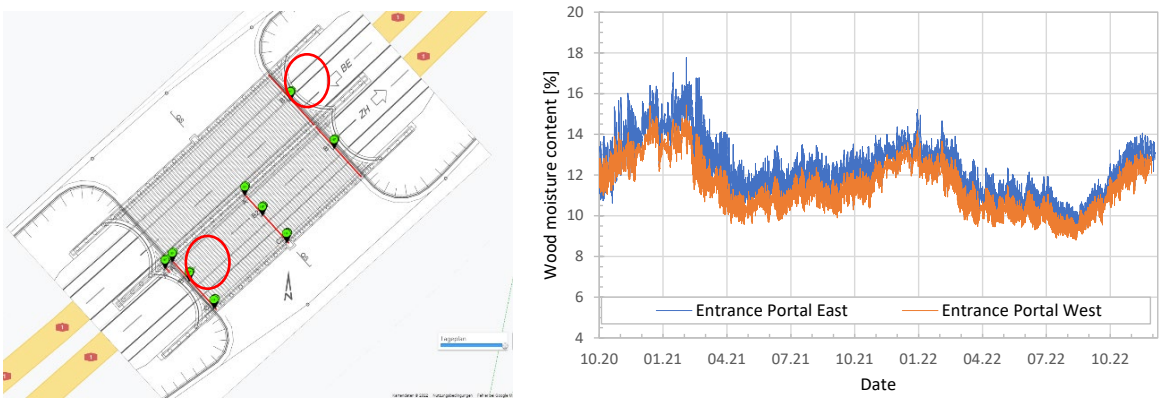

Figure 10. Measuring plan of Rynetel – wildlife overpass (left), measuring result of moisture content at the entrance portals

5 HEAVY TRAFFIC TIMBER ROAD BRIDGES – FEASIBILITY OF LARGE-SCALE APPLICATIONS

Recent feasibility study has explored the potential of realizing large-scale timber road bridges, including configurations with three traffic lanes plus a breakdown lane in one direction, as shown in Figure 11. These concepts are based on the hollow box girder type, a structural system commonly used in concrete and steel bridges, and now being adapted for timber construction. The design scenario assumes a main span of 60 meters within a multi-span configuration and load assumptions according to EN 1990:2010, including a design traffic load of 60 tonnes. Preliminary analyses indicate that the load-bearing capacity and serviceability requirements can be met using engineered timber products such as glulam and cross-laminated timber (CLT), potentially enhanced with reinforcing steel or wood-concrete composites, [6].

Compared to conventional steel or prestressed concrete solutions, timber box girders offer several advantages in terms of material sustainability, CO_2 footprint, and modular prefabrication. While steel and concrete bridges provide well-established solutions for long spans and high loads, they come with significant embodied energy and carbon emissions, especially during production and construction. In contrast, timber is a renewable material that stores carbon and supports climate-neutral construction goals, particularly when sourced from sustainably managed forests.

Structurally, concrete and steel allow for more compact cross-sections and often longer spans without intermediate supports. However, modern timber technologies are increasingly closing this gap through optimized geometry and advanced connection systems. For spans around 60 meters under heavy highway loads, timber hollow box girders present a viable alternative, especially when lifecycle considerations and environmental performance are prioritized. These developments mark a significant step toward the integration of timber in high-performance infrastructure, supporting a broader shift toward resource-efficient and climate-resilient constructions.

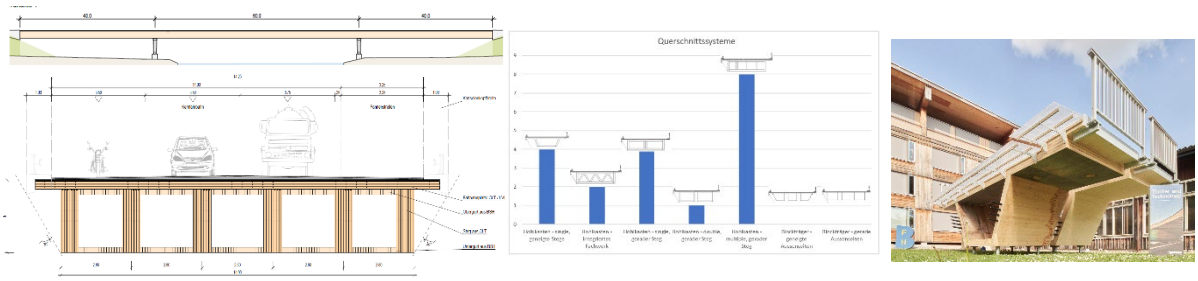

Figure 11. Feasibility study for heavy traffic timber bridges, structural system and cross section (left), evaluation of different cross sections (middle), and mock up for two lane bridge (right), source [6]

6 CONCLUSIONS

Modern timber bridges have proven to be a viable and competitive alternative to conventional concrete and steel structures. With excellent structural performance, timber bridges can meet the same static and functional requirements as their counterparts in other materials. At the same time, they offer distinct advantages in terms of sustainability, resource efficiency and construction speed.

Applications range from lightweight pedestrian bridges to heavily trafficked road bridges and large span wildlife overpasses. In all typologies, durability can be ensured through structural timber protection, without the need for chemical treatments for the European region. Intelligent

design solutions - such as protective cladding, covered structures and moisture management - have been shown to maintain timber components well below critical moisture content, as confirmed by long-term monitoring data.

The examples presented clearly demonstrate the long-term performance and resilience of engineered timber, even under challenging environmental conditions. In addition, the use of renewable materials, combined with prefabrication and minimal on-site labour, helps reduce carbon emissions, supports circular building practices and contributes to global climate and sustainability goals set out in international frameworks. Timber bridges are no longer a niche solution - they represent a forward-looking, climate-conscious approach to infrastructure development that is both technically sound and environmentally responsible.

7 REFERENCES

[1] Zöllig S. (2022) Infrastructure made of wood – opportunities for decarbonization of the public sector, Conference Proceedings, 4th ICTB, Biel/Bienne, https://doi.org/10.24451/s13g-td18

[2] Seidel A., Keil A., Hafner A., Özdemir Ö., Jacob-Freitag S. (2019) Drüber und Drunter, Brücken aus Holz, Qualitätsgemeinschaft Holzbrückenbau e.V., Germany

[3] Bachofer, R. and Conzett J. (2013) Brucken in Holz: Moeglichkeietn und Grenzen, Forschungsprojekt AGB 2003/012, Schweizer Verband der Strassen – und Verkehrsfachleute VSS, Switzerland.

[4] Besix (2020) Besix enters Norwegian market with bridge and road win, https://www.theconstructionindex.co.uk/news/view/besix-enters-norwegian-market-with-bridge-and-road-win, online 04.04.2025

[5] Schlosser K. (2020) Is wood the way to rebuild West Seattle Bridge? Architect shares idea to replace cracking roadway, https://www.geekwire.com/2020/wood-way-rebuild-west-seattle-bridge-architect-shares-idea-replace-cracking-roadway/, online 04.04.2025

[6] Franke S., Franke B., Pfindel C., Gkesouli V., Sigrist C. (2024) Machbarkeitstudie zu Schwerlastbrücken in Holz für Schweizer National- und Kantonsstrassen, Research Report, Bern University of Applied Sciences, Switzerland

[7] Aarberg Bridge (2025) documentation of aarberg bridge, http://swiss-timber-bridges.ch/detail/666.html, online 04.042025

[8] Franke B., Schiere M., Franke S. (2022) Climate and moisture induced stresses in block-glued glulam members of timber bridges, Conference Proceedings, 4th ICTB, Biel/Bienne

[9] Simon A., Arndt R., Jahreis M., Koch J. (2019) Musterbauzeichnungen für Holzbrücken, holzbau handbuch, Reihe 1, Teil 9, Folge 3, Qualitätsgemeinschaft Holzbrückenbau e.V., Germany

[10] Schwaner K. (2004) Protection and durability in the case of timber bridges, 10th International Forum Wood, Garmisch Partenkirchen, https://events.forum-holzbau.com/pdf/schutz_und_dauerhaftigkeit.pdf, online 03.04.2025

[11] Gerold M. (2006): Musterzeichnungen als Grundlage zur ZTV-ING 9.3 Holzbrücken. Abschlussbericht Forschungsvorhaben, DGfH Innovations- und Service GmbH, München. (Sample drawings to the German standard ZTV-ING 9-3 Timber Bridges. Final research report, DGfH Innovations and Service Ltd., Munich.

[12] Gerold M. (2010) Planungshinweise zum baulichen Holzschutz und zur Entwässerung von Brückenbauwerken, https://www.brettschichtholz.de/publish/binarydata/pdf_oeffentlich/musterz_holzbruecken.pdf, online 03.04.2025

[13] Müller A., Angst C., Bueche N., Schiere M., Huber L., Bonifacio S., Maurer J. (2021), VSS2016/326 Abdichtungssysteme und bitumenhaltige Schichten auf Brücken mit Fahrbahnplatten aus Holz, Bern University of Applied Sciences, Institute of Timber Construction, Structures and Architecture, Biel, Switzer

[14] Bernard and Lehmann (2014), Forschungspaket Brückenabdichtungen: EP6 - Anschlüsse von Brückenabdichtungen, Forschungsprojekt VSS 2006/516, Schweizerischen Verbands der Strassen- und Verkehrsfachleute, Switzerland

[15] VSS 40 451 (2019) Abdichtungssysteme und bitumenhaltige Schichten auf Brücken mit Fahrbahnbelägen aus Holz, Schweizer Verband der Strassen und Verkehrsfachleute VSS, Switzerland

[16] Schiere, M., Müller, A., Bueche, N., Angst, C. (2022), Creating a connecting between asphalt wearing surface and timber bridge decks, Conference Proceedings, 4th ICTB, Biel/Bienne

[17] Franke S., Franke B., Schiere M., Bonifacio S., Müller A. (2022) Monitoring systems for timber bridges – Moisture content and swinging behaviour, Conference Proceedings, 4th ICTB, Biel/Bienne, https://doi.org/10.24451/w5yg-j871

[18] Franke B., Franke S., and Müller A. (2015) Case studies: long-term monitoring of timber bridges, Journal of Civil Structural Health Monitoring 5, p. 195-202.

[19] Rüegsegger L. (2022) First Swiss wildlife bridge made with timber, Conference Proceedings, 4th ICTB, Biel/Bienne,

[20] Wakili K., Schiere M., Bonifacio S., Kauz U., Maurer J., Rüegsegger L., Müller A. (2023) Monitoring climatic impacts on the moisture uptake of the first Swiss wildlife bridge made of wood, European Journal of Wood and Wood Products, https://doi.org/10.1007/s00107-024-02052-8